Understanding interactions between phoma stem canker causal pathogens *Leptosphaeria maculans* and *Leptosphaeria biglobosa*

Evren Bingol, BSc. (Hons)

Submitted to the University of Hertfordshire in partial fulfilment of the requirements of the degree of Doctor of Philosophy

School of Health, Medicine and Life Sciences, University of Hertfordshire
Hatfield, Hertfordshire, AL10 9AB

May 2026

Abstract

This project aimed to improve the understanding of interspecific interactions between *Leptosphaeria maculans* and *Leptosphaeria biglobosa* and to provide valuable insights for future integrated strategies for control of phoma stem canker on oilseed rape (*Brassica napus*) in the UK. These aims were achieved by investigating interspecific interactions between *L. maculans* and *L. biglobosa in vitro*, *in planta* and in natural conditions.

In vitro experiments confirmed the ability of *L. biglobosa* to inhibit the production of sirodesmin PL by *L. maculans* under simultaneous co-inoculation. Further results showed differences between *L. maculans* and *L. biglobosa* in growth in liquid cultures; with *L. biglobosa* having a growth rate approximately three times greater than that of *L. maculans*. Growth of mycelia in simultaneously co-inoculated cultures showed a similar trend to that of *L. biglobosa* only, suggesting that the growth of *L. maculans* was inhibited by *L. biglobosa*. Sequential co-inoculation experiments showed that in liquid culture, *L. biglobosa* not only inhibits the production of sirodesmin PL by *L. maculans* but also inhibits the growth of *L. maculans* if inoculated before or up to one day after *L. maculans*, confirmed by quantitative polymerase chain reaction (qPCR) analyses. Interestingly, if *L. biglobosa* was co-inoculated three days after *L. maculans*, it was only able to partially inhibit the production of sirodesmin PL and the growth of *L. maculans* in liquid culture. Finally, if *L. biglobosa* was co-inoculated five days or later after *L. maculans*, enough time was provided for *L. maculans* to successfully produce sirodesmin PL, which in return led to inhibition of *L. biglobosa* growth by *L. maculans*. These results showed that the timing of interaction directly affects the outcome of interspecific interactions between *L. maculans* and *L. biglobosa*.

Results from *in planta* experiments showed that *L. biglobosa* can inhibit the production of sirodesmin PL by *L. maculans* when simultaneously co-inoculated on cotyledons of oilseed rape. In addition, the phenotype of lesions observed in the simultaneous co-inoculation treatment was similar to those of *L. biglobosa* only, suggesting that the growth of *L. maculans* was also inhibited by *L. biglobosa in planta*. Further results from *in planta* experiments with sequential co-inoculations showed similar results to those *in vitro*, with a small difference in the timeline. When *L. biglobosa* was inoculated before or

up to one day after *L. maculans* at the same site on cotyledons of oilseed rape, small, dark necrotic lesions appeared shortly after infection and expanded slowly under humid conditions, similar to those of *L. biglobosa* only. Furthermore, the growth of *L. maculans* was inhibited in those lesions, confirmed by qPCR. Conversely, when *L. biglobosa* was co-inoculated three days or later after *L. maculans*; small, grey lesions appeared by 7-10 days post inoculation (dpi) and rapidly expanded by 14-16 dpi, similar to those of *L. maculans* only and the growth of *L. biglobosa* was inhibited. Finally, the results for gene expression experiments in relation to plant defences indicated induction of systemic acquired resistance (SAR) through upregulation of *PR-1* and defence responses against a necrotrophic pathogen through upregulation of *WRKY33* but were otherwise inconclusive. These results showed that the timing of the interaction also plays a crucial role in determining the outcome of the competitive interactions between *L. maculans* and *L. biglobosa in planta*, which subsequently affects disease development and severity.

Observations made by monitoring the patterns of ascospore release of *L. maculans* and *L. biglobosa* at Bayfordbury, Hertfordshire over four growing seasons (2020/2021 to 2023/2024) showed the release of ascospores of both *Leptosphaeria* species at similar times. The first ascospore release was generally observed at the end of September, with the maximum release of ascospores generally observed in late-October/early-November, dependent on environmental conditions such as temperature and rainfall. Next, results of field experiments at Harpenden, Hertfordshire and Norwich, Norfolk over two growing seasons (2023/2024 and 2024/2025) showed little to no difference in overall disease incidence (% of plants affected) between different sites and different growing seasons for ten cultivars assessed. Interestingly, there were differences in the percentage of phoma leaf spot lesions caused by *L. maculans* and *L. biglobosa*. At both sites, a predominance of *L. biglobosa* in causing phoma leaf spot lesions was observed in the 2023/2024 growing season and *L. maculans* in the 2024/2025 season. These differences were most probably due to differences in weather conditions, stubble management practices and fungicide applications. Next, results of field experiments at Hereford, Herefordshire and Huntingdon, Cambridgeshire over two growing seasons (2021/2022 and 2022/2023) showed differences in overall phoma stem canker disease severity at different sites and in different growing seasons for two cultivars per assessment, despite showing little to no difference in percentage of *Leptosphaeria* species in stem cankers, where > 95 % of the DNA in stem basal cankers was of *L. maculans*, confirmed by qPCR. Finally, results

of field experiments at Wisbech, Cambridgeshire over two growing seasons (2021/2022 and 2022/2023) showed an increase in phoma stem canker disease severity in the latter season for cultivars with only the *Rlm7* resistance gene, with > 95 % of the DNA in stem basal cankers quantified as *L. maculans*, suggesting a breakdown of resistance event. Strikingly, for Line-A, which has both *Rlm7* and *RlmS*, the percentage of *L. biglobosa* DNA in stem basal cankers was the greatest across both growing seasons and increased to > 50 % in the latter season, suggesting that combining multiple resistance genes against *L. maculans* in oilseed rape cultivars may increase their susceptibility to *L. biglobosa*. These results showed that environmental and human factors, such as weather conditions and various disease control practices, may influence the interspecific interactions between *L. maculans* and *L. biglobosa*, which may subsequently affect proportions of pathogen populations and the course of disease epidemics.

This project improved the understanding of interspecific interactions between *L. maculans* and *L. biglobosa* by combining existing knowledge with novel findings from experiments and provided contemporary ideas to be incorporated into future integrated management strategies.

Acknowledgements

Firstly, I would like to thank my supervisory team: Prof Yong-Ju Huang, Dr Chinthani Karandeni-Dewage and Prof Bruce Fitt at the University of Hertfordshire and Dr Faye Ritchie at ADAS, for their unwavering support and encouragement during my PhD. I am grateful to the Centre for Agriculture, Food and Environmental Management Research (CAFEM) at the University of Hertfordshire, the Perry Foundation, Felix Thornley Cobbold Agricultural Trust and Chadacre Agricultural Trust for funding my PhD project and to ADAS for providing valuable in-kind contributions. I am also grateful to the British Society for Plant Pathology (BSPP) for providing travel grants.

I would like to thank Dr Aiming Qi for guidance and training in statistical analyses in all three of my research chapters. I would also like to thank Dr Avice Hall, Dr Cristina Barrero-Sicilia and Dr Shan Goh from the plant pathology and microbiology research laboratory for their support and encouragement. I extend my thanks to Mansukh Vadalia, Diana Francis, Aiden Bygrave, Jamie Stone and Hannah Fastenbauer for providing technical support for my experiments. I further extend my thanks to James Stanley and Christine Gigou for their help with method development for HPLC analyses and Dr Daniel Baker for doing LC-MS analyses used in Chapters 3 and 4. I thank Dr James Fortune for providing training in various methods I used during my PhD and our collaborative experiment presented in Chapter 4. I am grateful to Dr Mollie Langdon at Rothamsted Research and Carmel O'Neill at John Innes Centre for helping with field assessments in 2023/2024 and 2024/2025 growing seasons presented in Chapter 5. I would also like to thank Philip Walker and Andrew Francis at ADAS and Craig Padley and Dr Katherine Noel at LSPB for helping with field assessments in 2021/2022 and 2022/2023 presented in Chapter 5. I thank the MSc students Oluwasegun Ayobami Ademoyega, Fizza Basharat, Irfan Ali and Fathima Niyala for their help in processing stem samples used in Chapter 5.

I extend my gratitude to the members of the Crop Protection and Climate Change research group for their advice and support. Special thanks to my colleagues Valerija Parthala, Claire Wheeler, Dr Hannah Wileman and Dr Laura Sapelli, who all became close friends beyond the laboratory, for their tremendous support and encouragement throughout my PhD.

I am grateful to my dear friends Maya Dwane, Luke Oosterbaan and Emily Dwane for their positivity, uplifting energy and emotional support before and during my PhD. Finally, I would like to thank my family, Ozlem Gun, Atilay Bingol, Zeynep Bingol, Michael Duin and Agnes Morgan for their continuous love, support and encouragement.

Last but certainly not least, my final thank you is to my partner, Brandon Bourne, for his endless love, support and belief in me. I am incredibly grateful for his patience when our lives were being dictated by plants and his support during my most doubtful moments. I would not have been able to do this without you.

List of publications, presentations, events and awards

Publications

Fortune JA, **Bingol E**, Qi A, Baker D, Ritchie F, Karandeni-Dewage C, Fitt BDL, Huang YJ (2024). *Leptosphaeria biglobosa* inhibits the production of sirodesmin PL by *L. maculans*. *Pest Management Science 80:* 2416-2425. http://doi.org/10.1002/ps.7275. (Appendix O).

Bingol E, Qi A, Karandeni-Dewage C, Ritchie F, Fitt BDL, Huang YJ (2024). Co-inoculation timing affects the interspecific interactions between *Leptosphaeria maculans* and *Leptosphaeria biglobosa*. *Pest Management Science 80*: 2443-2452. http://doi.org/10.1002/ps.7799. (Appendix O).

Another manuscript is being prepared for submission to *Pest Management Science* for publication: **Bingol E,** Karandeni-Dewage C, Qi A, Ritchie F, Fitt BDL, Huang YJ (2026). Temporal dynamics of co-inoculation of *Leptosphaeria maculans* and *Leptosphaeria biglobosa* determine interspecific competition and disease development on oilseed rape.

Presentations

Internal

"*Leptosphaeria biglobosa* inhibits production of secondary metabolite sirodesmin PL by *L. maculans in planta*" – University of Hertfordshire Annual Life and Medical Sciences Conference in Hatfield, UK, June 2022 – Poster.

"Deciphering the influence of co-inoculation timing on antagonistic effects of *Leptosphaeria biglobosa* on *L. maculans*" – University of Hertfordshire Annual Life and Medical Sciences Conference in Hatfield, UK, June 2023 – Poster.

"Co-inoculation timing affects the interspecific interactions between phoma stem canker pathogens *Leptosphaeria maculans* and *L. biglobosa*" – University of Hertfordshire Annual Life and Medical Sciences Conference in Hatfield, UK, June 2023 – Oral presentation.

External (national)

"*Leptosphaeria biglobosa* inhibits production of secondary metabolite sirodesmin PL by *L. maculans in planta*" – Cereals in Hertfordshire, UK, June 2022 – Poster.

"Co-inoculation timing affects the interspecific interactions between phoma stem canker pathogens *Leptosphaeria maculans* and *L. biglobosa*" – AgriFood Charities Partnership (AFCP) Student Forum in Cambridge, Cambridgeshire, March 2024 – Oral presentation.

"Understanding interactions between *Leptosphaeria maculans* and *L. biglobosa* for improving control of phoma stem canker on oilseed rape in the UK" – British Crop Production Council (BCPC) Disease Review in Cambridge, Cambridgeshire, October 2024 – Oral presentation.

External (international)

"*Leptosphaeria biglobosa* inhibits production of secondary metabolite sirodesmin PL by *L. maculans in planta*" – British Society for Plant Pathology (BSPP) Annual Conference in Birmingham, West Midlands, UK, December 2021 – Poster.

"*Leptosphaeria biglobosa* inhibits production of secondary metabolite sirodesmin PL by *L. maculans in planta*" – International Organisation for Biological and Integrated Control (IOBC) Meeting on Integrated Control of Oilseed Crops, Online, May 2022 – Flash talk.

"Deciphering the influence of co-inoculation timing on antagonistic effects of *Leptosphaeria biglobosa* on *L. maculans*" – 16th International Congress of Plant Pathology (ICPP) in Lyon, France, August 2023 – Poster.

"Investigating the effects of co-inoculation timing on interspecific interactions between *Leptosphaeria maculans* and *L. biglobosa*" – British Mycological Society (BMS) Annual Conference, Newcastle, Northumberland, UK, September 2023 – Poster.

"Understanding the effects of co-inoculation timing on interspecific interactions between phoma stem canker pathogens (*Leptosphaeria maculans* and *L. biglobosa*)" – 16th International Rapeseed Congress (IRC) in Sydney, Australia, September 2023 – Poster.

"Co-inoculation timing affects the interspecific interactions between phoma stem canker pathogens *Leptosphaeria maculans* and *L. biglobosa*" – British Society for Plant Pathology (BSPP) Annual Conference in Oxford, Oxfordshire, September 2024 – Oral presentation.

Events

Internal

University of Hertfordshire Annual Life and Medical Sciences Conference in Hatfield, UK (June 2022)

University of Hertfordshire Annual Life and Medical Sciences Conference in Hatfield, UK (June 2023)

University of Hertfordshire Annual Life and Medical Sciences Conference in Hatfield, UK (June 2024)

External (national)

AgriFood Charities Partnership (AFCP) Forum on Oilseed Rape Pests and Diseases in Hatfield, UK (June 2021)

AgriFood Charities Partnership (AFCP) Forum on Young Minds and Ideas in Gloucester, Gloucestershire, UK (November 2021)

AgriFood Charities Partnership (AFCP) Student Forum in Cranfield, Bedfordshire, UK (March 2022)

Cereals in Hertfordshire, UK (June 2022)

AgriFood Charities Partnership (AFCP)/NIAB Meeting in Cambridge, Cambridgeshire (February 2023)

AgriFood Charities Partnership (AFCP) Student Forum in Cambridge, Cambridgeshire (March 2024)

Cereals in Hertfordshire, UK (June 2024)

British Crop Production Council (BCPC) Diseases Review Meeting in Cambridge, Cambridgeshire (October 2024)

External (international)

British Society for Plant Pathology (BSPP) Annual Conference in Birmingham, West Midlands, UK (December 2021)

International Organisation for Biological and Integrated Control (IOBC) Meeting – Integrated Control of Oilseed Crops, Online (May 2022)

British Society for Plant Pathology (BSPP) Annual Conference, Online (September 2022)

Association of Applied Biologists (AAB) – Climate Mitigation, Online (November 2022)

Association of Applied Biologists (AAB) – Biocontrol and IPM, Online (November 2022)

16th International Congress of Plant Pathology (ICPP) in Lyon, France (August 2023)

British Mycological Society (BMS) Annual Conference, Newcastle, Northumberland, UK (September 2023)

16th International Rapeseed Congress (IRC) in Sydney, Australia (September 2023)

British Society for Plant Pathology (BSPP) Annual Conference in Oxford, Oxfordshire (September 2024)

Awards

Best Poster Presentation (Flash talk) Award at International Organisation for Biological and Integrated Control (IOBC) Meeting on Integrated Control of Oilseed Crops, Online (May 2022)

Best Poster Presentation Award at University of Hertfordshire Annual Life and Medical Sciences Conference in Hatfield, UK (June 2022)

Best Oral Presentation Award at University of Hertfordshire Annual Life and Medical Sciences Conference in Hatfield, UK (June 2024)

Table of Contents

List of Figures

List of Tables

1 Chapter 1 – General introduction

1.1 Significance of oilseed rape

Oilseed rape or canola (*Brassica napus*) is a member of the mustard (*Brassicaceae*) family and originated as a result of a hybridisation event between turnip (*B. rapa*) and cabbage (*B. oleracea*), approximately 7.5 millennia ago (Nagaharu, 1935; Al-Shehbaz et al., 2006; Chalhoub et al., 2014; Lee et al., 2020) (Figure 1.1).

Production of oil being the most important, there are diverse applications of oilseed rape products across various industries (Orlovius & Kirkby, 2003). Oil extraction for human consumption, biodiesel production, production of lubricants to be used for engineering machinery and use of the by-products of these processes (i.e. oilseed rape meal) as animal feed are among applications of oilseed rape (van der Spiegel et al., 2013; Raboanatahiry et al., 2021). Additionally, a more recently conceived idea is utilising oilseed rape meal as a source of plant-based proteins for human consumption (Singh et al., 2022). Oilseed rape also plays an important role as a break crop.

The development of oilseed rape cultivars that contain reduced or no undesirable compounds (also called antinutritional factors), such as erucic acid and glucosinolates has led to an increase in the cultivation of oilseed rape (Friedt et al., 2018; Beszterda & Nogala-Kałucka, 2019). Furthermore, rapeseed oil is considered to have a greater nutritional value and health benefits compared to animal fats and several other vegetable oils, as it contains greater levels of unsaturated fatty acids, namely oleic acids, linolenic acid (omega-6) and α-linolenic acid (omega-3), and contains reduced levels of trans fats (Dubois et al., 2007; Ferguson et al., 2016; Beszterda & Nogala-Kałucka, 2019; Raboanatahiry et al., 2021). In addition, it was found in a clinical trial that dietary replacement of milk-fat-based cheese (containing saturated fats) with rapeseed oil-based cheese reduced overall total and especially low density lipoprotein cholesterol in participants (Karvonen et al., 2002).

Residue from the oil extraction processes is called oilseed rape meal (or cake) and contains an abundance of crude proteins (Chen et al., 2011). Oilseed rape meal can contain up to 40 % (400 g/kg) of crude proteins, depending on the growth conditions of

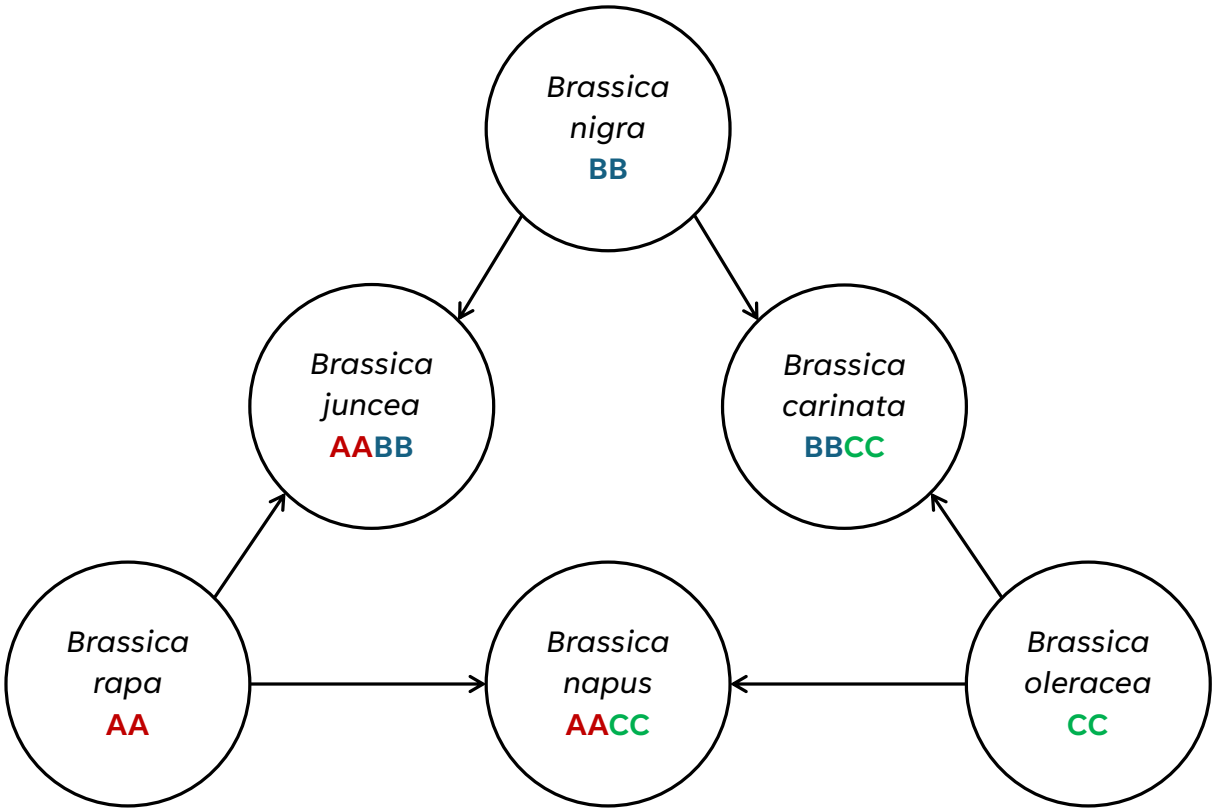

Figure 1.1: Speciation of *Brassica napus* (oilseed rape).

According to the 'Triangle of U' theory, *B. napus* (oilseed rape) originated from hybridisation of *B. rapa* (turnip) and *B. oleracea* (cabbage). These ancestors have also hybridised with *B. nigra*, which has led to the formation of *B. juncea* (brown mustard) and *B. carinata* (Ethiopian mustard). This figure was made based on the information in Nagaharu (1935) and Koh et al. (2017).

the crop and choice of method for oil extraction (Chen et al., 2011; Raboanatahiry et al., 2021). Moreover, oilseed rape meal has an amino acid profile of high methionine and cysteine, in addition to being a rich source of vitamins and minerals. Hence, it has been identified as a suitable candidate to be used in animal feed (Goding et al., 1972; Newkirk, 2011; Nega & Woldes, 2018).

Due to health and environmental sustainability concerns, there is currently an increasing trend in demand for plant-based proteins for human consumption instead of animal-derived proteins; particularly in the populations of developing and developed countries, where wide adoption of vegetarian and vegan diets is observed (Aiking, 2011; Henchion et al., 2017; Hoehnel et al., 2022). The needs for further societal and industrial transitions towards more sustainable ways of living and conducting business are also emphasised (Bruinsma, 2009; Henchion et al., 2017). Extrapolating from animal feed, development of methods to further reduce the antinutritional factors to trace amounts while retaining the protein content, such as the two-phase solvent method (Naczk et al., 1985) or protein micellar mass extraction method (Tzeng et al., 1990) have led to ideas of isolating proteins from oilseed rape meal for human consumption (Tan et al., 2010; Rodrigues et al., 2016; Ivanova et al., 2017). One example of a protein isolated from oilseed rape meal is Isolexx™, which was declared safe for human consumption as a plant-based protein (FSAI, 2012; EFSA, 2013). Furthermore, since livestock farming is a significant contributor to greenhouse gas emissions (Garnett, 2009; Bellarby et al., 2012; Yan et al., 2024) and has been targeted as one of the main areas to reduce greenhouse gas emissions, the potential for more protein isolates from oilseed rape meal for human consumption is likely to increase the importance of oilseed rape in the market (Carré & Pouzet, 2014). However, rapid urbanisation reducing arable land and the expected increase of 2.3 billion in world population by 2050 is likely to cause difficulties in meeting these demands (Bruinsma, 2009; Tiwari et al., 2017; Garg, 2020; Uniyal et al., 2020).

As fossil fuels are depleting daily, the importance of alternative fuels such as biodiesel is increasing. Edible oils, such as rapeseed, palm and coconut oil, have been identified as major candidates for production of biodiesel (Atabani et al., 2012). Over 90 % of biodiesel is produced from vegetable oils globally, with rapeseed oil estimated to account for approximately 85 % of biodiesel production (Hossain & Davies, 2010; Yunus-Khan et al., 2014). Using renewable biofuels may help mitigate the carbon emissions caused by the

use of fossil fuels and serve as a sustainable energy resource, especially when they are produced from recycled cooking oils (Gupta et al., 2022; Pande & Gahane, 2024). However, considering rapeseed oil is an edible oil with high nutritional value, some have argued that extensive pressing of rapeseed oil just to produce biodiesel could result in significant food shortages (Tenenbaum, 2008; Gasparatos et al., 2011; Altieri & Bravo, 2022). Moreover, as another alternative for industrial applications, bio-degradable lubricants for engineering machinery have also been produced from rapeseed oil (Wu et al., 2000; Carlsson et al., 2011; Arumugam & Sriram, 2012). Overall, with its increasing use in industry as well as animal and human nutrition, demand and importance of oilseed rape products are likely to increase in the future.

Oilseed rape is currently the second most cultivated oilseed in the world (after soybean), with an annual production of 89.9 million tonnes globally in 2024 (Zheng et al., 2020; USDA, 2025) (Figure 1.2). In addition, it is the third most important arable crop in the UK (after wheat and barley) (FAO, 2023). Major production of oilseed rape takes place in Canada, China, Australia, India, Europe (mainly France and Germany) and the United Kingdom (Carré & Pouzet, 2014: Zheng et al., 2020). With a five-year average of 18.1 million tonnes (Mt), Canada produces the greatest amount of oilseed rape, followed by China with 14.8 Mt, India with 10.6 Mt, then Australia, France, Germany and the United Kingdom with 1-5 Mt (FAOSTAT, 2023) (Figure 1.3). Furthermore, the production of oilseed rape has been increasing in United States, Russian Federation, Poland and Ukraine (Carré & Pouzet, 2014).

In the UK, oilseed rape production has increased between 2000 and 2011 and was maximal in 2011 with 2.8 Mt produced (FAOSTAT, 2023) (Figure 1.4A). Subsequently, oilseed rape cultivation area increased and was maximal in 2012, with 756 thousand hectares grown (DEFRA, 2023) (Figure 1.4B). However, both production and cultivation area of oilseed rape have had a downward overall trend since then, with smallest production (1.0 Mt) and area (307 thousand hectares) in 2021. The production value of oilseed rape in the UK has also increased substantially between 2000 and 2011 and was maximal in 2011, with £1.11 B production value. Since then, it has reduced to a thirteen-year low of £360 M in 2020; although a considerable increase to £876 M was noted in 2022, it was followed by a reduction to £483 M in 2023 (FAOSTAT, 2023) (Figure 1.4C).

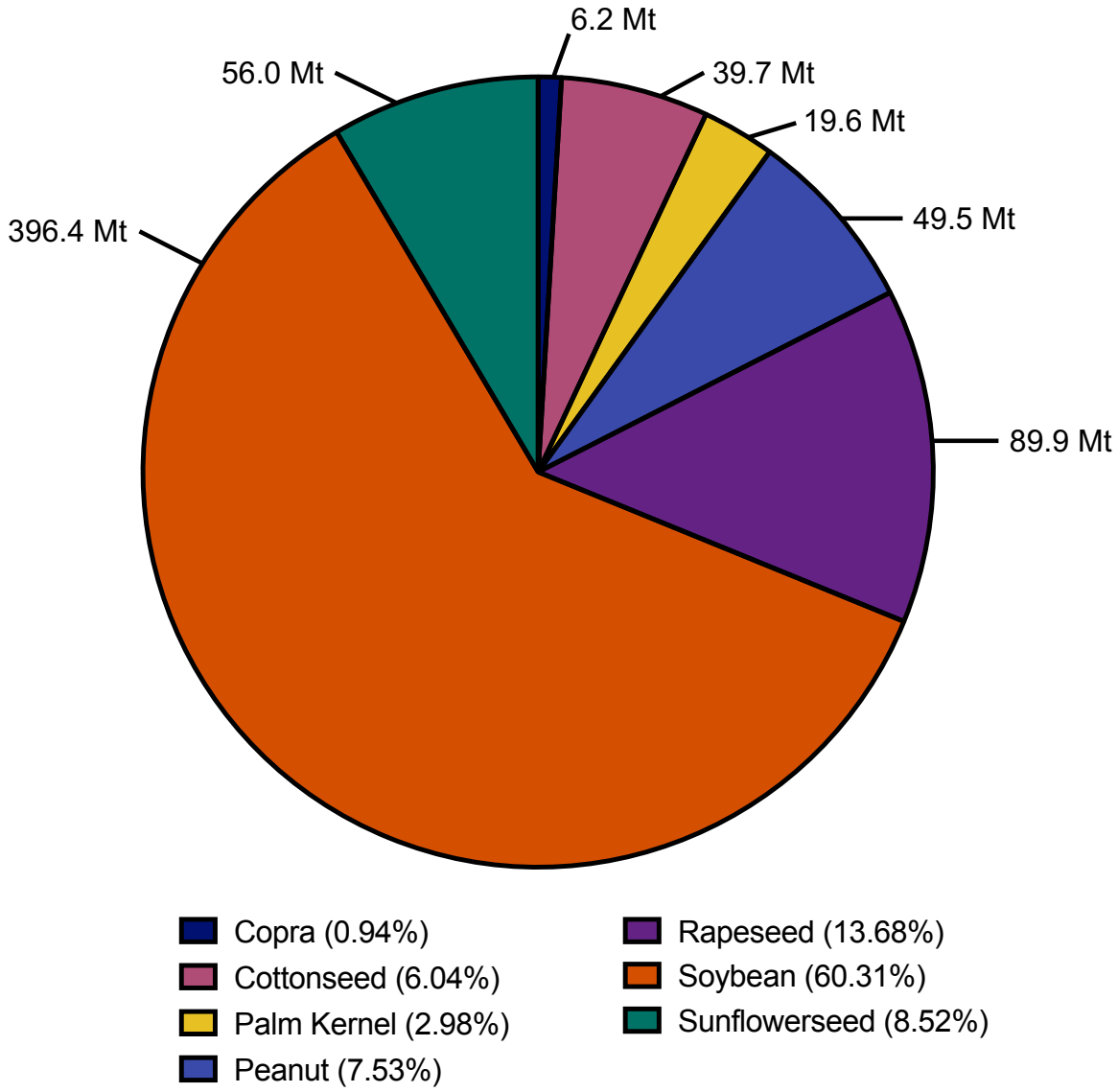

Figure 1.2: Global production of oilseed crops in 2023/2024 (in million metric tonnes).

The data were obtained from USDA, 2025.

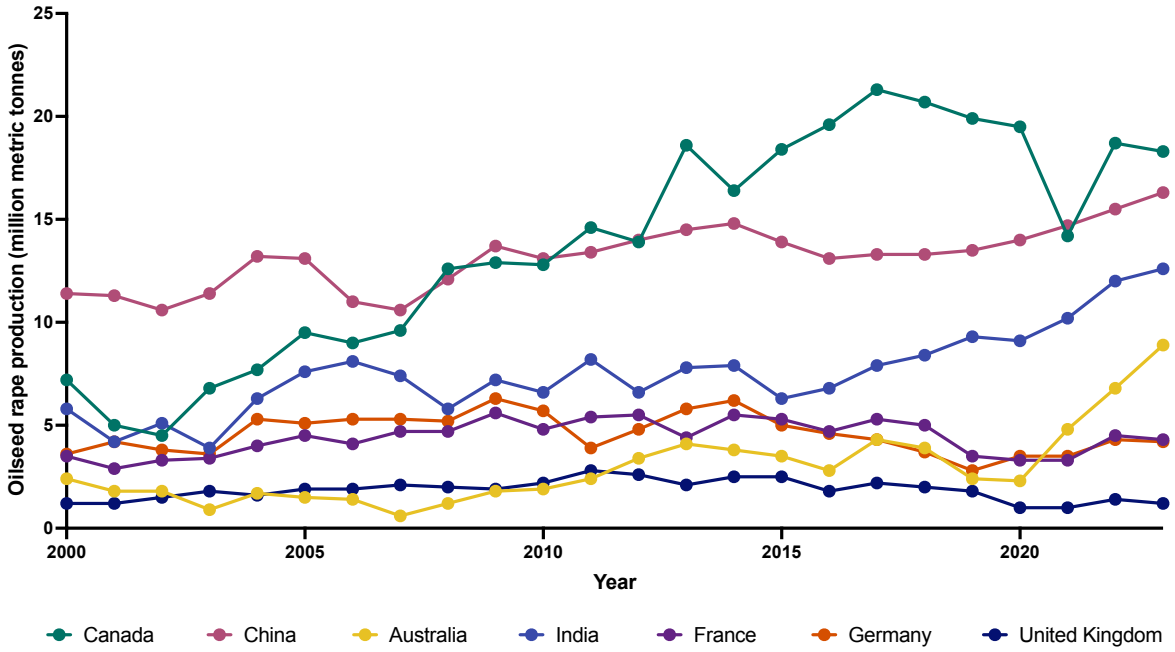

Figure 1.3: Oilseed rape production (million metric tonnes) in Canada, China, Australia, India, France, Germany and the United Kingdom between 2000 and 2023.

The data were obtained from FAOSTAT, 2023.

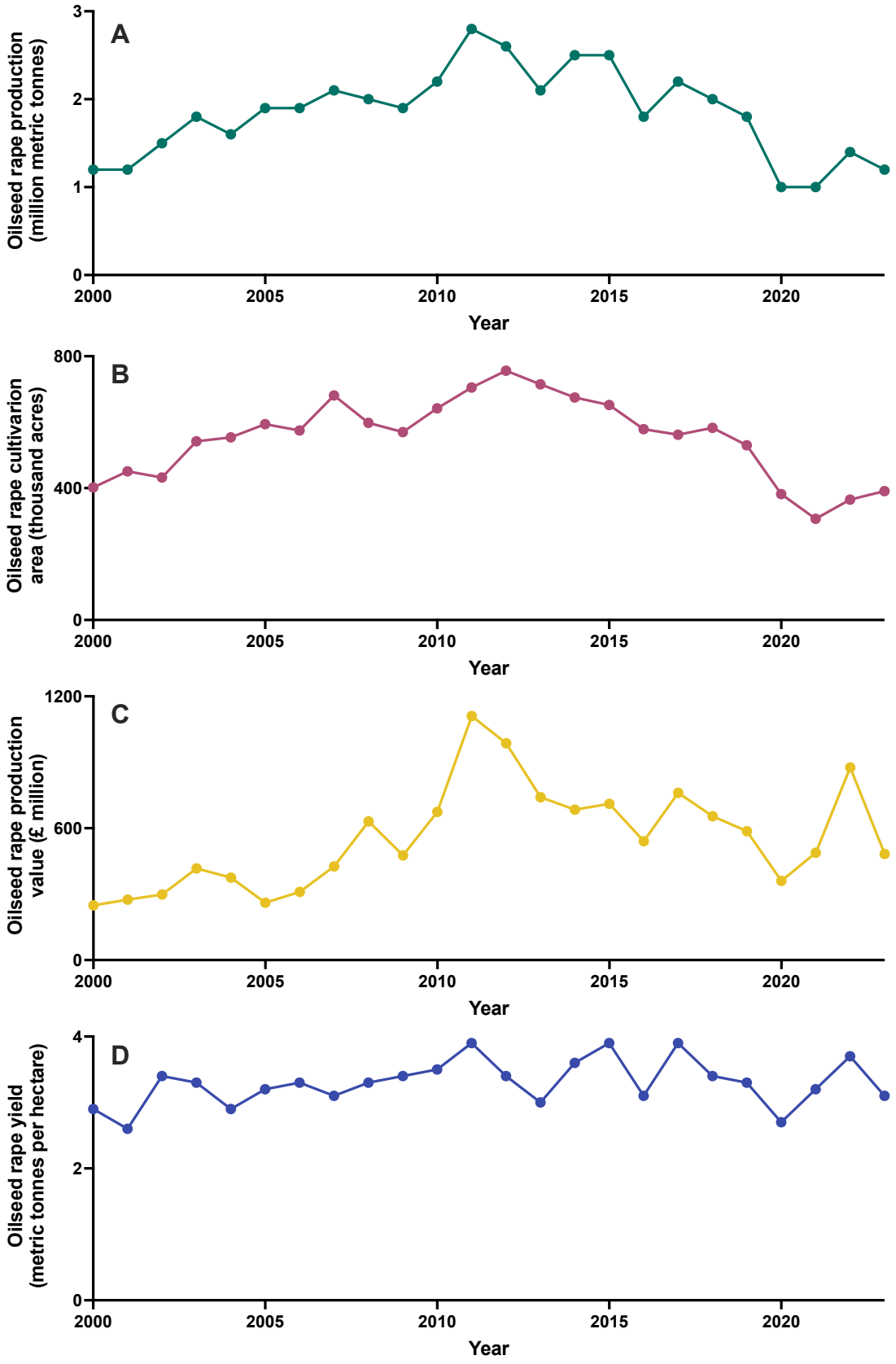

Figure 1.4: Oilseed rape (A) production (million metric tonnes), (B) cultivation area (thousand hectares), (C) production value (£ million) and (D) yield (metric tonnes per hectare) in United Kingdom between 2000 and 2023.

The data were obtained from FAOSTAT, 2023 and DEFRA, 2023.

Moreover, the yield of oilseed rape has remained unchanged in the past twenty-three years, ranging between 2.6 and 3.9 tonnes per hectare (DEFRA, 2023) (Figure 1.4D). The reduction in the production, cultivation area and average annual value of oilseed rape across Europe has been attributed to increasing temperatures as well as increasing insect pests and diseases (Zheng et al., 2020). Especially, the ban on neonicotinoids in Europe has left oilseed rape crops vulnerable to cabbage stem flea beetle (CSFB) (*Psylliodes chrysocephala*) attacks and led to a reduction in the cultivation area of oilseed rape (Andert et al., 2021; Ortega-Ramos et al., 2021).

Since there is a need to increase the plateaued yield of oilseed rape as a result of increasing population size and the anticipated increase in demand for novel plant-based proteins for human consumption, it is important to develop better control strategies against pests and diseases of oilseed rape (Bruinsma, 2009; Aiking, 2011; Henchion et al., 2017; Kumar et al., 2022).

1.2 Diseases of oilseed rape

Important diseases of oilseed rape in the UK include phoma stem canker (*Leptosphaeria maculans* and *Leptosphaeria biglobosa*), light leaf spot (*Pyrenopeziza brassicae*), Sclerotinia stem rot (*Sclerotinia sclerotiorum*), Verticillium stem striping (*Verticillium longisporum*) and clubroot (*Plasmodiophora brassicae*) (Zheng et al., 2020). Phoma stem canker and light leaf spot are the two most economically damaging diseases of oilseed rape in the UK, causing significant annual yield losses (Fitt et al., 2006a; Fitt et al., 2006b; CropMonitor, 2020; Zheng et al., 2020) (Figure 1.5).

1.2.1 Phoma stem canker

Phoma stem canker is one of the most damaging diseases of oilseed rape globally, as it can cause significant economic damage in different parts of the world, such as Australia, China, Europe and North America; with yield losses up to £1 B (billion) globally and £98 M in the UK (Fitt et al., 2006a; Barnes et al., 2010; Zhang et al., 2014). In fact, the average annual loss caused by phoma stem canker to growers in England between 2014 and 2018 was £80.9 M (million), with a twenty-year maximum of £98.7 M in 2016 (CropMonitor, 2020) (Figure 1.5). The incidence of phoma stem canker in England and Wales is greater in areas with higher temperatures, such as the east and south of England (Stonard et al., 2010).

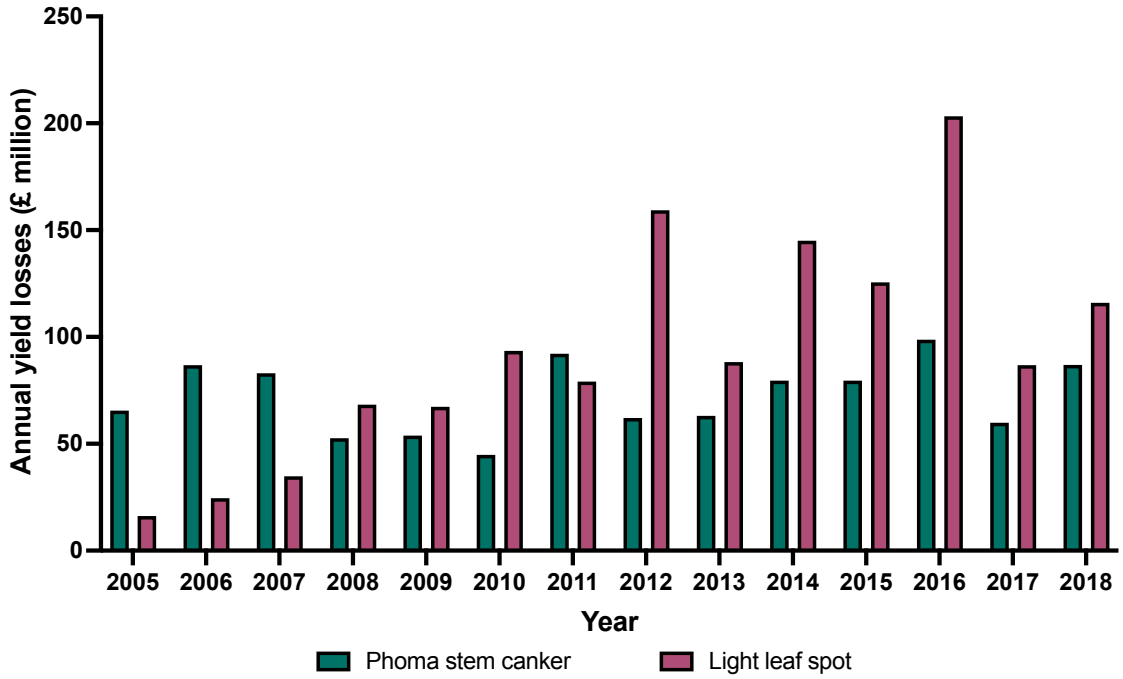

Figure 1.5: Annual yield losses (£ million) caused by phoma stem canker and light leaf spot in England and Wales between 2005 and 2018.

The data were obtained from CropMonitor, 2020.

Environmental factors (i.e. climate change) can potentially affect the incidence of pathogens and diseases in different parts of the same region. For example, even when low emission scenarios were applied, it was predicted that geographical location of phoma stem canker would expand in the UK, reaching northwards to Scotland by 2050 (Evans et al., 2007; Evans et al., 2010; Barnes et al., 2010).

In the UK, phoma stem canker is caused by two co-existing fungal pathogen species *L. maculans* and *L. biglobosa* (Shoemaker & Brun, 2001; West et al., 2001; Fitt et al., 2006b). Furthermore, the global distribution of these pathogens varies; *L. maculans* and *L. biglobosa* are found to co-infect oilseed rape in Europe, Canada and Australia, whereas only *L. biglobosa* is found in China (Fitt et al., 2006a; Dilmaghani et al., 2009; Cai et al., 2017). Invasion of oilseed rape crops in China by *L. maculans* could lead to increased economic damage, with additional yield losses estimated as high as £567 M (Fitt et al., 2008; Liu et al., 2014).

1.3 *Leptosphaeria* species complex

1.3.1 Taxonomy

Leptosphaeria maculans (Desm.) Ces. & De Not. 1863 [anamorph *Phoma lingam* (Tode:Fr) Desm.] (*Plenodomus lingam*) and *Leptosphaeria biglobosa* (*Plenodomus biglobosus*) (Shoemaker & Brun, 2001; de Gruyter et al., 2013) are in the kingdom of Fungi, phylum of *Ascomycota*, class of *Dothideomycetes*, order of *Pleosporales*, family of *Leptosphaeriaceae* and genus of *Leptosphaeria* (Schoch et al., 2009; Ohm et al., 2012; Grandaubert et al., 2014). They were initially considered to be different strains of a single species (*L. maculans*) and were differentiated through morphology of mycelia in culture, lesion phenotype on leaves and stems of oilseed rape plants and the ability to produce the phytotoxin sirodesmin PL (Koch et al., 1989; Pedras & Séguin-Swartz, 1990; Balesdent et al., 1992; Williams & Fitt, 1999). They were referred to as highly virulent, A group or Tox^{+} (for *L. maculans*) and weakly virulent, B group or Tox^{0} (for *L. biglobosa*) (Mahuku et al., 1996; Williams & Fitt, 1999; Toscano-Underwood et al., 2001; West et al., 2001). Through attempted inter-crossing of the isolates failing and development of molecular techniques, they have been distinguished as two closely related but separate species (Shoemaker & Brun, 2001; Mendes-Pereira et al., 2003; Grandaubert et al., 2014).

A comprehensive phylogenetic analysis of the phylum *Ascomycota* based on whole-genome sequencing data revealed that *L. maculans* and *L. biglobosa* have diverged approximately 22 million years ago, resulting in their speciation. Furthermore, subclades of *L. maculans* (*L. maculans* 'brassicae' and *L. maculans* 'lepidii') have diverged approximately 2-5 million years ago (Grandaubert et al., 2014; Figure 1.6). *L. maculans* has a larger genome size (45 Mb) and greater percentage of transposable elements (TEs) (25-33 %) in its genome in comparison to *L. biglobosa*, which has a genome size of 30 Mb and 2-4 % of TEs in its genome. Since TEs are known to contribute to evolution by promoting recombination, the relatively complex genetic make-up of *L. maculans* allowed closer adaptation to its host (Mendes-Pereira et al., 2003; Grandaubert et al., 2014; Musewska et al., 2019). Finally, *L. maculans* is considered to be a younger species that has evolved more recently, as it appears to be a more monomorphic species, with only two subclades identified and gene-for-gene interactions formed with its host. Whereas *L. biglobosa* has seven subclades identified and has a wider host range without gene-for-gene interactions formed (Mendes-Pereira et al., 2003; Vincenot et al., 2008; Dilmaghani et al., 2009; Zhou et al., 2023). The seven *L. biglobosa* subclades are *L. biglobosa* 'brassicae', 'canadensis', 'thalspii', erysmii', 'australensis', 'occiaustralensis' and 'americansis', distributed differently in different parts of the world. *L. biglobosa* 'brassicae' is the main subclade identified on oilseed rape in Europe, including the UK However, *L. biglobosa* 'canadensis' has been identified from wasabi (*Eutrema japonicum*) in the UK (King et al., 2022).

1.3.2 Epidemiology and life cycle

L. maculans and *L. biglobosa* have a similar life cycle that is monocyclic, meaning that the pathogens undergo only one full cycle in a single growing season (West et al., 2002b; Fitt et al., 2006b) (Figure 1.7).

Their life cycle is initiated by the release of ascospores (sexually produced spores) from the crop debris from the previous growing season. These ascospores get dispersed by wind and rain and land on leaf surfaces of oilseed rape plants (Huang et al., 2005; Lô-Pelzer et al., 2009). Ascospores of *Leptosphaeria* species germinate to develop germ tubes, which penetrate the leaves primarily through stomatal apertures, although they can also enter the leaves through wounds; leading to development of phoma leaf spotting (Toscano-Underwood et al., 2001; Huang et al., 2003b; Huang et al., 2005).

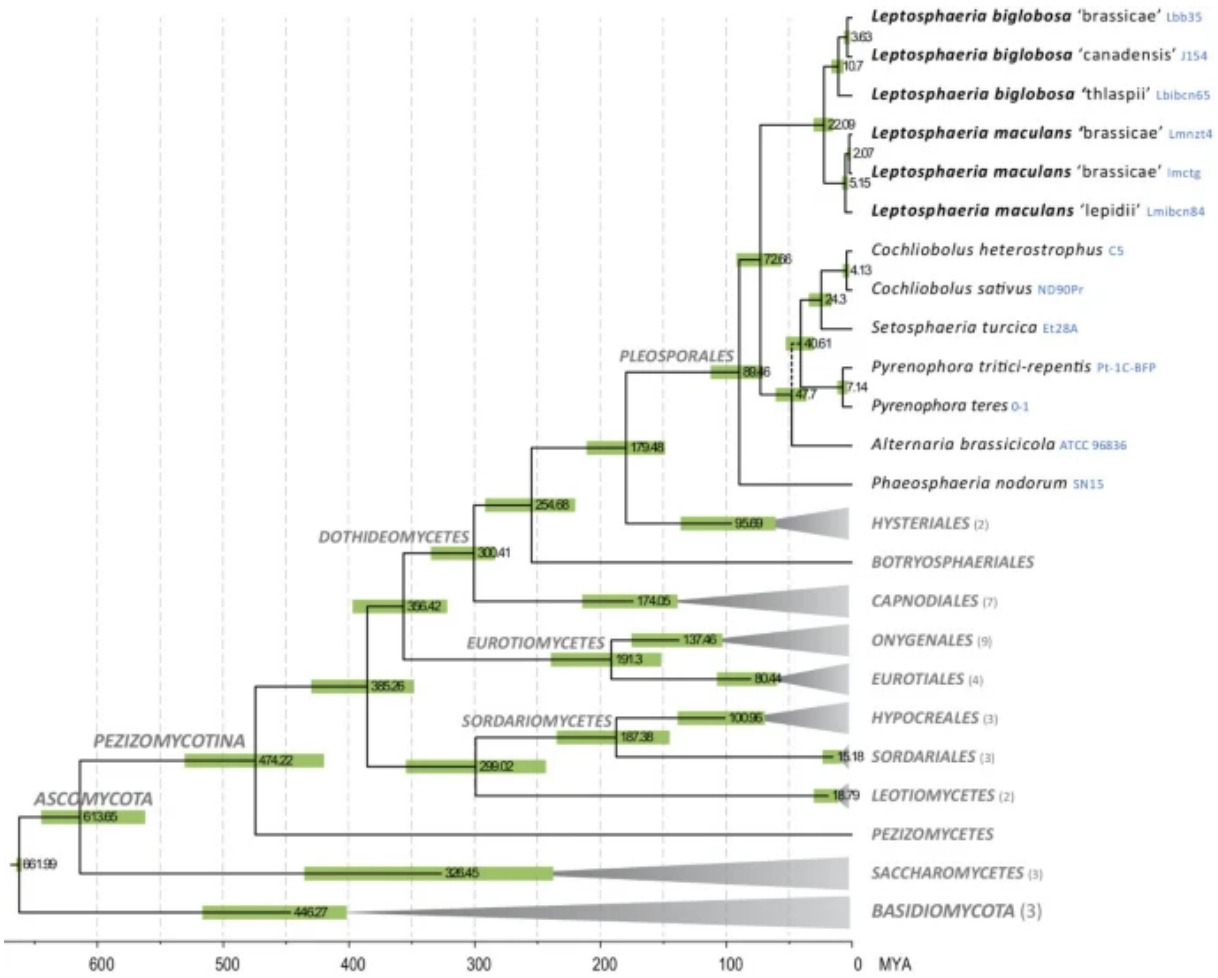

Figure 1.6: Phylogenetic analysis of the phylum *Ascomycota*, with focus on the order of *Pleosporales*, based on whole genome sequencing data.

Leptosphaeria maculans and *L. biglobosa* are shown to have diverged approximately 22 million years ago. The x axis of the chronogram shows evolutionary time in million years. This figure was adapted from Grandaubert et al., 2014.

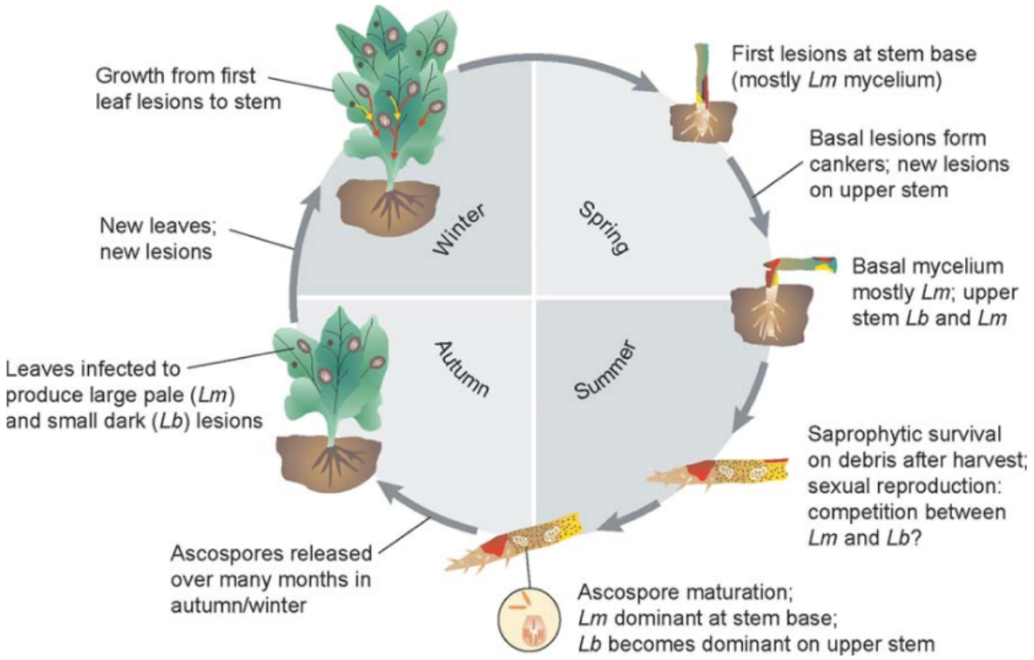

Figure 1.7: Life cycle of *Leptosphaeria maculans* and *L. biglobosa*.

Ascospores from mature pseudothecia are released throughout autumn and winter, infecting leaves and causing phoma leaf spotting. This is followed by the asymptomatic growth of the pathogens from infected leaves to the stem over the growing season. *L. maculans* is mainly associated with causing stem basal cankers and *L. biglobosa* is mainly associated with causing upper stem lesions. Following harvest, these pathogens can saprophytically survive on the crop debris during the summer, undergo sexual reproduction and form pseudothecia, which then release ascospores upon maturation in the autumn and winter of the next growing season, starting another disease cycle. This figure was adapted from West et al., 2002b.

Foliar lesions caused by *L. maculans* often develop asexual fruiting bodies called pycnidia, which can release conidia (asexual spores) and may cause secondary infections in Australia (Bokor et al., 1975; Toscano-Underwood et al., 2001; Travadon et al., 2007). Conidia do not often penetrate the plant tissues, however; they can cause lesions on oilseed rape if they enter through a wound (Huang et al., 2018). Therefore, practices that create wounds on the plants, such as defoliation of crops by grazing cattle (Sprague et al., 2015) can increase the risk of secondary infections by conidia of *L. maculans*.

Following the development of phoma leaf spotting, these pathogens asymptomatically grow along the leaf petiole down to the stem, where they continue spreading upwards and downwards. This is followed by colonisation of outer stem cortex and inner stem pith tissues, resulting in upper stem lesions or stem basal (crown) cankers (West et al., 2001; Fitt et al., 2006b; Sprague et al., 2007; Huang et al., 2009). Severe stem cankers interfere with water and nutrient uptake and transport throughout the plants, resulting in premature ripening or crop lodging, which leads to significant yield losses (West et al., 2001; Eckert et al., 2010). After harvest, *Leptosphaeria* species can undergo sexual reproduction on the crop debris to form pseudothecia (sexual fruiting bodies), which upon maturation under favourable conditions, release ascospores in autumn and winter of the next growing season, facilitating interseasonal transmission and starting their new life cycle (West et al., 2001; Fitt et al., 2006b; Fortune et al., 2021). The timing of pseudothecial maturation is dependent on environmental factors such as temperature and rainfall, which subsequently affect the onset of disease epidemics by release of ascospores (West et al., 2002b; Huang et al., 2003b; Toscano-Underwood et al., 2003; Fitt et al, 2006b; Huang et al., 2007; Salam et al., 2007).

1.3.3 Pathogen characteristics

L. maculans and *L. biglobosa* cause different symptoms on oilseed rape. *L. maculans* causes larger, grey lesions with many pycnidia on leaves of oilseed rape. In contrast, *L. biglobosa* causes smaller, black foliar lesions with very few or no pycnidia at all. Moreover, *L. maculans* has been associated with causing cankers at the stem base, which are considered more damaging, while *L. biglobosa* has been associated with causing lesions on the upper stem, which are considered less damaging (Toscano-Underwood et al., 2001; Huang, 2002; West et al., 2002a; Fitt et al., 2006b) (Figure 1.8).

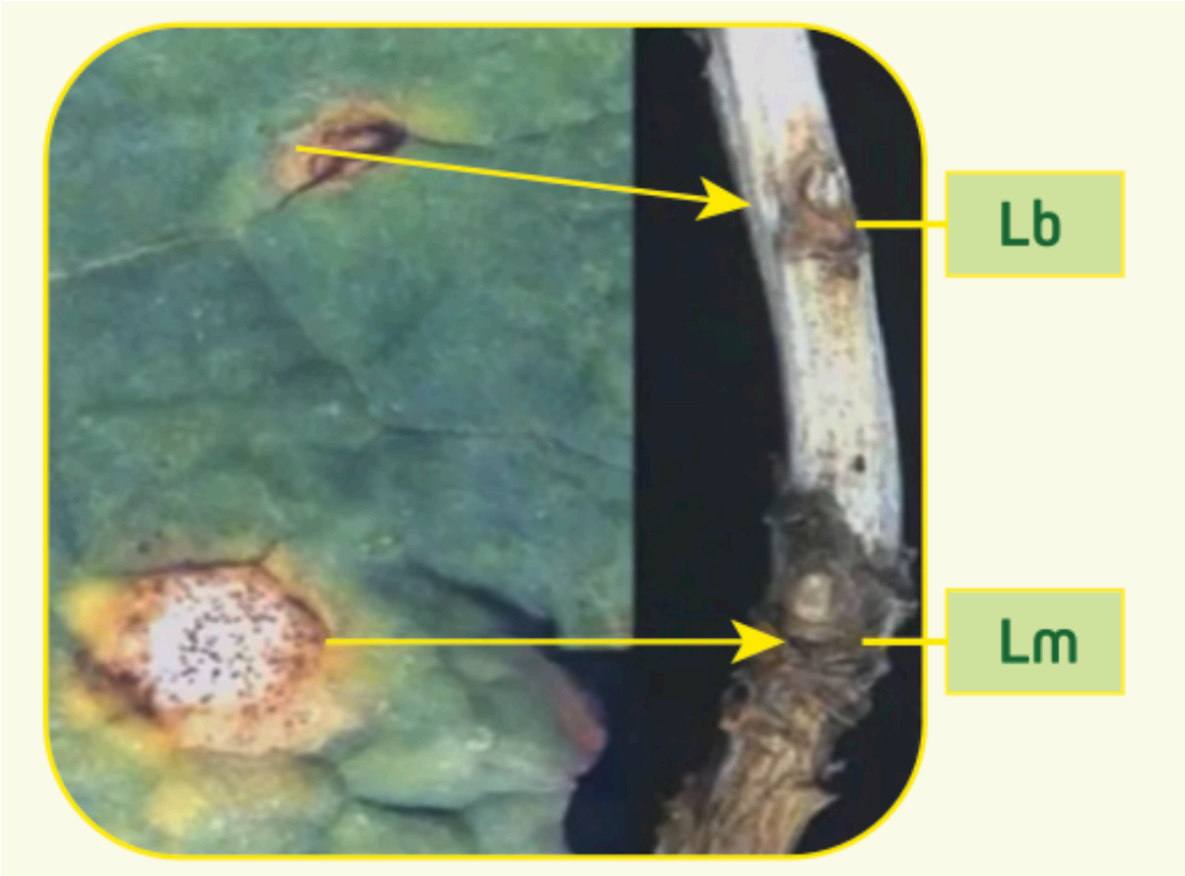

Figure 1.8: Phoma leaf spot and stem canker lesions caused by *Leptosphaeria maculans* (Lm) and *L. biglobosa* (Lb).

L. maculans causes large grey foliar lesions with black pycnidia present and later causes stem basal cankers. Whereas *L. biglobosa* causes small black foliar lesions with very few or no pycnidia at all and later causes upper stem lesions. This figure was adapted from Fitt et al., 2006b).

However, recent studies have reported that *L. biglobosa* DNA can also be detected in stem basal cankers of various oilseed rape cultivars in the UK, emphasising that *L. biglobosa* can also cause stem basal cankers (Javaid, 2019; Huang et al., 2024). Although it is not possible to visually distinguish between *L. maculans* and *L. biglobosa* in cankers in the stem base, molecular techniques (i.e. species-specific PCR and qPCR) allow identification and quantification of *Leptosphaeria* species in stem basal cankers.

There are several other characteristic differences identified between *L. maculans* and *L. biglobosa*, with small changes observed in some of them in recent years. It was found that pseudothecia of *L. maculans* were entirely exposed on the crop debris surface, where those of *L. biglobosa* were under the epidermis with only the ostiole (neck) exposed. Furthermore, although there were no differences at higher temperatures (15-20°C), pseudothecia of *L. maculans* were found to mature faster at lower temperatures (5-10°C) than those of *L. biglobosa* (Toscano-Underwood et al., 2003). As a result of this, it was thought that pseudothecial maturation and subsequent ascospore release of *L. maculans* takes place earlier in the growing season during early autumn and winter (lower temperatures), while pseudothecia of *L. biglobosa* complete maturation and release ascospores later in the season during late autumn/winter and spring (higher temperatures) (Huang, 2002; Huang et al., 2005). However, recent studies that monitored the release of ascospores measured by quantifying pathogen DNA using qPCR analyses of air samples showed that ascospores of both *L. maculans* and *L. biglobosa* are being released at similar times at multiple sites in England (Javaid, 2019; Fortune, 2022; Huang et al., 2024). This is most probably due to changes in winter weather conditions in the UK leading to milder and wetter winters, narrowing the time gap between the two *Leptosphaeria* species in maturation of pseudothecia and their consequent ascospore release.

Moreover, although ascospores of both *L. maculans* and *L. biglobosa* after germination penetrate the leaves of oilseed rape primarily through stomata, there are differences in the morphology of their germ tubes and hyphal formation. *L. maculans* has shorter germ tubes and forms its hyphae in a tortuous formation with large-scale branching, whereas *L. biglobosa* has longer germ tubes and forms its hyphae almost in a straight line formation with very little branching observed. Furthermore, *L. biglobosa* ascospores were

found to start germinating earlier than those of *L. maculans* at 5-20°C (Huang et al., 2001; Huang et al., 2003b).

Several *in vitro* studies to characterise the secondary metabolites produced by *L. maculans* and *L. biglobosa* identified the production of a major epipolythiodioxopiperazine (ETP) class phytotoxin called sirodesmin PL by *L. maculans* (Solelade et al., 1991; Pedras & Biesenthal, 1998; Rouxel et al., 1998; Gardiner et al., 2004). Later studies reported that *L. biglobosa* does not produce this phytotoxin (Pedras et al., 2007; Fortune, 2022); and although it produces a range of secondary metabolites, none of them were reported to have a major role (Pedras et al., 2007). Other *in vitro* studies have identified differences in colony morphology between *L. maculans* and *L. biglobosa*. Production of a yellow/orange pigment by *L. biglobosa* was observed in solid and liquid cultures (primarily potato dextrose agar and broth), and it was not produced by *L. maculans* (Williams & Fitt, 1999). Mycelia of *L. maculans* were found to be more structurally intact and round in liquid culture, in comparison to those of *L. biglobosa* having a less structurally defined and spread-out mycelial morphology (Zhang et al., 2014).

In order to evaluate the differences between pathogens, it is important to understand the nutritional strategies they use to infect and colonise their host (i.e. their trophic nature). Fungal pathogens of plants are classified in three distinct groups in terms of their trophic nature. Biotrophic pathogens obtain nutrients directly from the cells of their host, without causing cell death, often by developing specialised structures called haustoria (Latijnhouwers et al., 2003; Newton et al., 2010; Voegele & Mendgen, 2011; Kemen et al., 2015). They can secrete effectors to suppress plant defences to delay detection by the host (Mengden & Hahn, 2002; Delaye et al., 2013; Mapuranga et al., 2022). These pathogens have highly adapted to their host, require host viability for proliferation and cannot be grown on artificial media (Kemen & Jones, 2012; Tang et al., 2018; Mapuranga et al., 2022). Examples of biotrophic fungal plant pathogens are *Puccinia triticina* and *Blumeria graminis*, causing rusts and powdery mildews of wheat, respectively (Tang et al., 2018).

Necrotrophic pathogens cause cell death shortly after infection and obtain nutrients from necrotic cells and tissues; primarily through secretion of cell wall degrading enzymes and

phytotoxic metabolites and proteins to facilitate host cell death (van Kan, 2006; Shao et al., 2021). In addition, some necrotrophic pathogens can contribute to accumulation of reactive oxygen species (ROS) during colonisation of their host (Heller & Tudzynski, 2011; Foley et al., 2016). Some of them also carry enzymes such as superoxide dismutase (SOD), peroxidase and catalase, which may help them deal with the hostile environment as a result of colonisation (Mayer et al., 2001). Examples of necrotrophic fungal plant pathogens are *Botrytis cinerea* and *Sclerotinia sclerotiorum*, causing mould on various plant hosts; and as necrotrophic pathogens they have wider host ranges compared to biotrophic pathogens (Williamson et al., 2007; Newman et al., 2023).

Hemibiotrophic pathogens initially utilise an endophytic phase (similar to a biotrophic pathogen, but no visible symptoms or damage are observed on the host plant) for initial colonisation within the host, followed by a 'switch' to necrotrophy, where death of host cells and tissues is initiated (Oliver & Ipcho, 2004; De Silva et al., 2016; Shao et al., 2021). Molecular and metabolic changes occur and mediate the endotrophy-necrotrophy switch, such as increases in the expression of genes related to ROS scavenging and production of secondary metabolites and toxins (Chowdhury et al., 2017; Lee & Rose, 2020). Examples of hemibiotrophic fungal plant pathogens are *Magnaporthe oryzae* and *Fusarium graminearum*, causing rice blast and *Fusarium* head blight of wheat, respectively (Crouch & Kohn, 2001; Goswami & Kistler, 2004).

Initially, both *L. maculans* and *L. biglobosa* were considered as hemibiotrophic pathogens (Fitt et al., 2006a; Fitt et al., 2006b). However, more recent studies have identified *L. biglobosa* to be more of a necrotrophic pathogen (Lowe et al., 2014; Padmathilake & Fernando, 2022a; Padmathilake & Fernando, 2022b; Gay et al., 2023). *L. biglobosa* was found to start expression of cell wall degrading enzymes considerably earlier than *L. maculans*; this also leads to development of necrotic lesions earlier after inoculation (7 days post inoculation) compared to *L. maculans* (14 days post inoculation), as well as earlier activation of plant defences, more in line with necrotrophic behaviour (Eckert et al., 2005; Lowe et al., 2014). Furthermore, a recent transcriptomic study has also reported that the common differentially expressed genes as a response to both *L. maculans* and *L. biglobosa* infection were upregulated earlier as a response to *L. biglobosa* inoculation compared to *L. maculans* inoculation. The authors reported that *L. maculans* resulted in an upregulation of similar genes later in its colonisation upon

switching to necrotrophy (Gay et al., 2021; Gay et al., 2023). A comparison of pathogen characteristics of *L. maculans* and *L. biglobosa* is summarised in Table 1.1 (Fitt et al., 2006a; Stonard et al., 2010).

1.4 Induction of plant defences

Plant pathogens are faced with host defence responses upon infection. If the pathogens are not able to avoid recognition by the transmembrane pattern recognition receptors (PRRs), their pathogen-associated molecular patterns (PAMPs) get recognised by the host through these receptors, resulting in induction of PAMP-triggered immunity (PTI) (Zipfel & Felix, 2005; Dangl et al., 2013). This can halt further colonisation of the host by the pathogen by inducing a broad-spectrum response to infection (Jones & Dangl, 2006; Wang et al., 2014). Some pathogens can produce and deploy proteins or small molecules (effectors) to alter host cells and regulate PTI to contribute to pathogen virulence, which results in effector-triggered susceptibility (ETS) (Jones & Dangl, 2006; Oliva et al., 2010). In response, some plants have evolved intracellular proteins that can 'specifically recognise' these effectors, resulting in induction of effector-triggered immunity (ETI). This is more amplified compared to PTI and leads to hypersensitive response (HR) and cell death at the infection site, resulting in disease resistance, primarily effective against biotrophic and hemibiotrophic pathogens (Glazebrook, 2005; Jones & Dangl, 2006). Furthermore, due to differences in response mechanisms and consequent pathogen death, this type of resistance is described differently for haustoria-forming pathogens (HFP) and apoplastic pathogens (AP), as effector-triggered immunity (ETI) and effector-triggered defence (ETD), respectively (Stotz et al., 2014). ETI is triggered by intercellular receptors and leads to a faster resistance response, while ETD is triggered by apoplastic receptors and leads to a slower resistance response (Stotz et al., 2014). In some cases, natural selection may drive the pathogens to avoid ETI and ETD by mutations in the recognised effector genes, which would render the resistance triggered by those effectors ineffective (Jones & Dangl, 2006; Oliva et al., 2010; Stotz et al., 2014).

Plant immune/defence signalling pathways are mediated by induction of different phytohormones, which act as important regulators in stress responses against pathogens. The primary phytohormones involved in defence against pathogens are salicylic acid (SA), jasmonic acid (JA) and ethylene (ET) (Dong, 1998; Vlot et al., 2009; Bürger & Chory, 2019; Shafqat et al., 2024).

Table 1.1: Comparison of characteristics of *Leptosphaeria maculans* and *L. biglobosa*.

This table was modified and extended from Table 2 in Fitt et al. (2006b) and Table 1 in Stonard et al. (2010).

Observation	Parameter	*L. maculans*	*L. biglobosa*	Reference
Trophic nature	Infection strategy	Hemibiotrophic	More necrotrophic	a
Growth *in vitro*	Pigment production	N/A	Yellow/orange pigment in agar and broth	b
	Mycelial morphology	Structurally defined and circular	Not structurally defined	
Major phytotoxin production	Secondary metabolites	Production of sirodesmin PL	No production of major phytotoxins identified	c
Pseudothecial maturation	Maturation	Earlier at 5-10°C	Later at 5-10°C	d
	Position on debris	Exposed on the surface	Under the surface (just neck exposed)	
Ascospore release	Timing of release	Early autumn/winter	Previously thought late autumn/winter and spring but is commonly released at the same time as *L. maculans* recently	e
Ascospore germination	Start of germination	Later at 5-20°C	Earlier at 5-20°C	f
	Length of germ tubes	Short	Long	
	Growth of hyphae	Tortuous	Almost straight lines	
Penetration of leaf tissues	Mode of entry	Primarily through stomata	Primarily through stomata	g
Symptoms	Cotyledon lesions	Necrotic lesions appear 10-14 dpi	Necrotic lesions appear 3-7 dpi	h
	Leaf lesions	Larger, grey with pycnidia	Smaller, black with little or no pycnidia	
	Position of lesions on stem	Mainly stem base	Previously thought mainly upper stem but is frequently found at the stem base recently	

[a] (Lowe et al., 2014; Gay et al., 2023), [b] (Williams & Fitt, 1999; Zhang et al., 2014), [c] (Rouxel et al., 1988; Gardiner et al., 2004), [d] (Toscano-Underwood et al., 2003), [e] (West et al., 2002b; Huang et al., 2005; Javaid, 2019; Huang et al., 2024), [f] (Huang et al., 2001; Huang et al., 2003b), [g] (Hammond et al., 1985; Huang et al., 2003b), [h] (Toscano-Underwood et al., 2001; West et al., 2002a; Huang, 2002; Toscano-Underwood et al., 2003; Fitt et al., 2006a; Fitt et al., 2006b; Huang et al., 2024).

SA-mediated responses are important in local disease resistance and cell death, as well as induction of systemic acquired resistance (SAR) and expression of genes related to defence (Vlot et al., 2009; An & Mou, 2011). It was shown that an infection by a pathogen leads to accumulation of SA not only in the infected tissues locally, but also in uninfected leaves systemically in the case of SAR (Malamy & Klessig, 1992; Durrant & Dong, 2004). Furthermore, accumulation of SA in plant tissues is characterised to precede or parallel the increased expression of pathogenesis-related protein (*PR*) genes and signal for induction of SAR (Durrant & Dong, 2004; An & Mou, 2011). SA signalling has mainly been associated with mediating immune responses against obligate biotrophic or hemibiotrophic pathogens (Li et al., 2004; Lowe et al., 2014; Li et al., 2019). JA/ET-mediated responses are important in inducing the expression of other genes related to defence, such as plant defensins (*PDF*), by degrading its transcriptional suppressors (Penninckx et al., 1998; Zhu & Lee, 2015). Finally, JA/ET signalling has mainly been associated with mediating immune responses against necrotrophic pathogens and mechanical damage caused by insect pests (Farmer et al., 2003; Lowe et al., 2014; Li et al., 2019; Wang et al., 2021).

Important regulators of this phytohormone signalling and subsequent defence responses are several *WKRY* transcription factors, which are characterised to have various biological functions in plants (Bakshi & Oelmüller, 2014). WRKYs can act as activators or repressors, function upstream or downstream of phytohormones and are involved in antagonistic functions of SA and JA/ET (Pandey & Somssich, 2009; Agrawal et al., 2011; Bakshi & Oelmüller, 2014). WRKY70 is important for defence against biotrophic and hemibiotrophic pathogens, as it activates SA-induced genes and represses genes responsive to JA/ET signalling (Li et al., 2004; Li et al., 2019). Moreover, WRKY33 is indispensable for defence against necrotrophic pathogens, and loss of its function results in inappropriate accumulation of SA and subsequent downregulation of JA/ET-mediated responses (Zheng et al., 2006; Birkenbihl et al., 2012).

1.5 Interspecific interactions

A single host in nature is likely to get co-infected by multiple pathogens during different stages of its life cycle. This leads to interactions that take place between the co-infecting pathogens. These interactions can be characterised as competition, co-operation or co-existence (Abdullah et al., 2017; Dutt et al., 2021b).

All of the individuals need to obtain energy for growth, development, survival and reproduction. This energy can be obtained by utilising the resources available to them to facilitate expansion of their population size (Grover, 1997). However, since these resources are limited and consequently unavailable to an individual if already utilised by another, this limitation of resources leads resource competition to arise between the co-infecting pathogens. Resource competition can take place between different genotypes/isolates of a single species (intraspecific competition), or it can take place between individuals of multiple species (interspecific competition) (Grover, 1997; Hortal et al., 2016; Abdullah et al., 2017; Dutt et al., 2021b). This can lead to selection pressure; however, competition can lead to co-existence of closely related pathogens, if their biology permits for niche differentiation through a process called resource partitioning to minimise competition (MacArthur & Levins, 1967; Tilman, 1982; Fitt et al., 2006a).

The ecological niche is considered a hypervolume with multiple dimensions, where each dimension represents a specific condition (i.e. a nutrient resource or an environmental factor) that is critical for the survival and reproduction of a given species (Hutchinson, 1957). The range of a species' ability to survive and reproduce in different levels of those conditions forms its 'fundamental niche'. Furthermore, the effects of multi-pathogen interactions and resource partitioning arising from those interactions may limit the range of the species' fundamental niche, forming its 'realised niche' (Hutchinson, 1957; Begon et al., 2006; Gerz et al., 2018). Resource partitioning is an evolutionary response to selection pressure, where the competing pathogens utilise separations in space, time and resource use (forming their realised niches) to co-exist on their host (Schoener, 1974; Walter, 1991; Fitt et al., 2006a; Levine & HilleRisLambers, 2009). These separations can suggest different competitors occupy different tissues on their host (space); one of the competitors occurring earlier or later than another in a given growing season (time); or differences in the ability of the competitors in colonising viable and necrotic tissues of their host (resource use) (Fitt et al., 2006a). If the co-infecting pathogens are not able to partition the resource sufficiently, this would lead interspecific competition to take place, which may cause competitive exclusion of a competitor (Begon et al., 2006; Abdullah et al., 2017; Dutt et al., 2021b). This is explained by the competitive exclusion principle theory, which states that two different species cannot occupy the same niche and co-exist indefinitely, which would give the stronger competitor the advantage (Gause, 1934; Hardin, 1960; Fitt et al., 2006a).

If interspecific competition is taking place, the strategy of the competing pathogens can manifest in three different ways: resource-mediated (exploitative), host-mediated (apparent) or interference (Read & Taylor, 2001; Begon et al., 2006; Mideo, 2009; Tollenaere, 2016). Resource-mediated competition is observed when all competitors have access to a resource that is limited, whereby the competitor that can utilise the limited resource most efficiently would outcompete the others and survive (Tan et al., 2016; Dutt et al., 2021b). An example of this was shown in a study where effectiveness of the biocontrol strain of *Bacillus amylolequifaciens* T-5 in controlling a bacterial wilt pathogen (*Ralstonia solanacearum*) on tomato plants was investigated. It was reported that *B. amylolequifaciens* utilised the resources at the roots of the plants and colonised it more efficiently, which led to a local exclusion of *R. solanacearum* (Tan et al., 2016).

Host-mediated competition is observed when one of the competitors infects and develops in the host, leading to activation of plant defences, often resulting in the induction of systemic acquired resistance, which reduces the chances of other competitors successfully infecting and surviving on the host (Aimé et al., 2013; Dutt et al., 2021b). An example of this was shown in a study investigating interactions between the epiphytic fungi *Pseudozyma aphidis* and *Botrytis cinerea* on *Arabidopsis thaliana*. The authors reported that infection by *P. aphidis* induced the plant's defence systems locally and systemically against *B. cinerea* through activation of pathogenesis related protein-1 (*PR-1*) and plant defensin-1.2 (*PDF-1.2*) expression. Furthermore, similar observations were reported on mutant plants lacking SA and JA/ET signalling, suggesting that *P. aphidis* may also have activated the plant defences independent of phytohormone signalling (Buxdorf et al., 2013).

Interference competition is observed as a direct interaction, where one of the competitors produces molecules (e.g. toxins) to interfere with another competitor's access to a limited resource, growth and reproduction, to gain a competitive advantage (Mideo, 2009; Dutt et al., 2021b). An example of this was shown in a study investigating the endophytic fungi found in an African cereal crop finger millet, where it was found that one of the endophytic fungal species (predicted to be a species of the *Phoma* genus) produced antifungal compounds, which inhibited the growth of several pathogenic *Fusarium* species, including *F. graminearum* (Mousa et al., 2015).

L. maculans and *L. biglobosa* co-infect and co-exist on their host oilseed rape in the UK and Europe. Their co-existence is facilitated by the small differences in the niches they occupy. This is due to differences in their temperature optima required for pseudothecial maturation, where pseudothecia of *L. maculans* can mature faster at colder temperatures (< 10°C) compared to those of *L. biglobosa* (Toscano-Underwood et al., 2003). Although pseudothecial maturation of *L. maculans* and *L. biglobosa* are similar at higher temperatures (15-20°C), the difference at lower temperatures (which are observed in autumn and winter) favours earlier maturation of pseudothecia of *L. maculans*, leading to earlier release of its ascospores compared to those of *L. biglobosa* (Toscano-Underwood et al., 2003). This creates a temporal and spatial separation in the infection of oilseed rape between these two pathogens, where *L. biglobosa* arrives later in the growing season and colonises the newer leaves and upper stem tissues, as *L. maculans* colonises the older leaves and stem base (West et al., 2002a; Huang et al., 2005; Fitt et al., 2006a).

Some competitive interactions have also been reported to take place between *L. maculans* and *L. biglobosa*. Mahuku et al. (1996) first reported that a single pre-inoculation of oilseed rape plants with the weakly virulent isolate (now known to be *L. biglobosa*) sufficiently induced resistance against the highly virulent isolate (*L. maculans*) not only in pre-inoculated leaves, but also in other leaves without pre-inoculation of *L. biglobosa*. Interestingly, if *L. biglobosa* inoculation was done 64 h or later after *L. maculans*, the induction of resistance was lost. Liu et al. (2006) investigated induction of resistance against *L. maculans* using chemical defence activators and *L. biglobosa*, which showed that pre-inoculation of oilseed rape leaves with acibenzolar-*S*-methyl (ASM) or *L. biglobosa* ascospores in the autumn reduced the severity of stem cankers in the following summer before harvest. Following on, they have compared the mechanisms of resistance induced by those chemical defence activators and *L. biglobosa*. It was found that ASM-induced resistance was through earlier activation and enhancement of *PR-1* gene expression, and *PDF-1.2* expression was repressed. By contrast, *L. biglobosa*-induced resistance was predominantly through JA/ET signalling leading to earlier and enhanced expression of *PDF-1.2*, with upregulation in the expression of *PR-1* following afterwards (Liu et al., 2007). These observations indicate that *L. biglobosa* is able to deploy a host-mediated interspecific competition strategy

against *L. maculans*, by activating plant defences upon pre-inoculation, leading to a reduction in the severity of disease caused by *L. maculans*.

Another example from *Leptosphaeria* species is the phytotoxin sirodesmin PL produced by *L. maculans*, but not by *L. biglobosa* (Rouxel et al., 1988). Sirodesmin PL belongs to the class of epipolythiodioxopiperazine (ETP) secondary metabolites, which are characterised by containing a disulphide bridge (Curtis et al., 1977; Gardiner et al., 2005; Howlett et al., 2009) (Figure 1.9). There are 20 co-regulated genes in the biosynthetic gene cluster (BGC) responsible for production of sirodesmin PL, named *sir* genes (Gardiner et al., 2004; Urquhart et al., 2021). Biosynthesis of sirodesmin PL starts with two amino acid residues: tyrosine and serine (Gardiner et al., 2004; Gardiner et al., 2005). The first step is catalysed by a prenyl-transferase encoded by *sirD*, which is *O*-prenylation of the L-tyrosine residue by dimethylallyl pyrophosphate (Kremer & Li, 2010). This is followed by a condensation reaction of dimethylallyl-L-tyrosine and serine residues, which is catalysed by a two-module non-ribosomal peptide synthetase encoded by *sirP*, an enzyme reported to be essential for biosynthesis of sirodesmin PL (Gardiner et al., 2004; Elliott et al., 2007; Urquhart et al., 2021). These two reactions result in a known precursor of sirodesmin PL, called phomamide (318.4 Da) (Pedras & Yu, 2009). Following a series of other reactions (sulphurisation, oxidation, reduction, methylation, rearrangements and acetylation), sirodesmin PL (486.6 Da) is produced (Gardiner et al., 2004; Pedras & Yu, 2009). Furthermore, the expression of genes in the biosynthetic cluster is regulated by a Zn(II)2Cys6 transcription factor, encoded by a cross-control pathway gene *sirZ* (Elliott et al., 2007; Fox et al., 2008; Elliott et al., 2011).

Sirodesmin PL has antibacterial and antifungal properties (Rouxel et al., 1988). It was reported that a sirodesmin PL non-producing isolate of *L. maculans* had reduced antibiotic and antifungal activity. When cultures of wild-type and mutant *L. maculans* isolates were overlaid with molten agar containing *Bacillus subtilis* or *Fusarium graminearum* conidia, zones of inhibition were present near the wild-type *L. maculans* colony but were absent for the *sirP* mutant *L. maculans* colony. Furthermore, the mutant isolate was still able to produce the usual symptoms of wild-type *L. maculans* when applied directly on stems, but not as effective in colonising the stem when inoculated on leaves of oilseed rape. Finally, the *sirP* mutant isolate did not differ in spore germination, growth and fertility when compared to the wild-type isolate (Elliott et al, 2007).

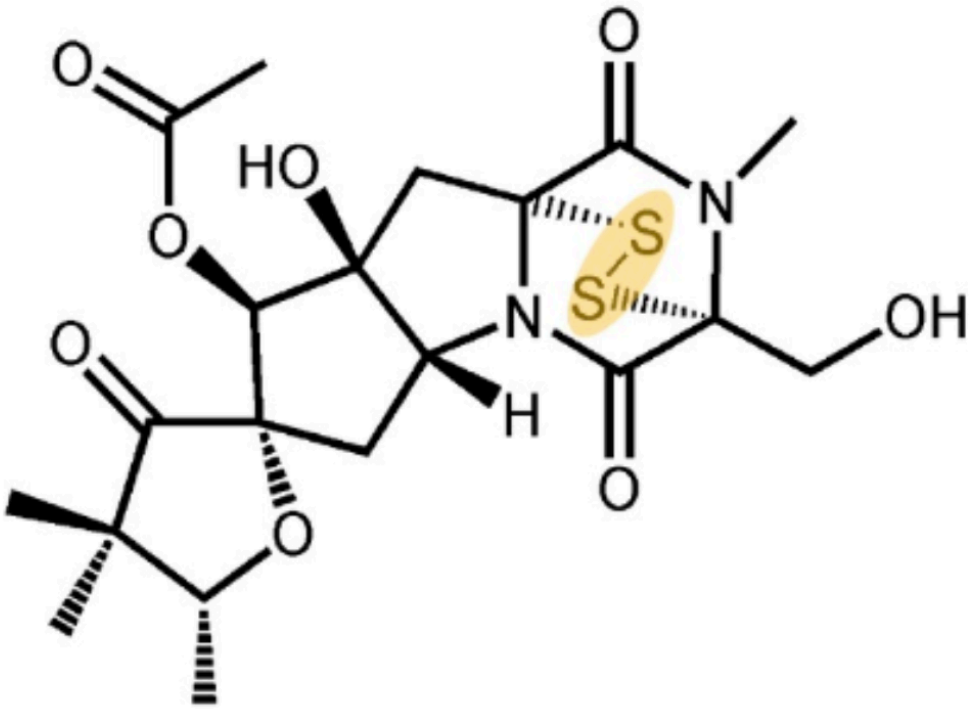

Figure 1.9: Chemical structure of the phytotoxin sirodesmin PL produced by *Leptosphaeria maculans*.

Sirodesmin PL belongs to the epipolythiodioxopiperazine class of secondary metabolites, characterised by a disulphide bridge, which is highlighted. This figure was adapted from Howlett et al., 2009.

These observations suggest that sirodesmin PL is not essential for the ability of *L. maculans* in causing disease on its host, but it is important during its asymptomatic phase when colonising the petiole and the upper stem tissues.

Interestingly, Elliott et al. (2007) also showed that the wild-type *L. maculans* isolate producing sirodesmin PL inhibited the germination of *L. biglobosa* conidia, which was not observed for the mutant isolate lacking sirodesmin PL production. These observations indicate that *L. maculans* is deploying an interference competition strategy against *L. biglobosa* (and other pathogens infecting oilseed rape) through the production of the phytotoxin sirodesmin PL. Although sirodesmin PL is thought to be important in competitive interactions, the toxin itself can still cause small yellow chlorotic lesions on cotyledons and leaves of oilseed rape when applied alone. Therefore, it was classified as a 'phytotoxin' and not as a 'fungitoxin' (Rouxel et al., 1998; Elliott et al., 2007).

1.6 Current disease control strategies for phoma stem canker

Phoma stem canker is an economically important disease leading to significant yield losses. Therefore it is important to control the disease through integrated pest management (IPM) strategies. IPM aims to have a sustainable approach of controlling pests and diseases through combination of chemical, cultural, varietal and biological methods in a manner that minimises environmental and economic risks (DEFRA, 2024).

1.6.1 Chemical control

Chemical control is based on application of fungicides, which is one of the most commonly used methods of controlling phoma stem canker on oilseed rape in the UK (West et al., 2001; Fortune et al., 2021). According to pesticide usage survey reports on arable crops in the UK for the past fourteen years, the fungicides applied in control of oilseed rape diseases included active substances with three different modes of action. Among these, the most commonly used active substances are prothioconazole and tebuconazole, with an increase in their usage in formulations over time (Garthwaite et al., 2012; 2014; 2016; 2018; 2020; 2022).

Prothioconazole and tebuconazole are triazole fungicides, which belong to the class of demethylase inhibitor fungicides (DMI). The mode of action of these DMI fungicides is the inhibition of the *CYP51* gene, encoding for a 14α-demethylase, an enzyme

responsible for catalysing ergosterol synthesis (Price et al., 2015). Inhibition of CYP51 disrupts the synthesis of ergosterol, which is an important component facilitating the stability of fungal cell membranes. Disruption of ergosterol synthesis therefore leads to accumulation of toxic compounds inside the cells, leading to fungal cell death (Lupetti et al, 2001; Sewell et al, 2017). Azole fungicides in general are used widely on UK oilseed rape crops (West et al., 2002b; Huang et al., 2011; King et al., 2021). This has led to a reduction in the effectiveness of azole fungicides through fungicide insensitivity development in the *Pyrenopeziza brassicae* (causing light leaf spot on oilseed rape) populations in the UK; through substitution mutations in the *CYP51* gene (Carter et al., 2014; King et al., 2021). For *L. maculans*, it was recently found that the modern western European isolates (collected in 2022-2023) had a reduction in their sensitivity to azole fungicides compared to older isolates (collected in 1992-2005), resulting from insertions of transposable elements in *CYP51* promoters (King et al., 2024). Furthermore, it was previously reported that *L. biglobosa* is less sensitive to azole fungicides compared to *L. maculans* (Eckert et al, 2010; Huang et al., 2011). Examples of DMI fungicides currently available in England include Proline 275® (prothioconazole) (Bayer Crop Science) and Toledo® (tebuconazole) (Albaugh Crop Protection).

Other modes of action of active ingredients often used in co-formulations with DMI fungicides are succinate dehydrogenase inhibitor fungicides (SDHI) and quinone outside inhibitor fungicides (QoI). SDHI fungicides work by inhibiting the succinate dehydrogenase enzyme, which is an important component in the mitochondrial electron transport chain. Blocking this enzyme halts fungal respiration, leading to fungal cell death (Avenot & Michailides, 2010). QoI fungicides work by inhibiting the electron transfer between cytochrome complexes, halting ATP production and leading to subsequent fungal cell death (Bartlett et al., 2002). Insensitivity development to SDHI or QoI fungicides has not been reported in field isolates of *L. maculans* and *L. biglobosa* (King et al., 2024). Examples of SDHI and QoI fungicides available in England include Filan® (boscalid) (BASF Agricultural Solutions UK) and Amistar® (azoxystrobin) (Syngenta).

In order to avoid fungicide insensitivity development in oilseed rape pathogens, it is advised to apply fungicides only when necessary (environmental factors favouring disease development, appearance of symptoms exceeding thresholds etc. increasing risk

of yield losses). Another important guidance is avoiding sequential use of fungicides with the same mode of action by alternating fungicides or using co-formulations with different modes of actions to preserve the effectiveness of fungicides (FRAG-UK, 2024). This is particularly important, as development of new fungicides is extremely costly and sometimes take over ten years (Leadbeater, 2015; Oliver & Beckerman, 2022). Thus, it is of great importance to also utilise alternative methods of disease control in rotation.

The current guidance from the Agriculture and Horticulture Development Board (AHDB) is to spray fungicide when 10 % to 20 % of plants show phoma leaf spot symptoms in the autumn (October and November). This is usually followed by another spray four to ten weeks after the first one to stop re-infection, if required. It is also advised that spray programmes are adjusted accordingly to account for fungicide spray required against *P. brassicae* (light leaf spot) in November to apply one spray to target both phoma leaf spot and light leaf spot (AHDB, 2020). It is important to note that the threshold for phoma leaf spot only includes lesions caused by *L. maculans* and not those caused by *L. biglobosa*.

1.6.2 Cultural practices

Cultural control aims to reduce interseasonal transmission by reducing pathogen inoculum by using common methods such as crop rotations, stubble management and earlier sowing (West et al., 2001). Crop rotations operate by rotating the sowing of oilseed rape seeds across different fields by sowing another crop for the next growing season, aiming to reduce inoculum in those particular fields. One important factor here is the time interval in rotations between the same crops. It is considered ideal to have a four year break for oilseed rape (West et al., 2001; Aubertot et al., 2006). Another important factor is the distance used between the fields with the same crop. In the UK, the current guidance is to isolate the fields with sequential oilseed rape cultivation by at least 200 – 500 m, as it was shown that the greatest risk of infection was within 500 m after the previous crop (Barbetti et al., 2000; West et al., 2001; FRAG-UK, 2024). Crop rotations with closer timing and distance from previous oilseed rape crops increase the pathogen inoculum in the soil, which may lead to an increase in the incidence of phoma leaf spots and subsequent stem cankers (West et al., 2001).

Stubble management works by using ploughing to bury the oilseed rape stubble from the previous growing season. This helps to reduce the exposure to infected stem stubble (containing pseudothecia of *Leptosphaeria* species) on the soil surface, reducing the number of ascospores released from the mature pseudothecia, leading to a reduction in the incidence of phoma leaf spots and subsequent stem cankers (Gladders & Musa, 1980; West et al., 2001; Aubertot et al., 2006). Other methods of reducing the inoculum on stem stubble include burying, burning and flooding after harvest (Ogle & Dale, 1997; West et al., 2001).

Earlier sowing of seeds allows oilseed rape crops to produce enough foliage before the release of ascospores of *Leptosphaeria* species (West et al., 2001; Aubertot et al., 2004). This method can be effective as it is easier to manage phoma leaf spot on larger plants with larger leaves (FRAG-UK, 2024). One reason for this is that the larger plants have longer leaves and longer petioles, and therefore the pathogens takes a longer time to reach the stem, leading to a reduction in disease severity (Sun et al., 2000; Sun et al., 2001). However, it is important to note that earlier sowing may increase the risk of another economically relevant disease of oilseed rape, called light leaf spot (*P. brassicae*), so regular monitoring of crops is recommended (FRAG-UK, 2024).

1.6.3 Cultivar resistance

Cultivar resistance is used extensively world-wide to control phoma stem canker (mainly targeting *L. maculans*). There are two types of cultivar resistance that can be bred into oilseed rape crops: qualitative (*R* gene-mediated) resistance and quantitative resistance (QR) (Balesdent et al., 2001; Delourme et al., 2006).

Qualitative resistance is mediated by single major resistance genes (*R* genes) and provides complete resistance and it usually operates early in the disease cycle, during initial colonisation of the leaves through stomatal penetration by germ tubes from ascospores (Ansan-Melayah et al., 1998; Balesdent et al., 2001). This type of resistance is race-specific and is effective only when pathogen populations carry the avirulent allele of the corresponding effector gene, allowing an incompatible interaction to occur between the pathogen and the host, leading to disease resistance (Delourme et al., 2006; Huang et al., 2018) (Figure 1.10). This is described as a gene-for-gene interaction (Flor, 1971).

	Genotype of *Leptosphaeria maculans* (pathogen)	
Genotype of *Brassica napus* (host)	***AvrLm1***	***avrLm1***
Rlm1	**Resistant**  **(incompatible interaction)**	**Susceptible**  **(compatible interaction)**
rlm1	**Susceptible**  **(compatible interaction)**	**Susceptible**  **(compatible interaction)**

Figure 1.10: Gene-for-gene interactions between the pathogen *Leptosphaeria maculans* and the host *Brassica napus* (oilseed rape) in qualitative resistance.

Dominant alleles of the resistance gene of the host (e.g. *Brassica napus Rlm1*) and the corresponding effector gene of the pathogen (e.g. *Leptosphaeria maculans AvrLm1*) result in an incompatible interaction, triggering local cell death mediated by a hypersensitive response (HR), restricting the pathogen at the inoculation site. Any other combinations of alleles result in a compatible interaction, where the pathogen can successfully infect and produce symptoms on the host (Delourme et al., 2006; Huang et al., 2018). Photos were taken by Prof. Yong-Ju Huang.

Successful recognition of pathogen effectors (encoded by *Avr* genes) by specific host receptors (encoded by *R* genes) leads to effector-triggered defence (ETD), resulting in localised cell death at the site infection, preventing the pathogen from causing further symptoms (Greenberg & Yao, 2004; Stotz et al., 2014). Since the restriction of the pathogen to the infection site is facilitated by cell death, this type of resistance is usually effective against biotrophic or hemibiotrophic pathogens, as they require living cells to establish themselves within the host (Stotz et al., 2014).

There have been several *Rlm* genes used against *L. maculans* in oilseed rape cultivars (Rouxel & Balesdent, 2017). An example of a particularly successful resistance gene is *Rlm7*, which has been widely deployed in the UK and France (Mitrousia et al., 2018; Balesdent et al., 2024). Although this type of resistance is very effective and provides complete resistance to the pathogen, it is not durable due to reliance on a single gene. There have been several reports of breakdown of *R* gene-mediated resistance in the *L. maculans-B. napus* pathosystem (Rouxel & Balesdent, 2017). Continuous use of a single *Rlm* gene in oilseed rape cultivars places an evolutionary pressure on local *L. maculans* populations. This leads to mutations in the *Avr* genes of *L. maculans*, which upon selection renders the resistance gene ineffective, resulting in its breakdown (Rouxel et al., 2003a; Rouxel et al., 2003b; Sprague et al., 2006; Fudal et al., 2009; Van de Wouw et al., 2010; Daverdin et al., 2012; Grandaubert et al., 2014). Breakdown of a resistance gene leads to severe phoma leaf spot and stem canker epidemics. This is described as a 'boom and bust' cycle (Pink & Puddephat, 1999). Therefore, it is advised that different *R* genes are used in combination or rotation, or combined with quantitative resistance (QR), which has been shown to increase the durability of *R* genes in field experiments (Brun et al., 2010; Huang et al., 2018). Currently, cultivars with qualitative resistance only target *L. maculans*, with no *R* genes identified for controlling *L. biglobosa* on oilseed rape. It was also reported that the cultivars with effective resistance against *L. maculans* are more susceptible to infection by *L. biglobosa* (Javaid, 2019; Huang et al., 2024).

Quantitative resistance (QR) is mediated by multiple genes in quantitative trait loci (QTLs), provides partial resistance and it usually operates later in the disease cycle, during the asymptomatic phase where pathogens grow along the petioles and colonise the stem tissues (Delourme et al., 2006; Huang et al., 2009). Due to its polygenic nature, this type of resistance is not race-specific (effective against various isolates/genotypes

of a pathogen species) and more durable compared to qualitative resistance (Boyd, 2006; Delourme et al., 2006). Furthermore, little is known about how QR operates, because it is mainly active in the asymptomatic phase of the disease. It is also challenging to investigate QR, as it relies on glasshouse experiments or field assessments with very large specific mapping populations of oilseed rape plants (Pilet et al., 1998; Huang et al., 2009). By contrast, qualitative resistance can be tested effectively and rapidly using cotyledon tests (Balesdent et al., 2001). Several stable QTLs have been identified for resistance against *L. maculans* (Huang et al., 2016). These QTLs are primarily thought to target *L. maculans*, but it was suggested that the background QTL in cultivar Fencer may also be conferring QR against *L. biglobosa* (Javaid, 2019). Moreover, Sapelli (2024) recently identified QTLs against *P. brassicae* (light leaf spot pathogen), some of which were overlapping with the QTLs identified against *L. maculans*. Some QTLs may have a general effect against disease development by multiple pathogens; and if common QTLs were identified against pathogens that are not closely related (*L. maculans* and *P. brassicae*), it may be that these QTLs are also effective against *L. biglobosa*, which is the closest relative of *L. maculans*. A summarised comparison of qualitative and quantitative cultivar resistance is given in Table 1.2.

1.6.4 Biocontrol

Biocontrol as a disease management method aims to limit or prevent the development of a disease (or a pathogen) by using other organisms (antagonists) (Cook & Baker, 1983; Jensen et al., 2016; Tronsmo et al., 2020; Stenberg et al., 2021). Biocontrol agents may antagonise the target pathogens through different mechanisms, by either direct or indirect competitive interactions (Köhl et al., 2019). These may include mycoparasitism, competition for resources and space (resource-mediated competition), induction of host defences (host-mediated competition) or antibiosis through secondary metabolites (interference competition) (Pieterse et al., 2014; Ghorbanpour et al., 2018; Köhl et al., 2019; Khan et al., 2020).

An example of a biocontrol agent is *Paenibacillus polymyxa PKB1* strain, which produces a peptide/metabolite (referred to as PKB1 antibiotic in the 2003 patent) that has antifungal activity against *L. maculans*, *Sclerotinia sclerotiorum* and *Alternaria brassicae*, inhibiting their growth on oilseed rape (Kharbanda et al., 1999).

Table 1.2: Comparison of qualitative (*R* gene-mediated) resistance and quantitative resistance (QR).

R gene-mediated resistance is race specific, monogenic, controlled by major *R* genes, provides complete resistance and is less durable. QR is non-race-specific, polygenic, controlled by minor genes or quantitative trait loci (QTLs), provides partial resistance and more durable (Balesdent et al., 2001; Delourme et al., 2006; Huang et al., 2009; Huang et al., 2016).

Qualitative (*R* gene-mediated) resistance	**Quantitative resistance (QR)**
Race specific	Non race specific
Monogenic	Polygenic
Controlled *R* genes	Controlled QTLs
Provides complete resistance	Provides partial resistance
Less durable	More durable

A more recent example of a biocontrol agent is *Bacillus amyloliquefaciens* MBI 600 strain, which was approved for use in the EU as a biocontrol agent against species of *Botrytis*, *Fusarium*, *Rhizoctonia* and powdery mildews (EU 2016/1429; EFSA, 2016). This biocontrol agent works by producing fungistatic and fungicidal compounds and suppressing the fungi through competition (EU 2016/1429).

The *B. amyloliquefaciens* MBI 600 strain was also shown to have promising results as a biocontrol agent against *L. maculans* (Chorleton, 2015). Furthermore, current guidance from the Fungicide Resistance Action Group – UK (FRAG-UK) includes consideration of *B. amyloliquefaciens* as a seed treatment to reduce levels of phoma (FRAG-UK, 2024). Some have also suggested the use of *L. biglobosa* as a biocontrol agent against *L. maculans*, since it induced systemic acquired resistance when pre-inoculated (Liu et al., 2006; Shah et al., 2020; Padmathilake & Fernando, 2022b).

1.6.5 Disease forecasting

Disease forecasting tools are commonly computational programs or equations often used to simulate and predict the development of crop diseases. In order to achieve maximum disease control, it is crucial to utilise the correct control methods appropriately into IPM strategies. These tools work by using the data input about the pathogen, plant, weather conditions, disease assessments and surveys, selection of cultivars and quantification of airborne inoculum (e.g. ascospores) (van den Bosch & Gilligan, 2003; Gilligan & van den Bosch, 2008). More technologically advanced models also often integrate the use of satellites (Newlands, 2018). These disease forecasting models are crucial for disease control, as they can contribute to the development of decision support systems (DSS), which provide valuable insights about disease progression to help guide growers on selection of cultivars and timing of fungicide applications (Audsley et al., 2005; Rupnik et al., 2019).

Weather-based models to predict the release of ascospores of *Leptosphaeria* species have been developed through input of previous temperature and rainfall data in relation to pseudothecial maturation leading to ascospore release. These models were considered useful to predict the first major release of ascospores in the autumn and effectively guide fungicide applications (Huang et al., 2007; Salam et al., 2007). Furthermore, a practical example of a disease prediction model is the phoma leaf spot

forecast provided by AHDB to UK growers, which was initially developed in the 2000s and updated in 2021 to increase its sensitivity to dampness/wetness (AHDB, 2025). Based on environmental data (temperature and rainfall), the model predicts the week when the advised threshold of 10 % incidence (% of plants affected) of phoma leaf spot for fungicide applications is likely to be observed, based on equation 2.1 presented in Evans et al. (2007). This tool also offers daily status of phoma leaf spot prediction, as well as comparison with the previous growing seasons to assess earliness or lateness (Figure 1.11).

These disease forecasting models are based on our understanding of the biology of the pathogens under different environmental conditions. Currently, these tools have limitations due to unpredictable nature of the environment and lack of complete understanding of the pathogens (Newbery et al., 2016) and lack of models specific for *L. maculans* or *L. biglobosa* ascospore release. Moreover, the interspecific interactions between multiple pathogens of a single crop are usually not considered in these models. These may introduce a degree of unreliability in the forecasts. Nevertheless, these tools hold great potential in guiding IPM strategies for effective control of crop diseases. Over time, further research on the pathogens, their interactions and how changes in the environment may affect them will improve the accuracy of these models in accurately predicting disease development.

1.7 Rationale

It has been previously reported in the past that in the UK, there is a difference between *L. maculans* and *L. biglobosa* in the timing of ascospore release, creating temporal and spatial separations between the pathogens on their host, allowing their co-existence (West et al., 2002; Toscano-Underwood et al., 2003; Huang et al., 2005; Fitt et al., 2006b; Huang et al., 2011). This is believed to be facilitated by the differences in their temperature optima for pseudothecial maturation, subsequently affecting and accounting for the difference in timing of ascospore release (Toscano-Underwood et al., 2003). However, there is increasing evidence that in recent years, a shift in the timings of ascospore release has occurred; and ascospores of both *L. maculans* and *L. biglobosa* are being released at similar times (Javaid, 2019; Huang et al., 2024). This is most probably due to effects of climate change, where warmer and wetter winters observed in the UK may be narrowing the time gap in pseudothecial maturation between

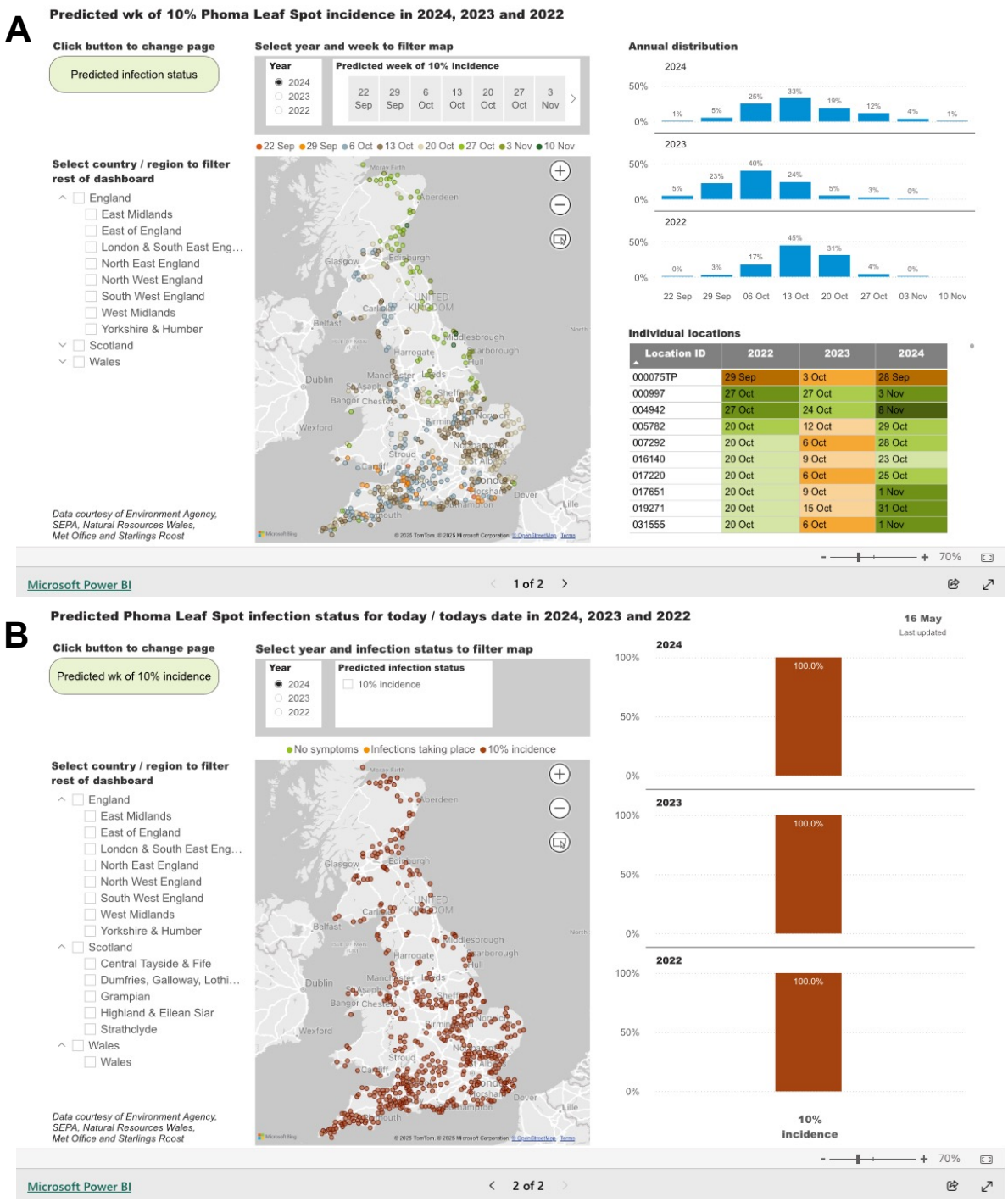

Figure 1.11: Phoma leaf spot forecast provided by the Agriculture and Horticulture Development Board (AHDB).

(A) Page One of the forecast: Prediction of when advised threshold of phoma leaf spot incidence (≥ 10 % of plants affected) based on environmental data (temperature and rainfall) in the UK. (B) Page Two of the forecast: Daily prediction of phoma leaf spot in the UK. Both pages also show comparison of phoma leaf spot prediction status on the same day(s) from the two previous growing seasons.

L. maculans and *L. biglobosa*. Consequently, ascospores of both pathogens are released at similar times, resulting in simultaneous and/or sequential co-inoculations with small time gaps (< 7 days) in natural conditions. This may lead to a disruption in the co-existence mechanisms (temporal and spatial separation) of these pathogens, resulting in interspecific competition between *L. maculans* and *L. biglobosa*.

Furthermore, a recent study (including some of the preliminary work in Chapter 4 of this PhD thesis done in collaboration with Dr. James Fortune) has shown that *L. biglobosa* can inhibit the production of sirodesmin PL by *L. maculans* under simultaneous co-inoculation, and this effect is lost if *L. biglobosa* is sequentially co-inoculated 7 days after *L. maculans* (Fortune et al., 2024). The strategy and timing of this antagonistic effect of *L. biglobosa* on *L. maculans* is not fully understood. Moreover, effects of the changing interspecific interactions between these pathogens on disease development and severity remain to be studied.

It is crucial to understand these pathogens – as well as their interactions – to implement appropriate and effective IPM strategies. Therefore, there is a need to investigate the interspecific interactions between *L. maculans* and *L. biglobosa* to understand the effects of these interactions on disease development and identify potential challenges – or opportunities – that may arise as a result of their different interactions.

1.8 Aims and objectives

This project aims to increase the understanding of interspecific interactions between *L. maculans* and *L. biglobosa* and to provide valuable insights into future integrated control strategies based on their interactions to improve control of phoma stem canker on oilseed rape in the UK. To meet the aims, there are three objectives:

1) To investigate interspecific interactions between *L. maculans* and *L. biglobosa in vitro* (Chapter 3)
2) To investigate interspecific interactions between *L. maculans* and *L. biglobosa in planta* (Chapter 4)
3) To investigate interspecific interactions between *L. maculans* and *L. biglobosa* in natural conditions (Chapter 5)

2 Chapter 2 – General materials and methods

2.1 Media preparation

All agar media were made to a volume of 400 mL and transferred into 500 mL Duran bottles for autoclaving. The lids of the Duran bottles were left loose to avoid explosion during the autoclave process. The bottles containing the media were autoclaved at 121°C for 15 min. Using an ErgoOne PipetBoy serological pipette (Starlab), 15 mL of autoclaved media were transferred into each Petri dish (9 cm diameter) in a biosafety cabinet (ThermoFisher) to standardise the agar media. After solidifying in the biosafety cabinet, the agar media dishes were labelled and sealed in plastic bags and stored at 5°C until required.

2.1.1 Preparation of V8 agar

Preparation of the medium was done by measuring the following components for making 400 mL:

- Agar Bacteriological Number 1 – 8 g
- $CaCO_3$ – 0.8 g
- V8 juice – 80 mL
- Distilled water – 320 mL

2.1.2 Preparation of clarified V8 (CV8) agar

Preparation of the medium was done by measuring the following components for making 400 mL:

- Agar Bacteriological Number 1 – 6 g
- $CaCO_3$ – 3 g
- Sucrose – 0.4 g
- CV8 supernatant – 80 mL
- Distilled water – 320 mL

The CV8 supernatant was prepared by the addition of 15 g/L $CaCO_3$ to V8 juice, mixing with a magnetic stirrer for 15 min, then centrifugation at 1,400 × *g* for 5 min. The pellet was discarded and the CV8 supernatant was used. This was followed by the addition of the remaining components listed above prior to autoclaving (Chapter 3).

2.1.3 Preparation of potato dextrose agar (PDA):

Preparation of the medium was done by measuring the following components for making 400 mL:

- Potato dextrose agar (PDA) – 15.6 g
- Distilled water – 400 mL

2.2 Preparation of isolates of *Leptosphaeria* species

L. maculans isolate ME24, obtained from phoma stem canker on oilseed rape cultivar Apex in 2002 (Huang et al., 2006; Eckert et al., 2010) and *L. biglobosa* isolate WH17 Why-1, obtained from phoma leaf spot on oilseed rape cultivar Whisky in 2017 (Fortune et al., 2024) were used in all experiments. *L. maculans* ME24 isolate carries three avirulence (*Avr*) effector genes *AvrLm1*, *AvrLm6* and *AvrLm7*.

Using sterilised forceps and scalpels, standardised V8 or CV8 agar media were inoculated with agar plugs of *L. maculans* or *L. biglobosa* isolates and incubated at 20°C for 6 days in continual darkness to obtain fungal mycelia. In order to avoid continuous sub-culturing of isolates, each isolate was initially cultured on V8 agar media to obtain agar plugs (8 mm diameter) and these were stored at 4°C until required for experiments.

2.3 DNA extraction from mycelia for standard DNA preparation

To grow mycelia of *L. maculans* and *L. biglobosa* for standard DNA preparation, V8 agar plates containing cellulose discs were made. This was done by autoclaving an empty beaker (600 mL capacity), distilled water (400 mL) and cellulose discs (9 cm diameter). In a biosafety cabinet, sterilised distilled water (SDW) was poured into the sterile beaker. Using sterile forceps, cellulose discs were collected one at a time, hydrated in SDW, and placed onto pre-made V8 agar plates. The addition of cellulose discs onto V8 agar media promotes mycelial growth and acts as a physical barrier between the mycelia and agar media during mycelial harvest. Using sterile corers (8 mm diameter), agar plugs of *L. maculans* or *L. biglobosa* were collected from pure cultures and placed onto these V8 agar plates with cellulose discs. After incubating at 20°C for 7 days in complete darkness, the mycelia were harvested into sterile 2 mL screw-cap tubes by scraping them off the surface covered with cellulose discs. The mycelia were then freeze-dried for 48 h prior to DNA extraction.

Freeze-dried mycelial samples were homogenised using a sterile mortar and pestle and approximately 20 mg of each ground sample were transferred into each of a series of 2 mL screw-cap tubes. DNA extractions from ground samples were done using the DNAmite Plant DNA Extraction Kit (Microzone Ltd). Three sterile metal beads were added to each tube containing a ground sample and 1 mL of lysis solution (Solution-LA) was added. The samples were processed using a FastPrep machine (MP Biomedicals) at 4.0 m/s for 40 s. This was followed by the addition of 100 μL of protein precipitant solution (Solution-PA) into each tube, vortexing for 10 s, and centrifugation at 8,000 × *g* for 5 min at 4°C. Following centrifugation, 500 μL of the supernatant from each tube were transferred into each of a new set of sterile 1.5 mL tubes containing 500 μL of capture solution (Solution-CA). These tubes were inverted ten times and incubated on the bench for 10 min before centrifugation at 11,300 × *g* for 7 min at 4°C to pellet the DNA. The supernatant was discarded, and any remnants were removed using a pipette. DNA pellets were re-suspended in 55 μL of nuclease-free water after air-drying in the fume hood for 30 min, then placed at -20°C for 16 h. Extracted DNA samples were then thawed at 20°C and centrifuged at 7,000 × *g* for 10 min at 4°C, and 50 μL of the supernatants containing the DNA were transferred into each of a new set of sterile 0.5 mL tubes (Figure 2.1).

2.4 DNA quality check and dilution

Following DNA extraction from various samples (mycelia in Chapter 3, cotyledons in Chapter 4 and stems in Chapter 5) using different protocols, all of the DNA samples obtained were subjected to quality checks and diluted to a standard concentration for quantitative polymerase chain reaction (qPCR) analyses.

2.4.1 DNA quality check by NanoDrop

DNA concentration, A260/A280 ratio and A260/A230 ratio in DNA samples were measured using a NanoDrop (ND-1000 Spectrophotometer, NanoDrop Technologies) by pipetting 1 μL of DNA sample following blanking of the spectrophotometer using nuclease-free water.

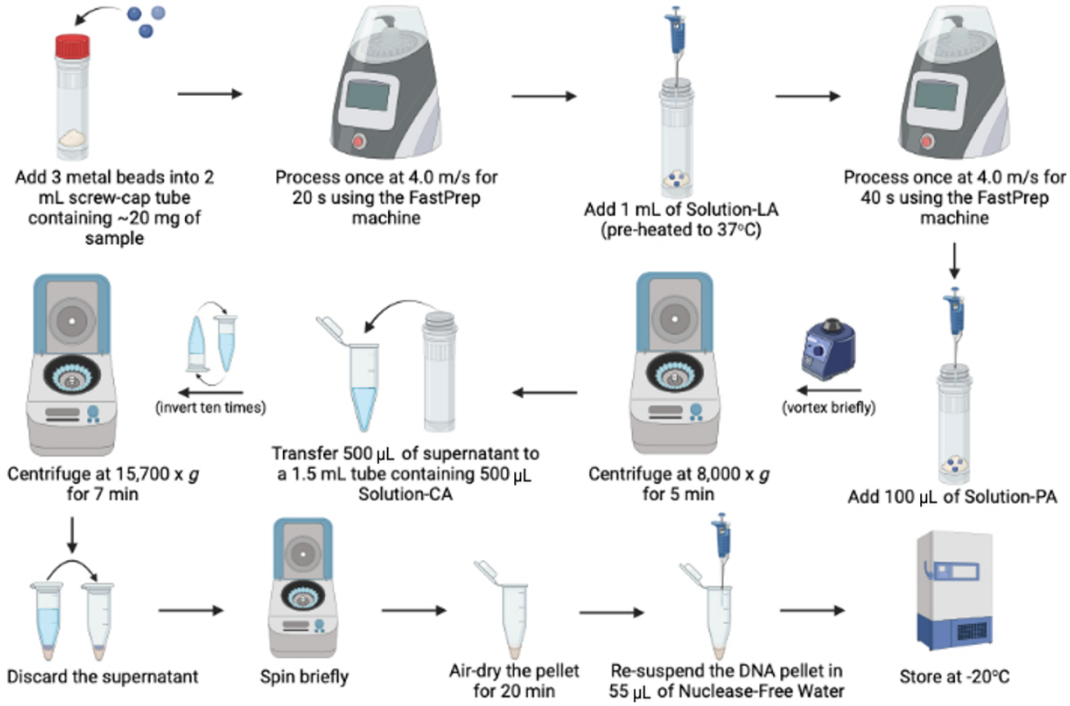

Figure 2.1: Workflow of DNA extraction from fungal mycelia using the DNAmite Kit (Microzone Ltd).

Samples were further homogenised by the addition of beads and use of a FastPrep machine (MP Biomedicals). Lysis solution was added, and the tubes were further processed in the FastPrep machine (MP Biomedicals). Protein precipitant solution was added, and the tubes were processed using a vortex and a centrifuge. The supernatant was moved into another tube containing DNA capture solution and inverted. The DNA was pelleted using a centrifuge. The supernatant was discarded, and the DNA pellet was air-dried before it was re-suspended in nuclease-free water and stored at -20°C until required for further steps. This figure was created using BioRender.com.

2.4.2 DNA quality check by Qubit

DNA concentrations of all samples were measured using Qubit DNA Broad Range Assay Kit (Invitrogen). This was done by preparing a master mix containing 199 μL of Qubit buffer and 1 μL of Qubit dye for each sample to be quantified. After vortexing, 190 μL of master mix was aliquoted for standards and 199 μL of master mix was aliquoted for samples into extra clear tubes for Qubit assays. This was followed by addition of 10 μL standard (for standards only) and 1 μL of sample (for samples only) to a final volume of 200 μL in all reactions. The tubes were vortexed for 2 s and incubated at 20°C for 2 min before DNA concentration readings were taken using a Qubit 3 Fluorometer (Invitrogen) (Figure 2.2).

2.4.3 DNA dilution

Based on the DNA concentrations measured using Qubit, all DNA samples were diluted to a standard concentration of 20 ng/μL and stored at -20°C until required for qPCR analyses.

2.5 Quantitative polymerase chain reaction (qPCR)

DNA samples were taken out of the freezer and thawed at 20°C then placed on ice. The qPCR analyses to quantify *L. maculans* DNA and *L. biglobosa* DNA were done using a Stratagene 3005P qPCR machine (Agilent).

2.5.1 Preparation of qPCR reactions

The amounts of *L. maculans* and *L. biglobosa* DNA in samples were quantified using SYBR Green (Agilent), with species-specific primers LmacF (5'-CTTGCCCACCAATTGGATCCCCTA-3') / LmacR (5'-GCAAAATGTGCTGCGCTCCAGG-3') for *L. maculans* and LbigF (5'-TCAGGGGATTGGTGTCAGCAGTTGA-3') / LmacR (5'-GCAAAATGTGCTGCGCTCCAGG-3') for *L. biglobosa* (Table 2.1) (Liu et al, 2006). The qPCR reaction mixtures were prepared at a total volume of 20 μL, containing 10 μL of SYBR Green (containing ROX as a reference dye), 6.3 μL of nuclease-free water, 0.6 μL of forward primer (10 μM), 0.6 μL of reverse primer (10 μM) and 2.5 μL of DNA standard or sample in duplicate wells in 96-well plates (Figure 2.3).

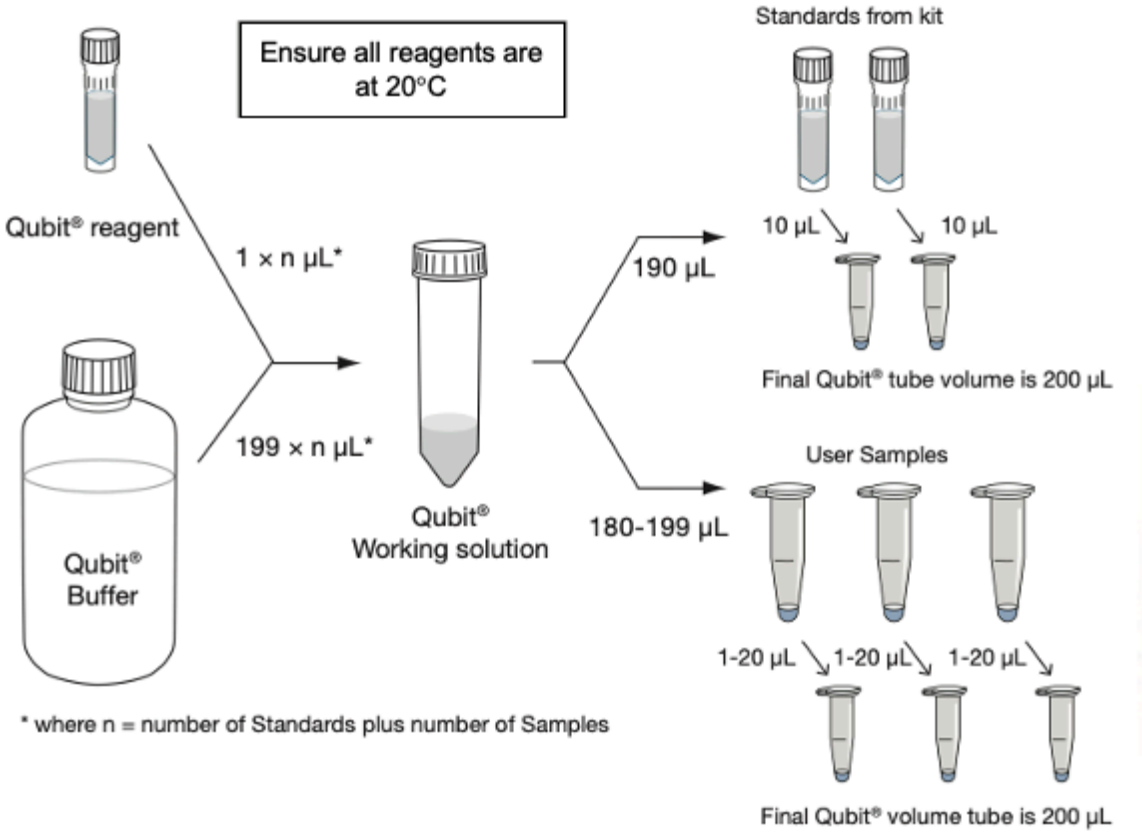

Figure 2.2: Workflow of reaction preparation for Qubit DNA Broad Range Assay Kit (Invitrogen).

Qubit buffer and reagent (dye) are used to prepare a working solution (or a master mix) and aliquoted according to the number of standards and samples to be tested. Once the standards and samples are added to the aliquots to a total volume of 200 µL, the tubes are vortexed for 2 s and incubated for 2 min at 20°C before readings are taken.

Table 2.1: Species-specific *Leptosphaeria maculans* (Lm) and *Leptosphaeria biglobosa* (Lb) forward and reverse primers used in quantitative polymerase chain reaction (qPCR) for quantification of *Leptosphaeria* species DNA.

Primer name, length (bp), sequence (5' to 3'), expected product size (bp) and reference are listed. These species-specific primers were designed to target the internal transcribed spacer (ITS) regions (Liu et al., 2006).

Primer name	Primer length (bp)	Primer sequence (5'-3')	Expected product size (bp)	Reference
LmacF (Lm forward)	24	CTTGCCCACCAATTGGATCCCCTA	331	Liu et al., 2006
LmacR (Lm reverse)	22	GCAAAATGTGCTGCGCTCCAGG		
LbigF (Lb forward)	26	TCAGGGGATTGGTGTCAGCAGTTGA	444	Liu et al., 2006
LmacR (Lb reverse)	22	GCAAAATGTGCTGCGCTCCAGG		

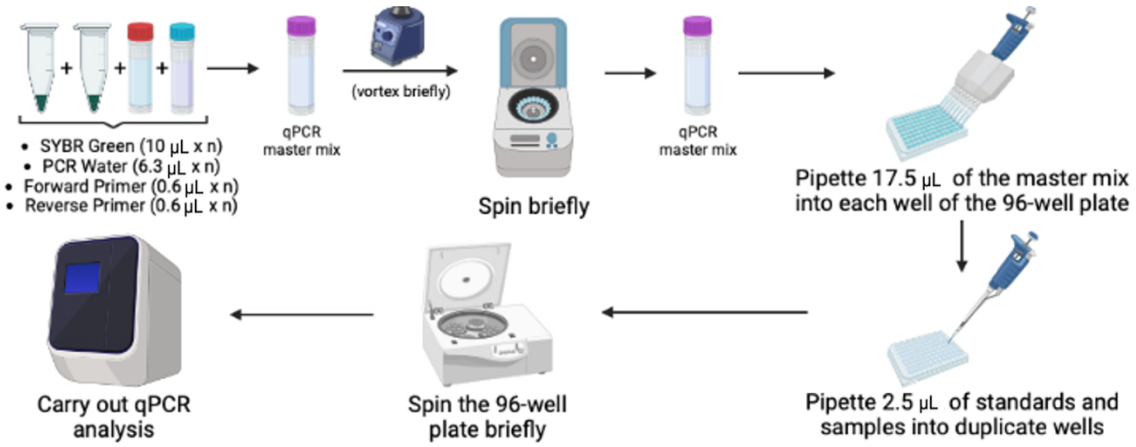

Figure 2.3: Workflow of quantitative polymerase chain reaction (qPCR) reaction preparation for DNA quantification.

SYBR Green, nuclease-free water, forward and reverse primers are combined to produce a qPCR master mix. After vortexing and spinning briefly, 17.5 µL of this qPCR master mix is aliquoted to wells of a 96-well plate, followed by the addition of 2.5 µL of standard or sample into each well. This figure was created using BioRender.com.

2.5.2 Preparation of standard DNA of *Leptosphaeria* species

To produce standard curves, sets of standards for each species were made using high quality DNA (> 1.8 A260/A280 ratio on NanoDrop), extracted from pure cultures. Standards were prepared in a 10-fold dilution series ranging from 10^4 to 1 pg of *L. maculans* DNA of isolate ME24 and 10^4 to 10^{-1} pg of *L. biglobosa* DNA of isolate WH17 Why-1. Standards were run alongside samples to produce standard curves in each 96-well plate. Images of standard curves used for quantification of *L. maculans* and *L. biglobosa* DNA can be found in Appendix A.

2.5.3 Thermocycling profiles for quantification of *Leptosphaeria* species

Thermocycling profiles for quantification of *L. maculans* and *L. biglobosa* DNA were as follows: 1 cycle of 95°C for 2 min, 40 cycles of 95°C for 15 s, 60°C (for *L. maculans*) or 55°C (for *L. biglobosa*) for 30 s, 72°C for 45 s and a reading step of 83°C for 15 s. Followed by 95°C for 1 min and a melting curve analysis by increasing the temperature from 60°C (for *L. maculans*) or 55°C (for *L. biglobosa*) to 95°C at 0.5°C increments at 3 s per step, finishing at 95°C for 15 s. Images of thermocycling profiles used for quantification of *L. maculans* and *L. biglobosa* DNA can be found in Appendix A.

2.6 High performance liquid chromatography (HPLC)

The HPLC methodology was adapted from Pedras & Biesenthal (1998). Analyses of samples were done using a Shimadzu Prominence HPLC machine, with a diode array detector (SPD-M20A), through taking 20 µL injections per sample, modified from Smedsgaard (1997). Separation was done using a C_{18} column (Varian pursuit 5, 150 x 4.6 mm) (Fortune et al., 2024).

A method with a linear gradient, starting at 85% water (Millipore) and 15% acetonitrile (FisherScientific, HPLC grade), going up to 100% acetonitrile over 40 min, maintaining there for 3 min and then starting a linear gradient back to 85% water and 15% acetonitrile over 5 min for each sample was used. The flow rate was 1 mL/min. Visualisations of HPLC chromatograms were done at 254 nm, using the Lab solution program [Version 5.92 (Shimadzu Corporation)] (Fortune et al., 2024).

2.6.1 Gliotoxin standard curve

Gliotoxin is a mycotoxin produced by some of the species of *Aspergillus*, *Penicillium*, *Alternaria* and *Trichoderma* (Scharf et al., 2012; Pratt-Hyatt, 2020). It is classified in the epipolythiodioxopiperazine (ETP) class of fungal secondary metabolites; which is the same class as sirodesmin PL produced by *L. maculans* (Kwon-Chung & Sugui, 2009; Gardiner et al., 2004). Previous studies have used gliotoxin standard curves to aid identification of sirodesmin PL through analytical techniques with a recovery efficiency of 91±7% (Gardiner et al., 2004; Elliott et al., 2007). In this study, the gliotoxin standard curve produced by Dr. James Fortune (Fortune, 2022), who used the same extraction and analytical methods as this study, was used.

This was done by preparation of a gliotoxin stock at 5 mg/mL concentration. This was followed by using a dilution series of 0.1 mg/mL, 0.25 mg/mL, 0.5 mg/mL and 1 mg/mL in a total volume of 1 mL. Three aliquots of 200 µL from each of these dilutions were taken into HPLC vials containing glass inserts and HPLC was run. The average areas of maxima for each concentration were plotted to produce the gliotoxin standard curve. The equation of the line was calculated as $y = 2E+06x - 56900$ and had an R^2 of 0.999 (Figure 2.4). The limit of detection was calculated at 70 mg/L, and the limit of quantification was calculated as 200 mg/L (Fortune, 2022). In addition, Fortune (2022) identified the maxima corresponding to sirodesmin PL and its precursors (deacetylsirodesmin PL and phomamide) using the information from Pedras & Biesenthal, (1998); and reported the retention times of sirodesmin PL and its precursors as ~16.2 min and ~11.2 min, respectively.

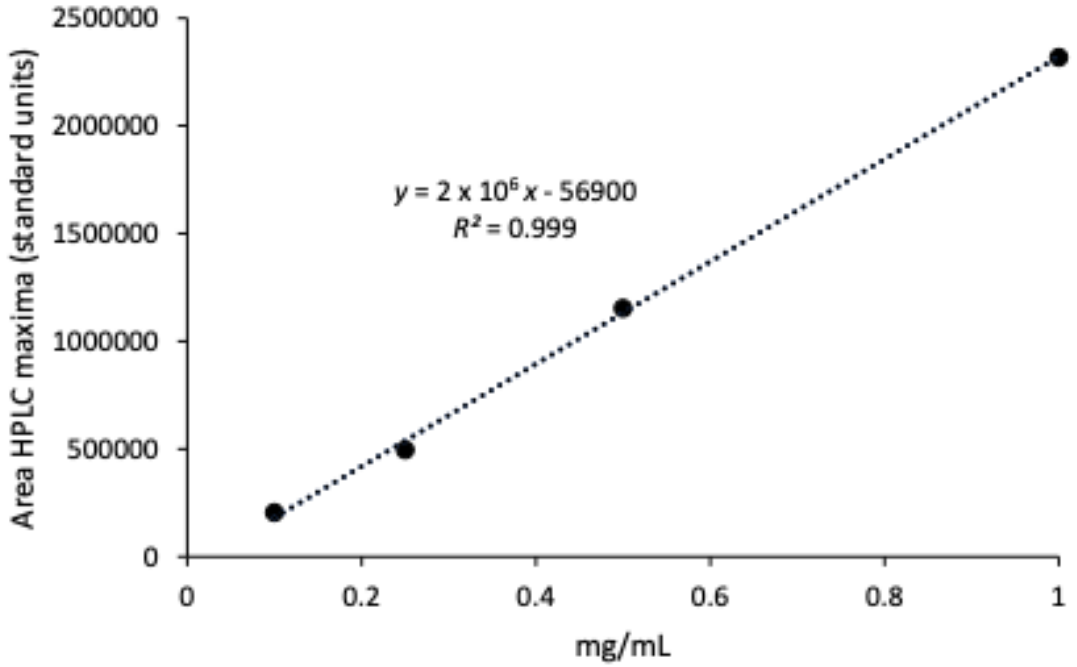

Figure 2.4: Gliotoxin standard curve produced by Fortune (2022).

Used for quantification of sirodesmin PL and its precursors using high performance liquid chromatography (HPLC) analyses.

3 Chapter 3 – Interspecific interactions between *Leptosphaeria maculans* and *Leptosphaeria biglobosa in vitro*

Acknowledgements – HPLC method used in this chapter was developed by James Stanley and Christine Gigou. Logistic equation analyses were done by Dr Aiming Qi.

Publications – The work presented in this chapter has been published: **Bingol E**, Qi A, Karandeni-Dewage C, Ritchie F, Fitt BDL, Huang YJ (2024). Co-inoculation timing affects the interspecific interactions between *Leptosphaeria maculans* and *Leptosphaeria biglobosa*. *Pest Management Science 80*: 2443-2452. http://doi.org/10.1002/ps.7799. A copy of this publication can be found in Appendix O.

3.1 Introduction

A plant host in nature is subjected to various pests and diseases throughout its life, often caused by plant pathogenic fungi (Dutt et al., 2021b). Oilseed rape, also known as canola (*Brassica napus*) is known to be affected by at least 16 different pathogens around the world; they infect different parts of the plant in different stages of its life cycle (Zheng et al., 2020).

Phoma stem canker is one of the most economically damaging diseases of oilseed rape globally (Zhang et al., 2014). In the UK alone, it can cause annual yield losses worth > £80 M, despite disease control efforts using fungicides and resistant cultivars (CropMonitor, 2020). In the UK, phoma stem canker has two causal agents, two closely related fungal pathogen species *Leptosphaeria maculans* (also known as *Plenodomus lingam*) and *Leptosphaeria biglobosa* (also known as *Plenodomus biglobosus*) (Shoemaker & Brun, 2001; Fitt et al., 2006a; de Gruyter et al., 2013). Although the global distribution of these pathogens varies, both *L. maculans* and *L. biglobosa* are found to co-infect oilseed rape across Europe and in the UK (Fitt et al., 2006b; Dilmaghani et al., 2009).

When co-infection of a single host by multiple pathogens occurs, interactions arise between them. All of these organisms require energy for survival, growth, development and reproduction; and they need to acquire that energy by utilising the nutrient resources

around them. These nutrient resources can be classified as materials consumed in the process of increasing population growth (Grover, 1997). Since these resources are finite and would not be available to an organism if already utilised by another, a limited availability of resources leads to resource competition arising between the co-infecting pathogens (Grover, 1997; Abdullah et al., 2017; Dutt et al., 2021b).

This resource competition can take place between different genotypes within the same species (intraspecific competition), or between different species (interspecific competition) (Hortal et al., 2016; Dutt et al., 2021b). The concept of interspecific competition is based on the competitive exclusion principle theory (Gause, 1934), which states that no two non-interbreeding species can continuously share a resource that is limited, leading to detriment and exclusion of the weaker competitor (Hardin, 1960; Fitt et al., 2006a).

When interspecific competition is taking place, the strategy which the competitors use can manifest in three different ways: resource-mediated (or exploitative) competition, host-mediated (or apparent) competition, or interference competition (Begon et al., 2006; Mideo, 2009; Read & Taylor, 2001; Tollenaere et al., 2016). Resource-mediated competition strategy is observed when a particular resource becomes limited. The species that can utilise the limited resource most efficiently outcompetes the other competitors and survives, often leading to competitive exclusion of other species (Gause, 1934; Tan et al., 2016; Dutt et al., 2021a). Host-mediated competition strategy is when the development of one of the competitors on the host primes the plant defence system by inducing systemic resistance against other competitors, reducing their chances of successfully infecting the host plant (Aimé et al., 2013; Dutt et al., 2021b). Interference competition strategy is when one of the competitors directly interferes with another's access to a limited resource, often by producing toxins (Dutt et al., 2021b).

Some of the observations done on *L. maculans* and *L. biglobosa* over many years can be attributed to some of these interspecific competition strategies. For example, it was found that if *L. biglobosa* infects oilseed rape before *L. maculans*, it primes the plant defence system and induces systemic acquired resistance, reducing the chances of *L. maculans* successfully infecting oilseed rape (Mahuku et al., 1996; Liu et al., 2006; Shah et al., 2020). It can be suggested that *L. biglobosa* uses a host-mediated interspecific

competition strategy against *L. maculans*. Furthermore, it was found that *L. maculans* produces a phytotoxin called sirodesmin PL, potentially as a part of an interference competition strategy (Rouxel et al., 1988).

Sirodesmin PL has antibacterial and antifungal properties (Rouxel et al., 1988). Moreover, it was shown that a mutant isolate of *L. maculans* without the ability to produce sirodesmin PL was still able to cause the associated symptoms of *L. maculans* caused by the wild type isolate when directly applied on stems; however, the mutant isolate was not as effective in colonising the stem tissues compared to the wild type isolate when inoculations were started in cotyledons or true leaves (Rouxel et al, 1988; Elliott et al., 2007; Gardiner et al., 2004), further suggesting that sirodesmin PL is not produced as a pathogenicity factor. Instead, it is important in the asymptomatic phase of pathogen growth, when *L. maculans* is colonising the petiole and the stem; where it would be interacting with other co-infecting pathogens in natural conditions. Furthermore, sirodesmin PL has been shown to have an inhibitory effect on the germination of *L. biglobosa* conidia (Elliott et al., 2007).

Usually in the UK, *L. maculans* is associated with stem basal cankers, whereas *L. biglobosa* is associated with upper stem lesions (West et al., 2001; Fitt et al., 2006b). This has mainly been attributed to differences in timing of ascospore release through pseudothecial maturation at different times in a cropping season; where pseudothecia of *L. maculans* mature at colder temperatures and lead to ascospore release earlier in the cropping season compared to those of *L. biglobosa* (West et al., 2002; Toscano-Underwood et al., 2003; Huang et al., 2011). Conversely, both *L. maculans* and *L. biglobosa* were found in stem basal cankers on oilseed rape in the UK (Huang et al., 2014b; Huang et al., 2024).

Interestingly, in recent years, it has been observed that ascospores of both *L. maculans* and *L. biglobosa* are being released at similar times (Javaid et al., 2021; Huang et al., 2024). This is most probably due to climate change, as increasing temperatures are narrowing the gap between the two *Leptosphaeria* species in maturation of pseudothecia. In addition, previous work has shown that there are no differences between *L. maculans* and *L. biglobosa* in terms of pseudothecial maturation at higher temperatures (Toscano-Underwood et al., 2003). Therefore, increasing temperatures

result in pseudothecial maturation of both *Leptosphaeria* species at similar times, leading to ascospore release at similar times, resulting in simultaneous and/or sequential co-inoculations by both of the pathogens in natural conditions, leading to interspecific interactions.

There has been little work on interspecific interactions between *L. maculans* and *L. biglobosa*, especially in the effects of timing on their interactions. It was reported that the induction of systemic acquired resistance by inoculation of oilseed rape leaves with *L. biglobosa* was affected by the timeline of co-inoculation of the two *Leptosphaeria* species. *L. biglobosa* was still able to reduce lesion severity caused by *L. maculans* if it was co-inoculated 48 h (2 days) after *L. maculans*; however, if *L. biglobosa* was co-inoculated 64 h (~2.5 days) after *L. maculans*, the induction of systemic acquired resistance was lost (Mahuku et al., 1996). Interestingly, recent studies (some of the work in Chapter 4 of this PhD thesis) have shown that *L. biglobosa* can inhibit the production of sirodesmin PL by *L. maculans* under simultaneous co-inoculation, and this effect is lost if *L. biglobosa* is sequentially co-inoculated 7 days after *L. maculans* (Fortune et al., 2024). The key mechanisms and important time points of interspecific interactions between *L. maculans* and *L. biglobosa* are unknown.

Therefore, this chapter focuses on pathogen-pathogen interactions and aims to characterise the interspecific interactions (and the effects of timing when the two pathogens are co-inoculated on these interactions) between phoma stem canker causal pathogens *L. maculans* and *L. biglobosa in vitro*. The hypotheses behind this study are:

1) Composition of secondary metabolites produced by *L. maculans* and growth rates of the two pathogens in terms of mycelial masses are different in liquid cultures simultaneously co-inoculated with *L. maculans* and *L. biglobosa* compared to sole cultures of *Leptosphaeria* species.

2) Morphology of mycelia, mycelial masses, composition of secondary metabolites produced by *L. maculans*, and relative percentages of pathogen DNA are different in liquid cultures sequentially co-inoculated with *L. maculans* and *L. biglobosa* compared to sole or simultaneously co-inoculated cultures of *Leptosphaeria* species.

3) *L. maculans* and *L. biglobosa* can outcompete each other and lead to competitive exclusion of one another based on the timing of their interaction in conditions with limited nutrients.

These hypotheses were addressed by the following objectives:

1) To investigate the effects of simultaneous co-inoculation of *L. maculans* and *L. biglobosa* on the production of sirodesmin PL and its precursors by *L. maculans* and growth of mycelial masses *in vitro*.

2) To investigate the effects of sequential co-inoculation of *L. maculans* and *L. biglobosa* on morphology of mycelia, mycelial masses, composition of secondary metabolites produced by *L. maculans* and relative growth of the two pathogens in terms of percentage of pathogen DNA *in vitro*.

3.2 Materials and methods

3.2.1 Setting up experiments for simultaneous and sequential co-inoculations

3.2.1.1 Preparation of media

Clarified V8 (CV8) agar and liquid media were used in the *in vitro* experiments. Preparation of CV8 agar media was done as described in section 2.1.2. Preparation of the CV8 liquid media was done by measuring the following components for making 1500 mL media:

- CV8 supernatant – 300 mL
- Sucrose – 1.5 g
- Distilled water – 1200 mL

CV8 supernatant was obtained as described in section 2.1.2. Using a measuring cylinder, 75 mL of broth was transferred into each 250 mL conical flask. Sponges were placed in the necks of conical flasks and each sponge was covered by four layers of tin foil (12 × 12 cm). Autoclave tapes were labelled and placed on top of each conical flask to observe the colour change, indicating that proper autoclaving had been done. Conical flasks were cooled at 20°C and were inoculated with agar plugs of each *Leptosphaeria* species on the same day.

3.2.1.2 Preparation of inoculum

To obtain inoculum, agar plugs of *L. maculans* and *L. biglobosa* (8 mm diameter) were taken from the initial stock at 4°C (as outlined in section 2.2) and were placed on CV8 agar media with the mycelial side of the plug in contact with the medium surface. After 6 days of culturing at 20°C in continual darkness, a sterilised corer (8 mm diameter) was used to obtain agar plugs from the front edges of the growing colonies to be used in experiments. This process was repeated for each experiment to obtain inoculum.

3.2.1.3 Inoculation of liquid cultures and experimental designs

3.2.1.3.1 Simultaneous co-inoculation experiments

CV8 broth (75 mL) in 250 mL conical flasks was inoculated with three different treatments: *L. maculans* only (Lm only), *L. biglobosa* only (Lb only) and *L. maculans* & *L. biglobosa* co-inoculated simultaneously (Lm&Lb) (Table 3.1). The experiments were arranged in a randomised block design in two blocks, with 18 conical flasks containing inoculated liquid media in each block (Appendix B). Inoculated liquid media were placed in a shaking incubator set at 18°C and 80 rpm with continual darkness. Sampling and separation of mycelia from the culture filtrate for measuring of mycelial masses and extraction of secondary metabolites from culture filtrates were done at 1, 3, 5, 7, 10, and 14 days post inoculation (dpi) (Figure 3.1). Three independent experiments were done. The composition of secondary metabolites was assessed in all three experiments. Mycelial masses were assessed in two experiments.

3.2.1.3.2 Sequential co-inoculation experiments

CV8 broth (75 mL) in 250 mL conical flasks was inoculated with eleven different treatments: *L. maculans* only (Lm only), *L. biglobosa* only (Lb only), *L. maculans* & *L. biglobosa* co-inoculated simultaneously (Lm&Lb), initial inoculation by *L. maculans* and then *L. biglobosa* co-inoculated sequentially at 1, 3, 5, or 7 days later (Lm+Lb-1, Lm+Lb-3, Lm+Lb-5, Lm+Lb-7), and initial inoculation by *L. biglobosa*, and then *L. maculans* co-inoculated sequentially at 1, 3, 5, or 7 days later (Lb+Lm-1, Lb+Lm-3, Lb+Lm-5, Lb+Lm-7) (Table 3.2, Figure 3.2).

Table 3.1: Treatments of inoculation with agar plugs (8 mm diameter) of *Leptosphaeria maculans* (Lm) and *Leptosphaeria biglobosa* (Lb) for *in vitro* simultaneous co-inoculation experiments.

For sole cultures, inoculations were done using three plugs of Lm or Lb. For simultaneously co-inoculated liquid cultures, inoculations were done using three plugs of Lm and Lb each at the same time.

Treatment	No of Lm agar plugs	No of Lb agar plugs
Lm only	3	0
Lb only	0	3
Lm&Lb	3	3

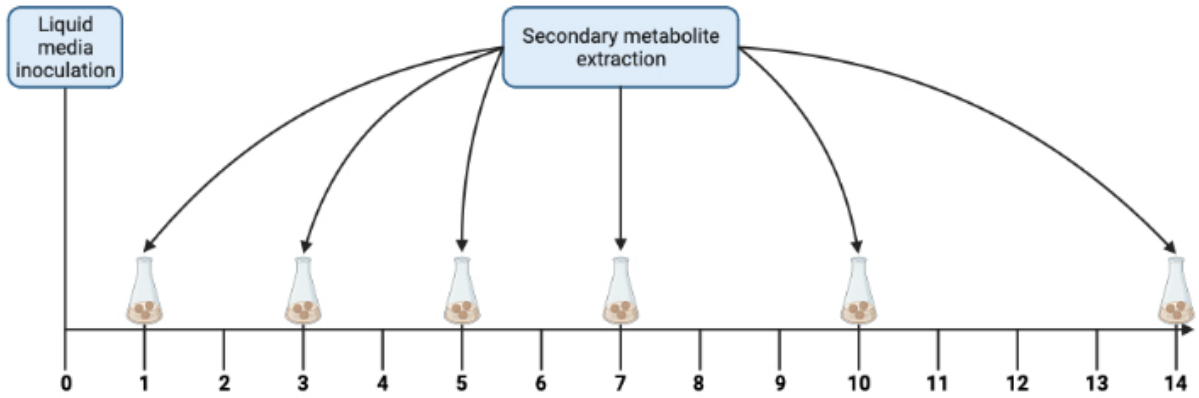

Figure 3.1: Timeline of inoculation and secondary metabolite extraction for *in vitro* simultaneous co-inoculation experiments.

Mycelia were collected from these liquid cultures at each time point alongside secondary metabolite extractions at 1, 3, 5, 7, 10 and 14 days post inoculation (dpi). This figure was created using BioRender.com.

Table 3.2: Treatments of inoculation with agar plugs (8 mm diameter) *of Leptosphaeria maculans* (Lm) and *Leptosphaeria biglobosa* (Lb) for *in vitro* sequential co-inoculation experiments.

For sole cultures, inoculations were done using three plugs of Lm or Lb. For simultaneously co-inoculated liquid cultures, inoculations were done using three plugs of Lm and Lb each at the same time. For sequentially co-inoculated cultures, inoculations were done initially with three plugs of Lm or Lb, followed by the addition of another three plugs of the other species at 1, 3, 5 and 7 days after the initial inoculation.

Treatment	No of Lm agar plugs (initial inoculation)	No of Lb agar plugs (initial inoculation)	No of Lm agar plugs (sequential co-inoculation)	No of Lb agar plugs (sequential co-inoculation)
Lm only	3	0	-	-
Lb only	0	3	-	-
Lm&Lb	3	3	-	-
Lm+Lb-1	3	0	-	3 (1 day after Lm)
Lm+Lb-3	3	0	-	3 (3 days after Lm)
Lm+Lb-5	3	0	-	3 (5 days after Lm)
Lm+Lb-7	3	0	-	3 (7 days after Lm)
Lb+Lm-1	0	3	3 (1 day after Lb)	-
Lb+Lm-3	0	3	3 (3 days after Lb)	-
Lb+Lm-5	0	3	3 (5 days after Lb)	-
Lb+Lm-7	0	3	3 (7 days after Lb)	-

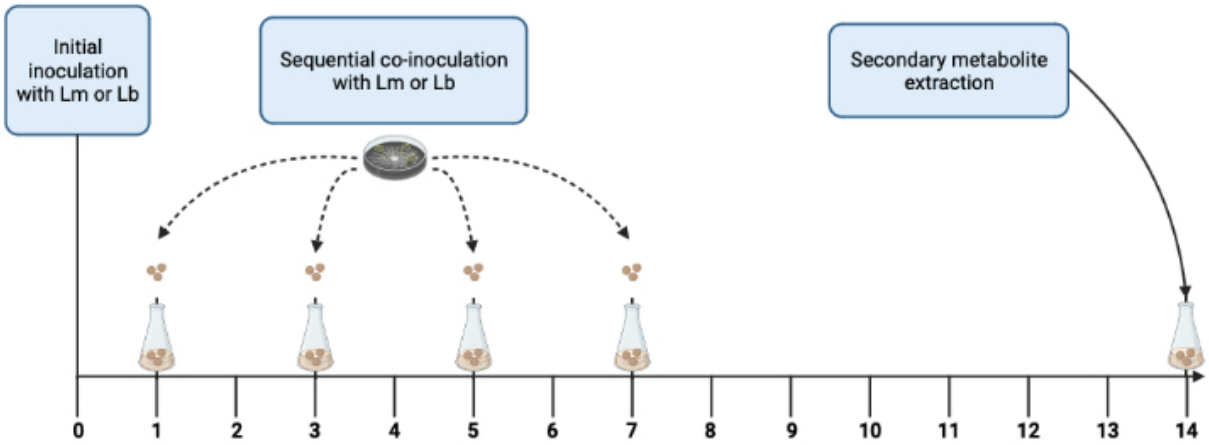

Figure 3.2: Timeline of inoculation and secondary metabolite extraction for *in vitro* sequential co-inoculation experiments.

Mycelia were collected from these liquid cultures at the end of the experiment at 14 days post inoculation (dpi). This figure was created using BioRender.com.

The experiments were arranged in a randomised design (Appendix B). Inoculated liquid media were placed in a shaking incubator set at 18°C and 80 rpm with continual darkness. Sampling and separation of mycelia from the culture filtrate for measuring of mycelial masses and extraction of secondary metabolites from culture filtrates were done at 14 dpi (Figure 3.2). Three independent experiments were done. Treatments were done in duplicate in two experiments and in triplicate in one experiment.

3.2.2 Effects of simultaneous co-inoculation on composition of secondary metabolites by *L. maculans*

3.2.2.1 Separation of fungal mycelia from liquid cultures

At each sampling day, multiple sets of sterile Buchner flasks and funnels (one set for each treatment) were set up inside a fume hood and cleaned with ethyl acetate. After ethyl acetate evaporated in approximately 5 min, filter papers (Whatman) were placed in the Buchner funnel and wetted with sterilised distilled water (SDW) and the vacuum was turned on. CV8 broth containing fungal mycelia was slowly poured on each Buchner funnel to separate fungal mycelia from liquid culture. When all the liquid culture was collected in the Buchner flask, the vacuum was turned off. Using sterilised forceps, fungal mycelia collected in the Buchner funnel were blot-dried with filter paper and transferred into sterile 15 mL Falcon tubes and stored at -20°C. Culture filtrate collected in the Buchner flask was transferred into two sterile 50 mL skirted Falcon tubes (35 mL in each) for secondary metabolite extraction (Figure 3.3). This process was repeated as required for all treatments at all sampling days.

3.2.2.2 Secondary metabolite extraction from culture filtrates and preparation of samples for high performance liquid chromatography (HPLC)

Inside a fume hood, 15 mL of ethyl acetate was added to each of the 50 mL skirted Falcon tubes containing 35 mL of culture filtrate. The tubes were then inverted 30 times to facilitate secondary metabolite uptake and left inside the fume hood for 10 min for the two liquid phases to settle. If there was emulsification observed, the tubes were centrifuged at 2,000 $\times$ *g* for 5 min. Using a pipette, 10 mL each of the upper phase were transferred into new sterile skirted 50 mL Falcon tubes for each treatment (20 mL in total for each treatment).

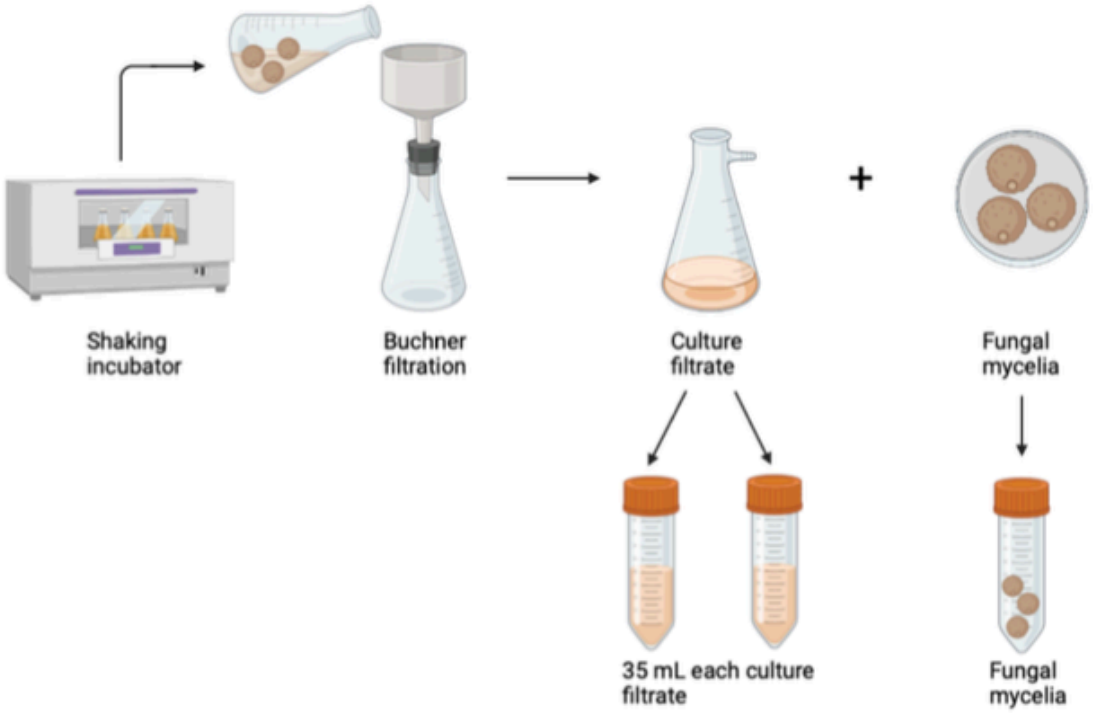

Figure 3.3: Workflow of separation of mycelia from liquid cultures.

Liquid cultures were taken from the shaking incubator. Separation of mycelia and culture filtrate were done using Buchner filtration. A total of 70 mL of culture filtrate (35 mL each in two tubes) were saved for downstream analysis. The mycelia were placed in tubes for storage at -20°C. This figure was created using BioRender.com.

The samples obtained were stored in a spark-free fridge at 4°C until required for HPLC sample preparation. The samples were placed under a constant stream of nitrogen for 6 h to allow ethyl acetate to evaporate. The samples were then re-suspended by adding 500 µL of ethyl acetate. Using 1 mL syringes (Terumo®), re-suspended samples were passed through 0.45 µm nylon syringe filters (ThermoFisher) into 2 mL HPLC vials to remove insoluble particles and create a stock. Using a pipette, 150 µL of stock samples were transferred into a new set of HPLC vials containing a 200 µL glass insert. All of the samples were stored in a spark-free fridge at 4°C until required for HPLC analysis (Figure 3.4).

3.2.2.3 High performance liquid chromatography (HPLC)

HPLC analyses were done as described in section 2.6.

3.2.3 Effects of simultaneous co-inoculation on growth rate of the pathogens

3.2.3.1 Freeze drying and weighing dry mycelia

The 15 mL Falcon tubes with mycelia were taken out of the -20°C freezer, the lids were removed, and the necks of the tubes were covered with Parafilm®. Using a sterilised needle, five small holes were created in the Parafilm® covering the neck of each tube, and all tubes were placed in a freeze-dryer for 48 h.

Once the freeze-drying was done, Parafilm® was removed from the neck of the tubes and the lids were placed back on. A 250 mL beaker was placed onto an analytical balance and was tared. Empty weights of five 15 mL Falcon tubes were recorded and an average was taken (all five tubes were of similar weight to two decimal points). The dry mycelial weight was obtained by subtracting the average weight of the five empty 15 mL Falcon tubes from the total measurement on the analytical balance.

3.2.4 Effects of sequential co-inoculation on morphology and pigmentation of the co-cultures

3.2.4.1 Separation of fungal mycelia from liquid cultures

The cultures were photographed for comparison before separating the mycelia from the culture filtrate. Separation of fungal mycelia from liquid cultures was done as described in section 3.2.2.1. Collected culture filtrates were also photographed for comparison.

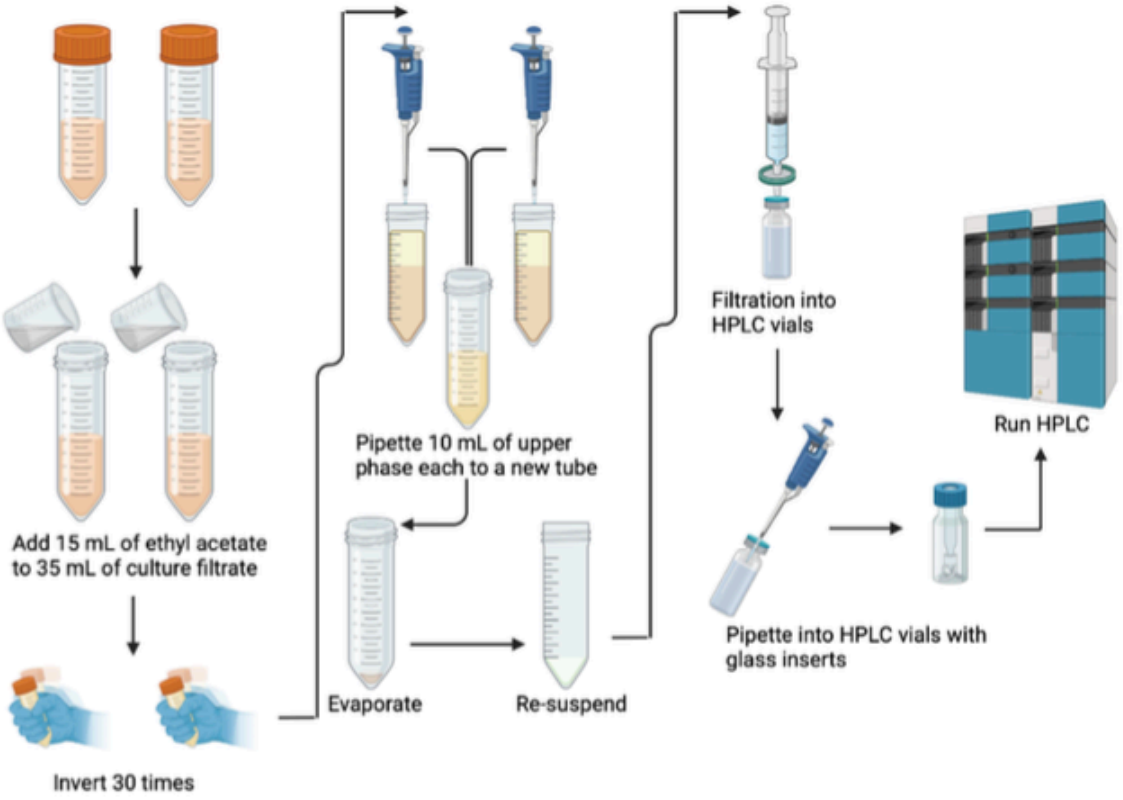

Figure 3.4: Workflow of secondary metabolite extraction from culture filtrates and preparation of samples for high performance liquid chromatography (HPLC).

Ethyl acetate (15 mL) was added to each tube containing 35 mL of culture filtrate. After inverting 30 times and waiting for the phases to settle, 10 mL each of the upper aqueous phases from each tube were combined into a new tube. After evaporation using a nitrogen stream, secondary metabolites were re-suspended in a standard reduced volume of ethyl acetate to increase their concentration. The re-suspended secondary metabolites were filtered into HPLC vials and small aliquots were taken into HPLC vials with glass inserts for analysis. This figure was created using BioRender.com.

3.2.5 Effects of sequential co-inoculation on dry mycelial weight of the co-cultures

3.2.5.1 Freeze-drying and weighing dry mycelia

Freeze-drying and weighing dry mycelia were done as described in section 3.2.3.1.

3.2.6 Effects of sequential co-inoculation on composition of secondary metabolites produced by *L. maculans*

3.2.6.1 Secondary metabolite extraction from culture filtrates and preparation of samples for high performance liquid chromatography (HPLC)

Secondary metabolite extraction from culture filtrates and preparation of samples for HPLC were done as described in section 3.2.2.2.

3.2.6.2 High performance liquid chromatography (HPLC)

HPLC analyses were done as described in section 2.6.

3.2.7 Effects of sequential co-inoculation on relative growth of the pathogens

3.2.7.1 DNA extraction from fungal mycelia using the DNAmite kit

DNA extraction from freeze-dried mycelial samples were done as described in section 2.3.

3.2.7.2 DNA quality checks and dilution for quantitative polymerase chain reaction (qPCR)

DNA quality check and dilutions were done as described in section 2.4.

3.2.7.3 Quantitative polymerase chain reaction (qPCR)

qPCR analyses were done as described in section 2.5.

3.2.8 Statistical analysis

3.2.8.1 Fitting a logistic equation to assess relative growth rates of the pathogens in simultaneously co-inoculated cultures

Using the GenStat program (22nd edition) (VSN International), a logistic equation was fitted to the data for dry mycelial weight against days post inoculation from simultaneous co-inoculation experiments, using the non-linear model directive. The fitted logistic equation was:

$$Y = \frac{A}{1 + e^{(-k*(t-t_0))}}$$

In this logistic equation, Y is the dry mycelial weight (g), t is the time (dpi), A is the upper asymptotic dry mycelial weight, k is the rate of increase in dry mycelial weight with time t, and t_0 is the time at which the dry mycelial weight reaches half the value of A.

3.2.8.2 Statistical tests used in analysis of the data

Statistical analyses of the data were done using the GenStat program (22nd edition) (VSN International). Since three repeated experiments were done for sequential co-inoculations for the same treatments, when the data from the experiments were analysed together, experiment number was assigned as a factor to assess whether the experiment had a significant effect. For measurements of sirodesmin PL and its precursors, data transformation was done with a common logarithm to homogenise the variances between treatments before they were subjected to two-way analysis of variance (ANOVA). Tukey's HSD post-hoc tests were done to separate the means of treatments at probability of 5% significance.

3.3 Results

3.3.1 Effects of simultaneous co-inoculation on composition of secondary metabolites produced by *L. maculans*

Production of sirodesmin PL and its precursors was assessed *in vitro*. 'Lb only' and 'Lm&Lb' treatments did not show any maxima corresponding to sirodesmin PL or its precursors in their HPLC chromatograms. However, for 'Lm only' treatment, the precursors of sirodesmin PL were first detected at 5 dpi at 70.4 mg/L concentration in HPLC analyses. The average concentration of the precursors increased from 5 dpi and was greatest at 10 dpi at 270.3 mg/L, before decreasing to 188.4 mg/L by 14 dpi (Figure 3.5).

Similarly, sirodesmin PL was first detected at 5 dpi at 91.6 mg/L concentration in HPLC analyses. The average concentration of sirodesmin PL increased steadily and was the greatest at 10 dpi at 884.3 mg/L concentration. It then decreased to 681.6 mg/L by 14 dpi (Figure 3.6).

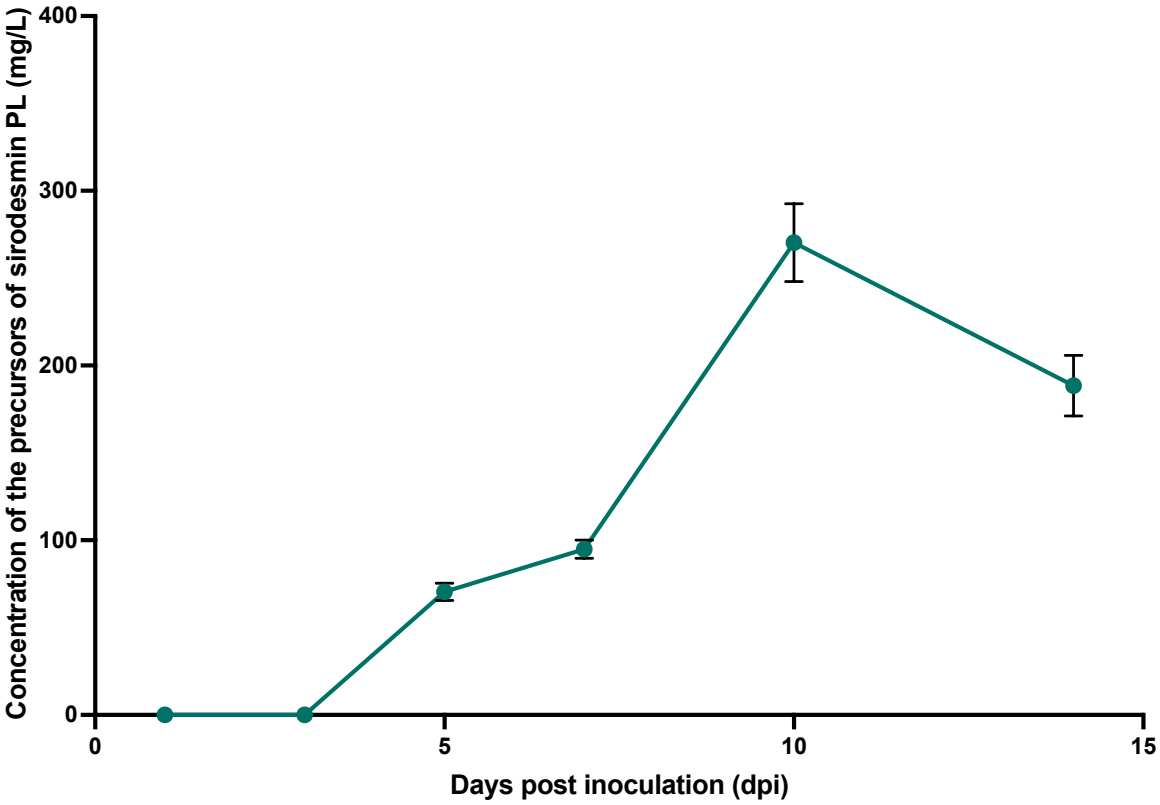

Figure 3.5: Average concentration of the precursors of sirodesmin PL (mg/L) for *Leptosphaeria maculans* only (Lm only) treatment from three experiments at 1, 3, 5, 7, 10 and 14 days post inoculation (dpi) *in vitro*.

Error bars show standard error of the mean (SEM) (n = 36).

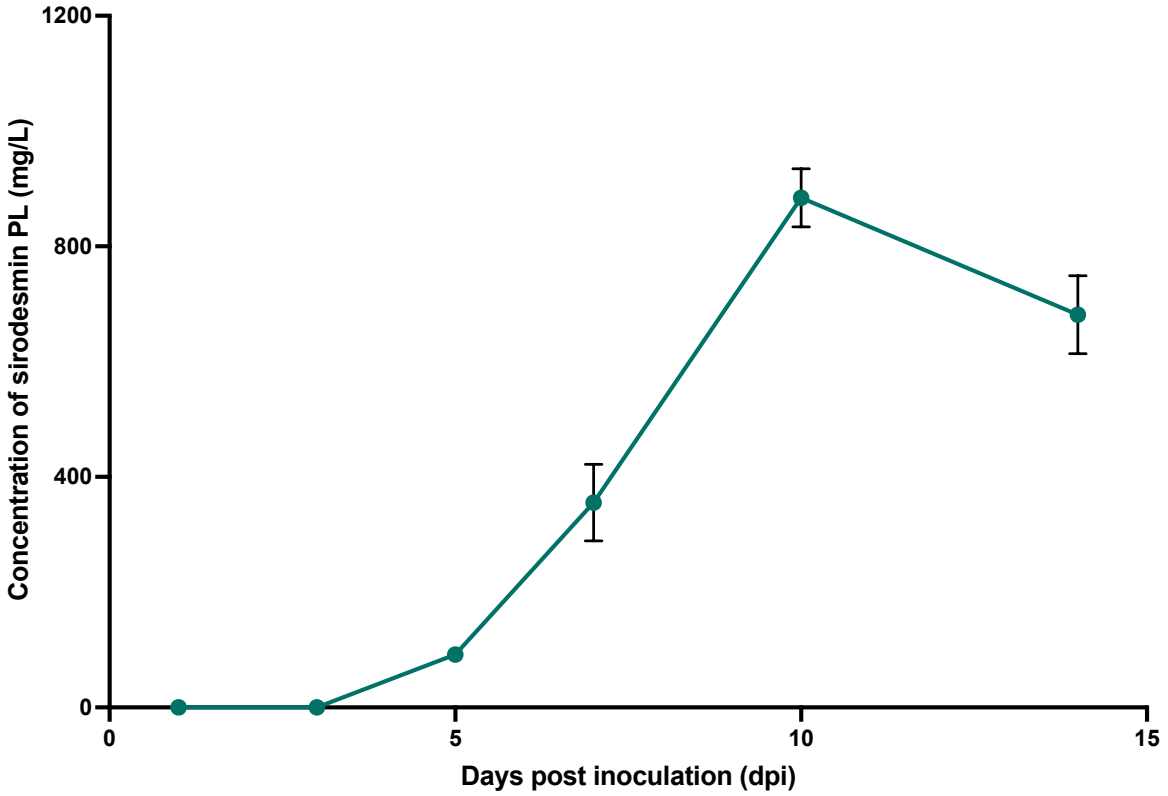

Figure 3.6: Average concentration of sirodesmin PL (mg/L) for *Leptosphaeria maculans* only (Lm only) treatment from three experiments at 1, 3, 5, 7, 10 and 14 days post inoculation (dpi) *in vitro*.

Error bars show standard error of the mean (SEM) (n = 36).

Overall, in all of the three experiments, sirodesmin PL and its precursors were detected only in the 'Lm only' treatment from 5 dpi, with their concentrations increasing until 10 dpi and then reducing from 10 dpi to 14 dpi. Trends in the production of sirodesmin PL and its precursors from individual experiments can be found in Appendix C.

3.3.2 Effects of simultaneous co-inoculation on growth rate of the pathogens

Mycelial growth of 'Lm only' increased steadily from day 0 to day 14, reaching an average dry mycelial weight of 0.22 g by 10 dpi and 0.30 g by 14 dpi. The k value estimated from the fitted logistic equation representing the rate of increase in dry mycelial weight with time was 0.38 for the 'Lm only' treatment (Figure 3.7).

For 'Lb only', mycelial growth occurred at a faster rate (k = 1.18) compared to 'Lm only', reaching an average dry mycelial weight of 0.20 g by 5 dpi. The mycelial growth for 'Lb only' treatment was greatest at 0.26 g by 7 dpi and did not increase any further from 7 dpi to 14 dpi (Figure 3.7).

Interestingly, albeit relatively faster between 1 dpi and 3 dpi, 'Lm&Lb' mycelial growth showed a similar rate (k = 1.03) to that of 'Lb only'. Average dry mycelial weight for 'Lm&Lb' treatment was greatest at 0.29 g by 7 dpi and did not increase any further from 7 dpi to 14 dpi (Figure 3.7). Trends in mycelial weight through the measurement of dry mycelial weight from individual experiments can be found in Appendix C.

3.3.3 Effects of sequential co-inoculation on morphology and pigmentation of the co-cultures

The morphology of mycelia in liquid cultures at 14 dpi was different between different treatments (Figure 3.8). The mycelia of 'Lm only' treatment were light brown, round in shape and had an intact structure. Whereas mycelia of 'Lb only' treatment were red and spread across the liquid media, without an intact structure. The morphology of mycelia in treatments with initial inoculation by *L. maculans*, followed by sequential co-inoculation with *L. biglobosa* at 1, 3, 5 and 7 days later (Lm+Lb-1, Lm+Lb-3, Lm+Lb-5, and Lm+Lb-7) was more similar to that of 'Lm only' treatment. Notably, the mycelia from 'Lm+Lb-5' and 'Lm+Lb-7' treatments looked almost identical to the mycelia from the 'Lm only' treatment.

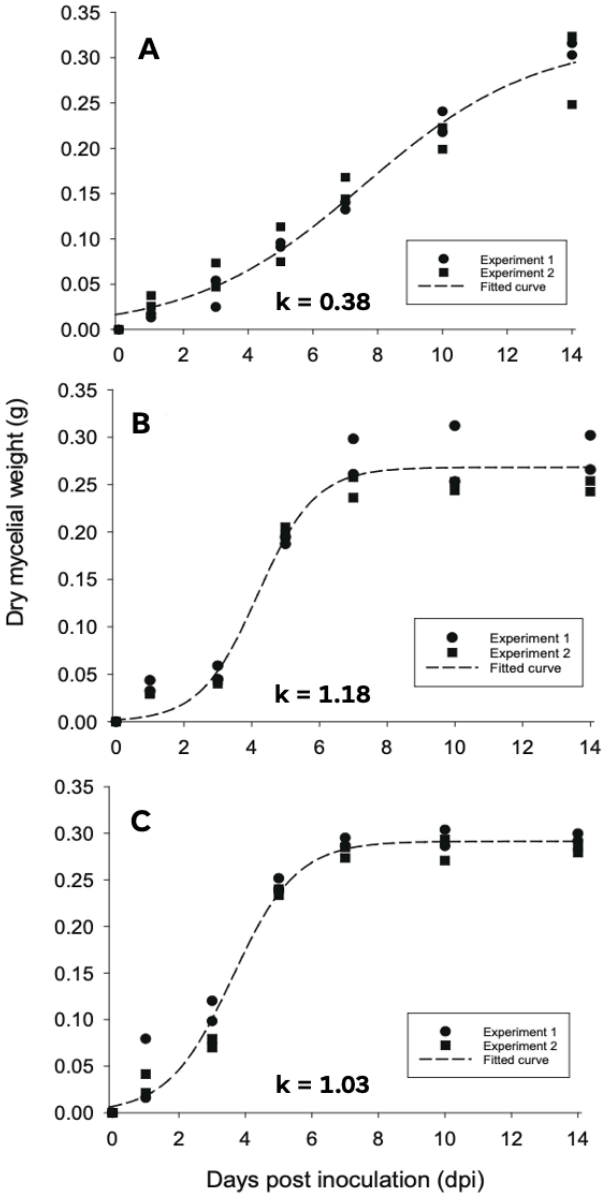

Figure 3.7: Fitted logistic curves for dry mycelial weight (g) of (A) *Leptosphaeria maculans* only (Lm only), (B) *Leptosphaeria biglobosa* only (Lb only) and (C) *L. maculans* & *L. biglobosa* co-inoculated simultaneously (Lm&Lb) treatments from two experiments at 1, 3, 5, 7, 10 and 14 days post inoculation (dpi) *in vitro*.

Dry mycelial weight in 'Lm only' treatment increased continuously from day 0 to day 14 with the growth rate coefficient *k* value of 0.38 and the coefficient of determination (R^2) 96.6%. Dry mycelial weight in 'Lb only' and 'Lm&Lb' treatments increased from day 0 to day 7 to reach an asymptote and maintained the plateau thereafter until the experiment ended on day 14, with the growth rate coefficient *k* values of 1.18 and 1.03 and coefficients of determination (R^2) 96.8% and 97.9%, respectively (Lm only, n = 24) (Lb only, n = 24) (Lm&Lb, n = 24).

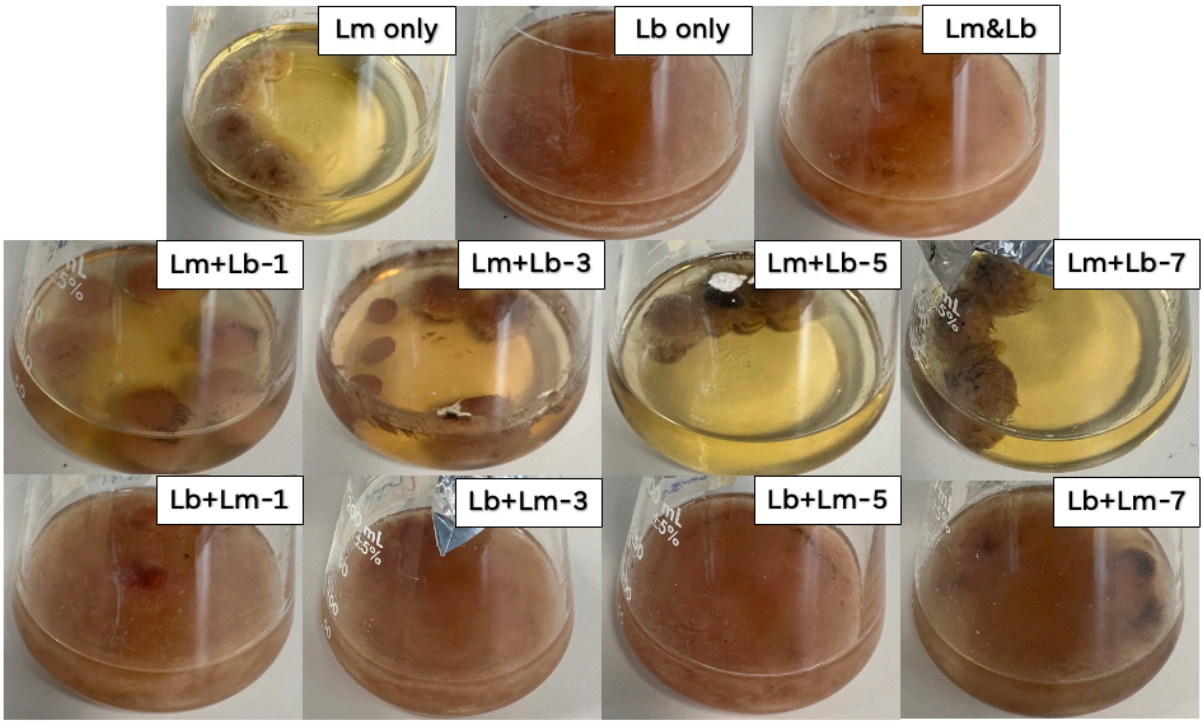

Figure 3.8: Morphology of mycelia in liquid cultures inoculated with *Leptosphaeria maculans* only (Lm only), *Leptosphaeria biglobosa* only (Lb only), *L. maculans* & *L. biglobosa* co-inoculated simultaneously (Lm&Lb), initial inoculation with *L. maculans* followed by co-inoculation with *L. biglobosa* sequentially at 1, 3, 5 and 7 days later (Lm+Lb-1, Lm+Lb-3, Lm+Lb-5, Lm+Lb-7) and initial inoculation with *L. biglobosa* followed by co-inoculation with *L. maculans* sequentially at 1, 3, 5 and 7 days later (Lb+Lm-1, Lb+Lm-3, Lb+Lm-5, Lb+Lm-7) at 14 days after the initial inoculation.

The mycelia of 'Lm only', 'Lm+Lb-5' and 'Lm+Lb-7' treatments looked similar; a light brown colour and intact round shaped structures. The mycelia of 'Lb only', 'Lm&Lb', 'Lb+Lm-1', 'Lb+Lm-3', 'Lb+Lm-5' and 'Lb+Lm-7' treatments looked similar; a red colour and spread across the liquid media without intact structures.

Moreover, the morphology of mycelia in treatments with initial inoculation with *L. biglobosa*, followed by sequential co-inoculation with *L. maculans* at 1, 3, 5 and 7 days later (Lb+Lm-1, Lb+Lm-3, Lb+Lm-5, and Lb+Lm-7) and *L. maculans* & *L. biglobosa* simultaneous co-inoculation (Lm&Lb) looked almost identical to that of the 'Lb only' treatment. The colour of culture filtrates from liquid cultures at 14 dpi differed between different treatments (Figure 3.9). Culture filtrate of 'Lm only' treatment had a light yellow colour. However, culture filtrate of 'Lb only' treatment had a dark yellow/orange colour. This difference was due to the production of a pigment by *L. biglobosa*, which was not produced by *L. maculans* (Williams & Fitt, 1999).

The colour of culture filtrates from liquid cultures where *L. maculans* was inoculated 3, 5 and 7 days before *L. biglobosa* (Lm+Lb-3, Lm+Lb-5, and Lm+Lb-7) was similar to that of the 'Lm only' treatment. The colour of culture filtrates from liquid cultures where *L. biglobosa* was inoculated at any time before (or at the same time as) *L. maculans* (Lm&Lb, Lb+Lm-1, Lb+Lm-3, Lb+Lm-5, and Lb+Lm-7) was similar to that of the 'Lb only' treatment. Interestingly, production of pigment was also noted in the 'Lm+Lb-1' treatment.

3.3.4 Effects of sequential co-inoculation on dry mycelial weight of co-cultures

There were significant differences in the average dry mycelial weight between the three experiments ($F(2,44) = 17.35$, $P < 0.001$) (Table 3.3, Table 3.4). The experiment mean for dry mycelial weight was significantly smaller in experiment 1 compared to experiments 2 and 3. Individual analyses of each of the three experiments can be found in Appendix C.

At 14 dpi, there was only one significant difference found in average dry mycelial weight between different treatments ($F(10,44) = 4.89$, $P < 0.001$), with 'Lm only' (0.33 g) being significantly greater than all other treatments. Average dry mycelial weight for the rest of the treatments ranged between 0.21 g (Lm+Lb-3) and 0.27 g (Lm+Lb-7) and they did not differ significantly from each other (Table 3.3, Table 3.4) (Figure 3.10). The interactions between experiments and treatments were not significant ($F(20,44) = 1.60$, $P = 0.095$) (Table 3.3).

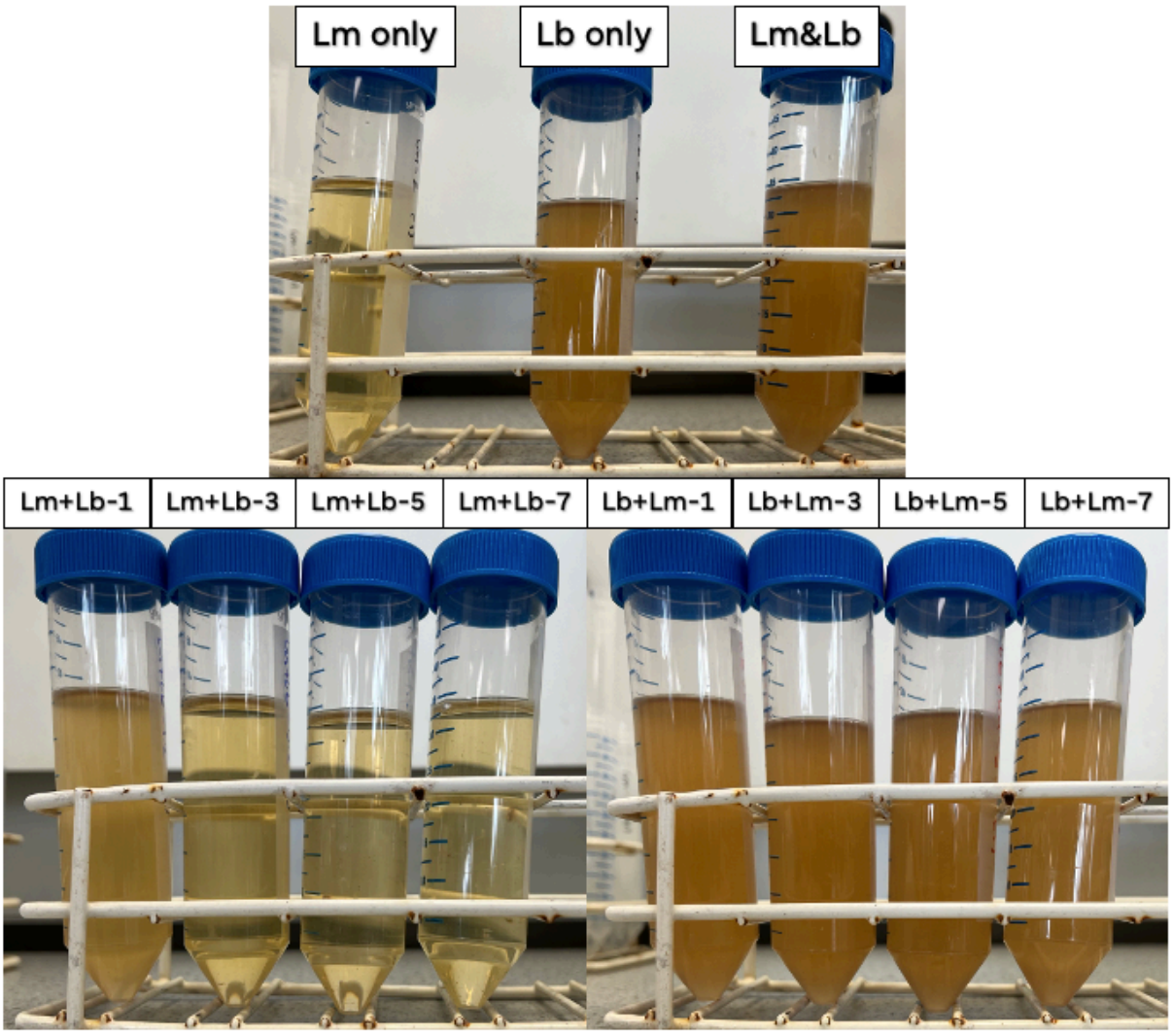

Figure 3.9: Colour of culture filtrates from liquid cultures inoculated with *Leptosphaeria maculans* only (Lm only), *Leptosphaeria biglobosa* only (Lb only), *L. maculans* & *L. biglobosa* co-inoculated simultaneously (Lm&Lb), initial inoculation with *L. maculans* followed by co-inoculation with *L. biglobosa* sequentially at 1, 3, 5 and 7 days later (Lm+Lb-1, Lm+Lb-3, Lm+Lb-5, Lm+Lb-7) and initial inoculation with *L. biglobosa* followed by co-inoculation with *L. maculans* sequentially at 1, 3, 5 and 7 days later (Lb+Lm-1, Lb+Lm-3, Lb+Lm-5, Lb+Lm-7) at 14 days after the initial inoculation.

Light yellow colour without orange pigmentation was observed in culture filtrates of 'Lm only', 'Lm+Lb-3', 'Lm+Lb-5' and 'Lm+Lb-7' treatments. Orange pigmentation was observed in culture filtrates of 'Lb only', 'Lm&Lb', 'Lm+Lb-1', 'Lb+Lm-1', 'Lb+Lm-3', 'Lb+Lm-5' and 'Lb+Lm-7' treatments.

Table 3.3: Statistical testing outputs for significant probability of the main effects of experiment, treatment and the two-way interactions on dry mycelial weight (g) for different treatments in sequential co-inoculation experiments.

Two-way analysis of variance (ANOVA) tests were done by selecting experiment number and treatment as factors.

Factor	*df*	F statistic	LSD	F probability
Experiment	2	17.35	0.019	< 0.001
Treatment	10	4.89	0.037	< 0.001
Experiment x Treatment	44	1.60	0.064	= 0.095

Table 3.4: Average dry mycelial weight (g) from liquid cultures inoculated with *Leptosphaeria maculans* only (Lm only), *Leptosphaeria biglobosa* only (Lb only), *L. maculans* & *L. biglobosa* co-inoculated simultaneously (Lm&Lb), initial inoculation with *L. maculans* followed by co-inoculation with *L. biglobosa* sequentially at 1, 3, 5 and 7 days later (Lm+Lb-1, Lm+Lb-3, Lm+Lb-5, Lm+Lb-7) and initial inoculation with *L. biglobosa* followed by co-inoculation with *L. maculans* sequentially at 1, 3, 5 and 7 days later (Lb+Lm-1, Lb+Lm-3, Lb+Lm-5, Lb+Lm-7) at 14 days post inoculation (dpi) from all experiments.

Tukey's HSD tests were used to separate the mean dry mycelial weight values across different treatments. Columns that do not share a letter are considered significantly different ($P < 0.05$).

Treatment	Expt-1	Expt-2	Expt-3	Mean
Lm only	0.26 **ab**	0.39 **a**	0.32 **ab**	0.33 **b**
Lb only	0.22 **b**	0.25 **b**	0.28 **ab**	0.25 **a**
Lm&Lb	0.22 **b**	0.28 **ab**	0.27 **ab**	0.26 **a**
Lm+Lb-1	0.24 **b**	0.29 **ab**	0.21 **b**	0.25 **a**
Lm+Lb-3	0.21 **b**	0.20 **b**	0.22 **b**	0.21 **a**
Lm+Lb-5	0.25 **ab**	0.25 **b**	0.26 **ab**	0.25 **a**
Lm+Lb-7	0.25 **ab**	0.27 **ab**	0.28 **ab**	0.27 **a**
Lb+Lm-1	0.19 **b**	0.30 **ab**	0.25 **b**	0.25 **a**
Lb+Lm-3	0.20 **b**	0.27 **ab**	0.29 **ab**	0.25 **a**
Lb+Lm-5	0.20 **b**	0.27 **ab**	0.31 **ab**	0.26 **a**
Lb+Lm-7	0.20 **b**	0.26 **b**	0.27 **ab**	0.25 **a**
Expt mean	0.22 **b**	0.28 **a**	0.27 **a**	-

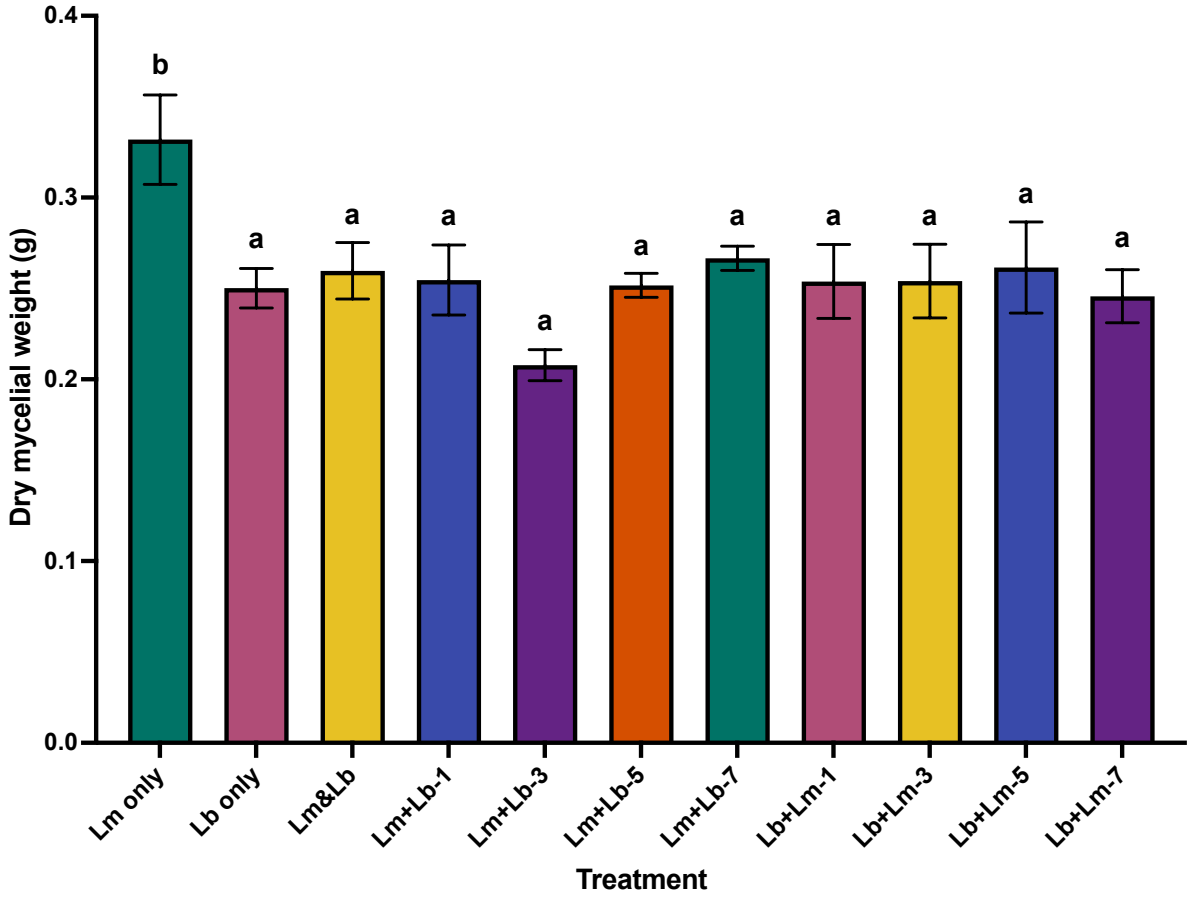

Figure 3.10: Average dry mycelial weight (g) of mycelia obtained from three experiments consisting of liquid cultures inoculated with *Leptosphaeria maculans* only (Lm only), *Leptosphaeria biglobosa* only (Lb only), *L. maculans* & *L. biglobosa* co-inoculated simultaneously (Lm&Lb), initial inoculation with *L. maculans* followed by co-inoculation with *L. biglobosa* sequentially at 1, 3, 5 and 7 days later (Lm+Lb-1, Lm+Lb-3, Lm+Lb-5, Lm+Lb-7) and initial inoculation with *L. biglobosa* followed by co-inoculation with *L. maculans* sequentially at 1, 3, 5 and 7 days later (Lb+Lm-1, Lb+Lm-3, Lb+Lm-5, Lb+Lm-7) at 14 days after the initial inoculation.

Tukey's HSD tests were used to separate the mean dry mycelial weight values across different treatments. Columns that do not share a letter are considered significantly different ($P < 0.05$). Error bars show standard error of the mean (SEM) (44 d.f.).

3.3.5 Effects of sequential co-inoculation on composition of secondary metabolites produced by *L. maculans*

There were no significant differences in the average concentration of the precursors of sirodesmin PL between the three experiments ($F(2,44) = 4.54$, $P = 0.016$) (Table 3.5, Table 3.6). Individual analyses of each of the three experiments can be found in Appendix C.

At 14 dpi, the average concentration of the precursors of sirodesmin PL was significantly different in different treatments ($F(10,44) = 1294.62$, $P < 0.001$). For the treatments 'Lb only', 'Lm&Lb', 'Lm+Lb-1', 'Lb+Lm-1', 'Lb+Lm-3', 'Lb+Lm-5', 'Lb+Lm-7', there were no significant differences between them, since no production of the precursors of sirodesmin PL was detected in those treatments. For the treatments 'Lm only' (381.4 mg/L), 'Lm+Lb-5' (358.2 mg/L), and 'Lm+Lb-7' (386.7 mg/L), there were no significant differences between them. Interestingly, 'Lm+Lb-3' (185.4 mg/L) treatment was significantly different from all other treatments (Table 3.5, Table 3.6) (Figure 3.11). The interactions between experiments and treatments were not significant ($F(20,44) = 0.88$, $P = 0.607$) (Table 3.5).

Likewise, there were no significant differences in the average concentration of sirodesmin PL between the three experiments ($F(2,44) = 1.13$, $P = 0.334$) (Table 3.7, Table 3.8). Individual analyses of each of the three experiments can be found in Appendix C.

At 14 dpi, the average concentration of sirodesmin PL was significantly different in different treatments ($F(10,44) = 1129.98$, $P < 0.001$). For the treatments 'Lb only', 'Lm&Lb', 'Lm+Lb-1', 'Lb+Lm-1', 'Lb+Lm-3', 'Lb+Lm-5' and 'Lb+Lm-7', there were no significant differences between them, since no production of sirodesmin PL was detected in those treatments. For the treatments 'Lm only' (892.9 mg/L), 'Lm+Lb-5' (832.2 mg/L) and 'Lm+Lb-7' (971.4 mg/L), there were no significant differences between them. As with the precursors, 'Lm+Lb-3' (334.5 mg/L) treatment was significantly different from all other treatments (Table 3.7, Table 3.8) (Figure 3.12). The interactions between experiments and treatments were not significant ($F(20,44) = 0.46$, $P = 0.969$) (Table 3.7).

Table 3.5: Statistical testing outputs for significant probability of the main effects of experiment, treatment and the two-way interactions on concentration of the precursors of sirodesmin PL (mg/L) for different treatments in sequential co-inoculation experiments.

Data were transformed using a common logarithm and two-way analysis of variance (ANOVA) tests were done by selecting experiment number and treatment as factors.

Factor	*df*	F statistic	LSD	F probability
Experiment	2	4.54	0.051	= 0.016
Treatment	10	1294.62	0.991	< 0.001
Experiment x Treatment	44	0.88	0.169	= 0.607

Table 3.6: Average concentration of the precursors of sirodesmin PL (mg/L) from liquid cultures inoculated with *Leptosphaeria maculans* only (Lm only), *Leptosphaeria biglobosa* only (Lb only), *L. maculans* & *L. biglobosa* co-inoculated simultaneously (Lm&Lb), initial inoculation with *L. maculans* followed by co-inoculation with *L. biglobosa* sequentially at 1, 3, 5 and 7 days later (Lm+Lb-1, Lm+Lb-3, Lm+Lb-5, Lm+Lb-7) and initial inoculation with *L. biglobosa* followed by co-inoculation with *L. maculans* sequentially at 1, 3, 5 and 7 days later (Lb+Lm-1, Lb+Lm-3, Lb+Lm-5, Lb+Lm-7) at 14 days post inoculation (dpi) from all experiments.

Tukey's HSD tests were used to separate the mean concentrations of the precursors of sirodesmin PL across different treatments. Columns that do not share a letter are considered significantly different ($P < 0.05$).

Treatment	Expt-1	Expt-2	Expt-3	Mean
Lm only	280.9 **ad**	426.5 **a**	414.2 **ab**	381.4 **c**
Lb only	0.0 **e**	0.0 **e**	0.0 **e**	0.0 **a**
Lm&Lb	0.0 **e**	0.0 **e**	0.0 **e**	0.0 **a**
Lm+Lb-1	0.0 **e**	0.0 **e**	0.0 **e**	0.0 **a**
Lm+Lb-3	120.9 **d**	241.5 **bd**	165.7 **cd**	185.4 **b**
Lm+Lb-5	278.9 **ad**	423.9 **a**	338.8 **abc**	358.2 **c**
Lm+Lb-7	255.3 **ad**	491.0 **a**	361.6 **abc**	368.7 **c**
Lb+Lm-1	0.0 **e**	0.0 **e**	0.0 **e**	0.0 **a**
Lb+Lm-3	0.0 **e**	0.0 **e**	0.0 **e**	0.0 **a**
Lb+Lm-5	0.0 **e**	0.0 **e**	0.0 **e**	0.0 **a**
Lb+Lm-7	0.0 **e**	0.0 **e**	0.0 **e**	0.0 **a**
Expt mean	85.1 **b**	143.9 **a**	116.4 **ab**	-

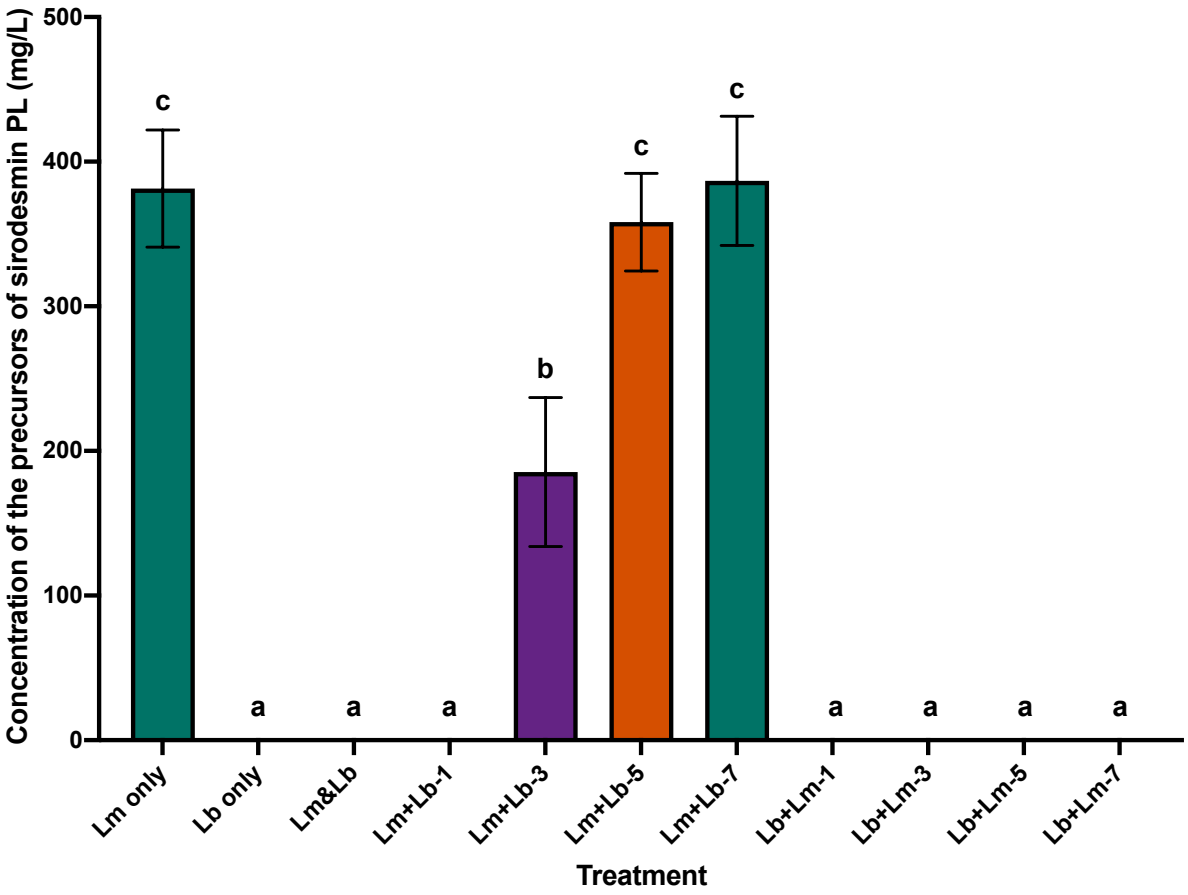

Figure 3.11: Average concentration of the precursors of sirodesmin PL (mg/L) in secondary metabolite extracts obtained from three experiments consisting of liquid cultures inoculated with *Leptosphaeria maculans* only (Lm only), *Leptosphaeria biglobosa* only (Lb only), *L. maculans* & *L. biglobosa* co-inoculated simultaneously (Lm&Lb), initial inoculation with *L. maculans* followed by co-inoculation with *L. biglobosa* sequentially at 1, 3, 5 and 7 days later (Lm+Lb-1, Lm+Lb-3, Lm+Lb-5, Lm+Lb-7) and initial inoculation with *L. biglobosa* followed by co-inoculation with *L. maculans* sequentially at 1, 3, 5 and 7 days later (Lb+Lm-1, Lb+Lm-3, Lb+Lm-5, Lb+Lm-7) at 14 days after the initial inoculation.

Tukey's HSD tests were used to separate the mean concentration of the precursors of sirodesmin PL across different treatments. Columns that do not share a letter are considered significantly different ($P < 0.05$). Error bars show standard error of the mean (SEM) (44 d.f.).

Table 3.7: Statistical testing outputs for significant probability of the main effects of experiment, treatment and the two-way interactions on concentration of sirodesmin PL (mg/L) for different treatments in sequential co-inoculation experiments.

Data were transformed using a common logarithm and two-way analysis of variance (ANOVA) tests were done by selecting experiment number and treatment as factors.

Factor	*df*	F statistic	LSD	F probability
Experiment	2	1.13	0.062	= 0.334
Treatment	10	1129.98	0.121	< 0.001
Experiment x Treatment	44	0.46	0.207	= 0.969

Table 3.8: Average concentration of sirodesmin PL (mg/L) from liquid cultures inoculated with *Leptosphaeria maculans* only (Lm only), *Leptosphaeria biglobosa* only (Lb only), *L. maculans* & *L. biglobosa* co-inoculated simultaneously (Lm&Lb), initial inoculation with *L. maculans* followed by co-inoculation with *L. biglobosa* sequentially at 1, 3, 5 and 7 days later (Lm+Lb-1, Lm+Lb-3, Lm+Lb-5, Lm+Lb-7) and initial inoculation with *L. biglobosa* followed by co-inoculation with *L. maculans* sequentially at 1, 3, 5 and 7 days later (Lb+Lm-1, Lb+Lm-3, Lb+Lm-5, Lb+Lm-7) at 14 days post inoculation (dpi) from all experiments.

Tukey's HSD tests were used to separate the mean concentration of sirodesmin PL across different treatments. Columns that do not share a letter are considered significantly different ($P < 0.05$).

Treatment	Expt-1	Expt-2	Expt-3	Mean
Lm only	839.2 **ab**	889.0 **ab**	952.2 **ab**	892.9 **c**
Lb only	0.0 **e**	0.0 **e**	0.0 **e**	0.0 **a**
Lm&Lb	0.0 **e**	0.0 **e**	0.0 **e**	0.0 **a**
Lm+Lb-1	0.0 **e**	0.0 **e**	0.0 **e**	0.0 **a**
Lm+Lb-3	175.6 **d**	416.1 **cd**	371.3 **bd**	334.5 **b**
Lm+Lb-5	779.0 **abc**	912.5 **ab**	765.0 **abc**	832.2 **c**
Lm+Lb-7	838.2 **abc**	1020.0 **ab**	1031.3 **ab**	971.4 **c**
Lb+Lm-1	0.0 **e**	0.0 **e**	0.0 **e**	0.0 **a**
Lb+Lm-3	0.0 **e**	0.0 **e**	0.0 **e**	0.0 **a**
Lb+Lm-5	0.0 **e**	0.0 **e**	0.0 **e**	0.0 **a**
Lb+Lm-7	0.0 **e**	0.0 **e**	0.0 **e**	0.0 **a**
Expt mean	239.3 **a**	294.3 **a**	283.6 **a**	-

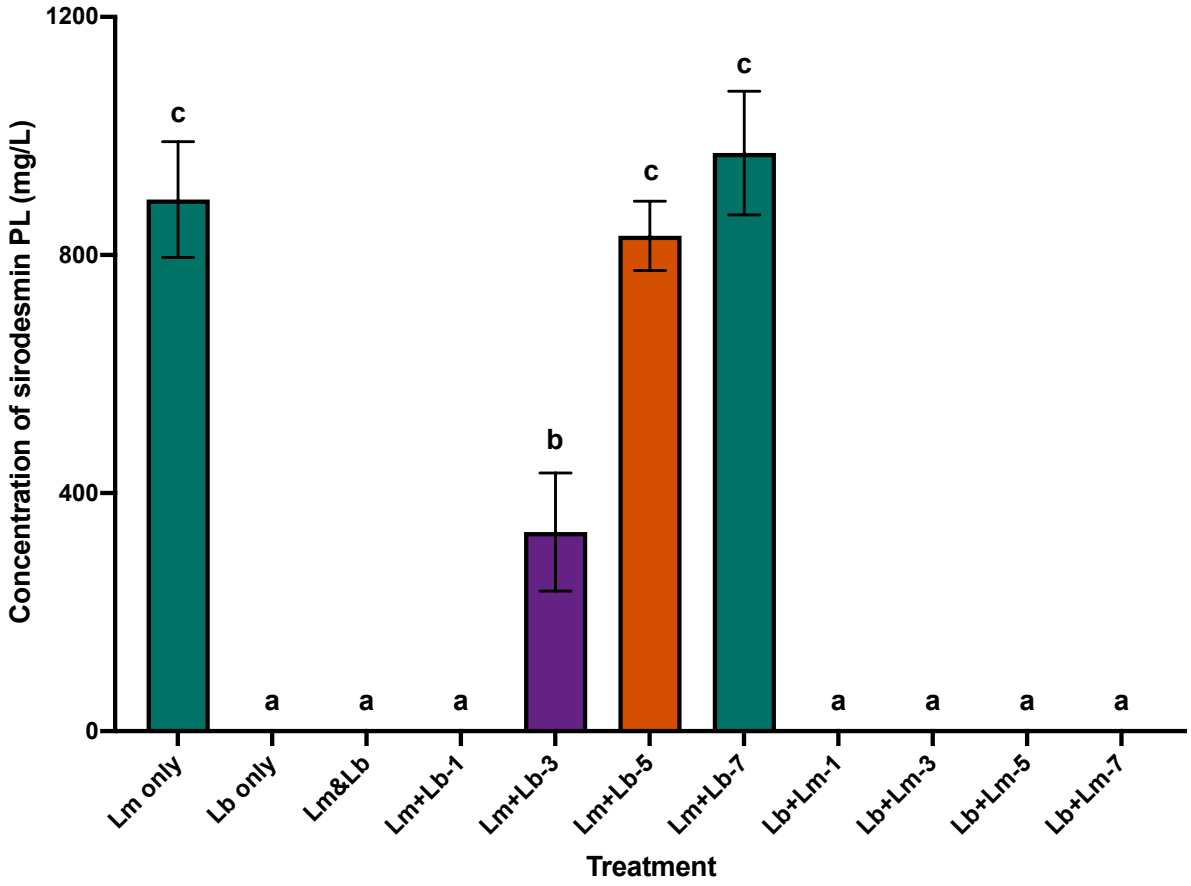

Figure 3.12: Average concentration of sirodesmin PL (mg/L) in secondary metabolite extracts obtained from three experiments consisting of liquid cultures inoculated with *Leptosphaeria maculans* only (Lm only), *Leptosphaeria biglobosa* only (Lb only), *L. maculans* & *L. biglobosa* co-inoculated simultaneously (Lm&Lb), initial inoculation with *L. maculans* followed by co-inoculation with *L. biglobosa* sequentially at 1, 3, 5 and 7 days later (Lm+Lb-1, Lm+Lb-3, Lm+Lb-5, Lm+Lb-7) and initial inoculation with *L. biglobosa* followed by co-inoculation with *L. maculans* sequentially at 1, 3, 5 and 7 days later (Lb+Lm-1, Lb+Lm-3, Lb+Lm-5, Lb+Lm-7) at 14 days after the initial inoculation.

Tukey's HSD tests were used to separate the mean concentration of sirodesmin PL across different treatments. Columns that do not share a letter are considered significantly different ($P < 0.05$). Error bars show standard error of the mean (SEM) (44 d.f.).

3.3.6 Effects of sequential co-inoculation on growth of the pathogens

There were no significant differences in the average percentage of *L. maculans* DNA in total extracted DNA between the three experiments ($F(2,44) = 1.43$, $P = 0.273$) (Table 3.9, Table 3.10). Individual analyses of each of the three experiments can be found in Appendix C.

At 14 dpi, the average percentage of *L. maculans* DNA in total extracted DNA was significantly different in different treatments ($F(10,44) = 545.86$, $P < 0.001$). For the treatments 'Lb only' (0.0 %), 'Lm&Lb' (3.1 %), 'Lm+Lb-1' (6.6 %), 'Lb+Lm-1' (1.1 %), 'Lb+Lm-3' (1.4 %), 'Lb+Lm-5' (1.3 %) and 'Lb+Lm-7' (1.4 %), there were no significant differences between them. For the treatments 'Lm only' (100.0 %), 'Lm+Lb-5' (97.4 %) and 'Lm+Lb-7' (97.4 %), there were no significant differences between them. In addition, 'Lm+Lb-3' (72.2 %) treatment was significantly different to all other treatments (Table 3.9, Table 3.10) (Figure 3.13). The interactions between experiments and treatments were not significant ($F(20,44) = 0.94$, $P = 0.546$) (Table 3.9).

3.4 Discussion

The results of these *in vitro* studies provide the first evidence that the timing of co-inoculation (i.e. the timing when *L. maculans* and *L. biglobosa* meet) strongly affects the interspecific interactions between them in terms of sirodesmin PL production and relative pathogen growth.

Under sequential co-inoculation *in vitro*, for the treatments where *L. biglobosa* was inoculated first, followed by *L. maculans* at 1, 3, 5 and 7 days later, the production of sirodesmin PL and its precursors by *L. maculans* was inhibited; however, when *L. maculans* was inoculated first, followed by *L. biglobosa* at 3, 5, or 7 days later, the production of sirodesmin PL and its precursors by *L. maculans* was not inhibited. These findings indicate that if there is to be any production of sirodesmin PL *in vitro*, *L. maculans* must be inoculated at least 3 days before *L. biglobosa*. Strikingly, *L. biglobosa* was still able to inhibit the production of sirodesmin PL and its precursors and retain its competitive advantage even when it was sequentially co-inoculated 1 day after *L. maculans*.

Table 3.9: Statistical testing outputs for significant probability of the main effects of experiment, treatment and the two-way interactions on percentage *Leptosphaeria maculans* DNA (%) for different treatments in sequential co-inoculation experiments.
Two-way analysis of variance (ANOVA) tests were done by selecting experiment number and treatment as factors.

Factor	*df*	F statistic	LSD	F probability
Experiment	2	1.34	2.878	= 0.273
Treatment	10	545.86	5.589	< 0.001
Experiment x Treatment	44	0.94	9.545	= 0.546

Table 3.10: Average percentage *Leptosphaeria maculans* DNA (%) from liquid cultures inoculated with *Leptosphaeria maculans* only (Lm only), *Leptosphaeria biglobosa* only (Lb only), *L. maculans* & *L. biglobosa* co-inoculated simultaneously (Lm&Lb), initial inoculation with *L. maculans* followed by co-inoculation with *L. biglobosa* sequentially at 1, 3, 5 and 7 days later (Lm+Lb-1, Lm+Lb-3, Lm+Lb-5, Lm+Lb-7) and initial inoculation with *L. biglobosa* followed by co-inoculation with *L. maculans* sequentially at 1, 3, 5 and 7 days later (Lb+Lm-1, Lb+Lm-3, Lb+Lm-5, Lb+Lm-7) at 14 days post inoculation (dpi) from all experiments.

Tukey's HSD tests were used to separate the mean percentage of *L. maculans* DNA in total extracted DNA different treatments. Columns that do not share a letter are considered significantly different ($P < 0.05$).

Treatment	Expt-1	Expt-2	Expt-3	Mean
Lm only	100.0 **a**	100.0 **a**	100.0 **a**	100.0 **c**
Lb only	0.0 **e**	0.0 **e**	0.0 **e**	0.0 **a**
Lm&Lb	5.0 **e**	2.8 **e**	1.7 **e**	3.1 **a**
Lm+Lb-1	4.3 **e**	9.0 **e**	5.1 **e**	6.6 **a**
Lm+Lb-3	60.2 **d**	80.9 **bc**	71.1 **cd**	72.2 **b**
Lm+Lb-5	99.3 **ab**	96.5 **ab**	98.8 **ab**	97.4 **c**
Lm+Lb-7	97.3 **ab**	97.4 **ab**	97.7 **ab**	97.4 **c**
Lb+Lm-1	0.6 **e**	1.7 **e**	0.7 **e**	1.1 **a**
Lb+Lm-3	1.4 **e**	1.5 **e**	1.4 **e**	1.4 **a**
Lb+Lm-5	0.7 **e**	1.8 **e**	1.2 **e**	1.3 **a**
Lb+Lm-7	0.4 **e**	2.2 **e**	1.2 **e**	1.4 **a**
Expt mean	33.6 **a**	35.8 **a**	34.3 **a**	-

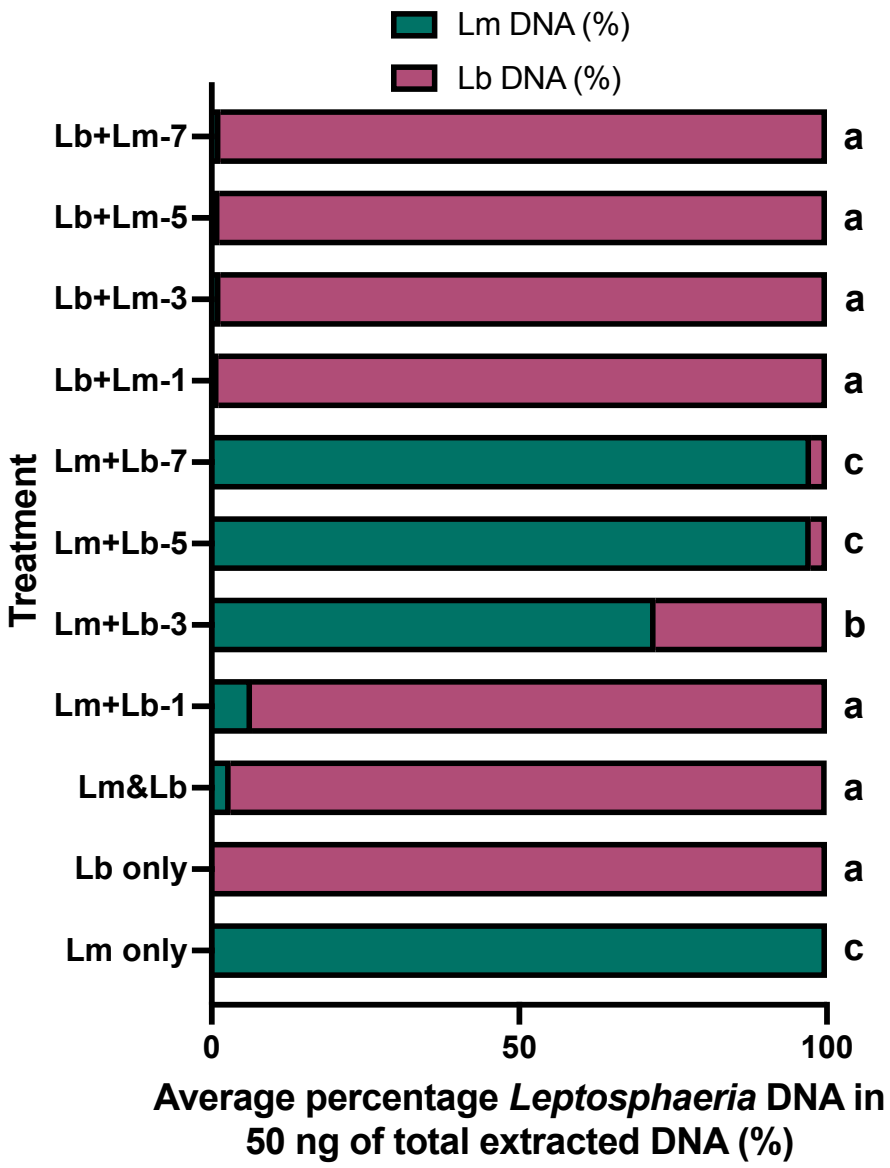

Figure 3.13: Average percentage of *Leptosphaeria* species DNA (%) in homogenised mycelia obtained from three experiments consisting of liquid cultures inoculated with *Leptosphaeria maculans* only (Lm only), *Leptosphaeria biglobosa* only (Lb only), *L. maculans* & *L. biglobosa* co-inoculated simultaneously (Lm&Lb), initial inoculation with *L. maculans* followed by co-inoculation with *L. biglobosa* sequentially at 1, 3, 5 and 7 days later (Lm+Lb-1, Lm+Lb-3, Lm+Lb-5, Lm+Lb-7) and initial inoculation with *L. biglobosa* followed by co-inoculation with *L. maculans* sequentially at 1, 3, 5 and 7 days later (Lb+Lm-1, Lb+Lm-3, Lb+Lm-5, Lb+Lm-7) at 14 days after the initial inoculation.

Tukey's HSD tests were used to separate the mean percentage of *L. maculans* DNA in total extracted DNA across different treatments. Columns that do not share a letter are considered significantly different ($P < 0.05$) (44 d.f.).

Interestingly, *L. biglobosa* started to lose its antagonistic effects on the production of sirodesmin PL when it was sequentially co-inoculated 3 days after *L. maculans*, as there was already some sirodesmin PL being produced, along with its precursors, even though it was significantly less compared to 'Lm only' control. Additionally, *L. biglobosa* completely lost its ability to inhibit the production of sirodesmin PL, when it was inoculated 5 or 7 days after *L. maculans*. These results show that *L. biglobosa* is affected even by the early stages of sirodesmin PL production by *L. maculans* (3 days) but can still have a partial antagonistic effect. These findings are supported by previous work, where it was shown that *L. maculans* takes approximately 3 days to produce sirodesmin PL *in vitro* (Gardiner et al., 2004; Elliott et al., 2007).

Furthermore, as production of sirodesmin PL progresses (5-7 days), *L. biglobosa* loses its antagonistic effects. This is also consistent with previous work, where it was shown that *L. biglobosa* could not inhibit the production of sirodesmin PL when it was sequentially co-inoculated 7 days after *L. maculans* (Fortune et al., 2024). This was mainly due to the presence of sirodesmin PL already produced by *L. maculans* by 5-7 dpi in culture inhibiting the growth of *L. biglobosa* and 'shifting' the competitive advantage in favour of *L. maculans*. Thus, it is suggested that *L. maculans* used an interference interspecific competition strategy against *L. biglobosa*, further supporting the proposed function of sirodesmin PL in previous research (Rouxel et al., 1988; Gardiner et al., 2004; Elliott et al., 2007; Fortune et al., 2024).

The findings regarding inhibition of sirodesmin PL were further contextualised through the analyses of relative pathogen DNA in homogenised mycelia from the co-cultures. For the first time, it was shown that *L. biglobosa* was not only able to inhibit the production of sirodesmin PL by *L. maculans* but also it was able to inhibit the growth of *L. maculans* entirely. Relative percentage of *L. maculans* DNA was consistently less than 3.0 % in all of the co-cultures inoculated with *L. biglobosa* before or at the same time as *L. maculans*. Although 'Lm+Lb-1' treatment had a greater percentage of *L. maculans* DNA, this difference was not significant from 'Lb only' or 'Lm&Lb'. These findings are further supported by the observations of morphology of mycelia and pigmentation production in the co-cultures. It was previously reported that *L. maculans* mycelia grew more intactly compared to *L. biglobosa* in liquid culture (Zhang et al., 2014) and *L. biglobosa* produced orange pigmentation whereas *L. maculans* did not (Williams & Fitt, 1999). Both

morphology of mycelia and pigmentation in culture filtrates suggest that *L. biglobosa* was predominant in the co-cultures where *L. biglobosa* was inoculated before or at the same time as *L. maculans*. Since these visual observations are consistent with the quantification of phytotoxin and relative pathogen DNA, it is suggested that future *in vitro* co-inoculation studies may use presence or absence of this orange pigment produced by *L. biglobosa* as a qualitative measure of assessing interspecific interactions between *L. maculans* and *L. biglobosa*. Furthermore, the production of this pigment may also be quantified by measuring the optical density of the liquid culture using a spectrophotometer, in a similar fashion to assessing growth in liquid bacterial cultures.

Although different speculations can be made about how these interactions occur, the exact mechanisms of the antagonistic effects of *L. biglobosa* on *L. maculans* are uncertain. The main speculations to explain these interactions are the differences between *L. maculans* and *L. biglobosa* in terms of metabolic capacity. *L. biglobosa* was recently shown to be more efficient in nutrient acquisition and utilisation of natural resources compared to *L. maculans* (Frąc et al., 2022). This is also consistent with past reports describing tissue colonisation by *L. biglobosa* occurring more rapidly compared to *L. maculans* (Huang et al., 2003; Eckert et al., 2005). The findings from the simultaneous co-inoculation experiments of this study also further support this idea, since the mycelial growth rate coefficient of *L. biglobosa* was more than three times greater than that of *L. maculans*. Furthermore, mycelial weight of 'Lb only' treatment reached its maximum by 7 dpi and did not increase any further. This can be due to *L. biglobosa* efficiently acquiring and utilising all of the nutrients in the limited liquid medium and therefore exhausting nutrients for further growth and development by 7 dpi. Moreover, 'Lb only' and 'Lm&Lb' had similar rates of mycelial growth *in vitro*, suggesting that *L. biglobosa* inhibited the growth of *L. maculans* by acquiring all of the vital nutrients required for growth and development. Thus, it is suggested that *L. biglobosa* used a resource-mediated (or exploitative) interspecific competition strategy against *L. maculans*. The differences in metabolic capacity between these pathogens may be due to differences in their nutritional strategies.

Although both *Leptosphaeria* species were characterised to have hemi-biotrophic lifestyles, differences between these two pathogens in terms of nutritional strategies have been reported, with some classifying *L. biglobosa* closer to nectrotrophy (Lowe et

al., 2014; Padmathilake & Fernando, 2022b). Additionally, a recent investigation into differences in metabolic capacity between *Leptosphaeria* species described *L. biglobosa* to be less specialised, and *L. maculans* co-evolving more strictly with the plant host (Frąc et al., 2022). Therefore, one of the speculations to explain the mechanisms of these interactions is that *L. biglobosa* utilised the resources in the limited liquid medium more efficiently and potentially caused competitive exclusion of *L. maculans* by employing a resource-mediated (or exploitative) interspecific competition strategy (Dutt et al., 2021b). In return, *L. maculans* inhibited the growth of *L. biglobosa* dependent upon successful production of sirodesmin PL by employing an interference interspecific competition strategy (Dutt et al., 2021b; Rouxel et al., 1988; Gardiner et al., 2004; Elliott et al., 2007; Fortune et al., 2024). Results of these *in vitro* studies supported this speculation and highlighted the significant influence of co-inoculation timing on the interspecific interactions between *L. maculans* and *L. biglobosa*.

An additional speculation to explain the mechanisms of these interactions is that *L. biglobosa* interferes with the gene expression related to production of sirodesmin PL by *L. maculans*. It was reported that 20 co-regulated genes are present in the sirodesmin PL biosynthetic gene cluster (BGC) in *L. maculans* (Gardiner et al., 2004; Urquhart et al., 2021). The results of this study showed that *L. biglobosa* inhibits the production of the precursors of sirodesmin PL; this suggests that if *L. biglobosa* were to interfere with the expression of genes involved in the production of sirodesmin PL, it would be interfering with the expression of genes that are active in early stages of sirodesmin PL biosynthesis. It is known that biosynthesis of sirodesmin PL starts with two amino acids, tyrosine and serine (Gardiner et al., 2004; Gardiner et al., 2005). The first step is the *O*-prenylation of L-tyrosine residue by dimethylallyl pyrophosphate, a reaction catalysed by a 4-*O*-dimethylallyl-L-tyrosine synthase, encoded by *sirD* (Kremer & Li, 2010). The second step is the condensation of dimethylallyl-L-tyrosine and serine, catalysed by a two-module non-ribosomal peptide synthetase known to be indispensable for sirodesmin PL biosynthesis, encoded by *sirP* (Gardiner et al., 2004; Elliott et al., 2007; Urquhart et al., 2021). Furthermore, this biosynthetic cluster is regulated by a cross-control pathway gene encoding for a Zn(II)2Cys6 transcription factor through *sirZ* (Gardiner et al., 2004; Elliott et al., 2007; Elliott et al., 2011; Fox et al., 2008). It can be suggested that if *L. biglobosa* interferes with the expression of one or more of these genes through an

interference interspecific competition strategy, it would inhibit the production of sirodesmin PL by *L. maculans* at the precursors stage.

On the contrary to this speculation, further interpretation of the findings in this chapter in conjunction with previous literature suggests that it is unlikely that *L. biglobosa* directly interferes with the expression of genes involved in the production of sirodesmin PL by *L. maculans*. To support this contradiction, this study showed that *L. biglobosa* inhibited the growth of *L. maculans* entirely. This is unlikely to be solely due to inhibition of sirodesmin PL; since it was shown that a mutant isolate of *L. maculans* that does not produce sirodesmin PL was still able to grow *in vitro* and cause disease symptoms *in planta* (Elliott et al., 2007); which shows that the growth of *L. maculans* is not reliant on its ability to produce sirodesmin PL. Additionally, from a technical point of view, if this speculation was to be further studied, it would have been nearly impossible to quantify the transcripts of genes involved in the production of this phytotoxin in an *in vitro* co-culture setting, since the growth of *L. maculans* is inhibited. Furthermore, *L. biglobosa* was shown to metabolise amino acids (especially L-serine in this context) more efficiently than *L. maculans* (Frąc et al., 2022); suggesting that *L. biglobosa* would utilise the building blocks of sirodesmin PL (tyrosine and serine) in the limited liquid medium before *L. maculans* gets to start the biosynthesis of sirodesmin PL. Therefore, this study concludes that *L. biglobosa* used a resource-mediated (or exploitative) interspecific competition strategy against *L. maculans in vitro*, rather than an interference interspecific competition strategy by secretion of peptides to directly interfere with the production of sirodesmin PL. Instead, it is believed that the antagonistic effects of *L. biglobosa* on sirodesmin PL production by *L. maculans* are observed as side-effects resulting from the actual interspecific competition strategy used by *L. biglobosa*; emphasising the emerging importance of this organism as a phoma stem canker pathogen.

Similar interspecific interactions between co-existing plant pathogens in other pathosystems have been reported as well. *Fusarium graminearum* and *Fusarium subglutinans* are fungal species, both infecting and causing ear and kernel rot in maize globally (di Menna et al., 1997; Görtz et al., 2008; Zhou et al., 2018). *F. graminearum* produces a mycotoxin called trichothecene, which is toxic to both plants and humans (Ueno, 1980; Lauren & di Menna, 1999; Brown et al. 2001). It was reported that early

inoculation with *F. subglutinans* significantly reduced the production of trichothecene by the more aggressive pathogen *F. graminearum* (Cooney et al. 2001). Although this aforementioned study did not investigate whether *F. subglutinans* inhibits the growth of *F. graminearum*; their findings in terms of toxin production inhibition are similar to the interactions observed between *L. maculans* and *L. biglobosa* in this chapter.

Another example is the interactions observed between *Sclerotinia sclerotiorum*, *Alternaria alternata* and *Trichoderma viridae*, all isolated from the phylloplane of lettuce plants. It was reported that *A. alternata* and *T. viridae* were able to reduce germ-tube elongation of *S. sclerotiorum* (Mercier & Reelder., 1987). The authors concluded that this was due to different mechanisms rather than direct parasitism of *A. alternata* and *T. viridae* on *S. sclerotiorum*. They further added that *T. viridae* was shown to produce antifungal compounds, which may have been present in their work (Mercier & Reelder., 1987; Dennis & Webster., 1971; Brian & Hemming., 1945). This is similar to *L. maculans* inhibiting the growth of *L. biglobosa* through successful production of sirodesmin PL.

The strengths of this *in vitro* study compared to previous *in vitro* studies on comparison of *L. maculans* and *L. biglobosa* growth are that in this study, liquid media were used, and experiments were done in shaking incubators to ensure equal distribution of nutrients within the liquid media. Previous studies have done this comparison by measuring radial growth of mycelia on agar plates (Shah et al., 2020; Fortune et al., 2024). Moreover, this *in vitro* study investigated several aspects of interspecific interactions in conjunction; which has led to identification of strong correlative relationships between toxin production, pathogen growth and even phenotypic observations of the pathogens in liquid co-cultures. This has allowed stronger arguments to be made regarding the interspecific competition strategies used by *L. maculans* and *L. biglobosa*. Finally, in this study, the number of time gaps in-between sequential co-inoculations tested was increased, leading to identification of the key time points affecting the outcome of the interspecific interactions between *L. maculans* and *L. biglobosa in vitro*.

The limitation of this study is that only one isolate of each pathogen was used due to time constraints and availability of equipment. There are six subclades of *L. biglobosa* (Dilmaghani et al., 2009; Zou et al., 2014). Future studies are required to investigate whether other subclades of *L. biglobosa* have similar antagonistic effects on *L. maculans*.

The *in vitro* studies presented in this chapter hold great importance in increasing our understanding of the interactions between *L. maculans* and *L. biglobosa*. Nevertheless, it is important to note that these interactions may occur differently when these pathogens are under interspecific competition on their host rather than on artificial media. Therefore, using the findings from this chapter as a foundation, future studies are required to further investigate the interspecific interactions between *L. maculans* and *L. biglobosa in planta* (Chapter 4).

The results of this work have potential practical importance for disease management. It is known that phoma leaf spot and subsequent stem canker epidemics are initiated by ascospores (Toscano-Underwood et al., 2003; Huang et al., 2005). In addition, it has been reported that ascospores of both *Leptosphaeria* species are being released at similar times in the UK (Javaid et al., 2021; Huang et al., 2024). Therefore, the findings of this study suggest that the changes in timing of ascospore release of *Leptosphaeria* species in natural conditions may increase the incidence of simultaneous and/or sequential co-inoculations (similar to this study); which may lead to changes in phoma stem canker management strategies in the UK.

4 Chapter 4 – Interspecific interactions between *Leptosphaeria maculans* and *Leptosphaeria biglobosa in planta*

Acknowledgements – HPLC method used in this chapter was developed by James Stanley and Christine Gigou. LC-MS analyses were done by Dr Daniel Baker. The *in planta* simultaneous co-inoculation work was done in collaboration with Dr James Fortune.

Publications – Part of the work presented in this chapter has been published: Fortune JA, **Bingol E**, Qi A, Baker D, Ritchie F, Karandeni-Dewage C, Fitt BDL, Huang YJ (2024). *Leptosphaeria biglobosa* inhibits the production of sirodesmin PL by *L. maculans*. *Pest Management Science 80:* 2416-2425. http://doi.org/10.1002/ps.7275. A copy of this publication can be found in Appendix O.

A second manuscript containing the rest of the work presented in this chapter is being prepared for submission to *Pest Management Science* for publication: **Bingol E,** Karandeni-Dewage C, Qi A, Ritchie F, Fitt BDL, Huang YJ (2026). Temporal dynamics of co-inoculation of *Leptosphaeria maculans* and *Leptosphaeria biglobosa* determine interspecific competition and disease development on oilseed rape.

4.1 Introduction

Oilseed rape (*Brassica napus*) is currently the second most important source of vegetable oil globally, making it an essential crop for international food security. Furthermore, oilseed rape is the third most important arable crop in the UK, after wheat and barley (Huang et al., 2021). Phoma stem canker (blackleg) is of worldwide importance, currently being one of the most damaging diseases of oilseed rape globally, with yield losses over £1 billion in a cropping season (Barnes et al., 2010; Zhang et al., 2014). Considering just the UK, phoma stem canker can result in annual yield losses more than £80 M, in addition to the disease control efforts by fungicide applications costing c. £20 M per annum (Fitt et al., 2008; Stonard et al., 2010; CropMonitor, 2020; Huang et al., 2024). The causal pathogens *Leptosphaeria maculans* and *L. biglobosa* are closely related co-existing fungal pathogens and are found to co-infect oilseed rape in the UK (Shoemaker & Brun, 2001; Fitt et al., 2006a; Fitt et al., 2006b) (Figure 4.1).

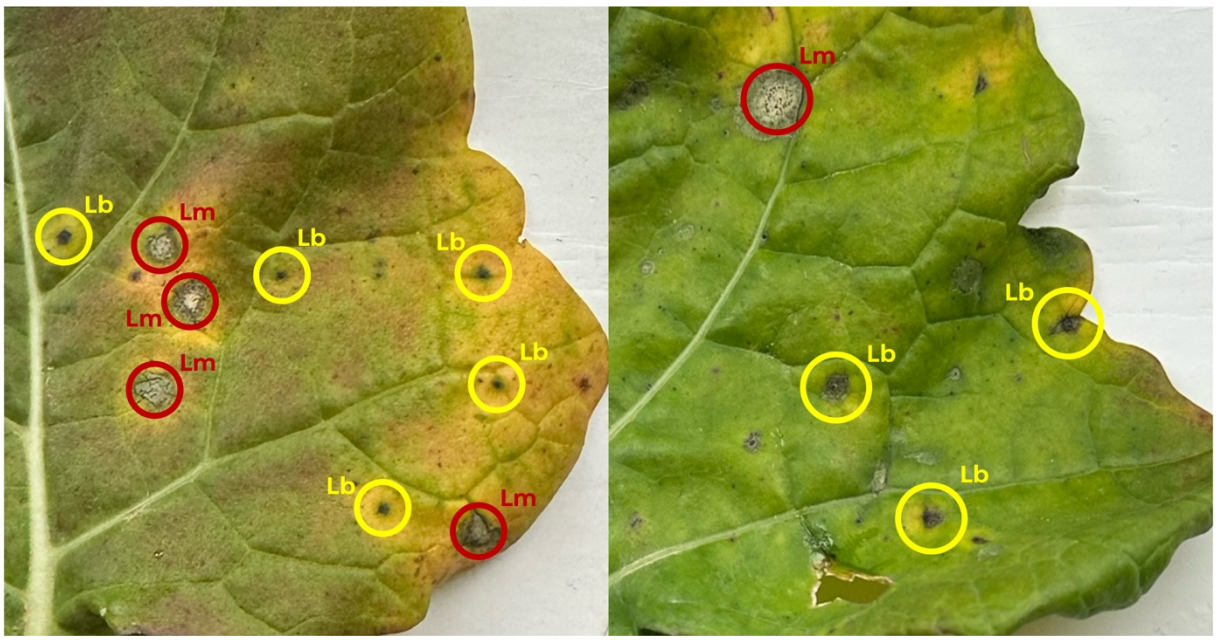

Figure 4.1: Phoma leaf spots caused by *Leptosphaeria maculans* (Lm) (circled in red) and *Leptosphaeria biglobosa* (Lb) (circled in yellow) on leaves of oilseed rape cultivar Campus grown near Norwich.

Photos were taken in November 2023.

It is thought that co-existence of *L. maculans* and *L. biglobosa* is facilitated by the differences between them in optimal temperatures for pseudothecial maturation. Pseudothecia of *L. maculans* can mature at colder temperatures compared to those of *L. biglobosa*, leading to ascospore release earlier in the cropping season (West et al., 2002a; Toscano-Underwood et al., 2003). However, recent studies report that ascospores of both *L. maculans* and *L. biglobosa* are sometimes being released at similar times in the UK (Javaid et al., 2021; Huang et al., 2024), because increasing temperatures are decreasing the time interval between the two species in pseudothecial maturation.

Furthermore, there are no differences in timing of pseudothecial maturation between these *Leptosphaeria* species at higher temperatures (Toscano-Underwood et al., 2003). In addition, detection of *L. biglobosa* also in stem basal cankers has become common (Huang et al., 2014b; Huang et al., 2024). The release of ascospores of both pathogens at similar times is resulting in simultaneous and/or sequential co-inoculations in natural conditions, which may lead to interspecific competition arising between these *Leptosphaeria* species.

During interspecific competition, pathogens can deploy three different interspecific competition strategies. The resource-mediated (or exploitative) competition strategy occurs when a species utilises a limited resource more efficiently than other species, potentially leading to competitive exclusion of other species (Gause, 1934; Tan et al., 2016; Dutt et al., 2021a). Host-mediated (or apparent) competition strategy is when the development of one species activates the plant defence system through induction of systemic acquired resistance and therefore reduces the chance of other species successfully infecting the host (Aimé et al., 2013; Dutt et al., 2021b). Interference competition strategy occurs when one of the species produces toxins to interfere with another competitor's access to a limited resource (Dutt et al., 2021b).

Although there have not been many studies directly investigating the interspecific competition strategies between *L. maculans* and *L. biglobosa*, previous *in planta* work focussing on induction of plant immune defences by either pathogen has also resulted in observations relevant to this study. First, it was reported that pre-inoculation of oilseed rape leaves with *L. biglobosa* activates the plant immune system through induction of systemic acquired resistance (SAR), which subsequently reduces the likelihood of *L.*

maculans successfully infecting oilseed rape (Mahuku et al., 1996). This could be an example of *L. biglobosa* deploying a host-mediated interspecific competition strategy against *L. maculans*. Interestingly, *L. biglobosa* maintained its effect to reduce lesion severity of *L. maculans* even when it was co-inoculated 48 h after *L. maculans* but completely lost this effect if it was co-inoculated 64 h after *L. maculans* (Mahuku et al., 1996). Moreover, pre-treatment with chemical defence activators and *L. biglobosa* ascospores were compared in inducing resistance to *L. maculans*. It was suggested that much like the chemical defence activators, pre-treatment with *L. biglobosa* ascospores could induce both local and systemic resistance against *L. maculans*, reducing the severity of phoma leaf spots and subsequent stem cankers (Liu et al., 2006).

Further studies have investigated the expression of genes related to plant immune signalling pathways (Liu et al., 2007; Padmathilake & Fernando, 2022b), which are activated by phytohormones, namely salicylic acid (SA), jasmonic acid (JA) and ethylene (ET) (Li et al., 2019; Shafqat et al., 2024). The target gene for SA is *PR-1* (pathogenesis-related protein 1) and for JA/ET it is *PDF-1.2* (plant defensin 1.2) (Dong, 1998; Li et al., 2019). Furthermore, SA and JA/ET pathways are associated with defence responses against hemibiotrophic and necrotrophic pathogens, respectively (Li et al., 2004; Lowe et al., 2014). Additionally, the transcription factors WRKY70 and WRKY33 are thought to be important regulators of the defence response pathways, with WRKY70 suggested to be an activator of SA-induced genes, and WRKY33 characterised to be critical for defence against pathogens that are necrotrophic (Li et al., 2004; Zheng et al., 2006; Birkenbihl et al., 2012). Both studies reported similar interpretations, with *L. biglobosa* inoculation resulting in upregulation of *PR-1*, attributed to induction of systemic acquired resistance (Durrant & Dong, 2004; Liu et al., 2007; Padmathilake & Fernando, 2022b). Additionally, an early upregulation of *PDF-1.2* expression was reported as a result of *L. biglobosa* inoculation (Liu et al., 2007).

In terms of other interspecific competition strategies between *L. maculans* and *L. biglobosa*, Elliott et al. (2007) first reported a zone of inhibition in a co-culture of *L. maculans* and *L. biglobosa*. This was attributed to antifungal properties of the phytotoxin sirodesmin PL, produced by *L. maculans*, preventing the *L. biglobosa* colony from growing towards the *L. maculans* colony. This was hypothesised to be due to *L. maculans* deploying an interference competition strategy against *L. biglobosa*. Interestingly, this

zone of inhibition was not present when *L. biglobosa* was co-cultured with a non-sirodesmin PL producing (mutant) isolate of *L. maculans* using the same method (Elliott et al., 2007). Conversely, Fortune et al. (2024) showed that *L. biglobosa* can in fact inhibit the production of sirodesmin PL by *L. maculans* if they are simultaneously co-inoculated, both *in vitro* and *in planta* (part of this *in planta* work was done in collaboration with Dr. James Fortune and is presented in the results of this chapter). In addition, it was also reported that if *L. biglobosa* was sequentially co-inoculated 7 days after *L. maculans in vitro*, then inhibition of sirodesmin PL would not occur (Fortune et al., 2024). Strikingly, further *in vitro* studies revealed that the timing when *L. maculans* and *L. biglobosa* interact was not only affecting the production of secondary metabolites but also was affecting the growth of the pathogens entirely (Bingol et al., 2024) (Chapter 3 of this PhD thesis). It was reported that if *L. biglobosa* was inoculated before or up to 1 day after *L. maculans*, it would inhibit the growth of *L. maculans* by acquiring all nutrients in the liquid media by deploying a resource-mediated interspecific competition strategy. Conversely, if *L. biglobosa* was co-inoculated 5 days or later after *L. maculans*, it would not be able to grow due to *L. maculans* successfully producing sirodesmin PL by deploying an interference interspecific competition strategy. Interestingly, if *L. biglobosa* was co-inoculated 3 days after *L. maculans*, it would be able only to cause partial inhibition of *L. maculans* growth, as it would co-incide with the start of sirodesmin PL production by *L. maculans in vitro* (Bingol et al., 2024).

A definitive way of assessing the outcome of interspecific competition between the *Leptosphaeria* species in experiments is quantification of pathogen DNA through qPCR, using species-specific primers. With this method, it can be assessed whether the pathogens are growing, or potentially a competitive exclusion event has occurred between them. This was easily achievable in *in vitro* part of the work (Chapter 3) by utilising the commonly used DNAmite Plant DNA Extraction Kit (Microzone Ltd.). However, it was not easy to extract DNA with sufficiently high quality for qPCR analyses from cotyledons extensively colonised with *L. maculans* and/or *L. biglobosa* using this kit.

Although the results of *in vitro* studies (Chapter 3) have allowed stronger arguments to be made regarding the interspecific interactions between *L. maculans* and *L. biglobosa*, these interactions may occur differently on their host. Therefore, this chapter focusses on

effects of pathogen-pathogen interactions on their host and aims to further characterise the interspecific interactions between *L. maculans* and *L. biglobosa in planta*. The hypotheses behind this study are:

1) Composition of secondary metabolites and lesion phenotypes are different between treatment of simultaneous co-inoculation with *L. maculans* & *L. biglobosa* and treatments of sole inoculation with *L. maculans* or *L. biglobosa* (in collaboration with Dr. James Fortune).

2) Lesion development and phenotype, pycnidia production on colonised cotyledons, and relative percentage of pathogen DNA in lesions are different between treatments of sequential co-inoculations with *L. maculans* & *L. biglobosa* and treatments of sole or simultaneous co-inoculation of the two *Leptosphaeria* species.

3) Oilseed rape (*Brassica napus*) defence responses are different between treatments of sequential co-inoculations with *L. maculans* & *L. biglobosa* and treatments of sole or simultaneous co-inoculation of the two *Leptosphaeria* species.

4) *L. maculans* and *L. biglobosa* can outcompete each other and this leads to competitive exclusion of one or another, based on the time when they meet and interact at the inoculation site.

These hypotheses were tested through the following objectives:

1) To investigate the effects of simultaneous co-inoculation on composition of secondary metabolites produced by *L. maculans* and lesion phenotypes.

2) To investigate the effects of simultaneous and sequential co-inoculations on lesion development and phenotype, pycnidia production on infected cotyledons, and relative growth of the two pathogens in lesions.

3) To test and optimise methods for DNA extraction from cotyledons of oilseed rape extensively colonised with *L. maculans* and/or *L. biglobosa*.

4) To investigate the effects of simultaneous and sequential co-inoculations on oilseed rape defence responses.

4.2 Materials and methods

4.2.1 Setting up experiment for simultaneous co-inoculation

4.2.1.1 Preparation of plants

To measure seed germination success (%), a pre-germination assay was done to ensure viability of seeds used in this experiment. This was done by placing 50 seeds on a moist Whatman filter paper placed in a Petri dish (both 9 cm diameter). These Petri dishes were then placed by a window for 48 h. The percentage of seeds that had successfully germinated was noted.

Seeds of oilseed rape cultivar Charger (AHDB Recommended List phoma stem canker resistance rating 4, susceptible to *L. maculans* with no known resistance genes) were sown in 8 × 5 well plug trays placed inside 20 cm × 32 cm plastic trays lined with absorbent soaking mats. A total of four plug trays were sown for a total of 160 plants to be used in the experiment. John Innes Number 3 soil and Miracle Gro All Purpose compost were mixed in 1:1 ratio to fill the wells. The soil/compost mixture was watered to create a moist environment to facilitate seed germination. Small pits of 1 cm depth were created using the bottom of a 15 mL Falcon tube in each well to place the seeds. The seeds were then covered with a moist soil/compost mixture and watered at the bottom of the tray on the absorbent soaking mats. The trays were placed in a controlled environment (CE) cabinet (Aralab, Rio de Mouro, Portugal) at 20°C light/18°C dark with 12 h light/12 h with 60% humidity for 14 days. Plants were regularly watered to ensure the soil/compost mixture stayed moist.

4.2.1.2 Preparation of conidial suspensions of *Leptosphaeria* species

L. maculans isolate ME24 and *L. biglobosa* 'brassicae' isolate WH17 Why-1 were sub-cultured on V8 agar plates for pycnidial production to make conidial suspensions. Two agar pieces were excised using sterilised scalpels from 12-day old cultures of the

Leptosphaeria isolates. These agar pieces were then placed on a new set of V8 agar plates, with the mycelial surface facing down to contact the surface of the agar. Using sterilised L-shaped spreaders, the mycelial surfaces of the agar pieces were smeared across the plates to cover the entire surface. This was followed by breaking the two agar pieces into smaller pieces and distributing them across the surfaces of the agar plates. The plates were stored in incubators at 20°C in darkness for 48 h, then transferred into CE cabinets (Aralab, Rio de Mouro, Portugal) at 20°C light/18°C dark with 12 h light/12 h dark and 60% humidity for 10 days (Figure 4.2).

After 12 days of incubation (48 h in the incubator plus 10 days in the CE cabinet), the plates were taken into a biosafety cabinet (ThermoFisher, Waltham, Massachusetts, United States) to prepare conidial suspensions. Sterilised distilled water (10 mL per plate) was added into the plates containing pycnidia. A sterilised L-shaped spreader was used to dislodge the spores from the plate surface into sterilised distilled water. The suspensions obtained from plates were filtered through a sterilised funnel lined with two layers of sterilised Miracloth (Sigma-Aldrich, Burlington, Massachusetts, United States), into sterile 15 mL Falcon tubes to separate the agar pieces and the mycelia from conidial suspensions obtained (Figure 4.3).

Once the harvesting of spores was completed for both *Leptosphaeria* species, the concentrations of spores were assessed using a haemocytometer (Superior®, Lauda-Königshofen, Germany) at 400 × magnification (Figure 4.4). Final concentrations of the suspensions were adjusted to 10^7 spores/mL using sterilised distilled water. For this experiment, conidial suspensions with adjusted concentrations were stored in sterilised 15 mL Falcon tubes and kept in a -20°C freezer until required for further use. However, for use in all other experiments presented in this chapter, separate, fresh batches of conidial suspensions of the same *Leptosphaeria* isolates were prepared, diluted to 10^7 spores/mL concentration and aliquoted into smaller batches in sterilised 2 mL screw-cap tubes for short-term storage in order to avoid reduction in spore viability through freeze-thaw cycles (Figure 4.3). All tubes were vortexed every time before any pipetting was done to ensure homogenous distribution of spores within the suspension.

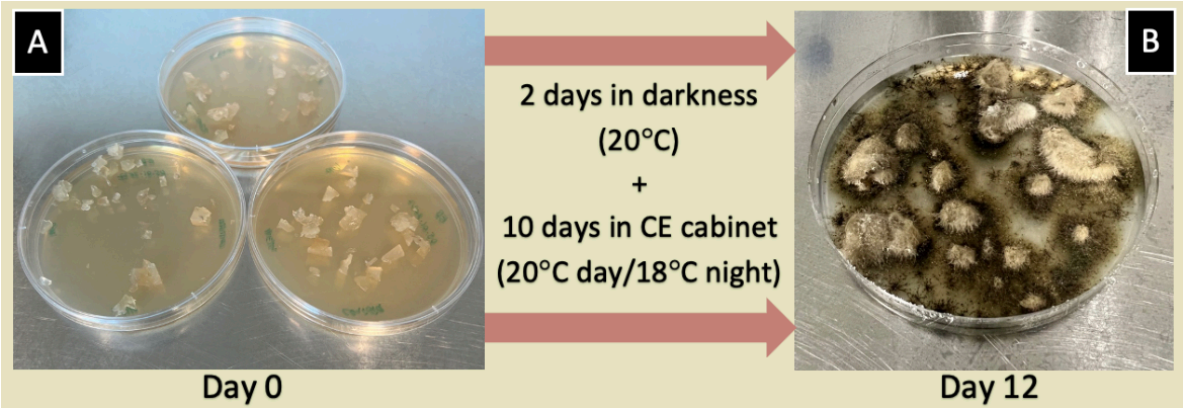

Figure 4.2: Sub-culturing *Leptosphaeria* species for conidial suspension preparation. (A) *L. maculans* on V8 agar plates on day 0. (B) *L. maculans* on a V8 agar plate on day 12. Agar pieces from previous cultures of *Leptosphaeria* species were collected and the sides of these pieces containing the mycelia were smeared across the entire surface of new V8 agar plates. This was followed by breaking down of the agar pieces into smaller pieces and spreading them across the V8 agar plates. After incubation at 20°C for 48 h in an incubator in darkness followed by 12 h light/12 h dark at 20°C light/18°C dark with 60% humidity for 10 days in a controlled environment (CE) cabinet, pycnidial production was observed and these plates were used for preparation of conidial suspensions of *Leptosphaeria* species.

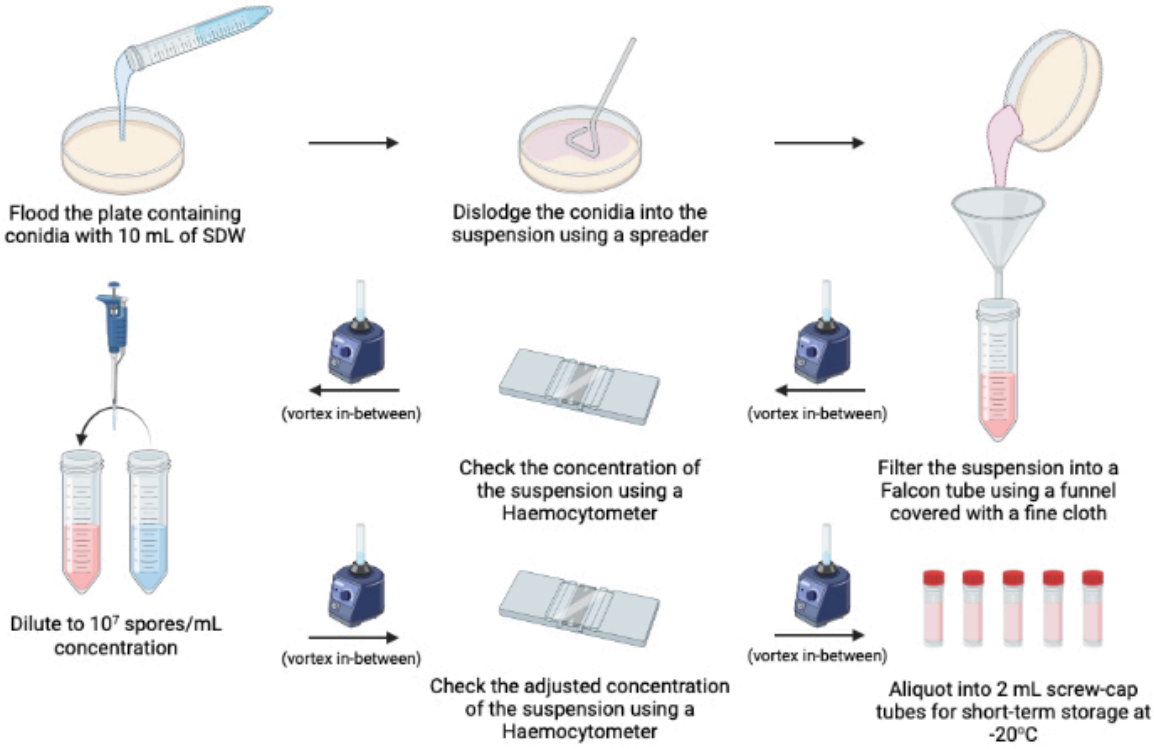

Figure 4.3: Workflow of harvesting and diluting inoculum from cultures of *Leptosphaeria* species incubated for preparation of conidial suspensions.

V8 agar plates containing conidia were flooded with 10 mL of sterilised distilled water. The spores were removed from the agar surface into suspension using sterilised L-shaped spreaders and filtered into 15 mL Falcon tubes through a sterilised funnel lined with a fine cloth. The concentrations of conidial suspensions were checked using a haemocytometer and diluted to 10^7 spores/mL using sterilised distilled water (SDW). The diluted conidial suspensions were aliquoted into sterilised 2 mL screw-cap tubes for short term storage in a -20°C freezer. The tubes were vortexed before each pipetting to ensure equal distribution of spores within the suspensions. This figure was created using BioRender.com.

The haemocytometer contains 25 large squares, with each containing 16 small squares (Figure 4.4). The area and volume of one large square are 0.04 mm^2 and 0.004 mm^3 (4×10^{-6} mL), respectively. Thus, the area and volume of one small square are 0.0025 mm^2 and 0.00025 mm^3 (2.5×10^{-7} mL), respectively. Therefore, the numbers of spores/mL were calculated using the following formula:

spores/mL = average number of spores in one large square / 4×10^{-6}

4.2.1.3 Inoculation of cotyledons and experimental design

Cotyledons of oilseed rape cultivar Charger were inoculated. There were four treatments: *L. maculans* only (Lm only), *L. biglobosa* only (Lb only), *L. maculans* and *L. biglobosa* co-inoculated simultaneously (Lm&Lb) and sterilised distilled water (SDW) as a control. The experiment was done in a randomised block design with 10 replicate plants per treatment in each of the four blocks.

When plants were 14 days old, any emerging true leaves were removed and support sticks (made by wrapping some metal wiring on parts of sterilised bacterial inoculation loops) were placed in the soil/compost mixture and adjusted accordingly to support the seedlings and keep the cotyledons upright. The cotyledons were point-inoculated, using the puncture-wound method (Huang et al. 2018). A sterilised microscope needle was used to create wounds on the cotyledons (two wounds per cotyledon, four wounds per plant), then a drop of 11 µL of spore suspension was pipetted onto each wound, according to treatments. A spore suspension for the Lm&Lb treatment was obtained by mixing spore suspensions of both *Leptosphaeria* species in a 1:1 ratio.

Following cotyledon inoculation, plants were watered and covered with misted propagator lids for 48 h to maintain high humidity. For the first 24 h, propagator lids were covered with black bags to ensure darkness (to optimise conditions for spore germination). The black bags were then removed and propagator lids were kept in place for another 24 h. All inoculated plants from the time of inoculation were kept in a CE cabinet (Aralab, Rio de Mouro, Portugal) at 18°C light/16°C dark with 12h light/12h dark and 60% humidity.

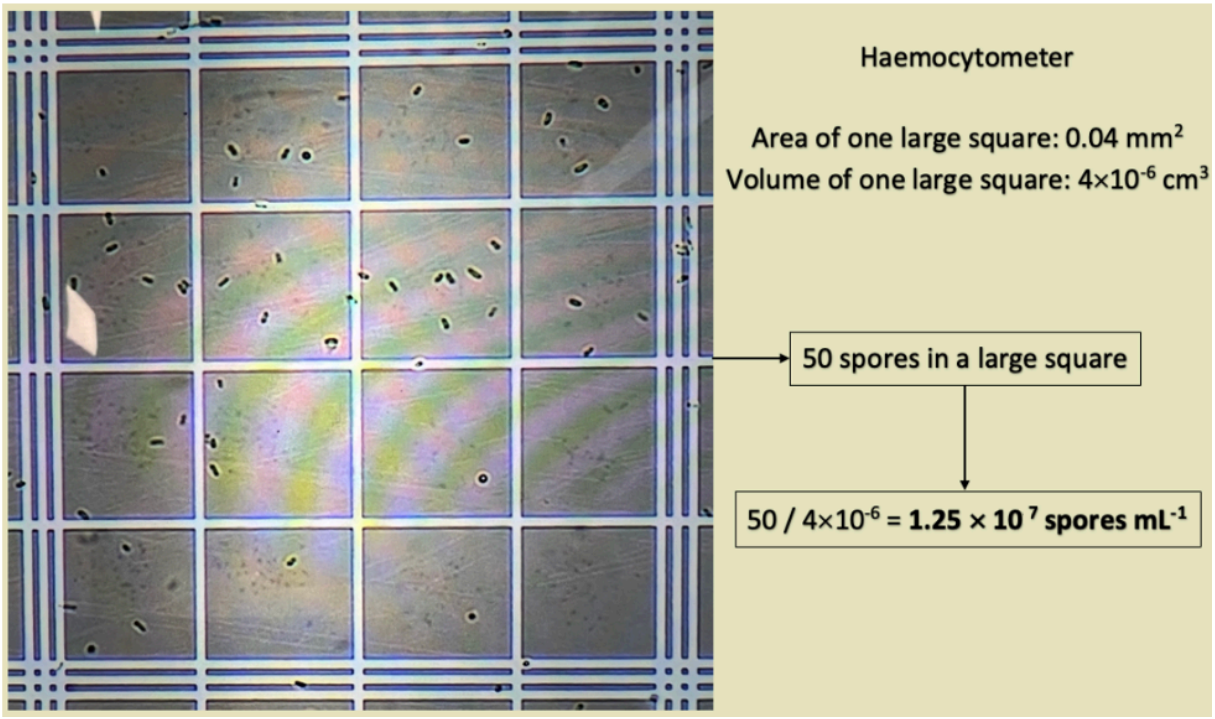

Figure 4.4: Calculation of the concentration of conidial suspensions using a haemocytometer.

A count of 50 spores in a large square of a haemocytometer (4×10^{-6} mL volume) corresponds to a spore suspension with a concentration of 1.25×10^{7} spores/mL.

Plants were watered regularly and misted with sterilised distilled water to ensure a moist environment for disease development. True leaves were removed regularly to increase the lifespan of cotyledons.

4.2.2 Effects of simultaneous co-inoculation on lesion phenotype and composition of secondary metabolites

4.2.2.1 Phenotypic assessment of lesions

At 26 days post inoculation (dpi), cotyledons from all plants were removed using scissors and photographed in standardised settings in an 8 cm × 8 cm square. All photographs were taken from a set distance, and all four corners of the square were clearly visible in all photographs. The lesion areas of all cotyledons were measured using the ImageJ image processing software (National Institutes of Health, Bethesda, United States) in pixels. The average number of pixels for each lesion were converted into mm^2 using the known area of the square.

4.2.2.2 Secondary metabolite extraction from cotyledons

As it is very difficult to detect secondary metabolites in infected oilseed rape cotyledons due to the relatively smaller fungal biomass compared to that in *in vitro* experiments, phenotypic assessment and secondary metabolite extractions were done at 26 dpi to ensure cotyledons were very severely diseased. After photographing the cotyledons, lesions from 30 plants per treatment were excised using sterilised scalpels. Lesions were distributed across six 2 mL screw-cap tubes (lesions from 5 plants per tube) and freeze-dried for 48 h. Afterwards, three small stainless-steel beads and 600 µL of ethyl acetate (HPLC grade, Fisher Scientific, Waltham, Massachusetts, United States) were added into each tube and processed three times using the FastPrep machine (MP Biomedicals, Irvine, California, United States) at 6.0 m/s for 40 s and samples were placed on ice for 5 min inbetween runs. The samples were then centrifuged at 1,100 × *g* for 5 min, then 500 µL of supernatant from each tube was taken and pooled into 50 mL skirted Falcon tubes according to treatments.

4.2.2.3 Sample preparation for high performance liquid chromatography (HPLC)

The 50 mL skirted Falcon tubes containing pooled secondary metabolite extracts were placed under a constant stream of nitrogen for 6 h to allow ethyl acetate to evaporate. The samples were then re-suspended by adding 500 μL of ethyl acetate. Using 1 mL syringes (Terumo®, Shibuya, Tokyo, Japan), re-suspended samples were passed through 0.45 μm nylon syringe filters (HPLC grade, Thermo Fisher, Waltham, Massachusetts, United States) into 2 mL HPLC vials to create stocks. Using a pipette, 200 μL of stock samples were transferred into a new set of HPLC vials each containing a 200 μL glass insert. All of the samples were stored in a spark-free fridge at 4°C until required for HPLC analysis.

4.2.2.4 High performance liquid chromatography (HPLC)

HPLC analyses were done as described in section 2.6. To identify unique maxima seen on HPLC chromatograms through liquid chromatography-mass spectrometry (LC-MS), 1.5 mL fractions were taken at 11-12.5 min and 16-17.5 min retention time for all samples and placed under a constant stream of nitrogen for 6 h to allow solvents to evaporate. Concentrated samples were re-suspended in 120 μL of ethyl acetate (for LC-MS analyses.

4.2.2.5 Liquid chromatography-mass spectrometry (LC-MS)

The samples were identified in a Waters I-Class ultra performance liquid chromatography (UPLC) system connected to a Xevo Micro TQ-S mass spectrometer. Separation was done on a Waters BEH C_{18} column (2.1 mm × 50 mm, 1.8 μm), holding samples at 40°C with mobile phases A and B, which were 0.2% formic acid in water and acetonitrile, respectively (both HPLC grade, Fisher Scientific, Waltham, Massachusetts, United States). Separation gradient was set to ramp initial conditions of 85% A and 15% B to 100% over 9 min, maintain them for 1 min and then return back to 85% A and 15% B in 0.1 min and maintain them for 4.9 min to equilibrate the column. The flow rate was 0.4 mL/min and an injection volume of 10 μL was used. It was followed by a mass scan in positive ion mode (range 50 *m/z* to 650 *m/z*) with a 0.2 s scan time. Probe capillary voltage was set at 3 kV, cone voltage was set and fixed at 20 V, with collision energy set and fixed at 3 V. Gas flow for desolvation was set at 10^3 L/hr at 500°C. Gas flow for the cone was set at 150 L/hr at 150°C (Fortune, 2022).

4.2.3 Setting up experiments for sequential co-inoculation

4.2.3.1 Preparation of plants

To ensure seedling emergence at similar times, seed were pre-germinated as described in section 4.2.1.1. Germination success was consistently > 90% for all experiments. Sowing of seeds was also done as described in section 4.2.1.1, with the following differences: a mixture with equal amounts of Miracle Gro Peat-Free All Purpose compost and Old Country Peat-Free compost was created and then mixed in a 1:1 ratio with John Innes Number 3 soil, pre-germinated seeds were placed into the pits using forceps, and the trays for some experiments were kept in glasshouse conditions at the University of Hertfordshire College Lane Campus for 12 days and then moved into a controlled environment (CE) cabinet (Conviron, Winnipeg, Manitoba, Canada) at 18°C light/16°C dark with 12 h light/12 h dark and 60% humidity for 2 days to acclimatise the plants before inoculation.

4.2.3.2 Preparation of conidial suspensions of *Leptosphaeria* species

Preparation of conidial suspensions of both *Leptosphaeria* species were done as described in section 4.2.1.2.

4.2.3.3 Inoculation of cotyledons and experimental designs

Five experiments (Figure 4.5) were done to investigate different aspects of interspecific competition between *L. maculans* and *L. biglobosa in planta*. In all experiments, cotyledons of oilseed rape cultivar Charger were inoculated with ten treatments: Sterilised Distilled Water (SDW) as a control, *L. maculans* only (Lm only), *L. biglobosa* only (Lb only), *L. maculans* & *L. biglobosa* co-inoculated simultaneously (Lm&Lb), initial inoculation by *L. maculans* and then *L. biglobosa* at 1, 3 or 5 days later (Lm+Lb-1, Lm+Lb-3, Lm+Lb-5), and initial inoculation by *L. biglobosa* and then *L. maculans* at 1, 3 or 5 days later (Lb+Lm-1, Lb+Lm-3, Lb+Lm-5) (Table 4.1).

When plants were 12 days old, any emerging true leaves were removed and support sticks (made by wrapping some metal wiring on parts of sterilised bacterial inoculation loops) were placed in the soil/compost mixture and adjusted accordingly to support the seedlings and keep the cotyledons upright. Two days later, the cotyledons of the plants (14 days old) were point-inoculated, using the puncture wound method (Huang et al. 2018).

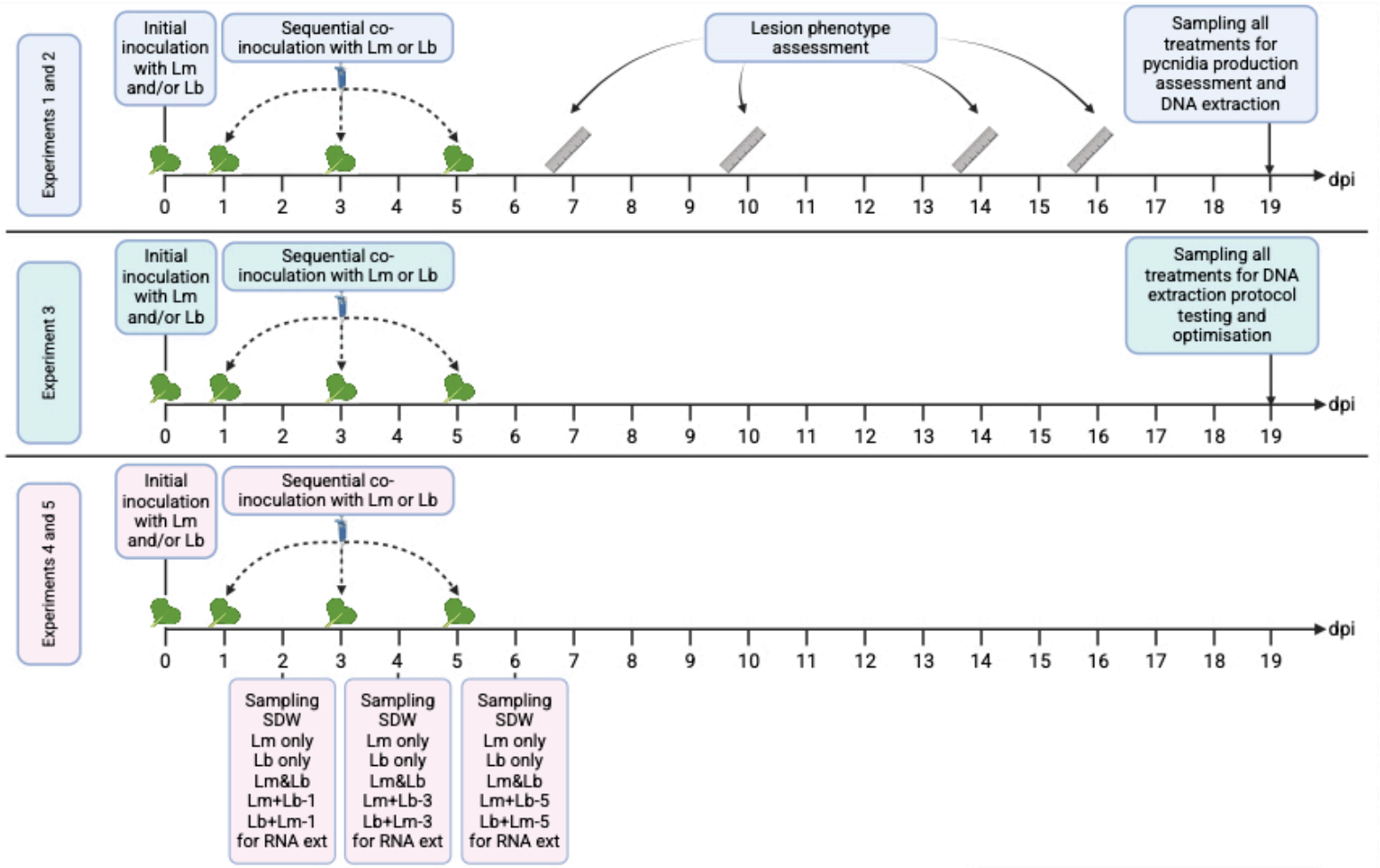

Figure 4.5: Graphical summary of *in planta* simultaneous and sequential co-inoculation experiments.

Experiments 1 and 2 were done to assess lesion development, lesion phenotype, pycnidial production and relative growth of the pathogens. Experiment 3 was done to test and optimise DNA extraction protocols. Experiments 4 and 5 were done to assess oilseed rape (*Brassica napus*) defence responses against *Leptosphaeria maculans* and/or *L. biglobosa*. This figure was created using BioRender.com.

Table 4.1: Treatments of inoculations with conidial suspensions (10^7 spores/mL concentration) of *Leptosphaeria maculans* (Lm) and *Leptosphaeria biglobosa* (Lb) for *in planta* experiments.

For control, 11 µL of Sterilised Distilled Water (SDW) was used per inoculation site. For solo inoculations, 11 µL of Lm or Lb conidial suspensions were used. For simultaneous co-inoculation, conidial suspensions of Lm and Lb were mixed in a 1:1 ratio and 11 µL was used. For sequential co-inoculations, initial inoculations were done with 11 µL of Lm or Lb conidial suspensions, followed by the addition of 11 µL of conidial suspension of the other species at 1, 3 or 5 days after the initial inoculation.

Treatment	Vol. of Lm conidial suspension for initial inoculation (µL)	Vol. of Lb conidial suspension for initial inoculation (µL)	Vol. of Lm conidial suspension for sequential co-inoculation (µL)	Vol. of Lb conidial suspension for sequential co-inoculation (µL)
SDW	-	-	-	-
Lm only	11	0	-	-
Lb only	0	11	-	-
Lm&Lb	5.5	5.5	-	-
Lm+Lb-1	11	0	-	11 (1 day after Lm)
Lm+Lb-3	11	0	-	11 (3 days after Lm)
Lm+Lb-5	11	0	-	11 (5 days after Lm)
Lb+Lm-1	0	11	11 (1 day after Lb)	-
Lb+Lm-3	0	11	11 (3 days after Lb)	-
Lb+Lm-5	0	11	11 (5 days after Lb)	-

On initial inoculation day, a sterilised microscope needle was used to create wounds on the cotyledons (two wounds per cotyledon, four wounds per plant), then a drop of 11 µL of spore suspension was pipetted onto each wound according to treatments (Table 4.1). Spore suspension for the Lm&Lb treatment was obtained by mixing spore suspensions of both *Leptosphaeria* species in a 1:1 ratio.

Following initial cotyledon inoculation, plants were covered and sealed with misted propagator lids and black bags for the first 24 h. The black bags were then removed, and the misted propagator lids were kept without sealing them for another 48 h to maintain high humidity. This was repeated for sequential co-inoculations. Inoculated plants were kept in a CE cabinet (either Aralab or Conviron) at 18°C light/16°C with 12 h light/12 h dark and 60% humidity. Plants were regularly watered and the true leaves were regularly removed to increase the lifespan of cotyledons.

4.2.3.3.1 Experiments to investigate lesion development and relative growth of the pathogens

Two experiments (1&2) were done using a randomised block design. For the treatments 'Lm only', 'Lb only', 'Lm+Lb-3', 'Lb+Lm-3', 'Lm+Lb-5' and 'Lb+Lm-5', there were 5 replicate plants per treatment in three blocks. For the treatments 'Lm+Lb-1' and 'Lb+Lm-1', there were 5 replicates per treatment in four blocks. For the treatments 'SDW' and 'Lm&Lb', there were 15 replicates per treatment in one block (Appendix D). Lesion phenotypes were assessed at 7, 10, 14 and 16 days post inoculation (dpi). Cotyledons were randomly removed from each treatment for assessment of pycnidial production (2 cotyledons per treatment) and DNA extraction at 19 dpi (6 cotyledons per treatment) (Figure 4.5).

4.2.3.3.2 Experiment to optimise a protocol for DNA extraction from cotyledons extensively colonised by *L. maculans* and/or *L. biglobosa*

One experiment (3) was done to obtain samples to test and optimise different DNA extraction kits and protocols for DNA extraction from oilseed rape cotyledons extensively colonised by *L. maculans* and/or *L. biglobosa*. The same experimental design as in section 4.2.3.3.1 was used. Cotyledons were randomly removed from each treatment for DNA extraction at 19 dpi (10 cotyledons per treatment) (Figure 4.5).

4.2.3.3.3 Experiments to investigate plant defence responses against co-inoculation by *L. maculans* and *L. biglobosa*

Two experiments (4&5) were done. In order to accommodate the sample size required and to avoid mistakes when sampling, the treatments were separated into two groups, and a randomised block design was applied to each group. For the treatments 'SDW', 'Lm only', 'Lb only' and 'Lm&Lb', there were 10 replicates per treatment in four blocks. For the treatments 'Lm+Lb-1', 'Lb+Lm-1', 'Lm+Lb-3', 'Lb+Lm-3', 'Lm+Lb-5' and 'Lb+Lm-5', there were 10 replicates per treatment in two blocks (Appendix D).

For the treatments 'SDW', 'Lm only', 'Lb only' and 'Lm&Lb', cotyledons were randomly removed from individual plants from each treatment for RNA extraction at 2, 4 and 6 dpi. For the treatments 'Lm+Lb-3' and 'Lb+Lm-3', this was done at 4 dpi; and for 'Lm+Lb-5' and 'Lb+Lm-5' at 6 dpi (i.e. 1 day after *L. maculans* and *L. biglobosa* met). At each sampling point, five cotyledons per treatment were removed, placed in 2 mL screw-cap tubes individually and immediately placed in liquid nitrogen, followed by storage in a - 80°C freezer until required for RNA extraction. Due to time constraints, 'Lm+Lb-1' and 'Lb+Lm-1' treatments were excluded and three cotyledons per treatment were used from RNA extraction and further downstream analyses.

4.2.4 Effects of sequential co-inoculation on lesion development and phenotype

Lesion development was assessed by measuring the lesion area (length by width) twice on all lesions for all treatments at 7, 10, 14 and 16 dpi (Figure 4.6). Up to 60 lesions per treatment were measured at each time point in each experiment.

4.2.5 Effects of sequential co-inoculation on pycnidial production on infected cotyledons

At 19 dpi, 2 cotyledons per treatment were randomly selected, removed and placed on 2% Water Agar (WA) plates and the lids were sprayed with SDW before placing them on top of the plates. This was followed by incubation at 20°C in darkness for 72 h. Using a Nikon YS100 light microscope (Minato City, Tokyo, Japan) at 100 × magnification, for each lesion, the number of mature pycnidia in a view area of 0.100 mm^2 was counted for three view areas and averages were taken to calculate pycnidial density (Figure 4.7).

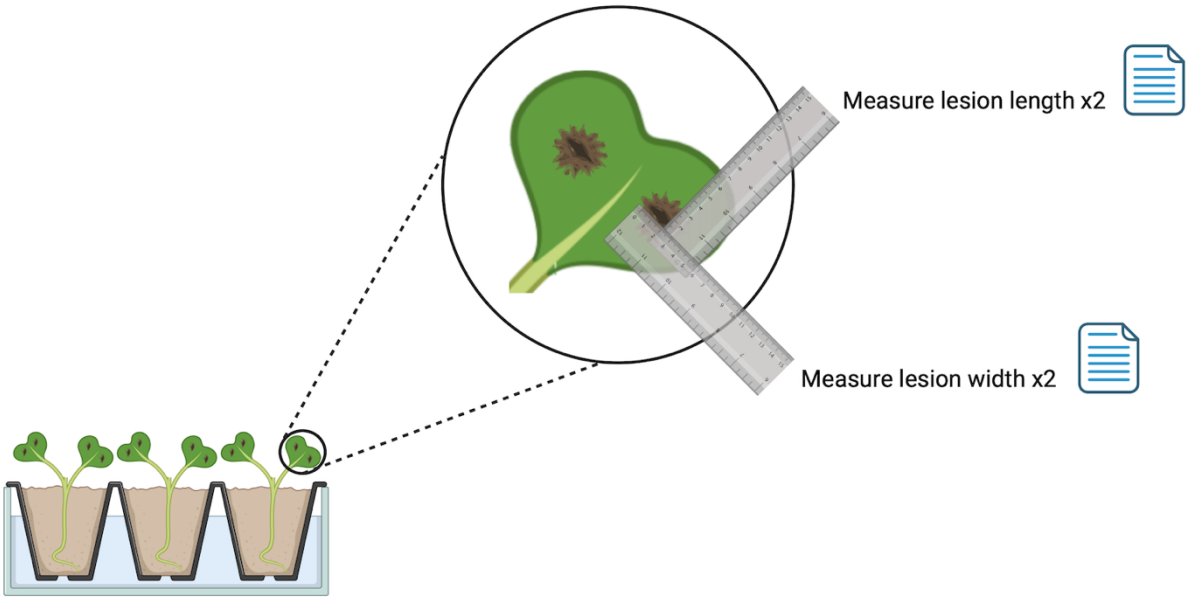

Figure 4.6: Workflow of phenotypic assessment of lesions.

Lesion phenotypes were assessed by measuring the lesion area (length by width) twice at 7, 10, 14 and 16 days post inoculation (dpi). This figure was created using BioRender.com.

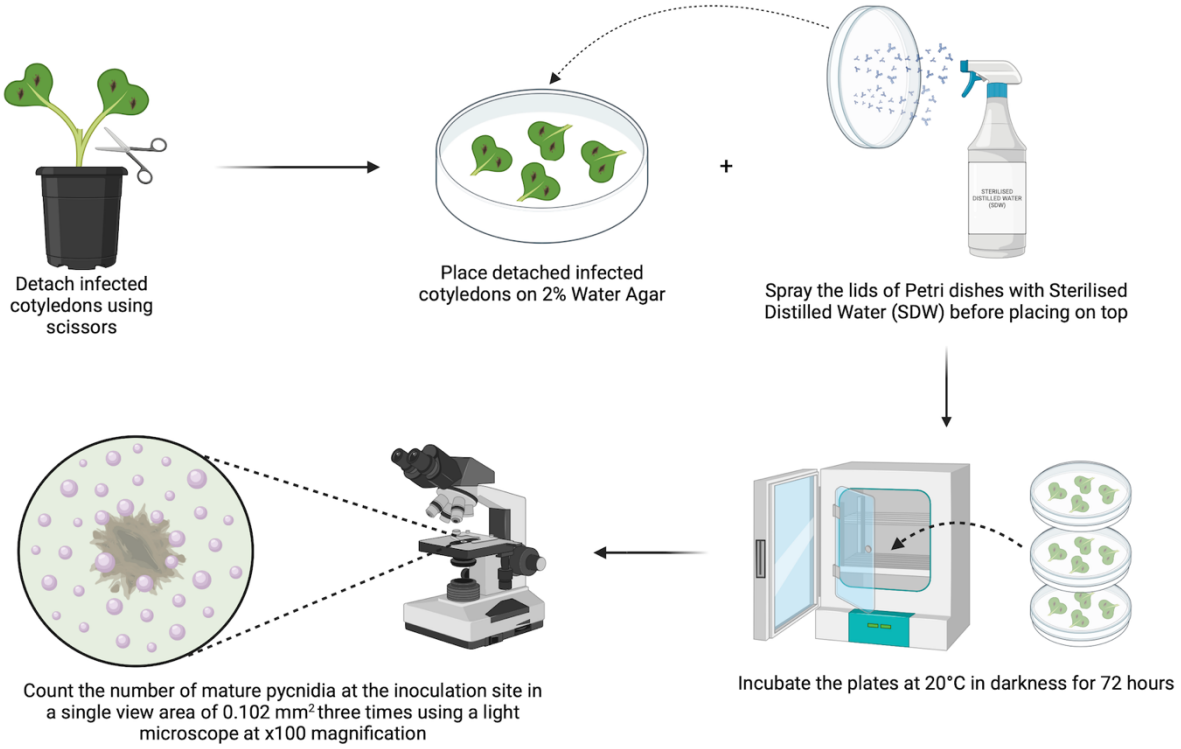

Figure 4.7: Workflow of assessment of pycnidial production.

Infected cotyledons were detached using scissors at 19 days post inoculation (dpi). These cotyledons were placed on 2% Water Agar (WA) plates and the lids of the Petri dishes were sprayed with Sterilised Distilled Water (SDW) before placing them on top of the plates. This was followed by incubation at 20°C in the dark for 72 h. The density of pycnidial production was calculated by counting the number of mature pycnidia at the inoculation site in a single view area of 0.100 mm^2 using a light microscope at 100 × magnification three times and taking an average. This figure was created using BioRender.com.

4.2.6 Testing and optimising methods for DNA extraction from oilseed rape cotyledons extensively colonised by *L. maculans* and/or *L. biglobosa*

It was proven difficult to extract good enough quality and quantity of DNA from oilseed rape cotyledons extensively colonised by *L. maculans* and/or *L. biglobosa* by the commonly used DNAmite Plant DNA Extraction Kit (Microzone Ltd.). Therefore, different kits and protocols were tested. One protocol was selected and optimised to extract good quality (A260/A280 > 1.8 and A260/A230 > 2.0) and quantity (> 100 ng/μL) of DNA from infected cotyledons (Table 4.2). The infected cotyledons were considered in two groups: Group 1 (Lm only, Lm+Lb-3 and Lm+Lb-5) and Group 2 (Lb only, Lb+Lm-3 and Lb+Lm-5). DNA samples obtained from all kits and protocols were quality checked by NanoDrop and Qubit as described in sections 2.4.1 and 2.4.2.

4.2.6.1 DNA extraction from infected cotyledons using the DNAmite Plant DNA Extraction Kit

DNA extraction using the DNAmite Plant DNA Extraction Kit (Microzone Ltd.) was done as described in section 2.3, using cotyledon samples instead of mycelial samples.

4.2.6.2 DNA extraction from infected cotyledons using the DNeasy Plant Pro Kit

DNA extraction using the DNeasy Plant Pro Kit (Qiagen, Venlo, The Netherlands) was done according to the manufacturer's guidelines, with minor modifications. Two cotyledons of the same treatment were taken out of the -20°C freezer and placed in 2 mL screw cap tubes alongside one sterile Zirconia bead. The samples were homogenised by processing using the TissueLyser (Qiagen) at 30 Hz for 1 min. This was followed by the addition of 450 μL of Solution CD1 and 50 μL of Solution PS and vortexing briefly. The samples were then processed again using the TissueLyser at 30 Hz for 1 min and centrifuged at 12,000 × *g* for 2 min. Following centrifugation, 320 μL of the supernatant from each tube was transferred into a new set of sterile 1.5 mL tubes. Then, 180 μL of Solution CD2 was added, and samples were vortexed for 5 s before centrifugation at 12,000 × *g* for 1 min. This was followed by transferring 350 μL of the supernatant from each tube into a new set of sterile 1.5 mL tubes. Buffer APP (450 μL) was added, and the samples were vortexed for 5 s. Using a pipette, 500 μL of each of the lysates at a time were loaded and passed through the MB spin column by centrifuging at 12,000 × *g* for 1 min.

Table 4.2: List of different DNA extraction kits and protocols tested for DNA extraction from cotyledons extensively colonised by *Leptosphaeria maculans* and/or *Leptosphaeria biglobosa*.

Two kits [DNAmite Plant DNA Extraction Kit (Microzone Ltd.) and DNeasy Plant Pro Kit (Qiagen)], two modified versions of the spore tape DNA extraction protocol (Huang et al., 2011; Kaczmarek et al., 2009) and the sorbitol pre-wash DNA extraction protocol (Inglis et al., 2018) were tested. Only the sorbitol pre-wash DNA extraction protocol was suitable and was therefore optimised for use in these experiments.

Kit/Protocol name	Manufacturer/Reference	Suitability
DNAmite Plant DNA Extraction Kit	Microzone Ltd.	✗
DNeasy Plant Pro Kit	Qiagen	✗
Modified spore tape DNA extraction protocol version one	Huang et al., 2011 Kaczmarek et al., 2009	✗
Modified spore tape DNA extraction protocol version two	Huang et al., 2011 Kaczmarek et al., 2009	✗
Sorbitol pre-wash DNA extraction protocol	Inglis et al., 2018	✓

Flow-through from all of the columns were discarded and the columns were placed in a new set of sterile 2 mL collection tubes. The columns were washed by adding 500 µL of Buffers AW1 and centrifuging at 12,000 × *g* for 1 min. This was repeated with Buffer AW2. The columns were then placed in a new set of sterile 2 mL collection tubes and were centrifuged at 16,000 × *g* for 2 min. This was followed by transferring the columns into a new set of sterile 1.5 mL tubes, adding 40 µL of Buffer EB directly into the centre of the membrane inside the columns and centrifuging at 12,000 × *g* for 1 min to elute the DNA. The eluted DNA samples were stored in a -20°C freezer until required (Figure 4.8).

4.2.6.3 DNA extraction form infected cotyledons using modified versions of the spore tape DNA extraction protocol

The spore tape DNA extraction protocol was developed by Kaczmarek et al. (2009) and further optimised by Huang et al. (2011).

Minor modifications to this protocol were made in this study to produce modified spore tape DNA extraction protocols versions one and two for DNA extraction from infected cotyledons. The protocol consists of two parts, done on two different days. Firstly, two cotyledons of the same treatment were taken out of the -20°C freezer and placed in 2 mL screw cap tubes alongside three sterile stainless steel beads. This was followed by the addition of 500 µL of DNA extraction buffer into each tube.

The samples were then processed three times using the FastPrep machine (MP Biomedicals) at 6.0 m/s for 40 s, keeping them on ice for 5 min between runs. After homogenisation of the samples, 500 µL of 2% SDS was added, followed by vortexing briefly and incubating in a 65°C water bath for 1 h. Next, 800 µL of the bottom phase of phenol:chloroform:isoamyl alcohol (25:24:1) (version one) or chloroform:isoamyl alcohol (24:1) (version two) was added into each tube, vortexed briefly, and centrifuged at 15,700 × *g* for 10 min at 4°C. In the meantime, a new set of sterile 1.5 mL tubes was prepared, and 1 µL of glycogen, 30 µL of 7.5 M ammonium acetate and 480 µL of isopropanol (all taken from a -20°C freezer) were added into this new set of tubes. After centrifugation, 650 µL of the upper phase from each original tube was transferred into each of the new set of tubes and mixed by inverting ten times. These tubes were incubated at -20°C for 16 h (Figure 4.9).

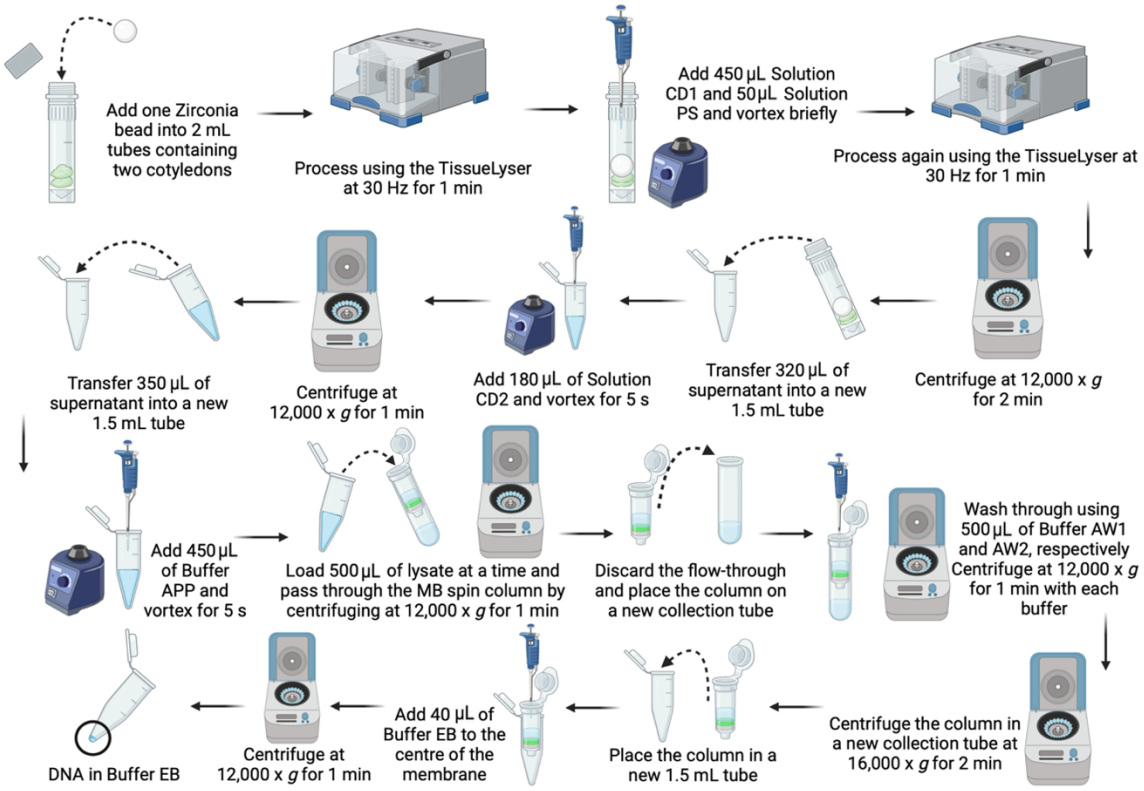

Figure 4.8: Workflow of DNA extraction using the DNeasy Plant Pro Kit (Qiagen).
Two cotyledons were homogenised using one Zirconia bead and processing the samples using the TissueLyser (Qiagen). This was followed by addition of solutions CD1 and PS and vortexing before processing the samples using the TissueLyser. The plant debris was pelleted by centrifugation and the supernatant was transferred into a new tube. Solution CD2 was added, and the samples were vortexed before pelleting of further debris by centrifugation. The supernatant was transferred into a new tube and buffer APP was added and the tubes were vortexed to mix. The lysate was passed through the MB spin column, the flow-through was discarded and the spin column was placed in a new collection tube. The spin column was then washed through using buffers AW1 and AW2 and a centrifuge. The spin column was again placed in a new collection tube and then centrifuged at a higher speed to collect all buffers remaining in the spin column membrane. The spin column was then placed in a new tube and the DNA was eluted through addition of Buffer EB and subsequent centrifugation. This figure was created using BioRender.com.

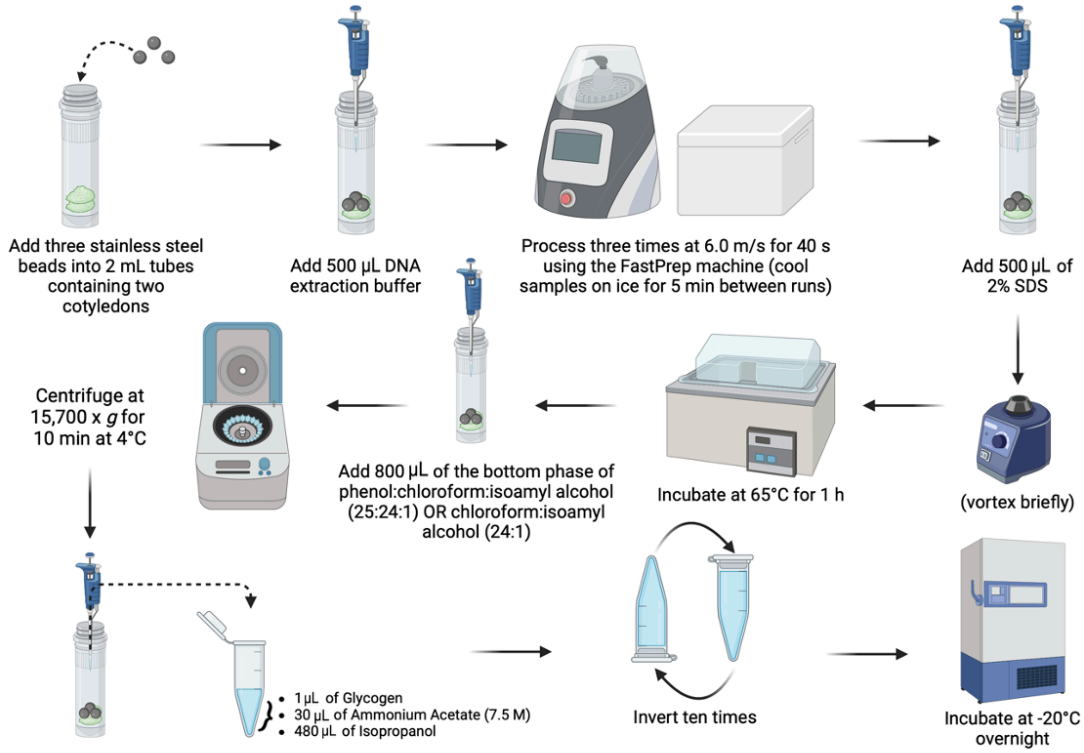

Figure 4.9: Workflow of the first part of the modified spore tape DNA extraction protocol. Three stainless steel beads were added to each of two cotyledon samples alongside DNA extraction buffer. Samples were homogenised in the buffer using the FastPrep machine (MP Biomedicals). After homogenisation, 2% SDS was added, mixed by vortexing and incubated in a water bath. Next, phenol:chloroform:isoamyl alcohol (25:24:1) or chloroform:isoamyl alcohol (24:1) was added (depending on the version of the protocol) and samples were separated into two phases through centrifugation. The upper phase was then transferred into a new tube containing glycogen, 7.5 M ammonium acetate and isopropanol, mixed by inverting and incubated in the -20°C freezer for 16 h. This figure was created using BioRender.com.

In the second part, the tubes were taken from the -20°C freezer and centrifuged at 15,700 × *g* for 30 min at 4°C. The supernatant was discarded and the DNA pellet was washed twice by adding 500 µL of 70% ethanol (taken from a -20°C freezer) and centrifuging at 15,700 × *g* for 8 min at 4°C. The supernatant was discarded again, and the tubes were spun briefly to collect the remaining ethanol in the bottom of the tubes. Using a pipette, the remaining ethanol was removed, and the tubes were left open in a fume hood for 20 min for the DNA pellets to dry. Finally, the DNA pellets were re-suspended by adding 30 µL of nuclease-free water and flicking them gently. The extracted DNA samples were stored in a -20°C freezer until required (Figure 4.10). Recipes of all buffers used in this protocol can be found in Appendix E.

4.2.6.4 DNA extraction from infected cotyledons using the sorbitol pre-wash DNA extraction protocol

The sorbitol pre-wash DNA extraction protocol was developed by Inglis et al. (2018). The optimised version of the protocol consists of two parts. One infected cotyledon was taken out of the -20°C freezer and each one was placed in a 2 mL screw-cap tube, alongside three sterile stainless steel beads. The samples were homogenised by processing using the FastPrep machine (MP Biomedicals) at 4.0 m/s for 20 s. An abundance of sorbitol pre-wash buffer (1.5 mL) was added to each tube and then vortexed for 5 s to ensure re-suspension of all powdered material in the buffer. This was followed by centrifugation at 5,000 × *g* for 5 min at 20°C. The supernatants (containing polyphenols and polysaccharides) were aspirated using a pipette. Next, 700 µL of lysis buffer (pre-warmed to 65°C) was added into each tube and the tubes were vortexed for 5 s. The samples were incubated in a 65°C water bath for 40 min and mixed by inverting five times once in every 10 min of the incubation time. The samples were then cooled at 20°C for 5 min (Figure 4.11).

In the second part, 700 µL of chloroform:isoamyl alcohol (24:1) was added into each tube and the tubes were vortexed for 10 s to mix well before centrifugation at 5,000 × *g* for 10 min at 20°C. Following centrifugation, 700 µL of the upper phase from each tube were transferred into a new set of sterile 1.5 mL tubes. This was followed by the addition of 70 µL of 3 M sodium acetate (pH 5.2) and 460 µL of isopropanol (taken from a -20°C freezer) into each tube and mixing by inverting ten times.

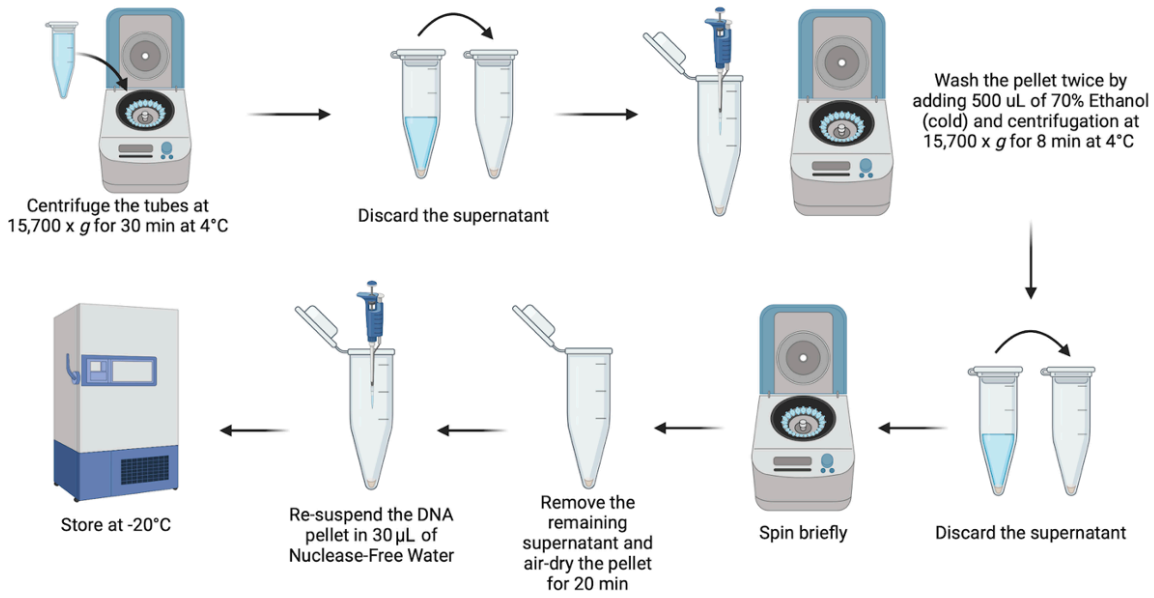

Figure 4.10: Workflow of the second part of the modified spore tape DNA extraction protocol.

The tubes were centrifuged to pellet the DNA and the supernatant was discarded. The DNA pellets were washed twice by the addition of 70% ethanol followed by centrifugation. The supernatant was discarded after each wash. The tubes were spun briefly to collect the remaining ethanol at the bottom of the tube, which was then removed using a pipette. After drying in the fume hood, the DNA pellets were re-suspended in nuclease-free water and stored in the -20°C freezer until required. This figure was created using BioRender.com.

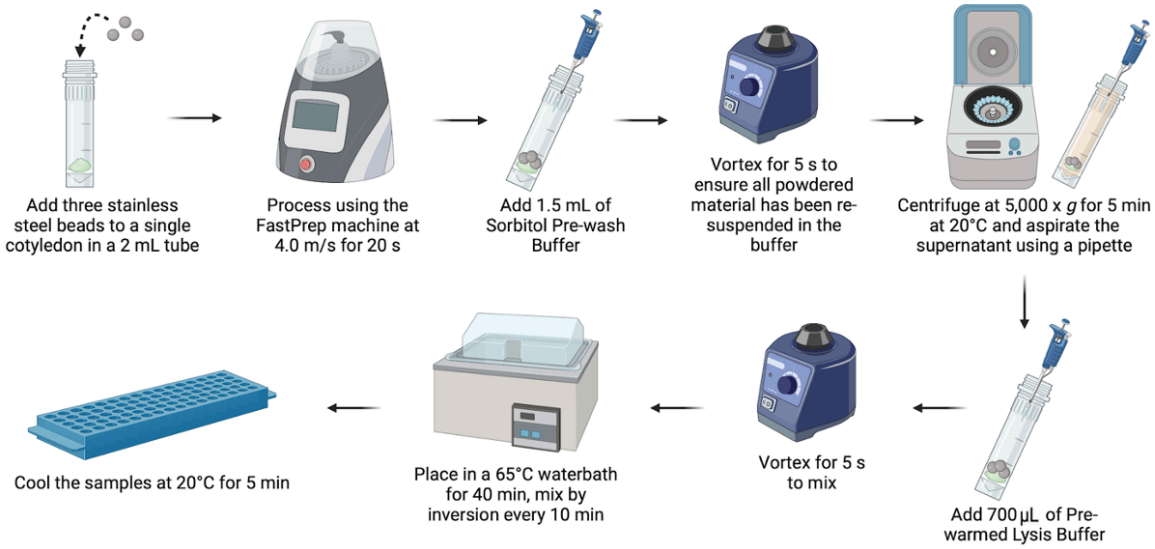

Figure 4.11: Workflow of the first part of the sorbitol pre-wash DNA extraction protocol. Three stainless steel beads were added to a single cotyledon sample and homogenisation was done using the FastPrep machine (MP Biomedicals). An excess of sorbitol pre-wash buffer was added, and the samples were vortexed to mix the plant material with the buffer. Centrifugation was then done to pellet the plant material, and the supernatant was removed using a pipette. Pre-warmed lysis buffer was added, and the samples were vortexed to mix the pre-washed plant material with the lysis buffer. The samples were then incubated in a water bath with regular mixing by inversion, followed by cooling at the bench before proceeding to the second part. This figure was created using BioRender.com.

The samples were then incubated in a -20°C freezer for 1 h and then centrifuged at 13,000 × *g* for 10 min at 20°C. The supernatants were discarded, and the DNA pellets were washed by adding 700 µL of 70% ethanol (taken from a -20°C freezer) and centrifuging at 13,000 × *g* for 10 min at 20°C. The supernatant was discarded again, and the tubes were spun briefly to collect the remaining ethanol in the bottom of the tubes. Using a pipette, the remaining ethanol was removed, and the tubes were left open in a fume hood for 20 min for the DNA pellets to dry. The DNA pellets were re-suspended in 40 µL of nuclease-free water. The extracted DNA samples were stored in a -20°C freezer until required (Figure 4.12). Recipes of all buffers used in this protocol can be found in Appendix E.

4.2.7 Effects of sequential co-inoculation on relative growth of the pathogens

4.2.7.1 DNA extraction from infected cotyledons

DNA extractions from infected cotyledons were done using the protocol modified from sorbitol pre-wash protocol developed by Inglis et al., (2018), as described in section 4.2.6.4.

4.2.7.2 DNA quality checks and dilution for quantitative polymerase chain reaction (qPCR)

DNA quality checks and dilutions were done as described in section 2.4.

4.2.7.3 Quantitative polymerase chain reaction (qPCR)

qPCR analyses were done as described in section 2.5.

4.2.8 Effects of sequential co-inoculation on oilseed rape (*Brassica napus*) defence responses

4.2.8.1 RNA extraction from cotyledons

RNA extraction using the RNeasy Plant Mini Kit (Qiagen, Venlo, The Netherlands) was done according to the manufacturer's guidelines, with minor modifications. Single cotyledon samples were each taken out of the -80°C freezer and one Zirconia bead (cooled in liquid nitrogen) was added to each tube. The samples were homogenised using the TissueLyser (Qiagen) at 30 Hz for 20 s. This was followed by the addition of 450 µL of Buffer RLT and processing once more using the TissueLyser at 30 Hz for 20 s.

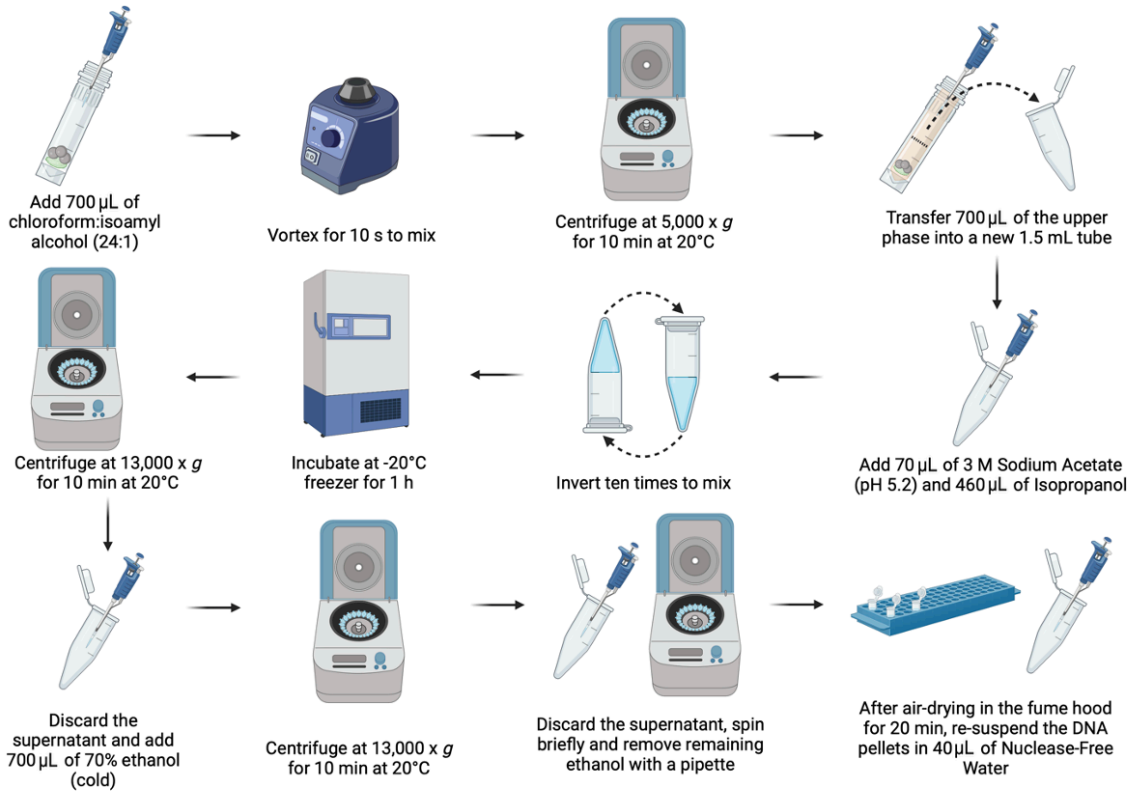

Figure 4.12: Workflow of the second part of the sorbitol pre-wash DNA extraction protocol.

After cooling the samples, chloroform:isoamyl alcohol (24:1) was added, and the samples were vortexed to mix. The samples were then separated into two phases by centrifugation, and the upper phase was transferred into a new tube. Sodium acetate (3 M, pH 5.2) and isopropanol were added and mixed by inverting, followed by incubation in the -20°C freezer. The DNA was pelleted using a centrifuge. Washing of the DNA pellets was done using 70% ethanol and centrifugation. The supernatant was discarded, and the tubes were spun briefly to collect the remaining ethanol at the bottom of the tube, which was then removed using a pipette. After drying in the fume hood, the DNA pellets were re-suspended in nuclease-free water and stored in the -20°C freezer until required. This figure was created using BioRender.com.

The lysates were then transferred into QIAshredder columns (purple), using wide-bore pipette tips to ensure transfer of the entire lysate, including any clumps or precipitates. The samples were centrifuged at 15,700 × *g* for 2 min at 20°C and the flow through was transferred into a new set of sterile 1.5 mL tubes. Next, 0.5 volume of 100% ethanol was added into each sample and immediately mixed by pipetting up and down. The samples were then transferred into RNeasy spin columns (pink) and centrifuged at 10,000 × *g* for 15 s at 20°C. The flow-through was discarded, 700 µL of Buffer RW1 was added, and the tubes were spun using a centrifuge with the same settings. The flow-through was discarded again, 500 µL of Buffer BPE was added and the tubes were spun again using a centrifuge with the same settings. The flow-through was discarded again, another 500 µL of Buffer BPE was added and the tubes were centrifuged at 10,000 × *g* for 2 min at 20°C. The RNeasy spin columns were then placed in a new set of sterile 1.5 mL tubes. The RNA was eluted by adding 50 µL of nuclease-free water directly into the centre of the membrane inside the columns and centrifuging at 10,000 × *g* for 1 min at 20°C. The eluted RNA samples were stored in a -80°C freezer until required (Figure 4.13).

4.2.8.2 RNA quality checks

Following RNA extraction using the RNeasy Plant Mini Kit (Qiagen), all of the RNA samples obtained were subjected to quality checks before DNase treatment and cDNA synthesis for gene expression analyses using quantitative polymerase chain reaction (qPCR).

4.2.8.2.1 RNA quality check by NanoDrop

RNA concentration, A260/A280 ratio and A260/A230 ratio in RNA samples were measured using a NanoDrop (ND-1000 Spectrophotometer, NanoDrop Technologies) by pipetting 1 µL of RNA sample following blanking of the spectrophotometer using nuclease-free water.

4.2.8.2.2 RNA quality check by Qubit

RNA concentrations of all samples were measured using Qubit RNA Broad Range Assay Kit (Invitrogen). The protocol used was the same as described in section 2.4.2, with using Qubit RNA reagents instead of Qubit DNA reagents and RNA samples instead of DNA samples.

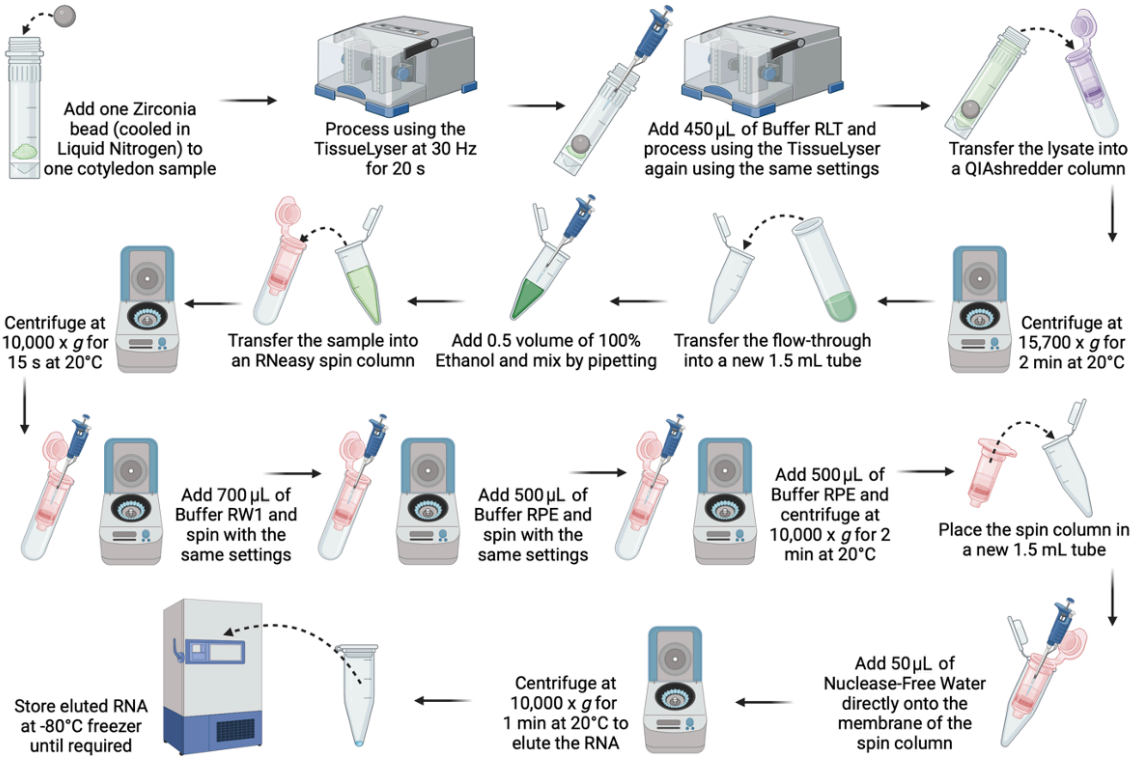

Figure 4.13: Workflow of RNA extraction using the RNeasy Plant Mini Kit (Qiagen). Each single cotyledon was homogenised using one Zirconia bead and the samples were processed using the TissueLyser (Qiagen). This was followed by the addition of Buffer RLT and processing again using the TissueLyser. The lysate was transferred into a QIAshredder column (purple) and centrifuged to filter out the plant debris. The flow-through was transferred into a new tube and mixed with 100% ethanol and then loaded onto the RNeasy spin column (pink). Centrifugation was done and Buffer RW1 was added and passed through the column through centrifugation. This was repeated twice using Buffer RPE. The RNeasy spin column was then placed in a new tube and the RNA was eluted by adding nuclease-free water into the column and centrifugation. The eluted RNA samples were stored in a -80°C freezer until required. This figure was created using BioRender.com.

4.2.8.3 DNase treatment and cDNA synthesis

DNase treatment was done using the RQ1 RNase-Free DNase Kit (Promega, Madison, Wisconsin, United States). Firstly, a DNase treatment master mix was prepared by mixing 1 μL each of RQ1 Reaction Buffer and RQ1 RNase-Free DNase per sample in a sterile 2 mL screw-cap tube. Second, based on the RNA concentrations measured using Qubit (Invitrogen), all RNA samples were diluted to contain 1 μg of total RNA in sterile PCR tubes (200 μL capacity), using DEPC-treated water. This was followed by aliquoting 2 μL of DNase treatment master mix into each tube and incubating at 37°C. Finally, 1 μL of RQ1 Stop Solution was aliquoted into each tube and the samples were incubated at 65°C for 10 min. Both incubation steps were done using a Bio-Rad T100 thermocycler (Bio-Rad, Hercules, California, United States) (Figure 4.14). Absence of DNA was tested through a gel electrophoresis.

cDNA synthesis was done using the UltraScript 2.0 Reverse Transcriptase Kit (PCR Biosystems, Wayne, Pennsylvania, United States). A cDNA synthesis master mix was prepared by mixing 4 μL of cDNA synthesis mix and 1 μL of UltraScript 2.0 per sample in a sterile 2 mL screw-cap tube. Following that, 5 μL of cDNA synthesis master mix was aliquoted into each tube. Using a Bio-Rad T100 thermocycler (Bio-Rad), the samples were incubated at 55°C for 30 min and then at 95°C for 10 min. cDNA samples were stored in a -20°C freezer until required (Figure 4.15).

4.2.8.4 cDNA dilution

All cDNA samples were diluted in a 1:10 ratio before qPCR analyses were done by pipetting 10 μL of cDNA sample and 90 μL of nuclease-free water into a new set of sterile PCR tubes.

4.2.8.5 Quantitative polymerase chain reaction (qPCR)

The expressions of genes related to oilseed rape defence responses: pathogenesis-related protein (*PR-1*), plant defensin (*PDF-1.2*) and two WRKY transcription factors (*WKRY70* and *WRKY33*) were analysed using actin (*ACTIN*) as a reference gene. The sequences of primers used in this study are presented in Table 4.3.

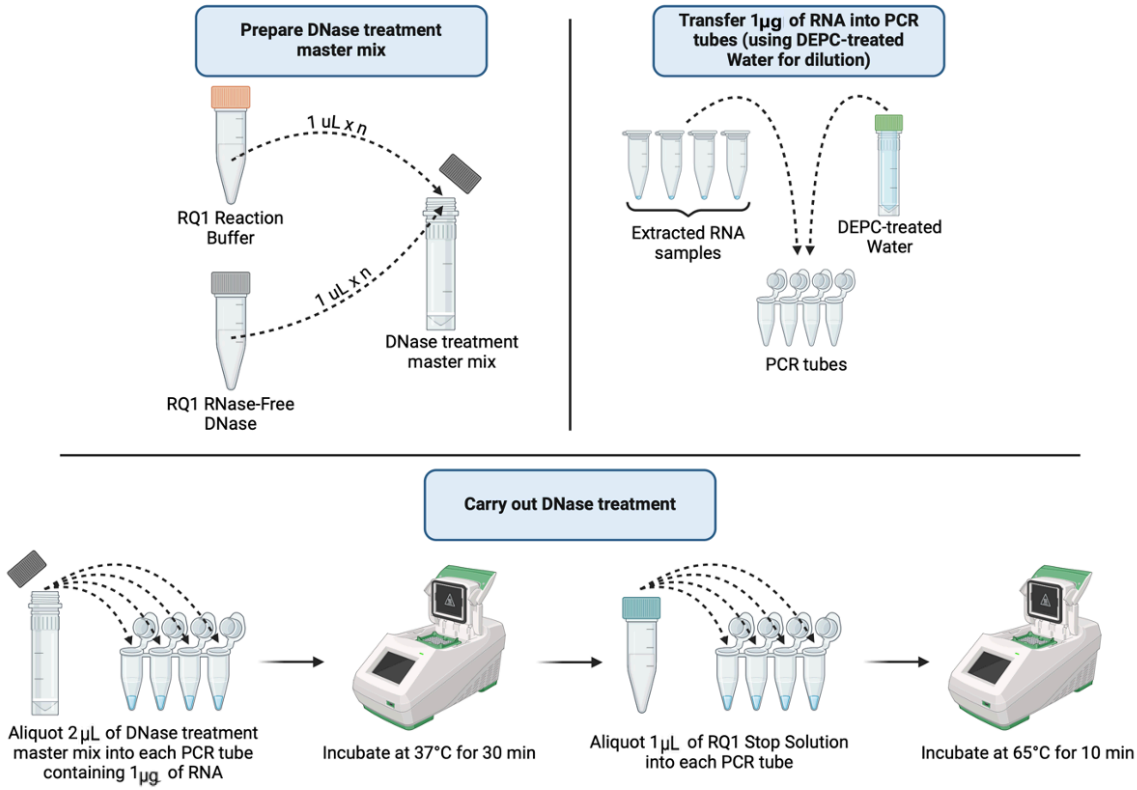

Figure 4.14: Workflow of DNase treatment using the RQ1 RNase-Free DNase Kit (Promega).

A DNase treatment master mix was prepared by mixing RQ1 Reaction Buffer and RQ1 RNase-Free DNase. RNA samples were diluted into PCR tubes using DEPC-treated water to contain 1 µg of total RNA per tube. This was followed by aliquoting 2 µL of DNase treatment master mix into the tubes containing 1 µg of total RNA. These samples were incubated according to the protocol and then 1 µL of RQ1 Stop Solution was added, followed by another incubation as described. This figure was created using BioRender.com.

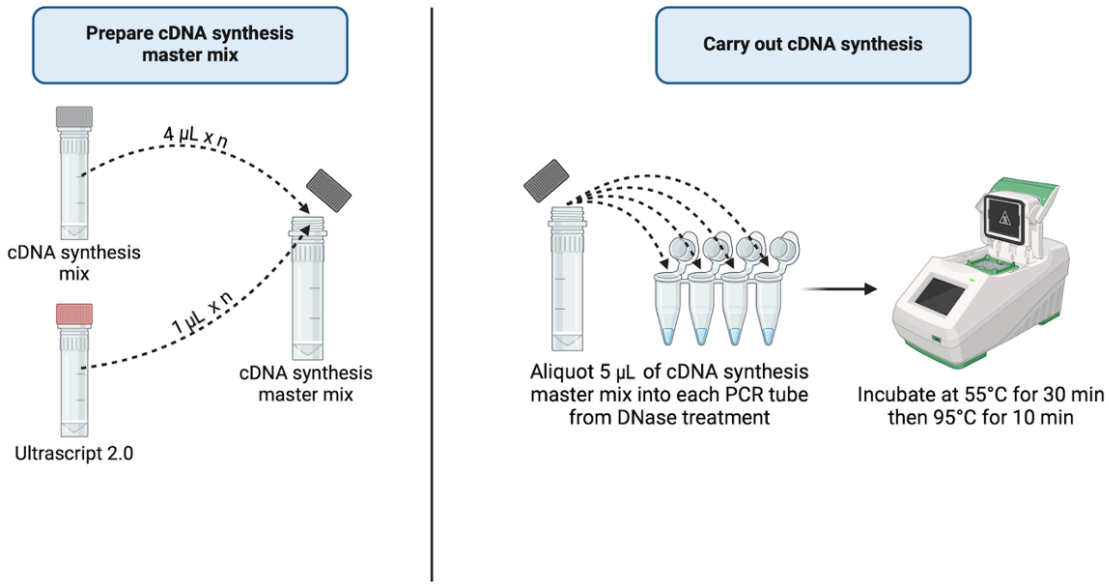

Figure 4.15: Workflow of cDNA synthesis using the UltraScript 2.0 Reverse Transcriptase Kit (PCR Biosystems).

A cDNA synthesis master mix was prepared by mixing the cDNA synthesis mix and UltraScript 2.0 according to the protocol. This was followed by aliquoting 5 µL of cDNA synthesis master mix into tubes obtained at the end of DNase treatment. These samples were then incubated as described. The cDNA samples obtained were stored in the -20°C freezer until required. This figure was created using BioRender.com.

Table 4.3: Primers used in gene expression analyses using quantitative polymerase chain reaction (qPCR).

Primer name, length (bp), sequence (5' to 3'), expected product size and reference are listed. These were previously published primers taken from literature (Liu et al., 2007; Padmathilake & Fernando, 2022b).

Primer name	Primer length (bp)	Primer sequence (5'-3')	Expected product size (bp)	Reference
PR-1-F	21	GGCTAACTATAACCACGATTC	79	Padmathilake & Fernando, 2022b
PR-1-R	19	GTTCCACCATTGTTACACC		
PDF-1.2-F	22	GCTAAGTTGTGCGAGAGGTCAA	72	Liu et al., 2007
PDF-1.2-R	22	CTGATTCTTGCAGGCGTTATTG		
WRKY70-F	21	ACATACATAGGAAACCACACG	105	Padmathilake & Fernando, 2022b
WRKY70-R	22	ACTTGGACTATCTTCAGAATGC		
WRKY33-F	20	TGTCGGACAGCTTGGGAAAG	100	Padmathilake & Fernando, 2022b
WRKY33-R	24	AGAGGACGGTTACAACTGGAGAAA		
ACTIN-F	22	CTGGAATTGCTGACCGTATGA G	65	Padmathilake & Fernando, 2022b
ACTIN-R	21	GTTGGAAAGTGCTGAGGGATG		

cDNA samples were taken out of the freezer and thawed at 20°C then placed on ice. The qPCR analyses to compare relative expression of the genes in samples were done using a CFX Opus 96 Real-Time PCR System (Bio-Rad, Hercules, California, United States). Amounts of transcripts of the genes of interest and the reference gene were quantified using SYBR Green (Agilent), with primers listed in Table 4.3. The qPCR reaction mixtures were prepared at a total volume of 10 μL, containing 5 μL of SYBR Green, 2.2 μL nuclease-free water, 0.4 μL of forward primer (10 μM), 0.4 μL of reverse primer (10 μM) and 2 μL of cDNA sample in triplicate wells in 96-well plates.

Thermocycling profiles were as follows: 1 cycle of 95°C for 2 min, 40 cycles of 95°C for 5 s, 60°C for 10 s and a reading step of 72°C for 30 s. Followed by a melting curve analysis by increasing the temperature from 60°C to 95°C in 0.5°C increments at 3 s per step. Images of thermocycling profiles used for gene expression analyses can be found in Appendix F. In order to validate the suitability and specificity of these primers with the thermocycling profile, the qPCR efficiency of all primers was tested on a dilution series. Images of standard curves and melting curves for all primers can be found in Appendix F. The relative expressions of genes were calculated using the $2^{-\Delta\Delta Ct}$ method (Livak & Schmittgen, 2001).

4.2.9 Statistical analysis

All of the statistical analyses of the data in this chapter were done using GraphPad Prism (version 10 for masOS) (GraphPad Software, Boston, Massachusetts, United States). To analyse the differences in lesion area in the initial simultaneous co-inoculation experiment, a one-way analysis of variance (ANOVA) was done. Since repeated experiments were done for simultaneous and sequential co-inoculation experiments with the same treatments, when the data from the experiments were analysed together, experiment number was assigned as a factor (where applicable) to assess whether the experiment had a significant effect. To analyse the differences in lesion development, the data were transformed using a natural logarithm to homogenise the variances before simple linear equations were fitted to the data for lesion area against days post inoculation. The rates of lesion development in different treatments were analysed by comparing the slopes of the regression lines using a one-way ANOVA. To analyse the differences in lesion area, pycnidial production and percentage of *L. maculans* DNA in

lesions, two-way ANOVA tests were done. To analyse relative gene expression, the data were transformed using a common logarithm to homogenise the variances before they were subjected to two-way ANOVA. Tukey's HSD post-hoc tests were done to separate the means of treatments at a probability of 5% significance.

4.3 Results

4.3.1 Effects of simultaneous co-inoculation on lesion phenotype and composition of secondary metabolites produced by *L. maculans*

4.3.1.1 Phenotypic assessment of lesions at 26 days post inoculation (dpi)

There were significant differences in lesion area between different treatments ($F(3,458) = 690.10$, $P < 0.0001$). For the treatments 'Lb only' (24.6 mm^2) and 'Lm&Lb' (27.1 mm^2), there were no significant differences between them. However, the lesion area of the 'Lm only' (153.3 mm^2) treatment was significantly greater than that of all other treatments (Table 4.4, Table 4.5) (Figure 4.16). Representative images of cotyledons inoculated with different treatments are shown in Figure 4.17.

4.3.1.2 Assessment of the composition of secondary metabolites produced by *L. maculans*

There were maxima unique to the 'Lm only' treatment in the HPLC chromatograms at 16.3 and 16.8 min retention times, which were consistent with the retention time of sirodesmin PL from *in vitro* studies. However, these maxima were less than the limit of detection (70 mg/L). Therefore, HPLC fractions were taken at 16 – 17.5 min retention time to confirm presence or absence of sirodesmin PL using LC-MS.

In the HPLC chromatograms of these fractions, there were three unique maxima identified only in the 'Lm only' treatment, at 4.95, 5.03 and 5.11 min retention times. At 4.95 min retention time, the positive ion spectra showed ions detected at *m/z* 242.29, which could correspond to a monocation of a molecule with a molecular weight of 241.3 Da. These ions remain unidentified.

At 5.03 min retention time, the positive ion spectra showed ions detected at *m/z* 319.26 (Figure 4.18), which could correspond to a monocation of a molecule with a molecular weight of 318.4 Da.

Table 4.4: Statistical testing output for significant propability of the main effects of treatment on average lesion area (mm²) for different treatments in one simultaneous co-inoculation experiment.

One-way analysis of variance (ANOVA) test was done by selecting treatment as a factor.

Factor	*df*	F statistic	F probability
Treatment	3	690.10	< 0.0001

Table 4.5: Average lesion area (mm^2) on cotyledons inoculated with sterilised distilled water (SDW) for control, *Leptosphaeria maculans* only (Lm only), *Leptosphaeria biglobosa* only (Lb only) and *L. maculans* & *L. biglobosa* co-inoculated simultaneously (Lm&Lb) at 26 days post inoculation (dpi) from one simultaneous co-inoculation experiment.

Tukey's HSD tests were used to compare the mean lesion area between different treatments. Treatments that do not share a letter are considered significantly different ($P < 0.05$).

Treatment	Expt-1
SDW	0.0 **a**
Lm only	153.3 **c**
Lb only	24.6 **b**
Lm&Lb	27.1 **b**

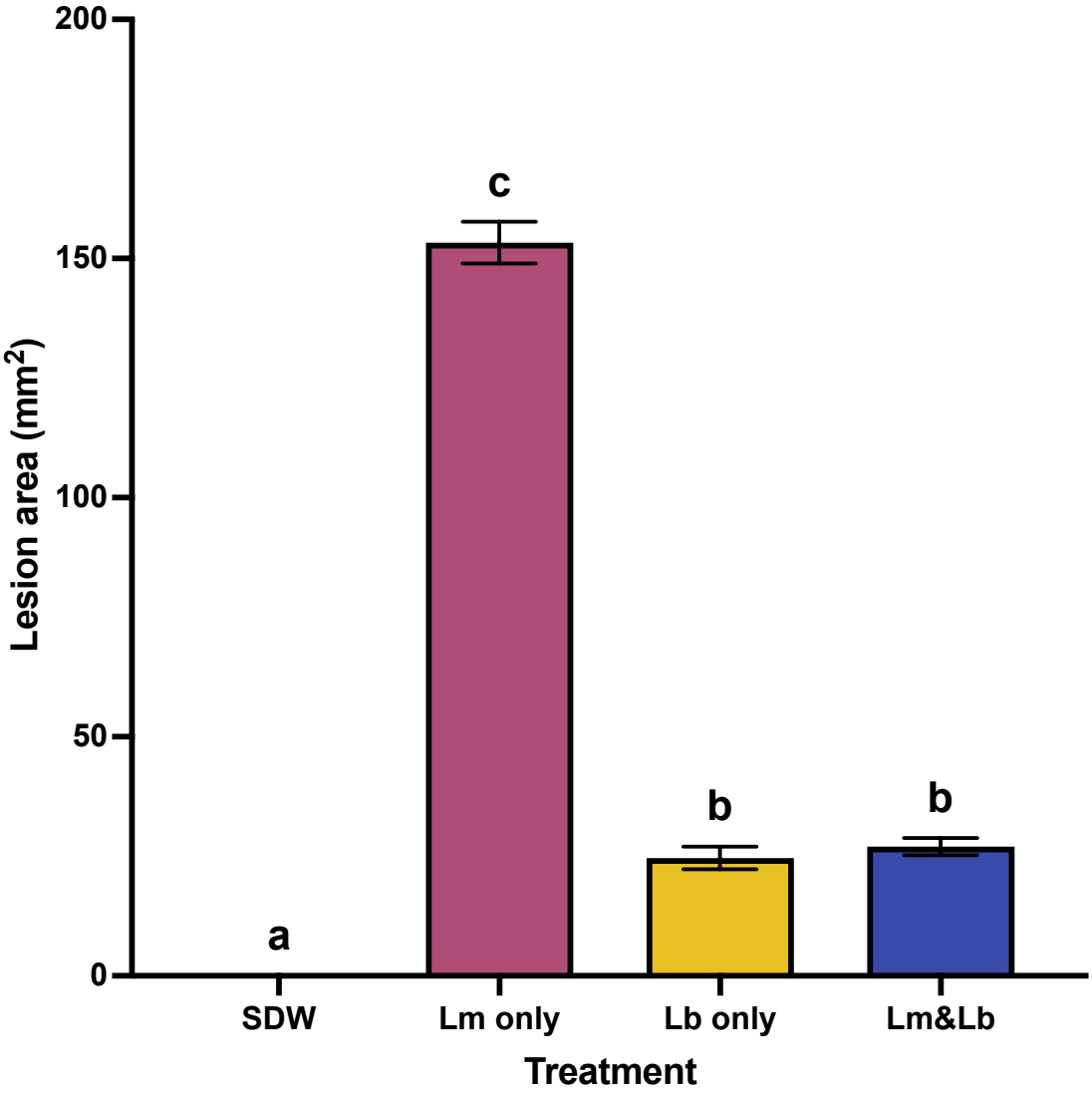

Figure 4.16: Average lesion area (mm²) on cotyledons inoculated with sterilised distilled water for control (SDW), *Leptosphaeria maculans* only (Lm only), *Leptosphaeria biglobosa* only (Lb only) and *L. maculans* & *L. biglobosa* co-inoculated simultaneously (Lm&Lb) at 26 days post inoculation (dpi).

Tukey's HSD tests were used to compare the mean lesion area between different treatments. Treatments that do not share a letter are considered significantly different ($P < 0.05$). Error bars show standard error of the mean (SEM) (461 d.f.). This figure was published in Fortune et al. (2024).

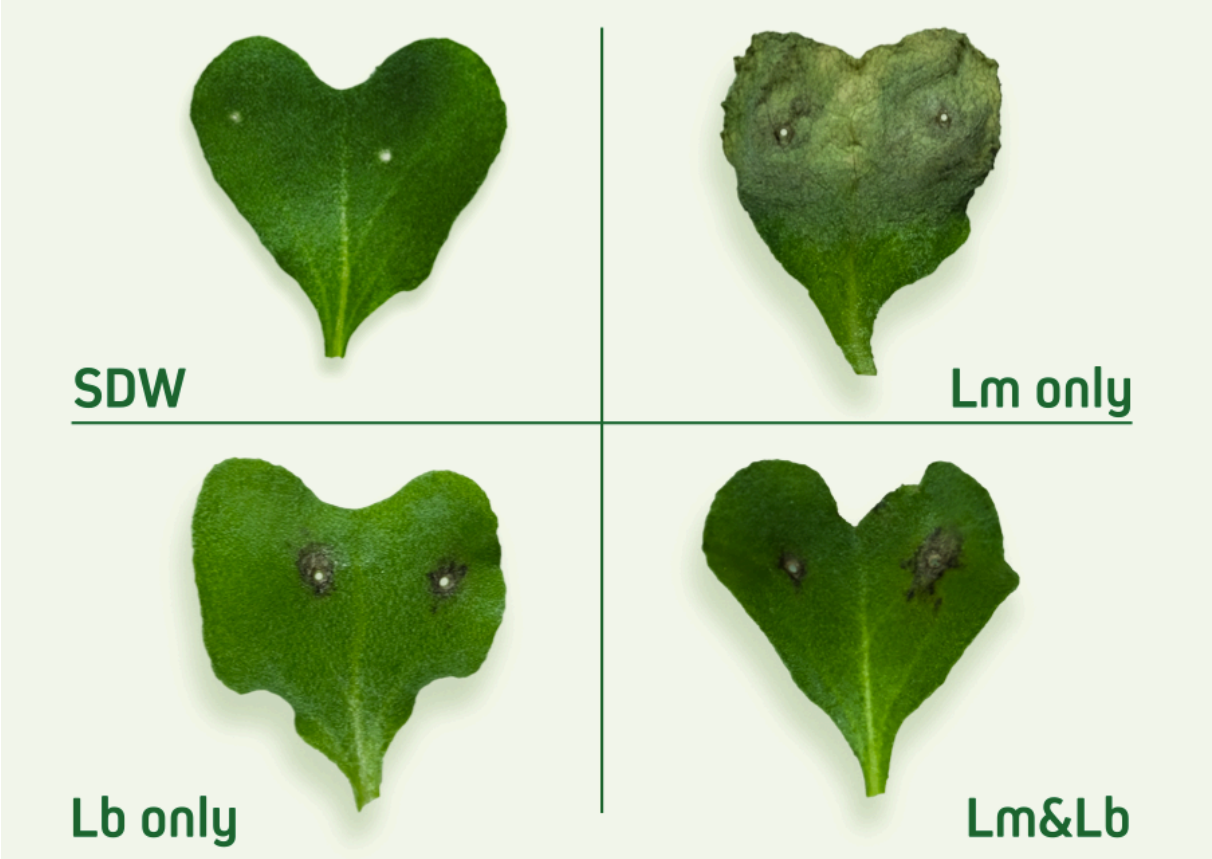

Figure 4.17: Representative images of lesions on cotyledons of oilseed rape (*Brassica napus*) cultivar Charger inoculated with sterilised distilled water for control (SDW), *Leptosphaeria maculans* only (Lm only), *Leptosphaeria biglobosa* only (Lb only) and *L. maculans* & *L. biglobosa* co-inoculated simultaneously (Lm&Lb) at 26 days post inoculation (dpi).

Cotyledons were photographed in standardised settings. This figure was published in Fortune et al. (2024).

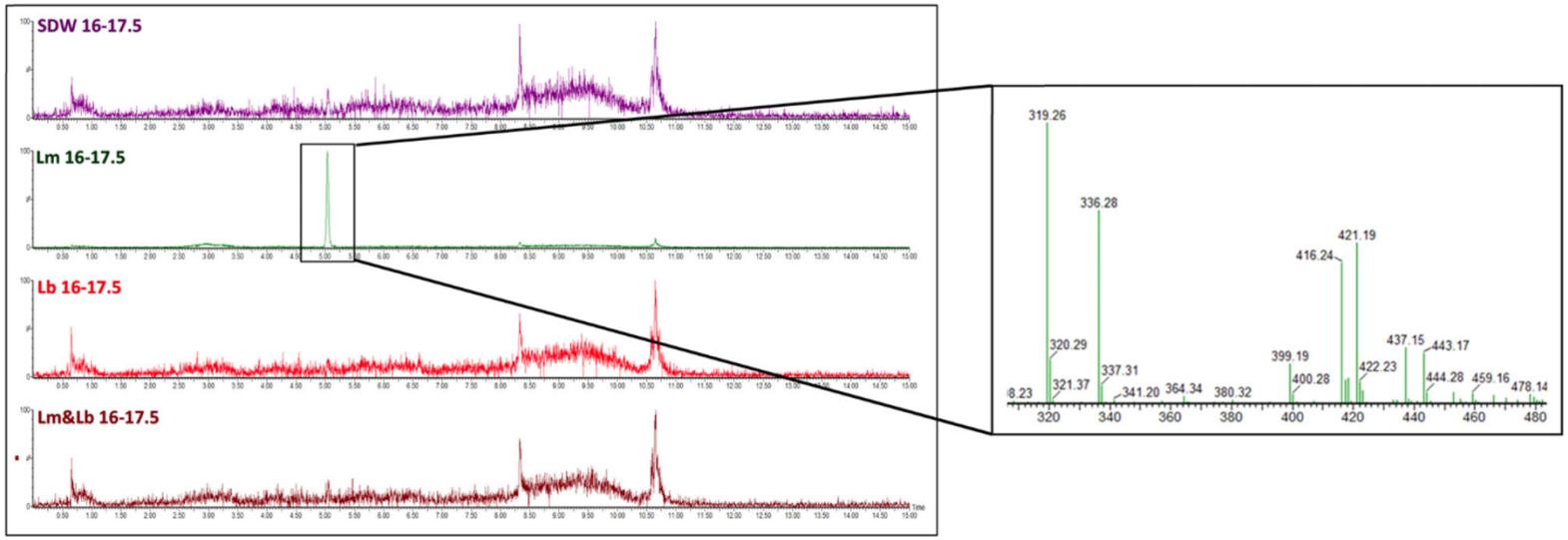

Figure 4.18: LC-MS chromatograms for *m/z* 319.2 of HPLC fractions taken at retention time 16 – 17.5 min of secondary metabolite extracts obtained from cotyledons of oilseed rape (*Brassica napus*) cultivar Charger inoculated with sterilised distilled water for control (SDW), *Leptosphaeria maculans* only (Lm only), *Leptosphaeria biglobosa* only (Lb only) or *L. maculans* & *L. biglobosa* co-inoculated simultaneously (Lm&Lb).

The unique maximum found only in the 'Lm only' treatment (Lm 16 – 17.5 sample) at 5.03 min retention time is highlighted and its positive ion spectra is zoomed in between *m/z* 310 and 480. This figure was published in Fortune et al. (2024).

Interestingly, phomamide is a secondary metabolite produced by *L. maculans* with a molecular weight of 318.4 Da and is considered to be one of the precursors of sirodesmin PL (Pedras & Yu, 2009).

At 5.11 min retention time, the positive ion spectra showed ions detected at *m/z* 487.18 (Figure 4.19), which could correspond to a monocation of a molecule with a molecular weight of 486.6 Da. Sirodesmin PL has a molecular weight of 486.6 Da (Elliott et al., 2007; Pedras & Yu, 2009; PubChem, 2024). In addition, the positive ion spectra (Figure 4.19) also showed detection of ions that could correspond to several of its adducts and molecular ions; sirodesmin PL lacking two sulphur atoms at *m/z* 424.33 $[M - S_2 + H]^+$, and its sodium, potassium and acetonitrile adducts at *m/z* 445.24 $[M - S_2 + Na]^+$, *m/z* 460.24 $[M - S_2 + K]^+$ and *m/z* 465.20 $[M - S_2 + CH_3CN]^+$, respectively. Additionally, ammonium adduct of sirodesmin PL was observed at *m/z* 504.25 $[M + NH_4]^+$ (Elliott et al., 2007; Pedras & Yu, 2009).

4.3.2 Effects of sequential co-inoculation on lesion development and lesion phenotype

Simple linear equations were fitted to describe the relationship between lesion area and days post inoculation (dpi) (Figure 4.20). There was no lesion development in the 'SDW' control at any time point. For 'Lb only', 'Lm&Lb', 'Lm+Lb-1', 'Lb+Lm-1', 'Lb+Lm-3' and 'Lb+Lm-5' treatments, lesion development progressed steadily from 7 dpi to 16 dpi (Figure 4.20 B, C, D, G, H, I). Interestingly, despite sharing a similar trend in lesion development with the rest of the treatments in this group, the 'Lm+Lb-1' treatment had smaller lesion areas at all time points. For 'Lm only', 'Lm+Lb-3' and 'Lm+Lb-5', lesion development did not progress significantly between 7 dpi and 10 dpi. However, a rapid increase in lesion area was observed between 10 dpi and 14 dpi for these treatments. The lesions kept expanding rapidly from 14 dpi to 16 dpi (Figure 4.20 A, E, F).

Slopes of the fitted simple linear equations were compared to assess the rates of lesion development between the different treatments. There were significant differences in the rates of lesion development between different treatments ($F(9,236) = 47.67$, $P < 0.0001$) (Table 4.6). The 'SDW' treatment was significantly different to all other treatments, since no lesion development was observed.

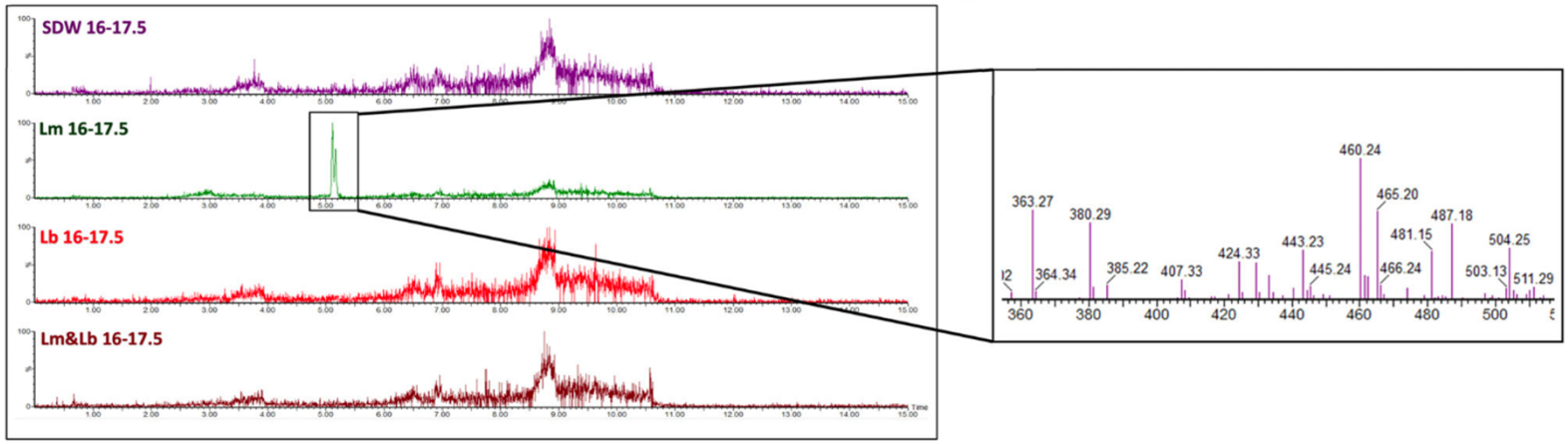

Figure 4.19: LC-MS chromatograms for *m/z* 487.2 of HPLC fractions taken at retention time 16 – 17.5 min of secondary metabolite extracts obtained from cotyledons of oilseed rape (*Brassica napus*) cultivar Charger inoculated with sterilised distilled water for control (SDW), *Leptosphaeria maculans* only (Lm only), *Leptosphaeria biglobosa* only (Lb only) or *L. maculans* & *L. biglobosa* co-inoculated simultaneously (Lm&Lb).

The unique maximum found only in the 'Lm only' treatment (Lm 16 – 17.5 sample) at 5.11 min retention time is highlighted and its positive ion spectra is zoomed in between *m/z* 360 and 510. This figure was published in Fortune et al. (2024).

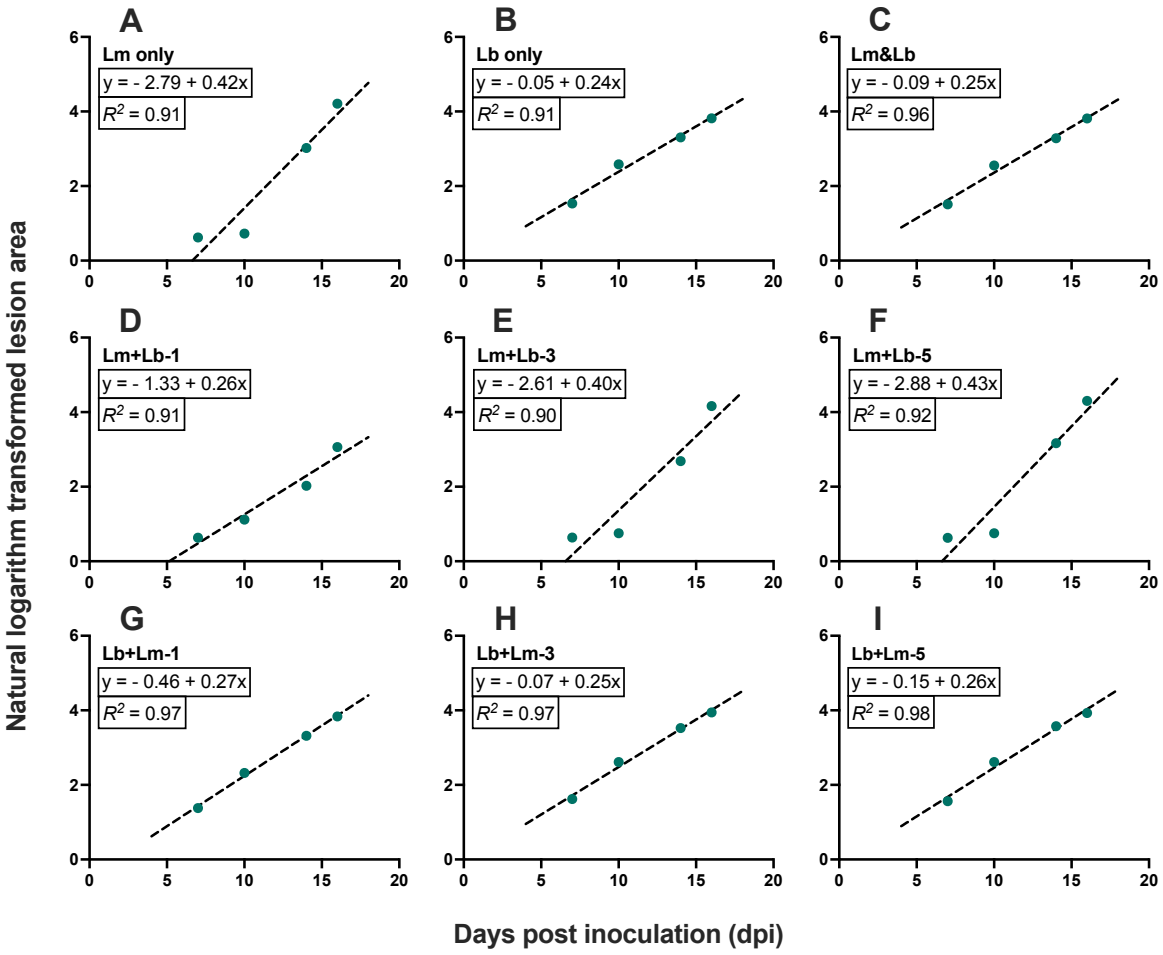

Figure 4.20: Simple linear equations (y = a + b*x) showing the relationships between the lesion area (natural logarithm transformed) and days post inoculation (dpi) from two experiments for different treatments.

Cotyledons of oilseed rape (*Brassica napus*) cultivar Charger were inoculated with; (A) *Leptosphaeria maculans* only (Lm only), (B) *Leptosphaeria biglobosa* only (Lb only), (C) *L. maculans* & *L. biglobosa* co-inoculated simultaneously (Lm&Lb), (D, E, F) initial inoculation with *L. maculans* followed by co-inoculation with *L. biglobosa* at 1, 3 or 5 days later (Lm+Lb-1, Lm+Lb-3, Lm+Lb-5) and (G, H, I) initial inoculation with *L. biglobosa* followed by co-inoculation with *L. maculans* at 1, 3 or 5 days later (Lb+Lm-1, Lb+Lm-3, Lb+Lm-5). Lesion areas were assessed at 7, 10, 14 and 16 dpi for all treatments (Lm only, Lb only, Lm+Lb-3, Lm+Lb-5, Lb+Lm-3, Lb+Lm-5, n = 24 each) (Lm+Lb-1, Lb+Lm-1, n = 32 each).

Table 4.6: The estimated parameter values of intercept (a) and slope (b) in the simple linear equation y = a + b*x fitted to describe the relationship between the natural logarithm transformed lesion area and days post inoculation (dpi) from two experiments for different treatments.

Cotyledons of oilseed rape (*Brassica napus*) were inoculated with; sterilised distilled water (control), *Leptosphaeria maculans* only (Lm only), *Leptosphaeria biglobosa* only (Lb only), *L. maculans* & *L. biglobosa* co-inoculated simultaneously (Lm&Lb), initial inoculation with *L. maculans* followed by co-inoculation with *L. biglobosa* at 1, 3 or 5 days later (Lm+Lb-1, Lm+Lb-3, Lm+Lb-5) and initial inoculation with *L. biglobosa* followed by co-inoculation with *L. maculans* at 1, 3 or 5 days later (Lb+Lm-1, Lb+Lm-3, Lb+Lm-5). Lesion areas were assessed at 7, 10, 14 and 16 dpi for all treatments. In order to compare the rate of lesion development, line parallel comparisons were done by using Tukey's HSD tests to compare the mean slope values between different treatments. Treatments that do not share a letter are considered significantly different ($P < 0.05$).

Treatment	Intercept (a)	Slope (b)	Line comparisons
SDW	0.00	0.00	**c**
Lm only	-2.79	0.42	**a**
Lb only	-0.05	0.24	**b**
Lm&Lb	-0.09	0.25	**b**
Lm+Lb-1	-1.33	0.26	**b**
Lm+Lb-3	-2.61	0.40	**a**
Lm+Lb-5	-2.88	0.43	**a**
Lb+Lm-1	-0.46	0.27	**b**
Lb+Lm-3	-0.07	0.25	**b**
Lb+Lm-5	-0.15	0.26	**b**

For the rate of lesion development (slope), there were no significant differences between 'Lb only' (0.24), 'Lm&Lb' (0.25), 'Lm+Lb-1' (0.26), 'Lb+Lm-1' (0.27), 'Lb+Lm-3' (0.25) and 'Lb+Lm-5' (0.26) (Table 4.6). There were no significant differences between treatments 'Lm only' (0.42), 'Lm+Lb-3' (0.40) and 'Lm+Lb-5' (0.43) (Table 4.6). Representative images of cotyledons inoculated with different treatments at four time points are shown in Figure 4.21. The analyses of individual experiments can be found in Appendix G.

There were no significant differences in the average lesion area at 16 dpi between different experiments ($F(1,44) = 0.31$, $P = 0.583$) (Table 4.7, Table 4.8). Therefore, the data from the two experiments were analysed together. The analyses of individual experiments can be found in Appendix G.

At 16 dpi, the average lesion areas were significantly different between different treatments ($F(9,44) = 57.38$ $P < 0.0001$). For the treatments 'Lb only' (45.0 mm^2), 'Lm&Lb' (44.5 mm^2), 'Lb+Lm-1' (45.8 mm^2), 'Lb+Lm-3' (51.0 mm^2) and 'Lb+Lm-5' (50.1 mm^2), there were no significant differences between them. For the treatments 'Lm only' (67.1 mm^2), 'Lm+Lb-3' (63.6 mm^2) and 'Lm+Lb-5' (73.4 mm^2), there were no significant differences between them. Interestingly, 'Lm+Lb-1' (20.6 mm^2) treatment was significantly different to all other treatments (Table 4.7, Table 4.8) (Figure 4.22). The interactions between experiments and treatments were not significant ($F(9,44) = 0.04$, $P = 0.999$).

There were differences in lesion phenotypes between different treatments. Lesion phenotype for 'Lm only', 'Lm+Lb-3' and 'Lm+Lb-5' appeared to be larger, grey and less defined than the lesion phenotype for 'Lb only', 'Lm&Lb', 'Lm+Lb-1', 'Lb+Lm-1', 'Lb+Lm-3' and 'Lb+Lm-5' which was smaller, darker and more defined (Figure 4.21).

4.3.3 Effects of sequential co-inoculation on pycnidial production on infected cotyledons

After removing the cotyledons at 19 dpi and incubating for 72 h, there were no differences between different experiments in density of mature pycnidia ($F(1,40) = 0.51$, $P = 0.481$) (Table 4.9, Table 4.10). Therefore, the data from the two experiments were analysed together. The analyses of individual experiments can be found in Appendix G.

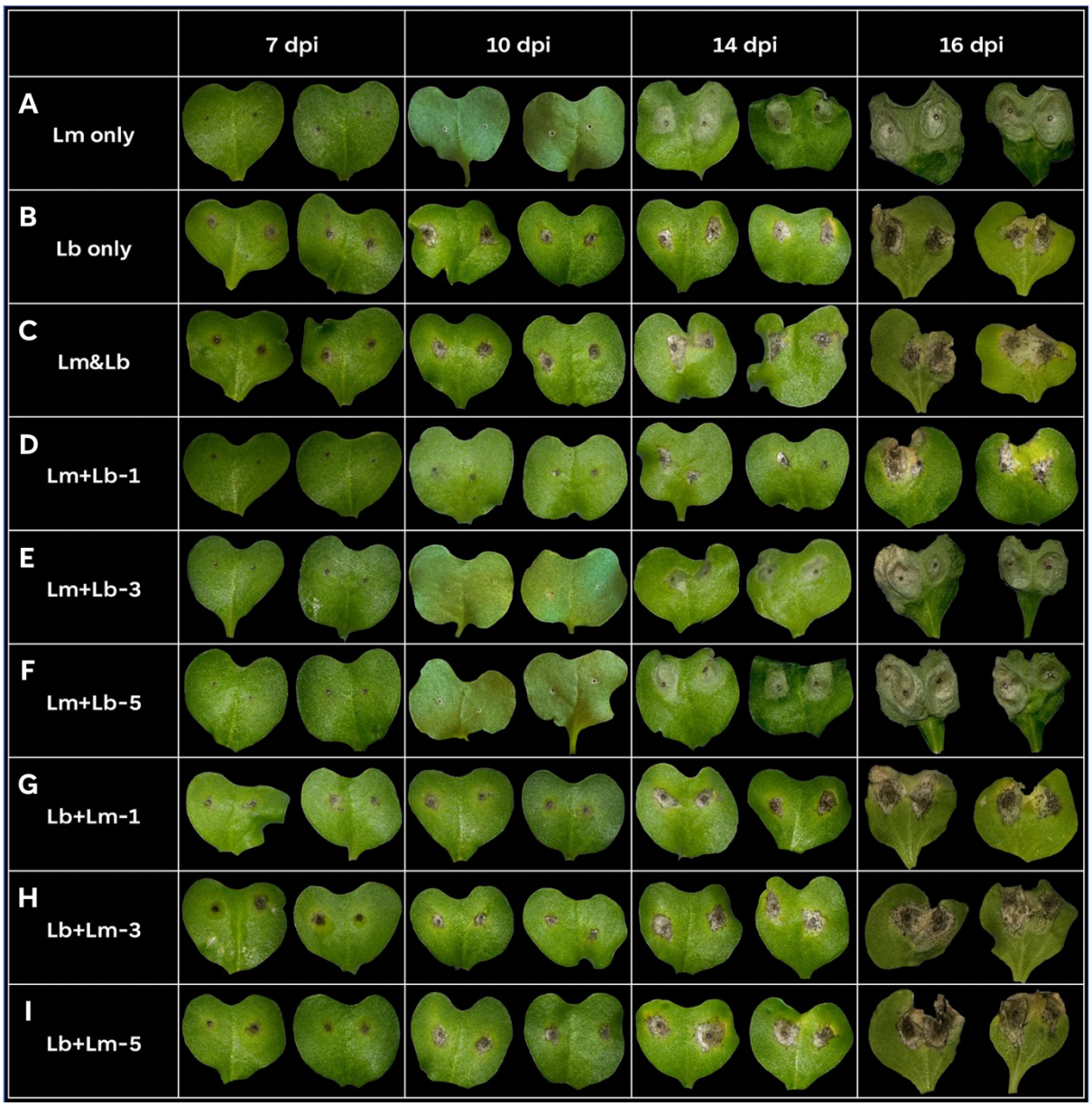

Figure 4.21: Representative images of lesions on cotyledons of oilseed rape (B*rassica napus*) cultivar Charger.

Plants were inoculated with; (A) *Leptosphaeria maculans* only (Lm only), (B) *Leptosphaeria biglobosa* only (Lb only), (C) *L. maculans* & *L. biglobosa* co-inoculated simultaneously (Lm&Lb), (D, E, F) initial inoculation with *L. maculans* followed by co-inoculation with *L. biglobosa* at 1, 3 or 5 days later (Lm+Lb-1, Lm+Lb-3, Lm+Lb-5) and (G, H, I) initial inoculation with *L. biglobosa* followed by co-inoculation with *L. maculans* at 1, 3 or 5 days later (Lb+Lm-1, Lb+Lm-3, Lb+Lm-5). Lesion phenotypes were assessed at 7, 10, 14 and 16 days post inoculation (dpi). Cotyledons were photographed in standardised settings.

Table 4.7: Statistical testing outputs for significant probability of the main effects of experiment, treatment and the two-way interactions on lesion area (mm^2) from two experiments for different treatments.

Two-way analysis of variance (ANOVA) tests were done by selecting experiment number and treatment as factors.

Factor	*df*	F statistic	F probability
Experiment	1	0.31	= 0.583
Treatment	9	57.38	< 0.0001
Experiment x Treatment	9	0.04	= 0.999

Table 4.8: Average lesion area (mm²) on cotyledons from two experiments for different treatments.

Cotyledons of oilseed rape (*Brassica napus*) were inoculated with sterilised distilled water (control), *Leptosphaeria maculans* only (Lm only), *Leptosphaeria biglobosa* only (Lb only), *L. maculans* & *L. biglobosa* co-inoculated simultaneously (Lm&Lb), initial inoculation with *L. maculans* followed by co-inoculation with *L. biglobosa* at 1, 3 or 5 days later (Lm+Lb-1, Lm+Lb-3, Lm+Lb-5) and initial inoculation with *L. biglobosa* followed by co-inoculation with *L. maculans* at 1, 3 or 5 days later (Lb+Lm-1, Lb+Lm-3, Lb+Lm-5). Final lesion area was measured at 16 days post inoculation (dpi). Tukey's HSD tests were used to compare the mean lesion area between different treatments. Treatments that do not share a letter are considered significantly different ($P < 0.05$).

Treatment	Expt-1	Expt-2	Mean
SDW	0.0 **g**	0.0 **g**	0.0 **d**
Lm only	68.2 **abc**	66.1 **abcd**	67.1 **a**
Lb only	45.7 **de**	44.3 **de**	45.0 **b**
Lm&Lb	45.3 **de**	43.6 **e**	44.5 **b**
Lm+Lb-1	21.6 **f**	19.6 **fg**	20.6 **c**
Lm+Lb-3	64.2 **ae**	63.0 **ae**	63.6 **a**
Lm+Lb-5	72.8 **ab**	74.1 **a**	73.4 **a**
Lb+Lm-1	45.9 **de**	45.7 **de**	45.8 **b**
Lb+Lm-3	51.0 **be**	51.0 **be**	51.0 **b**
Lb+Lm-5	51.4 **be**	48.8 **ce**	50.1 **b**
Expt mean	46.6 **a**	45.6 **a**	-

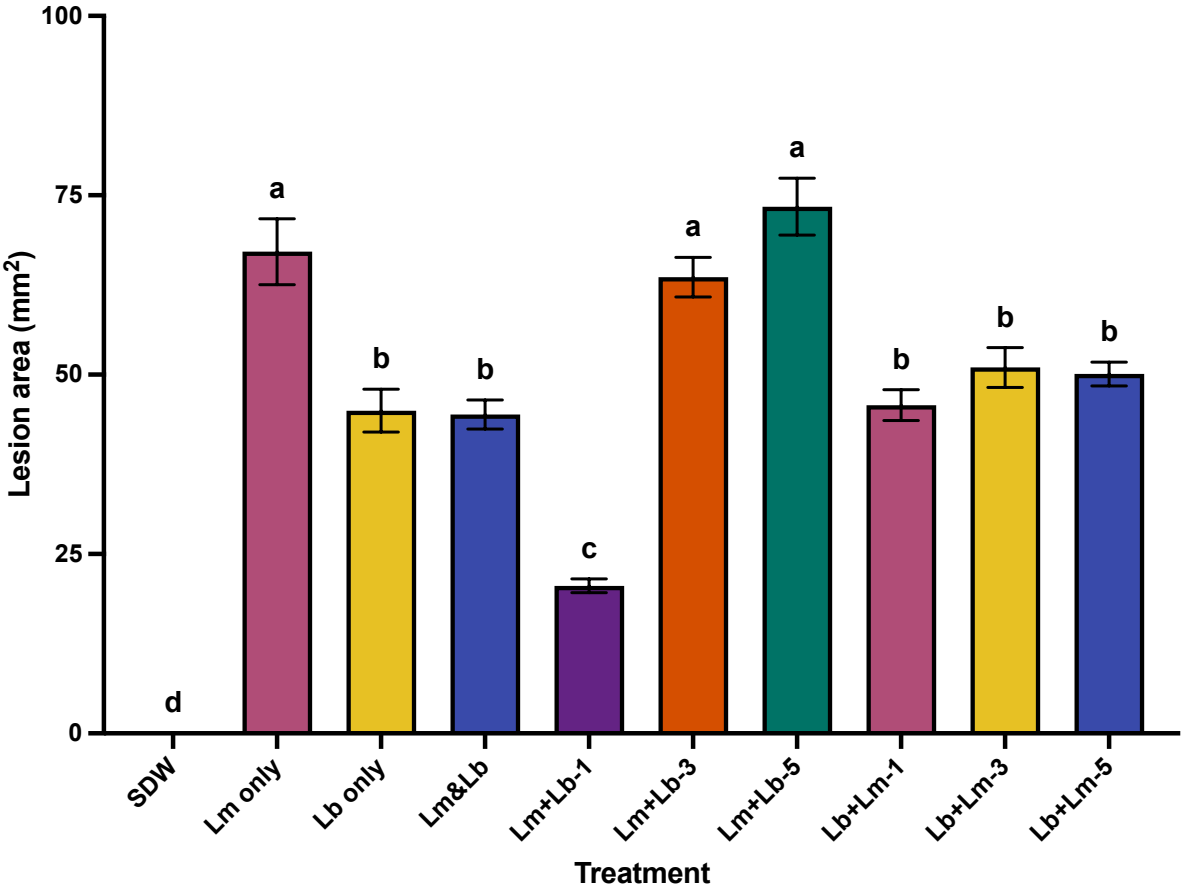

Figure 4.22: Average lesion area (mm²) from two experiments for different treatments. Cotyledons of oilseed rape (*Brassica napus*) were inoculated with; sterilised distilled water (control), *Leptosphaeria maculans* only (Lm only), *Leptosphaeria biglobosa* only (Lb only), *L. maculans* & *L. biglobosa* co-inoculated simultaneously (Lm&Lb), initial inoculation with *L. maculans* followed by co-inoculation with *L. biglobosa* at 1, 3 or 5 days later (Lm+Lb-1, Lm+Lb-3, Lm+Lb-5) and initial inoculation with *L. biglobosa* followed by co-inoculation with *L. maculans* at 1, 3 or 5 days later (Lb+Lm-1, Lb+Lm-3, Lb+Lm-5). Final lesion area was measured at 16 days post inoculation (dpi). Tukey's HSD tests were used to compare the mean lesion area between different treatments. Treatments that do not share a letter are considered significantly different ($P < 0.05$). Error bars show standard error of the mean (SEM) (44 d.f.).

Table 4.9: Statistical testing outputs for significant probability of the main effects of experiment, treatment and the two-way interactions on density of pycnidial production (Number of mature pycnidia/mm^2×10^{-1}) from two experiments for different treatments. Two-way analysis of variance (ANOVA) tests were done by selecting experiment number and treatment as factors.

Factor	*df*	F statistic	F probability
Experiment	1	0.51	= 0.481
Treatment	9	550.40	< 0.0001
Experiment x Treatment	9	0.47	= 0.885

Table 4.10: Average density of pycnidial production (Number of mature pycnidia/mm^2×10^{-1}) from two experiments for different treatments.

Cotyledons of oilseed rape (*Brassica napus*) were inoculated with; sterilised distilled water (control), *Leptosphaeria maculans* only (Lm only), *Leptosphaeria biglobosa* only (Lb only), *L. maculans* & *L. biglobosa* co-inoculated simultaneously (Lm&Lb), initial inoculation with *L. maculans* followed by co-inoculation with *L. biglobosa* at 1, 3 or 5 days later (Lm+Lb-1, Lm+Lb-3, Lm+Lb-5) or initial inoculation with *L. biglobosa* followed by co-inoculation with *L. maculans* at 1, 3 or 5 days later (Lb+Lm-1, Lb+Lm-3, Lb+Lm-5). Cotyledons were removed at 19 days post inoculation (dpi) and incubated at 20°C in darkness for 72 h before microscopic assessment. Tukey's HSD tests were used to compare the mean density of pycnidial production between different treatments. Treatments that do not share a letter are considered significantly different ($P < 0.05$).

Treatment	Expt-1	Expt-2	Mean
SDW	0 **b**	0 **b**	0 **b**
Lm only	37 **a**	36 **a**	37 **a**
Lb only	0 **b**	0 **b**	0 **b**
Lm&Lb	0 **b**	0 **b**	0 **b**
Lm+Lb-1	0 **b**	0 **b**	0 **b**
Lm+Lb-3	34 **a**	36 **a**	35 **a**
Lm+Lb-5	35 **a**	37 **a**	36 **a**
Lb+Lm-1	0 **b**	0 **b**	0 **b**
Lb+Lm-3	0 **b**	0 **b**	0 **b**
Lb+Lm-5	0 **b**	0 **b**	0 **b**
Expt mean	11 **a**	11 **a**	-

The average pycnidial density (number of pycnidia/$mm^2 \times 10^{-1}$ area) was significantly different between different treatments ($F(9,40) = 550.40$, $P < 0.0001$). For the treatments 'Lb only', 'Lm&Lb', 'Lm+Lb-1', 'Lb+Lm-1', 'Lb+Lm-3' and 'Lb+Lm-5', there were no significant differences between them. Although there were lesions that developed for these treatments, no production of mature pycnidia was observed in microscopic analyses.

For the treatments 'Lm only' (37 mature pycnidia/$mm^2 \times 10^{-1}$), 'Lm+Lb-3' (35 mature pycnidia/$mm^2 \times 10^{-1}$) and 'Lm+Lb-5' (36 mature pycnidia/$mm^2 \times 10^{-1}$), there were no significant differences between them (Table 4.9, Table 4.10) (Figure 4.23). The interactions between experiment and treatment were not significant ($F(9,40) = 0.47$, $P = 0.885$) (Table 4.9). Representative microscopy images of lesion areas near the inoculation sites on cotyledons inoculated with different treatments are shown in Figure 4.24.

4.3.4 Testing different methods for DNA extraction from oilseed rape cotyledons extensively colonised by *L. maculans* and/or *L. biglobosa*

Different kits and protocols were tested in order to optimise a robust method for DNA extraction from extensively colonised cotyledons to assess relative percentages of *Leptosphaeria* species DNA in lesions.

Using the DNAmite Plant DNA Extraction Kit (Microzone Ltd.) for both groups of samples, low quality (mean A260/A230 ratio of 0.38 for both groups) and quantity (mean Qubit concentration of 27.4 ng/μL for Group 1 and 21.4 ng/μL for Group 2) of DNA were extracted (Table 4.11). The DNA samples obtained using this kit were not suitable for qPCR analyses.

Using the DNeasy Plant Pro Kit (Qiagen) for both groups of samples, low quality (mean A260/A230 ratio of 0.41 for Group 1 and 0.29 for Group 2) and low quantity (mean Qubit concentration of < 0.4 ng/μL for both groups) of DNA were extracted (Table 4.11). The DNA samples obtained using this kit were not suitable for qPCR analyses.

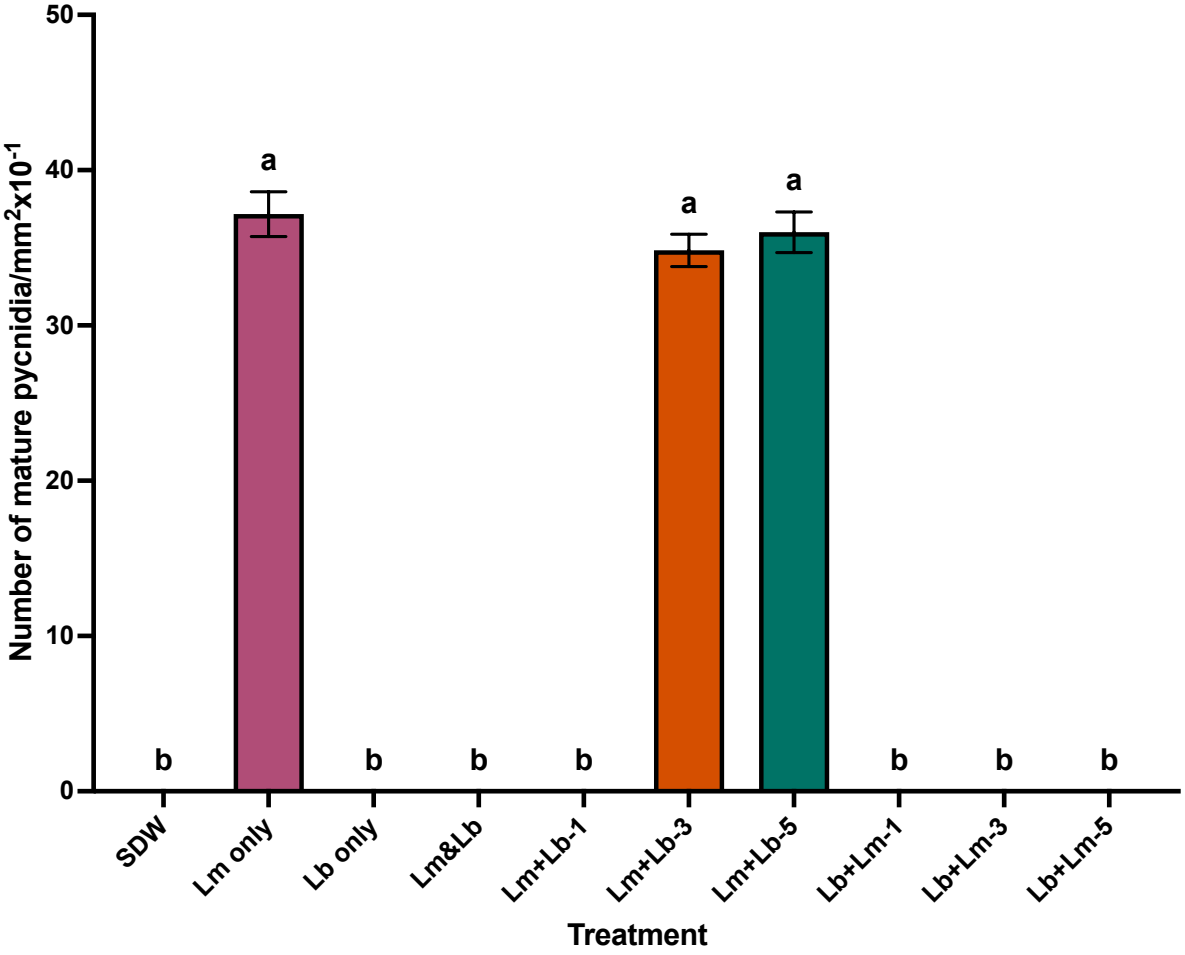

Figure 4.23: Average density of pycnidial production (Number of mature pycnidia/mm²×10⁻¹) from two experiments for different treatments.

Cotyledons of oilseed rape (*Brassica napus*) were inoculated with; sterilised distilled water (control), *Leptosphaeria maculans* only (Lm only), *Leptosphaeria biglobosa* only (Lb only), *L. maculans* & *L. biglobosa* co-inoculated simultaneously (Lm&Lb), initial inoculation with *L. maculans* followed by co-inoculation with *L. biglobosa* at 1, 3 or 5 days later (Lm+Lb-1, Lm+Lb-3, Lm+Lb-5) or initial inoculation with *L. biglobosa* followed by co-inoculation with *L. maculans* at 1, 3 or 5 days later (Lb+Lm-1, Lb+Lm-3, Lb+Lm-5). Cotyledons were removed at 19 days post inoculation (dpi) and incubated at 20°C in darkness for 72 h before microscopic assessment. Tukey's HSD tests were used to compare the mean density of pycnidial production between different treatments. Treatments that do not share a letter are considered significantly different ($P < 0.05$). Error bars show standard error of the mean (SEM) (40 d.f.).

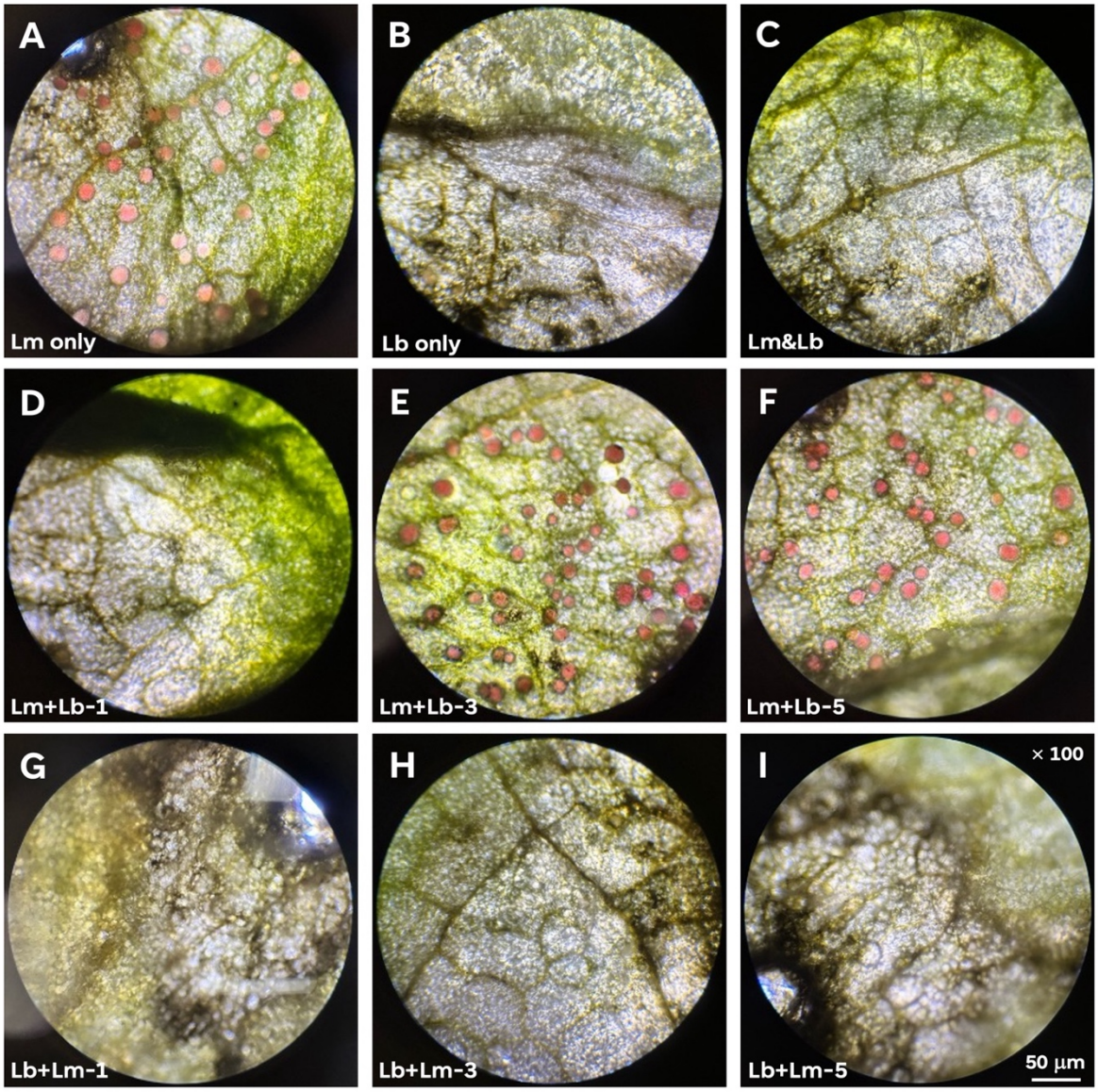

Figure 4.24: Representative microscopy images (at × 100 magnification) of lesion areas (0.1 mm²) near the inoculation site showing production of pycnidia in different treatments.

Cotyledons of oilseed rape (*Brassica napus*) cultivar Charger were inoculated with; (A) *Leptosphaeria maculans* only (Lm only), (B) *Leptosphaeria biglobosa* only (Lb only), (C) *L. maculans* & *L. biglobosa* co-inoculated simultaneously (Lm&Lb), (D, E, F) initial inoculation with *L. maculans* followed by co-inoculation with *L. biglobosa* at 1, 3 or 5 days later (Lm+Lb-1, Lm+Lb-3, Lm+Lb-5) or (G, H, I) initial inoculation with *L. biglobosa* followed by co-inoculation with *L. maculans* at 1, 3 or 5 days later (Lb+Lm-1, Lb+Lm-3, Lb+Lm-5). Cotyledons were removed at 19 days post inoculation (dpi) and incubated at 20°C in darkness for 72 h before microscopic assessment. Production of mature pycnidia (circular structures with pink cirri) was observed only in (A) 'Lm only', (E) 'Lm+Lb-3' and (F) 'Lm+Lb-5' treatments.

Table 4.11: Quality and quantity of DNA extracted from cotyledons of oilseed rape (*Brassica napus*) extensively colonised by *Leptosphaeria maculans* and/or *Leptosphaeria biglobosa* using different DNA extraction methods. Samples were considered in two groups: cotyledons showing characteristic symptoms of severe infection by *L. maculans* (Group 1) or *L. biglobosa* (Group 2).

Kit/Protocol	Sample group	Replicates	Mean A260/A280	Mean A260/A230	Mean concentration – NanoDrop (ng/µL)	Mean concentration – Qubit (ng/µL)
DNAmite Plant DNA Extraction Kit[a]	1	3	1.88	0.38	99.7	27.4
	2	3	1.43	0.38	90.6	21.4
DNeasy Plant Pro Kit[b]	1	3	1.78	0.41	9.9	< 4.0
	2	3	1.48	0.29	6.9	< 4.0
Modified spore tape DNA protocol version one[c]	1	2	1.96	1.64	1221.2	89.3
	2	2	1.61	0.90	1726.8	92.7
Modified spore tape DNA protocol version two[c]	1	2	1.92	1.70	1144.4	72.3
	2	2	1.79	1.30	390.5	6.9
Sorbitol pre-wash protocol[d]	1	3	1.93	2.02	3988.3	325.0
	2	3	2.08	2.10	2259.4	201.7

[a] Microzone Ltd., Stourbridge, United Kingdom.

[b] Qiagen, Venlo, The Netherlands.

[c] Huang at al., 2011; Kaczmarek et al., 2009.

[d] Inglis et al., 2018.

Version one of the modified spore tape DNA extraction protocol (Huang et al., 2011; Kaczmarek et al., 2009) for both sample groups yielded low quality (mean A260/A230 ratio of 1.64 for Group 1 and 0.90 for Group 2) but acceptable quantity (mean Qubit concentration of 89.3 ng/μL for Group 1 and 92.7 ng/μL for Group 2) of DNA (Table 4.11). Interestingly, the DNA quality check metrics of Group 1 samples were closer to be considered 'pure' compared to Group 2 samples. Ultimately, the DNA samples obtained using version one of this protocol were not suitable for qPCR analyses.

Version two of the modified spore tape DNA extraction protocol (Huang et al., 2011; Kaczmarek et al., 2009) yielded DNA of low quality for both sample groups (mean A260/A230 ratio of 1.70 for Group 1 and 1.30 for Group 2), acceptable quantity for Group 1 (mean Qubit concentration of 72.3 ng/μL) and low quantity for Group 2 (mean Qubit concentration of 6.9 ng/μL) (Table 4.11). Interestingly, once again, the DNA quality check metrics of Group 1 samples were closer to be considered 'pure' compared to Group 2 samples. Ultimately, the DNA samples obtained using version two of this protocol were not suitable for qPCR analyses. Additionally though, the DNA quality check metrics of Group 2 samples were closer to be considered 'pure' in version two as opposed to version one of the protocol.

The sorbitol pre-wash protocol (Inglis et al., 2018) for both sample groups yielded high quality (mean A260/A230 ratio of 2.02 for Group 1 and 2.10 for Group 2) and high quantity (mean Qubit concentration of 325.0 ng/μL for Group 1 and 201.7 ng/μL for Group 2) of DNA (Table 4.11). The DNA samples obtained using this protocol were suitable for qPCR analyses. Therefore, this method was used for DNA extraction from cotyledons of oilseed rape extensively colonised by *L. maculans* and/or *L. biglobosa*, which were subsequently used for qPCR analyses.

4.3.5 Effects of sequential co-inoculation on relative growth of the pathogens

There were no significant differences in the average percentage of *L. maculans* DNA on total extracted DNA of *Leptosphaeria* species from lesions between different experiments ($F(1,70) = 0.01$, $P = 0.938$) (Table 4.12, Table 4.13). Therefore, the data from the two experiments were analysed together. The analyses of individual experiments can be found in Appendix G.

Table 4.12: Statistical testing outputs for significant probability of the main effects of experiment, treatment and the two-way interactions on percentage *Leptosphaeria maculans* DNA (%) from two experiments for different treatments.

Two-way analysis of variance (ANOVA) tests were done by selecting experiment number and treatment as factors.

Factor	*df*	F statistic	F probability
Experiment	1	0.01	= 0.938
Treatment	8	18648.00	< 0.0001
Experiment x Treatment	8	1.16	= 0.337

Table 4.13: Average percentage of *Leptosphaeria maculans* DNA (%) in total DNA extracted from inoculated cotyledons from two experiments for different treatments.

Cotyledons of oilseed rape (*Brassica napus*) were inoculated with; sterilised distilled water (control), *Leptosphaeria maculans* only (Lm only), *Leptosphaeria biglobosa* only (Lb only), *L. maculans* & *L. biglobosa* co-inoculated simultaneously (Lm&Lb), initial inoculation with *L. maculans* followed by co-inoculation with *L. biglobosa* at 1, 3 or 5 days later (Lm+Lb-1, Lm+Lb-3, Lm+Lb-5) or initial inoculation with *L. biglobosa* followed by co-inoculation with *L. maculans* at 1, 3 or 5 days later (Lb+Lm-1, Lb+Lm-3, Lb+Lm-5). Cotyledons were removed at 19 days post inoculation (dpi). Tukey's HSD tests were used to compare the mean percentage of *L. maculans* DNA between different treatments. Treatments that do not share a letter are considered significantly different ($P < 0.05$).

Treatment	Expt-1	Expt-2	Mean
Lm only	100.0 **a**	100.0 **a**	100.0 **a**
Lb only	0.0 **b**	0.0 **b**	0.0 **b**
Lm&Lb	1.8 **b**	2.0 **b**	1.9 **b**
Lm+Lb-1	1.4 **b**	1.9 **b**	1.6 **b**
Lm+Lb-3	97.3 **a**	98.3 **a**	97.8 **a**
Lm+Lb-5	98.6 **a**	97.1 **a**	97.9 **a**
Lb+Lm-1	1.1 **b**	1.1 **b**	1.1 **b**
Lb+Lm-3	1.1 **b**	0.7 **b**	0.9 **b**
Lb+Lm-5	0.6 **b**	0.9 **b**	0.8 **b**
Expt mean	33.5 **a**	33.6 **a**	-

At 19 dpi, the average percentage of *L. maculans* DNA in total DNA of *Leptosphaeria* species extracted from lesions was significantly different between different treatments ($F(8,70) = 18648.00$, $P < 0.0001$). For the treatments 'Lb only' (0.0 %), 'Lm&Lb' (1.9 %), 'Lm+Lb-1' (1.6 %), 'Lb+Lm-1' (1.1 %), 'Lb+Lm-3' (0.9 %) and 'Lb+Lm-5' (0.8 %), there were no significant differences between them. For the treatments 'Lm only' (100.00 %), 'Lm+Lb-3' (97.8 %) and 'Lm+Lb-5' (97.9 %), there were no significant differences between them (Table 4.12, Table 4.13) (Figure 4.25). The interactions between experiments and treatments were not significant ($F(8,70) = 1.16$, $P = 0.337$) (Table 4.12).

4.3.6 Effects of sequential co-inoculation on *Brassica napus* defence responses

Overall, there were significant differences in relative expression of genes related to *Brassica napus* defence responses between different experiments. However, the expressions of all four genes at all three time points in different experiments were not significantly different in the SDW (control) treatment. Therefore, the data from the two experiments were analysed together. The analyses of individual experiments can be found in Appendix G.

There were significant differences in relative expression of the *PR-1* gene in different treatments at 2 dpi ($F(1,3) = 105.20$, $P < 0.0001$) (Table 4.14) (Figure 4.26). All of the remaining treatments were significantly different from each other, with 'Lm&Lb' resulting in the greatest upregulation of this gene, followed by 'Lb only', 'Lm only' and 'SDW', respectively.

There were also significant differences in relative expression of the *PR-1* gene in different treatments at 4 dpi ($F(1,5) = 996.50$, $P < 0.0001$) (Table 4.14) (Figure 4.26). For the treatments 'SDW', 'Lm only' and 'Lm+Lb-3', there were no significant differences between them, with all resulting in a very small upregulation. All of the remaining treatments were significantly different from each other, with 'Lb only' resulting in the greatest upregulation of this gene, followed by 'Lm&Lb' and 'Lb+Lm-3', respectively.

Similarly, there were significant differences in relative expression of the *PR-1* gene in different treatments at 6 dpi ($F(1,5) = 662.80$, $P < 0.0001$) (Table 4.14) (Figure 4.26).

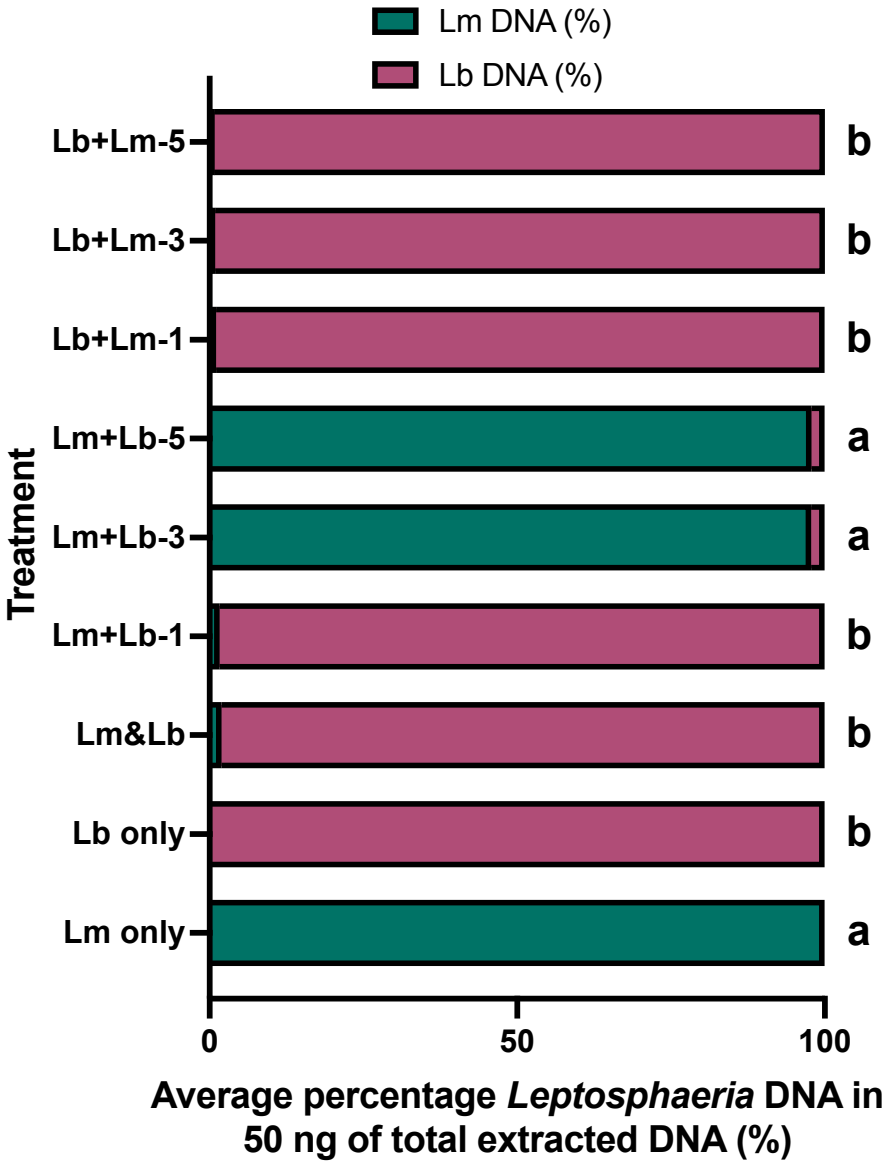

Figure 4.25: Average percentage of *Leptosphaeria* species DNA (%) in cotyledons from two experiments for different treatments.

Cotyledons of oilseed rape (*Brassica napus*) were inoculated with; sterilised distilled water (control), *Leptosphaeria maculans* only (Lm only), *Leptosphaeria biglobosa* only (Lb only), *L. maculans* & *L. biglobosa* co-inoculated simultaneously (Lm&Lb), initial inoculation with *L. maculans* followed by co-inoculation with *L. biglobosa* at 1, 3 or 5 days later (Lm+Lb-1, Lm+Lb-3, Lm+Lb-5) or initial inoculation with *L. biglobosa* followed by co-inoculation with *L. maculans* at 1, 3 or 5 days later (Lb+Lm-1, Lb+Lm-3, Lb+Lm-5). Cotyledons were removed at 19 days post inoculation (dpi). Tukey's HSD tests were used to compare the mean percentages of *L. maculans* DNA in total extracted DNA of both *Leptosphaeria* species between different treatments. Treatments that do not share a letter are considered significantly different ($P < 0.05$) (70 d.f.).

Table 4.14: Statistical testing outputs for significant probability of the main effects of experiment, treatment and the two-way interactions on relative expression of *PR-1* gene from two experiments for different treatments at 2, 4 or 6 days post inoculation (dpi).

Two-way analysis of variance (ANOVA) tests were done by selecting experiment number and treatment as factors.

Days post inoculation (dpi)	Factor	*df*	F statistic	F probability
2 dpi	Experiment	1	0.02	= 0.900
	Treatment	3	105.20	< 0.0001
	Experiment x Treatment	3	2.59	= 0.089
4 dpi	Experiment	1	85.05	< 0.0001
	Treatment	5	996.80	< 0.0001
	Experiment x Treatment	5	17.27	< 0.0001
6 dpi	Experiment	1	51.90	< 0.0001
	Treatment	5	662.80	< 0.0001
	Experiment x Treatment	5	11.95	< 0.0001

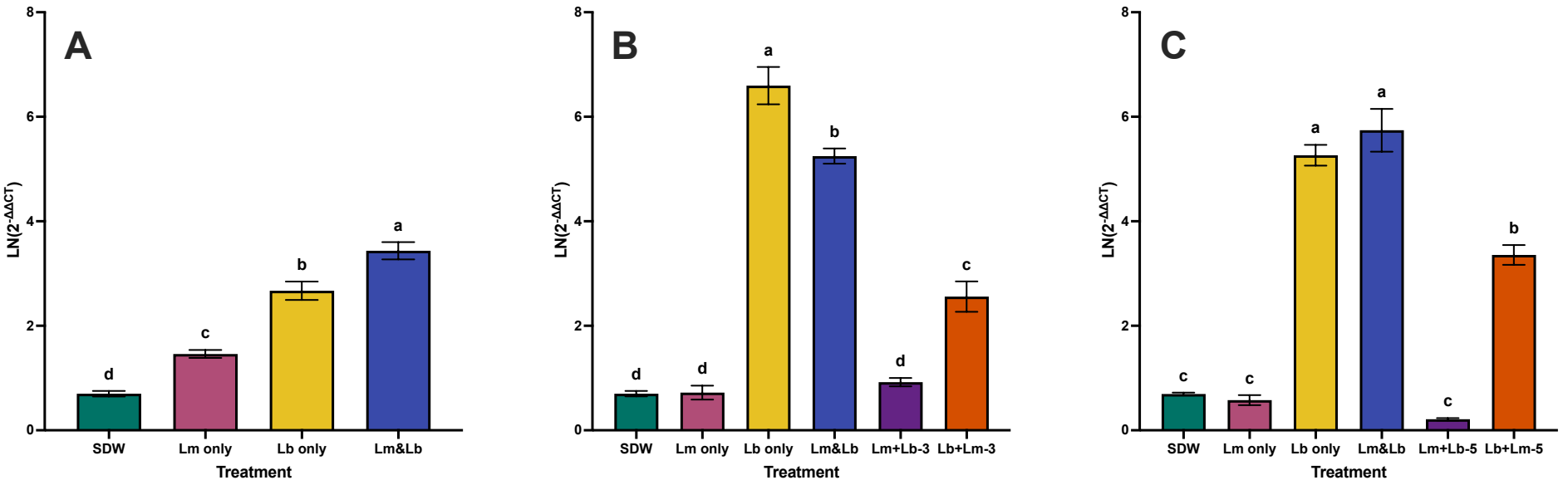

Figure 4.26: Relative expression of the *PR-1* gene in cotyledons obtained from two experiments examining interactions between *Leptosphaeria maculans* and *L. biglobosa* inoculated onto cotyledons of oilseed rape (*Brassica napus*).

Cotyledons were inoculated with Sterilised Distilled Water (SDW) for control, *Leptosphaeria maculans* only (Lm only), *Leptosphaeria biglobosa* only (Lb only), *L. maculans* & *L. biglobosa* co-inoculated simultaneously (Lm&Lb), initial inoculation with *L. maculans* followed by co-inoculation with *L. biglobosa* sequentially at 3 or 5 days later (Lm+Lb-3, Lm+Lb-5) or initial inoculation with *L. biglobosa* followed by sequential co-inoculation with *L. maculans* sequentially at 3 or 5 days later (Lb+Lm-3, Lb+Lm-5) at (A) 2 days post inoculation (dpi), (B) 4 dpi and (C) 6 dpi. Tukey's HSD tests were used to separate the mean relative expression of the *PR-1* gene in across different treatments. Columns that do not share a letter are considered significantly different ($P < 0.05$). Error bars show standard error of the mean (SEM) (2 dpi 23 d.f., 4 dpi 35 d.f., 6 dpi 35 d.f.).

For the treatments ‘SDW’, ‘Lm only’ and ‘Lm+Lb-5’, there were no significant differences between them, with all resulting in a very small upregulation. For the treatments ‘Lb only’ and ‘Lm&Lb’, there were no significant differences between them, both resulting in the greatest upregulation of this gene, followed by ‘Lb+Lm-5’, which was significantly different to all other treatments.

In summary, ‘Lb only’ and ‘Lm&Lb’ treatments resulted in the greatest upregulation of the *PR-1* gene at all time points. Additionally, this upregulation was also detected in sequential co-inoculation treatments but only where *L. biglobosa* was the first pathogen to be inoculated (Lb+Lm-3 and Lb+Lm-5) (Figure 4.26).

There were significant differences in relative expression of the *PDF-1.2* gene in different treatments at 2 dpi ($F(1,3) = 51.77$, $P < 0.0001$) (Table 4.15) (Figure 4.27). ‘Lm only’ and ‘SDW’ resulted in the greatest upregulation of this gene, which were greater than ‘Lm&Lb’ but not significantly different to ‘Lb only’.

There were also significant differences in relative expression of the *PDF-1.2* gene in different treatments at 4 dpi ($F(1,5) = 77.02$, $P < 0.0001$) (Table 4.15) (Figure 4.27). For the treatments ‘SDW’, ‘Lm only’, ‘Lb only’ and ‘Lm&Lb’, there were no significant differences between them, with all resulting in a very small upregulation. ‘Lm+Lb-3’ resulted in the greatest upregulation of this gene, which was significantly greater than any other treatment. This was followed by ‘Lb+Lm-3’, which was significantly smaller than ‘Lm+Lb-3’ but greater than the rest of the treatments.

Similarly, there were significant differences in relative expression of the *PDF-1.2* gene in different treatments at 6 dpi ($F(1,5) = 28.40$, $P < 0.0001$) (Table 4.15) (Figure 4.27). ‘Lm+Lb-5’ and ‘Lb+Lm-5’ resulted in the greatest upregulation of this gene and were significantly greater than ‘Lb only’ but not significantly different to the rest of the treatments or each other.

In summary, despite the statistically significant differences, it is difficult to identify trends in relative expression of the *PDF-1.2* gene as a response to simultaneous and/or sequential co-inoculations from these data (Figure 4.27).

Table 4.15: Statistical testing outputs for significant probability of the main effects of experiment, treatment and the two-way interactions on relative expression of *PDF-1.2* gene from two experiments for different treatments at 2, 4 or 6 days post inoculation (dpi).

Two-way analysis of variance (ANOVA) tests were done by selecting experiment number and treatment as factors.

Days post inoculation (dpi)	Factor	*df*	F statistic	F probability
2 dpi	Experiment	1	53.03	< 0.0001
	Treatment	3	51.77	< 0.0001
	Experiment x Treatment	3	32.10	< 0.0001
4 dpi	Experiment	1	16.26	= 0.021
	Treatment	5	77.02	< 0.0001
	Experiment x Treatment	5	3.29	= 0.0005
6 dpi	Experiment	1	48.74	< 0.0001
	Treatment	5	28.40	< 0.0001
	Experiment x Treatment	5	21.66	< 0.0001

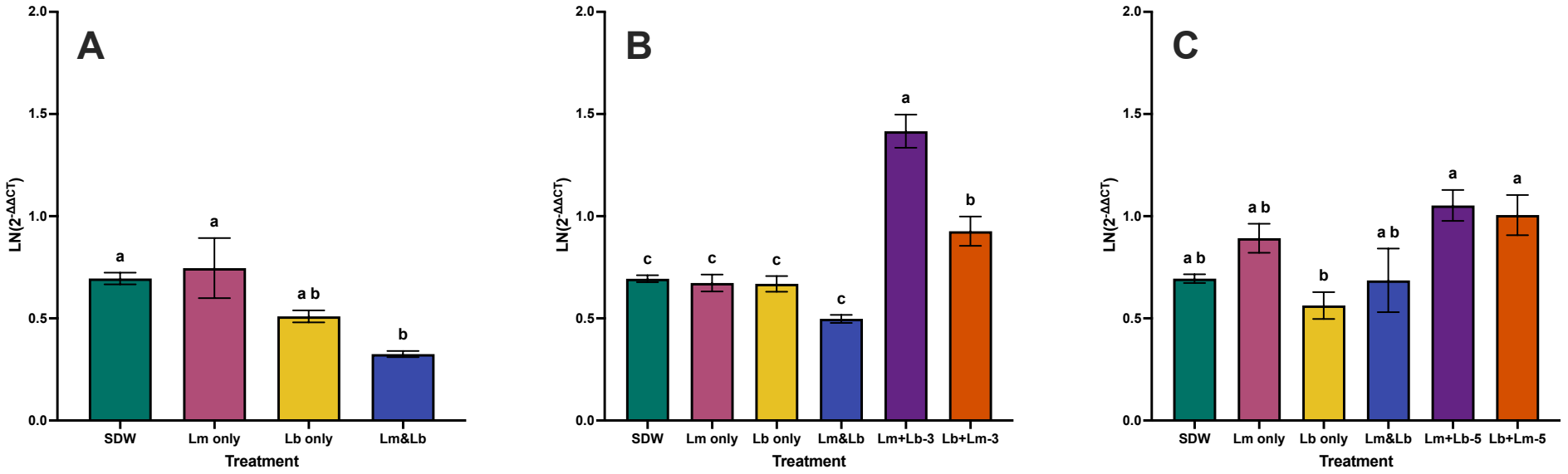

Figure 4.27: Relative expression of the *PDF-1.2* gene in cotyledons obtained from two experiments examining interactions between *Leptosphaeria maculans* and *L. biglobosa* inoculated onto cotyledons of oilseed rape (*Brassica napus*).

Cotyledons were inoculated with Sterilised Distilled Water (SDW) for control, *Leptosphaeria maculans* only (Lm only), *Leptosphaeria biglobosa* only (Lb only), *L. maculans* & *L. biglobosa* co-inoculated simultaneously (Lm&Lb), initial inoculation with *L. maculans* followed by co-inoculation with *L. biglobosa* sequentially at 3 or 5 days later (Lm+Lb-3, Lm+Lb-5) or initial inoculation with *L. biglobosa* followed by sequential co-inoculation with *L. maculans* sequentially at 3 or 5 days later (Lb+Lm-3, Lb+Lm-5) at (A) 2 days post inoculation (dpi), (B) 4 dpi and (C) 6 dpi. Tukey's HSD tests were used to separate the mean relative expression of the *PDF-1.2* gene in across different treatments. Columns that do not share a letter are considered significantly different ($P < 0.05$). Error bars show standard error of the mean (SEM) (2 dpi 23 d.f., 4 dpi 35 d.f., 6 dpi 35 d.f.).

There were significant differences in relative expression of the *WRKY70* gene in different treatments at 2 dpi ($F(1,3) = 43.66$, $P < 0.0001$) (Table 4.16) (Figure 4.28). 'Lb only' resulted in the greatest upregulation of this gene, followed by 'Lm&Lb', which was significantly smaller than 'Lb only' but significantly greater than 'SDW' and 'Lm only'.

There were also significant differences in relative expression of the *WRKY70* gene in different treatments at 4 dpi ($F(1,5) = 89.58$, $P < 0.0001$) (Table 4.16) (Figure 4.28). Treatments 'Lb only' and 'Lm&Lb' resulted in the greatest upregulation of this gene and were significantly greater than the rest of the treatments, but not significantly different from each other. 'Lb+Lm-3' was significantly greater than 'SDW', but not significantly different to 'Lm only' and 'Lm+Lb-3'.

Similarly, there were significant differences in relative expression of the *WRKY70* gene between different treatments at 6 dpi ($F(1,5) = 216.50$, $P < 0.0001$) (Table 4.16) (Figure 4.28). Treatments 'Lm&Lb' and 'Lb+Lm-5' resulted in the greatest upregulation of this gene and were significantly greater than 'SDW' and 'Lm only', but not significantly different to the rest of the treatments or each other.

In summary, similar to the *PDF-1.2* gene, despite the statistically significant differences, it is difficult to identify trends in relative expression of the *WRKY70* gene as a response to simultaneous and/or sequential co-inoculations from these data (Figure 4.28).

There were significant differences in relative expression of the *WRKY33* gene in different treatments at 2 dpi ($F(1,3) = 347.20$, $P < 0.0001$) (Table 4.17) (Figure 4.29). 'Lb only' resulted in the greatest upregulation of this gene and was significantly greater than the rest of the treatments.

There were also significant differences in relative expression of the *WRKY33* gene in different treatments at 4 dpi ($F(1,5) = 422.60$, $P < 0.0001$) (Table 4.17) (Figure 4.29). Treatments 'Lm+Lb-3' and 'Lb+Lm-3' resulted in the greatest upregulation of this gene and were significantly greater than the other treatments, but not significantly different from each other.

Table 4.16: Statistical testing outputs for significant probability of the main effects of experiment, treatment and the two-way interactions on relative expression of *WRKY70* gene from two experiments for different treatments at 2, 4 or 6 days post inoculation (dpi).

Two-way analysis of variance (ANOVA) tests were done by selecting experiment number and treatment as factors.

Days post inoculation (dpi)	Factor	*df*	F statistic	F probability
2 dpi	Experiment	1	6.02	= 0.025
	Treatment	3	43.66	< 0.0001
	Experiment x Treatment	3	3.08	= 0.057
4 dpi	Experiment	1	30.61	< 0.0001
	Treatment	5	89.58	< 0.0001
	Experiment x Treatment	5	9.82	< 0.0001
6 dpi	Experiment	1	367.50	< 0.0001
	Treatment	5	216.50	< 0.0001
	Experiment x Treatment	5	152.10	< 0.0001

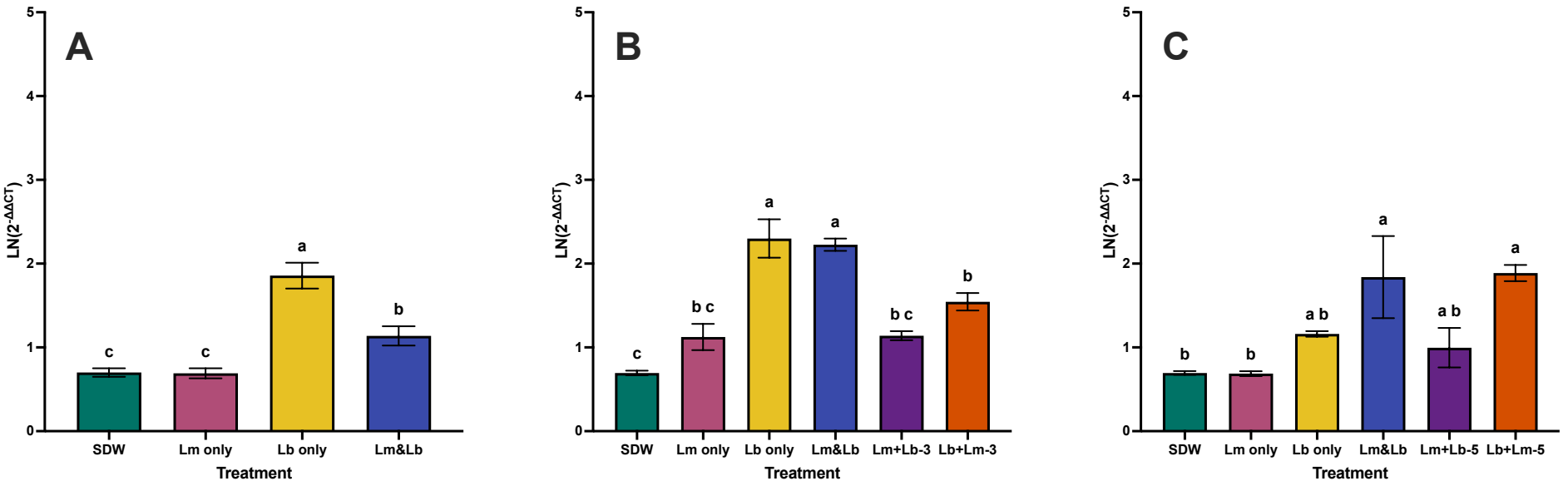

Figure 4.28: Relative expression of the *WRKY70* gene in cotyledons obtained from two experiments examining interactions between *Leptosphaeria maculans* and *L. biglobosa* inoculated onto cotyledons of oilseed rape (*Brassica napus*).

Cotyledons were inoculated with Sterilised Distilled Water (SDW) for control, *Leptosphaeria maculans* only (Lm only), *Leptosphaeria biglobosa* only (Lb only), *L. maculans* & *L. biglobosa* co-inoculated simultaneously (Lm&Lb), initial inoculation with *L. maculans* followed by co-inoculation with *L. biglobosa* sequentially at 3 or 5 days later (Lm+Lb-3, Lm+Lb-5) or initial inoculation with *L. biglobosa* followed by sequential co-inoculation with *L. maculans* sequentially at 3 or 5 days later (Lb+Lm-3, Lb+Lm-5) at (A) 2 days post inoculation (dpi), (B) 4 dpi and (C) 6 dpi. Tukey's HSD tests were used to separate the mean relative expression of the *WRKY70* gene in across different treatments. Columns that do not share a letter are considered significantly different ($P < 0.05$). Error bars show standard error of the mean (SEM) (2 dpi 23 d.f., 4 dpi 35 d.f., 6 dpi 35 d.f.).

Table 4.17: Statistical testing outputs for significant probability of the main effects of experiment, treatment and the two-way interactions on relative expression of *WRKY33* gene from two experiments for different treatments at 2, 4 or 6 days post inoculation (dpi).

Two-way analysis of variance (ANOVA) tests were done by selecting experiment number and treatment as factors.

Days post inoculation (dpi)	Factor	*df*	F statistic	F probability
2 dpi	Experiment	1	226.30	< 0.0001
	Treatment	3	347.20	< 0.0001
	Experiment x Treatment	3	51.71	< 0.0001
4 dpi	Experiment	1	42.29	< 0.0001
	Treatment	5	422.60	< 0.0001
	Experiment x Treatment	5	103.40	< 0.0001
6 dpi	Experiment	1	14.42	< 0.0001
	Treatment	5	299.90	< 0.0001
	Experiment x Treatment	5	50.33	< 0.0001

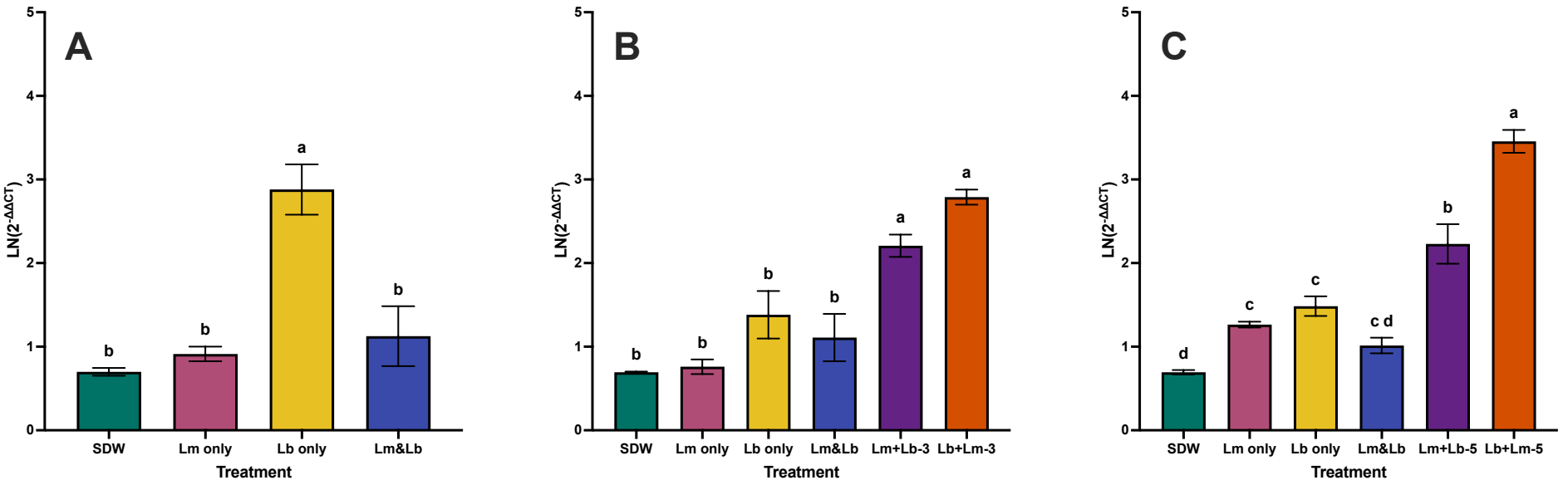

Figure 4.29: Relative expression of the *WRKY33* gene in cotyledons obtained from two experiments examining interactions between *Leptosphaeria maculans* and *L. biglobosa* inoculated onto cotyledons of oilseed rape (*Brassica napus*).

Cotyledons were inoculated with Sterilised Distilled Water (SDW) for control, *Leptosphaeria maculans* only (Lm only), *Leptosphaeria biglobosa* only (Lb only), *L. maculans* & *L. biglobosa* co-inoculated simultaneously (Lm&Lb), initial inoculation with *L. maculans* followed by co-inoculation with *L. biglobosa* sequentially at 3 or 5 days later (Lm+Lb-3, Lm+Lb-5) or initial inoculation with *L. biglobosa* followed by sequential co-inoculation with *L. maculans* sequentially at 3 or 5 days later (Lb+Lm-3, Lb+Lm-5) at (A) 2 days post inoculation (dpi), (B) 4 dpi and (C) 6 dpi. Tukey's HSD tests were used to separate the mean relative expression of the *WRKY33* gene in across different treatments. Columns that do not share a letter are considered significantly different ($P < 0.05$). Error bars show standard error of the mean (SEM) (2 dpi 23 d.f., 4 dpi 35 d.f., 6 dpi 35 d.f.).

Similarly, there were significant differences in relative expression of the *WRKY33* gene in different treatments at 6 dpi ($F(1,5) = 299.90$, $P < 0.0001$) (Table 4.17) (Figure 4.29). Treatment 'Lb+Lm-5' resulted in the greatest upregulation of this gene and was significantly greater than the other treatments. This was followed by 'Lm+Lb-5', which was significantly different to all other treatments. Treatments 'Lm only' and 'Lb only' were significantly greater than 'SDW' but not significantly different to 'Lm&Lb'. In addition, 'SDW' and 'Lm&Lb' were not significantly different from each other.

In summary, greatest upregulation of the *WRKY33* gene was detected as a result of sequential co-inoculations, especially where *L. biglobosa* was the first pathogen to be inoculated (Lb+Lm-3 and Lb+Lm-5), as well as where *L. maculans* was the first pathogen to be inoculated, followed by *L. biglobosa* later on (Lm+Lb-3 and Lm+Lb-5). Additionally, a similar upregulation event was detected in 'Lb only' at 2 dpi (Figure 4.29).

4.4 Discussion

The results of the studies in this chapter provide further evidence that the timing of co-inoculation (i.e. the timing when *L. maculans* and *L. biglobosa* meet) strongly affects the interspecific interactions between them in terms of relative pathogen growth not only *in vitro* but also *in planta*.

In the simultaneous co-inoculation experiment, it was found that the lesion size and phenotype for the 'Lm&Lb' treatment were similar to 'Lb only', suggesting that *L. biglobosa* might have inhibited the growth of *L. maculans* (Fortune et al., 2024). This was further supported by the observations regarding phytotoxin production by *L. maculans*, where no production of sirodesmin PL or its precursors was detected in the 'Lm&Lb' treatment. These initial results, taken together with the previous work reporting a faster colonisation rate of *L. biglobosa* compared to *L. maculans* (Huang et al., 2001; Huang et al., 2003; Fitt et al., 2006a), indicates that *L. biglobosa* is potentially deploying a resource-mediated interspecific competition strategy against *L. maculans*. An *in vitro* study (Chapter 3) (Bingol et al., 2024) has supported this hypothesis, as inoculation with *L. biglobosa* only and *L. maculans* & *L. biglobosa* simultaneously had a similar growth rate in liquid culture, which was nearly three times faster than inoculation with *L. maculans* only.

Following on from these initial findings (Fortune et al., 2024), as well as the findings in Chapter 3 (Bingol et al., 2024), further investigations were done on the interactions between *L. maculans* and *L. biglobosa in planta* (this chapter), through simultaneous and sequential co-inoculations on cotyledons of oilseed rape (*Brassica napus*). In these experiments, for the treatments where *L. biglobosa* was inoculated any time before *L. maculans*, as well as for the treatment where the two pathogens were co-inoculated simultaneously, the kinetics of lesion development were similar to that of *L. biglobosa* only inoculation; as shown by the growth of lesions observed from 7 dpi to 16 dpi. This is consistent with the trends in lesion development previously reported for *L. biglobosa* (Lowe et al., 2014; Shah et al., 2020). This suggests that in these treatments, *L. biglobosa* might have inhibited the growth of *L. maculans*, as with observations from the *in vitro* experiments. To further support this, the trends in lesion development for these treatments observed in this study were also in agreement with previous work, where similar trends were reported on leaves of oilseed rape pre-treated with *L. biglobosa* ascospores prior to *L. maculans* inoculation at the same site (Liu et al., 2006; Liu et al., 2007). Interestingly, the treatment where *L. biglobosa* was sequentially co-inoculated 1 day after *L. maculans* (Lm+Lb-1) also showed a similar trend to that of *L. biglobosa* only. This suggests that *L. biglobosa* might have still been able to inhibit the growth of *L. maculans*, even when it was sequentially co-inoculated 1 day after *L. maculans*, which is also similar to observations from the *in vitro* experiments. This particular trend in lesion development of *L. biglobosa* (appearance of necrotic lesions early after inoculation and expansion of these necrotic lesions under relatively high humidity) fit well into the characteristics of a necrotrophic plant pathogen (Talley et al., 2002; Laluk & Mengiste, 2010; Précigout et al., 2020).

In addition, for the treatments where *L. biglobosa* was sequentially co-inoculated at 3 or 5 days after *L. maculans*, the kinetics of lesion development were similar to that of *L. maculans* only inoculation; where little to no lesion development was observed from 7 dpi to 10 dpi, followed by a sudden appearance of relatively large lesions at 14 dpi and further expansion of these lesions at 16 dpi. This is consistent with the trends in lesion development previously reported for *L. maculans* (Lowe et al., 2014; Haddadi et al., 2019). This suggests that in these treatments, *L. maculans* might have inhibited the growth of *L. biglobosa*, similar to observations from the *in vitro* experiments. Furthermore, this particular trend in lesion development of *L. maculans* (lack of visible

symptoms, associated with a biotrophic (or endophytic) phase, followed by sudden appearance of large lesions, associated with switching to a necrotrophic phase) fits well into the characteristics of a hemi-biotrophic plant pathogen (Horbach et al., 2011; Koeck et al., 2012; Seybold et al., 2020).

For the treatments that showed a similar trend in lesion development to *L. biglobosa*, the lesions appeared to be relatively smaller, darker and defined, which was also similar to lesions observed in *L. biglobosa* only inoculation. This further suggests that *L. biglobosa* was growing predominantly in those lesions, with *L. maculans* being inhibited. Interestingly, despite showing a similar lesion phenotype to *L. biglobosa*, the 'Lm+Lb-1' treatment had the smallest lesion size out of all treatments in the experiment. This suggests that, although *L. biglobosa* can still inhibit the growth of *L. maculans* locally even if it is co-inoculated 1 day after *L. maculans*, this comes with a cost, leading to a reduction in the severity of lesions caused by *L. biglobosa*. This was most probably due to the start of endophytic colonisation by *L. maculans* at the inoculation site reducing the availability of nutrients to *L. biglobosa*. Although *L. biglobosa* can overcome this one day advantage of *L. maculans*, because it has a faster metabolic rate (Frąc et al., 2022), it is likely that the initial reduction in nutrient resources at the inoculation site is disadvantageous to lesion development of *L. biglobosa*.

Additionally, at 16 dpi, for the treatments that showed a similar trend in lesion development to *L. maculans*, the lesions appeared to be relatively larger, lighter (grey) and less defined, which was also similar to lesions observed in *L. maculans* only inoculation. This further suggests that *L. maculans* was growing predominantly in those lesions, with *L. biglobosa* being inhibited. Moreover, the sizes of lesions observed in these experiments were greater than the sizes of lesions in the initial simultaneous co-inoculation experiment, where inhibition of sirodesmin PL was investigated. This is attributed to technical differences between these experiments. Since there are multiple inoculation events in the experiments with sequential co-inoculations, there was a longer incubation period at high humidity, promoting the development of larger lesions of the same phenotypes resulting from these treatments.

Further investigation on production of pycnidia on detached infected cotyledons showed a similar trend of lesion development and phenotype to *L. biglobosa*, there were no

mature pycnidia produced (same as *L. biglobosa* only inoculation). Conversely, for the treatments that showed a similar trend of lesion development and phenotype to *L. maculans*, there were similar numbers of mature pycnidia counted under the microscope (same as *L. maculans* only inoculation). It is widely known that *L. biglobosa* is associated with smaller, darker lesions with very few or no pycnidia; whereas *L. maculans* is associated with larger, grey lesions with pycnidia on leaves of oilseed rape (West et al., 2001; Fitt et al., 2006a). This further supports the hypothesis that *L. maculans* and *L. biglobosa* might have completely inhibited each other's growth, depending on co-inoculation timing, in a similar fashion to the results of *in vitro* studies.

In order to further contextualise and confirm the results of lesion development, phenotype and pycnidial production, the relative amounts of *Leptosphaeria* species DNA in these lesions were analysed. To obtain good quality and quantity of DNA for qPCR analyses, different DNA extraction methods were tested. The commercial kits tested were not applicable for these samples and yielded low quality and quantity of DNA. Therefore, previously published protocols were evaluated. Out of the two versions of modified spore tape DNA extraction protocol tested (Huang et al., 2011; Kaczmarek et al., 2009), the version using chloroform:isoamyl alcohol without the phenol has yielded higher quality of DNA for all samples, with a notable improvement for *L. biglobosa*-type lesions. Nonetheless, the quality of DNA extracted was still low.

Further research suggested that the reason behind these quality issues could be the presence of polyphenols and polysaccharides in the samples interfering with DNA extraction by binding to the DNA (Aljanabi et al., 1999; Sahu et al., 2012). Presence of these compounds could have increased in the cotyledons used in this experiment as a result of advanced colonisation. It was previously reported that some polyphenols (e.g. flavonoids) are involved in plant defence responses against pathogens (Mierizak et al., 2014; Stiller et al., 2021; Patil et al., 2024). Furthermore, it was also reported that flavonoids are incorporated into the cell walls of necrotic and adjacent cells (Beckman, 2000; Mierizak et al., 2014). This could explain the reduced quality of DNA extracted from these cotyledons, as advanced lesions causing extensive tissue necrosis are likely to increase the amounts of these compounds in the necrotic tissues, which would subsequently interfere with DNA extraction. Moreover, the observation that quality of DNA extracted from *L. biglobosa*-type lesions was more sensitive to added phenol could

be attributed to the necrotrophic lifestyle of *L. biglobosa*, as necrosis would take place for a longer time compared to *L. maculans*, leading to more accumulation of these compounds in the advanced lesions. Therefore, a protocol with a sorbitol pre-wash step for removing polyphenols and polysaccharides from the samples prior to addition of lysis buffer for DNA extraction was tested (Inglis et al., 2018). This protocol has led to immediate improvements and allowed extraction of high quality DNA at high concentrations, allowing subsequent qPCR analyses to be done. Hence, it was selected as the method for DNA extraction in this study.

Through the analyses of relative amounts of pathogen DNA in lesions of oilseed rape cotyledons inoculated with *L. maculans* and/or *L. biglobosa*, it was first confirmed here that *L. biglobosa* was indeed able to inhibit the growth of *L. maculans* entirely locally. The observation that the 'Lm+Lb-1' treatment had a similar amount of *L. maculans* DNA to the 'Lm&Lb' treatment (< 2.0 %) further supports the idea that *L. biglobosa* is still able to overcome *L. maculans* locally even if it is co-inoculated 1 day after *L. maculans*. This is somewhat contradictory to the findings of Mahuku et al. (1996), as the authors reported that both species were isolated from the leaf lesions irrespective of the co-inoculation timeline. Although DNA of both pathogens can certainly be detected in lesions of all co-inoculation treatments, the relative quantities of *L. maculans* and *L. biglobosa* DNA differed greatly. Furthermore, the lack of pycnidial production in *L. biglobosa*-type lesions in this study suggests that the residual amount of *L. maculans* detected in those lesions was not able to produce viable conidia. These discrepancies between the studies are most probably due to use of different pathogen isolates or subclades and oilseed rape cultivars. Mahuku et al. (1996) most probably used an *L. biglobosa* 'canadensis' isolate. By contrast, this study used an *L. biglobosa* 'brassicae' isolate. Nevertheless, it is concluded here that it would be unlikely for *L. maculans* to be pathogenic under these specific conditions. This is further supported by another recent study, where it was reported that development of *L. maculans* was stopped before primary hyphal development in the presence of *L. biglobosa* at the same site (Gay et al., 2023).

One explanation for this could be that the faster metabolic rate of *L. biglobosa* (Frąc et al., 2022) leads to depletion of nutrient resources at the inoculation site, reducing the availability of nutrients required for growth of *L. maculans* (similar to *in vitro* studies).

Another explanation could be that the necrotic tissues formed early on by *L. biglobosa* are not suitable for *L. maculans* to obtain nutrients from during its early endophytic phase (Gay et al., 2023). Although *L. maculans* is able to cause necrosis on tissues and obtain nutrients from them in its late necrotrophic phase, this recent study suggests that *L. maculans* might not be able to adapt its transcriptomic programme to change its lifestyle as a response to nutritional changes caused by *L. biglobosa* (Gay et al., 2021; Gay et al., 2023). Both of these potential explanations indicate that *L. biglobosa* might be able to deploy a resource-mediated interspecific competition strategy (local effect, nutrient depletion), in addition to its host-mediated interspecific competition strategy (systemic effect, induction of SAR) against *L. maculans* (Mahuku et al., 1996; Liu et al., 2006; Dutt et al., 2021b). This would suggest that *L. biglobosa* might have more strategies for competition against *L. maculans* than previously thought.

Oilseed rape defence responses against these simultaneous and/or sequential co-inoculations were investigated, which provided some results supporting the interspecific competition strategies used by *L biglobosa*. At all sampling points, the greatest upregulation of the *PR-1* gene was induced as a result of 'Lb only' or 'Lm&Lb' treatments. This was followed by 'Lb+Lm-3' at 4 dpi and 'Lb+Lm-5' at 6 dpi. It is known that induction of systemic acquired resistance (SAR) through salicylic acid (SA) leads to accumulation of pathogenesis-related proteins (i.e. PR-1) (Durrant & Dong, 2004; Ali et al., 2017). Furthermore, similar findings in upregulation of *PR-1* expression in *L. biglobosa*-infected cotyledons attributed to induction of SAR have also been reported (Padmathilake & Fernando, 2022b). On the other hand, Liu et al. (2007) reported an earlier upregulation of *PDF-1.2* expression in *L. biglobosa*-infected leaves and suggested that *L. biglobosa*-induced acquired resistance is predominantly mediated through jasmonic acid/ethylene (JA/ET) instead, with upregulated expression of *PR-1* following shortly after. Considering the JA/ET pathways (and upregulation of *PDF-1.2*) are associated with resistance against necrotrophic pathogens (Li et al., 2004), this trend would fit better with the characteristics of *L. biglobosa* as a necrotrophic pathogen.

To further elucidate these mechanisms, the expression of two transcription factors thought to be regulators of SA and JA/ET pathways (*WRKY70* and *WKRY33*, respectively) was also investigated. The greatest upregulation of *WRKY33* was observed in the sequential co-inoculations at all time points, and in 'Lb only' at 2 dpi. The latter was

expected, as WRKY33 is known to be important in responding to infections by necrotrophic pathogens (Zheng et al., 2006; Birkenbihl et al., 2012). Interestingly, even though expression of *WRKY33* was reduced at 4 dpi and 6 dpi in 'Lb only', it was still highly expressed in 'Lb+Lm-3' and 'Lb+Lm-5' treatments at 24 h after sequential co-inoculation with *L. maculans*. This could suggest that *L. biglobosa* could be increasing its necrotrophic activity, such as secretion of enzymes to degrade host cell walls upon detection of *L. maculans*, resulting in upregulation of *WRKY33* expression. However, the lack of upregulation in *WRKY33* expression in 'Lm&Lb' at 2 dpi contrasts with this speculation. Interestingly, at 4 dpi, expression of *WRKY33* in 'Lm+Lb-3' was similar to that of 'Lb+Lm-3'. Moreover, at 6 dpi, although 'Lm+Lb-5' was smaller than 'Lb+Lm-5', it was still greater than the rest of the treatments. These could suggest that *L. biglobosa* is still recognised as a pathogen by the host even if it is co-inoculated 3 or 5 days after *L. maculans*. Gene expression analyses in this study were not suitable to assess host defence responses against *L. maculans*. This was because the genes selected are usually not responsive to *L. maculans* infection until it switches from biotrophy to necrotrophy later on in its colonisation (7-10 dpi) (Borhan et al., 2022; Gay et al., 2023), as indicated by consistently low transcript levels in all time points for 'Lm only' treatment. Overall, the gene expression component of this study is considered insufficient in significantly improving our understanding of molecular aspects of the host during interspecific interactions between the *Leptosphaeria* species *in planta*. Nonetheless, the possibility of *L. biglobosa* deploying multiple interspecific competition strategies against *L. maculans* is not ruled out. Perhaps, the mechanisms of these strategies can be further investigated in future transcriptomic studies, focusing on the pathogens as well as the host.

The analyses of relative amounts of pathogen DNA in infected cotyledons for the first time confirmed that *L. maculans* was indeed able to inhibit the growth of *L. biglobosa* entirely locally, provided that it was inoculated at least 3 days before *L. biglobosa*. These results are similar to the results of *in vitro* experiments, with a slightly different timeline, where no inhibition of *L. maculans* was observed in the 'Lm+Lb-3' treatment *in planta* compared to the partial inhibition of phytotoxin production and pathogen growth observed *in vitro* (Bingol et al., 2024). This was most probably due to the differences in nutrients and environment in oilseed rape cotyledons compared to liquid culture, as well as the involvement of plant defence systems. This inhibitory effect of *L. maculans* on *L. biglobosa* was attributed to the production timeline of sirodesmin PL in the *in vitro*

studies. However, it is difficult to know whether it was the production of sirodesmin PL by *L. maculans* that was inhibiting the growth of *L. biglobosa* in these treatments *in planta*. In the initial simultaneous co-inoculation work, 30 cotyledons with very large *L. maculans* lesions were pooled for secondary metabolite extraction and subsequent HPLC and LC-MS analyses. Even then, we were able only to confirm presence or absence of sirodesmin PL using the more sensitive LC-MS and were not able to quantify the phytotoxin. Therefore, from a technical point of view, it would be very difficult to investigate the production of sirodesmin PL *in planta* during early stages of infection to test this hypothesis. Furthermore, it is known that production of phytotoxins is mainly associated with necrotrophic pathogens or with the 'later necrotrophic phase' of hemi-biotrophic pathogens (Horbach et al., 2011; Stergiopoulos et al., 2013). Thus, although not for certain, it can be argued that *L. maculans* would not be producing sirodesmin PL during early stages of infection *in planta* during its endophytic phase, but it would be producing it in its later necrotrophic phase when lesions appear on cotyledons. This is also supported by the results of a large-scale transcriptomic study, where upregulation of genes related to production of sirodesmin PL was associated with the later necrotrophic phase of *L. maculans*, especially during colonisation of stems (Gay et al., 2021). These interpretations suggest that the mechanisms causing inhibition of pathogens might be different *in vitro* from *in planta*, albeit leading to similar visual observations (similar morphology of mycelia in *in vitro* studies and similar lesion phenotypes in *in planta* studies).

An alternative way to explain the inhibitory effect of *L. maculans* on *L. biglobosa in planta* locally is based on the timing advantage. It was suggested here that the start of endophytic colonisation by *L. maculans* leads to reduction in nutrients required by *L. biglobosa*, resulting in smaller *L. biglobosa*-type lesions in the 'Lm+Lb-1' treatment. Although *L. biglobosa* was still able to overcome the 1 day advantage of *L. maculans* (Lm+Lb-1), it might not be able to overcome a 3 or 5 day advantage of *L. maculans* (Lm+Lb-3 and Lm+Lb-5). This suggests that the endophytic colonisation of *L. maculans* for at least 3 days might lead to a local environment unsuitable for *L. biglobosa* to produce lesions on cotyledons. Although this is similar to the resource-mediated interspecific competition strategy suggested for *L. biglobosa*, it is not considered to be a direct interspecific competition strategy for *L. maculans*. This is because the faster metabolic rate of *L. biglobosa* (Frąc et al., 2022) confers the ability to successfully cause

symptoms even at a timing disadvantage when competing with *L. maculans*. Conversely, for *L. maculans*, this is totally timing-dependent and any inoculation of *L. biglobosa* without a 3 day timing advantage would result in the loss of its inhibitory effects on *L. biglobosa*.

Interestingly, from an evolutionary point of view, *L. maculans* did co-evolve more closely with the host *Brassica napus* compared to *L. biglobosa* (Grandaubert et al., 2014; Frąc et al., 2022) and developed the ability to complete pseudothecial maturation at colder temperatures, leading to ascospore release earlier in the growing season than that of *L. biglobosa* (Toscano-Underwood et al., 2003). These could have been a part of a more fundamental interspecific competition strategy for *L. maculans* to have the timing advantage over *L. biglobosa*. Furthermore, *L. maculans* is also detected later to activate plant defence systems as it switches from endotrophy to necrotrophy (Padmathilake & Fernando, 2022b; Gay et al., 2023). Therefore, if *L. maculans* has a timing advantage in infection of oilseed rape, with *L. biglobosa* arriving considerably later in the growing season, the plant defence system could be activated by the necrotrophic phase of *L. maculans*. This could lead to a reduction in the severity of *L. biglobosa* lesions, mimicking a host-mediated interspecific competition strategy, similar to that of *L. biglobosa* in inducing SAR against *L. maculans*. Overall, *L. maculans* requires a timing advantage for its potential local and systemic effects against *L. biglobosa in planta*. However, with the reports of ascospores of both *Leptosphaeria* species being released at similar times in the UK in recent years (Javaid et al., 2021; Fortune, 2022), alongside the emphasis on controlling *L. maculans* increasing the prevalence of *L. biglobosa* at stem basal cankers (Huang et al., 2024), it is unlikely that the inhibitory effects of *L. maculans* on *L. biglobosa* will be observed in natural conditions.

Perhaps, *L. biglobosa* has a wider 'fundamental niche', which can be observed when the competitive advantage of *L. maculans* is reduced by natural and human factors, and that *L. biglobosa* being predominant in the upper stem is its 'realised niche' to facilitate co-existence when factors favour *L. maculans* during their interspecific interactions on oilseed rape (Fitt et al., 2006a; Begon et al., 2006; Sadava et al., 2012; Dutt et al., 2021b).

Similar interactions between other co-infecting plant pathogens have also been observed. One example is the interactions between *Puccinia hordei* and *Erysiphe*

graminis, causing leaf rust and powdery mildew on barley, respectively (Chin & Wolfe, 1984; Clifford, 1985). It was reported that pre-inoculation of barley seedlings with *P. hordei* reduced the severity of symptoms caused by *E. graminis* by reducing its colony size and number of conidia produced. Conversely, pre-inoculation of barley seedlings with *E. graminis* at least 2 days before *P. hordei* reduced the severity of symptoms caused by *P. hordei* by reducing the size and number of rust pustules produced (Round & Wheeler, 1978). Although competitive exclusion of neither pathogen was reported by the authors, their findings in terms of the importance of timing of co-inoculation were similar to the observations between *L. maculans* and *L. biglobosa* in this study.

Another example of interactions between co-infecting plant pathogens are the interactions between *Cochliobolus sativus* and *Pyrenophora tritici-repentis*, both involved in wheat leaf spot diseases in the North American continent (Hosford, 1976; Tekauz, 1976; da Luz & Bergstrom, 1987). It was found that upon simultaneous co-inoculation, *C. sativum* can suppress conidial germination and germ tube elongation of *P. tritici-repentis* on the leaf surface. Furthermore, *C. sativus* could still exert these antagonistic effects as long as it was co-inoculated up to 6 h after *P. tritici-repentis*. Additionally, higher percentages of *P. tritici-repentis* were recovered when it was inoculated 12-168 h before *C. sativus* (da Luz & Bergstrom, 1987). This is similar to *L. maculans* evading the antagonistic effects of *L. biglobosa* when provided with a 3 day timing advantage in this study.

The strengths of this *in planta* study compared to previous similar *in planta* studies are that in this study, several fundamental characteristics of the pathogens were investigated in relation to interspecific interactions; which has highlighted correlations between visual symptoms and relative growth of the pathogens, while further expanding the ideas regarding the interspecific competition strategies used by *L. maculans* and *L. biglobosa*. Moreover, this study identified a protocol suitable for DNA extraction from cotyledons of oilseed rape extensively colonised by *Leptosphaeria* species. This has allowed confirmation of pathogen inhibition *in planta*. In addition, in this study, sequential co-inoculations with multiple time gaps in-between were tested, leading to identification of key time points affecting the outcome of the interspecific interactions between *L. maculans* and *L. biglobosa in planta*.

The limitation of this study is that only one isolate of each pathogen and one cultivar of oilseed rape were used due to time constraints and availability of equipment. There are six identified subclades of *L. biglobosa* (Dilmaghani et al., 2009; Zou et al., 2014). Future studies need to investigate whether other subclades of *L. biglobosa* have similar antagonistic effects on *L. maculans* and whether these effects are observed on other cultivars of oilseed rape. This study further characterised the interspecific interactions between *L. maculans* and *L. biglobosa* locally on cotyledons of oilseed rape in specific experimental conditions, such as same concentration of inoculum of both pathogens inoculated at the same site. However, these specific conditions are unlikely to occur in natural conditions. Nevertheless, the results of this study, analysed and interpreted in conjunction with previous literature regarding both local and systemic effects created by these pathogens, provide critical insights into potential future disease dynamics.

The timing of ascospore release in natural conditions is mainly dependent on temperature and rainfall, and it has been reported that ascospores of both species are being released at similar times in the UK (Javaid et al., 2021; Fortune et al, 2022; Huang et al., 2024). Therefore, out of all the potential strategies discussed in this chapter, the current timing of ascospore release is most likely to favour the systemic effects of *L. biglobosa*, with it inducing systemic acquired resistance against *L. maculans* by deploying a host-mediated interspecific competition strategy. Furthermore, if the proximity of stomatal penetration by *L. maculans* and *L. biglobosa* on the same leaf is narrow, *L. biglobosa* could also possibly cause faster necrotic colonisation and deplete the nutrient resources, by also deploying a resource-mediated interspecific competition strategy against *L. maculans*. Maybe, the characteristics that make *L. biglobosa* a 'weaker' pathogen; such as earlier detection by plant defence systems and smaller necrotic lesions, are the very characteristics that make it a 'fierce' competitor against *L. maculans*.

Some studies have suggested the use of *L. biglobosa* as a biocontrol agent against *L. maculans* in Europe and Canada (Liu et al., 2006; Shah et al., 2020; Padmathilake & Fernando, 2022b). However, more detailed analyses need to be done with great caution before such application can be considered. It is important to remember that *L. biglobosa* is the only phoma stem canker pathogen in China and can cause yield losses up to 40 % (Cai et al., 2017). Furthermore, *L. biglobosa* has been reported to be less sensitive to

azole fungicides than *L. maculans* (Eckert et al, 2010; Huang et al., 2011; Sewell et al., 2017). Moreover, effective control of *L. maculans* has already increased the incidence of *L. biglobosa* in stem basal cankers (Huang et al., 2024). These results suggest that *L. biglobosa* might have the potential to become more damaging to oilseed rape crops in the UK.

Finding a novel strategy of disease management to incorporate into integrated pest management (IPM) strategies is a commercially exciting prospect. Nonetheless, these pathogens do not exist in isolation in natural conditions and also interact with other pathogens, such as the currently most damaging pathogen of oilseed rape in the UK, *Pyrenopeziza brassicae*, causing light leaf spot. Hence, great caution must be taken to avoid unintentional off-target effects. For example, Fortune (2022) suggested that the adoption of integrated control against *L. maculans* leading to a reduction in phoma leaf spots caused by *L. maculans* resulted in later or no application of fungicides in the autumn; and this has led to an increase in incidence and severity of light leaf spot, as the fungicide applications in the autumn to control *L. maculans* were also protecting the crops against *P. brassicae*. Later or no application of fungicides in the autumn have therefore allowed *P. brassicae* to complete its asymptomatic phase through the autumn and winter without disruption, leading to devastating yield loses in the next summer. Thus, before any suggestions can be made regarding the use of *L. biglobosa* as a biocontrol agent, interactions between *L. biglobosa* and other economically relevant pathogens of oilseed rape must also be investigated.

The *in planta* studies presented in this chapter have advanced our understanding of the interspecific interactions between *L. maculans* and *L. biglobosa*. In order to understand the effects of these interactions on the course of the disease in crops, it is important to keep monitoring the ascospore release and related weather conditions, as well as the incidence and severity of phoma leaf spotting and stem canker caused by *L. maculans* and *L. biglobosa* in natural conditions (Chapter 5).

5 Chapter 5 – Interspecific interactions between *Leptosphaeria maculans* and *Leptosphaeria biglobosa* in natural conditions

5.1 Introduction

Oilseed rape (*Brassica napus*) us the second most important oil crop in the world and the third most important arable crop in the UK. Phoma stem canker is one of the most damaging diseases of oilseed rape, caused by two closely related fungal pathogens *Leptosphaeria maculans* and *Leptosphaeria biglobosa*, annually causing yield losses over £1 billion globally and £80 M in the UK (West et al., 2001; Fitt et al., 2006a; Barnes et al., 2010; Zhang et al., 2014). These two pathogens can co-infect and co-exist on oilseed rape in Europe and in the UK (Shoemaker & Brun, 2001; Fitt et al., 2006b; Dilmaghani et al., 2009).

Co-existence of *L. maculans* and *L. biglobosa* has mainly been attributed to the differences between them in optimal environmental conditions (i.e. temperature and rainfall) for pseudothecial maturation, leading to temporal and spatial separation in ascospore release of the two species, creating a gap between them in the starts of their life cycles in the autumn (Fitt et al., 2006a). Pseudothecia of *L. maculans* can mature faster at colder temperatures (< 10°C) compared to those of *L. biglobosa*, leading to earlier release of *L. maculans* ascospores (West et al., 2002a; Toscano-Underwood et al., 2003). Nevertheless, recent research observed the release of ascospores of both *Leptosphaeria* species at similar times across different field sites and growing seasons in the UK (Javaid et al., 2021; Fortune, 2022; Huang et al., 2024). These observations were ascribed to the effects of climate change, with increasing temperatures leading to a reduction in the time gap between these two pathogens in the completion of pseudothecial maturation, resulting in the release of their ascospores at similar times.

Moreover, rainfall is another important factor for the process of pseudothecial maturation and subsequent ascospore release. Rainfall in August and September was reported to facilitate progression of pseudothecial maturation (Huang et al., 2005; Huang et al., 2007). Conversely, dry weather in August and September was reported to stop pseudothecial maturation, leading to release of ascospores later in the growing season (Huang et al., 2011; Huang et al., 2024). Furthermore, the timing of the first major release

of ascospores was reported to be related to rainfall in the summer and early autumn, when increased rainfall in August and September led to earlier first major release of ascospores of both *Leptosphaeria* species (West et al., 2002b; Huang et al., 2005; Huang et al., 2007).

Although *L. maculans* is generally associated with more damaging stem basal cankers and *L. biglobosa* is often associated with less damaging upper stem lesions, the frequency of *L. biglobosa* DNA being detected in stem basal cankers in the UK has increased from 14 % in 2000 to 95 % in 2013 (West et al., 2001; Fitt et al., 2006a; Huang et al., 2014b; Huang et al., 2024). One of the main reasons for this is most probably the changes in the timing and pattern of ascospore release, with the pathogens starting their life cycles on their host at similar times. This could be providing *L. biglobosa* with the time to colonise a greater area on oilseed rape stems and contribute to development of stem basal cankers.

Another reason for this increased frequency of *L. biglobosa* in stem basal cankers in the UK could be the emphasis on controlling *L. maculans* through various disease control methods, with no specific focus on *L. biglobosa*. The main method of disease control for phoma stem canker in the UK is azole fungicides (i.e. prothiconazole and tebuconazole), applied based on the frequency of phoma leaf spot lesions caused by *L. maculans* (West et al., 2002b; Fortune et al., 2021; https://ahdb.org.uk/knowledge-library/how-to-manage-phoma-in-oilseed-rape). Furthermore, previous research reported that *L. biglobosa* was less sensitive to azole fungicides compared to *L. maculans* (Eckert et al., 2010; Huang et al, 2011). If the timing of fungicide applications is based on the frequency of *L. maculans* lesions and *L. biglobosa* is less sensitive to these fungicides than *L. maculans*, this could also favour *L. biglobosa* over *L. maculans*.

A different method of disease control is breeding resistance against *Leptosphaeria* species into cultivars of oilseed rape. There are two resistance types that can be bred into oilseed rape: quantitative resistance (QR) and qualitative resistance (*R*-gene mediated resistance). QR is complex, non-race-specific and polygenic, where several genes in regions of the genome called quantitative trait loci (QTLs) confer partial resistance against pathogens. Furthermore, QR has been reported to be durable and mainly in operation at later stages of colonisation, when pathogens are colonising the

stem tissues (Delourme et al., 2006; Huang et al., 2009). *R*-gene mediated resistance against *L. maculans* is race-specific and monogenic, where a gene-for-gene interaction occurs (with a corresponding *Avr* gene in *L. maculans* populations) and confers complete resistance against pathogens (Flor, 1971; Ansan-Melayah et al, 1998; Rouxel et al., 2003a). Unlike QR, it is active in early stages of colonisation, when pathogens are entering the plants through stomata (Balesdent et al., 2002; Fitt et al., 2006b). Although very effective, *R*-gene mediated resistance has been reported to be much less durable than QR, as continuous use of the same *R*-genes puts evolutionary pressure on *L. maculans* populations, leading to the selection of mutations in the corresponding *Avr* genes and subsequent breakdown of resistance (Rouxel et al., 2003b; Sprague et al., 2006). There have been more than fifteen *R*-genes identified against *L. maculans* (Van de Wouw et al., 2023). Currently, *Rlm7* is the most effective and common *R*-gene used against *L. maculans* in the UK (Huang et al., 2011; Mitrousia et al., 2018). There are no *R*-genes against *L. biglobosa* identified. One of the main reasons for this is most probably the association of *Avr* genes with transposable elements (TEs). *L. biglobosa* has a smaller percentage of TEs in its genome (< 4 %) compared to *L. maculans* (32.5 %) (Grandaubert et al., 2014). This could reduce the number of potential *Avr* genes that may be present in *L. biglobosa*. Even then, the majority of practices in breeding resistance against phoma stem canker pathogens in oilseed rape cultivars have been focussed on targeting *L. maculans*, with very little consideration on *L. biglobosa*. This could be altering the local proportions of pathogen populations, also in favour of *L. biglobosa* over *L. maculans*.

Aside from these factors, interspecific interactions between *L. maculans* and *L. biglobosa* could also be playing a role in *L. biglobosa* becoming more commonly detected in stem basal cankers. Recent studies reported that *L. biglobosa* can have antagonistic effects on *L. maculans in vitro* (Bingol et al., 2024) (Chapter 3) and *in planta* (Fortune et al., 2024) (further studied in Chapter 4), through deploying different interspecific competition strategies. Moreover, it was also reported that *L. biglobosa* can induce systemic acquired resistance against *L. maculans* in oilseed rape (Mahuku et al., 1996; Liu et al., 2006; Liu et al., 2007). Furthermore, *L. biglobosa* is the only phoma stem canker pathogen present in China and is responsible for significant yield losses (Liu et al., 2014; Cai et al., 2017; Du et al., 2021). In addition, studies done in Europe (Poland) have also reported more frequent isolation of *L. biglobosa* from stem basal cankers compared to *L. maculans* (Brachaczek et al., 2016; Brachaczek et al., 2021).

The course of the disease epidemics and proportions of *Leptosphaeria* species causing disease symptoms under current conditions (environmental factors, disease control methods focussed on *L. maculans*), where *L. biglobosa* may be favoured needs to be evaluated. Therefore, this chapter aims to characterise factors that can affect the interspecific interactions between *L. maculans* and *L. biglobosa*, and the individual contributions of the two *Leptosphaeria* species to disease development in natural conditions. The hypotheses behind this study are:

1) Ascospores of *L. maculans* and *L. biglobosa* are released at similar times throughout different growing seasons under current environmental conditions.

2) There are differences between cultivars in phoma leaf spots caused by *L. maculans* and *L. biglobosa*.

3) There are differences between cultivars in phoma stem cankers caused by *L. maculans* and *L. biglobosa*.

4) Oilseed rape cultivars with resistance against *L. maculans* (i.e. using *Rlm7*) are more susceptible to *L. biglobosa*.

These hypotheses were tested through the following objectives:

1) To monitor weather conditions (temperature and rainfall) and ascospore release of *L. maculans* and *L. biglobosa* in different growing seasons.

2) To assess the severity of phoma leaf spot by measuring incidence of phoma leaf spots and the number of phoma leaf spots caused by *L. maculans* and *L. biglobosa* on different cultivars in different sites and growing seasons.

3) To assess severity of phoma stem canker by measuring severity score of phoma stem canker and the quantities of *L. maculans* and *L. biglobosa* DNA in stem basal cankers on different cultivars in different sites and growing seasons.

5.2 Materials and methods

5.2.1 Timing and pattern of ascospore release by *L. maculans* and *L. biglobosa*

To monitor the timing and proportions of ascospore release of both *Leptosphaeria* species at Bayfordbury, Hertfordshire, a Burkard spore sampler was used (Burkard Manufacturing Company Limited, Rickmansworth, United Kingdom) (Figure 5.1). This was done for four growing seasons (2020/2021, 2021/2022, 2022/2023 and 2023/2024) (Table 5.1).

5.2.1.1 Burkard drum preparation

The Burkard drums and their containers were swabbed with 70% IMS (industrial methylated spirit) before any tape was placed onto them. A strip of double-sided sticky tape was placed at the start site of the drum, and then the Melinex tape was wound around the drum, with both ends being secured on the strip of double-sided sticky tape (Lacey & West, 2006). The drums were then taken into a fume hood for coating and placed on the Burkard drum coating apparatus. The coating solution (10 g petroleum jelly:20 mL hexane) container was shaken to homogenise the components before they were poured into the reservoir of the apparatus, followed by placing a small rolling pin on top of the reservoir (Figure 5.2). The drums were then rotated against the rolling pin to transfer the coating solution onto the Melinex tape, covering its whole surface (Lacey & West, 2006). After leaving them to dry in the fume hood for 2 min, the drums were placed into their labelled containers and stored at 10°C until required for use.

5.2.1.2 Burkard spore sampler set-up

In each growing season, after harvest (in August), infected oilseed rape stubble was collected from the Rothamsted Research farm at Harpenden, Hertfordshire and placed around the Burkard spore sampler (Huang et al., 2005) at Bayfordbury, Hertfordshire (Table 5.1) (Figure 5.3).

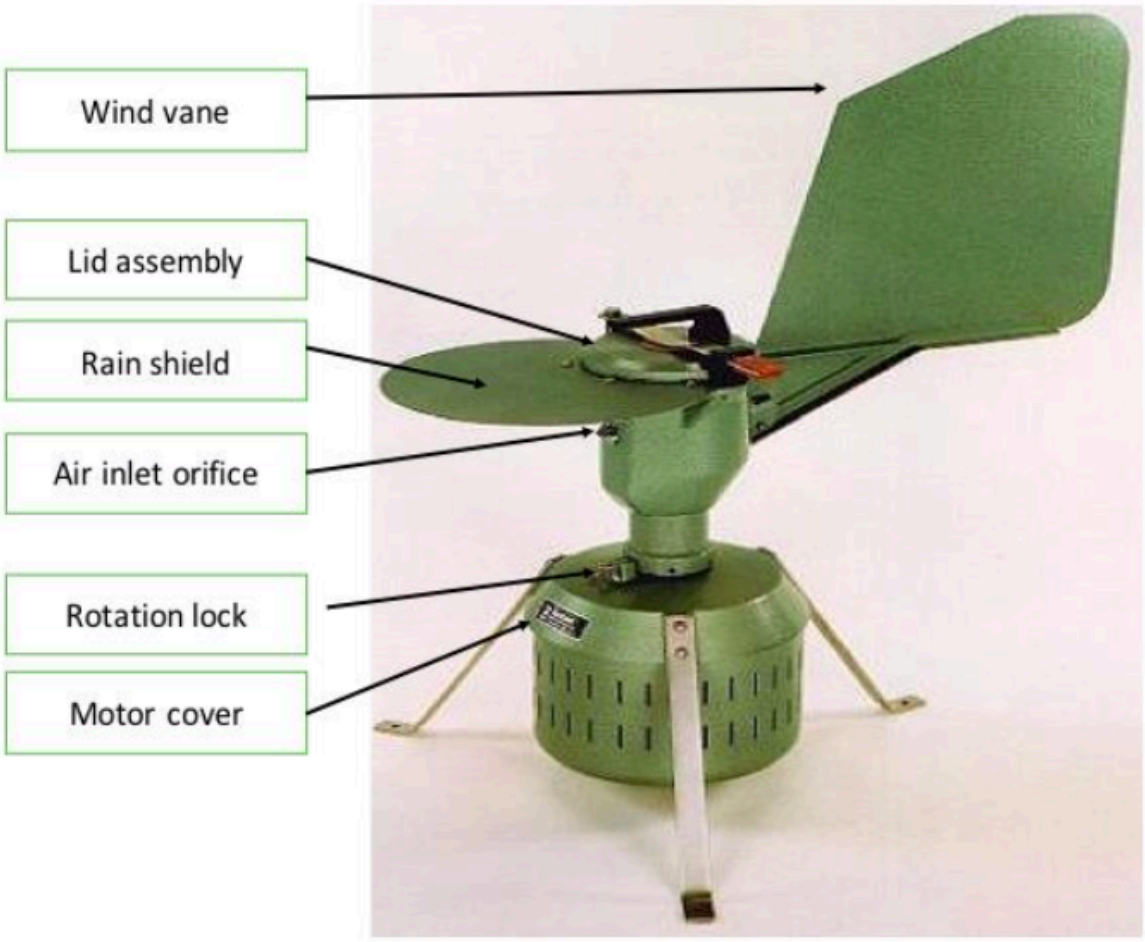

Figure 5.1: Burkard spore sampler.

Various components of the equipment are illustrated by arrows. Air samples are collected through the air inlet orifice at a rate of 10 L/min for 7 days. This figure was taken from Lacey & West, 2006.

Table 5.1: Dates of Burkard spore sampler operation in different growing seasons.

The Burkard spore sampler was used in four growing seasons (2020/2021, 2021/2022, 2022/2023 and 2023/2024).

Growing season	Start – Burkard spore sampler	End – Burkard spore sampler
2020/2021	24 September 2020	30 March 2021
2021/2022	02 September 2021	29 March 2022
2022/2023	01 September 2022	31 March 2023
2023/2024	01 September 2023	31 March 2024

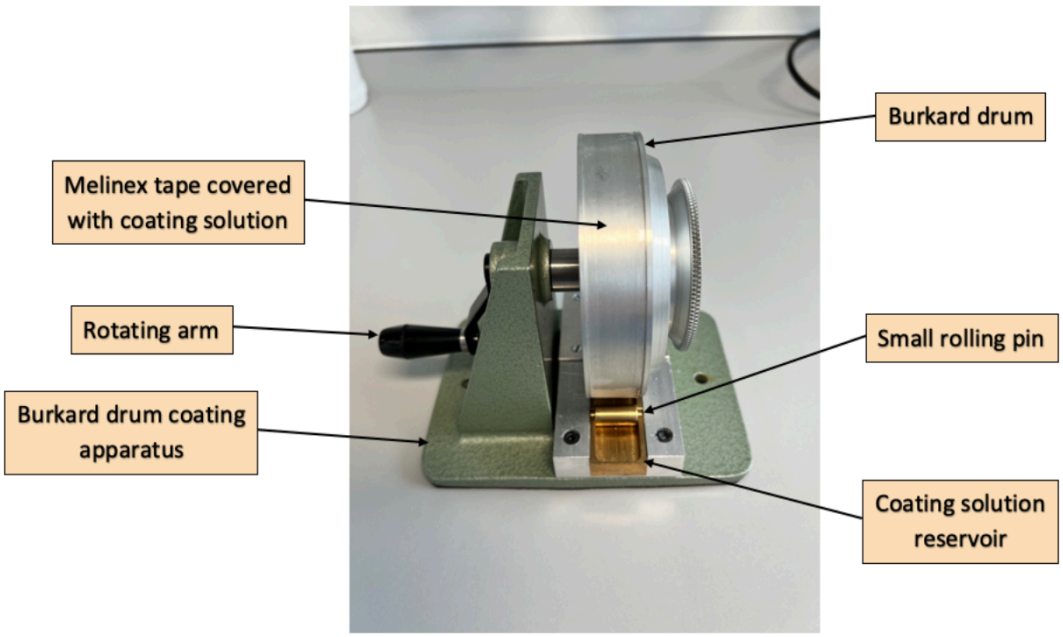

Figure 5.2: Burkard drum and the coating apparatus.

Various components of the apparatus are illustrated by arrows. Melinex tape is tightly wound around the Burkard drum. Coating solution (10 g petroleum jelly:20 mL hexane) is poured into the reservoir, followed by placing the small pin on top. Rotating arm is used to rotate the drums against the rolling pin to cover the whole surface of the Melinex tape with the coating solution (Lacey & West, 2006).

Figure 5.3: Infected oilseed rape stubble from the previous growing season placed around the Burkard spore sampler set-up at Bayfordbury, Hertfordshire.

The stubble was collected in August from Rothamsted Research farm at Harpenden, Hertfordshire.

A prepared Burkard drum was secured into the Burkard spore sampler and the clock mechanism was wound up. Through the air inlet of the spore sampler, air samples were collected on the drums at a rate of 10 L/min for 7 days, followed by replacing the drum and resetting the clock mechanism to rotate for another 7 days. After completing a full rotation, the used drums were processed for microscopic and molecular analyses. The Burkard spore sampler was in operation from September to March in each growing season (Table 5.1).

5.2.1.3 Burkard drum processing

Using clean forceps, the tapes were removed from the used Burkard drums and were placed onto a Perspex cutting ruler. Using clean scissors, the tapes were cut into seven equal pieces (48 mm each, corresponding to a 24 h time period), and each piece was cut longitudinally into two equal pieces. One of the pieces was placed on a labelled microscope slide containing a drop of fungal mounting fluid, taken into the fume hood and stained by placing 2 drops of cotton blue on cover slips prior to placing them over the tapes. Stained spore tapes were left in the fume hood for 2 h to dry. These samples were used for counting the ascospores of *Leptosphaeria* species, using a Nikon YS100 light microscope (Minato City, Tokyo, Japan) at 100 × magnification (Huang et al., 2005; Lacey & West, 2006) (Figure 5.4). The other piece was placed in a labelled 2 mL screw-cap tube and stored in a -20°C freezer. These samples were used for DNA extraction and qPCR to quantify the proportions of *L. maculans* and *L. biglobosa* DNA collected on each day (Huang et al., 2011) (Figure 5.4).

5.2.1.4 Ascospore counting using a light microscope

Starting from one of the corners in the longitudinally cut side of the tape, ascospores of *Leptosphaeria* species were counted by slowly moving the field of vision along the corner using the stage control knobs. Once the other end was reached, the field of vision was moved towards the inner side of the tape, avoiding an overlap with the previous field. This time, the ascospores of *Leptosphaeria* species were counted by slowly moving the field of vision in the other direction to obtain a second count (Figure 5.5). The average of these two counts was taken and used for calculating the number of *Leptosphaeria* species ascospores/m^3.

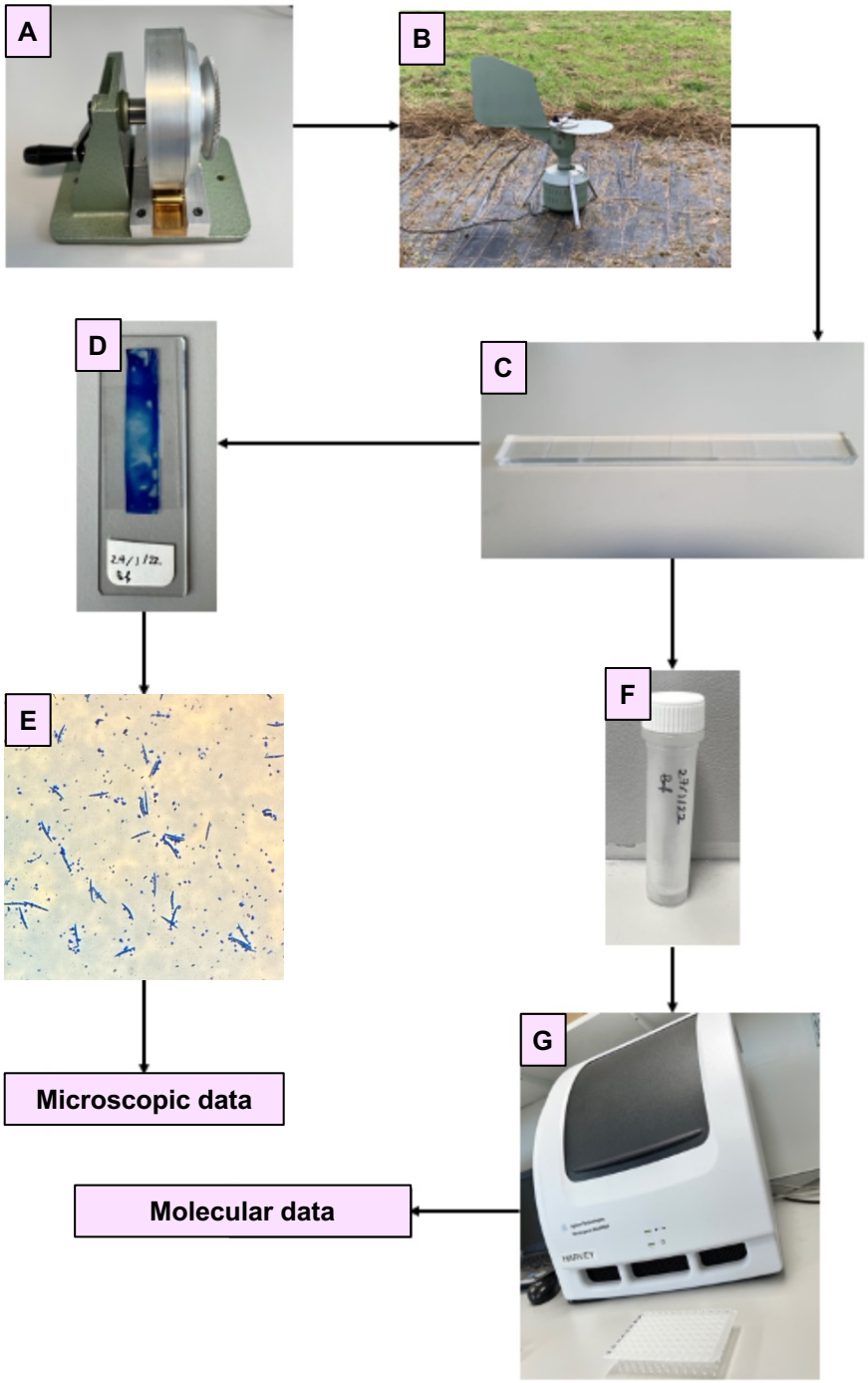

Figure 5.4: Workflow of Burkard spore tape processing.

(A) Prepared Burkard drum is placed into (B) the Burkard spore sampler at Bayfordbury, Hertfordshire. After rotating for 7 days, the tape is placed on (C) the Perspex cutting ruler, where it is cut into seven equal pieces, each corresponding to one day. These pieces are then longitudinally cut into two equal pieces, where one half (D, E) is stained for counting of *Leptosphaeria* species ascospores under the microscope, and the other half (F, G) is used for DNA extraction and qPCR to quantify proportions of *L. maculans* and *L. biglobosa* DNA in the air samples.

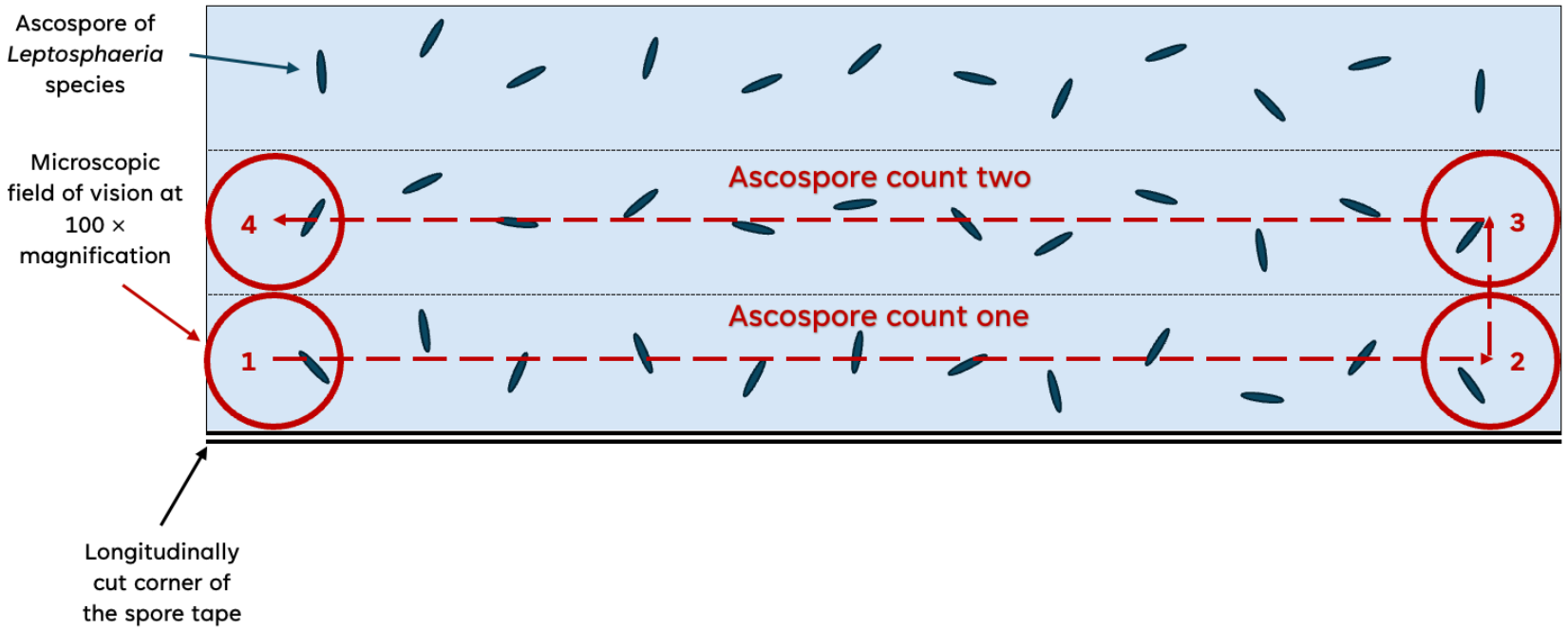

Figure 5.5: Process of counting ascospores of *Leptosphaeria* species using a light microscope.

Field of vision (at 100 × magnification) seen through the eyepiece of the light microscope is initially set at position 1, at one of the longitudinally cut corners of the stained spore tape. Ascospores of *Leptosphaeria* species are counted by slowly moving the field of vision by using the stage control knobs of the microscope until reaching position 2, giving the first count of ascospores. This was followed by moving the field of vision to position 3 and repeating the previous step in the other direction until reaching position 4, giving the second count of ascospores.

5.2.1.5 DNA extraction from spore tapes

The spore tape DNA extraction protocol was developed by Kaczmarek et al. (2009) and further optimised by Huang et al. (2011). Modified versions of this protocol were introduced in section 4.2.6.3. For DNA extraction from spore tapes, the original version of this protocol without any modifications was used. Approximately 0.5 g of acid-washed Ballotini glass beads (Sigma, Saint Louis, Missouri, United States) were added to each 2 mL screw-cap tube containing a spore tape sample and 440 µL of DNA extraction buffer was added into each tube. Samples were processed using the FastPrep machine (MP Biomedicals, California, United States) three times at 6.0 m/s for 40 s, with cooling on ice for 5 min in-between the runs. This was followed by the addition of 400 µL of 2% SDS into each tube. After vortexing briefly, the tubes were incubated in a 65°C water bath for 30 min. Next, 800 µL of the bottom phase of phenol:chloroform:isoamyl alcohol (25:24:1) was added into each tube, vortexed briefly, and centrifuged at 15,700 × *g* for 10 min at 4°C. In the meantime, a new set of 1.5 mL tubes was labelled, and 1 µL of glycogen, 30 µL of 7.5 M sodium acetate, and 480 µL of isopropanol (all taken from a -20°C freezer) were added into this new set of tubes. After centrifugation, 650 µL of the supernatant from each of the original tubes was transferred into one of the new set of tubes and mixed by inverting ten times. These tubes were then incubated in a -20°C freezer for 16 h (Figure 5.6).

The tubes were taken from the -20°C freezer and centrifuged at 15,700 × *g* for 30 min at 4°C. The supernatant was discarded and 300 µL of 70% ethanol (taken from a -20°C freezer) was added onto the pellets and centrifuged at 15,700 × *g* for 8 min at 4°C. The supernatant was discarded again, and the tubes were spun briefly to collect the remaining ethanol in the bottom of the tube. Using a pipette, the remaining ethanol was removed and the tubes were left open in the fume hood for 20 min for the DNA pellets to dry. The DNA pellets were re-suspended by adding 30 µL of nuclease-free water and flicking them gently. The extracted DNA samples were stored in a -20°C freezer until required for further use (Figure 5.7). Recipes of all buffers used in this protocol can be found in Appendix E.

5.2.1.6 Quantitative polymerase chain reaction (qPCR)

qPCR analyses were done as described in section 2.5.

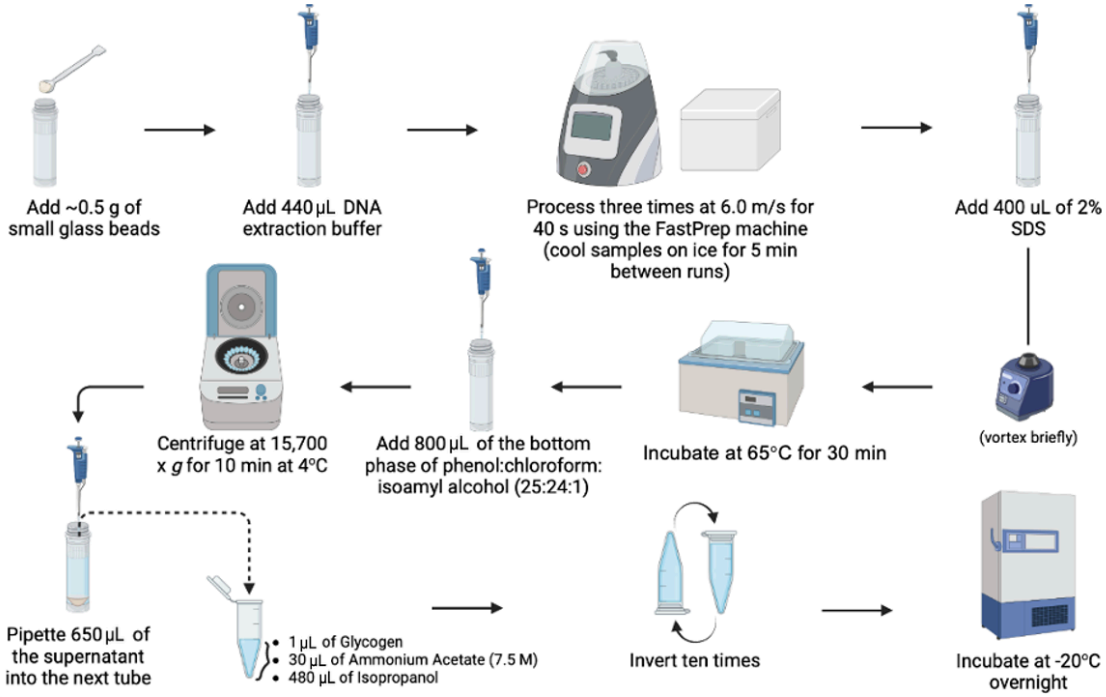

Figure 5.6: Workflow of the first part of spore tape DNA extraction protocol.

Approximately 0.5 g of Ballotini glass beads and DNA extraction buffer were added to each tube containing a spore tape sample. Samples were homogenised using the FastPrep machine (MP Biomedicals). After homogenisation, 2% SDS was added, mixed by vortexing and incubated in a 65°C water bath. Next, the bottom phase of phenol:chloroform:isoamyl alcohol (25:24:1) was added, samples were vortexed and then separated into two phases through centrifugation. The upper phase was transferred into a new tube containing glycogen, 7.5 M ammonium acetate and isopropanol, mixed by inverting and incubated in the -20°C for 16 h. This figure was created using BioRender.com.

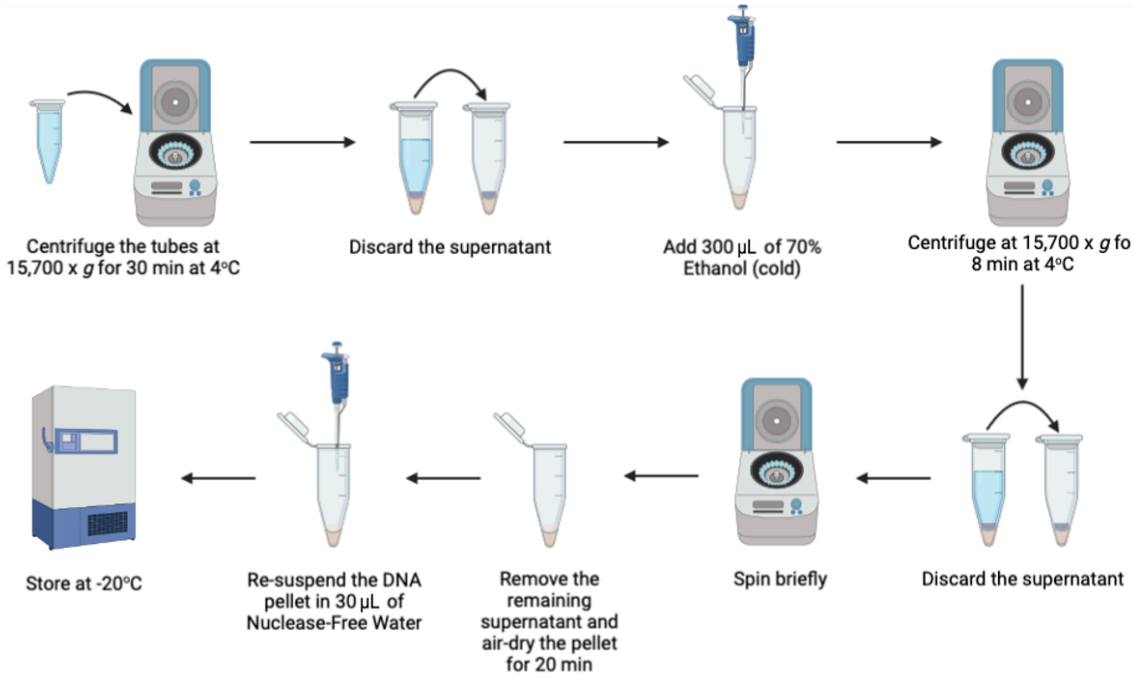

Figure 5.7: Workflow of the second part of spore tape DNA extraction protocol.

The tubes were centrifuged to pellet the DNA and the supernatant was discarded. The DNA pellets were washed once by the addition of 70% ethanol followed by centrifugation. The supernatant was discarded. The tubes were spun briefly to collect the remaining ethanol at the bottom of the tube, which was then removed using a pipette. After drying in the fume hood, the DNA pellets were re-suspended in nuclease-free water and stored in the -20°C freezer until required. This figure was created using BioRender.com.

5.2.1.7 Weather conditions related to ascospore release by *L. maculans* and *L. biglobosa*

To investigate the effects of weather conditions on timing and pattern of ascospore release of *Leptosphaeria* species, temperature and rainfall data were collected from the on-site weather station at Bayfordbury, Hertfordshire. Using these data, daily and monthly averages of temperature and rainfall were calculated from August to the following April for the 2020/2021, 2021/2022, 2022/2023 and 2023/2024 growing seasons.

5.2.2 Phoma leaf spots caused by *L. maculans* and *L. biglobosa*

Field experiments at two sites (Rothamsted Research and the John Innes Centre) over two growing seasons (2023/2024 and 2024/2025) were used to assess phoma leaf spots caused by *L. maculans* and *L. biglobosa* (Table 5.2).

5.2.2.1 Field experiments at Harpenden and Norwich in the 2023/2024 and 2024/2025 growing seasons

Ten cultivars, consisting of eight parent lines and two control lines (Table 5.3) were selected for field experiments at Rothamsted Research and John Innes Centre. Parent lines were selected due to their variability in several traits, to be tested and analysed over a set period of time with an aim to develop multi-parent advanced generation inter-crossed (MAGIC) populations of oilseed rape.

The field experiments were set up by Rothamsted Research at Harpenden, Hertfordshire and John Innes Centre at Norwich, Norfolk in the 2023/2024 and 2024/2025 growing seasons. The experiments were set up with a randomised block design with five replicates (Appendix H). Seeds were sown in early or late August at both sites for both growing seasons (Table 5.2). At the Harpenden site, no fungicides were applied in the autumn of 2023, but Soratel® (prothioconazole) was applied in the autumn of 2024. At the Norwich site, Filan® (boscalid) was applied in the autumn of 2023, and Shepherd® (boscalid and pyraclostrobin) was applied in the autumn of 2024 (Table 5.2).

5.2.2.2 Assessment of phoma leaf spots

For this project, three replicates of each cultivar were assessed for phoma leaf spots caused by *L. maculans* and *L. biglobosa* in the autumn of 2023 and 2024.

Table 5.2: Summary of field experiments for phoma leaf spot assessments.

Dates of sowing, fungicide application and phoma leaf spot assessment for field experiments at Rothamsted Research at Harpenden, Hertfordshire and John Innes Centre at Norwich, Norfolk.

Rothamsted Research, Harpenden, Hertfordshire (AL5 2JQ)		
Task	**2023/2024**	**2024/2025**
Sowing	19 August 2023	08 August 2024
Fungicide application	N/A	13 November 2024[a]
Phoma leaf spot assessment	15 November 2023	26 November 2024
John Innes Centre, Norwich, Norfolk (NR4 7UH)		
Task	**2023/2024**	**2024/2025**
Sowing	30 August 2023	22 August 2024
Fungicide application	16 October 2023[b]	23 October 2024[c]
Phoma leaf spot assessment	15 November 2023	26 November 2024

[a] Fungicide applied: Soratel® (active ingredient: prothioconazole)

[b] Fungicide applied: Filan® (active ingredient: boscalid)

[c] Fungicide applied: Shepherd® (active ingredient: boscalid and pyraclostrobin)

Table 5.3: Cultivars used in field experiments at Harpenden and Norwich in the 2023/2024 and 2024/2025 growing seasons.

For the cultivars that are present in the AHDB Recommended Lists (RL) archives (covering between 2005 and 2025), the most recent resistance rating against *L. maculans* is listed. Resistance rating range is between 0 and 9, with 0 being very susceptible and 9 being very resistant.

Cultivar	Present in AHDB RL archives	Most recent resistance rating for phoma stem canker
Acacia	✓	5[a]
Apex	✗	N/A
Campus	✓	6[b]
Castille	✓	6[c]
Catana	✓	4[d]
Kielder	✓	3[e]
Kromerska	✗	N/A
POH Bolko	✗	N/A
Rocket	✗	N/A
Yudal	✗	N/A

[a] AHDB RL for winter oilseed rape 2025/2026

[b] AHDB RL for winter oilseed rape 2019/2020

[c] AHDB RL East/West for winter oilseed rape 2012/2023

[d] AHDB RL East/West for winter oilseed rape 2011/2012

[e] AHDB RL for winter oilseed rape 2020/2021

To assess the incidence of phoma leaf spots at each site, twenty plants were randomly selected from each experimental plot and the numbers of plants with phoma leaf spot lesions caused by *L. maculans* and/or *L. biglobosa* were counted. The average of disease incidence (% of plants affected) was then calculated for each cultivar. In order to assess the severity of phoma leaf spots caused by individual *Leptosphaeria* species, at each site ten plants were randomly selected from each experimental plot and the numbers of plants with phoma leaf spots caused by *L. maculans* or *L. biglobosa* were counted separately. The differentiation between the two types of lesions was based on the morphological characteristics of the lesions on leaves of oilseed rape, where *L. maculans* caused large pale lesions with pycnidia and *L. biglobosa* caused small dark lesions with very few or no pycnidia (West et al., 2001; Fitt et al., 2006b). The average percentages of phoma leaf spots caused by *L. maculans* and *L. biglobosa* were then calculated for each cultivar.

5.2.2.3 Weather conditions

Temperature and rainfall data were collected from the on-site weather stations at Rothamsted Research at Harpenden, Hertfordshire and John Innes Centre at Norwich, Norfolk. Using these data, daily and monthly averages of temperature and rainfall were calculated from August to the following April for the 2023/2024 and 2024/2025 growing seasons.

5.2.3 Phoma stem canker caused by *L. maculans* and *L. biglobosa*

Field experiments at three sites (two sites of ADAS and one site of LSPB) over two growing seasons (2021/2022 and 2022/2023) were used to assess phoma stem canker caused by *L. maculans* and *L. biglobosa* (Table 5.4).

5.2.3.1 Field experiments at Hereford and Huntingdon in the 2021/2022 and 2022/2023 growing seasons

Field experiments were set-up by ADAS at Hereford, Herefordshire and Huntingdon, Cambridgeshire using oilseed rape cultivars with different levels of resistance (Table 5.5). The experiments were set-up with two replicates at both sites. In the 2021/2022 growing season, cultivars Aquila and Flamingo were used. In the 2022/2023 growing season, due to poor establishment of Flamingo, it was replaced by cultivar Acacia at the Huntingdon site (Table 5.5).

Table 5.4: Summary of field experiments for phoma stem canker assessments.

ADAS (Hereford, Herefordshire and Huntingdon, Cambridgeshire) and LSPB (Wisbech, Cambridgeshire) field experiments were independent of each other. Severity of phoma stem canker was assessed and stem samples were taken for DNA extraction and qPCR.

Phoma stem canker assessment date		
Site	**2021/2022**	**2022/2023**
Hereford, Herefordshire (ADAS) (HR1 3PG)	05 July 2022	23 June 2023
Huntingdon, Cambridgeshire (ADAS) (CB23 4NN)	06 July 2022	26 June 2023
Wisbech, Cambridgeshire (LSPB) (CB24 9NG)	03 July 2022	07 July 2023

Table 5.5: Cultivars used in field experiments at Hereford and Huntingdon in the 2021/2022 and 2022/2023 growing seasons.

For the cultivars that are present in the AHDB Recommended Lists (RL) archives (covering between 2005 and 2025), the most recent resistance rating for phoma stem canker is listed. Resistance rating range is between 0 and 9, with 0 being very susceptible and 9 being very resistant. At the Hereford site, cultivars Aquila and Flamingo were assessed in both growing seasons. At the Huntingdon site, cultivar Flamingo was poorly established in the 2022/2023 growing season and was therefore substituted with cultivar Acacia.

Cultivar	Present in AHDB RL archives	Most recent resistance rating for phoma stem canker
Acacia	✓	5[a]
Aquila	✓	8[b]
Flamingo	✓	4[b]

[a] AHDB RL for winter oilseed rape 2025/2026

[b] AHDB RL for winter oilseed rape 2019/2020

No fungicides were applied at both sites in both growing seasons. Two replicates of each cultivar were assessed for severity of phoma stem canker and sampled for quantification of *L. maculans* and *L. biglobosa* DNA in stem basal cankers at both sites in the summer of 2022 and 2023.

5.2.3.2 Field experiments at Wisbech in the 2021/2022 and 2022/2023 growing seasons

Field experiments were set-up by LSPB at Wisbech, Cambridgeshire using different oilseed rape breeding lines or cultivars (with different types of resistance: QR and/or *R*-genes) to test resistance against phoma stem canker pathogens in the 2021/2022 and 2022/2023 growing seasons. Due to changes in commercial interest of the company, cultivar Aurelia was replaced by cultivar Adonis in the 2022/2023 growing season (Table 5.6). In terms of fungicide applications, Pictor® (boscalid and dimoxystrobin) was applied in the early to mid-flowering growth stage to control sclerotinia stem rot in both growing seasons. In the summers of 2022 and 2023, plants from one replicate of cultivars Crocodile, Cromat, Line-A (not yet commercially available at the time), Murray and Turing (and one other as mentioned above) were assessed for phoma stem canker and relative percentages of *L. maculans* and *L. biglobosa* DNA in stem basal cankers.

5.2.3.3 Assessment of phoma stem canker

To assess the severity of phoma stem canker on different cultivars, for all ADAS and LSPB field experiments, ten plants per cultivar were randomly selected for assessment in both growing seasons. The plants were uprooted and cut near the stem base to assess the severity of stem basal cankers. The severity score ranged between 0 and 7, depending on the percentages of necrotic area in cross-sections of stems (0 for no canker, 1 for <5%, 2 for 5-25%, 3 for 26-50%, 4 for 51-75%, 5 for 76-99% of affected stem area, 6 for 100% of stem area affected but the stem is not broken, and 7 for 100% of stem area affected and the stem is broken) (modified from the 1-6 scale introduced by Lô-Pelzer et al., 2009) (Figure 5.8). An average phoma stem canker severity score was then calculated for each cultivar.

5.2.3.4 Sampling of stems for DNA extraction

To assess the contribution of individual *Leptosphaeria* species to stem basal cankers, for all ADAS and LSPB field experiments assessed, five to ten diseased plants per cultivar were

Table 5.6: Cultivars used in field experiments at Wisbech in the 2021/2022 and 2022/2023 growing seasons.

For the cultivars that are present in the AHDB Recommended Lists (RL) archives (covering between 2005 and 2025), the most recent resistance rating for phoma stem canker is listed. Resistance rating range is between 0 and 9, with 0 being very susceptible and 9 being very resistant. Resistance type(s) and gene(s) are also listed. In the 2021/2022 growing season, cultivars Adonis, Crocodile, Cromat, Line-A (not yet commercially available at the time), Murray and Turing were assessed. In the 2022/2023 season, cultivar Adonis was substituted with Aurelia due to changes in commercial interest of the company.

Cultivar	Present in AHDB RL archives	Most recent resistance rating for phoma stem canker	Resistance type(s) and gene(s)
Adonis	✗	N/A	Qualitative (*Rlm7*)
Aurelia	✓	4[a]	Qualitative (*Rlm7*)
Crocodile	✓	4[a]	No known resistance
Cromat	✗	N/A	Qualitative (*Rlm7*)
Line-A	✗	N/A	Qualitative (*Rlm7* & *RlmS)*
Murray	✓	8[a]	Qualitative (*RlmS*)
Turing	✓	4[a]	Quantitative

[a] AHDB RL for winter oilseed rape 2025/2026

Figure 5.8: Phoma stem canker assessment scale (0-7).

The severity score is based on the percentage area of cross-sections of stems that was necrotic, 0 for no canker, 1 for <5%, 2 for 5-25%, 3 for 26-50%, 4 for 51-75%, 5 for 76-99% of affected stem area, 6 for 100% of stem area affected but the stem is not broken, and 7 for 100% of stem area affected and the stem is broken. This scale was modified from the 1-6 scale of Lô-Pelzer et al. 2009. Photos for scores 0 to 6 were taken by Dr. Asna Javaid and photo for score 7 was taken by Prof. Yong-Ju Huang in July 2016. This figure was adapted from Javaid, 2019.

randomly selected for DNA extraction and qPCR to identify the relative amounts of *L. maculans* and *L. biglobosa* DNA in stem basal cankers. The plants were uprooted and cut 20 cm above the stem base and taken to the laboratory for sampling. Using clean scalpels, shavings of necrotic tissues at the stem base were taken, placed in labelled 2 mL screw-cap tubes and placed in a -20°C freezer prior to freeze drying. The caps were removed, and the necks of the tubes were covered with Parafilm®. Using a sterilised needle, five small holes were punctured in the Parafilm® covering the neck of each tube and all tubes were placed in a freeze-dryer for 72 h. Once the freeze-drying was done, Parafilm® was removed from the necks of the tubes. Using a clean pestle and mortar, the freeze dried samples were homogenised until they were in a fine powder texture and placed back into their labelled tubes. The pestle and mortar were cleaned in between each sample.

5.2.3.5 DNA extraction from stems

DNA extraction was done using the DNAmite Plant DNA Extraction Kit (Microzone Ltd.) as described in section 2.3, using homogenised stem samples instead of mycelial samples.

5.2.3.6 DNA quality checks and dilution for quantitative polymerase chain reaction (qPCR)

DNA quality checks and dilutions were done as described in section 2.4.

5.2.3.7 Quantitative polymerase chain reaction (qPCR)

qPCR analyses were done as described in section 2.5.

5.2.4 Statistical analysis

All of the statistical analyses of the data in this chapter were done using GraphPad Prism (version 10 for macOS) (GraphPad Software, Boston, Massachusetts, United States). To analyse the differences in incidence of phoma leaf spot (% of plants affected), and percentages of phoma leaf spot lesions caused by *L. maculans* on ten different cultivars assessed at Rothamsted Research and John Innes Centre in the 2023/2024 and 2024/2025 growing seasons; one-way analysis of variance (ANOVA) tests were done for each growing season and site individually. To compare the overall means of different growing seasons, paired t-tests were done for each site. To analyse the severity of phoma

stem canker and percentage of *L. maculans* DNA in stem basal cankers of two different cultivars assessed at ADAS at Hereford, Herefordshire in the 2021/2022 and 2022/2023 growing seasons, a two-way ANOVA test was done. To analyse the same data from ADAS at Huntingdon, Cambridgeshire, unpaired t-tests were done for each growing season individually. To analyse the severity of phoma stem canker and percentage of *L. maculans* DNA in stem basal cankers of six different cultivars assessed at LSPB in Wisbech, Cambridgeshire, one-way ANOVA tests were done for each growing season individually. For data from ADAS at Huntingdon, Cambridgeshire and LSPB at Wisbech, Cambridgeshire, it was not possible to test for more factors due to differences in cultivars used in different growing seasons. Where applicable, Tukey's HSD post-hoc tests were done to separate the means of the cultivars at a probability of 5 % significance.

5.3 Results

5.3.1 Timing and pattern of ascospore release by *L. maculans* and *L. biglobosa*

5.3.1.1 Release of ascospores

Ascospore release data were obtained both by microscopic counting of ascospores of *Leptosphaeria* species to calculate the number of ascospores per m^3 of air, and by DNA extraction followed by qPCR analyses to quantify the amounts of *L. maculans* and *L. biglobosa* DNA in air samples obtained at Bayfordbury, Hertfordshire. This was done for four growing seasons; from 2020/2021 to 2023/2024.

5.3.1.1.1 2020/2021 growing season

In the 2020/2021 growing season, the first major release of ascospores (which is ≥ 10% of the maximum number of ascospores released in the season) was observed on 30 September 2020 (Figure 5.9A). The maximum release of ascospores was on 27 October 2020, with 1058 ascospores per m^3 of air. Number of ascospores released declined from December to January and remained small until the end of March.

Upon quantification of DNA using species-specific primers, it was observed that ascospores of *L. maculans* and *L. biglobosa* were both released at similar times throughout the 2020/2021 growing season (Figure 5.10A). Although there was less *L. biglobosa* DNA quantified compared to *L. maculans* DNA in this season, the maximum amounts of DNA quantified from both *L. maculans* and *L. biglobosa* were on the same day, 21 October 2020, with 4663.8 pg and 618.1 pg, respectively.

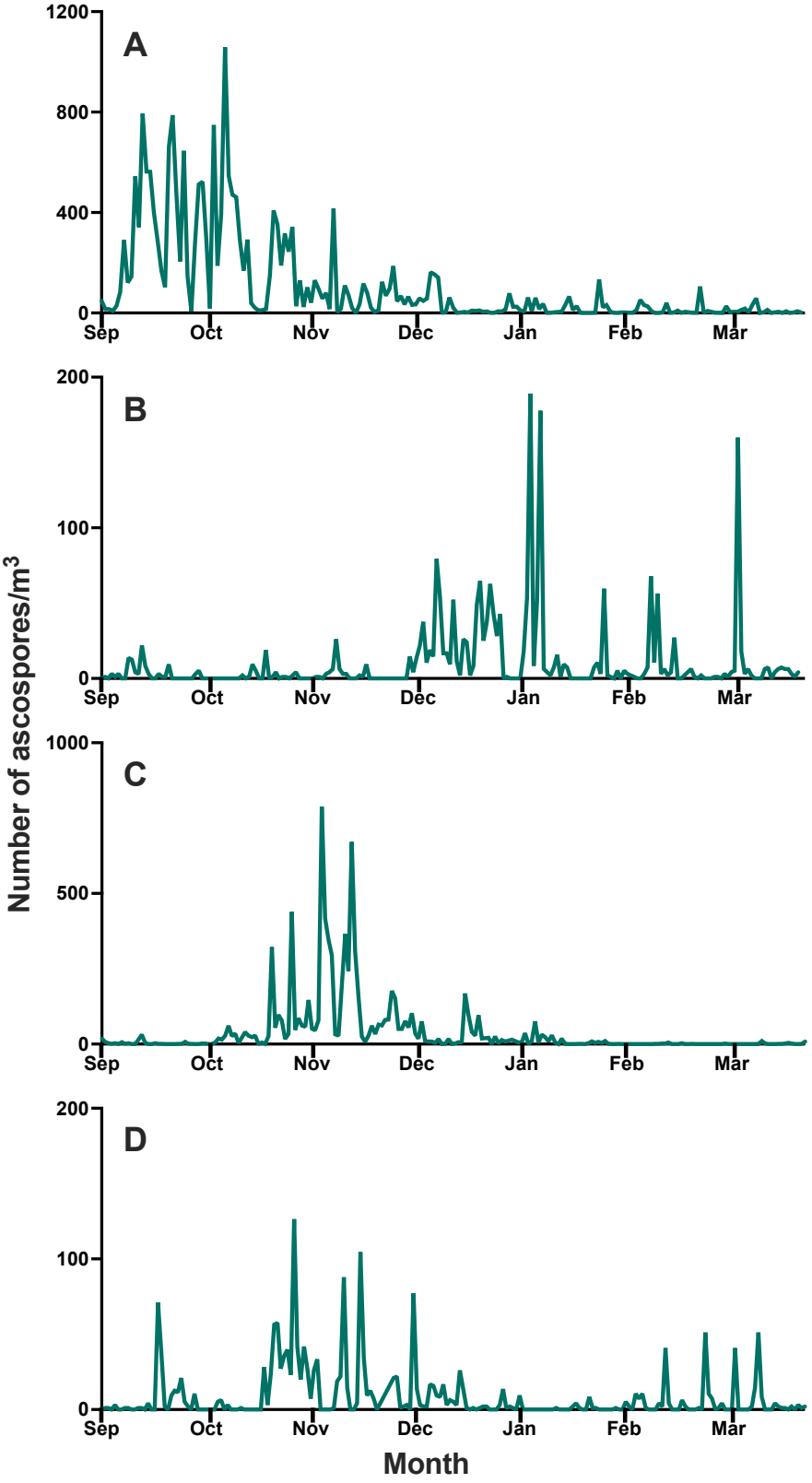

Figure 5.9: Patterns of ascospore release of *Leptosphaeria* species at Bayfordbury, Hertfordshire between September and March in (A) 2020/2021, (B) 2021/2022, (C) 2022/2023 and (D) 2023/2024 growing seasons.

Air samples were collected using a Burkard spore sampler and ascospores of *Leptosphaeria* species on spore tape samples were counted using a light microscope.

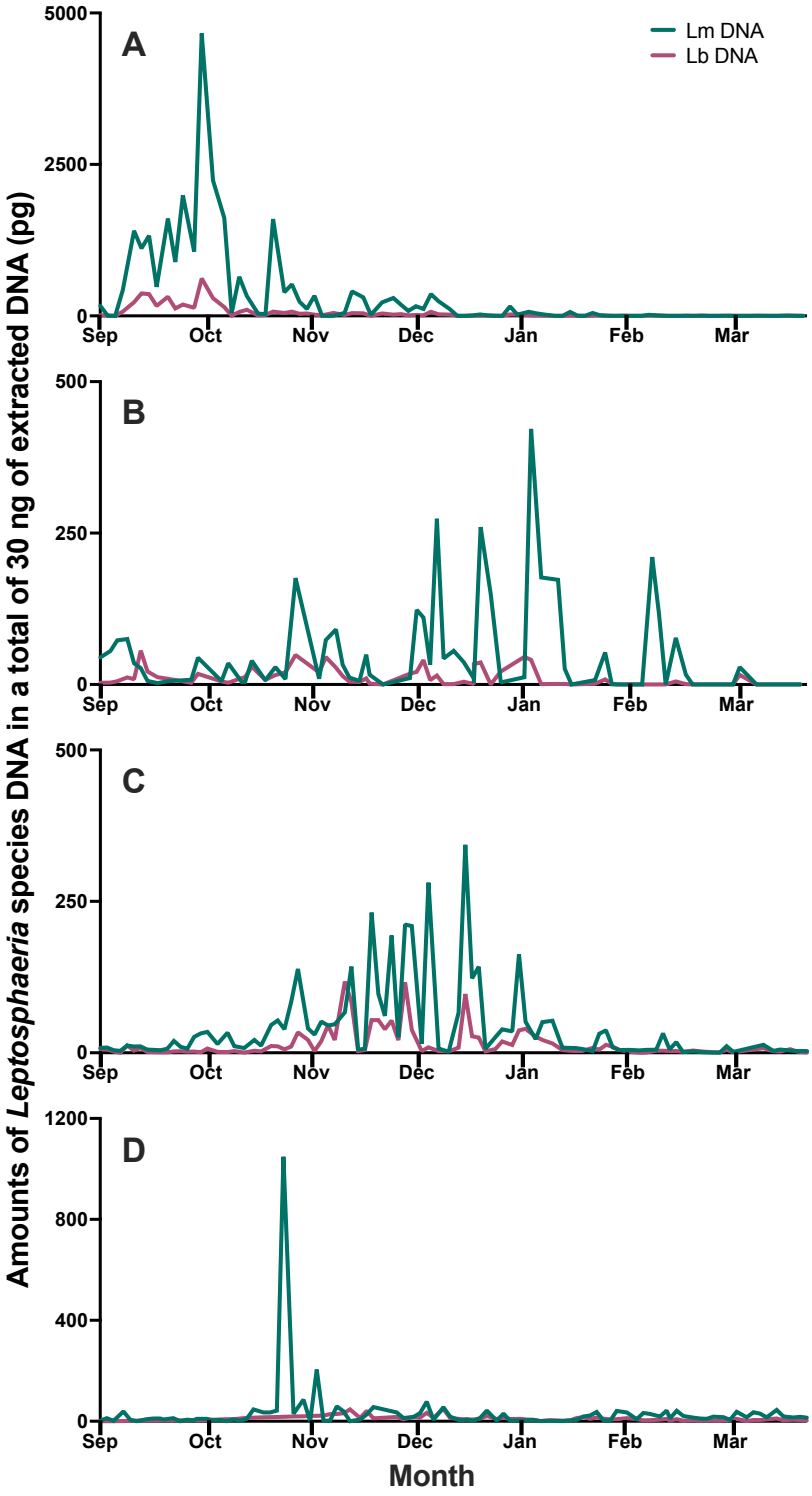

Figure 5.10: Amounts of *Leptosphaeria* species DNA (pg) in a total of 30 µL of extracted DNA at Bayfordbury, Hertfordshire between September and March in (A) 2020/2021, (B) 2021/2022, (C) 2022/2023 and (D) 2023/2024 growing seasons.

Air samples were collected using a Burkard spore sampler and amounts of *L. maculans* and *L. biglobosa* in spore tape samples were quantified using quantitative polymerase chain reactions (qPCR).

5.3.1.1.2 2021/2022 growing season

In the 2021/2022 growing season, the first major release of ascospores was observed on 14 September 2021 (Figure 5.9B). Although release of ascospores increased throughout the autumn, the maximum release of ascospores was observed relatively late in the growing season on 08 January 2022, with 189 ascospores per m^3 of air. The number of ascospores released decreased throughout February, with another major release observed on 03 March 2022, then reducing and remaining small until the end of March.

Upon quantification of DNA, it was observed that ascospores of *L. maculans* and *L. biglobosa* were released at similar times throughout the 2021/2022 growing season (Figure 5.10B). However, there were instances in winter (mid-January and mid-February) where the DNA from ascospores in the air corresponded to a major ascospore release event by *L. maculans*, with very little or no *L. biglobosa* DNA quantified. Overall, there was less *L. biglobosa* DNA quantified compared to *L. maculans* DNA in this season. The maximum amount of *L. maculans* DNA was quantified on 08 January 2022 with 422.2 pg (quantity of *L. biglobosa* DNA was 40.7 pg on the same day). The maximum amount of *L. biglobosa* DNA was quantified on 14 September 2021, with 55.9 pg (quantity of *L. maculans* DNA was 27.2 pg on the same day).

5.3.1.1.3 2022/2023 growing season

In the 2022/2023 growing season, the first major release of ascospores was observed on 22 October 2022 (Figure 5.9C). The maximum release of ascospores was on 06 November 2022, with 787 ascospores per m^3 of air. There was also another major ascospore release event in mid-November. Release of ascospores then declined throughout winter and remained small until the end of March.

Upon quantification of DNA, it was observed that ascospores of *L. maculans* and *L. biglobosa* were released at similar times throughout the 2022/2023 growing season (Figure 5.10C). Although there was less *L. biglobosa* DNA quantified compared to *L. maculans* DNA in this season, the maximum amount of *L. biglobosa* DNA was quantified before *L. maculans* DNA. The maximum amount of *L. maculans* DNA was quantified on 19 December 2022 with 343.4 pg (quantity of *L. biglobosa* DNA was 97.0 pg on the same day). The maximum amount of *L. biglobosa* DNA was quantified on 13 November 2022 with 117.5 pg (quantity of *L. maculans* DNA was 66.8 pg on the same day).

5.3.1.1.4 2023/2024 growing season

In the 2023/2024 growing season, the first major release of ascospores was observed on 18 September 2023 (Figure 5.9D). The maximum release of ascospores was on 29 October 2023, with 126 ascospores per m^3 of air. Major ascospore release events continued throughout November and December. Number of ascospores released then reduced and remained small throughout January and early-February, followed by a few small ascospore release events from mid-February to mid-March. Release of ascospores then declined and remained small until the end of March.

Upon quantification of DNA, it was observed that the majority of ascospores released in the 2023/2024 growing season were those of *L. maculans*, since very little *L. biglobosa* DNA was quantified between September and March (Figure 5.10D). The maximum amount of *L. maculans* DNA was quantified on 26 October 2023 with 1048.1 pg (quantity of *L. biglobosa* DNA was 17.5 pg on the same day). The maximum amount of *L. biglobosa* DNA was quantified on 13 December 2023 with 49.1 pg (quantity of *L. maculans* DNA was 55.7 pg on the same day).

5.3.1.1.5 Summary of all four growing seasons

Overall, the first major release of ascospores of *Leptosphaeria* species was observed in mid-late-September, with the exception of the 2022/2023 growing season, where this was observed in late-October. Maximum release of ascospores of *Leptosphaeria* species was observed in late-October or early-November, with the exception of 2021/2022 growing season, where this was observed in early-January. In all four growing seasons, there was more *L. maculans* DNA quantified in the air compared to *L. biglobosa* DNA. According to DNA quantification data, maximum release of ascospores of both *L. maculans* and *L. biglobosa* was observed on the same day in the 2020/2021 growing season. Interestingly, maximum release of ascospores of *L. biglobosa* was observed approximately three and a half months earlier than the maximum for *L. maculans* in 2021/2022 and approximately a month earlier than *L. maculans* in 2022/2023 growing seasons. Finally, maximum release of ascospores of *L. maculans* was observed approximately a month and a half earlier than that of *L. biglobosa* in the 2023/2024 growing season.

5.3.1.2 Weather conditions

5.3.1.2.1 2020/2021 growing season

In the 2020/2021 growing season, the average daily temperature at Bayfordbury, Hertfordshire ranged from a maximum of 18.5°C in August to a minimum of 3.7°C in January. In August-September, the average daily temperature was 16.6°C, ranging between 25.0°C on 11 August and 9.3°C on 26 September. In October-November, it was 9.8°C, ranging between 14.9°C on 21 October and 1.4°C on 27 November. In December-January, it was 4.6°C, ranging between 11.1°C on 18 December and -0.9°C on 09 January. In February-March, the average daily temperature was 6.4°C, with fluctuations observed in February, ranging between -1.9°C on 11 February and 13.0°C on 24 February (Figure 5.11A) (Table 5.7).

There was a total of 272.0 mm rainfall recorded at Bayfordbury, Hertfordshire in the 2020/2021 growing season. In August-September, there was a total of 66.5 mm rainfall across thirty rain days (≥ 0.1 mm rainfall), with one day of heavy rain (>10 mm) (14 August, 17.2 mm). In October-November, there was a total of 83.8 mm rainfall across fifty-six rain days, with two days of heavy rain (02 and 03 October with 12.7 mm and 16.9 mm, respectively). In December-January, 93.8 mm of rainfall was recorded across fifty-nine rain days, with two days of heavy rain (27 December and 14 January with 13.0 mm and 10.8 mm, respectively). In February-March, 27.8 mm of rainfall was recorded across thirty-eight rain days, with the heaviest recorded as 2.9 mm on 13 March (Figure 5.11A) (Table 5.8).

The ascospore data showed that major releases of ascospores were observed from October to December, especially following increases in temperature and rainfall. In addition, It was observed that dry periods without regular rainfall alongside temperatures < 5°C led to a reduction in ascospores of *Leptosphaeria* species in the air.

5.3.1.2.2 2021/2022 growing season

In the 2021/2022 growing season, the average daily temperature at Bayfordbury, Hertfordshire ranged from a maximum of 16.1°C in August to a minimum of 4.8°C in January. In August-September, the average daily temperature was 16.0°C, between 19.6°C on 07 September and 10.5°C on 29 September.

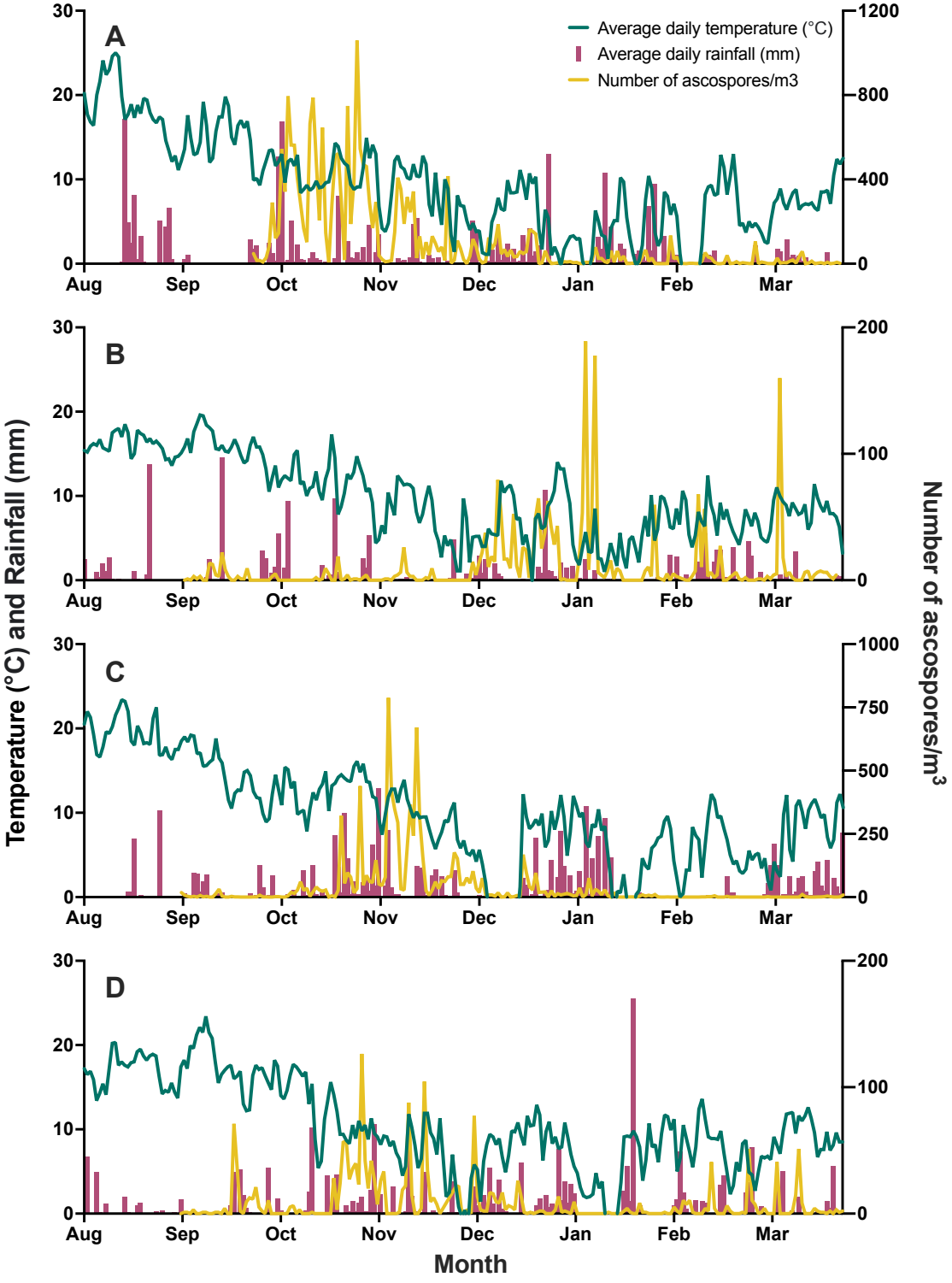

Figure 5.11: Daily release of ascospores of *Leptosphaeria* species in relation to average daily temperature (°C) and rainfall (mm) at Bayfordbury, Hertfordshire from August to March in (A) 2020/2021, (B) 2021/2022, (C) 2022/2023 and (D) 2023/2024 growing seasons.

Air samples were collected using a Burkard spore sampler and ascospores of *Leptosphaeria* species on spore tape samples were counted using a light microscope. Daily weather data were collected from the weather station located on-site.

Table 5.7: Minimum, maximum and average daily temperature (°C) at Bayfordbury, Hertfordshire between August and March in the 2020/2021, 2021/2022, 2022/2023 and 2023/2024 growing seasons.

Weather data were collected from the on-site weather station at Bayfordbury, Hertfordshire.

Month	2020/2021			2021/2022			2022/2023			2023/2024		
	Minimum daily temp (°C)	Maximum daily temp (°C)	Average daily temp (°C)	Minimum daily temp (°C)	Maximum daily temp (°C)	Average daily temp (°C)	Minimum daily temp (°C)	Maximum daily temp (°C)	Average daily temp (°C)	Minimum daily temp (°C)	Maximum daily temp (°C)	Average daily temp (°C)
Aug	11.1	25.0	18.5	13.6	18.5	16.1	16.3	23.4	19.4	13.7	20.3	16.9
Sep	9.3	19.8	14.6	10.5	19.6	15.9	8.9	19.2	14.6	12.2	23.4	17.5
Oct	8.4	14.9	10.9	7.8	17.3	12.1	7.8	16.1	13.1	5.4	18.2	12.6
Nov	1.4	14.1	8.7	1.1	12.4	7.4	5.7	13.9	9.6	-0.4	11.9	7.4
Dec	-0.3	11.1	5.5	-0.3	14.0	7.1	-5.2	12.2	4.0	-1.3	12.9	7.8
Jan	-0.9	10.4	3.7	1.0	13.2	4.8	-2.6	12.0	5.0	-2.0	10.8	5.1
Feb	-1.9	13.0	5.6	3.9	12.4	7.4	0.0	12.2	6.0	2.3	13.6	8.3
Mar	2.4	12.5	7.2	3.2	11.4	7.8	0.8	12.1	7.4	2.7	12.6	8.5
Mean			**9.3**			**9.8**			**9.9**			**10.5**

Table 5.8: Average daily / total monthly rainfall (mm) and total monthly rain days (days) at Bayfordbury, Hertfordshire between August and March in the 2020/2021, 2021/2022, 2022/2023 and 2023/2024 growing seasons.

Weather data were collected from the on-site weather station at Bayfordbury, Hertfordshire.

Month	2020/2021			2021/2022			2022/2023			2023/2024		
	Average daily rainfall (mm)	Total monthly rainfall (mm)	Total monthly rain days (days)	Average daily rainfall (mm)	Total monthly rainfall (mm)	Total monthly rain days (days)	Average daily rainfall (mm)	Total monthly rainfall (mm)	Total monthly rain days (days)	Average daily rainfall (mm)	Total monthly rainfall (mm)	Total monthly rain days (days)
Aug	1.7	53.8	16	0.8	25.9	20	0.6	18.8	5	0.6	18.6	20
Sep	0.4	12.7	14	0.8	25.3	14	0.7	21.2	21	0.7	21.7	15
Oct	2.0	63.2	29	1.4	42.5	21	1.4	43.8	29	1.2	37.1	24
Nov	0.7	20.6	27	0.2	6.9	21	1.8	55.4	27	1.4	40.5	28
Dec	1.5	46.6	29	1.0	30.7	26	0.9	28.6	24	1.3	41.3	24
Jan	1.5	47.2	30	0.3	8.4	20	1.7	51.7	28	1.6	49.4	20
Feb	0.5	13.3	21	1.1	31.8	22	0.2	4.6	12	1.0	29.2	21
Mar	0.5	14.5	17	0.5	15.4	18	1.7	51.3	27	1.0	32.1	24
Total		**272.0**	**183**		**186.9**	**162**		**275.2**	**173**		**269.9**	**176**
Mean	**1.1**	**33.9**	**23**	**0.8**	**23.4**	**20**	**1.1**	**34.4**	**22**	**1.3**	**33.7**	**22**

Each day with over 0.1 mm rain recorded was counted as a rain day.

In October-November, it was 9.8°C, ranging between 17.3°C 19 in October and 1.1°C on 29 November. In December-January, it was 6.0°C, with fluctuations observed, ranging between -0.3°C on 22 December and 14.0°C on 30 December. In February-March, the average daily temperature was 7.6°C, ranging between 12.4°C on 16 February and 3.2°C on 31 March (Figure 5.11B, Table 5.7).

There was a total of 186.9 mm rainfall recorded at Bayfordbury, Hertfordshire in the 2021/2022 growing season. In August-September, there was a total of 51.2 mm rainfall across thirty-four rain days, with two days of heavy rain (22 August and 14 September with 13.7 mm and 14.6 mm, respectively). In October-November, there was a total of 49.4 mm rainfall across forty-two rain days, with the heaviest rainfall recorded as 9.7 mm on 20 October. In December-January, 39.1 mm of rainfall was recorded across forty-six rain days, with one day of heavy rain (26 December, 10.7 mm). In February-March, 47.2 mm of rainfall was recorded across forty rain days, with the heaviest rainfall recorded as 4.6 mm on 01 March (Figure 5.11B) (Table 5.8).

The ascospore data showed that the major releases of ascospores were observed following increases in temperature and rainfall intermittently from December to March, which was later than in the previous growing season. Additionally, it was observed that the dry autumn (relatively dryer than the previous growing season despite having similar autumn and warmer winter temperatures) delayed the release of ascospores of *Leptosphaeria* species.

5.3.1.2.3 2022/2023 growing season

In the 2022/2023 growing season, the average daily temperature at Bayfordbury, Hertfordshire ranged from a maximum of 19.4°C in August to 4.0°C in December. In August-September, the average daily temperature was 17.0°C, ranging between 23.4°C on 13 August and 8.9°C on 28 September. In October-November, it was 11.4°C, ranging between 16.1°C on 27 October and 5.7°C on 21 November. In December-January, it was 4.5°C, with fluctuations observed and ten consecutive days of sub-zero temperatures recorded in December, ranging between -5.2°C on 15 December and 12.2°C on 19 December. In February-March, the average daily temperature was 6.7°C, with

fluctuations observed in February, ranging between 0.0°C on 07 February and 12.2°C on 17 February (Figure 5.11C) (Table 5.7).

There was a total of 275.2 mm rainfall recorded at Bayfordbury, Hertfordshire in the 2022/2023 growing season. In August-September, there was a total of 40.0 mm rainfall across twenty-six rain days, with one day of heavy rain (25 August, 10.3 mm). In October-November, there was a total of 99.2 mm rainfall across fifty-six rain days, with two days of heavy rain (23 October and 03 November with 10.0 mm and 12.3 mm, respectively). In December-January, 80.3 mm of total rainfall was recorded across fifty-one rain days, with one day of heavy rain (08 January, 10.8 mm). In February-March, 55.9 mm of total rainfall was recorded across thirty-nine rain days, with the heaviest rainfall recorded as 7.6 mm on 31 March (Figure 5.11C) (Table 5.8).

The ascospore release data showed that the major releases of ascospores were observed following increases in temperature and especially a few days after heavy rainfall events from late-October to December. In addition, it was observed that dry periods without regular rainfall alongside temperatures < 5°C (especially sub-zero temperatures) led to a reduction of ascospores of *Leptosphaeria* species in the air, in a similar fashion to the 2020/2021 growing season.

5.3.1.2.4 2023/2024 growing season

In 2023/2024 growing season, the average daily temperature at Bayfordbury, Hertfordshire ranged from a maximum of 17.5°C in September to a minimum of -2.0°C in January. In August-September, the average daily temperature was 17.2°C, ranging between 23.4°C on 09 September and 12.2°C on 22 September. In October-November, it was 10.0°C, ranging between 18.2°C on 01 October and -0.4°C on 30 November. In December-January, it was 6.5°C, ranging between 12.9°C on 24 December and -2.0°C on 18 January. In February-March, the average daily temperature was 8.4°C, with fluctuations observed in February, ranging between 13.6°C on 15 February and 2.3°C on 24 February (Figure 5.11D) (Table 5.7).

There was a total of 269.9 mm rainfall recorded at Bayfordbury, Hertfordshire in the 2023/2024 growing season. In August-September, there was a total of 40.3 mm rainfall

across thirty-five rain days, with the heaviest recorded as 6.7 mm on 02 August. In October-November, there was a total of 77.6 mm rainfall across fifty-two rain days, with two days of heavy rain (13 October and 02 November with 10.2 mm and 10.6 mm, respectively). In December-January, 90.7 mm of rainfall was recorded across forty-four rain days, with one day of heavy rain (24 January, 25.5 mm). In February-March, 61.3 mm of rainfall was recorded across forty-five rain days, with the heaviest rainfall recorded as 7.9 mm on 02 March (Figure 5.11D) (Table 5.8).

The ascospore release data showed that the major releases of ascospores were observed from late-September to mid-December, and then from mid-February to mid-March, following increases in temperature and rainfall. Additionally, it was observed that, despite being followed by a heavy rainfall event, temperatures < 5°C led to a reduction in ascospores of *Leptosphaeria* species in the air.

5.3.1.2.5 Summary of all four growing seasons

Although daily average temperature of different months fluctuated from one growing season to another, the overall mean of daily average temperature between September and March has increased over time, from 9.3°C in 2020/2021 to 10.5°C in the 2023/2024 growing season. Similarly, total rainfall of different months (ranging between 269.9 mm – 275.2 mm), except 2021/2022 (186.9 mm), which also had the dryest autumn-winter period across all four growing seasons, as well as number of rain days from 01 August until the first major ascospore release (ranging between 17 – 35 days) differed from one growing season to another.

5.3.2 Phoma leaf spots caused by *L. maculans* and *L. biglobosa*

5.3.2.1 Field experiments at Harpenden in the 2023/2024 and 2024/2025 growing seasons

5.3.2.1.1 Incidence and severity of phoma leaf spot

At Harpenden, in the 2023/2024 growing season, there were no significant differences in average incidence of phoma leaf spot (% of plants affected) between different cultivars ($F(9,20) = 1.17$, $P = 0.362$) (Table 5.9). The average incidence of phoma leaf spots ranged between 20.0 % (Kromerska) and 41.7 % (Yudal) for all ten cultivars assessed (Table 5.10) (Figure 5.12A).

Table 5.9: Statistical testing outputs for significant probability of the main effects of cultivar on average incidence of phoma leaf spots (% of plants affected) and average percentage of phoma leaf spot lesions caused by *Leptosphaeria maculans* (%) for ten different cultivars at Harpenden in the 2023/2024 and 2024/2025 growing seasons.

One-way analysis of variance (ANOVA) tests were done for each growing season separately by selecting cultivar as a factor. Overall means from different growing seasons were compared using a paired t-test.

Average incidence of phoma leaf spots (% of plants affected)			
2023/2024			
Factor	***df***	**F statistic**	**F probability**
Cultivar	29	1.17	= 0.362
2024/2025			
Factor	***df***	**F statistic**	**F probability**
Cultivar	29	2.32	= 0.056
2023/2024 × 2024/2025			
Factor	***df***	**t statistic**	**t probability**
Season	29	1.62	= 0.116
Average percentage of phoma leaf spots caused by *L. maculans* (%)			
2023/2024			
Factor	***df***	**F statistic**	**F probability**
Cultivar	299	9.18	< 0.0001
2024/2025			
Factor	***df***	**F statistic**	**F probability**
Cultivar	299	2.81	< 0.05
2023/2024 × 2024/2025			
Factor	***df***	**t statistic**	**t probability**
Season	299	37.79	< 0.0001

Table 5.10: Average incidence of phoma leaf spots (% of plants affected) for ten different cultivars at Harpenden in the 2023/2024 and 2024/2025 growing seasons.

Tukey's HSD tests were used for each growing season separately to compare the mean incidence of phoma leaf spots between different cultivars for each growing season. Overall means from different growing seasons were compared using a paired t-test. Cultivars that do not share a letter are considered significantly different ($P < 0.05$).

Cultivar	Average incidence of phoma leaf spots (% of plants affected)	
	2023/2024	2024/2025
Acacia	25.0 **a**	30.0 **a**
Apex	33.3 **a**	46.7 **a**
Campus	40.0 **a**	23.3 **a**
Castille	30.0 **a**	30.0 **a**
Catana	38.3 **a**	31.7 **a**
Kielder	28.3 **a**	40.0 **a**
Kromerska	20.0 **a**	48.3 **a**
POH Bolko	40.0 **a**	45.0 **a**
Rocket	25.0 **a**	38.3 **a**
Yudal	41.7 **a**	50.0 **a**
Mean	**32.2 a**	**38.3 a**

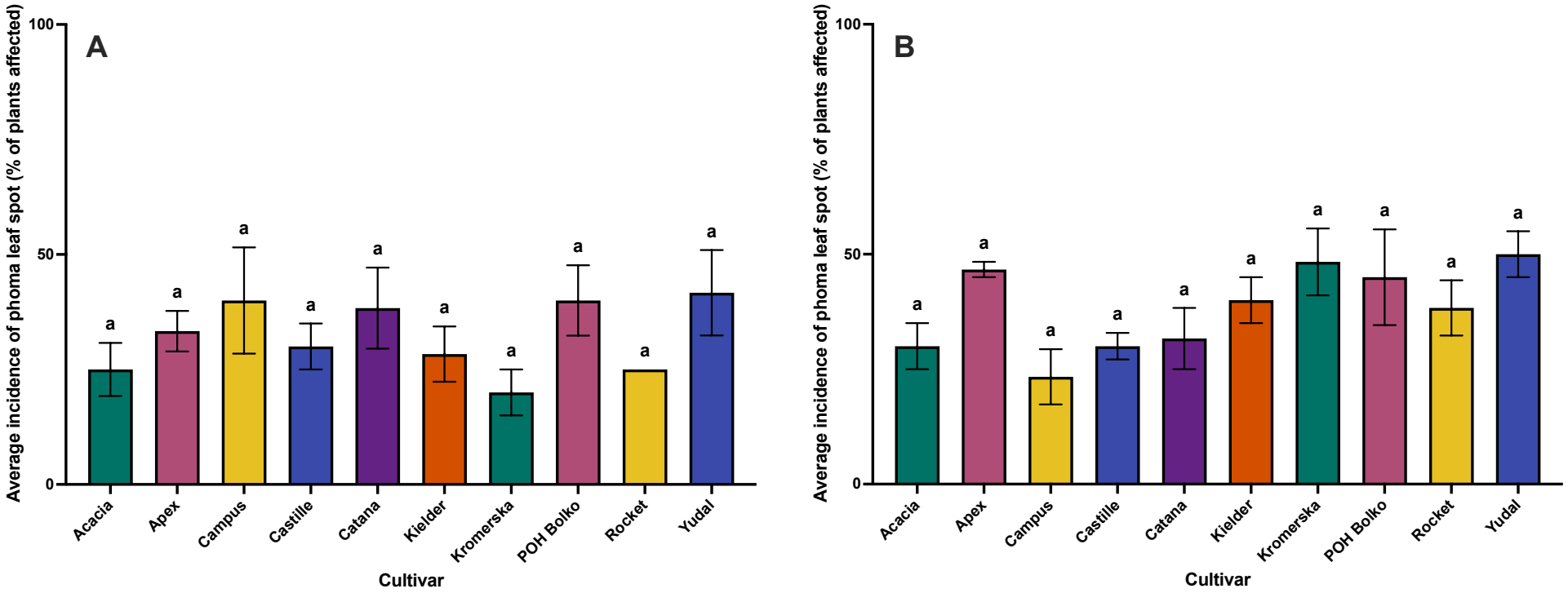

Figure 5.12: Average incidence of phoma leaf spots (% of plants affected) for ten different cultivars at Harpenden in the (A) 2023/2024 and (B) 2024/2025 growing seasons.

Tukey's HSD tests were used for each growing season separately to compare the mean incidence of phoma leaf spots between different cultivars for each growing season. Cultivars that do not share a letter are considered significantly different ($P < 0.05$). Error bars show standard error of the mean (SEM) (2023/2024 growing season, 59 d.f.; 2024/2025 growing season 59 d.f.).

In the 2024/2025 growing season, there were also no significant differences in average incidence of phoma leaf spots (% of plants affected) between different cultivars ($F(9,20) = 2.32$, $P = 0.056$) (Table 5.9). The average incidence of phoma leaf spots ranged between 23.3 % (Campus) and 50.0 % (Yudal) for all ten cultivars assessed (Table 5.10) (Figure 5.12B).

At Harpenden, in the 2023/2024 growing season, average percentage of phoma leaf spot lesions caused by *L. maculans* was significantly different between different cultivars ($F(9,290) = 9.18$, $P < 0.0001$) (Table 5.9). For the cultivars Apex (9.8 %), Campus (7.1 %), Catana (11.4 %), Kromerska (16.4 %), POH Bolko (7.0 %) and Rocket (16.9 %), there were no significant differences between them (Table 5.11) (Figure 5.13A). Castille (26.9 %) was not significantly different to these cultivars, despite being significantly different to Acacia (6.2 %) and Kielder (4.4 %), which were not significantly different to each other or to the cultivars initially mentioned. Finally, Yudal (50.0 %) was significantly different to all other cultivars, with the greatest average percentage of phoma leaf spot lesions caused by *L. maculans* (Table 5.11).

In the 2024/2025 growing season, average percentage of phoma leaf spot lesions caused by *L. maculans* was also significantly different between different cultivars ($F(9,290) = 2.81$, $P < 0.05$) (Table 5.9). For the cultivars Apex (87.5 %), Castille (91.4 %), Catana (89.4 %), Kielder (87.5 %), POH Bolko (90.2 %), Rocket (85.7 %) and Yudal (84.3 %), there were no significant differences between them (Table 5.11) (Figure 5.13B). Kromerska (98.0 %) was not significantly different to these cultivars, despite being significantly different to Acacia (77.3 %) and Campus (82.4 %), which were not significantly different to each other or to the initially mentioned cultivars (Table 5.11).

In summary, at Harpenden, overall incidence of phoma leaf spots (% of plants affected) increased from 32.2 % in the 2023/2024 growing season to 38.3 % in the 2024/2025 growing season, but this was not significant ($t(29) = 1.62$, $P = 0.116$) (Table 5.9, Table 5.10). In addition, the overall average percentage of phoma leaf spot lesions caused by *L. maculans* (%) increased significantly from 15.6 % in the 2023/2024 growing season to 87.1 % in the 2024/2025 growing season ($t(299) = 37.79$, $P < 0.0001$) (Table 5.9, Table 5.11).

Table 5.11: Average percentage of phoma leaf spot lesions caused by *Leptosphaeria maculans* (%) for ten different cultivars at Harpenden in the 2023/2024 and 2024/2025 growing seasons.

Tukey's HSD tests were used for each growing season separately to compare the mean percentage of phoma leaf spot lesions caused by *L. maculans* between different cultivars for each growing season. Overall means from different growing seasons were compared using a paired t-test. Cultivars that do not share a letter are considered significantly different ($P < 0.05$).

Cultivar	**Average percentage of phoma leaf spots caused by *L. maculans* (%)**	
	2023/2024	**2024/2025**
Acacia	6.2 **c**	77.3 **b**
Apex	9.8 **bc**	87.5 **ab**
Campus	7.1 **bc**	82.4 **b**
Castille	26.9 **b**	91.4 **ab**
Catana	11.4 **bc**	89.4 **ab**
Kielder	4.4 **c**	87.5 **ab**
Kromerska	16.4 **bc**	98.0 **a**
POH Bolko	7.0 **bc**	90.2 **ab**
Rocket	16.9 **bc**	85.7 **ab**
Yudal	50.0 **a**	84.3 **ab**
Mean	**15.6 b**	**87.1 a**

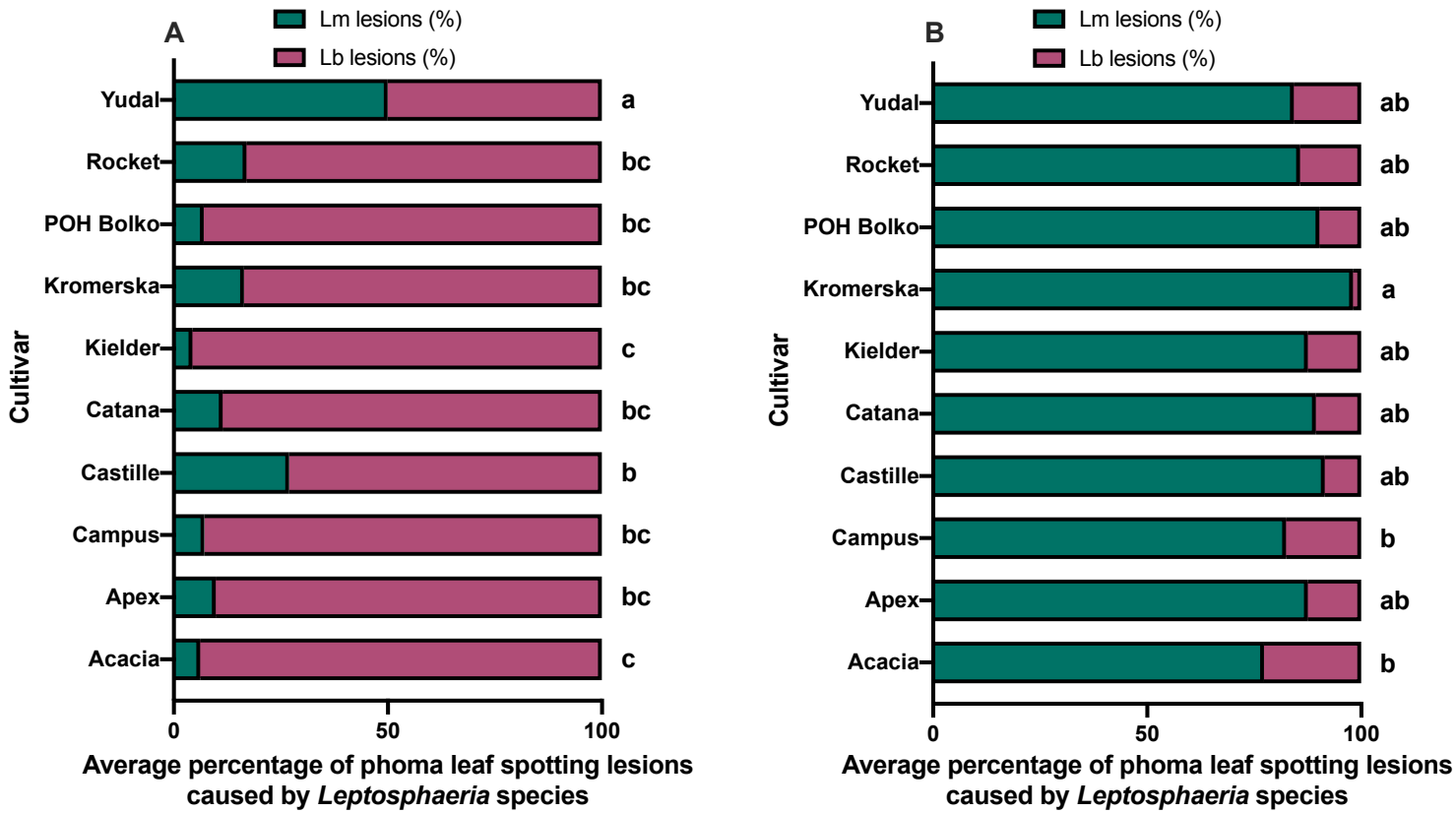

Figure 5.13: Average percentage of phoma leaf spot lesions caused by *Leptosphaeria* species (%) for ten different cultivars at Harpenden in the (A) 2023/2024 and (B) 2024/2025 growing seasons.

Tukey's HSD tests were used for each growing season separately to compare the mean percentage of phoma leaf spots caused by *L. maculans* between different cultivars for each growing season. Cultivars that do not share a letter are considered significantly different ($P < 0.05$) (2023/2024 growing season, 299 d.f.; 2024/2025 growing season, 299 d.f.).

5.3.2.1.2 Weather conditions

In the 2023/2024 growing season between August and March, the average daily maximum temperature at Harpenden ranged from 25.2°C in August to 8.9°C in January, and minimum temperature ranged from 13.9°C in August to -1.7°C in January (Figure 5.14A) (Table 5.12). In August-September, the daily temperature ranged between 25.2°C (23 August) and 12.7°C (23 September), with an average temperature of 17.4°C. In October-November, the daily temperature ranged between 18.5°C (09 October) and 0.2°C (30 November), with an average temperature of 9.9°C. In December-January, the daily temperature ranged between 11.5°C (24 December) and -1.7°C (18 January), with an average temperature of 5.7°C. In February-March, the daily temperature ranged between 13.7°C (15 February) and 2.6°C (24 February), with an average temperature of 7.9°C (Figure 5.14A) (Table 5.12).

There was a total of 670.0 mm rainfall recorded at Harpenden in the 2023/2024 growing season between August and March (Table 5.13). In August-September, there was a total of 100.1 mm rainfall across twenty-seven rain days, with one day of heavy rain (> 10 mm) (20 September, 34.0 mm). In October-November, there was a total of 176.4 mm rainfall across forty rain days, with six days of heavy rain (12 October, 14.8 mm; 18 October, 14.6 mm; 19 October, 13.1 mm; 28 October, 16.6 mm; 01 November, 16.6 mm; 02 November, 11.5 mm; 12 November, 11.9 mm). In December-January, 173.6 mm of rainfall was recorded across forty-one rain days, with six days of heavy rain. In February-March, 219.9 mm of rainfall was recorded across forty rain days, with eight days of heavy rain (Figure 5.14A) (Table 5.13).

In the 2024/2025 growing season between August and March, the average daily maximum temperature at Harpenden ranged from 31.2°C in August to 9.4°C in January, and minimum temperature ranged between 13.6°C in August to -2.7°C in January (Figure 5.14B) (Table 5.12). In August-September, the daily temperature ranged between 24.2°C (12 August) and 8.7°C (29 September), with an average temperature of 16.2°C. In October-November, the daily temperature ranged between 16.0°C (16 October) and 0.6°C (21 November), with an average temperature of 9.3°C. In December-January, the daily temperature ranged between 11.2°C (01 December) and -2.7°C (10 January), with an average temperature of 4.8°C.

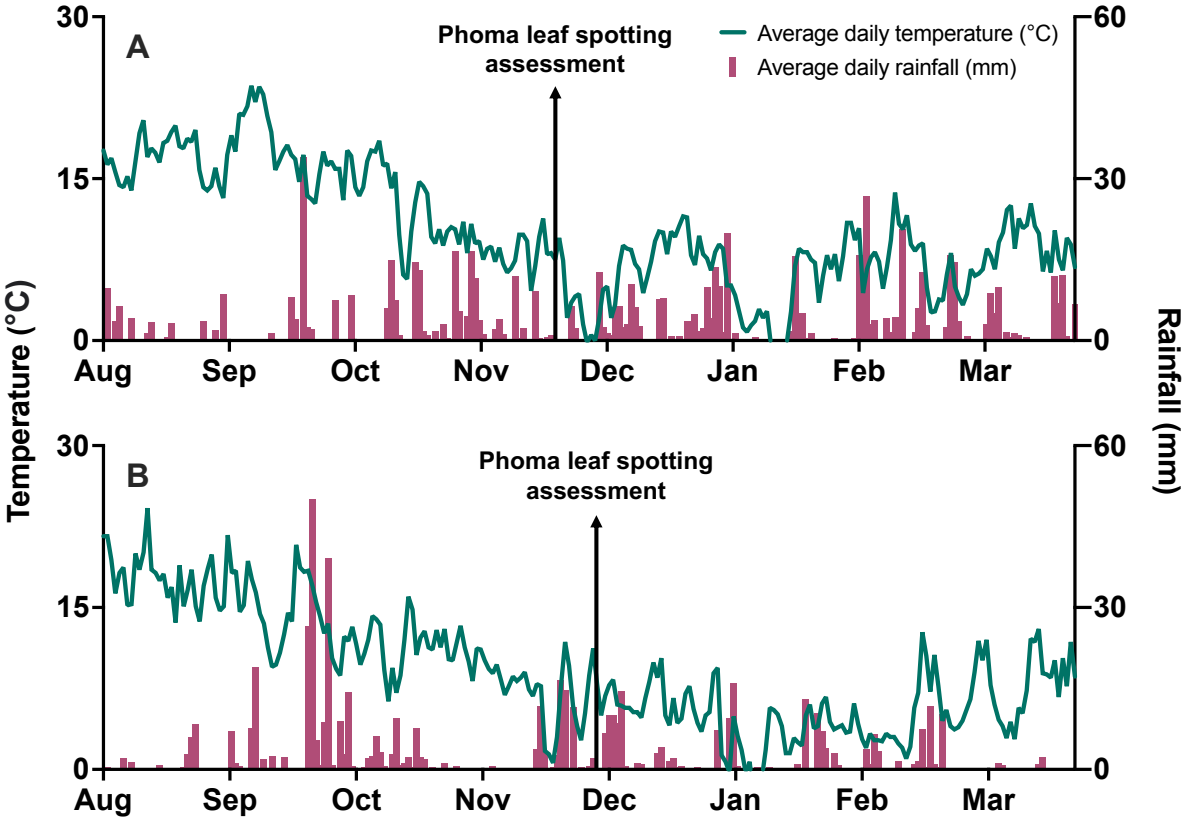

Figure 5.14: Average daily temperature (°C) and rainfall (mm) at Harpenden from August to March in the (A) 2023/2024 and (B) 2024/2025 growing seasons.

Daily weather data were collected from the weather station located on-site. Timings of phoma leaf spot assessments are indicated.

Table 5.12: Minimum, maximum and average daily temperature (°C) at Harpenden between August and March in the 2023/2024 and 2024/2025 growing seasons.

Weather data were collected from the on-site weather station.

Month	2023/2024			2024/2025		
	Minimum daily temp (°C)	Maximum daily temp (°C)	Average daily temp (°C)	Minimum daily temp (°C)	Maximum daily temp (°C)	Average daily temp (°C)
Aug	13.9	25.2	17.1	13.6	31.2	17.9
Sep	12.7	23.6	17.7	8.7	21.7	14.7
Oct	5.7	18.5	12.6	6.3	16.0	11.4
Nov	-0.2	11.3	7.1	0.6	11.8	7.2
Dec	0.0	11.5	7.0	3.5	11.2	6.5
Jan	-1.7	8.9	4.3	-2.7	9.4	3.0
Feb	2.6	13.7	7.7	1.0	12.7	4.6
Mar	3.3	12.7	8.1	2.9	13.0	7.6
Mean			**10.2**			**9.1**

Table 5.13: Average daily / total monthly rainfall (mm) and total rain days (days) at Harpenden between August and March in the 2023/2024 and 2024/2025 growing seasons.

Weather data were collected from the on-site weather station.

Month	2023/2024			2024/2025		
	Average daily rainfall (mm)	Total monthly rainfall (mm)	Total monthly rain days (days)	Average daily rainfall (mm)	Total monthly rainfall (mm)	Total monthly rain days (days)
Aug	1.6	39.8	16	0.7	22.6	12
Sep	2.0	60.3	11	6.2	185.4	18
Oct	3.2	100.7	19	2.0	61.8	27
Nov	2.5	75.7	21	2.2	66.5	14
Dec	3.3	101.3	26	2.2	67.9	21
Jan	2.3	72.3	15	2.4	74.5	17
Feb	4.5	130.0	21	1.8	51.2	18
Mar	2.9	89.9	19	0.2	6.2	9
Total		**670.0**	**148**		**536.1**	**136**
Mean	**2.8**	**83.8**	**19**	**2.2**	**67.0**	**17**

Each day with over 0.1 mm rain recorded was counted as a rain day.

In February-March, the daily temperature ranged between 2.0°C (17 February) and 13.0°C (22 March), with an average temperature of 6.1°C (Figure 5.14B) (Table 5.12).

There was a total of 536.1 mm rainfall recorded at Harpenden in the 2024/2025 growing season between August and March (Table 5.13). In August-September, there was a total of 208.0 mm rainfall across thirty rain days, with four days of heavy rain (08 September, 18.9 mm; 21 September, 26.5 mm; 22 September, 50.1 mm; 26 September, 39.2 mm). In October-November, there was a total of 128.3 mm rainfall across forty-one rain days, with five days of heavy rain (01 October, 14.3 mm; 18 November, 11.7 mm; 23 November, 16.6 mm; 24 November, 14.7 mm; 26 November, 11.5 mm). In December-January, 142.2 mm of rainfall was recorded across thirty-eight rain days, with six days of heavy rain. In February-March, 57.4 mm of rainfall was recorded across twenty-seven rain days, with two days of heavy rain (Figure 5.14B) (Table 5.13).

Overall, between August and November (period of ascospore release and phoma leaf spot development), the average daily temperature was greater in the 2023/2024 growing season (13.5°C) compared to the 2024/2025 growing season (12.7°C). Conversely, the total rainfall in this period was greater in the 2024/2025 growing season (336.8 mm) compared to the 2023/2024 growing season (287.0 mm).

5.3.2.2 Field experiments at Norwich in the 2023/2024 and 2024/2025 growing seasons

5.3.2.2.1 Incidence and severity of phoma leaf spot

At Norwich, in the 2023/2024 growing season, there were no significant differences in average incidence of phoma leaf spots (% of plants affected) between different cultivars ($F(9,20) = 0.97$, $P = 0.492$) (Table 5.14). The average incidence of phoma leaf spots ranged between 25.0 % (Catana and Kromerska) and 45.0 % (Yudal) for all ten cultivars assessed (Table 5.15) (Figure 5.15A).

In the 2024/2025 growing season, there were also no significant differences in average incidence of phoma leaf spots (% of plants affected) between different cultivars ($F(9,20) = 1.83$, $P = 0.124$) (Table 5.14). The average incidence of phoma leaf spots ranged between 15.0 % (Rocket) and 45.0 % (Yudal) for all ten cultivars assessed (Table 5.15) (Figure 5.15B).

Table 5.14: Statistical testing outputs for significant probability of the main effects of cultivar on average incidence of phoma leaf spots (% of plants affected) and average percentage of phoma leaf spot lesions caused by *Leptosphaeria maculans* (%) for ten different cultivars at Norwich in the 2023/2024 and 2024/2025 growing seasons.

One-way analysis of variance (ANOVA) tests were done for each growing season separately by selecting cultivar as a factor. Overall means from different growing seasons were compared using a paired t-test.

Average incidence of phoma leaf spots (% of plants affected)			
2023/2024			
Factor	***df***	**F statistic**	**F probability**
Cultivar	29	0.97	= 0.492
2024/2025			
Factor	***df***	**F statistic**	**F probability**
Cultivar	29	1.83	= 0.124
2023/2024 × 2024/2025			
Factor	***df***	**t statistic**	**t probability**
Season	29	2.26	< 0.05
Average percentage of phoma leaf spots caused by *L. maculans* (%)			
2023/2024			
Factor	***df***	**F statistic**	**F probability**
Cultivar	299	3.25	< 0.001
2024/2025			
Factor	***df***	**F statistic**	**F probability**
Cultivar	299	1.35	= 0.211
2023/2024 × 2024/2025			
Factor	***df***	**t statistic**	**t probability**
Season	299	18.13	< 0.0001

Table 5.15: Average incidence of phoma leaf spots (% of plants affected) for ten different cultivars at Norwich in the 2023/2024 and 2024/2025 growing seasons.

Tukey's HSD tests were used for each growing season separately to compare the mean incidence of phoma leaf spots between different cultivars for each growing season. Overall data from different growing seasons were compared using a paired t-test. Cultivars that do not share a letter are considered significantly different ($P < 0.05$).

Cultivar	Average incidence of phoma leaf spots (% of plants affected)	
	2023/2024	2024/2025
Acacia	31.6 **a**	23.3 **a**
Apex	33.3 **a**	38.3 **a**
Campus	33.3 **a**	23.3 **a**
Castille	28.3 **a**	16.6 **a**
Catana	25.0 **a**	23.3 **a**
Kielder	35.0 **a**	21.6 **a**
Kromerska	25.0 **a**	33.3 **a**
POH Bolko	31.6 **a**	21.6 **a**
Rocket	36.6 **a**	15.0 **a**
Yudal	45.0 **a**	45.0 **a**
Mean	**32.5 a**	**26.1 b**

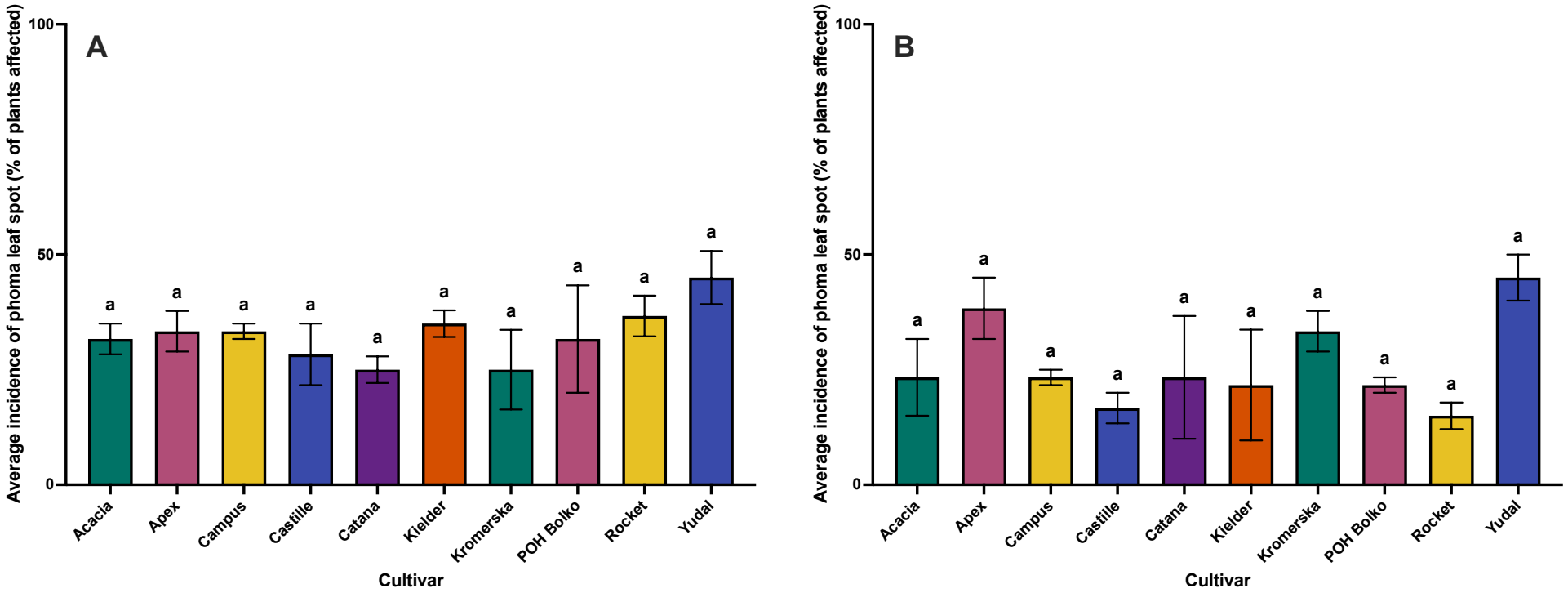

Figure 5.15: Average incidence of phoma leaf spots (% of plants affected) for ten different cultivars at Norwich in the (A) 2023/2024 and (B) 2024/2025 growing seasons.

Tukey's HSD tests were used for each growing season separately to compare the mean incidence of phoma leaf spots between different cultivars for each growing season. Cultivars that do not share a letter are considered significantly different ($P < 0.05$). Error bars show standard error of the mean (SEM) (2023/2024 growing season, 59 d.f.; 2024/2025 growing season, 59 d.f.).

At Norwich, in the 2023/2024 growing season, average percentage of phoma leaf spot lesions caused by *L. maculans* was significantly different between different cultivars ($F(9,290) = 3.25$, $P < 0.001$) (Table 5.14). For the cultivars Acacia (53.1 %), Campus (45.5 %), Castille (43.1 %), Catana (37.1 %), Kromerska (35.6 %) and Rocket (32.1 %), there were no significant differences between them (Table 5.16) (Figure 5.16A). Apex (55.8 %), Kielder (57.6 %) and Yudal (55.3 %) were not significantly different to these cultivars or to each other, despite being significantly different to POH Bolko (27.1 %), which was not significantly different to the initially mentioned cultivars (Table 5.16).

In 2024/2025 growing season, average percentage of phoma leaf spot lesions caused by *L. maculans* was not significantly different between different cultivars ($F(9,290) = 1.35$, $P = 0.211$) (Table 5.14). The average percentage of phoma leaf spot lesions caused by *L. maculans* ranged between 82.9 % (Acacia) and 93.1 % (Yudal) (Table 5.16) (Figure 5.16B).

In summary, at Norwich, overall incidence of phoma leaf spots (% of plants affected) decreased significantly from 32.5 % in the 2023/2024 growing season to 26.1 % in the 2024/2025 growing season ($t(29) = 2.26$, $P < 0.05$) (Table 5.14, Table 5.15). Additionally, the overall average percentage of phoma leaf spot lesions caused by *L. maculans* (%) increased significantly from 44.2 % in the 2023/2024 growing season to 86.3 % in the 2024/2025 growing season ($t(299) = 18.13$, $P < 0.0001$) (Table 5.14, Table 5.16).

5.3.2.2.2 Weather conditions

In the 2023/2024 growing season between August and March, the average daily maximum temperature at Norwich ranged from 24.1°C in September to 9.4°C in January, and minimum temperature ranged from 13.3°C in August to -2.1°C in December (Figure 5.17A) (Table 5.17) (there are gaps in the data for December and January due to equipment malfunctions). In August-September, the daily temperature ranged between 24.1°C (10 September) and 13.1°C (24 September), with an average temperature of 18.0°C. In October-November, the daily temperature ranged between 18.3°C (10 October) and 0.6°C (30 November), with an average temperature of 10.2°C. In December-January, the daily temperature ranged between -2.1°C (03 December) and 9.9°C (19 December), with an average temperature of 4.9°C (based on the available data).

Table 5.16: Average percentage of phoma leaf spot lesions caused by *Leptosphaeria maculans* (%) for ten different cultivars at Norwich in the 2023/2024 and 2024/2025 growing seasons.

Tukey's HSD tests were used for each growing season separately to compare the mean percentage of phoma leaf spot lesions caused by *L. maculans* between different cultivars for each growing season. Overall data from different growing seasons were compared using a paired t-test. Cultivars that do not share a letter are considered significantly different ($P < 0.05$).

Cultivar	**Average percentage of phoma leaf spots caused by *L. maculans* (%)**	
	2023/2024	**2024/2025**
Acacia	53.1 **ab**	82.9 **a**
Apex	55.8 **a**	88.8 **a**
Campus	45.5 **ab**	89.0 **a**
Castille	43.1 **ab**	88.5 **a**
Catana	37.1 **ab**	83.2 **a**
Kielder	57.6 **a**	84.2 **a**
Kromerska	35.6 **ab**	91.7 **a**
POH Bolko	27.1 **b**	78.3 **a**
Rocket	32.1 **ab**	82.8 **a**
Yudal	55.3 **a**	93.1 **a**
Mean	**44.2 b**	**86.3 a**

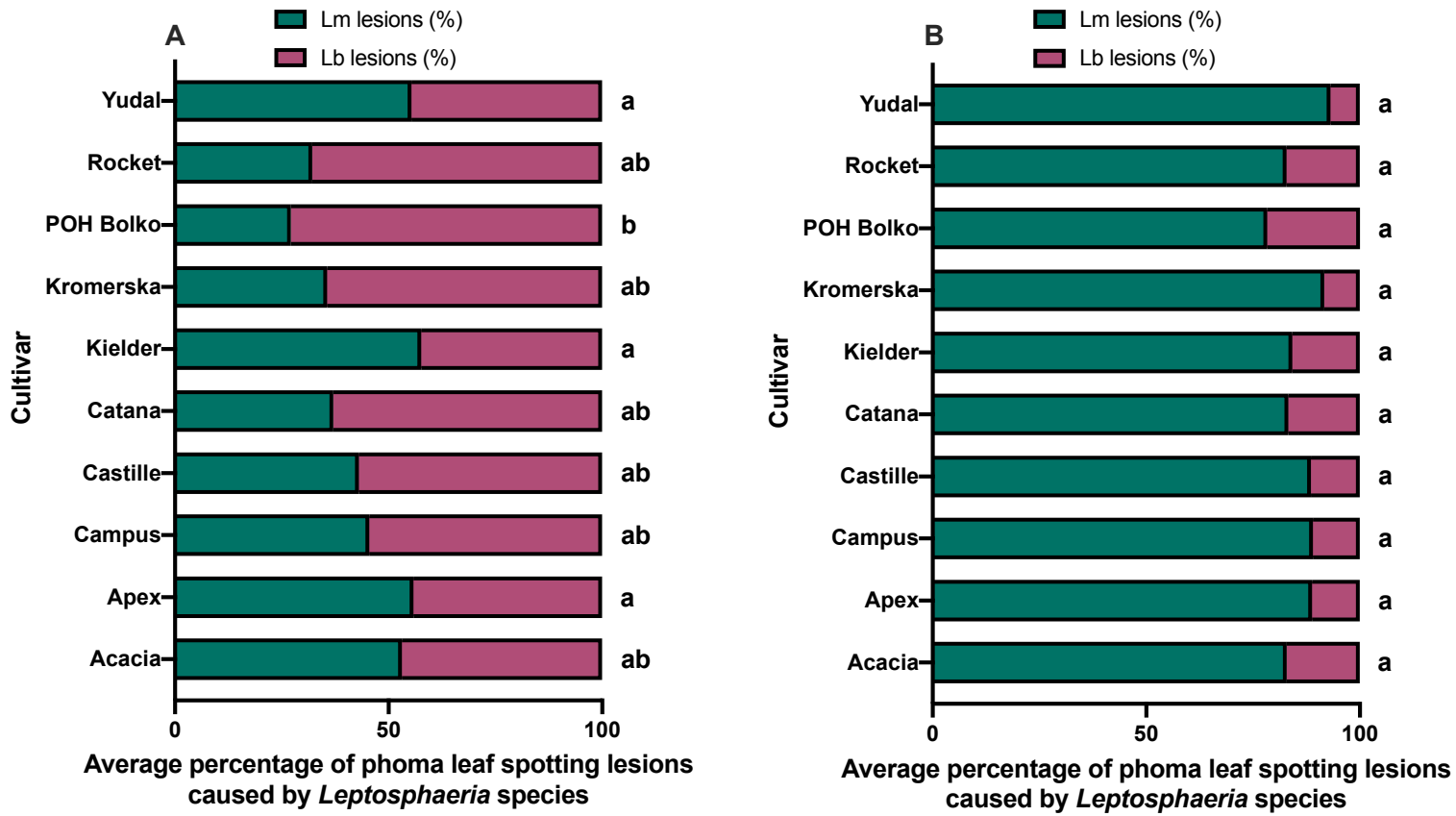

Figure 5.16: Average percentage of phoma leaf spot lesions caused by *Leptosphaeria* species (%) for ten different cultivars at Norwich in the (A) 2023/2024 and (B) 2024/2025 growing seasons.

Tukey's HSD tests were used for each growing season separately to compare the mean percentage of phoma leaf spots caused by *L. maculans* between different cultivars for each growing season. Cultivars that do not share a letter are considered significantly different ($P < 0.05$) (2023/2024 growing season, 299 d.f.; 2024/2025 growing season, 299 d.f.).

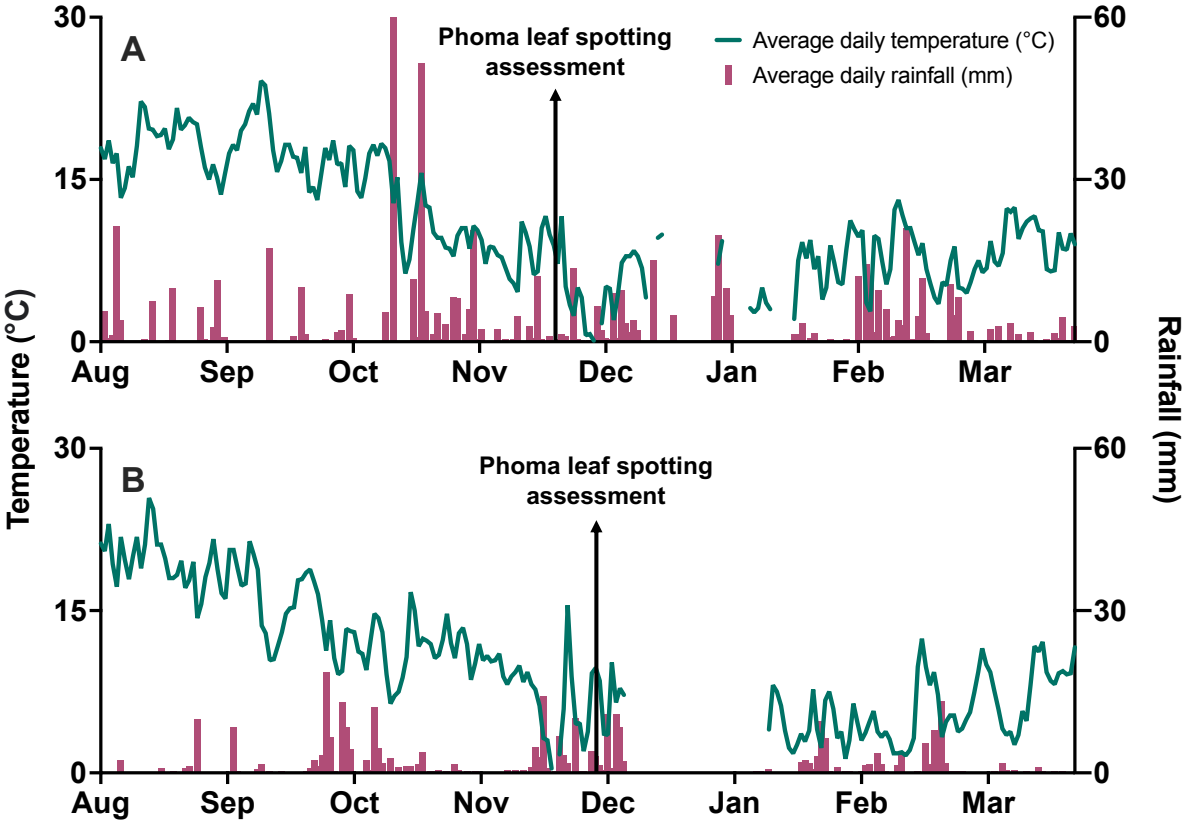

Figure 5.17: Average daily temperature (°C) and rainfall (mm) at Norwich from August to March in the (A) 2023/2024 and (B) 2024/2025 growing seasons.

Daily weather data were collected from the weather station located on-site. Timings of phoma leaf spot assessments are indicated.

Table 5.17: Minimum, maximum and average daily temperature (°C) at Norwich between August and March in the 2023/2024 and 2024/2025 growing seasons.

Weather data were collected from the on-site weather station.

Month	2023/2024			2024/2025		
	Minimum daily temp (°C)	Maximum daily temp (°C)	Average daily temp (°C)	Minimum daily temp (°C)	Maximum daily temp (°C)	Average daily temp (°C)
Aug	13.3	22.2	18.0	14.3	25.4	19.6
Sep	13.1	24.1	18.0	9.1	21.4	15.5
Oct	6.3	18.3	12.9	6.4	16.7	11.7
Nov	0.6	11.6	7.5	-1.6	15.5	7.3
Dec *	-2.1	9.9	5.1	3.5	10.2	7.4
Jan *	-2.0	9.4	4.7	-1.1	8.1	3.6
Feb	2.8	13.1	7.9	1.3	12.4	4.7
Mar	4.5	12.4	8.6	2.6	12.1	7.4
Mean			**10.3**			**9.7**

(*) There are gaps in the data for December and January for both growing seasons due to equipment malfunctions.

In February-March, the daily temperature ranged between 2.8°C (09 February) and 13.1°C (16 February), with an average temperature of 8.3°C (Figure 5.17A) (Table 5.17).

There was a total of 619.1 mm rainfall recorded at Norwich in the 2023/2024 growing season between August and March (Table 5.18). In August-September, there was a total of 107.7 mm rainfall across twenty-five rain days, with four days of heavy rain (> 10 mm) (05 August, 21.4 mm; 30 August, 11.4 mm; 12 September, 17.3 mm; 20 September, 10.0 mm). In October-November, there was a total of 246 mm rainfall across thirty-six rain days, with six days of heavy rain (13 October, 61.6 mm; 18 October, 11.6 mm; 20 October, 51.4 mm; 02 November, 20.6 mm; 18 November, 12.2 mm; 27 November, 13.5 mm). In December-January (based on the data available), 112.6 mm of rainfall was recorded across twenty-five rain days, with two days of heavy rain. In February-March, 152.8 mm of rainfall was recorded across thirty-four rain days, with six days of heavy rain (Figure 5.17A) (Table 5.18).

In the 2024/2025 growing season between August and March, the average daily maximum temperature at Norwich ranged from 25.4°C in August to 8.1°C in January, and minimum temperature ranged from 14.3°C in August to -1.1°C in January (Figure 5.17B) (Table 5.17) (there are gaps in the data for December and January due to equipment malfunctions). In August-September, the daily temperature ranged between 25.4°C (13 August) and 9.1°C (29 September), with an average temperature of 17.6°C. In October-November, the daily temperature ranged between -1.6°C (22 November) and 15.5°C (25 November), with an average temperature of 9.5°C. In December-January, the daily temperature ranged between 10.2°C (06 December) and -1.1°C (11 January), with an average temperature of 5.5°C (based on the available data). In February-March, the daily temperature ranged between 1.3°C (02 February) and 12.4°C (21 February), with an average temperature of 6.1°C (Figure 5.17B) (Table 5.17).

There was a total of 288.4 mm rainfall recorded at Norwich in the 2024/2025 growing season between August and March (Table 5.18). In August-September, there was a total of 72.8 mm rainfall across twenty-one rain days, with two days of heavy rain (26 September, 18.6 mm; 30 September, 13.1 mm).

Table 5.18: Average daily / total monthly rainfall (mm) and total rain days (days) at Norwich between August and March in the 2023/2024 and 2024/2025 growing seasons. Weather data were collected from the on-site weather station.

Month	2023/2024			2024/2025		
	Average daily rainfall (mm)	Total monthly rainfall (mm)	Total monthly rain days (days)	Average daily rainfall (mm)	Total monthly rainfall (mm)	Total monthly rain days (days)
Aug	2.3	72.2	15	0.5	15.3	6
Sep	1.2	35.5	10	1.9	57.5	15
Oct	5.6	174.2	16	1.6	49.2	22
Nov	2.4	71.8	20	1.6	47.3	16
Dec *	2.4	60.8	14	4.6	41.8	9
Jan *	1.7	51.8	11	1.2	28.0	12
Feb	4.0	115.3	19	1.6	43.9	17
Mar	1.2	37.5	15	0.2	5.4	12
Total		**619.1**	**120**		**288.4**	**109**
Mean	**2.6**	**77.4**	**15**	**1.6**	**36.0**	**14**

(*) There are gaps in the data for December and January for both growing seasons due to equipment malfunctions.

Each day with over 0.1 mm rain recorded was counted as a rain day.

In October-November, there was a total of 96.5 mm rainfall recorded across thirty-eight rain days, with three days of heavy rain (08 October, 12.2 mm; 19 November, 14.1 mm; 26 November, 10.0 mm). In December-January (based on the data available), 69.8 mm of rainfall was recorded across twenty-one rain days, with two days of heavy rain. In February-March, 49.3 mm of rainfall was recorded across twenty-nine rain days, with one day of heavy rain (Figure 5.17B) (Table 5.18).

Overall, between August and November (period of ascospore release and phoma leaf spot development), the average daily temperature was greater in the 2023/2024 growing season (14.1°C) compared to the 2024/2025 growing season (12.5°C). Additionally, the total rainfall in this time period was also greater in the 2023/2024 growing season (354.0 mm) compared to the 2024/2025 growing season (169.3 mm).

5.3.3 Phoma stem canker caused by *L. maculans* and *L. biglobosa*

5.3.3.1.1 Field experiments at Hereford in the 2021/2022 and 2022/2023 growing seasons

In the 2021/2022 and 2022/2023 growing seasons, there were significant differences in average phoma stem canker disease score (0-7) between different growing seasons ($F(1,36) = 16.20$, $P < 0.0001$) (Table 5.19). Overall disease score was 4.2 for the 2021/2022 and 5.7 for the 2022/2023 growing seasons (Table 5.20) .

In the 2021/2022 and 2022/2023 growing seasons, there were no significant differences in average phoma stem canker disease score (0-7) between different cultivars ($F(1,36) = 0.65$, $P = 0.426$) (Table 5.19). Average disease score was 4.1 for Aquila and 4.3 for Flamingo in the 2021/2022 growing season. Average disease score was 6.1 for Aquila and 5.3 for Flamingo in the 2022/2023 growing season (Table 5.20) (Figure 5.18). The interactions between cultivars and growing seasons were not significant ($F(1,36) = 1.80$, $P = 0.188$) (Table 5.19).

In the 2021/2022 and 2022/2023 growing seasons, there were significant differences in the average percentage of *L. maculans* DNA (%) in stem basal cankers between different growing seasons ($F(1,32) = 16.38$, $P < 0.001$) (Table 5.19). Overall average percentage of *L. maculans* DNA was 99.9 % for the 2021/2022 growing season and 96.2 % for the 2022/2023 growing season (Table 5.21).

Table 5.19: Statistical testing outputs for the significant probability of the main effects of cultivar, season, and the two-way interactions on phoma stem canker disease score (0-7) and percentage of *Leptosphaeria maculans* DNA (%) in stem basal cankers in field experiments at Hereford in the 2021/2022 and 2022/2023 growing seasons.

Two-way analysis of variance (ANOVA) tests were done by selecting cultivar and season as factors.

Average phoma stem canker disease score (0-7)			
Factor	***df***	**F statistic**	**F probability**
Cultivar	1	0.65	= 0.426
Season	1	16.20	< 0.001
Cultivar x Season	1	1.80	= 0.188
Average percentage of *L. maculans* DNA in stem basal cankers (%)			
Factor	***df***	**F statistic**	**F probability**
Cultivar	1	1.85	= 0.184
Season	1	16.38	< 0.001
Cultivar x Season	1	2.27	= 0.142

Table 5.20: Average phoma stem canker disease score (0-7) for oilseed rape cultivars Aquila and Flamingo in field experiments at Hereford in the 2021/2022 and 2022/2023 growing seasons.

Tukey's HSD tests were used to compare the mean disease score between different cultivars and seasons. Cultivars and/or seasons that do not share a letter are considered significantly different ($P < 0.05$).

Average phoma stem canker disease score (0-7)			
Cultivar	**2021/2022**	**2022/2023**	**Mean**
Aquila	4.1 **b**	6.1 **a**	5.1 **a**
Flamingo	4.3 **b**	5.3 **ab**	4.8 **a**
Season mean	4.2 **b**	5.7 **a**	**-**

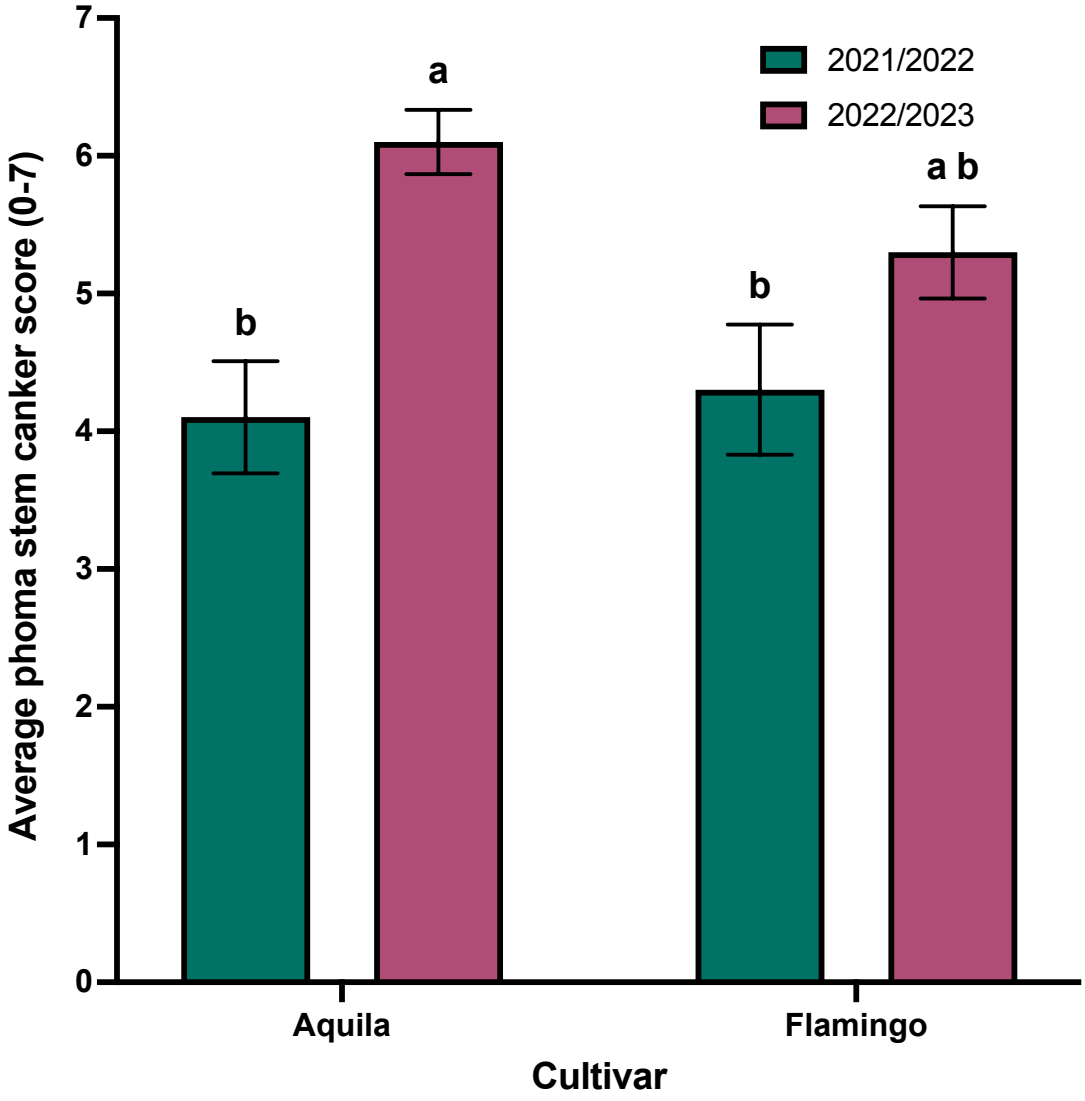

Figure 5.18: Average phoma stem canker disease score (0-7) for oilseed rape cultivars Aquila and Flamingo in field experiments at Hereford in the 2021/2022 and 2022/2023 growing seasons.

Tukey's HSD tests were used to compare the mean disease score between different cultivars and seasons. Columns that do not share a latter are considered significantly different ($P < 0.05$). Error bars show standard error of the mean (SEM) (44 d.f.).

Table 5.21: Average percentage of *Leptosphaeria maculans* DNA (%) in stem basal cankers of oilseed rape cultivars Aquila and Flamingo samples from field experiments at Hereford in the 2021/2022 and 2022/2023 growing seasons.

Tukey's HSD tests were used to compare the mean disease score between different cultivars and seasons. Cultivars and/or seasons that do not share a letter are considered significantly different ($P < 0.05$).

Average percentage of *L. maculans* DNA in stem basal cankers (%)			
Cultivar	**2021/2022**	**2022/2023**	**Mean**
Aquila	99.9 **a**	97.5 **ab**	98.7 **a**
Flamingo	99.9 **a**	94.8 **b**	97.4 **a**
Season mean	99.9 **a**	96.2 **b**	**-**

In the 2021/2022 and 2022/2023 growing seasons, there were no significant differences in average percentage of *L. maculans* DNA (%) in stem basal cankers between different cultivars ($F(1,32) = 1,85$, $P = 0.184$) (Table 5.19). Average percentage of *L. maculans* DNA was 99.9 % for both Aquila and Flamingo in the 2021/2022 growing season. Average percentage of *L. maculans* DNA was 97.5 % for Aquila and 94.8 % for Flamingo in the 2022/2023 growing season (Table 5.21) (Figure 5.19).

In summary, at Hereford, the overall phoma stem canker disease score was greater in the 2022/2023 (5.7) than in the 2021/2022 (4.2) growing season. While the overall average percentage of *L. maculans* DNA in stem basal cankers was smaller in the 2022/2023 (96.2 %) than in the 2021/2022 (99.9 %) growing season (Appendix J).

5.3.3.2 Field experiments at Huntingdon in the 2021/2022 and 2022/2023 growing seasons

In the 2021/2022 growing season, there were no significant differences in average phoma stem canker disease score (0-7) between different cultivars ($t(18) = 0.37$, $P = 0.714$) (Table 5.22). Average disease score was 5.9 for Aquila and 5.8 for Flamingo (Table 5.23) (Figure 5.20A).

In the 2022/2023 growing season, there were also no significant differences in average phoma stem canker disease score (0-7) between different cultivars ($t(18) = 0.25$, $P = 0.806$) (Table 5.22). Average disease score was 2.1 for Acacia and 2.2 for Aquila (Table 5.23) (Figure 5.20B).

In the 2021/2022 growing season, there were no differences in average percentage of *L. maculans* DNA (%) in stem basal cankers between different cultivars ($t(14) = 1.16$, $P = 0.264$) (Table 5.22). Average percentage of *L. maculans* DNA was 98.5 % for Aquila and 99.7 % for Flamingo (Table 5.24) (Figure 5.21A).

In the 2022/2023 growing season, there were also no significant differences in average percentage of *L. maculans* DNA (%) in stem basal cankers between different cultivars ($t(8) = 1.44$, $P = 0.187$) (Table 5.22). Average percentage of *L. maculans* DNA was 99.1 % for Acacia and 96.5 % for Aquila (Table 5.24) (Figure 5.21B).

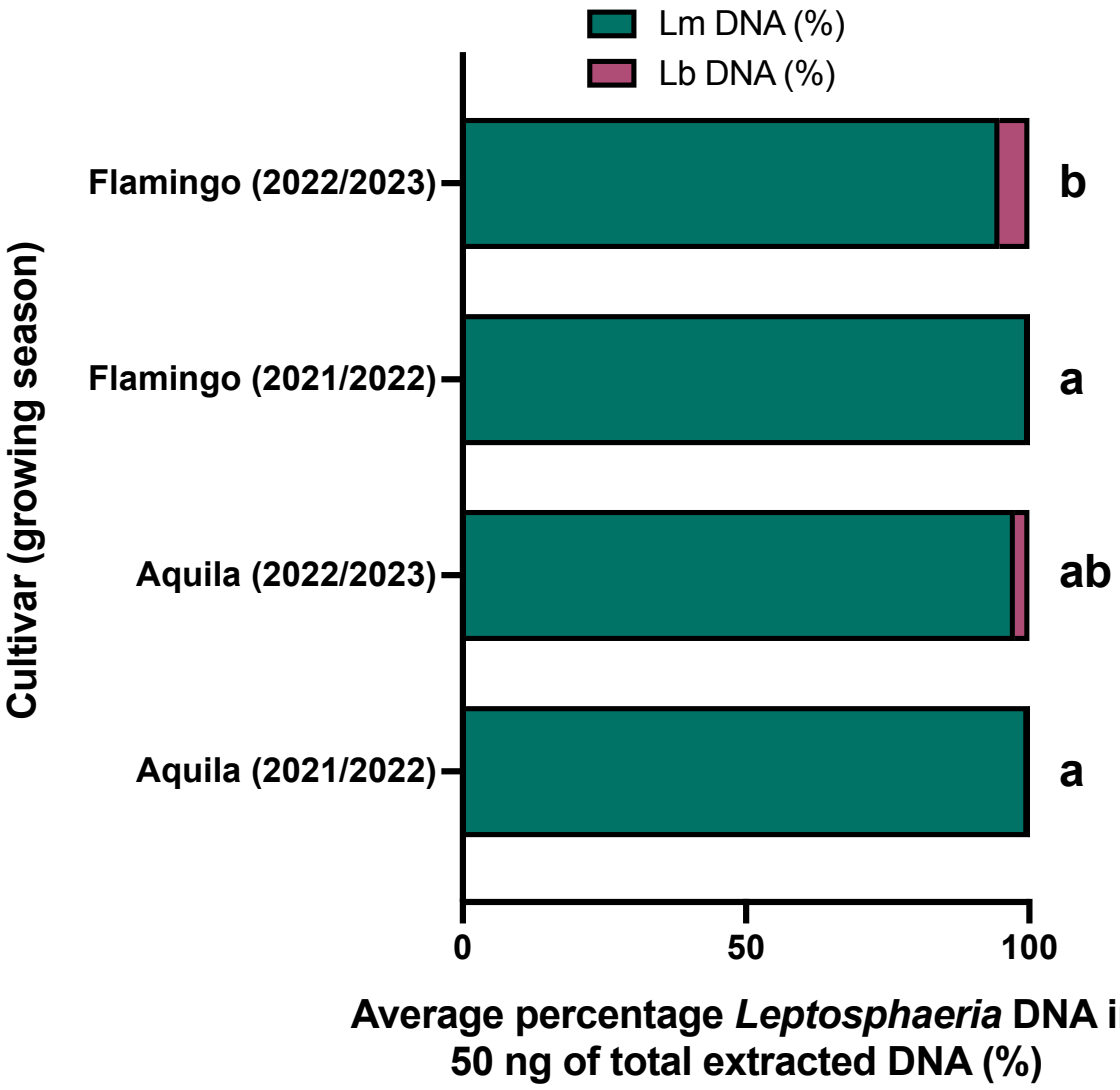

Figure 5.19: Average percentages of *Leptosphaeria* species DNA (%) in stem basal cankers of oilseed rape cultivars Aquila and Flamingo sampled from field experiments at Hereford in the 2021/2022 and 2022/2023 growing seasons.

Tukey's HSD tests were used to compare the percentages of *Leptosphaeria* species DNA (%) between different cultivars and seasons. Columns that do not share a letter are considered significantly different ($P < 0.05$) (32 d.f.).

Table 5.22: Statistical testing outputs for the main effects of cultivar on average phoma stem canker disease score (0-7) and percentage of *Leptosphaeria maculans* DNA (%) in stem basal cankers in field experiments at Huntingdon in the 2021/2022 and 2022/2023 growing seasons.

Due to differences in cultivars used in assessments, it is not possible to test the effects of growing season. Unpaired t-tests were done for each growing season separately to test the effects of cultivar.

Average phoma stem canker disease score (0-7)			
2021/2022			
Factor	***df***	**t statistic**	**t probability**
Cultivar	18	0.37	= 0.714
2022/2023			
Factor	***df***	**t statistic**	**t probability**
Cultivar	18	0.25	= 0.806
Average percentage of *L. maculans* DNA in stem basal cankers (%)			
2021/2022			
Factor	***df***	**t statistic**	**t probability**
Cultivar	14	1.16	= 0.264
2022/2023			
Factor	***df***	**t statistic**	**t probability**
Cultivar	8	1.44	= 0.187

Table 5.23: Average phoma stem canker disease score (0-7) for oilseed rape cultivars Aquila and Flamingo (2021/2022 growing season) and Aquila and Acacia (2022/2023 growing season) in field experiments at Huntingdon.

Due to differences in cultivars used in assessments, it is not possible to test the effects of growing season. Unpaired t-tests were done for each growing season separately to test the effects of cultivar. Cultivars that do not share a letter are considered significantly different ($P < 0.05$).

Average phoma stem canker disease score (0-7)		
Cultivar	**2021/2022**	**2022/2023**
Acacia	-	2.1 **a**
Aquila	5.9 **a**	2.2 **a**
Flamingo	5.8 **a**	-
Season mean	5.9	2.2

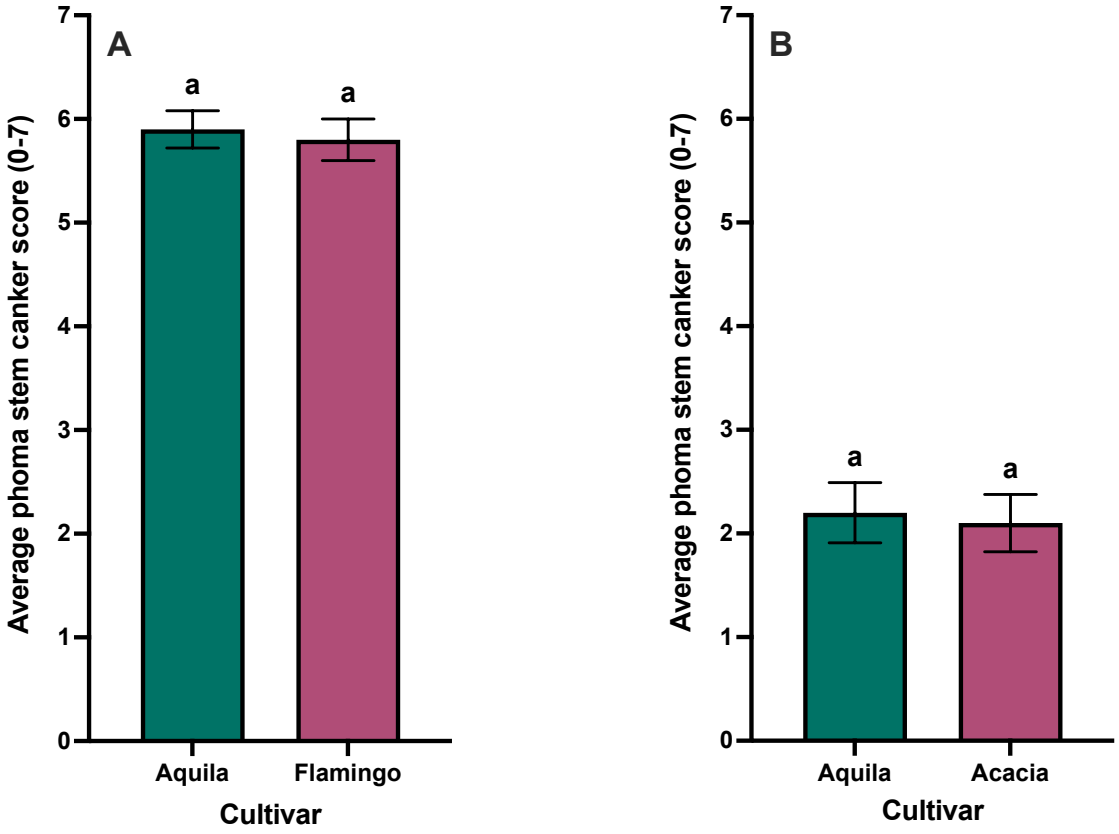

Figure 5.20: Average phoma stem canker disease score (0-7) for oilseed rape cultivars (A) Aquila and Flamingo in the 2021/2022 and (B) Aquila and Acacia in the 2022/2023 growing seasons in field experiments at Huntingdon.

Due to differences in cultivars used in assessments, it is not possible to test the effects of growing season. Unpaired t-tests were done for each growing season separately to test the effects of cultivar. Cultivars that do not share a letter are considered significantly different ($P < 0.05$). Error bars show standard error of the mean (SEM) (2021/2022 growing season, 18 d.f.; 2022/2023 growing season, 18 d.f.).

Table 5.24: Average percentage of *Leptosphaeria maculans* DNA (%) in stem basal cankers of oilseed rape cultivars Aquila and Flamingo (2021/2022 growing season) and Aquila and Acacia (2022/2023 growing season) in field experiments at Huntingdon.

Due to differences in cultivars used in assessments, it is not possible to test the effects of growing season. Unpaired t-tests were done for each growing season separately to test the effects of cultivar. Cultivars that do not share a letter are considered significantly different ($P < 0.05$).

Average percentage of *L. maculans* DNA in stem basal cankers (%)		
Cultivar	**2021/2022**	**2022/2023**
Acacia	-	99.1 **a**
Aquila	98.5 **a**	96.5 **a**
Flamingo	99.7 **a**	-
Season mean	99.1	97.8

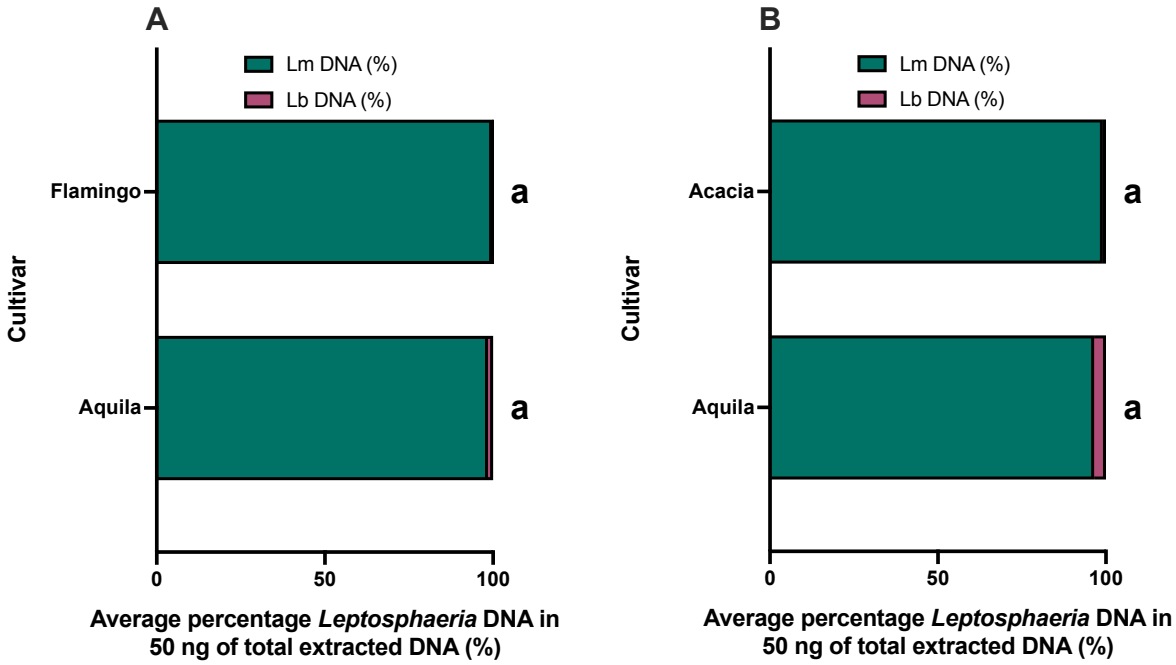

Figure 5.21: Average percentages of *Leptosphaeria* species DNA (%) in stem basal cankers of oilseed rape cultivars (A) Aquila and Flamingo in 2021/2022 and (B) Aquila and Acacia in 2022/2023 growing seasons in field experiments at Huntingdon.

Due to differences in cultivars used in assessments, it is not possible to test the effects of growing season. Unpaired t-tests were done for each growing season separately to test the effects of cultivar. Cultivars that do not share a letter are considered significantly different ($P < 0.05$) (2021/2022 growing season, 14 d.f.; 2022/2023 growing season, 8 d.f.).

In summary, at Huntingdon, overall phoma stem canker disease score was greater in the 2022/2023 (5.9) than in the 2021/2022 (2.2) growing season. While the overall average percentage of *L. maculans* DNA in stem basal cankers was smaller in the 2022/2023 (97.8 %) than in the 2021/2022 (99.1 %) growing season (Appendix J). Comparisons of similar cultivars between the two growing seasons can be found in Appendix I.

5.3.3.3 Field experiments at Wisbech in the 2021/2022 and 2022/2023 growing seasons

In the 2021/2022 growing season, there were significant differences in average phoma stem canker disease score (0-7) between different cultivars ($F(5,54) = 15.42$, $P < 0.0001$) (Table 5.25). For cultivars Adonis (2.9), Crocodile (3.1), Cromat (2.7) and Turing (2.9), there were no significant differences between them. Line-A (1.2) and Murray (1.9) were significantly different to the rest of the cultivars but were not significantly different to each other (Table 5.26) (Figure 5.22A).

In the 2022/2023 growing season, there were also significant differences in average phoma stem canker disease score (0-7) between different cultivars ($F(5,54) = 39.10$, $P < 0.0001$) (Table 5.25). For cultivars Aurelia (4.7) and Crocodile (4.9), there were no significant differences between them. Turing (3.1) was significantly different to all other cultivars except Cromat (4.4), which was not significantly different to the cultivars initially mentioned. Line-A (0.7) and Murray (0.7) were significantly different to the rest of the cultivars but were not significantly different from each other (Table 5.26) (Figure 5.22B).

In the 2021/2022 growing season, there were significant differences in average percentage of *L. maculans* DNA (%) in stem basal cankers between different cultivars ($F(5,35) = 4.53$, $P < 0.001$) (Table 5.25). For cultivars Adonis (97.3 %), Cromat (96.6 %), Murray (98.4 %) and Turing (99.0 %), there were no significant differences between them. Line-A (90.5 %) was significantly different to all other cultivars except Crocodile (95.3 %), which was not significantly different to the cultivars initially mentioned (Table 5.27) (Figure 5.23A).

In the 2022/2023 growing season, there were also significant differences in average percentage of *L. maculans* DNA (%) in stem basal cankers between different cultivars ($F(5,36) = 348.50$, $P < 0.0001$) (Table 5.25).

Table 5.25: Statistical testing outputs for significant probability of the main effects of cultivar on average phoma stem canker disease score (0-7) and percentage of *Leptosphaeria maculans* DNA (%) in stem basal cankers in field experiments at Wisbech in the 2021/2022 and 2022/2023 growing seasons.

Due to differences in cultivars used in assessments, it is not possible to test the effects of growing season. One-way analysis of variance (ANOVA) tests were done for each growing season by selecting cultivar as a factor.

Average phoma stem canker disease score (0-7)			
2021/2022			
Factor	***df***	**F statistic**	**F probability**
Cultivar	59	15.42	< 0.0001
2022/2023			
Factor	***df***	**F statistic**	**F probability**
Cultivar	59	39.10	< 0.0001
Average percentage of *L. maculans* DNA in stem basal cankers (%)			
2021/2022			
Factor	***df***	**F statistic**	**F probability**
Cultivar	40	4.53	< 0.001
2022/2023			
Factor	***df***	**F statistic**	**F probability**
Cultivar	41	348.50	<0.0001

Table 5.26: Average phoma stem canker disease score (0-7) for different oilseed rape cultivars in field experiments at Wisbech in the 2021/2022 and 2022/2023 growing seasons.

Due to differences in cultivars used in assessments, it is not possible to test the effects of growing season. Tukey's HSD tests were used compare the mean disease score between different cultivars. Cultivars that do not share a letter are considered significantly different ($P < 0.05$).

Average phoma stem canker disease score (0-7)		
Cultivar	**2021/2022**	**2022/2023**
Adonis	2.9 **a**	**-**
Aurelia	**-**	4.7 **a**
Crocodile	3.1 **a**	4.9 **a**
Cromat	2.7 **a**	4.4 **ab**
Line-A	1.2 **b**	0.7 **c**
Murray	1.9 **b**	0.7 **c**
Turing	2.9 **a**	3.1 **b**
Season mean	2.5	3.1

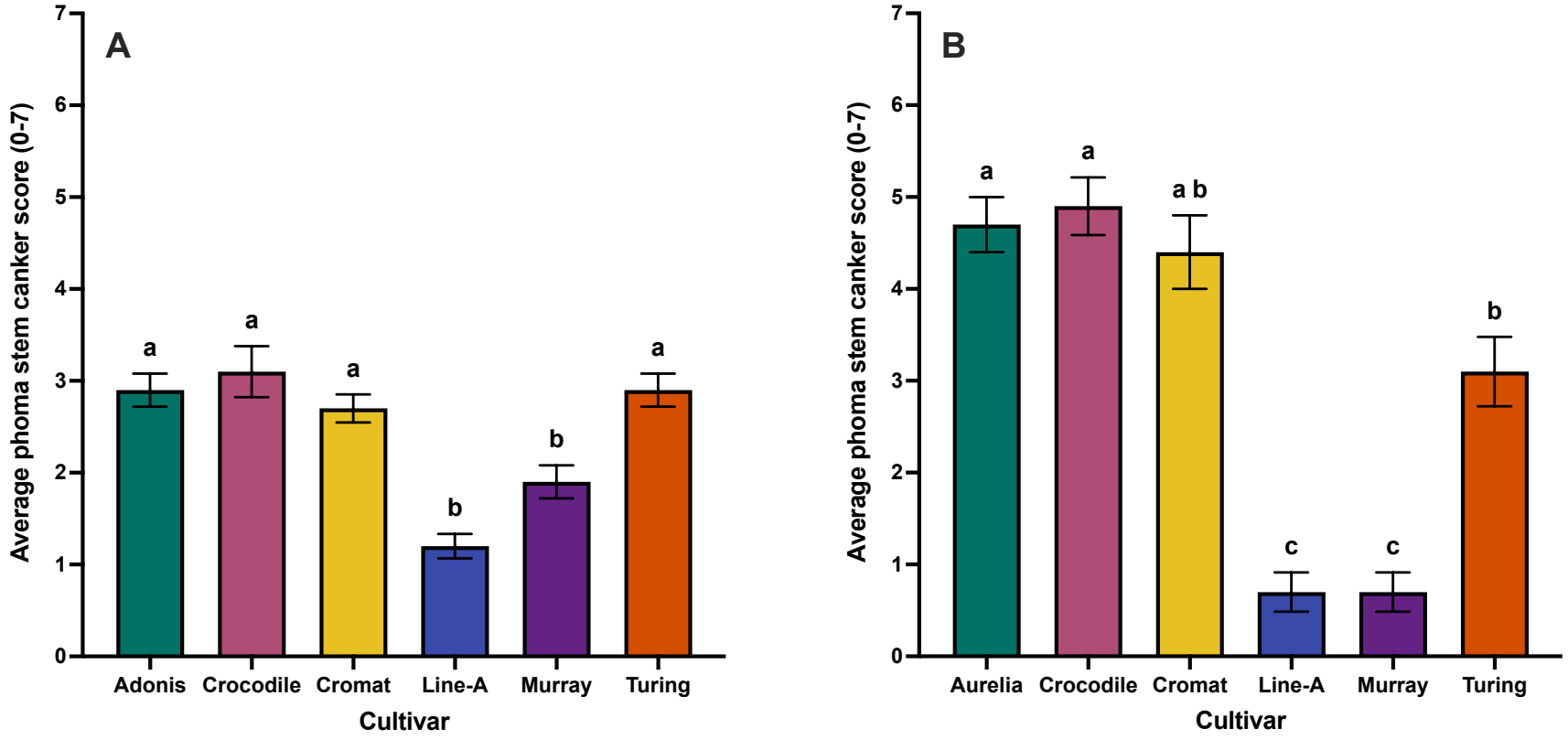

Figure 5.22: Average phoma stem canker disease score (0-7) for different oilseed rape cultivars in the (A) 2021/2022 growing season and (B) 2022/2023 growing season in field experiments at Wisbech.

Due to differences in cultivars used in assessments, it is not possible to test the effects of growing season. Tukey's HSD tests were used compare the mean disease score between different cultivars. Cultivars that do not share a letter are considered significantly different ($P < 0.05$). Error bars show standard error of the mean (SEM) (2021/2022 growing season, 59 d.f.; 2022/2023 growing season, 59 d.f.).

Table 5.27: Average percentage of *Leptosphaeria maculans* DNA (%) for different oilseed rape cultivars in field experiments at Wisbech in the 2021/2022 and 2022/2023 growing seasons.

Due to differences in cultivars used in assessments, it is not possible to test the effects of growing season. Tukey's HSD tests were used compare the mean disease score between different cultivars. Cultivars that do not share a letter are considered significantly different ($P < 0.05$).

Average percentage of *L. maculans* DNA in stem basal cankers (%)		
Cultivar	**2021/2022**	**2022/2023**
Adonis	97.3 **a**	-
Aurelia	-	98.9 **a**
Crocodile	95.3 **ab**	98.5 **a**
Cromat	96.6 **a**	98.2 **a**
Line-A	90.5 **b**	41.4 **b**
Murray	98.4 **a**	98.0 **a**
Turing	99.0 **a**	95.3 **a**
Season mean	96.2	88.4

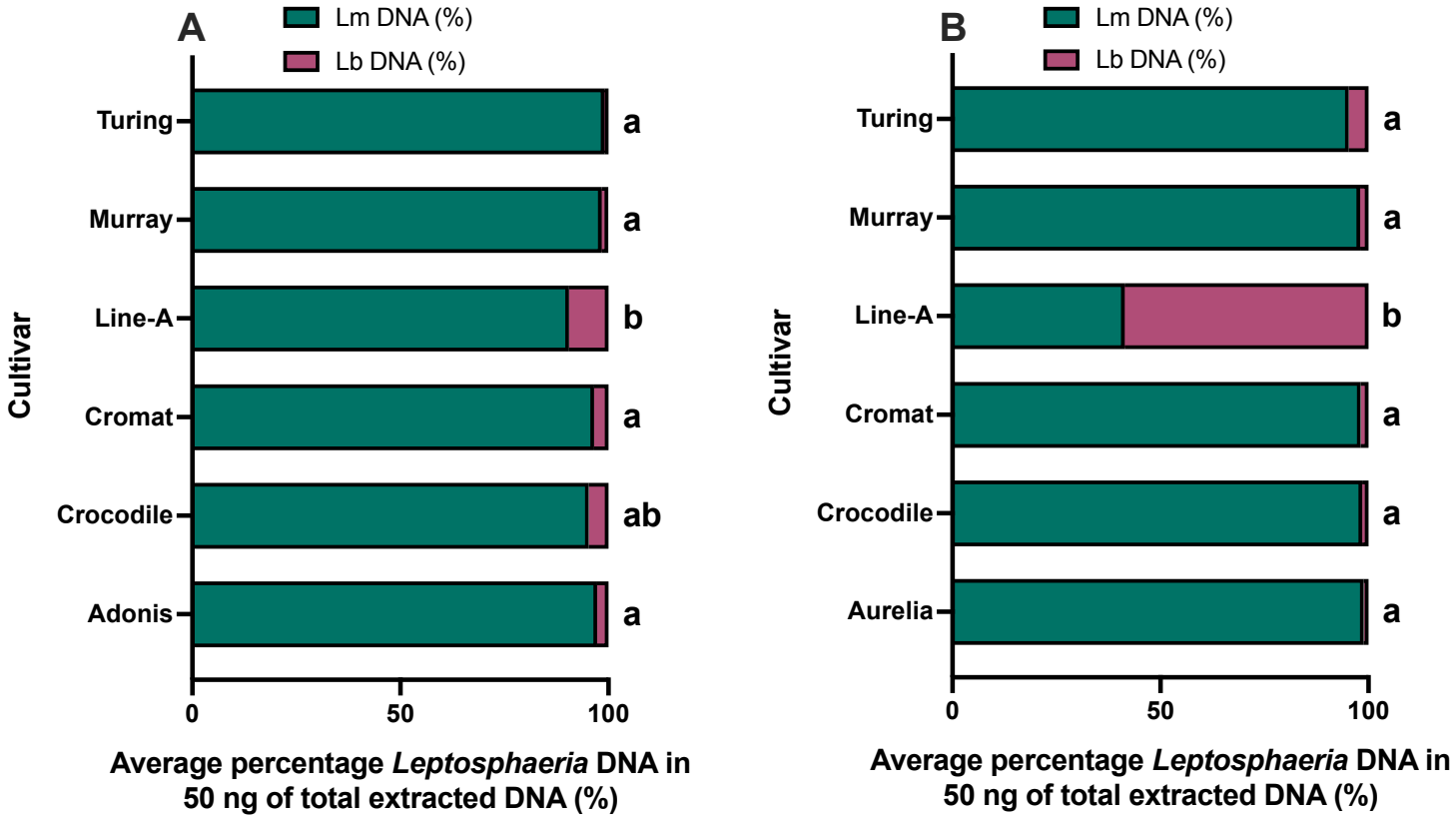

Figure 5.23: Average percentages of *Leptosphaeria* species DNA (%) in stem basal cankers of different oilseed rape cultivars in the (A) 2021/2022 growing season and (B) 2022/2023 growing season in field experiments at Wisbech.

Due to differences in cultivars used in assessments, it is not possible to test the effects of growing season. Tukey's HSD tests were used compare the mean disease score between different cultivars. Cultivars that do not share a letter are considered significantly different ($P < 0.05$) (2021/2022 growing season, 40 d.f.; 2022/2023 growing season, 41 d.f.).

For cultivars Aurelia (98.9 %), Crocodile (98.5 %), Cromat (98.2 %), Murray (98.0 %) and Turing (95.3 %), there were no significant differences between them. Line-A (41.4 %) was significantly different to all other cultivars (Table 5.27) (Figure 5.23B).

In summary, at Wisbech, overall phoma stem canker disease score was greater in the 2022/2023 (3.1) than in the 2021/2022 (2.5) growing season. While the overall average percentage of *L. maculans* DNA in stem basal cankers was smaller in the 2022/2023 (88.4 %) than in the 2021/2022 (96.2 %) growing season (Appendix J). Comparisons of similar cultivars between the two growing seasons can be found in Appendix I.

5.4 Discussion

The results of the studies in this chapter provide a brief summary of the current proportions of the two *Leptosphaeria* species responsible for phoma stem canker disease symptoms in England, and the factors that may affect these proportions as well as the interspecific interactions between *L. maculans* and *L. biglobosa* in natural conditions.

Results on ascospore release at Bayfordbury, Hertfordshire in four growing seasons (between 2020/2021 and 2023/2024) showed differences in the timing and pattern of ascospore release of *Leptosphaeria* species between different seasons, which were mainly affected by weather conditions, especially temperature and rainfall.

The timing of first major release of ascospores differed between the four growing seasons. The onset of ascospore release is dependent on the timing of pseudothecial maturation, which is affected by temperature and rainfall (West et al., 2001; Toscano-Underwood et al., 2003; Huang et al., 2007; Salam et al., 2007). After maturation of pseudothecia, the release of ascospores of *Leptosphaeria* species is triggered by rainfall (Huang et al., 2005). The first major release of ascospores was observed at the end of October in the 2022/2023 growing season, approximately a month later than the other three seasons. The 2022/2023 growing season had the least number of rain days in August compared to the other three seasons, which is suggested to have caused the delay in the first major release of ascospores of *Leptosphaeria* species. This is supported by a study done in Poland, where it was reported that the first major release of ascospores was related to the number of rain days over the summer (July-September) (Dawidziuk et al., 2012a).

The timing of maximum release of ascospores differed between the four growing seasons. The maximum release of ascospores was observed in late-October/early-November, except in the 2021/2022 growing season where it was observed in early-January, approximately two months later than in the other three seasons. This is also attributed to weather conditions. The average temperature between August and November in the 2021/2022 growing season was slightly less than in other seasons, which could have slowed down the pseudothecial maturation process. However, this is unlikely to have had a significant impact on the timing of ascospore release, as temperatures were >10°C, at a level where pseudothecia of both *Leptosphaeria* species are able to go through the stages of maturation (Toscano-Underwood et al., 2003). Instead, the reduced amount of rainfall between October and January of the 2021/2022 growing season (30 % to 50 % less than in other seasons) can be the main reason to have caused the delay in the maximum release of ascospores of *Leptosphaeria* species. Although excessive rain is not thought to accelerate the process, frequent debris wetness has been reported to be a pre-requisite for pseudothecial maturation (Petrie, 1994; Salam et al., 2007). Interestingly, even though the first major release of ascospores was delayed in the 2022/2023 growing season due to reduced number of rain days in August, the maximum release of ascospores was not delayed. This was because of weather conditions in October-November being conducive and providing the frequent debris wetness required for pseudothecial maturation. In fact, the greatest amount of total rainfall (as well as the highest average temperature) for the October-November period was recorded in the 2022/2023 growing season among all four seasons monitored.

There was a variation in the number of ascospores of *Leptosphaeria* species between different growing seasons. There may be several reasons for this. The amount of debris collected from plots of the previous growing season and the amount of disease (i.e. pseudothecia) on the debris could affect the number of ascospores (similar to stubble management methods to reduce inoculum in the next season) (Bousset et al., 2015; Fortune et al., 2024). In addition, the use of resistant cultivars leading to reduction in disease severity can also reduce the number of ascospores produced on the crop debris (Bousset et al., 2021). Similar results were also reported in previous studies, where fluctuations were observed in the number of ascospores of *Leptosphaeria* species between different seasons (Huang et al., 2011; Huang et al., 2024).

Ascospores of *L. maculans* and *L. biglobosa* were released at similar times at Bayfordbury, Hertfordshire throughout the four growing seasons, which was in agreement with recent reports (Javaid et al., 2021; Fortune, 2022; Huang et al., 2024). Interestingly, in the 2022/2023 growing season, maximum release of ascospores of *L. biglobosa* was observed approximately one month before maximal release of *L. maculans* ascospores. This suggests that under the same temperature, *L. biglobosa* might have required less amount of rainfall after a relatively dry August-September period to complete its pseudothecial maturation and release its ascospores. A similar observation was made, where relatively dryer weather conditions resulted in increased proportion of *L. biglobosa* ascospores compared to *L. maculans* ascospores at multiple sites in the UK (Javaid, 2019). This is further supported by the results that the greatest proportion of *L. biglobosa* ascospores was observed in the 2022/2023 growing season, which had the dryest August-September period. Although models have been developed to predict ascospore release, there was no distinction between *L. maculans* and *L. biglobosa* (Huang et al., 2007; Salam et al., 2007). Further studies are needed to investigate the effects of temperature and rainfall on *L. maculans* and *L. biglobosa* pseudothecial maturation. With increasing importance of *L. biglobosa* as a phoma stem canker pathogen, such investigations may be useful in improving current ascospore release models.

Interestingly, an example of factors affecting the proportions and interactions of *L. maculans* and *L. biglobosa* – perhaps in a beneficial way for disease control – has been observed. It was reported that in field experiments done at Rothamsted Research in Harpenden, Hertfordshire, ascospores of *L. biglobosa* were released earlier and in greater abundance in 2007 autumn compared to 2006 autumn; and this has led to a reduced stem canker severity score in 2008 summer compared to 2007 in untreated plots of two oilseed rape cultivars (Huang et al., 2011). This observation could have been a result of factors favouring *L. biglobosa*, and as mentioned before, providing it with the time to deploy its interspecific competition strategy to induce systemic acquired resistance, subsequently reducing the potential damage caused by *L. maculans* (Mahuku et al., 1996; Liu et al., 2006; Liu et al., 2007) (Chapter 4).

In this study, there was a variation in the proportions of *L. maculans* and *L. biglobosa* DNA between different growing seasons. There may be several reasons for this. Different weather conditions in different growing seasons may favour pseudothecial maturation

of one pathogen over the other (Toscano-Underwood et al., 2003; Huang et al., 2007; Dawidziuk et al., 2010; Dawidziuk et al., 2012b). Furthermore, disease control methods, such as efficacy and timing of fungicide applications and use of resistant cultivars may also have an effect on the proportions of *L. maculans* and *L. biglobosa* in stem lesions, which could subsequently affect the proportions of inoculum of these pathogens transmitted to the next growing season (Eckert et al., 2010; Huang et al., 2011; Sewell et al., 2016). There was less *L. biglobosa* DNA quantified on spore tapes throughout all four growing seasons in this study. However, fluctuating patterns in consecutive growing seasons, where more *L. biglobosa* DNA was quantified after a season with more *L. maculans* DNA (and *vice versa*) have also been documented (Huang et al., 2011; Javaid, 2019; Fortune, 2022; Huang et al., 2024).

In phoma leaf spot assessments done at Harpenden and Norwich in the 2023/2024 and 2024/2025 growing seasons, all ten cultivars had similar incidence in each individual assessment, but some differences were observed between different growing seasons and sites. These differences may be due to differences in fungicide applications in different growing seasons at the two sites. For phoma leaf spots caused by *L. maculans* and *L. biglobosa*, both sites showed a dominance of lesions caused by *L. biglobosa* in the 2023/2024 growing season and by *L. maculans* in the 2024/2025 season. Although weather data were collected at both sites for both growing seasons, distinct differences in temperature and rainfall that could result in such a change in the proportions of *L. maculans* and *L. biglobosa* in causing leaf lesions were not identified. However, if there were any differences in weather conditions that could have resulted in this change in proportions of *L. maculans* and *L. biglobosa* by affecting timing of ascospore release; these may be identified in further studies to investigate the effects of weather conditions on ascospore release by *L. maculans* and *L. biglobosa* separately (Toscano-Underwood et al., 2003; Huang et al., 2003b; Huang et al., 2005; Huang et al., 2007; Salam et al., 2007; Dawidziuk et al., 2012b).

Furthermore, there are other factors that could have had an effect on the proportions of phoma leaf spot lesions caused by *L. maculans* and *L. biglobosa*. Crop rotations and tillage are common disease control methods in efforts to isolate crops from infected stubble from the previous growing season, and to reduce transmission of inoculum in the field to subsequent growing seasons, respectively (West et al., 2001; Guo et al., 2005;

Fitt et al., 2006b; Hossard et al., 2018). It was previously reported that ascospores of *L. maculans* were still discharged from infected crop debris after the majority of the original infected stubble had disappeared, for three to five years in Canada (low tillage) and for two to four years in France (burial of stubble) (Petrie, 1995). Moreover, it was also reported that *L. maculans* survives longer in buried stubble compared to *L. biglobosa* (Huang et al., 2003a; Fitt et al., 2006a). If the field management practices were not sufficiently executed; it could explain the increase in the proportion of phoma leaf spot lesions caused by *L. maculans* from the 2023/2024 to the 2024/2025 season. This could have been due to *L. maculans* surviving on oilseed rape debris in those fields for longer and producing viable ascospores, leading to an increase in its foliar lesions compared to the previous growing season.

Alternatively, if the field management practices were insufficient, interspecific competition between *L. maculans* and *L. biglobosa* on infected crop debris could be considered as another factor. It is known that *L. maculans* produces the phytotoxin sirodesmin PL, which has been characterised to be involved in competition, and mainly produced when the pathogen is colonising the stem and crown during its necrotrophic phase (Rouxel et al., 1998; Elliott et al., 2007; Fortune et al., 2024; Bingol et al., 2024; Pombe et al., 2024). However, in this instance, *L. maculans* inhibiting *L. biglobosa* on infected crop debris through production of sirodesmin PL is not considered very likely. This is for two reasons. First, there was an abundance of phoma leaf spot lesions caused by *L. biglobosa* (greater than *L. maculans*) on crops at the time of assessment in 2023/2024 growing season. And if ascospores of both *Leptosphaeria* species were released at similar times in the East of England (as observed at Bayfordbury, Hertfordshire), this would give *L. biglobosa* the opportunity to deploy its host-mediated interspecific competition strategy. It could induce systemic acquired resistance and reduce the success of *L. maculans* in infecting oilseed rape. Secondly, *L. biglobosa* was shown to have more flexibility in timing of infecting oilseed rape alongside *L. maculans* to deploy its interspecific competition strategies to create local and systemic effects against *L. maculans* (Mahuku et al., 1996; Liu et al., 2006; Liu et al., 2007) (Chapter 4). Therefore, *L. maculans* would have required a considerable timing advantage (which is unlikely to occur in current climatic conditions in the UK) over *L. biglobosa* to outcompete it. It is suggested here that other previously mentioned factors (fungicides, resistance genes, crop rotations, tillage, etc.), either individually or collectively, have resulted in the

differences of pathogen proportions in causing phoma leaf spot lesions between the two growing seasons.

Phoma stem canker severity on the two cultivars at Hereford was smaller in the 2021/2022 than in the 2022/2023 growing season. Furthermore, there was a reduction in the percentage of *L. maculans* DNA in stem basal cankers in the 2021/2022 compared to the 2022/2023 growing season. Nevertheless, over 95 % of the DNA in stem basal cankers was of *L. maculans* for both cultivars. This could have been a result of environmental or human factors (except fungicide applications, as these experiments were untreated). Interestingly, although having a high phoma stem canker resistance score of 8 in the 2019/2020 AHDB recommended list (AHDB, 2019), cultivar Aquila had high phoma stem canker disease scores, which also increased from the 2021/2022 to the 2022/2023 growing season. Although no information is available on the resistance type in cultivar Aquila (e.g. *Rlm7* etc.), it is likely that a breakdown of resistance event has occurred due to changes in local *L. maculans* populations in Hereford. This could have been due other local farms growing cultivar Aquila extensively, as it was in the AHDB recommended lists for three consecutive years (AHDB, 2017; AHDB, 2018; AHDB, 2019). Breakdown of resistance mediated by *R*-genes against *L. maculans* after large scale commercial use over a short period of time (i.e. less than five years) has been documented previously (Rouxel et al., 2003b; Zhang et al., 2015; Van de Wouw et al., 2022).

Contrary to the site at Hereford, results from the field experiments done at Huntingdon in the same growing seasons showed a reduced overall disease severity in the 2022/2023 season. Further investigation showed that over 95 % of the DNA in stem basal cankers was of *L. maculans* for both cultivars in each growing season. It was not possible to statistically test whether cultivar or growing season had an effect on severity of phoma stem canker and proportions of pathogens in stem basal cankers, because there were differences between the cultivars used in each growing season. The reduction in disease severity in the 2022/2023 growing season at Huntingdon could be due to environmental or human factors (except fungicide applications, as these experiments were also untreated). One example to these could be that if there were several days in autumn/winter of the 2022/2023 growing season that were cold and dry (< 5°C with no rainfall) compared to the 2021/2022 season, this could have reduced and/or delayed the release of ascospores of *Leptosphaeria* species locally (Toscano-Underwood et al., 2003;

Javaid, 2019; Brachaczek et al., 2021). It has been documented that warm and wet autumn/winter periods promote ascospore release and result in greater disease severity and yield losses; as infection of cotyledons or the first few true leaves early in the growing season increases the severity of stem cankers, as the pathogens take less time to reach the stem and crown (Barbetti, 1975; Petrie, 1995; Sun et al., 2001; Li et al., 2006; Ghanbarnia et al., 2011; Brachaczek et al., 2021).

Results from field experiments at Wisbech with six cultivars showed an increase in the overall disease severity in the 2022/2023 growing season, similar to the results from field experiments at Hereford. This was the case for all cultivars assessed in both growing seasons, except Line-A (*Rlm7* + *RlmS*) and Murray (*RlmS*). Nevertheless, it was not possible to statistically test whether the growing season had an effect on the severity of phoma stem canker and proportions of pathogens in stem basal cankers, because there were differences in the cultivars used between each growing season.

The pathogen DNA in stem basal cankers of cultivars with just the *Rlm7* resistance gene was mainly *L. maculans* (> 95 %), which suggests that the local *L. maculans* populations at Wisbech might have mutated to virulence against *Rlm7*, rendering the resistance gene ineffective (Fudal et al., 2009; Van de Wouw et al., 2010; Idnurm et al., 2024). A study in 2018 first reported isolates of *L. maculans* becoming virulent against *Rlm7* at multiple sites in England (Mitrousia et al., 2018), indicating the start of the breakdown of *Rlm7* in the UK (Van de Wouw et al., 2022). Furthermore, although still mostly caused by *L. maculans*, cultivar Murray (which has *RlmS*) had less severe stem basal cankers. The *RlmS* resistance gene has a different genetic background and is related to adult plant resistance against stem lesions and was suggested to be used alongside *Rlm7* to increase its longevity (Neik et al., 2022; NPZ UK, 2023; Farmers Weekly, 2023; Balesdent et al., 2024). Strikingly, cultivar Line-A (which has *Rlm7* and *RlmS*), had the least overall disease severity across the two growing seasons assessed. However, the greatest proportion of *L. biglobosa* DNA was observed in cultivar Line-A, with > 50 % of *L. biglobosa* DNA in stem basal cankers in the 2022/2023 growing season. This supports the findings of Huang et al. (2024), which reported that the focus on effective control of *L. maculans* is increasing the importance of *L. biglobosa* as a phoma stem canker pathogen. This is an example of disease control methods affecting the relative proportions of pathogen

populations and interspecific interactions by giving advantage to one pathogen over the other.

Considering these abilities and the competitive strength of *L. biglobosa*, some have suggested to incorporate *L. biglobosa* into integrated pest management practices as a biocontrol agent against *L. maculans* (Liu et al., 2006; Shah et al., 2020; Padmathilake & Fernando, 2022b). However, apart from being the only phoma stem canker pathogen in China responsible for significant yield losses, *L. biglobosa* was also suggested to contribute to yield losses in Poland (Huang et al., 2005; Brachaczek et al., 2016; Cai et al., 2017; Brachaczek et al., 2021). Taken together with its decreased sensitivity to azole fungicides compared to *L. maculans* and its increased frequency in stem basal cankers, these reports suggest that *L. biglobosa* has the potential to cause severe disease epidemics and reduce yields of oilseed rape in the UK (Eckert et al., 2010; Sewell et al., 2017; Huang et al., 2024). To use *L. biglobosa* as a potential biocontrol agent against *L. maculans*, less aggressive isolates of *L. biglobosa* will need to be identified.

Moreover, a new subclade of *L. biglobosa* 'canadensis' was identified on wasabi (*Eutrema japonicum*) in England and Ireland; and was also shown to be pathogenic to oilseed rape (King & West, 2022). This adds to the risks already caused by the common *L. biglobosa* 'brassicae' subclade to oilseed rape growers in the UK. There is also no information available on interspecific interactions of either subclade of *L. biglobosa* with other relevant pathogens of oilseed rape, such as *Pyrenopeziza brassicae* (causing light leaf spot). Therefore, the risks of *L. biglobosa* causing significant yield losses, and the potential consequences of its interactions with pathogens other than *L. maculans* must be evaluated before considering its use as a biocontrol agent in any setting.

Proportions of other co-existing pathogens in causing disease being affected by natural and human factors have also been documented. For example, it was found that the proportions of *Oculimacaula yallundae* and *O. acuformis* (causing eyespot disease in wheat) were affected by the application of fungicides; where proportion of *O. acuformis* increasing to over 80 % in fields treated with prochloraz or prochloraz plus carbendazim (Bierman et al., 2002; Fitt et al., 2006a). This was due to the greater range of prochloraz-sensitivity found within the populations of *O. acuformis*, leading to differences in the efficacy of fungicide in reducing the mycelial growth of the two species, increasing the

proportion of *O. acuformis* over *O. yallundae* (Bateman et al., 1995; Bateman, 2002; Fitt et al., 2006a).

The strength of the study presented in this chapter is that *L. maculans* and *L. biglobosa* were evaluated separately in relation to ascospore release and their contributions to development of phoma leaf spot and phoma stem canker symptoms. The results have provided further insight into prevalence and potential interspecific interactions of the two *Leptosphaeria* species in natural conditions at various sites in England, while also emphasising the factors that could affect their proportions in causing disease on oilseed rape crops.

The limitation of this study is that these field experiments were not set up just for this project, but also for other purposes (e.g. assessment of other diseases, yield related and agronomically relevant characteristics, etc.). Further research is required to test the independent and combined effects of natural and/or human factors on the proportional populations and interspecific interactions of *Leptosphaeria* species on various cultivars of oilseed rape, both in controlled environment and in natural conditions.

The results of this work have potential practical importance for UK growers. It is understood that the release of ascospores of *Leptosphaeria* species at similar times will result in co-inoculations of both pathogens; which may lead to unexpected challenges – or opportunities – in the management strategies of phoma stem canker in the UK.

Since multiple factors are affecting pathogen co-existence and disease severity in natural conditions, it is unlikely that a set of strategies (e.g. utilisation of fungicides and resistant cultivars with *Rlm* genes) would sufficiently control diseases and prevent yield losses in each growing season. Instead, a holistic approach will most likely need to be taken, where disease control strategies are evaluated on a season-by-season basis, depending on the expected course of the epidemics to be caused by individual pathogens and their interactions. Perhaps, a step towards this direction can be taken through development of a decision support system (DSS), and its continued improvement by adding more data and utilising the emerging technological advancements, such as artificial intelligence and machine learning. Undertaking such efforts will require vast

inter-community collaborations, with academic researchers in various disciplines working with companies and growers.

6 Chapter 6 – General discussion

The aims of this project were to increase the understanding on interspecific interactions between *Leptosphaeria maculans* and *Leptosphaeria biglobosa* and to provide valuable insights for future integrated control strategies based on their interactions to improve control of phoma stem canker on oilseed rape (*Brassica napus*) in the UK. These aims were achieved by investigating interspecific interactions between *L. maculans* and *L. biglobosa in vitro* (Chapter 3), *in planta* (Chapter 4) and in natural conditions (Chapter 5).

6.1 Co-inoculation timing directly affects the interspecific interactions between *Leptosphaeria maculans* and *Leptosphaeria biglobosa*

Investigations done on the timing of co-inoculation of the two *Leptosphaeria* species *in vitro* (Chapter 3) revealed that *L. maculans* and *L. biglobosa* are both able to have antagonistic effects on the growth and development of each other, depending on the timing of their co-inoculation. The results of this study showed that in liquid co-cultures of *Leptosphaeria* species, morphology of mycelia and production of pigment are indicative of their interspecific interactions. Presence of a dark yellow/orange pigmentation in culture filtrates in treatments where *L. biglobosa* was inoculated before or up to 1 day after *L. maculans* suggested a predominance of *L. biglobosa* growth in those co-cultures. This was further supported by the results on inhibition by *L. biglobosa* of the production of sirodesmin PL and its precursors by *L. maculans*. In all treatments where morphology and pigmentation associated with *L. biglobosa* were observed, no sirodesmin PL or its precursors were detected in culture filtrates, suggesting that *L. biglobosa* had inhibited the production of this phytotoxin by *L. maculans*. Interestingly, a partial inhibition of phytotoxin production by *L. maculans* was observed when *L. biglobosa* was sequentially co-inoculated 3 days after *L. maculans*. Furthermore, if *L. biglobosa* was sequentially co-inoculated 5 days or later after *L. maculans*, it was not able to inhibit the production of sirodesmin PL at all. The results for DNA of the two pathogens in co-cultures revealed that the antagonistic effects were beyond just phytotoxin production, but the growth of pathogens themselves was being inhibited. *L. biglobosa* was able to inhibit the growth of *L. maculans* entirely if it was co-inoculated before or up to 1 day after *L. maculans*, and partially if it was co-inoculated 3 days after *L. maculans*. Conversely, as the time gap between the co-inoculations increased, the

competitive advantage 'shifted' in favour of *L. maculans* (upon successful production of sirodesmin PL), and *L. maculans* was able to inhibit the growth of *L. biglobosa* entirely when *L. biglobosa* was co-inoculated 5 days or later after *L. maculans in vitro*. Elliott et al. (2007) reported similar findings, where thirteen day old colonies of a sirodesmin PL producing isolate of *L. maculans* were able to inhibit germination of *L. biglobosa* conidia. However, Fortune et al. (2024) (part of Chapter 4) and Bingol et al. (2024) (Chapter 3) were the first to identify such significant antagonistic effects of *L. biglobosa* on *L. maculans* under interspecific competition.

The mechanisms of these interactions and interspecific competition strategies deployed by *L. maculans* and *L. biglobosa* were evaluated based on literature and findings of this study. It is suggested that *L. maculans* uses an interference interspecific competition strategy by producing sirodesmin PL, which inhibits the growth of *L. biglobosa* through its fungitoxic effects. This can take place only when *L. maculans* successfully produces its toxin, which was shown to be at detectable levels *circa* 5 days post inoculation (dpi) *in vitro* (Gardiner et al., 2004; Fortune et al., 2024). Therefore, the ability of *L. maculans* to successfully inhibit the growth of *L. biglobosa in vitro* relies on its successful production of sirodesmin PL. On the other hand, it is suggested that *L. biglobosa* uses a resource-mediated interspecific competition strategy, where it utilises the limited nutrient resources more efficiently than *L. maculans*. Previous work has reported that *L. biglobosa* colonises the host tissues more rapidly than *L. maculans* (Huang et al., 2003; Eckert et al., 2005). Moreover, Frąc et al. (2022) recently reported that *L. biglobosa* is more efficient in utilising natural carbon resources compared to *L. maculans*. The results for mycelial growth rate in this study were consistent with these reports, where mycelia of *L. biglobosa* grew at a rate nearly three times greater than that of *L. maculans*. Therefore, if *L. biglobosa* utilises the resource before *L. maculans* produces sirodesmin PL, it can inhibit the growth of *L. maculans in vitro*. This study has provided important insights into the importance of timing on interspecific interactions between *L. maculans* and *L. biglobosa*.

Suggestions for future work are:

(1) Optimising *in vitro* assays using conidial suspensions as inoculum and smaller volumes of liquid media to reduce time and resources required to carry out future investigations.

(2) Testing isolates from other subclades of *L. biglobosa* to investigate whether they have similar antagonistic effects on *L. maculans* to understand potential interactions that may take place in different regions of the world where *L. maculans* and different subclades of *L. biglobosa* co-infect oilseed rape.

(3) Testing nutrient uptake of different *L. biglobosa* isolates in the International Blackleg of Crucifers Network (IBCN) isolate collection to identify isolates with potential for future investigations.

6.2 Interspecific interactions between *Leptosphaeria maculans* and *Leptosphaeria biglobosa* affect disease development and severity

Investigations done on the effects of co-inoculation timing on interspecific interactions between the two *Leptosphaeria* species *in planta* (Chapter 4) also revealed reciprocal antagonistic effects between *L. maculans* and *L. biglobosa* in terms of pathogen growth, which were also dependent on the timing of their co-inoculation and influenced the development and severity of disease on oilseed rape. The results of this study showed that the pattern of lesion development for all treatments where *L. biglobosa* was inoculated before or up to 1 day after *L. maculans* was similar to that of *L. biglobosa*. This was characterised by the appearance of small necrotic lesions shortly after inoculation and expansion of lesions slowly under humid conditions, which was previously reported for *L. biglobosa* (Lowe et al., 2014; Shah et al., 2020) and consistent with the pattern of lesion development by a necrotrophic plant pathogen (Talley et al., 2002; Laluk & Mengiste, 2010; Précigout et al., 2020). These have suggested a predominance of *L. biglobosa* in those lesions. The results also showed that the pattern of lesion development for the treatments where *L. biglobosa* was sequentially co-inoculated 3 days or later after *L. maculans* was similar to that of *L. maculans*. This was characterised by a lack of lesion development from 7 dpi to 10 dpi (indicating endophytic colonisation of tissues), followed by appearance of large lesions at 14 dpi and expansion of lesions at 16 dpi (indicating the switch to necrotrophy), which was previously reported for *L. maculans* (Lowe et al., 2014; Haddadi et al., 2019) and is also consistent with the pattern of lesion development by a hemi-biotrophic plant pathogen (Horbach et al., 2011; Koeck et al., 2012; Seybold et al., 2020). These results have suggested a predominance of *L. maculans* in those lesions.

The results for lesion phenotype and mature pycnidia on infected cotyledons further supported the results for lesion development. The treatments showing a similar lesion development pattern to *L. biglobosa* also showed similar lesion phenotype and size to *L. biglobosa* only. Interestingly, the only exception was the treatment where *L. biglobosa* was sequentially co-inoculated 1 day after *L. maculans*, where smaller lesions of the same phenotype were observed. Furthermore, upon incubation of these infected cotyledons, no pink cirri of conidia released from mature pycnidia were observed in any of these treatments. In contrast, the treatments showing a similar lesion development pattern to *L. maculans* also showed similar lesion phenotype and size to *L. maculans* only. Moreover, upon incubation of these infected cotyledons, similar amounts of pink cirri of conidia released from mature pycnidia were observed for these treatments. On foliar tissues of oilseed rape, *L. biglobosa* is associated with smaller and darker lesions with very few or no pycnidia, while *L. maculans* is associated with larger and lighter lesions with pycnidia (West et al., 2001; Fitt et al., 2006a). These results suggested that *L. maculans* and *L. biglobosa* may be inhibiting the growth and development of each other locally when inoculated at the same site, depending on the timing of their co-inoculation, similar to results of *in vitro* studies presented in Chapter 3.

Quantification of relative pathogen DNA in lesions confirmed that *L. maculans* and *L. biglobosa* can indeed inhibit each other when inoculated at the same site on their host, based on the co-inoculation timeline. The results of *in planta* studies slightly differed from those of *in vitro* studies; although *L. biglobosa* was still able to inhibit the growth of *L. maculans* when sequentially co-inoculated 1 day after *L. maculans*, the partial antagonistic effect of *L. biglobosa* when co-inoculated 3 days after *L. maculans* was not observed *in planta*. Instead, the growth of *L. biglobosa* was inhibited by *L. maculans* if *L. maculans* was at a timing advantage of 3 or more days. Nevertheless, growth of *L. maculans* was inhibited in all treatments which showed *L. biglobosa*-type lesions.

The mechanisms of these interactions and the interspecific competition strategies deployed by *L. maculans* and *L. biglobosa* (resulting in the changes in disease development and severity on their host) were evaluated based on literature and findings of this study. It was concluded in *in vitro* studies that the antagonistic effects of *L. maculans* were as a result of the production of sirodesmin PL. However, it is not thought to be the reason in such early interactions (1 dpi to 5 dpi) *in planta*. This is because *L.*

maculans is unlikely to produce sirodesmin PL during its 'early endophytic phase', as production of phytotoxins is associated with the 'late necrotrophic phase' of hemi-biotrophic pathogens (Stergiopoulos et al., 2013). In addition, a recent transcriptomic study reported that the upregulation of genes related to production of sirodesmin PL was associated with the necrotrophic phase of *L. maculans*, specifically in colonisation of stem tissues (Gay et al., 2021). Another explanation of the antagonistic effects of *L. maculans* on *L. biglobosa* in these experiments is that the endophytic colonisation of *L. maculans* created an unsuitable environment or reduced the nutrients required for the growth of *L. biglobosa* locally. Although this is mimicking of a resource-mediated interspecific competition strategy deployed by *L. biglobosa*, it is not considered to be an interspecific competition strategy for *L. maculans* here. This is because *L. biglobosa* can use this strategy and still inhibit the growth of *L. maculans* even when at a timing disadvantage of 1 day. By contrast for *L. maculans*, this is solely dependent on having 3 or more days of timing advantage when competing with *L. biglobosa*, and loss of this timing advantage would result in the inhibition of *L. maculans* growth.

It is suggested that *L. biglobosa* uses a host-mediated interspecific competition strategy by systematically activating plant defences early, which reduces the success of *L. maculans* in establishing itself on the host. This phenomenon was previously documented, where pre-inoculation of oilseed rape leaves with *L. biglobosa* was shown to induce systemic acquired resistance (SAR) in oilseed rape and reduced the damage caused by *L. maculans* (Mahuku et al., 1996; Liu et al., 2006; Padmathilake & Fernando, 2022b). Liu et al. (2007) reported that *L. biglobosa*-induced SAR primarily functioned through jasmonic-acid/ethylene (JA/ET) signalling and upregulation of plant defensins (*PDF-1.2*), with accumulation of salicylic acid (SA) and pathogenesis related proteins (*PR-1*) following subsequently. Although the results of gene expression experiments in this study agreed with those reported by Liu et al. (2007) in terms of *PR-1* expression, an early upregulation of *PDF-1.2* as a result of *L. biglobosa* infection was not observed. However, an early upregulation of a marker gene for defence against necrotrophic pathogens (*WRKY33*) (Zheng et al., 2006; Birkenbihl et al., 2012) was observed in response to *L. biglobosa* inoculation.

It is also suggested that *L. biglobosa* uses a resource-mediated interspecific competition strategy locally by depleting or modifying the nutrient resources at the inoculation site,

reducing the availability of nutrients required by *L. maculans* for growth and development. This can be facilitated through *L. biglobosa* depleting the nutrient resources through its faster metabolic rate (Frąc et al., 2022) (similar to *in vitro* studies). Alternatively, the early necrotic colonisation of *L. biglobosa* resulting in death of the cells may not be suitable for *L. maculans* to use as nutrient resources during its 'early endophytic phase'. *L. maculans* itself is able to cause necrotic tissues and obtain nutrients from them during its 'late necrotrophic phase'. However, the results of this study, as well as a recent transcriptomic study suggests that *L. maculans* may not be able to adapt its trophic nature during its endophytic phase as a response to changes in nutritional resources (i.e. necrotic tissues) caused by *L. biglobosa* (Gay et al., 2021; Gay et al., 2023). This is reminiscent of tissue necrosis arresting *L. maculans* at the inoculation site through a cell death response as a result of an incompatible interaction between *L. maculans* and *B. napus* (qualitative resistance) (Balesdent et al., 2006; Huang et al., 2018). The results of this study suggest that *L. biglobosa* may have more strategies in competition against *L. maculans* than previously thought, through systemic (induction of SAR) and local (changes in nutrient availability) effects. With ascospores of both *L. maculans* and *L. biglobosa* being released at similar times, infection timelines of these pathogens on oilseed rape crops are likely to favour *L. biglobosa* to have a competitive advantage over *L. maculans* (summarised in Figure 6.1). This study has provided important insights into the effects of interspecific interactions between *L. maculans* and *L. biglobosa* on disease development and disease severity on their host.

Suggestions for future work are:

(1) Testing other subclades and isolates of *L. biglobosa* identified to have potential for future investigations.

(2) Executing experiments at greater scales with increased sampling timeline to investigate host defences during interspecific competition in greater detail, including systemic effects.

(3) Developing methods to investigate interspecific interactions of *L. maculans* and *L. biglobosa* with other important pathogens of oilseed rape, such as *Pyrenopeziza brassicae* (causing light leaf spot) and *Sclerotinia sclerotiorum* (causing sclerotinia stem rot).

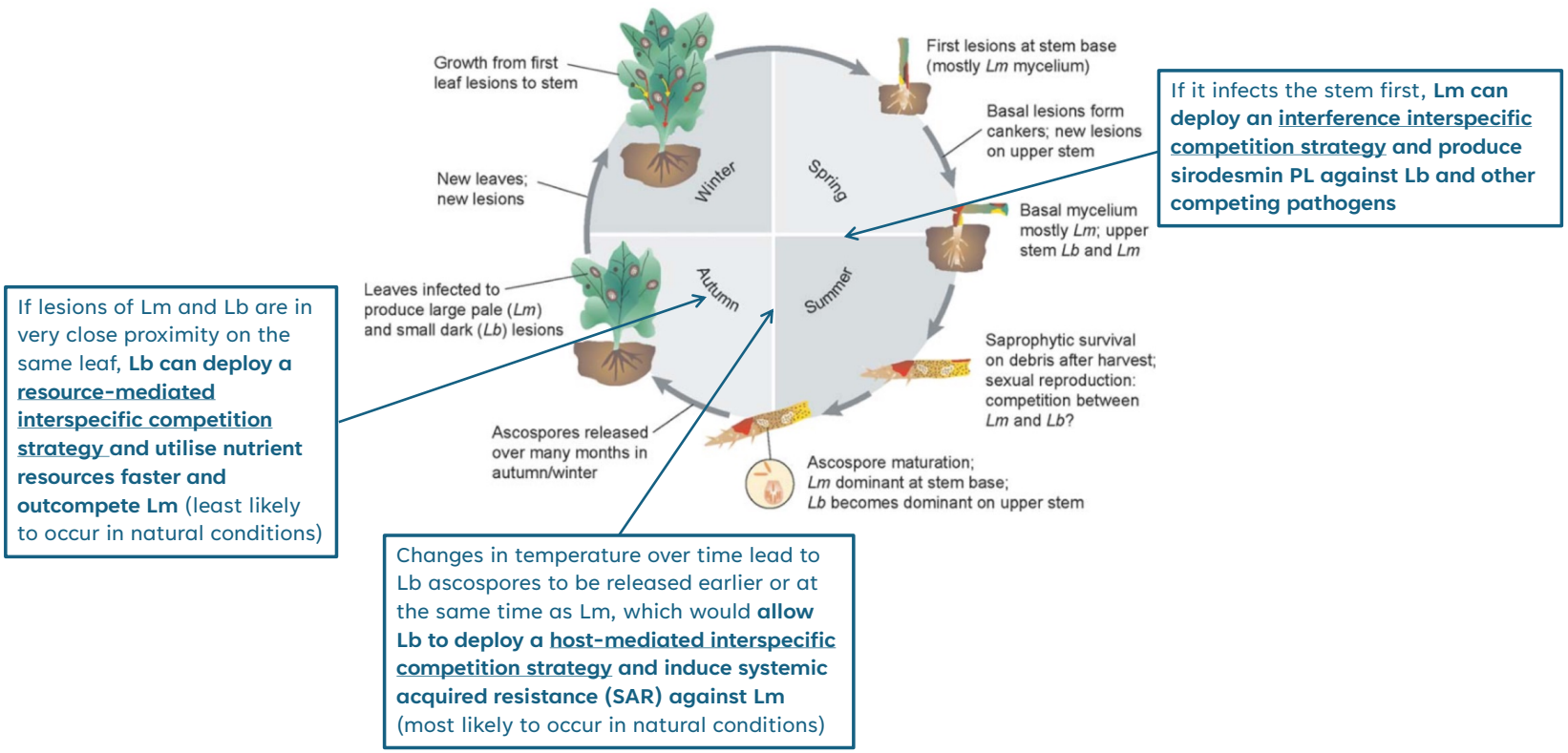

Figure 6.1:Summary of different interspecific competition strategies taking place between *Leptosphaeria maculans* (Lm) and *Leptosphaeria biglobosa* (Lb).

During spring/summer, if Lm colonises the stem tissues first, it can deploy an interference interspecific competition strategy against Lb and other competing pathogens. During autumn, if ascospores of Lm and Lb are germinating and causing lesions in very close proximity on the same leaf, Lb can deploy a resource-mediated interspecific competition strategy against Lm (least likely to occur in natural conditions) .During summer/autumn, increases in temperature lead to ascospores of Lb to be released before or at the same time as Lm, which would allow Lb to deploy a host-mediated interspecific competition strategy against Lm (most likely to occur in natural conditions.

6.3 Environmental and human factors may influence the interspecific interactions between *Leptosphaeria maculans* and *Leptosphaeria biglobosa*, which may affect the course of disease epidemics

Results from the investigations on the timing of ascospore release and the disease caused by the two *Leptosphaeria* species in field experiments (Chapter 5) emphasised the influence of environmental and human factors on the interspecific interactions between *L. maculans* and *L. biglobosa*, and their potential subsequent effects on disease epidemics in natural conditions. The results of this study showed that ascospores of *L. maculans* and *L. biglobosa* were released at similar times in four consecutive growing seasons at Bayfordbury, Hertfordshire. This agrees with recent reports describing similar trends of ascospore release of *Leptosphaeria* species at several sites in England (Javaid, 2019; Fortune, 2022; Huang et al., 2024). The first major release of ascospores was generally observed at the end of September, except in the 2022/2023 growing season, where the first major release of ascospores was delayed due to a smaller number of rain days in August of the 2022/2023 season. The maximum release of ascospores was mainly observed in late-October/early-November, except in the 2021/2022 growing season, where the maximum release of ascospores was delayed due to smaller amount of rainfall between October and January of the 2021/2022 season. These observations are in agreement with previous reports describing ascospore release of *L. maculans* or *L. biglobosa* in relation to temperature and rainfall. There were differences in the timing of ascospore release of *L. maculans* and *L. biglobosa* (with pseudothecia of *L. maculans* maturing faster at < 10°C), creating a temporal and spatial separation between the pathogens to facilitate their co-existence (Toscano-Underwood et al., 2003; Huang et al., 2005; Fitt et al., 2006b). However, the trend for UK winters becoming milder and wetter (as also documented in this study) leads to increases in the number of days where pseudothecial maturation of both *L. maculans* and *L. biglobosa* can proceed, resulting in ascospore release of both pathogens at similar times. This is likely to disrupt the interspecific interactions between *L. maculans* and *L. biglobosa*, causing them to change from 'co-existence' to 'competition'. It is important to keep monitoring the ascospore release of *L. maculans* and *L. biglobosa* in relation to environmental factors to better understand how changes in climatic conditions might affect their interspecific interactions.

The results of phoma leaf spot assessments at Harpenden and Norwich for the 2023/2024 and 2024/2025 growing seasons showed differences in percentage of phoma leaf spot lesions caused by *L. maculans* and *L. biglobosa* at different sites and in different growing seasons, despite having little to no difference in overall disease incidence (% of plants affected) for all ten cultivars assessed. There was a predominance of *L. biglobosa* in the 2023/2024 growing season and *L. maculans* in the 2024/2025 growing season in causing phoma leaf spot lesions at both sites. These differences in pathogen proportions in causing phoma leaf spots may have been due to environmental factors, however; no clear differences in temperature and rainfall that could affect proportions of *L. maculans* and *L. biglobosa* between the different growing seasons were identified. There are also human factors that may have affected the proportions of these pathogens, such as fungicide applications (which were different in different sites and growing seasons), crop rotations and soil/stubble management. *L. biglobosa* is less sensitive to azole fungicides (Eckert et al., 2010; Huang et al., 2011) and *L. maculans* survives longer on buried crop debris (Huang et al., 2003a; Fitt et al., 2006a). Recently, reduced sensitivity to DMI fungicide prothioconazole-desthio in *L. biglobosa* isolates has been reported (King et al., 2025). These disease management strategies differing in their efficacy against different pathogens may affect their interspecific interactions by favouring one over the other.

The results of phoma stem canker assessments at Hereford and Huntingdon for the 2021/2022 and 2022/2023 growing seasons showed differences in overall disease severity at different sites and in different growing seasons, despite having little to no difference in percentage of stem basal cankers caused by *L. maculans* (over 95 % of pathogen DNA in stem basal cankers was of *L. maculans*) for all cultivars assessed. Fluctuations in disease severity between different growing seasons can occur as a result of environmental and human factors as explained above. In addition to those, there is evidence of *R* gene-mediated (qualitative resistance) against *L. maculans* as well as quantitative resistance (QR). By contrast, there is no evidence of qualitative resistance against *L. biglobosa*, with only QR contributing to cultivar resistance against *L. biglobosa*. The increase in disease severity at Hereford (especially for cultivar Aquila with a resistance score of 8 out of 9) may have been due to a breakdown of resistance event. If cultivar Aquila was widely cultivated in consecutive growing seasons at sites near Hereford, local *L. maculans* populations may have mutated to virulence in response to selection. This phenomenon has been documented previously in the *L. maculans*/*B. napus*

pathosystem (Rouxel et al., 2003a; Van de Wouw et al., 2022). The results of similar assessments for the same growing seasons at Wisbech highlighted the effects of cultivar selection might have on proportions of pathogens in stem basal cankers. All cultivars with only the *Rlm7* resistance gene had increased disease severity scores in the second growing season (with over 95 % of pathogen DNA in stem basal cankers quantified as *L. maculans*), suggesting that local *L. maculans* populations might also have mutated to virulence at Wisbech, rendering *Rlm7* ineffective. Although still primarily caused by *L. maculans*, cultivar Murray (containing the new *RlmS* resistance gene, with an alternative mechanism of targeting stem colonisation phase of *L. maculans*) had less severe stem basal cankers in comparison to cultivars with only *Rlm7*. Line-A (which has both *Rlm7* and *RlmS* – a combination of two resistance genes against *L. maculans*) was the most resistant cultivar in both growing seasons. However, there was more *L. biglobosa* DNA quantified in stem basal cankers of Line-A compared to all other cultivars; especially in the second growing season, over 50 % of the DNA in stem basal cankers was of *L. biglobosa*. These results are consistent with those of Huang et al. (2024), who reported that the focus on controlling *L. maculans* using various disease control strategies is increasing the importance of *L. biglobosa* in causing stem basal cankers. This study has provided important insights into how environmental and human factors may influence the interspecific interactions between *L. maculans* and *L. biglobosa*, and how these interactions may affect local proportions of pathogen populations and the course of disease epidemics.

Suggestions for future work are:

(1) Running field experiments dedicated to monitoring ascospore release and assessing disease development of *L. maculans* and *L. biglobosa* (as well as other economically relevant pathogens of oilseed rape) in relation to temperature, rainfall, fungicide applications, cultural practices and cultivar resistance.

(2) Collaborating with academic and industrial institutions to develop more advanced disease forecasting models separately for *L. maculans* and *L. biglobosa*, which take into account potential effects of interspecific interactions.

6.4 Implications for disease management

Following the reports of *L. biglobosa* being able to reduce the damage caused by *L. maculans* through systemic effects (Mahuku et al., 1996; Liu et al., 2006; Liu et al., 2007), some studies have investigated this mechanism further and suggested to use *L. biglobosa* as a biocontrol agent against *L. maculans* (Shah et al., 2020; Padmathilake & Fernando, 2022b). Although results of this study supported the findings of these previous studies and also suggested a novel local mechanism for *L. biglobosa* in inhibiting the growth of *L. maculans*, such suggestions for incorporating *L. biglobosa* into IPM strategies as a biocontrol agent must not be rushed. *L. biglobosa* may already exist in nature, but altering its proportion – especially when it is already being altered by environmental and human factors – may result in unprecedented off-target effects. It is known that *L. biglobosa* is responsible for significant yield losses as the only phoma stem canker pathogen present in China (Cai et al., 2017). It was also considered to cause yield losses in Poland (Huang et al., 2005; Brachaczek et al., 2016; Brachaczek et al., 2021). Considering its reduced sensitivity to azole fungicides (Eckert et al., 2010; Huang et al., 2011; King et al., 2025) and its increasing importance in causing stem basal cankers (Huang et al., 2024), *L. biglobosa* may also have the potential to cause significant yield losses in the UK. The pathogenic potential of *L. biglobosa*, as well its interactions with other pathogens of oilseed rape present in the UK must be thoroughly evaluated before further suggestions can be made regarding its use as a biocontrol agent.

Effective disease control can be achieved through targeted approaches, where strategies are informed based on environmental and human factors, as well as their combined effects on pathogen interactions and disease development on a local, season-by-season basis. This may be achieved by developing a decision support system (DSS) for oilseed rape diseases using the latest technological tools. The DSS would then be regularly updated with annual improvements based on environmental and experimental data, which would facilitate the integration and co-ordination of control strategies against several diseases by providing holistic, specialised and targeted guidance on disease management.

6.5 Conclusion

This project increased the understanding of interspecific interactions between *L. maculans* and *L. biglobosa* and provided valuable insights into future integrated control strategies based on their interactions to improve control of phoma stem canker on oilseed rape in the UK. Results showed that different mechanisms and strategies are deployed by these two pathogens depending on the timing of their interaction and may affect disease severity. Environmental and human factors may also influence their interactions and lead to unexpected changes in phoma leaf spot and stem canker epidemics. Effective disease control strategies must be integrated with consideration to target all important (and with potential to become important) pathogens of oilseed rape.

7 References

Abdullah, A. S., Moffat, C. S., Lopez-Ruiz, F. J., Gibberd, M. R., Hamblin, J., & Zerihun, A. (2017). Host–Multi-Pathogen Warfare: Pathogen interactions in co-infected plants. *Frontiers in Plant Science*, *8*. https://doi.org/10.3389/fpls.2017.01806

Agarwal, P., Reddy, M. P., & Chikara, J. (2011). WRKY: its structure, evolutionary relationship, DNA-binding selectivity, role in stress tolerance and development of plants. *Molecular Biology Reports*, *38*, 3883–3896. https://doi.org/10.1007/s11033-010-0504-5

How to manage phoma in oilseed rape | AHDB. (2021). Retrieved 05 February 2022, from https://ahdb.org.uk/knowledge-library/how-to-manage-phoma-in-oilseed-rape

AHDB. 2017: Recommended Lists. Retrieved 16 April 2025, from https://projectblue.blob.core.windows.net/media/Default/Imported%20Publication%20Docs/AHDB%20Cereals%20&%20Oilseeds/Varieties/RL2017-18/Table%2013a%20Winter%20oilseed%20rape%20Recommended%20List%20-%20EastWest.pdf

AHDB. 2018: Recommended Lists. Retrieved 16 April 2025, from https://projectblue.blob.core.windows.net/media/Default/Imported%20Publication%20Docs/AHDB%20Cereals%20&%20Oilseeds/Varieties/RL2018-19/Table-13-Winter-oilseed-rape-AHDB-Recommended-List-2018-19.pdf

AHDB. 2019: Recommended Lists. Retrieved 16 April 2025, from https://projectblue.blob.core.windows.net/media/Default/Imported%20Publication%20Docs/AHDB%20Cereals%20&%20Oilseeds/Varieties/RL2019-20/Table%2013.%20Winter%20oilseed%20rape%20Recommended%20List%202019-20-1.pdf

AHDB. 2020: Recommended Lists. Retrieved 16 April 2025, from https://projectblue.blob.core.windows.net/media/Default/Imported%20Publication%20Docs/AHDB%20Cereals%20&%20Oilseeds/Varieties/RL2020-21/Winter%20oilseed%20rape%202020-21.pdf

AHDB. 2025: Recommended Lists. Retrieved 16 April 2025, from https://projectblue.blob.core.windows.net/media/Default/RL%20harvest%20results/16.%20Winter%20oilseed%20rape%20recommended%20list%20(2025-26)-1.pdf

Phoma leaf spot forecast. (2024). AHDB. Retrieved 05 May 2025, from https://ahdb.org.uk/phoma-leaf-spot-forecast

Aiking, H. (2011). Future protein supply. *Trends in Food Science & Technology*, *22*, 112–120. https://doi.org/10.1016/j.tifs.2010.04.005

Aimé, S., Alabouvette, C., Steinberg, C., & Olivain, C. (2013). The endophytic strain *Fusarium oxysporum* FO47: a good candidate for priming the defense responses in tomato roots. *Molecular Plant-Microbe Interactions*, *26*, 918–926. https://doi.org/10.1094/mpmi-12-12-0290-r

Al-Shehbaz, I. A., Beilstein, M. A., & Kellogg, E. A. (2006). Systematics and phylogeny of the *Brassicaceae* (Cruciferae): an overview. *Plant Systematics and Evolution, 259*, 89–120. https://doi.org/10.1007/s00606-006-0415-z

Ali, S., Mir, Z. A., Bhat, J. A., Tyagi, A., Chandrashekar, N., Yadav, P., Rawat, S., Sultana, M., & Grover, A. (2017). Isolation and characterization of systemic acquired resistance marker gene *PR1* and its promoter from *Brassica juncea*. *3 Biotech*, *8*. https://doi.org/10.1007/s13205-017-1027-8

Aljanabi, S., Forget, L., & Dookun, A. (1999). An Improved and rapid protocol for the isolation of polysaccharide- and polyphenol-free sugarcane DNA. *Plant Molecular Biology Reporter, 17*, 281. https://doi.org/10.1023/a:1007692929505

Altieri, M. A., & Bravo, E. (2007). The ecological and social tragedy of crop-based biofuel production in the Americas. Retrieved 21 April 2025, from http://hdl.handle.net/10919/67545

An, C., & Mou, Z. (2011). Salicylic acid and its function in plant immunity. *Journal of Integrative Plant Biology, 53*, 412–428. https://doi.org/10.1111/j.1744-7909.2011.01043.x

Andert, S., Ziesemer, A., & Zhang, H. (2021). Farmers' perspectives of future management of winter oilseed rape (*Brassica napus* L.): A case study from north-eastern Germany. *European Journal of Agronomy*, *130*, 126350. https://doi.org/10.1016/j.eja.2021.126350

Ansan-Melayah, D., Balesdent, M. H., Delourme, R., Pilet, M. L., Tanguy, X., Renard, M., & Rouxel, T. (1998). Genes for race-specific resistance against blackleg disease in *Brassica napus* L. *Plant Breeding*, *117*, 373–378. https://doi.org/10.1111/j.1439-0523.1998.tb01956.x

Arumugam, S., & Sriram, G. (2012). Synthesis and characterisation of rapeseed oil bio-lubricant – its effect on wear and frictional behaviour of piston ring–cylinder liner combination. *Proceedings of the Institution of Mechanical Engineers Part J Journal of Engineering Tribology*, *227*, 3–15. https://doi.org/10.1177/1350650112458398

Atabani, A., Silitonga, A., Badruddin, I. A., Mahlia, T., Masjuki, H., & Mekhilef, S. (2012). A comprehensive review on biodiesel as an alternative energy resource and its characteristics. *Renewable and Sustainable Energy Reviews*, *16*, 2070–2093. https://doi.org/10.1016/j.rser.2012.01.003

Aubertot, J., Pinochet, X., & Doré, T. (2004). The effects of sowing date and nitrogen availability during vegetative stages on *Leptosphaeria maculans* development on winter oilseed rape. *Crop Protection*, *23*, 635–645. https://doi.org/10.1016/j.cropro.2003.11.015

Aubertot, J. N., West, J. S., Bousset-Vaslin, L., Salam, M. U., Barbetti, M. J., & Diggle, A. J. (2006). Improved resistance management for durable disease control: a case study of phoma stem canker of oilseed rape (*Brassica napus*). *European Journal of Plant Pathology*, *114*, 91–106. https://doi.org/10.1007/s10658-005-3628-z

Audsley, E., Milne, A., & Paveley, N. (2005). A foliar disease model for use in wheat disease management decision support systems. *Annals of Applied Biology*, *147*, 161–172. https://doi.org/10.1111/j.1744-7348.2005.00023.x

Avenot, H. F., & Michailides, T. J. (2010). Progress in understanding molecular mechanisms and evolution of resistance to succinate dehydrogenase inhibiting (SDHI) fungicides in phytopathogenic fungi. *Crop Protection*, *29*, 643–651. https://doi.org/10.1016/j.cropro.2010.02.019

Bakshi, M., & Oelmüller, R. (2014). WRKY transcription factors. *Plant Signaling & Behavior*, *9*, e27700. https://doi.org/10.4161/psb.27700

Balesdent, M., Gall, C., Robin, P., & Rouxel, T. (1992). Intraspecific variation in soluble mycelial protein and esterase patterns of *Leptosphaeria maculans* French isolates. *Mycological Research*, *96*, 677–684. https://doi.org/10.1016/s0953-7562(09)80497-8

Balesdent, M., Attard, A., Ansan-Melayah, D., Delourme, R., Renard, M., & Rouxel, T. T. (2001). Genetic control and host range of avirulence toward *Brassica napus* cultivars Quinta and Jet Neuf in *Leptosphaeria maculans*. *Phytopathology*, *91*, 70–76. https://doi.org/10.1094/phyto.2001.91.1.70

Balesdent, M. H., Attard, A., Kühn, M. L., & Rouxel, T. (2002). New avirulence genes in the phytopathogenic fungus *Leptosphaeria maculans*. *Phytopathology*, *92*, 1122–1133. https://doi.org/10.1094/phyto.2002.92.10.1122

Balesdent, M., Laval, V., Noah, J. M., Bagot, P., Mousseau, A., & Rouxel, T. (2024). Large-scale population survey of *Leptosphaeria maculans* in France highlights both on-going breakdowns and potentially effective resistance genes in oilseed rape. *Pest Management Science, 80*, 2426–2434. https://doi.org/10.1002/ps.7401

Barbetti MJ, Carmody P, Khangura RK, Sweetingham M & Walton G. (2000). *Managing blackleg in 2000.* Perth, WA: Agriculture Western Australia, Bulletin no. 4400.

Barbetti, M. (1975). Late blackleg infections in rape are important. *Australasian Plant Pathology*, *4*(1), 3. https://doi.org/10.1071/app9750003

Barnes, A. P., Wreford, A., Butterworth, M. H., Semenov, M. A., Moran, D., Evans, N., & Fitt, B. D. L. (2010). Adaptation to increasing severity of phoma stem canker on winter oilseed rape in the UK under climate change. *The Journal of Agricultural Science*, *148*, 683–694. https://doi.org/10.1017/s002185961000064x

Bartlett, D. W., Clough, J. M., Godwin, J. R., Hall, A. A., Hamer, M., & Parr-Dobrzanski, B. (2002). The strobilurin fungicides. *Pest Management Science*, *58*, 649–662. https://doi.org/10.1002/ps.520

Bateman, G. L., Landau, S., & Welham, S. J. (1995). Sensitivity to prochloraz in populations of the eyespot fungus, *Pseudocercosporella herpotrichoides*, in relation to fungicide treatments and their efficacy in continuous winter wheat. *Annals of Applied Biology*, *126*, 235–247. https://doi.org/10.1111/j.1744-7348.1995.tb05362.x

Bateman, G. L. (2002). Long-term performance of fungicides applied to control eyespot in winter wheat. *Annals of Applied Biology*, *141*, 29–33. https://doi.org/10.1111/j.1744-7348.2002.tb00192.x

Beckman, C. H. (2000). Phenolic-storing cells: keys to programmed cell death and periderm formation in wilt disease resistance and in general defence responses in plants? *Physiological and Molecular Plant Pathology*, *57*, 101–110. https://doi.org/10.1006/pmpp.2000.0287

Begon, M., Townsend, C. R., & Harper, J. L. (2006). *Ecology: From individuals to ecosystems*. http://ci.nii.ac.jp/ncid/BA72657172

Bellarby, J., Tirado, R., Leip, A., Weiss, F., Lesschen, J. P., & Smith, P. (2012). Livestock greenhouse gas emissions and mitigation potential in Europe. *Global Change Biology*, *19*, 3–18. https://doi.org/10.1111/j.1365-2486.2012.02786.x

Beszterda, M., & Nogala-Kałucka, M. (2019). Current research developments on the processing and improvement of the nutritional quality of rapeseed (*Brassica napus* L.). *European Journal of Lipid Science and Technology*, *121*. https://doi.org/10.1002/ejlt.201800045

Bierman, S. M., Fitt, B. D. L., Van Den Bosch, F., Bateman, G. L., Jenkyn, J. F., & Welham, S. J. (2002). Changes in populations of the eyespot fungi *Tapesia yallundae* and *T. acuformis* under different fungicide regimes in successive crops of winter wheat, 1984–2000. *Plant Pathology*, *51*, 191–201. https://doi.org/10.1046/j.1365-3059.2002.00673.x

Bingol, E., Qi, A., Karandeni-Dewage, C., Ritchie, F., Fitt, B. D. L., & Huang, Y. (2024). Co-inoculation timing affects the interspecific interactions between phoma stem canker pathogens *Leptosphaeria maculans* and *Leptosphaeria biglobosa*. *Pest Management Science*, *80*, 2443–2452. https://doi.org/10.1002/ps.7799

Birkenbihl, R. P., Diezel, C., & Somssich, I. E. (2012). *Arabidopsis* WRKY33 is a key transcriptional regulator of hormonal and metabolic responses toward *Botrytis cinerea* infection. *Plant Pathology*, *159*, 266–285. https://doi.org/10.1104/pp.111.192641

Borhan, M. H., Van De Wouw, A. P., & Larkan, N. J. (2022). Molecular interactions between *Leptosphaeria maculans* and *Brassica* Species. *Annual Review of Phytopathology*, *60*, 237–257. https://doi.org/10.1146/annurev-phyto-021621-120602

Bousset, L., Jumel, S., Garreta, V., Picault, H., & Soubeyrand, S. (2015). Transmission of *Leptosphaeria maculans* from a cropping season to the following one. *Annals of Applied Biology*, *166*, 530–543. https://doi.org/10.1111/aab.12205

Bousset, L., Vallée, P., Delourme, R., Parisey, N., Palerme, M., & Leclerc, M. (2021). Besides stem canker severity, oilseed rape host genotype matters for the production of *Leptosphaeria maculans* fruit bodies. *Fungal Ecology*, *52*, 101076. https://doi.org/10.1016/j.funeco.2021.101076

Boyd, L. A. (2006). Can the durability of resistance be predicted? *Journal of the Science of Food and Agriculture*, *86*, 2523–2526. https://doi.org/10.1002/jsfa.2648

Brachaczek, A., Kaczmarek, J., & Jedryczka, M. (2016). Monitoring blackleg (*Leptosphaeria* spp.) ascospore release timing and quantity enables optimal fungicide application to improved oilseed rape yield and seed quality. *European Journal of Plant Pathology*, *145*, 643–657. https://doi.org/10.1007/s10658-016-0922-x

Brachaczek, A., Kaczmarek, J., & Jedryczka, M. (2021). Warm and wet autumns favour yield losses of oilseed rape caused by phoma stem canker. *Agronomy*, *11*, 1171. https://doi.org/10.3390/agronomy11061171

Brian, P. W., & Hemming, H. G. (1945). Gliotoxin, a fungistatic metabolic product of *Trichoderma viride*. *Annals of Applied Biology*, *32*, 214–220. https://doi.org/10.1111/j.1744-7348.1945.tb06238.x

Brown, D. W., McCormick, S. P., Alexander, N. J., Proctor, R. H., & Desjardins, A. E. (2001). A genetic and biochemical approach to study trichothecene diversity in *Fusarium sporotrichioides* and *Fusarium graminearum*. *Fungal Genetics and Biology*, *32*, 121–133. https://doi.org/10.1006/fgbi.2001.1256

Bruinsma, J., Food and Agriculture Organization of the United Nations, Economic and Social Development Department, Fischer, G., Boedeker, G., Faures, J.-M., Frenken, K., & Hoogeveen, J. (2009). The resource outlook to 2050: By how much do land, water and crop yields need to increase by 2050? *Expert Meeting on How to Feed the World in 2050*. https://www.fao.org/3/ak971e/ak971e.pdf

Brun, H., Chèvre, A., Fitt, B. D., Powers, S., Besnard, A., Ermel, M., Huteau, V., Marquer, B., Eber, F., Renard, M., & Andrivon, D. (2010). Quantitative resistance increases the durability of qualitative resistance to *Leptosphaeria maculans* in *Brassica napus*. *New Phytologist*, *185*, 285–299. https://doi.org/10.1111/j.1469-8137.2009.03049.x

Bürger, M., & Chory, J. (2019). Stressed out about hormones: How plants orchestrate immunity. *Cell Host & Microbe*, *26*, 163–172. https://doi.org/10.1016/j.chom.2019.07.006

Buxdorf, K., Rahat, I., Gafni, A., & Levy, M. (2013). The epiphytic fungus *Pseudozyma aphidis* induces jasmonic Acid- and salicylic Acid/nonexpressor of *PR1*-independent local and systemic resistance. *Plant Physiology*, *161*, 2014–2022. https://doi.org/10.1104/pp.112.212969

Cai, X., Huang, Y., Jiang, D., Fitt, B. D., Li, G., & Yang, L. (2017). Evaluation of oilseed rape seed yield losses caused by *Leptosphaeria biglobosa* in central China. *European Journal of Plant Pathology*, *150*, 179–190. https://doi.org/10.1007/s10658-017-1266-x

Carlsson, A. S., Yilmaz, J. L., Green, A. G., Stymne, S., & Hofvander, P. (2011). Replacing fossil oil with fresh oil – with what and for what? *European Journal of Lipid Science and Technology*, *113*, 812–831. https://doi.org/10.1002/ejlt.201100032

Carré, P., & Pouzet, A. (2014). Rapeseed market, worldwide and in Europe. *OCL*, *21*, D102. https://doi.org/10.1051/ocl/2013054

Carter, H. E., Fraaije, B. A., West, J. S., Kelly, S. L., Mehl, A., Shaw, M. W., & Cools, H. J. (2014). Alterations in the predicted regulatory and coding regions of the sterol 14α-demethylase gene (CYP51) confer decreased azole sensitivity in the oilseed rape pathogen *Pyrenopeziza brassicae*. *Molecular Plant Pathology*, *15*, 513–522. https://doi.org/10.1111/mpp.12106

Chalhoub, B., Denoeud, F., Liu, S., Parkin, I. a. P., Tang, H., Wang, X., Chiquet, J., Belcram, H., Tong, C., Samans, B., Corréa, M., Da Silva, C., Just, J., Falentin, C., Koh, C. S., Clainche, I. L., Bernard, M., Bento, P., Noel, B., Wincker, P. (2014). Early allopolyploid evolution in the post-Neolithic *Brassica napus* oilseed genome. *Science*, *345*, 950–953. https://doi.org/10.1126/science.1253435

Chen, G., Zhang, B., Wu, J., & Shi, C. (2011). Nondestructive assessment of amino acid composition in rapeseed meal based on intact seeds by near-infrared reflectance spectroscopy. *Animal Feed Science and Technology*, *165*, 111–119. https://doi.org/10.1016/j.anifeedsci.2011.02.004

Chin, K. M., & Wolfe, M. S. (1984). Selection on *Erysiphe graminis* in pure and mixed stands of barley. *Plant Pathology*, *33*, 535–546. https://doi.org/10.1111/j.1365-3059.1984.tb02878.x

Cholerton, L. (2015). *Biological control of Leptosphaeria maculans on Brassica napus and quantification of the microbes in planta using qPCR* (PhD Thesis). University of Nottingham.

Chowdhury, S., Basu, A., & Kundu, S. (2017). Biotrophy-necrotrophy switch in pathogen evoke differential response in resistant and susceptible sesame involving multiple signalling pathways at different phases. *Scientific Reports*, *7*. https://doi.org/10.1038/s41598-017-17248-7

Clifford, B. (1985). Barley Leaf Rust. *Elsevier eBooks* (pp. 173–205). https://doi.org/10.1016/b978-0-12-148402-6.50014-6

Cook, R. J., & Baker, K. F. (1983). *The nature and practice of biological control of plant pathogens*.

Cooney, J. M., Lauren, D. R., & Di Menna, M. E. (2001). Impact of competitive fungi on trichothecene production by *Fusarium graminearum*. *Journal of Agricultural and Food Chemistry, 49*, 522–526. https://doi.org/10.1021/jf0006372

Couch, B. C., & Kohn, L. M. (2001). A multilocus gene genealogy concordant with host preference indicates segregation of a new species, *Magnaporthe oryzae*, from *M. grisea*. *Mycologia, 94*, 683–693. https://doi.org/10.1080/15572536.2003.11833196

CropMonitor. Secure.fera.defra.gov.uk. (2022). Retrieved 24 February 2022, from https://secure.fera.defra.gov.uk/cropmonitor/

Curtis, P. J., Greatbanks, D., Hesp, B., Cameron, A. F., & Freer, A. A. (1977). Sirodesmins A, B, C, and G, antiviral epipolythiopiperazine-2,5-diones of fungal origin: X-ray analysis of sirodesmin A diacetate. *Journal of the Chemical Society. Perkin Transactions I/Journal of the Chemical Society. Perkin Transactions. I*, *2*, 180. https://doi.org/10.1039/p19770000180

da Luz, W. C. (1987). Interactions between *Cochliobolus sativus* and *Pyrenophora tritici-repentis* on wheat leaves. *Phytopathology*, *77*, 1355. https://doi.org/10.1094/phyto-77-1355

Dangl, J. L., Horvath, D. M., & Staskawicz, B. J. (2013). Pivoting the plant immune system from dissection to deployment. *Science*, *341*, 746–751. https://doi.org/10.1126/science.1236011

Daverdin, G., Rouxel, T., Gout, L., Aubertot, J., Fudal, I., Meyer, M., Parlange, F., Carpezat, J., & Balesdent, M. (2012). Genome structure and reproductive behaviour influence the evolutionary potential of a fungal phytopathogen. *PLoS Pathogens*, *8*, e1003020. https://doi.org/10.1371/journal.ppat.1003020

Dawidziuk, A., Kasprzyk, I., Kaczmarek, J., & Jędryczka, M. (2010). Pseudothecial maturation and ascospore release of *Leptosphaeria maculans* and *L. biglobosa* in south-east Poland. *Acta Agrobotanica*, *63*, 107–120. https://doi.org/10.5586/aa.2010.013

Dawidziuk, A., Kaczmarek, J., Podlesna, A., Kasprzyk, I., & Jedryczka, M. (2012a). Influence of meteorological parameters on *Leptosphaeria maculans* and *L. biglobosa* spore release in central and eastern Poland. *Grana*, *51*, 240–248. https://doi.org/10.1080/00173134.2011.649016

Dawidziuk, A., Kaczmarek, J., & Jedryczka, M. (2012b). The effect of winter weather conditions on the ability of pseudothecia of *Leptosphaeria maculans* and *L. biglobosa* to release ascospores. *European Journal of Plant Pathology*, *134*, 329–343. https://doi.org/10.1007/s10658-012-9992-6

de Gruyter, J., Woudenberg, J., Aveskamp, M., Verkley, G., Groenewald, J., & Crous, P. (2013). Redisposition of phoma-like anamorphs in *Pleosporales*. *Studies in Mycology*, *75*, 1–36. https://doi.org/10.3114/sim0004

De Silva, N., Lumyong, S., Hyde, K., Bulgakov, T., Phillips, A., Yan, J., & Mycosphere. (2016). Mycosphere Essays 9: Defining biotrophs and hemibiotrophs. *Mycosphere*, *5*, 545–559. https://doi.org/10.5943/mycosphere/7/5/2

Agriculture in the United Kingdom data sets. DEFRA. (2023). Retrieved 22 April 2025, from https://www.gov.uk/government/statistical-data-sets/agriculture-in-the-united-kingdom

Integrated Pest Management (IPM) in farming. GOV.UK. (2024). Retrieved 22 April 2025, from https://www.gov.uk/guidance/integrated-pest-management-ipm-in-farming

Delaye, L., García-Guzmán, G., & Heil, M. (2013). Endophytes versus biotrophic and necrotrophic pathogens—are fungal lifestyles evolutionarily stable traits? *Fungal Diversity*, *60*, 125–135. https://doi.org/10.1007/s13225-013-0240-y

Delourme, R., Chèvre, A. M., Brun, H., Rouxel, T., Balesdent, M. H., Dias, J. S., Salisbury, P., Renard, M., & Rimmer, S. R. (2006). Major gene and polygenic resistance to *Leptosphaeria maculans* in oilseed rape (*Brassica napus*). *Springer eBooks* (pp. 41–52). https://doi.org/10.1007/1-4020-4525-5_4

Deng, Y., Li, J. C., Lyv, X., Xu, J. W., Wu, M. D., Zhang, J., Yang, L., & Li, G. Q. (2023). Large-scale surveys of blackleg of oilseed rape (*Leptosphaeria biglobosa*) revealed new Insights into epidemics of this disease in China. *Plant Disease*, *107*, 1408–1417. https://doi.org/10.1094/pdis-08-22-1765-re

Dennis, C., & Webster, J. (1971). Antagonistic properties of species-groups of *Trichoderma*. *Transactions of the British Mycological Society*, *57*, 25-IN3. https://doi.org/10.1016/s0007-1536(71)80077-3

di Menna, M., Lauren, & Hardacre, A. (1997). *Fusaria* and *Fusarium* toxins in New Zealand maize plants. *Mycopathologia*, *139*, 165–173. https://doi.org/10.1023/a:1006863908275

Dilmaghani, A., Balesdent, M. H., Didier, J. P., Wu, C., Davey, J., Barbetti, M. J., Li, H., Moreno-Rico, O., Phillips, D., Despeghel, J. P., Vincenot, L., Gout, L., & Rouxel, T. (2009). The *Leptosphaeria maculans – Leptosphaeria biglobosa* species complex in the American continent. *Plant Pathology*, *58*, 1044–1058. https://doi.org/10.1111/j.1365-3059.2009.02149.x

Dong, X. (1998). SA, JA, ethylene, and disease resistance in plants. *Current Opinion in Plant Biology*, *1*, 316–323. https://doi.org/10.1016/1369-5266(88)80053-0

Du, R., Huang, Y., Zhang, J., Yang, L., Wu, M., & Li, G. (2021). LAMP Detection and identification of the blackleg pathogen *Leptosphaeria biglobosa* 'brassicae.' *Plant Disease*, *105*, 3192–3200. https://doi.org/10.1094/pdis-08-20-1819-re

Dubois, V., Breton, S., Linder, M., Fanni, J., & Parmentier, M. (2007). Fatty acid profiles of 80 vegetable oils with regard to their nutritional potential. *European Journal of Lipid Science and Technology*, *109*, 710–732. https://doi.org/10.1002/ejlt.200700040

Durrant, W., & Dong, X. (2004). Systemic acquired resistance. *Annual Review of Phytopathology*, *42*, 185–209. https://doi.org/10.1146/annurev.phyto.42.040803.140421

Dutt, A., Anthony, R., Andrivon, D., Jumel, S., Roy, G. L., Baranger, A., Leclerc, M., & May, C. L. (2021a). Competition and facilitation among fungal plant parasites affect their life-history traits. *Oikos*, *130*, 652–667. https://doi.org/10.1111/oik.07747

Dutt, A., Andrivon, D., & May, C. L. (2021b). Multi-infections, competitive interactions, and pathogen coexistence. *Plant Pathology*, *71*, 5–22. https://doi.org/10.1111/ppa.13469

Eckert, M., Maguire, K., Urban, M., Foster, S., Fitt, B., Lucas, J., & Hammond-Kosack, K. (2005). *Agrobacterium tumefaciens*-mediated transformation of *Leptosphaeria* spp. and *Oculimacula* spp. with the reef coral gene DsRed and the jellyfish gene gfp. *FEMS Microbiology Letters*, *253*, 67–74. https://doi.org/10.1016/j.femsle.2005.09.041

Eckert, M. R., Rossall, S., Selley, A., & Fitt, B. D. (2010). Effects of fungicides on *in vitro* spore germination and mycelial growth of the phytopathogens *Leptosphaeria maculans* and *L. biglobosa* (phoma stem canker of oilseed rape). *Pest Management Science*, *66*, 396–405. https://doi.org/10.1002/ps.1890

Scientific Opinion on the safety of “rapeseed protein isolate” as a novel food ingredient. (2013). *EFSA Journal*, *11*. https://doi.org/10.2903/j.efsa.2013.3420

Peer review of the pesticide risk assessment of the active substance *Bacillus amyloliquefaciens* strain MBI 600. (2016). *EFSA Journal*, *14*. https://doi.org/10.2903/j.efsa.2016.4359

Elliott, C. E., Gardiner, D. M., Thomas, G., Cozijnsen, A., Van De Wouw, A., & Howlett, B. J. (2007). Production of the toxin sirodesmin PL by *Leptosphaeria maculans* during infection of *Brassica napus*. *Molecular Plant Pathology*, *8*, 791–802. https://doi.org/10.1111/j.1364-3703.2007.00433.x

Elliott, C. E., Fox, E. M., Jarvis, R. S., & Howlett, B. J. (2011). The cross-pathway control system regulates production of the secondary metabolite toxin, sirodesmin PL, in the ascomycete, *Leptosphaeria maculans*. *BMC Microbiology*, *11*, 169. https://doi.org/10.1186/1471-2180-11-169

EU, 2016/1429 (2016). Commission implementing regulation (EU) 2016/1429 of 26 August 2016 approving the active substance *Bacillus amyloliquefaciens* strain MBI 600, in accordance with Regulation (EC) No 1107/2009 of the European Parliament and of the Council concerning the placing of plant protection products on the market, and amending the Annex to Commission Implementing Regulation (EU) No 540/2011. Retrieved 21 April 2025, from https://eur-lex.europa.eu/eli/reg_impl/2016/1429/oj/eng

Evans, N., Baierl, A., Semenov, M. A., Gladders, P., & Fitt, B. D. (2007). Range and severity of a plant disease increased by global warming. *Journal of the Royal Society Interface*, *5*, 525–531. https://doi.org/10.1098/rsif.2007.1136

Evans, N., Butterworth, M. H., Baierl, A., Semenov, M. A., West, J. S., Barnes, A., Moran, D., & Fitt, B. D. L. (2010). The impact of climate change on disease constraints on production of oilseed rape. *Food Security*, *2*, 143–156. https://doi.org/10.1007/s12571-010-0058-3

FAO. (2023). Retrieved 18 January 2025, from https://www.fao.org/faostat/en/#rankings/countries_by_commodity

FAOSTAT. (2023). Retrieved 18 January 2025, from https://www.fao.org/faostat/en/#compare

Farmer, E. E., Alméras, E., & Krishnamurthy, V. (2003). Jasmonates and related oxylipins in plant responses to pathogenesis and herbivory. *Current Opinion in Plant Biology*, *6*, 372–378. https://doi.org/10.1016/s1369-5266(03)00045-1

Winning returns with Murray – Top oilseed rape on the east/west only recommended list. Farmers Weekly. (2023) Retrieved 21 April 2025, from https://www.fwi.co.uk/arable/winning-returns-with-murray-top-oilseed-rape-on-the-east-west-only-recommended-list

Ferguson, J. J., Stojanovski, E., MacDonald-Wicks, L., & Garg, M. L. (2016). Fat type in phytosterol products influence their cholesterol-lowering potential: A systematic review and meta-analysis of RCTs. *Progress in Lipid Research*, *64*, 16–29. https://doi.org/10.1016/j.plipres.2016.08.002

Fitt, B. D., Huang, Y., Van Den Bosch, F., & West, J. S. (2006a). Coexistence of related pathogen species on arable crops in space and time. *Annual Review of Phytopathology*, *44*, 163–182. https://doi.org/10.1146/annurev.phyto.44.070505.143417

Fitt, B. D. L., Brun, H., Barbetti, M. J., & Rimmer, S. R. (2006b). World-wide importance of phoma stem canker (*Leptosphaeria maculans* and *L. biglobosa*) on oilseed rape (*Brassica napus*). *European Journal of Plant Pathology*, *114*, 3–15. https://doi.org/10.1007/s10658-005-2233-5

Fitt, B. D. L., Hu, B. C., Li, Z. Q., Liu, S. Y., Lange, R. M., Kharbanda, P. D., Butterworth, M. H., & White, R. P. (2008). Strategies to prevent spread of *Leptosphaeria maculans* (phoma stem canker) onto oilseed rape crops in China; costs and benefits. *Plant Pathology*, *57*, 652–664. https://doi.org/10.1111/j.1365-3059.2008.01841.x

Flor, H. (1971). Current status of the gene-for-gene concept. *Annual Review of Phytopathology*, *9*, 275-296. https://doi.org/10.1146/annurev.py.09.090171.001423

Foley, R. C., Kidd, B. N., Hane, J. K., Anderson, J. P., & Singh, K. B. (2016). Reactive oxygen species play a role in the Infection of the necrotrophic fungi, *Rhizoctonia solani* in wheat. *PLoS ONE*, *11*, e0152548. https://doi.org/10.1371/journal.pone.0152548

Fortune, J. A., Qi, A., Ritchie, F., Dewage, C. S. K., Fitt, B. D. L., & Huang, Y. (2021). Effects of cultivar resistance and fungicide application on stem canker of oilseed rape (*Brassica napus*) and potential interseasonal transmission of *Leptosphaeria* spp. inoculum. *Plant Pathology*, *70*, 2115–2124. https://doi.org/10.1111/ppa.13453

Fortune, J. A., Bingol, E., Qi, A., Baker, D., Ritchie, F., Dewage, C. S. K., Fitt, B. D. L., & Huang, Y. (2024). *Leptosphaeria biglobosa* inhibits the production of sirodesmin PL by *L. maculans*. *Pest Management Science*, *80*, 2416–2425. https://doi.org/10.1002/ps.7275

Fortune, J.A. (2022). *Understanding the interactions between phoma stem canker (Leptosphaeria maculans and L. biglobosa) and light leaf spot (Pyrenopeziza brassicae) pathogens of oilseed rape (Brassica napus)*. (PhD thesis). University of Hertfordshire.

Fox, E. M., Gardiner, D. M., Keller, N. P., & Howlett, B. J. (2008). A Zn(II)2Cys6 DNA binding protein regulates the sirodesmin PL biosynthetic gene cluster in *Leptosphaeria maculans*. *Fungal Genetics and Biology*, *45*, 671–682. https://doi.org/10.1016/j.fgb.2007.10.005

Frąc, M., Kaczmarek, J., & Jędryczka, M. (2022). Metabolic capacity differentiates *Plenodomus lingam* from *P. biglobosus* subclade 'brassicae', the causal agents of phoma leaf spotting and stem canker of oilseed rape (*Brassica napus*) in agricultural ecosystems. *Pathogens*, *11*, 50. https://doi.org/10.3390/pathogens11010050

The Fungicide Resistance Action Group (FRAG-UK) | AHDB. (2024). Retrieved 18 January 2025, from https://ahdb.org.uk/knowledge-library/the-fungicide-resistance-action-group-frag-uk

Friedt, W., Tu, J., & Fu, T. (2018). Academic and economic importance of *Brassica napus* rapeseed. In *Compendium of plant genomes* (pp. 1–20). https://doi.org/10.1007/978-3-319-43694-4_1

Safety assessment of rapeseed protein (IsolexxTM). Food Safety Authority of Ireland. FSAI. (2012). Retrieved 18 January 2025, from https://www.fsai.ie/uploadedFiles/Science_and_Health/Novel_Foods/Applications/2012%20Rapeseed%20protein.pdf

Fudal, I., Ross, S., Brun, H., Besnard, A., Ermel, M., Kuhn, M., Balesdent, M., & Rouxel, T. (2009). Repeat-induced point mutation (RIP) as an alternative mechanism of evolution toward virulence in *Leptosphaeria maculans*. *Molecular Plant-Microbe Interactions*, *22*, 932–941. https://doi.org/10.1094/mpmi-22-8-0932

Gardiner, D. M., Cozijnsen, A. J., Wilson, L. M., Pedras, M. S. C., & Howlett, B. J. (2004). The sirodesmin biosynthetic gene cluster of the plant pathogenic fungus *Leptosphaeria maculans*. *Molecular Microbiology*, *53*, 1307–1318. https://doi.org/10.1111/j.1365-2958.2004.04215.x

Gardiner, D. M., Waring, P., & Howlett, B. J. (2005). The epipolythiodioxopiperazine (ETP) class of fungal toxins: distribution, mode of action, functions and biosynthesis. *Microbiology*, *151*, 1021–1032. https://doi.org/10.1099/mic.0.27847-0

Garg, S. (2020). Impact of overpopulation on land use pattern. In *IGI Global eBooks* (pp. 1517–1534). https://doi.org/10.4018/978-1-5225-9621-9.ch069

Garnett, T. (2009). Livestock-related greenhouse gas emissions: impacts and options for policy makers. *Environmental Science & Policy*, *12*, 491–503. https://doi.org/10.1016/j.envsci.2009.01.006

Garthwaite, D.G., Hudson, S., Barker, I., Parrish, G., Smith, L. & Pietravalle, S. (2012). Pesticide usage survey report 250: Arable crops in the United Kingdom 2012. Retrieved 21 April 2025, from https://pusstats.fera.co.uk/published-reports

Garthwaite, D.G., Barker, I., Laybourn, R., Huntly, A., Parrish, G., Huson, S. & Thygesen, H. (2014). Pesticide usage survey report 263: Arable crops in the United Kingdom 2014. Retrieved 21 April 2025, from https://pusstats.fera.co.uk/published-reports

Garthwaite, D.G., Barker, I., Ridley, L., Mace, A., Parrish, G., MacArthur, R. & Lu, Y. (2016). Pesticide usage survey report 271: Arable crops in the United Kingdom 2016. Retrieved 21 April 2025, from https://pusstats.fera.co.uk/published-reports

Garthwaite, D.G., Ridley, L., Mace, A., Parrish, G., Barker, I., Rainford, J. & MacArthur, R. (2018). Pesticide usage survey report 284: Arable crops in the United Kingdom 2018. Retrieved 21 April 2025, from https://pusstats.fera.co.uk/published-reports

Garthwaite, D.G., Ridley, L., Mace, A., Stroda, E., Parrish, G., Rainford, J. & MacArthur, R. (2020). Pesticide usage survey report 295: Arable crops in the United Kingdom 2020. Retrieved 21 April 2025, from https://pusstats.fera.co.uk/published-reports

Garthwaite, D.G., Ridley, L., Parrish, G., Chantry, T., Richmond, A. & MacArthur, R. (2022). Pesticide usage survey report 309: Arable crops in the United Kingdom 2022. Retrieved 21 April 2025, from https://pusstats.fera.co.uk/published-reports

Gasparatos, A., Stromberg, P., & Takeuchi, K. (2011). Biofuels, ecosystem services and human wellbeing: Putting biofuels in the ecosystem services narrative. *Agriculture Ecosystems & Environment*, *142*, 111–128. https://doi.org/10.1016/j.agee.2011.04.020

Gause, G.F. (1934). The struggle for existence. Baltimore The Williams & Wilkins Company

Gay, E. J., Soyer, J. L., Lapalu, N., Linglin, J., Fudal, I., Da Silva, C., Wincker, P., Aury, J., Cruaud, C., Levrel, A., Lemoine, J., Delourme, R., Rouxel, T., & Balesdent, M. (2021). Large-scale transcriptomics to dissect 2 years of the life of a fungal phytopathogen interacting with its host plant. *BMC Biology*, *19*. https://doi.org/10.1186/s12915-021-00989-3

Gay, E. J., Jacques, N., Lapalu, N., Cruaud, C., Laval, V., Balesdent, M., & Rouxel, T. (2023). Location and timing govern tripartite interactions of fungal phytopathogens and host in the stem canker species complex. *BMC Biology*, *21*. https://doi.org/10.1186/s12915-023-01726-8

Gerz, M., Bueno, C. G., Ozinga, W. A., Zobel, M., & Moora, M. (2018). Niche differentiation and expansion of plant species are associated with mycorrhizal symbiosis. *Journal of Ecology*, *106*, 254–264. https://doi.org/10.1111/1365-2745.12873

Ghanbarnia, K., Fernando, W. G. D., & Crow, G. (2011). Comparison of disease severity and incidence at different growth stages of naturally infected canola plants under field conditions by pycnidiospores of *Phoma lingam* as a main source of inoculum. *Canadian Journal of Plant Pathology*, *33*, 355–363. https://doi.org/10.1080/07060661.2011.593189

Ghorbanpour, M., Omidvari, M., Abbaszadeh-Dahaji, P., Omidvar, R., & Kariman, K. (2018). Mechanisms underlying the protective effects of beneficial fungi against plant diseases. *Biological Control*, *117*, 147–157. https://doi.org/10.1016/j.biocontrol.2017.11.006

Gilligan, C. A., & Van Den Bosch, F. (2008). Epidemiological models for invasion and persistence of pathogens. *Annual Review of Phytopathology*, *46*, 385–418. https://doi.org/10.1146/annurev.phyto.45.062806.094357

Gladders, P., & Musa, T. M. (1980). Observations on the epidemiology of *Leptosphaeria maculans* stem canker in winter oilseed rape. *Plant Pathology*, *29*, 28–37. https://doi.org/10.1111/j.1365-3059.1980.tb01134.x

Gladders, P., Roques, S., Moore, A., Smith, J. A., Ritchie, F., Oxley, S. J. P., Torrance, J., Dyer, C. (2009). Practical implications of fungicide performance data from winter oilseed rape. *Aspects of Applied Biology*, *91*, 33–35.

Glazebrook, J. (2005). Contrasting mechanisms of defense against biotrophic and necrotrophic pathogens. *Annual Review of Phytopathology, 43*, 205–227. https://doi.org/10.1146/annurev.phyto.43.040204.135923

Goding, L. A., Downey, R. K., & Finlayson, A. J. (1972). Seed protein amino acid compositions resulting from crosses between two *Brassica campestris* cultivars. *Canadian Journal of Plant Science*, *52*, 63–71. https://doi.org/10.4141/cjps72-008

Görtz, A., Oerke, E., Steiner, U., Waalwijk, C., Vries, I., & Dehne, H. (2008). Biodiversity of *Fusarium* species causing ear rot of maize in Germany. *Cereal Research Communications*, *36*, 617–622. https://doi.org/10.1556/crc.36.2008.suppl.b.51

Goswami, R. S., & Kistler, H. C. (2004). Heading for disaster: *Fusarium graminearum* on cereal crops. *Molecular Plant Pathology*, *5*, 515–525. https://doi.org/10.1111/j.1364-3703.2004.00252.x

Grandaubert, J., Lowe, R. G., Soyer, J. L., Schoch, C. L., Van De Wouw, A. P., Fudal, I., Robbertse, B., Lapalu, N., Links, M. G., Ollivier, B., Linglin, J., Barbe, V., Mangenot, S., Cruaud, C., Borhan, H., Howlett, B. J., Balesdent, M., & Rouxel, T. (2014). Transposable element-assisted evolution and adaptation to host plant within the *Leptosphaeria maculans-Leptosphaeria biglobosa* species complex of fungal pathogens. *BMC Genomics*, *15*, 891. https://doi.org/10.1186/1471-2164-15-891

GraphPad Prism. (2024). Prism 10 for macOS (Version 10.4.1) [Computer software]

Greenberg, J. T., & Yao, N. (2004). The role and regulation of programmed cell death in plant-pathogen interactions. *Cellular Microbiology*, *6*, 201–211. https://doi.org/10.1111/j.1462-5822.2004.00361.x

Grover, J. P. (1997). *Resource competition*. Springer Science & Business Media.

Guo, X., Fernando, W., & Entz, M. (2005). Effects of crop rotation and tillage on blackleg disease of canola. *Canadian Journal of Plant Pathology*, *27*, 53–57. https://doi.org/10.1080/07060660509507193

Gupta, R., McRoberts, R., Yu, Z., Smith, C., Sloan, W., & You, S. (2022). Life cycle assessment of biodiesel production from rapeseed oil: Influence of process parameters and scale. *Bioresource Technology*, *360*, 127532. https://doi.org/10.1016/j.biortech.2022.127532

Haddadi, P., Larkan, N. J., & Borhan, M. H. (2019). Dissecting R gene and host genetic background effect on the *Brassica napus* defense response to *Leptosphaeria maculans*. *Scientific Reports*, *9*. https://doi.org/10.1038/s41598-019-43419-9

Haddadi, P., Larkan, N. J., Van de Wouw, A., Zhang, Y., Neik, T. X., Beynon, E., Bayer, P., Edwards, D., Batley, J., & Borhan, M. H. (2022). *Brassica napus* genes *Rlm4* and *Rlm7*, conferring resistance to *Leptosphaeria maculans*, are alleles of the *Rlm9* wall-associated kinase-like resistance locus. *Plant Biotechnology Journal*, *20*, 1229–1231. https://doi.org/10.1111/pbi.13818

Hammond, K. E., Lewis, B. G., & Musa, T. M. (1985). A systemic pathway in the infection of oilseed rape plants by *Leptosphaeria maculans*. *Plant Pathology*, *34*, 557–565. https://doi.org/10.1111/j.1365-3059.1985.tb01407.x

Hardin, G. (1960). The competitive exclusion principle. *Science*, *131*, 1292–1297. https://doi.org/10.1126/science.131.3409.1292

Heller, J., & Tudzynski, P. (2011). Reactive oxygen species in phytopathogenic fungi: signaling, development, and disease. *Annual Review of Phytopathology*, *49*, 369–390. https://doi.org/10.1146/annurev-phyto-072910-095355

Henchion, M., Hayes, M., Mullen, A., Fenelon, M., & Tiwari, B. (2017). Future protein Supply and demand: Strategies and factors influencing a sustainable equilibrium. *Foods*, *6*, 53. https://doi.org/10.3390/foods6070053

Hoehnel, A., Zannini, E., & Arendt, E. K. (2022). Targeted formulation of plant-based protein-foods: Supporting the food system's transformation in the context of human health, environmental sustainability and consumer trends. *Trends in Food Science & Technology*, *128*, 238–252. https://doi.org/10.1016/j.tifs.2022.08.007

Horbach, R., Navarro-Quesada, A. R., Knogge, W., & Deising, H. B. (2011). When and how to kill a plant cell: Infection strategies of plant pathogenic fungi. *Journal of Plant Physiology*, *168*, 51–62. https://doi.org/10.1016/j.jplph.2010.06.014

Hortal, S., Powell, J. R., Plett, J. M., Simonin, A., & Anderson, I. C. (2016). Intraspecific competition between ectomycorrhizal *Pisolithus microcarpus* isolates impacts plant and fungal performance under elevated CO2 and temperature. *FEMS Microbiology Ecology*, *92*, fiw113. https://doi.org/10.1093/femsec/fiw113

Hosford, R. M. (1976). *Fungal leaf spot diseases of wheat in North Dakota: nature, importance and control*. Fargo: North Dakota Agricultural Experiment Station, North Dakota State University.

Hossain, A., & Davies, P. (2109). Plant oils as fuels for compression ignition engines: A technical review and life-cycle analysis. *Renewable Energy*, *35*, 1–13. https://doi.org/10.1016/j.renene.2009.05.009

Hossard, L., Souchere, V., & Jeuffroy, M. (2018). Effectiveness of field isolation distance, tillage practice, cultivar type and crop rotations in controlling phoma stem canker on oilseed rape. *Agriculture Ecosystems & Environment*, *252*, 30–41. https://doi.org/10.1016/j.agee.2017.10.001

Howlett, B. J., Fox, E. M., Cozijnsen, A. J., Van De Wouw, A. P., & Elliott, C. E. (2009). The secondary metabolite toxin, sirodesmin PL, and its role in virulence of the blackleg fungus. In *Springer eBooks* (pp. 89–95). https://doi.org/10.1007/978-1-4020-8932-9_8

Huang, Y. J., Toscano-underwood, C., Fitt, B. D. L., Todd, A. D., West, J. S., Koopmann, B., & Balesdent, M. H. (2001). Effects of temperature on germination and hyphal growth from ascospores of A-group and B-group *Leptosphaeria maculans* (phoma stem canker of oilseed rape). *Annals of Applied Biology*, *139*, 193–207. https://doi.org/10.1111/j.1744-7348.2001.tb00396.x

Huang, Y. J., Fitt, B. D. L., & Hall, A. M. (2003a). Survival of A-group and B-group *Leptosphaeria maculans* (phoma stem canker) ascospores in air and mycelium on oilseed rape stem debris. *Annals of Applied Biology*, *143*, 359–369. https://doi.org/10.1111/j.1744-7348.2003.tb00305.x

Huang, Y. J., Toscano-Underwood, C., Fitt, B. D. L., Hu, X. J., & Hall, A. M. (2003b). Effects of temperature on ascospore germination and penetration of oilseed rape (*Brassica napus*) leaves by A- or B-group *Leptosphaeria maculans* (phoma stem canker). *Plant Pathology*, *52*, 245–255. https://doi.org/10.1046/j.1365-3059.2003.00813.x

Huang, Y., Fitt, B. D. L., Jedryczka, M., Dakowska, S., West, J. S., Gladders, P., Steed, J. M., & Li, Z. (2005). Patterns of ascospore release in relation to phoma stem canker epidemiology in England (*Leptosphaeria maculans*) and Poland (*Leptosphaeria biglobosa*). *European Journal of Plant Pathology*, *111*, 263–277. https://doi.org/10.1007/s10658-004-4421-0

Huang, Y. J., Li, Z., Evans, N., Rouxel, T., Fitt, B. D. L., & Balesdent, M. (2005). Fitness cost associated with loss of the *AvrLm4* avirulence function in *Leptosphaeria maculans* (phoma stem canker of oilseed rape). *European Journal of Plant Pathology*, *114*, 77–89. https://doi.org/10.1007/s10658-005-2643-4

Huang, Y., Liu, Z., West, J., Todd, A., Hall, A., & Fitt, B. (2007). Effects of temperature and rainfall on date of release of ascospores of *Leptosphaeria maculans* (phoma stem canker) from winter oilseed rape (*Brassica napus*) debris in the UK. *Annals of Applied Biology*, *151*, 99–111. https://doi.org/10.1111/j.1744-7348.2007.00157.x

Huang, Y. J., Pirie, E. J., Evans, N., Delourme, R., King, G. J., & Fitt, B. D. L. (2009). Quantitative resistance to symptomless growth of *Leptosphaeria maculans* (phoma stem canker) in *Brassica napus* (oilseed rape). *Plant Pathology*, *58*, 314–323. https://doi.org/10.1111/j.1365-3059.2008.01957.x

Huang, Y. J., Hood, J. R., Eckert, M. R., Stonard, J. F., Cools, H. J., King, G. J., Rossall, S., Ashworth, M., & Fitt, B. D. L. (2011). Effects of fungicide on growth of *Leptosphaeria maculan*s and *L. biglobosa* in relation to development of phoma stem canker on oilseed rape (*Brassica napus*). *Plant Pathology*, *60*, 607–620. https://doi.org/10.1111/j.1365-3059.2010.02416.x

Huang, Y. J., Karandeni-Dewage, C. S., Fitt, B. D. L. (2014b). Importance of *Leptosphaeria biglobosa* as a cause of phoma stem canker on winter oilseed rape in the UK. *Aspects of Applied Biology, 127*, 117-122. https://uhra.herts.ac.uk/id/eprint/15285/1/HUANGAABPub2014.pdf

Huang, Y. J., Jestin, C., Welham, S. J., King, G. J., Manzanares-Dauleux, M. M., Fitt, B. D. L., & Delourme, R. (2016). Identification of environmentally stable QTL for resistance against *Leptosphaeria maculans* in oilseed rape (*Brassica napus*). *Theoretical and Applied Genetics*, *129*, 169–180. https://doi.org/10.1007/s00122-015-2620-z

Huang, Y., Mitrousia, G. K., Sidique, S. N. M., Qi, A., & Fitt, B. D. L. (2018). Combining R gene and quantitative resistance increases effectiveness of cultivar resistance against *Leptosphaeria maculans* in *Brassica napus* in different environments. *PLoS ONE*, *13*, e0197752. https://doi.org/10.1371/journal.pone.0197752

Huang, Y. J., Karandeni-Dewage, C. S., Fitt, B. D. L. (2021). Current understanding of phoma stem canker and light leaf spot on oilseed rape in the UK. In *Management of Diseases and Pests of Oilseed Rape* (p. 1). University of Hertfordshire; AgriFood Charities Partnership. Retrieved 19 April 2022, from https://www.youtube.com/watch?v=GwmkAUX9JV0

Huang, Y. J. (2002). *Comparative biology and epidemiology of A-group and B-group Leptosphaeria maculans on winter oilseed rape*. (PhD thesis). University of Hertfordshire.

Hutchinson, G. E. (1957). Concluding Remarks. *Cold Spring Harbor Symposia on Quantitative Biology*, *22*, 415–427. https://doi.org/10.1101/sqb.1957.022.01.039

Idnurm, A., McCallum, A. J., & Van De Wouw, A. P. (2024). No safe haven: Loss of avirulence in the plant pathogen *Leptosphaeria maculans* by DNA duplication and repeat-induced point mutation. *Plant Pathology*, *73*, 1127–1135. https://doi.org/10.1111/ppa.13889

Inglis, P. W., De Castro R Pappas, M., Resende, L. V., & Grattapaglia, D. (2018). Fast and inexpensive protocols for consistent extraction of high quality DNA and RNA from challenging plant and fungal samples for high-throughput SNP genotyping and sequencing applications. *PLoS ONE*, *13*, e0206085. https://doi.org/10.1371/journal.pone.0206085

Ivanova, P., Kalaydzhiev, H., Rustad, T., Silva, C., & Chalova, V. (2017). Comparative biochemical profile of protein-rich products obtained from industrial rapeseed meal. *Emirates Journal of Food and Agriculture*, *29*, 170. https://doi.org/10.9755/ejfa.2016-11-1760

Javaid, A., Gajula, L., & Huang, Y. (2021). Regional differences in the proportions of *Leptosphaeria maculans* and *L. biglobosa* (the cause of phoma stem canker on oilseed rape) in Eastern England. In Management of Diseases and Pests of Oilseed Rape (p. 28). University of Hertfordshire; AgriFood Charities Partnership. Retrieved 19 April 2022, from https://www.youtube.com/watch?v=GwmkAUX9JV0

Javaid, A. (2019). *Importance of Leptosphaeria maculans and L. biglobosa in causing phoma stem canker on winter oilseed rape in England*. (PhD thesis). University of Hertfordshire.

Jensen, D. F., Karlsson, M., Sarrocco, S., & Vannacci, G. (2016). Biological control ssing microorganisms as an alternative to disease resistance. *Plant Pathogen Resistance Biotechnology*, 341–363. https://doi.org/10.1002/9781118867716.ch18

Johnson, R. D., & Lewis, B. G. (1994). Variation in host range, systemic infection and epidemiology of *Leptosphaeria maculans*. *Plant Pathology*, *43*, 269–277. https://doi.org/10.1111/j.1365-3059.1994.tb02685.x

Jones, J. D. G., & Dangl, J. L. (2006). The plant immune system. *Nature*, *444*, 323–329. https://doi.org/10.1038/nature05286

Kaczmarek, J., Jędryczka, M., Fitt, B. D. L., Lucas, J. A., & Latunde-Dada, A. O. (2009). Analyses of air samples for ascospores of *Leptosphaeria maculans* and *L. biglobosa* by light microscopy and molecular techniques. *Journal of Applied Genetics*, *50*, 411–419. https://doi.org/10.1007/bf03195702

Karvonen, H., Tapola, N., Uusitupa, M., & Sarkkinen, E. (2002). The effect of vegetable oil-based cheese on serum total and lipoprotein lipids. *European Journal of Clinical Nutrition*, *56*, 1094–1101. https://doi.org/10.1038/sj.ejcn.1601452

Kemen, E., & Jones, J. D. (2012). Obligate biotroph parasitism: can we link genomes to lifestyles? *Trends in Plant Science*, *17*, 448–457. https://doi.org/10.1016/j.tplants.2012.04.005

Kemen, A. C., Agler, M. T., & Kemen, E. (2015). Host–microbe and microbe–microbe interactions in the evolution of obligate plant parasitism. *New Phytologist*, *206*, 1207–1228. https://doi.org/10.1111/nph.13284

Khan, R. a. A., Najeeb, S., Hussain, S., Xie, B., & Li, Y. (2020). Bioactive secondary metabolites from *Trichoderma* spp. against phytopathogenic fungi. *Microorganisms*, *8*, 817. https://doi.org/10.3390/microorganisms8060817

Kharbanda, P. D., Yang, J., Beatty, P., Jensen, S. & Tewari, J. P. (1999). Biocontrol of *Leptosphaeria maculans* and other pathogens of canola with *Paenibacillus polymyxa PKB1*. in *Proceedings of the 10th International Rapeseed Congress. Canberra, Australia. http://www. regional. org. au/au/gcirc*.

King, K. M., & West, J. S. (2022). Detection of the Phoma pathogens *Plenodomus biglobosus* subclades 'brassicae' and 'canadensis' on wasabi, and 'canadensis' in Europe. *European Journal of Plant Pathology*, *162*, 751–756. https://doi.org/10.1007/s10658-021-02428-z

King, K. M., Bucur, D. E., Ritchie, F., Hawkins, N. J., Kaczmarek, A. M., Duan, Y., Kildea, S., West, J. S., & Fraaije, B. A. (2021). Fungicide resistance status and chemical control options for the brassica pathogen *Pyrenopeziza brassicae*. *Plant Pathology*, *70*, 2086–2103. https://doi.org/10.1111/ppa.13441

King, K. M., Barr, L., Bousquet, L., Glaab, A., Canning, G., Ritchie, F., Kildea, S., Fraaije, B. A., & West, J. S. (2024). Evolution of decreased sensitivity to azole fungicides in western European populations of *Plenodomus lingam* (Phoma stem canker on oilseed rape). *Plant Pathology*, *73*, 1517–1532. https://doi.org/10.1111/ppa.13897

King, K. M., González-Rodríguez, L. M., Kaczmarek, J., Jędryczka, M., & West, J. S. (2025). Decreased DMI sensitivity of *Plenodomus biglobosus* (phoma of oilseed rape) associated with CYP51 substitution G476S. *Pest Management Science*. https://doi.org/10.1002/ps.8926

Koch, E., Badawy, H. M. A., & Hoppe, H. H. (1989). Differences between aggressive and non-aggressive single spore lines of *Leptosphaeria maculans* in cultural characteristics and phytotoxin production. *Journal of Phytopathology*, *124*, 52–62. https://doi.org/10.1111/j.1439-0434.1989.tb04894.x

Koeck, M., Hardham, A. R., & Dodds, P. N. (2012). The role of effectors of biotrophic and hemibiotrophic fungi in infection. *Cellular Microbiology*, *13*, 1849–1857. https://doi.org/10.1111/j.1462-5822.2011.01665.x

Koh, J. C. O., Barbulescu, D. M., Norton, S., Redden, B., Salisbury, P. A., Kaur, S., Cogan, N., & Slater, A. T. (2017). A multiplex PCR for rapid identification of *Brassica* species in the triangle of U. *Plant Methods*, *13*. https://doi.org/10.1186/s13007-017-0200-8

Köhl, J., Kolnaar, R., & Ravensberg, W. J. (2019). Mode of action of microbial biological control agents against plant diseases: relevance beyond efficacy. *Frontiers in Plant Science*, *10*. https://doi.org/10.3389/fpls.2019.00845

Kremer, A., & Li, S. (2010). A tyrosine *O*-prenyltransferase catalyses the first pathway-specific step in the biosynthesis of sirodesmin PL. *Microbiology*, *156*, 278–286. https://doi.org/10.1099/mic.0.033886-0

Kumar, M., Tomar, M., Punia, S., Dhakane-Lad, J., Dhumal, S., Changan, S., Senapathy, M., Berwal, M. K., Sampathrajan, V., Sayed, A. A., Chandran, D., Pandiselvam, R., Rais, N., Mahato, D. K., Udikeri, S. S., Satankar, V., Anitha, T., Reetu, N., Radha, N., Kennedy, J. F. (2022). Plant-based proteins and their multifaceted industrial applications. *LWT*, *154*, 112620. https://doi.org/10.1016/j.lwt.2021.112620

Kwon-Chung, K. J., & Sugui, J. A. (2009). What do we know about the role of gliotoxin in the pathobiology of *Aspergillus fumigatus*? *Medical Mycology*, *47*, S97–S103. https://doi.org/10.1080/13693780802056012

Lacey, M., & West, J. (2006). *The air spora: A manual for catching and identifying airborne biological particles* (1st ed., pp. 1-156). Springer.

Laluk, K., & Mengiste, T. (2010). Necrotroph attacks on plants: Wanton destruction or covert Eetortion? *The Arabidopsis Book*, *8*, e0136. https://doi.org/10.1199/tab.0136

Larkan, N. J., Ma, L., & Borhan, M. H. (2015). The *Brassica napus* receptor-like protein *Rlm2* is encoded by a second allele of the *LepR3/Rlm2* blackleg resistance locus. *Plant Biotechnology Journal*, *13*, 983–992. https://doi.org/10.1111/pbi.12341

Larkan, N. J., Ma, L., Haddadi, P., Buchwaldt, M., Parkin, I. A., Djavaheri, M., & Borhan, M. H. (2020). The *Brassica napus* wall-associated kinase-like (WAKL) gene *Rlm9* provides race-specific blackleg resistance. *The Plant Journal*, *104*, 892–900. https://doi.org/10.1111/tpj.14966

Latijnhouwers, M., De Wit, P. J., & Govers, F. (2003). Oomycetes and fungi: similar weaponry to attack plants. *Trends in Microbiology*, *11*, 462–469. https://doi.org/10.1016/j.tim.2003.08.002

Lauren, D. R., & Di Menna, M. E. (1999). *Fusaria* and *Fusarium* mycotoxins in leaves and ears of maize plants 2. A time course study made in the Waikato region, New Zealand, in 1997. *New Zealand Journal of Crop and Horticultural Science*, *27*, 215–223. https://doi.org/10.1080/01140671.1999.9514099

Leadbeater, A. (2015). Recent developments and challenges in chemical disease control - a review. *Plant Protection Science*, *51*, 163–169. https://doi.org/10.17221/83/2015-pps

Lee, S., & Rose, J. K. (2010). Mediation of the transition from biotrophy to necrotrophy in hemibiotrophic plant pathogens by secreted effector proteins. *Plant Signaling & Behavior*, *5*, 769–772. https://doi.org/10.4161/psb.5.6.11778

Lee, H., Chawla, H. S., Obermeier, C., Dreyer, F., Abbadi, A., & Snowdon, R. (2020). Chromosome-scale assembly of winter oilseed rape *Brassica napus*. *Frontiers in Plant Science*, *11*. https://doi.org/10.3389/fpls.2020.00496

Levine, J. M., & HilleRisLambers, J. (2009). The importance of niches for the maintenance of species diversity. *Nature*, *461*, 254–257. https://doi.org/10.1038/nature08251

Li, J., Brader, G., & Palva, E. T. (2004). The WRKY70 transcription factor: a node of convergence for jasmonate-mediated and salicylate-mediated signals in plant defense. *The Plant Cell*, *16*, 319–331. https://doi.org/10.1105/tpc.016980

Li, H., Smyth, F., Barbetti, M., & Sivasithamparam, K. (2006). Relationship between *Brassica napus* seedling and adult plant responses to *Leptosphaeria maculans* is determined by plant growth stage at inoculation and temperature regime. *Field Crops Research*, *96*, 428–437. https://doi.org/10.1016/j.fcr.2005.08.006

Li, N., Han, X., Feng, D., Yuan, D., & Huang, L. (2019). Signaling srosstalk between salicylic acid and ethylene/jasmonate in plant defense: Do We Understand What They Are Whispering? *International Journal of Molecular Sciences*, *20*, 671. https://doi.org/10.3390/ijms20030671

Liu, S. Y., Liu, Z., Fitt, B. D. L., Evans, N., Foster, S. J., Huang, Y. J., Latunde-Dada, A. O., & Lucas, J. A. (2006). Resistance to *Leptosphaeria maculans* (phoma stem canker) in *Brassica napus* (oilseed rape) induced by *L. biglobosa* and chemical defence activators in field and controlled environments. *Plant Pathology*, *55*, 401–412. https://doi.org/10.1111/j.1365-3059.2006.01354.x

Liu, S., Liu, R., Latunde-Dada, A. O., Cools, H. J., Foster, S. J., Huang, Y., & Fitt, B. D. L. (2007). Comparison of *Leptosphaeria biglobosa*-induced and chemically induced systemic resistance to *L. maculans* in *Brassica napus*. *Chinese Science Bulletin*, *52*, 1053–1062. https://doi.org/10.1007/s11434-007-0181-5

Livak, K. J., & Schmittgen, T. D. (2001). Analysis of relative gene expression data using real-time quantitative PCR and the 2−ΔΔCT method. *Methods*, *25*, 402–408. https://doi.org/10.1006/meth.2001.1262

Lô-Pelzer, E., Aubertot, J. N., David, O., Jeuffroy, M. H., & Bousset, L. (2009). Relationship between severity of blackleg (*Leptosphaeria maculans/L. biglobosa* species complex) and subsequent primary inoculum production on oilseed rape stubble. *Plant Pathology*, *58*, 61–70. https://doi.org/10.1111/j.1365-3059.2008.01931.x

Lowe, R. G. T., Cassin, A., Grandaubert, J., Clark, B. L., Van De Wouw, A. P., Rouxel, T., & Howlett, B. J. (2014). Genomes and transcriptomes of partners in plant-fungal-interactions between canola (*Brassica napus*) and two *Leptosphaeria* species. *PLoS ONE*, *9*, e103098. https://doi.org/10.1371/journal.pone.0103098

Lupetti, A., Danesi, R., Campa, M., Del Tacca, M., & Kelly, S. L. (2002). Molecular basis of resistance to azole antifungals. *Trends in Molecular Medicine*, *8*, 76–81. https://doi.org/10.1016/s1471-4914(02)02280-3

Levins, R. M. a. R. (1967). The limiting similarity, convergence, and divergence of coexisting species. *The American Naturalist*, *101*, 377–385. https://www.jstor.org/stable/2459090

MacArthur, R. H. (1984). *Geographical ecology: Patterns in the Distribution of Species*.

Mahuku, G., Hall, R., & Goodwin, P. (1996). Co-infection and induction of systemic acquired resistance by weakly and highly virulent isolates of *Leptosphaeria maculans* in oilseed rape. *Physiological And Molecular Plant Pathology*, *49*, 61-72. https://doi.org/10.1006/pmpp.1996.0039

Malamy, J., & Klessig, D. F. (1992). Salicylic acid and plant disease resistance. *The Plant Journal*, *2*, 643–654. https://doi.org/10.1111/j.1365-313x.1992.tb00133.x

Mapuranga, J., Zhang, N., Zhang, L., Chang, J., & Yang, W. (2022). Infection strategies and pathogenicity of biotrophic plant fungal pathogens. *Frontiers in Microbiology*, *13*. https://doi.org/10.3389/fmicb.2022.799396

Mayer, A. M., Staples, R. C., & Gil-Ad, N. L. (2001). Mechanisms of survival of necrotrophic fungal plant pathogens in hosts expressing the hypersensitive response. *Phytochemistry*, *58*, 33–41. https://doi.org/10.1016/s0031-9422(01)00187-x

Mendes-Pereira, E., Balesdent, M., Brun, H., & Rouxel, T. (2003). Molecular phylogeny of the *Leptosphaeria maculans-L. biglobosa* species complex. *Mycological Research*, *107*, 1287–1304. https://doi.org/10.1017/s0953756203008554

Mendgen, K., & Hahn, M. (2002). Plant infection and the establishment of fungal biotrophy. *Trends in Plant Science*, *7*, 352–356. https://doi.org/10.1016/s1360-1385(02)02297-5

Mercier, J., & Reeleder, R. D. (1987). Interactions between *Sclerotinia sclerotiorum* and other fungi on the phylloplane of lettuce. *Canadian Journal of Botany*, *65*, 1633–1637. https://doi.org/10.1139/b87-223

Mideo, N. (2009). Parasite adaptations to within-host competition. *Trends in Parasitology*, *25*, 261–268. https://doi.org/10.1016/j.pt.2009.03.001

Mierziak, J., Kostyn, K., & Kulma, A. (2014). Flavonoids as important molecules of plant interactions with the environment. *Molecules*, *19*, 16240–16265. https://doi.org/10.3390/molecules191016240

Mitrousia, G. K., Huang, Y. J., Qi, A., Sidique, S. N. M., & Fitt, B. D. L. (2018). Effectiveness of *Rlm7* resistance against *Leptosphaeria maculans* (phoma stem canker) in UK winter oilseed rape cultivars. *Plant Pathology*, *67*, 1339–1353. https://doi.org/10.1111/ppa.12845

Mousa, W. K., Schwan, A., Davidson, J., Strange, P., Liu, H., Zhou, T., Auzanneau, F., & Raizada, M. N. (2015). An endophytic fungus isolated from finger millet (*Eleusine coracan*a) produces anti-fungal natural products. *Frontiers in Microbiology*, *6*. https://doi.org/10.3389/fmicb.2015.01157

Muszewska, A., Steczkiewicz, K., Stepniewska-Dziubinska, M., & Ginalski, K. (2019). Transposable elements contribute to fungal genes and impact fungal lifestyle. *Scientific Reports*, *9*. https://doi.org/10.1038/s41598-019-40965-0

Naczk, M., Diosady, L. L., & Rubin, L. J. (1985). Functional properties of canola meals produced by a two-phase solvent extraction system. *Journal of Food Science*, *50*, 1685–1688. https://doi.org/10.1111/j.1365-2621.1985.tb10565.x

Nagaharu U. (1935). Genome analysis in *Brassica* with special reference to the experimental formation of *B. napus* and peculiar mode of fertilization. *Japanese Journal of Botany, 7*, 389-452.

Nega, T., Woldes, Y. (2018). Review on nutritional limitations and opportunities of using rapeseed meal and other rape seed by - products in animal feeding. *Journal of Nutritional Health & Food Engineering*, *8*. https://doi.org/10.15406/jnhfe.2018.08.00254

Neik, T. X., Ghanbarnia, K., Ollivier, B., Scheben, A., Severn-Ellis, A., Larkan, N. J., Haddadi, P., Fernando, D. W. G., Rouxel, T., Batley, J., Borhan, H. M., & Balesdent, M. (2022). Two independent approaches converge to the cloning of a new *Leptosphaeria maculans* avirulence effector gene, *AvrLmS-Lep2*. *Molecular Plant Pathology*, *23*, 733–748. https://doi.org/10.1111/mpp.13194

Newbery, F., Qi, A., & Fitt, B. D. (2016). Modelling impacts of climate change on arable crop diseases: progress, challenges and applications. *Current Opinion in Plant Biology*, *32*, 101–109. https://doi.org/10.1016/j.pbi.2016.07.002

Newkirk, R. (2011). Meal nutrient composition. In *Elsevier eBooks* (pp. 229–244). https://doi.org/10.1016/b978-0-9818936-5-5.50012-7

Newlands, N. K. (2018). Model-based forecasting of agricultural crop disease risk at the regional scale, integrating airborne inoculum, environmental, and satellite-based monitoring data. *Frontiers in Environmental Science*, *6*. https://doi.org/10.3389/fenvs.2018.00063

Newman, T. E., Kim, H., Khentry, Y., Sohn, K. H., Derbyshire, M. C., & Kamphuis, L. G. (2023). The broad host range pathogen *Sclerotinia sclerotiorum* produces multiple effector proteins that induce host cell death intracellularly. *Molecular Plant Pathology*, *24*, 866–881. https://doi.org/10.1111/mpp.13333

Newton, A. C., Fitt, B. D., Atkins, S. D., Walters, D. R., & Daniell, T. J. (2010). Pathogenesis, parasitism and mutualism in the trophic space of microbe–plant interactions. *Trends in Microbiology*, *18*, 365–373. https://doi.org/10.1016/j.tim.2010.06.002

Genetic improvements to oilseed rape varieties bring improved resistance to phoma, light leaf spot and Verticillium. NPZ UK. (2023). Retrieved 21 April 2025, from https://npz-uk.com/2023/08/04/genetic-improvements-to-oilseed-rape-varieties-bring-improved-resistance-to-phoma-light-leaf-spot-and-verticillium/

Ogle, Helen, and Dale, Michele (1997). *Disease management: cultural practices*. In: Brown, J.F., and Ogle, H.J., (eds.) Plant Pathogens and Plant Diseases. Rockvale Publications, Armidale, NSW, Australia, pp. 390-404.

Ohm, R. A., Feau, N., Henrissat, B., Schoch, C. L., Horwitz, B. A., Barry, K. W., Condon, B. J., Copeland, A. C., Dhillon, B., Glaser, F., Hesse, C. N., Kosti, I., LaButti, K., Lindquist, E. A., Lucas, S., Salamov, A. A., Bradshaw, R. E., Ciuffetti, L., Hamelin, R. C., Grigoriev, I. V. (2012). Diverse lifestyles and strategies of plant pathogenesis encoded in the genomes of eighteen *Dothideomycetes* fungi. *PLoS Pathogens*, *8*, e1003037. https://doi.org/10.1371/journal.ppat.1003037

Oliva, R., Win, J., Raffaele, S., Boutemy, L., Bozkurt, T. O., Chaparro-Garcia, A., Segretin, M. E., Stam, R., Schornack, S., Cano, L. M., Van Damme, M., Huitema, E., Thines, M., Banfield, M. J., & Kamoun, S. (2010). Recent developments in effector biology of filamentous plant pathogens. *Cellular Microbiology*, *12*, 705–715. https://doi.org/10.1111/j.1462-5822.2010.01471.x

Oliver, R. P., & Beckerman, J. L. (2022). The fungicide industry. In *CABI eBooks* (pp. 20–29). https://doi.org/10.1079/9781789246926.0003

Oliver, R. P., & Ipcho, S. V. S. (2004). *Arabidopsis* pathology breathes new life into the necrotrophs-vs.-biotrophs classification of fungal pathogens. *Molecular Plant Pathology*, *5*, 347–352. https://doi.org/10.1111/j.1364-3703.2004.00228.x

Orlovius, K. & Kirkby, E. A. (2003). Oilseed rape: fertilizing for high yield and quality. International Potash Institute. Basel: Switzerland, 1-125.

Ortega-Ramos, P. A., Coston, D. J., Seimandi-Corda, G., Mauchline, A. L., & Cook, S. M. (2021). Integrated pest management strategies for cabbage stem flea beetle (*Psylliodes chrysocephala*) in oilseed rape. *GCB Bioenergy*, *14*, 267–286. https://doi.org/10.1111/gcbb.12918

Padmathilake, K. R. E., & Fernando, W. G. D. (2022a). *Leptosphaeria maculans-Brassica napus* battle: a comparison of incompatible vs. compatible interactions using dual RNASeq. *International Journal of Molecular Sciences, 23*, 3964. https://doi.org/10.3390/ijms23073964

Padmathilake, K. R. E., & Fernando, W. G. D. (2022b). Less virulent *Leptosphaeria biglobosa* immunizes the canola plant to resist highly virulent *L. maculans*, the blackleg pathogen. *Plants*, *11*, 996. https://doi.org/10.3390/plants11070996

Pande, S., & Gahane, S. (2024). Waste cooking oil to biodiesel - a review. *Bentham Science Publishers eBooks*, 308–339. https://doi.org/10.2174/9789815196740124060012

Pandey, S. P., & Somssich, I. E. (2009). The Role of WRKY transcription factors in plant immunity. *Plant Phytsiology*, *150*, 1648–1655. https://doi.org/10.1104/pp.109.138990

Patil, J. R., Mhatre, K. J., Yadav, K., Yadav, L. S., Srivastava, S., & Nikalje, G. C. (2024). Flavonoids in plant-environment interactions and stress responses. *Discover Plants.*, *1*. https://doi.org/10.1007/s44372-024-00063-6

Pedras, M. S. C., & Biesenthal, C. J. (1998). Production of the host-selective phytotoxin phomalide by isolates of *Leptosphaeria maculans* and its correlation with sirodesmin PL production. *Canadian Journal of Microbiology*, *44*, 547–553. https://doi.org/10.1139/w98-034

Pedras, M. C., & Séguin-Swartz, G. (1990). Rapid high-performance liquid chromatographic analysis of phytotoxins from *Phoma lingam*. *Journal of Chromatography A*, *519*, 383–386. https://doi.org/10.1016/0021-9673(90)85168-u

Pedras, M. S. C., & Yu, Y. (2009). Phytotoxins, elicitors and other secondary metabolites from phytopathogenic “blackleg” fungi: structure, phytotoxicity and biosynthesis. *Natural Product Communications*, *4*. https://doi.org/10.1177/1934578x0900400927

Pedras, M. S. C., Chumala, P. B., & Yu, Y. (2007). The phytopathogenic *fungi Leptosphaeria maculan*s and *Leptosphaeria biglobosa*: chemotaxonomical characterization of isolates and metabolite production in different culture media. *Canadian Journal of Microbiology*, *53*, 364–371. https://doi.org/10.1139/w06-133

Penninckx, I., M. A., Thomma, B. P. H. J., Buchala, A., Métraux, J., & Broekaert, W. F. (1998). Concomitant activation of jasmonate and ethylene response pathways is required for induction of a plant defensin gene in *Arabidopsis*. *The Plant Cell*, *10*, 2103–2113. https://doi.org/10.1105/tpc.10.12.2103

Petrie G.A. (1994) Effects of temperature and moisture on the number, size and septation of ascospores produced by *Leptosphaeria maculans* (blackleg) on rapeseed stubble. *Canadian Plant Disease Survey*, *74*, 141–151

Petrie G.A. (1995) Patterns of ascospore discharge by *Leptosphaeria maculans* (blackleg) from 9- to 13-month-old naturally infected rapeseed/canola stubble from 1977 to 1993 in Saskatchwan. *Canadian Plant Disease Survey, 75*, 35–43

Pieterse, C. M., Zamioudis, C., Berendsen, R. L., Weller, D. M., Van Wees, S. C., & Bakker, P. A. (2014). Induced systemic resistance by beneficial microbes. *Annual Review of Phytopathology*, *52*, 347–375. https://doi.org/10.1146/annurev-phyto-082712-102340

Pilet, M. L., Delourme, R., Foisset, N., & Renard, M. (1998). Identification of loci contributing to quantitative field resistance to blackleg disease, causal agent *Leptosphaeria maculans* (Desm.) Ces. et de Not., in Winter rapeseed (*Brassica napus* L.). *Theoretical and Applied Genetics*, *96*, 23–30. https://doi.org/10.1007/s001220050704

Pink, D., & Puddephat, I. (1999). Deployment of disease resistance genes by plant transformation – a 'mix and match' approach. *Trends in Plant Science*, *4*, 71–75. https://doi.org/10.1016/s1360-1385(98)01372-7

Pombo, M. A., Rosli, H. G., Maiale, S., Elliott, C., Stieben, M. E., Romero, F. M., Garriz, A., Ruiz, O. A., Idnurm, A., & Rossi, F. R. (2024). Unveiling the virulence mechanism of *Leptosphaeria maculans* in the *Brassica napus* interaction: the key role of sirodesmin PL in cell death induction. *Journal of Experimental Botany*. https://doi.org/10.1093/jxb/erae498

Pratt-Hyatt, M. (2020). Mycotoxin exposure. In *Elsevier eBooks* (pp. 1026-1034.e3). https://doi.org/10.1016/b978-0-323-43044-9.00138-2

Précigout, P., Claessen, D., Makowski, D., & Robert, C. (2020). Does the latent period of leaf fungal pathogens reflect their trophic type? a meta-analysis of biotrophs, hemibiotrophs, and necrotrophs. *Phytopathology*, *110*, 345–361. https://doi.org/10.1094/phyto-04-19-0144-r

Price, C. L., Parker, J. E., Warrilow, A. G., Kelly, D. E., & Kelly, S. L. (2015). Azole fungicides - understanding resistance mechanisms in agricultural fungal pathogens. *Pest Management Science*, *71*, 1054–1058. https://doi.org/10.1002/ps.4029

Kim, S., Chen, J., Cheng, T., Gindulyte, A., He, J., He, S., Li, Q., Shoemaker, B. A., Thiessen, P. A., Yu, B., Zaslavsky, L., Zhang, J., & Bolton, E. E. (2025). PubChem 2025 update. *Nucleic Acids Res., 53*, D1516–D1525. https://doi.org/10.1093/nar/gkae1059

Raboanatahiry, N., Li, H., Yu, L., & Li, M. (2021). Rapeseed (*Brassica napus*): Processing, utilization, and genetic improvement. *Agronomy*, *11*, 1776. https://doi.org/10.3390/agronomy11091776

Read, A. F., & Taylor, L. H. (2001). The ecology of genetically diverse infections. *Science*, *292*(5519), 1099–1102. https://doi.org/10.1126/science.1059410

Rodrigues, I. M., Carvalho, M. G. V., & Rocha, J. M. (2016). Increase of protein extraction yield from rapeseed meal through a pretreatment with phytase. *Journal of the Science of Food and Agriculture*, *97*, 2641–2646. https://doi.org/10.1002/jsfa.8087

Round, P. A., & Wheeler, B. E. J. (1978). Interactions of *Puccinia hordei* and *Erysiphe graminis* on seedling barley. *Annals of Applied Biology*, *89*, 21–35. https://doi.org/10.1111/j.1744-7348.1978.tb02563.x

Rouxel, T., & Balesdent, M. (2017). Life, death and rebirth of avirulence effectors in a fungal pathogen of *Brassica* crops, *Leptosphaeria maculans*. *New Phytologist*, *214*, 526–532. https://doi.org/10.1111/nph.14411

Rouxel, T., Chupeau, Y., Fritz, R., Kollmann, A., & Bousquet, J. (1988). Biological effects of sirodesmin PL, a phytotoxin produced by *Leptosphaeria maculans*. *Plant Science*, *57*, 45–53. https://doi.org/10.1016/0168-9452(88)90140-9

Rouxel, T., Willner, E., Coudard, L., & Balesdent, M. (2003a). Screening and identification of resistance to *Leptosphaeria maculans* (stem canker) in *Brassica napus* accessions. *Euphytica*, *133*, 219–231. https://doi.org/10.1023/a:1025597622490

Rouxel, T., Penaud, A., Pinochet, X., Brun, H., Gout, L., Delourme, R., Schmit, J., & Balesdent, M. (2003b). A 10-year survey of populations of *Leptosphaeria maculans* in France indicates a rapid adaptation towards the *Rlm1* resistance gene of oilseed rape. *European Journal of Plant Pathology*, *109*, 871–881. https://doi.org/10.1023/a:1026189225466

Rupnik, R., Kukar, M., Vračar, P., Košir, D., Pevec, D., & Bosnić, Z. (2018). AgroDSS: A decision support system for agriculture and farming. *Computers and Electronics in Agriculture*, *161*, 260–271. https://doi.org/10.1016/j.compag.2018.04.001

Sadava, D., Hillis, D. ., Heller, H. and Berenbaum, M. (2012). Life: The science of biology (10th ed.). Sinauer Associates.

Sahu, S. K., Thangaraj, M., & Kathiresan, K. (2012). DNA extraction protocol for plants with high levels of secondary metabolites and polysaccharides without using liquid nitrogen and phenol. *ISRN Molecular Biology*, *2012*, 1–6. https://doi.org/10.5402/2012/205049

Salam, M. U., Fitt, B. D. L., Aubertot, J. -., Diggle, A. J., Huang, Y. J., Barbetti, M. J., Gladders, P., Jędryczka, M., Khangura, R. K., Wratten, N., Fernando, W. G. D., Penaud, A., Pinochet, X., & Sivasithamparam, K. (2007). Two weather-based models for predicting the onset of seasonal release of ascospores of *Leptosphaeria maculans* or *L. biglobosa*. *Plant Pathology*, *56*, 412–423. https://doi.org/10.1111/j.1365-3059.2006.01551.x

Sapelli, L. (2024). *Understanding Pyrenopeziza brassicae pathogen populations to improve control of light leaf spot on oilseed rape (Brassica napus)*. (PhD thesis). University of Hertfordshire.

Savage, D., Barbetti, M. J., MacLeod, W. J., Salam, M. U., & Renton, M. (2013). Temporal patterns of ascospore release in *Leptosphaeria maculans* vary depending on geographic region and time of observation. *Microbial Ecology*, *65*, 584–592. https://doi.org/10.1007/s00248-012-0165-0

Scharf, D. H., Heinekamp, T., Remme, N., Hortschansky, P., Brakhage, A. A., & Hertweck, C. (2012). Biosynthesis and function of gliotoxin in *Aspergillus fumigatus*. *Applied Microbiology and Biotechnology*, *93*, 467–472. https://doi.org/10.1007/s00253-011-3689-1

Schoener, T. W. (1974). Resource Partitioning in Ecological Communities. *Science*, *185*, 27–39. https://doi.org/10.1126/science.185.4145.27

Schoch, C., Crous, P., Groenewald, J., Boehm, E., Burgess, T., De Gruyter, J., De Hoog, G., Dixon, L., Grube, M., Gueidan, C., Harada, Y., Hatakeyama, S., Hirayama, K., Hosoya, T., Huhndorf, S., Hyde, K., Jones, E., Kohlmeyer, J., Kruys, Å., Spatafora, J. (2009). A class-wide phylogenetic assessment of *Dothideomycetes*. *Studies in Mycology*, *64*, 1–15. https://doi.org/10.3114/sim.2009.64.01

Sewell, T. R., Moloney, S., Ashworth, M., Ritchie, F., Mashanova, A., Huang, Y. J., Stotz, H. U., & Fitt, B. D. L. (2016). Effects of a penthiopyrad and picoxystrobin fungicide mixture on phoma stem canker (*Leptosphaeria* spp.) on UK winter oilseed rape. *European Journal of Plant Pathology*, *145*, 675–685. https://doi.org/10.1007/s10658-016-0916-8

Sewell, T. R., Hawkins, N. J., Stotz, H. U., Huang, Y., Kelly, S. L., Kelly, D. E., Fraaije, B., & Fitt, B. D. L. (2017). Azole sensitivity in *Leptosphaeria* pathogens of oilseed rape: the role of lanosterol 14α-demethylase. *Scientific Reports*, *7*. https://doi.org/10.1038/s41598-017-15545-9

Seybold, H., Demetrowitsch, T. J., Hassani, M. A., Szymczak, S., Reim, E., Haueisen, J., Lübbers, L., Rühlemann, M., Franke, A., Schwarz, K., & Stukenbrock, E. H. (2020). A fungal pathogen induces systemic susceptibility and systemic shifts in wheat metabolome and microbiome composition. *Nature Communications*, *11*. https://doi.org/10.1038/s41467-020-15633-x

Shafqat, A., Abbas, S., Ambreen, M., Bhatti, A. S., Kausar, H., & Gull, T. (2024). Exploring the vital role of phytohormones and plant growth regulators in orchestrating plant immunity. *Physiological and Molecular Plant Pathology*, *133*, 102359. https://doi.org/10.1016/j.pmpp.2024.102359

Shah, U. A., Kotta-Loizou, I., Fitt, B. D. L., & Coutts, R. H. A. (2020). Mycovirus-induced hypervirulence of *Leptosphaeria biglobosa* enhances systemic acquired resistance to *Leptosphaeria maculans* in *Brassica napus*. *Molecular Plant-Microbe Interactions, 33*, 98–107. https://doi.org/10.1094/mpmi-09-19-0254-r

Shao, D., Smith, D. L., Kabbage, M., & Roth, M. G. (2021). Effectors of plant necrotrophic fungi. *Frontiers in Plant Science*, *12*. https://doi.org/10.3389/fpls.2021.687713

Shoemaker, R., & Brun, H. (2001). The teleomorph of the weakly aggressive segregate of *Leptosphaeria maculans*. *Canadian Journal Of Botany*, *79*, 412-419. https://doi.org/10.1139/b01-019

Singh, R., Langyan, S., Sangwan, S., Rohtagi, B., Khandelwal, A., & Shrivastava, M. (2022). Protein for human consumption from oilseed cakes: a review. *Frontiers in Sustainable Food Systems*, *6*. https://doi.org/10.3389/fsufs.2022.856401

Smedsgaard J. (1997). Micro-scale extraction procedure for standardized screening of fungal metabolite production in cultures. Journal of Chromatography A. 760, 264–270.

Pedras, M. S. C., & Séguin-Swartz, G. (1991). The blackleg fungus: phytotoxins and phytoalexins. *Canadian Journal of Plant Pathology*, *14*, 67–75. https://doi.org/10.1080/07060669209500907

Sprague, S. J., Balesdent, M., Brun, H., Hayden, H. L., Marcroft, S. J., Pinochet, X., Rouxel, T., & Howlett, B. J. (2006). Major gene resistance in *Brassica napus* (oilseed rape) is overcome by changes in virulence of populations of *Leptosphaeria maculans* in France and Australia. In *Springer eBooks* (pp. 33–40). https://doi.org/10.1007/1-4020-4525-5_3

Sprague, S. J., Kirkegaard, J. A., Graham, J. M., Bell, L. W., Seymour, M., & Ryan, M. (2015). Forage and grain yield of diverse canola (*Brassica napus*) maturity types in the high-rainfall zone of Australia. *Crop and Pasture Science*, *66*, 260. https://doi.org/10.1071/cp14319

Stenberg, J. A., Sundh, I., Becher, P. G., Björkman, C., Dubey, M., Egan, P. A., Friberg, H., Gil, J. F., Jensen, D. F., Jonsson, M., Karlsson, M., Khalil, S., Ninkovic, V., Rehermann, G., Vetukuri, R. R., & Viketoft, M. (2021). When is it biological control? a framework of definitions, mechanisms, and classifications. *Journal of Pest Science*, *94*, 665–676. https://doi.org/10.1007/s10340-021-01354-7

Stergiopoulos, I., Collemare, J., Mehrabi, R., & De Wit, P. J. (2013). Phytotoxic secondary metabolites and peptides produced by plant pathogenic *Dothideomycete* fungi. *FEMS Microbiology Reviews*, *37*, 67–93. https://doi.org/10.1111/j.1574-6976.2012.00349.x

Stiller, A., Garrison, K., Gurdyumov, K., Kenner, J., Yasmin, F., Yates, P., & Song, B. (2021). From fighting critters to saving lives: Polyphenols in plant defense and human health. *International Journal of Molecular Sciences*, *22*, 8995. https://doi.org/10.3390/ijms22168995

Stonard, J. F., Latunde-Dada, A. O., Huang, Y., West, J. S., Evans, N., & Fitt, B. D. L. (2010). Geographic variation in severity of phoma stem canker and *Leptosphaeria maculans/ L. biglobosa* populations on UK winter oilseed rape (*Brassica napus*). *European Journal of Plant Pathology*, *126*, 97–109. https://doi.org/10.1007/s10658-009-9525-0

Stotz, H. U., Mitrousia, G. K., De Wit, P. J., & Fitt, B. D. (2014). Effector-triggered defence against apoplastic fungal pathogens. *Trends in Plant Science*, *19*, 491–500. https://doi.org/10.1016/j.tplants.2014.04.009

Sun, P., Fitt, B. D. L., Gladders, P., & Welham, S. J. (2000). Relationships between phoma leaf spot and development of stem canker (*Leptosphaeria maculans*) on winter oilseed rape (*Brassica napus*) in southern England. *Annals of Applied Biology*, *137*, 113–125. https://doi.org/10.1111/j.1744-7348.2000.tb00043.x

Sun, P., Fitt, B. D. L., Steed, J. M., Underwood, C. T., & West, J. S. (2001). Factors affecting development of phoma canker (*Leptosphaeria maculans*) on stems of winter oilseed rape (*Brassica napus*) in southern England. *Annals of Applied Biology*, *139*, 227–242. https://doi.org/10.1111/j.1744-7348.2001.tb00399.x

Talley, S. M., Coley, P. D., & Kursar, T. A. (2002). The effects of weather on fungal abundance and richness among 25 communities in the Intermountain West. *BMC Ecology*, *2*. https://doi.org/10.1186/1472-6785-2-7

Tan, S. H., Mailer, R. J., Blanchard, C. L., & Agboola, S. O. (2010). Canola proteins for human consumption: extraction, profile, and functional properties. *Journal of Food Science*, *76*. https://doi.org/10.1111/j.1750-3841.2010.01930.x

Tan, S., Gu, Y., Yang, C., Dong, Y., Mei, X., Shen, Q., & Xu, Y. (2016). *Bacillus amyloliquefaciens* T-5 may prevent *Ralstonia solanacearum* infection through competitive exclusion. *Biology and Fertility of Soils*, *52*, 341–351. https://doi.org/10.1007/s00374-015-1079-z

Tang, C., Xu, Q., Zhao, M., Wang, X., & Kang, Z. (2018). Understanding the lifestyles and pathogenicity mechanisms of obligate biotrophic fungi in wheat: The emerging genomics era. *The Crop Journal*, *6*, 60–67. https://doi.org/10.1016/j.cj.2017.11.003

Tekauz, A. (1976). Distribution, severity, and relative importance of leaf spot diseases of wheat in western Canada in 1974. *Canadian plant disease survey, 56*, 36-40.

Tenenbaum, D. J. (2008). Food vs. fuel: diversion of crops could cause more hunger. *Environmental Health Perspectives*, *116*. https://doi.org/10.1289/ehp.116-a254

Pimm, S. L. (1982). Tilman, D. 1982. Resource competition and community structure. Monogr. Pop. Biol. 17. Princeton University Press, Princeton, N.J. 296 p. *Limnology and Oceanography*, *28*, 1043–1045. https://doi.org/10.4319/lo.1983.28.5.1043

Tiwari, S., Vaish, B., & Singh, P. (2017). Population and global food security. In *Advances in environmental engineering and green technologies book series* (pp. 40–63). https://doi.org/10.4018/978-1-5225-1683-5.ch003

Tollenaere, C., Susi, H., & Laine, A. (2016). Evolutionary and epidemiological implications of multiple infection in plants. *Trends in Plant Science*, *21*, 80–90. https://doi.org/10.1016/j.tplants.2015.10.014

Toscano-Underwood, C., Huang, Y. J., Fitt, B. D. L., & Hall, A. M. (2003). Effects of temperature on maturation of pseudothecia of *Leptosphaeria maculans* and *L. biglobosa* on oilseed rape stem debris. *Plant Pathology*, *52*, 726–736. https://doi.org/10.1111/j.1365-3059.2003.00930.x

Toscano-Underwood, C., West, J. S., Fitt, B. D. L., Todd, A. D., & Jedryczka, M. (2001). Development of phoma lesions on oilseed rape leaves inoculated with ascospores of A-group or B-group *Leptosphaeria maculans* (stem canker) at different temperatures and wetness durations. *Plant Pathology*, *50*, 28–41. https://doi.org/10.1046/j.1365-3059.2001.00526.x

Travadon, R., Bousset, L., Saint-Jean, S., Brun, H., & Sache, I. (2007). Splash dispersal of *Leptosphaeria maculans* pycnidiospores and the spread of blackleg on oilseed rape. *Plant Pathology*, *56*, 595–603. https://doi.org/10.1111/j.1365-3059.2007.01572.x

Tronsmo, A., Collinge, D. B., Alabouvette, C., & Jensen, D. F. (2020). Biological control of plant diseases. In *CABI eBooks* (pp. 289–306). https://doi.org/10.1079/9781789243185.0289

Tzeng, Y., Diosady, L. L., & Rubin, L. J. (1990). Production of canola protein materials by alkaline extraction, precipitation, and membrane processing. *Journal of Food Science*, *55*, 1147–1151. https://doi.org/10.1111/j.1365-2621.1990.tb01619.x

Ueno, Y. (1980). Toxicological evaluation trichothecene mycotoxins. In *Elsevier eBooks* (pp. 663–671). https://doi.org/10.1016/b978-0-08-024952-0.50084-3

Uniyal, S., Paliwal, R., Kaphaliya, B., & Sharma, R. K. (2019). Human overpopulation. In *IGI Global eBooks* (pp. 20–30). https://doi.org/10.4018/978-1-5225-9276-1.ch002

Urquhart, A. S., Elliott, C. E., Zeng, W., & Idnurm, A. (2021). Constitutive expression of transcription factor *SirZ* blocks pathogenicity in *Leptosphaeria maculans* independently of sirodesmin production. *PLoS ONE*, *16*, e0252333. https://doi.org/10.1371/journal.pone.0252333

United States Department of Agriculture Foreign Agricultural Service & World Agricultural Outlook Board/USDA. (2025). *Oilseeds: World Markets and trade*.

Van De Wouw, A. P., Cozijnsen, A. J., Hane, J. K., Brunner, P. C., McDonald, B. A., Oliver, R. P., & Howlett, B. J. (2010). Evolution of linked avirulence effectors in *Leptosphaeria maculans* is affected by genomic environment and exposure to resistance genes in host plants. *PLoS Pathogens*, *6*, e1001180. https://doi.org/10.1371/journal.ppat.1001180

Van De Wouw, A. P., Scanlan, J. L., Al-Mamun, H. A., Balesdent, M., Bousset, L., Burketová, L., Del Rio Mendoza, L., Fernando, W. G. D., Franke, C., Howlett, B. J., Huang, Y., Jones, E. E., Koopmann, B., Lob, S., Mirabadi, A. Z., Nugent, B. C., Peng, G., Rossi, F. R., Schreuder, H., Idnurm, A. (2023). A new set of international *Leptosphaeria maculans* isolates as a resource for elucidation of the basis and evolution of blackleg disease on Brassica napus. *Plant Pathology*, *73*, 170–185. https://doi.org/10.1111/ppa.13801

Van De Wouw, A. P., Sheedy, E. M., Ware, A. H., Marcroft, S. J., & Idnurm, A. (2022). Independent breakdown events of the *Brassica napus Rlm7* resistance gene including via the off-target impact of a dual-specificity avirulence interaction. *Molecular Plant Pathology*, *23*, 997–1010. https://doi.org/10.1111/mpp.13204

Van Den Bosch, F., & Gilligan, C. A. (2003). Measures of durability of resistance. *Phytopathology*, *93*, 616–625. https://doi.org/10.1094/phyto.2003.93.5.616

Van Der Spiegel, M., Noordam, M., & Van Der Fels-Klerx, H. (2013). Safety of novel protein sources (Insects, microalgae, seaweed, duckweed, and rapeseed) and legislative aspects for their application in food and feed production. *Comprehensive Reviews in Food Science and Food Safety*, *12*, 662–678. https://doi.org/10.1111/1541-4337.12032

Van Kan, J. A. (2006). Licensed to kill: the lifestyle of a necrotrophic plant pathogen. *Trends in Plant Science*, *11*, 247–253. https://doi.org/10.1016/j.tplants.2006.03.005

Vincenot, L., Balesdent, M. H., Li, H., Barbetti, M. J., Sivasithamparam, K., Gout, L., & Rouxel, T. (2008). Occurrence of a new subclade of *Leptosphaeria biglobosa* in western Australia. *Phytopathology*, *98*, 321–329. https://doi.org/10.1094/phyto-98-3-0321

Vlot, A. C., Dempsey, D. A., & Klessig, D. F. (2009). Salicylic acid, a multifaceted hormone to combat disease. *Annual Review of Phytopathology*, *47*, 177–206. https://doi.org/10.1146/annurev.phyto.050908.135202

Voegele, R. T., & Mendgen, K. W. (2011). Nutrient uptake in rust fungi: how sweet is parasitic life? *Euphytica*, *179*, 41–55. https://doi.org/10.1007/s10681-011-0358-5

VSN International, Genstat for Windows, 22nd edn. VSN International, Hemel Hempstead, UK (2022) Web page: genstat.co.uk.

Walter, G. (1991). What is resource partitioning? *Journal of Theoretical Biology*, *150*, 137–143. https://doi.org/10.1016/s0022-5193(05)80327-3

Wang, X., Jiang, N., Liu, J., Liu, W., & Wang, G. (2014). The role of effectors and host immunity in plant–necrotrophic fungal interactions. *Virulence*, 722–732. https://doi.org/10.4161/viru.29798

Wang, Y., Mostafa, S., Zeng, W., & Jin, B. (2021). Function and mechanism of jasmonic acid in plant responses to abiotic and biotic stresses. *International Journal of Molecular Sciences*, *22*, 8568. https://doi.org/10.3390/ijms22168568

West, J., Kharbanda, P., Barbetti, M., & Fitt, B. (2001). Epidemiology and management of *Leptosphaeria maculans* (phoma stem canker) on oilseed rape in Australia, Canada and Europe. *Plant Pathology*, *50*, 10-27. https://doi.org/10.1046/j.1365-3059.2001.00546.x

West, J. S., Balesdent, M., Rouxel, T., Narcy, J. P., Huang, Y., Roux, J., Steed, J. M., Fitt, B. D. L., & Schmit, J. (2002a). Colonization of winter oilseed rape tissues by A/Tox+ and B/Tox0 *Leptosphaeria maculans* (phoma stem canker) in France and England. *Plant Pathology*, *51*, 311–321. https://doi.org/10.1046/j.1365-3059.2002.00689.x

West, J. S., Fitt, B. D. L., Leech, P. K., Biddulph, J. E., Huang, Y., & Balesdent, M. (2002b). Effects of timing of *Leptosphaeria maculans* ascospore release and fungicide regime on phoma leaf spot and phoma stem canker development on winter oilseed rape (*Brassica napus*) in southern England. *Plant Pathology*, *51*, 454–463. https://doi.org/10.1046/j.1365-3059.2002.00726.x

Williams, N., & Fitt, N. (1999). Differentiating A and B groups of *Leptosphaeria maculans*, causal agent of stem canker (blackleg) of oilseed rape. *Plant Pathology*, *48*, 161–175. https://doi.org/10.1046/j.1365-3059.1999.00333.x

Williams, P. H. (1991). Biology of *Leptosphaeria maculans*. *Canadian Journal of Plant Pathology*, *14*, 30–35. https://doi.org/10.1080/07060669209500903

Williamson, B., Tudzynski, B., Tudzynski, P., & Van Kan, J. a. L. (2007). *Botrytis cinerea*: the cause of grey mould disease. *Molecular Plant Pathology*, *8*, 561–580. https://doi.org/10.1111/j.1364-3703.2007.00417.x

Wu, X., Zhang, X., Yang, S., Chen, H., & Wang, D. (2000). The study of epoxidized rapeseed oil used as a potential biodegradable lubricant. *Journal of the American Oil Chemists Society*, *77*, 561–563. https://doi.org/10.1007/s11746-000-0089-2

Yan, X., Ying, Y., Li, K., Zhang, Q., & Wang, K. (2024). A review of mitigation technologies and management strategies for greenhouse gas and air pollutant emissions in livestock production. *Journal of Environmental Management*, *352*, 120028. https://doi.org/10.1016/j.jenvman.2024.120028

Yunus-Khan, T. Y., Atabani, A., Badruddin, I. A., Badarudin, A., Khayoon, & Triwahyono, S. (2014). Recent scenario and technologies to utilize non-edible oils for biodiesel production. *Renewable and Sustainable Energy Reviews*, *37*, 840–851. https://doi.org/10.1016/j.rser.2014.05.064

Zhang, X., White, R. P., Demir, E., Jedryczka, M., Lange, R. M., Islam, M., Li, Z. Q., Huang, Y. J., Hall, A. M., Zhou, G., Wang, Z., Cai, X., Skelsey, P., & Fitt, B. D. L. (2014). *Leptosphaeria* spp., phoma stem canker and potential spread of *L. maculans* on oilseed rape crops in China. *Plant Pathology*, *63*, 598–612. https://doi.org/10.1111/ppa.12146

Zhang, X., Peng, G., Kutcher, H. R., Balesdent, M., Delourme, R., & Fernando, W. G. D. (2015). Breakdown of *Rlm3* resistance in the *Brassica napus–Leptosphaeria maculans* pathosystem in western Canada. *European Journal of Plant Pathology*, *145*, 659–674. https://doi.org/10.1007/s10658-015-0819-0

Zheng, Z., Qamar, S. A., Chen, Z., & Mengiste, T. (2006). *Arabidopsis* WRKY33 transcription factor is required for resistance to necrotrophic fungal pathogens. *The Plant Journal*, *48*, 592–605. https://doi.org/10.1111/j.1365-313x.2006.02901.x

Zheng, X., Koopmann, B., Ulber, B., & von Tiedemann, A. (2020). A global survey on diseases and pests in oilseed rape—current challenges and innovative strategies of control. *Frontiers In Agronomy*, *2*. https://doi.org/10.3389/fagro.2020.590908

Zhou, D., Wang, X., Chen, G., Sun, S., Yang, Y., Zhu, Z., & Duan, C. (2018). The major *Fusarium* species causing maize ear and kernel rot and their toxigenicity in Chongqing, China. *Toxins*, *10*, 90. https://doi.org/10.3390/toxins10020090

Zhou, K., Zhang, J., Yang, L., Li, G., & Wu, M. (2023). Genetic diversity and population structure of *Leptosphaeria biglobosa* from the winter oilseed rape region in China. *Journal of Fungi*, *9*, 1092. https://doi.org/10.3390/jof9111092

Zhu, Z., & Lee, B. (2015). Friends or foes: New insights in jasmonate and ethylene co-actions. *Plant and Cell Physiology*, *56*, 414–420. https://doi.org/10.1093/pcp/pcu171

Zipfel, C., & Felix, G. (2005). Plants and animals: a different taste for microbes? *Current Opinion in Plant Biology*, *8*, 353–360. https://doi.org/10.1016/j.pbi.2005.05.004

Zou, Z., Zhang, X., Parks, P., Du Toit, L. J., Van De Wouw, A. P., & Fernando, W. G. D. (2019). A new subclade of *Leptosphaeria biglobosa* identified from *Brassica rapa*. *International Journal of Molecular Sciences*, *20*, 1668. https://doi.org/10.3390/ijms20071668

8 Appendices

8.1 Appendix A – Thermocycling profiles and standard curves for quantification of *Leptosphaeria* species DNA using quantitative polymerase chain reaction (qPCR) with species-specific primers

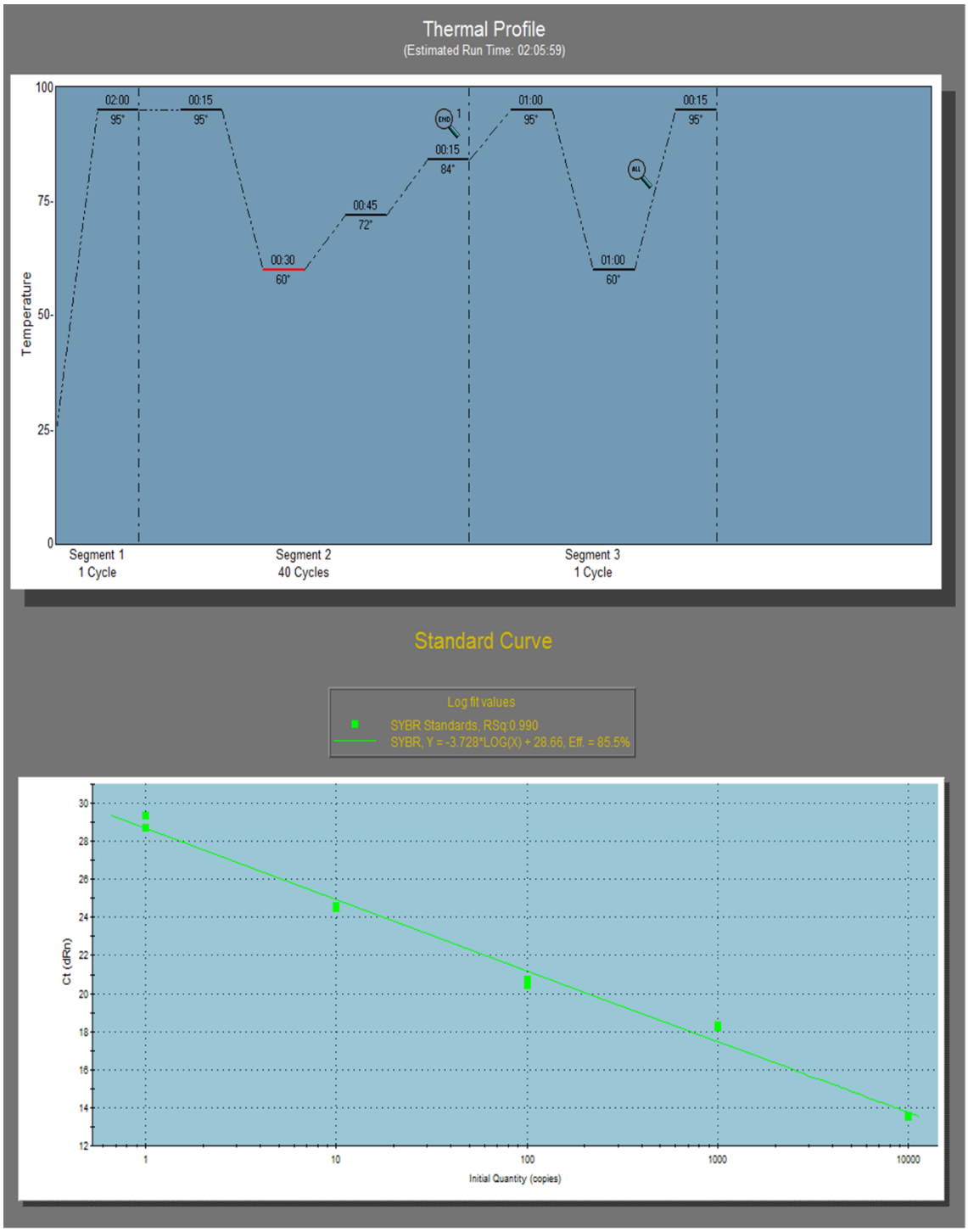

Figure A.1: Thermocycling profile and standard curve for quantification of *Leptosphaeria maculans* DNA using quantitative polymerase chain reaction (qPCR) with species-specific primers.

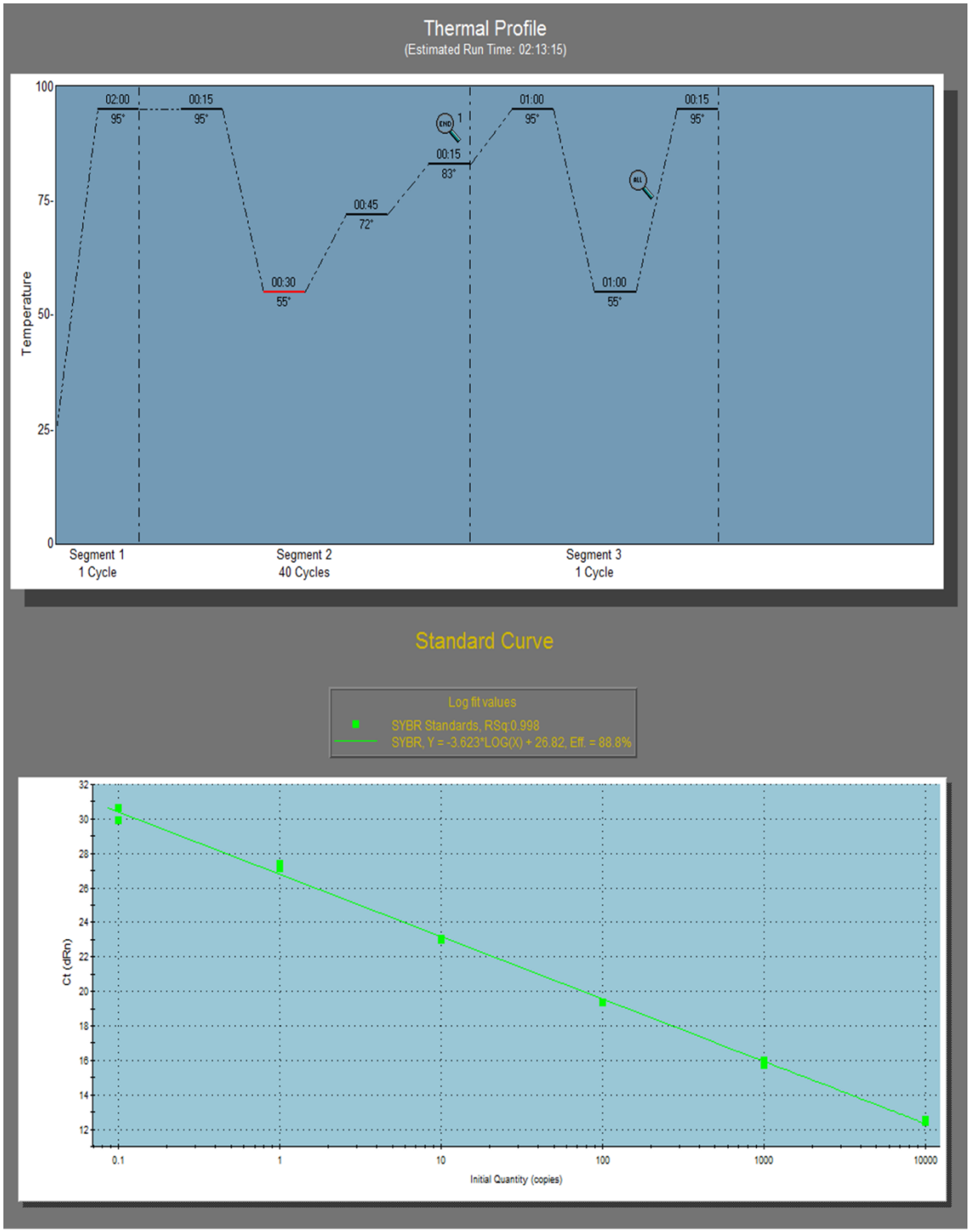

Figure A.2: Thermocycling profile and standard curve for quantification of *Leptosphaeria biglobosa* DNA using quantitative polymerase chain reaction (qPCR) with species-specific primers.

8.2 Appendix B - Experimental designs and layouts of experiments in Chapter 3

Randomisation of conical flasks for the *in vitro* simultaneous co-inoculation experiments

The experiments were done in a randomised block design, with three replicates per treatment in each block (Table B.1). The flasks were incubated in two shaking incubators with each considered as a block. The randomisation was done by assigning a number for each sample using a random number generator and samples were placed in shaking incubators accordingly.

Table B.1: Layout of *in vitro* simultaneous co-inoculation experiments

Shaking incubator 1 (Block 1)					
LmLb-5.1	Empty-6	Lb-10.1	Empty-5	Lm-7.1	Lb-5.1
LmLb-10.1	Lm-14.1	Lm-10.1	Empty-2	Lm-1.1	Empty-4
Empty-3	Lb-7.1	Lb-3.1	LmLb-1.1	LmLb-14.1	Lb-1.1
Lb-14.1	LmLb-3.1	Lm-3.1	LmLb-7.1	Lm-5.1	Empty-1
Shaking incubator 2 (Block 2)					
Lm-5.2	Empty-2	LmLb-7.2	Lb-5.2	Lb-1.2	LmLb-3.2
LmLb-1.2	LmLb-14.2	Lb-7.2	LmLb-10.2	Empty-3	Lm-7.2
LmLb-5.2	Empty-4	Lb-14.2	Lm-14.2	Lm-1.2	Lm-3.2
Empty-1	Lm-10.2	Lb-10.2	Empty-5	Lb-3.2	Empty-6

Randomisation of conical flasks for the *in vitro* sequential co-inoculation experiments

Experiments 1 and 3 were done in one shaking incubator and experiment 2 was done in two shaking incubators due to the greater number of samples. The experiments were done in a randomised design with two (experiments 1 and 3) or three (experiment 2) replicates for each treatment (Table B.2). The randomisation was done by assigning a number for each sample using a random number generator and samples were placed in shaking incubators accordingly.

Table B.2: Layout of *in vitro* sequential co-inoculation experiments

Experiments 1 and 3					
Shaking incubator 1					
Lb+Lm-5.2	**Lb**+Lm-3.1	Lb-2	**Lm**+Lb-3.1	Lm-2	**Lm**+Lb-1.2
Lm&Lb-1	**Lm**+Lb-5.2	**Lb**+Lm-3.2	**Lb**+Lm-7.1	Empty-2	**Lb**+Lm-5.1
Lm+Lb-7.2	Lm&Lb-2	Empty-1	Lb-1	**Lb**+Lm-1.1	**Lm**+Lb-7.1
Lb+Lm-7.2	**Lm**+Lb-1.1	**Lm**+Lb-5.1	**Lb**+Lm-1.2	**Lm**+Lb-3.2	Lm-1

Experiment 2					
Shaking incubator 1					
Lb+Lm-3.1	Empty-4	**Lm**+Lb-5.3	Blank	**Lm**+Lb-7.3	**Lb**+Lm-7.2
Lm-2	Lb-2	Empty-5	**Lm**+Lb-3.3	**Lb**+Lm-5.1	Empty-1
Empty-6	Lm-3	LmLb-2	**Lm**+Lb-7.1	**Lm**+Lb-1.1	Empty-2
Lb+Lm-1.3	**Lm**+Lb-5.1	**Lm**+Lb-3.1	Empty-7	**Lm**+Lb-1.2	Empty-3
Shaking incubator 2					
Lb+Lm-3.3	Empty-1	**Lb**+Lm-7.3	LmLb-1	Empty-2	**Lb**+Lm-5.3
Empty-3	**Lb**+Lm-5.2	**Lm**+Lb-5.2	**Lm**+Lb-7.2	LmLb-3	**Lm**+Lb-3.2
Lb-3	**Lm**+Lb-1.3	Empty-4	**Lb**+Lm-1.2	Empty-5	**Lb**+Lm-1.1
Lb+Lm-7.1	Empty-6	**Lb**+Lm-3.2	Lm-1	Lb-2	Empty-7

8.3 Appendix C – Individual analyses of experiments in Chapter 3

Effects of simultaneous co-inoculation on composition of secondary metabolites produced by *L. maculans*

Experiment 1

In experiment 1, 'Lb only' and 'Lm&Lb' treatments did not show any maxima corresponding to sirodesmin PL or its precursors in their HPLC chromatograms. For 'Lm only' treatment, the precursors of sirodesmin PL were first detected at 5 dpi at 71.3 mg/L concentration. From 5 dpi the concentration of the precursors of sirodesmin PL increased and was the greatest at 10 dpi at 303.2 mg/L concentration, before decreasing to 224.3 mg/L by 14 dpi (Figure C.1).

Similarly, sirodesmin PL was first detected at 5 dpi at 74.6 mg/L concentration. The concentration of sirodesmin PL increased steadily and was the greatest at 10 dpi at 940.6 mg/L concentration. It then decreased to 766.0 mg/L by 14 dpi (Figure C.1).

Experiment 2

In experiment 2, 'Lb only' and 'Lm&Lb' treatments did not show any maxima corresponding to sirodesmin PL or its precursors in their HPLC chromatograms. For 'Lm only' treatment, the precursors of sirodesmin PL were first detected at 5 dpi at 70.0 mg/L concentration. From 5 dpi the concentration of the precursors of sirodesmin PL increased and was the greatest at 10 dpi at 235.4 mg/L concentration, before decreasing to 201.9 mg/L by 14 dpi (Figure C.2).

Similarly, sirodesmin PL was first detected at 5 dpi at 123.5 mg/L concentration. The concentration of sirodesmin PL increased steadily and was the greatest at 10 dpi at 933.6 mg/L concentration. It then decreased to 732.0 mg/L by 14 dpi (Figure C.2).

Experiment 3

In experiment 3, 'Lb only' and 'Lm&Lb' treatments did not show any maxima corresponding to sirodesmin PL or its precursors in their HPLC chromatograms. For 'Lm only' treatment, the precursors of sirodesmin PL were first detected at 5 dpi at 70.4 mg/L concentration. From 5 dpi the concentration of the precursors of sirodesmin PL increased and was the greatest at 10 dpi at 272.4 mg/L concentration, before decreasing to 139.1 mg/L by 14 dpi (Figure C.3).

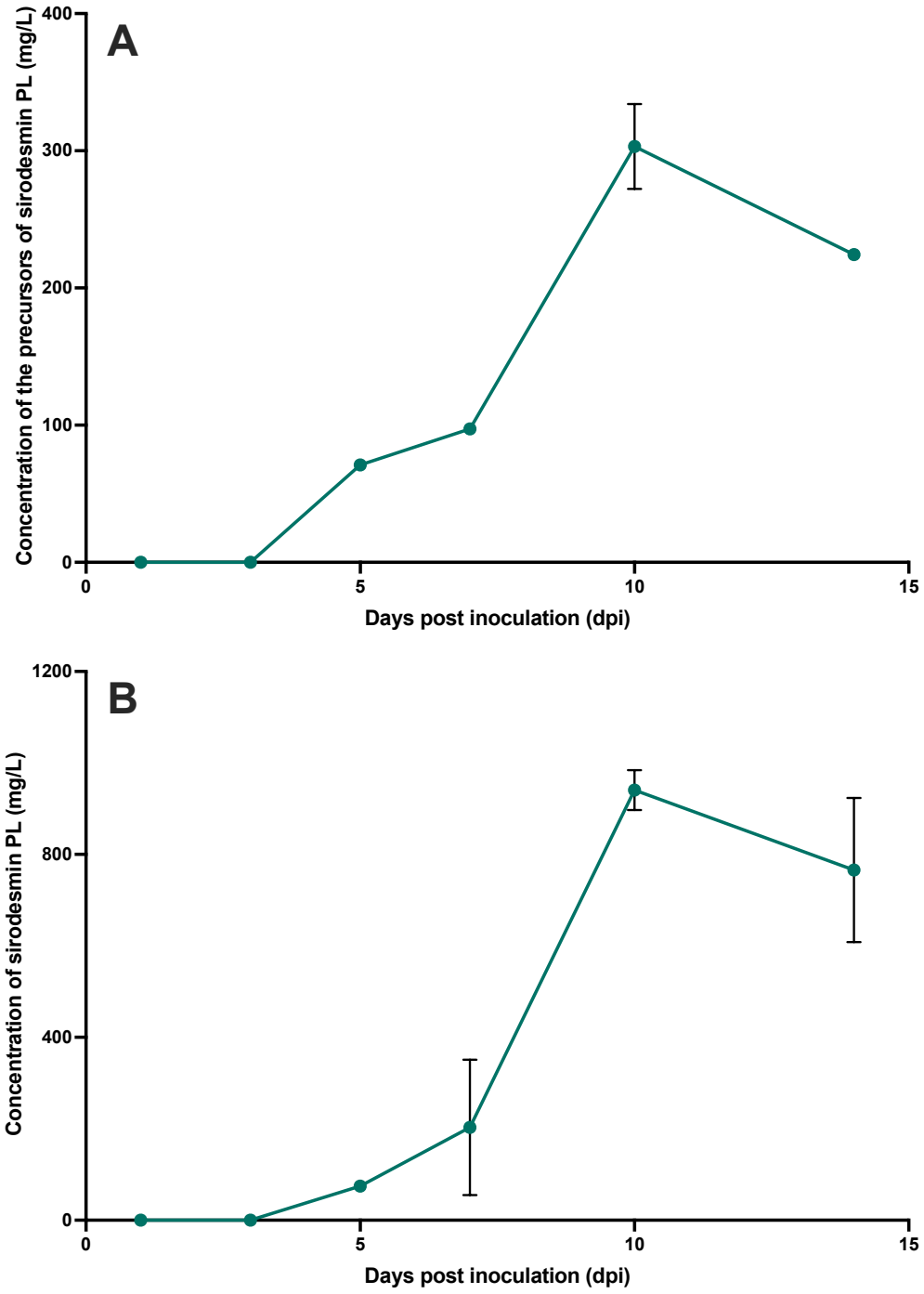

Figure C.1: Concentration of (A) the precursors of sirodesmin PL (mg/L) and (B) sirodesmin PL (mg/L) for *Leptosphaeria maculans* only (Lm only) treatment from *in vitro* simultaneous co-inoculation experiment-1 at 1, 3, 5, 7, 10 and 14 days post inoculation (dpi).

Error bars show standard error of the mean (SEM) (n = 12).

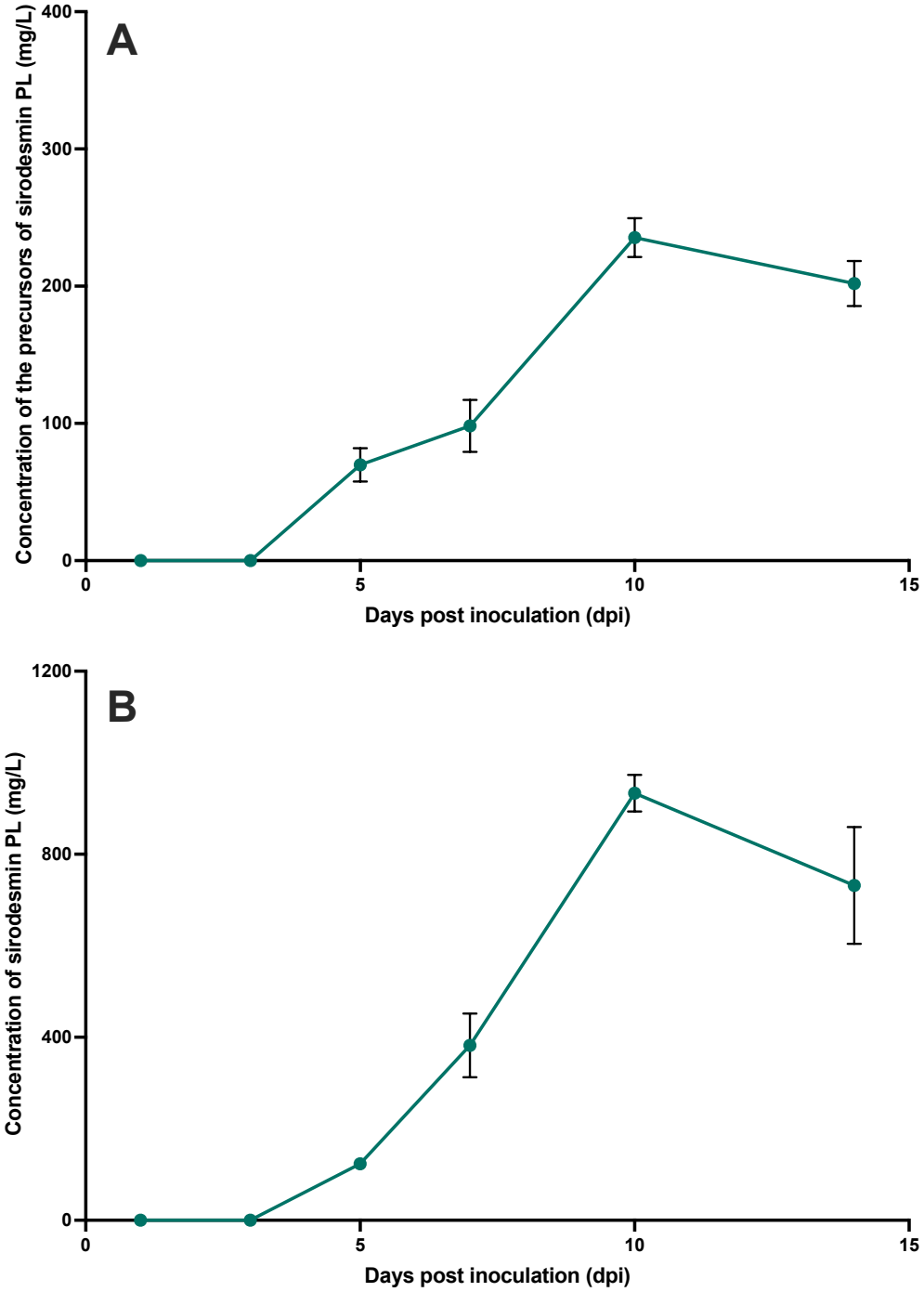

Figure C.2: Concentration of (A) the precursors of sirodesmin PL (mg/L) and (B) sirodesmin PL (mg/L) for *Leptosphaeria maculans* only (Lm only) treatment from *in vitro* simultaneous co-inoculation experiment-2 at 1, 3, 5, 7, 10 and 14 days post inoculation (dpi).

Error bars show standard error of the mean (SEM) (n = 12).

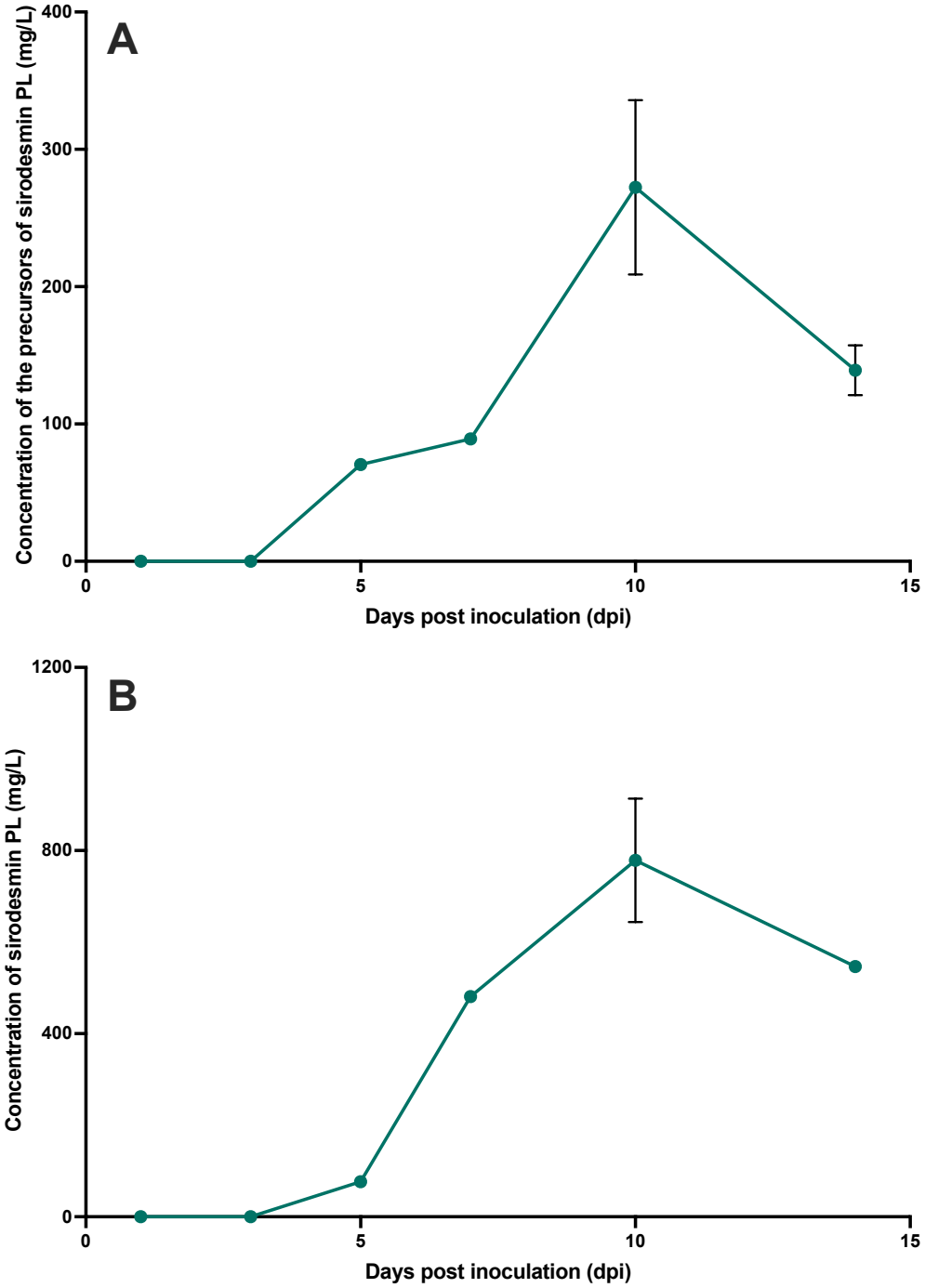

Figure C.3: Concentration of (A) the precursors of sirodesmin PL (mg/L) and (B) sirodesmin PL (mg/L) for *Leptosphaeria maculans* only (Lm only) treatment from *in vitro* simultaneous co-inoculation experiment-3 at 1, 3, 5, 7, 10 and 14 days post inoculation (dpi).

Error bars show standard error of the mean (SEM) (n = 12).

Similarly, sirodesmin PL was first detected at 5 dpi at 76.7 mg/L concentration. The concentration of sirodesmin PL increased steadily and was the greatest at 10 dpi at 778.7 mg/L concentration. It then decreased to 546.7 mg/L by 14 dpi (Figure C.3).

Effects of simultaneous co-inoculation on growth rate of the pathogens

Experiment 1

In experiment 1, mycelial growth of 'Lm only' increased steadily from day 0 to day 14, reaching a dry mycelial weight of 0.23 g by 10 dpi and 0.31 g by 14 dpi. For 'Lb only', mycelial growth occurred faster compared to 'Lm only', reaching a dry mycelial weight of 0.20 g by 5 dpi. The weight for 'Lb only' treatment was the greatest at 0.28 g by 7 dpi and did not significantly increase any further from 7 dpi to 14 dpi. Interestingly, 'Lm&Lb' treatment had a similar trend to 'Lb only', reaching a dry mycelial weight of 0.25 g by 5 dpi. The weight for 'Lm&Lb' treatment was the greatest at 0.29 g by 7 dpi and did not significantly increase any further from 7 dpi to 14 dpi (Figure C.4)

Experiment 2

In experiment 2, mycelial growth of 'Lm only' increased steadily from day 0 to day 14, reaching a dry mycelial weight of 0.21 g by 10 dpi and 0.29 g by 14 dpi. For 'Lb only', mycelial growth occurred faster compared to 'Lm only', reaching a dry mycelial weight of 0.20 g by 5 dpi. The weight for 'Lb only' treatment was the greatest at 0.25 g by 7 dpi and did not significantly increase any further from 7 dpi to 14 dpi. Interestingly, 'Lm&Lb' treatment had a similar trend to 'Lb only', reaching a dry mycelial weight of 0.24 g by 5 dpi. The weight for 'Lm&Lb' treatment was the greatest at 0.28 g by 7 dpi and did not significantly increase any further from 7 dpi to 14 dpi (Figure C.5).

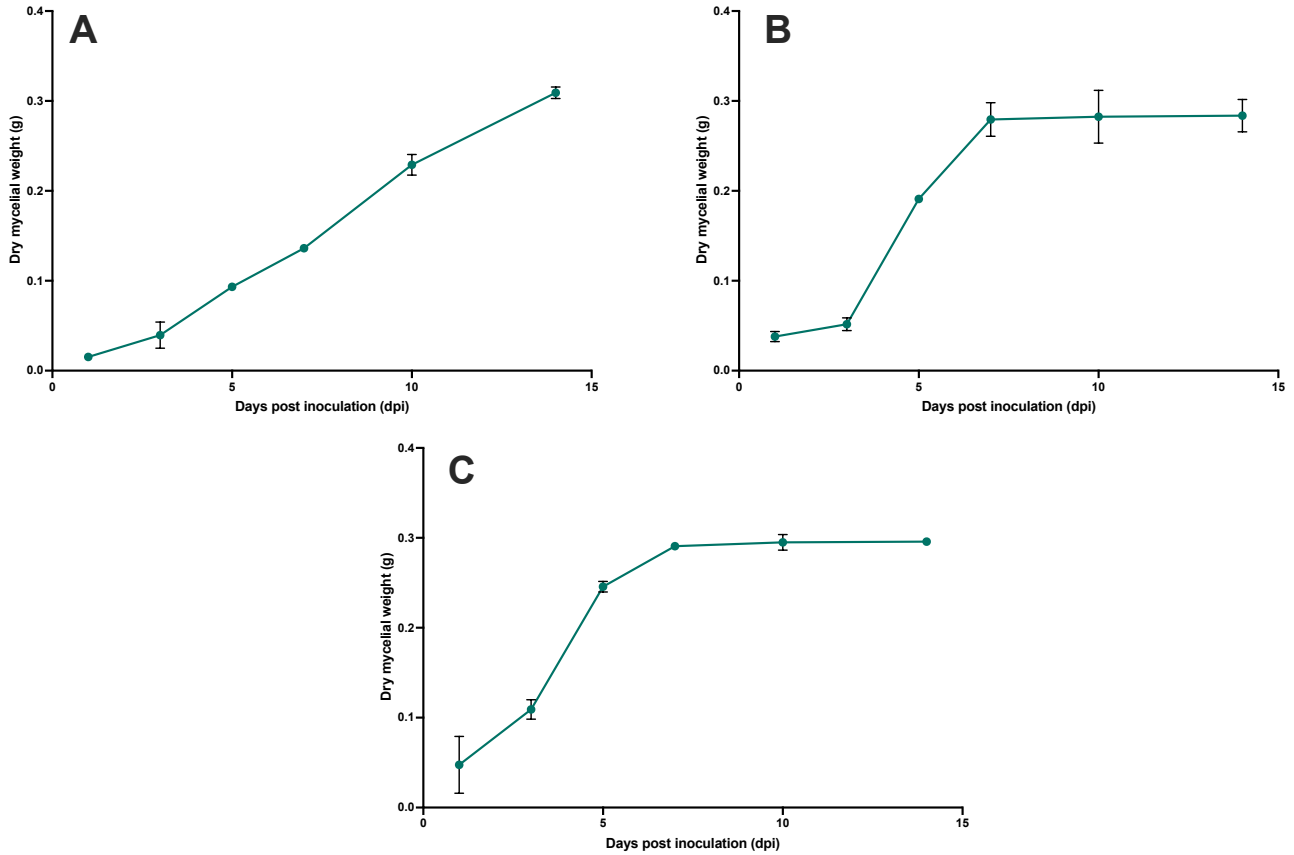

Figure C.4: Development of dry mycelial weight (g) of (A) *Leptosphaeria maculans* only (Lm only), (B) *Leptosphaeria biglobosa* only (Lb only) and (C) *L. maculans* & *L. biglobosa* co-inoculated simultaneously (Lm&Lb) treatments from *in vitro* simultaneous co-inoculation experiment-1 at 1, 3, 5, 7, 10 and 14 days post inoculation (dpi).

Error bars show standard error of the mean (SEM) (Lm only, n = 12) (Lb only, n = 12) (Lm&Lb, n = 12).

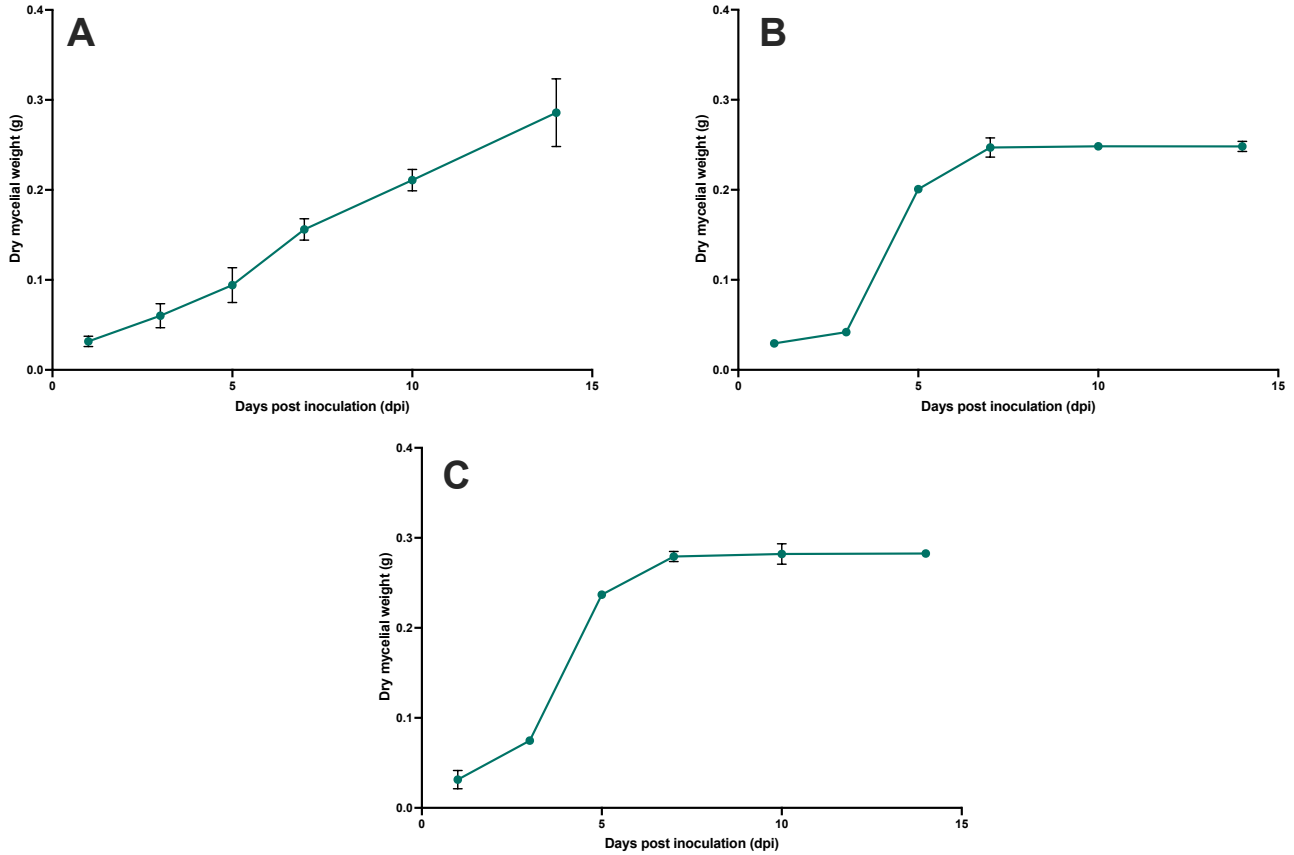

Figure C.5: Development of dry mycelial weight (g) of (A) *Leptosphaeria maculans* only (Lm only), (B) *Leptosphaeria biglobosa* only (Lb only) and (C) *L. maculans* & *L. biglobosa* co-inoculated simultaneously (Lm&Lb) treatments from *in vitro* simultaneous co-inoculation experiment-2 at 1, 3, 5, 7, 10 and 14 days post inoculation (dpi).

Error bars show standard error of the mean (SEM) (Lm only, n = 12) (Lb only, n = 12) (Lm&Lb, n = 12).

Effects of sequential co-inoculation on dry mycelial weight of co-cultures

Experiment 1

In experiment 1, at 14 dpi, there were significant differences in the dry mycelial weight measurements between different treatments ($F(10,11) = 5.09$, $P < 0.05$). 'Lm only' (0.26 g) was significantly different from 'Lb+Lm-1' (0.19 g) and 'Lb+Lm-7' (0.20 g). The rest of the treatments were not significantly different from each other (Figure C.6).

Experiment 2

In experiment 2, at 14 dpi, there were significant differences in the dry mycelial weight measurements between different treatments ($F10,22) = 3.09$, $P < 0.05$). 'Lm only' (0.38 g) was significantly different from 'Lb only' (0.25 g), 'Lm+Lb-3' (0.20 g), and 'Lm+Lb-5' (0.25 g). The rest of the treatments were not significantly different from each other (Figure C.6).

Experiment 3

In experiment 3, at 14 dpi, there were no significant differences in the dry mycelial weight measurements between different treatments ($F(10,11) = 2.5$, $P = 0.075$) (Figure C.6).

Effects of sequential co-inoculation on composition of secondary metabolites produced by *L. maculans*

Experiment 1

In experiment 1, at 14 dpi, the concentration of the precursors of sirodesmin PL were significantly different in different treatments ($F10,11) = 969.2$, $P < 0.001$). For the treatments Lb only', 'Lm&Lb', 'Lm+Lb-1', 'Lb+Lm-1', 'Lb+Lm-3', 'Lb+Lm-5', 'Lb+Lm-7', there were no significant differences between them, since no production of the precursors of sirodesmin PL was detected in those treatments. For the treatments Lm only' (280.9 mg/L), 'Lm+Lb-5' (278.9 mg/L) and 'Lm+Lb-7' (255.3 mg/L), there were no significant differences between them. Interestingly, Lm+Lb-3' (120.9 mg/L) treatment was significantly different from all other treatments (Figure C.7).

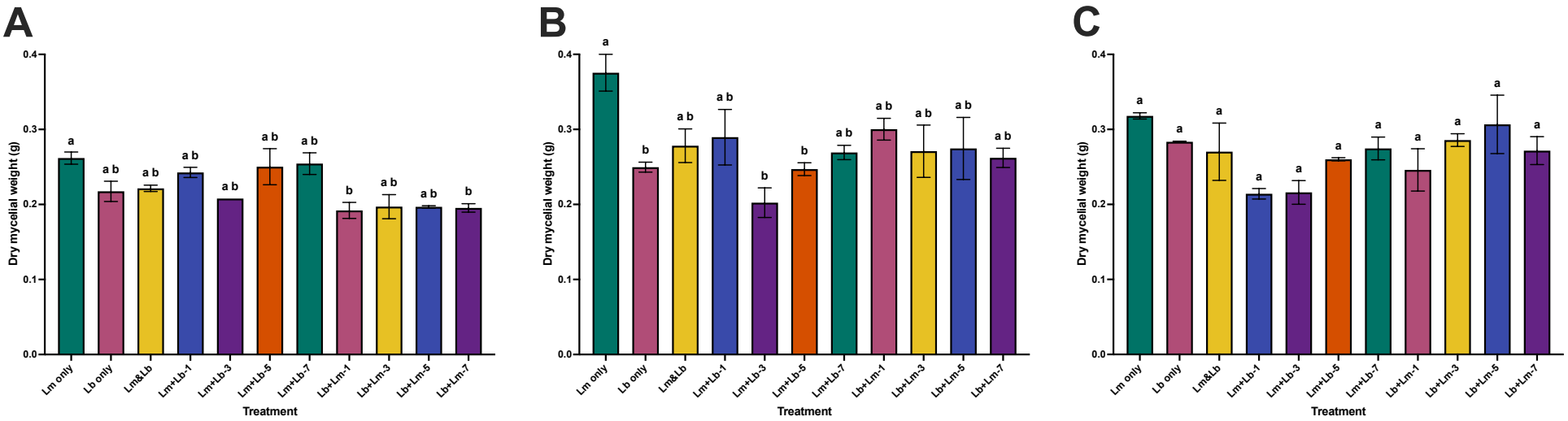

Figure C.6: Average dry mycelial weight (g) of mycelia obtained from (A) experiment-1, (B) experiment-2, and (C) experiment-3 consisting of liquid cultures inoculated with *Leptosphaeria maculans* only (Lm only), *Leptosphaeria biglobosa* only (Lb only), *L. maculans* & *L. biglobosa* co-inoculated simultaneously (Lm&Lb), initial inoculation with *L. maculans* followed by co-inoculation with *L. biglobosa* sequentially at 1, 3, 5 and 7 days later (Lm+Lb-1, Lm+Lb-3, Lm+Lb-5, Lm+Lb-7) and initial inoculation with *L. biglobosa* followed by co-inoculation with *L. maculans* sequentially at 1, 3, 5 and 7 days later (Lb+Lm-1, Lb+Lm-3, Lb+Lm-5, Lb+Lm-7) at 14 days after the initial inoculation.

Tukey's HSD tests were used to separate the mean dry mycelial weight values across different treatments. Columns that do not share a letter are considered significantly different ($P < 0.05$). Error bars show standard error of the mean (SEM) (experiment-1 21 d.f., experiment-2 32 d.f., experiment-3 21 d.f.).

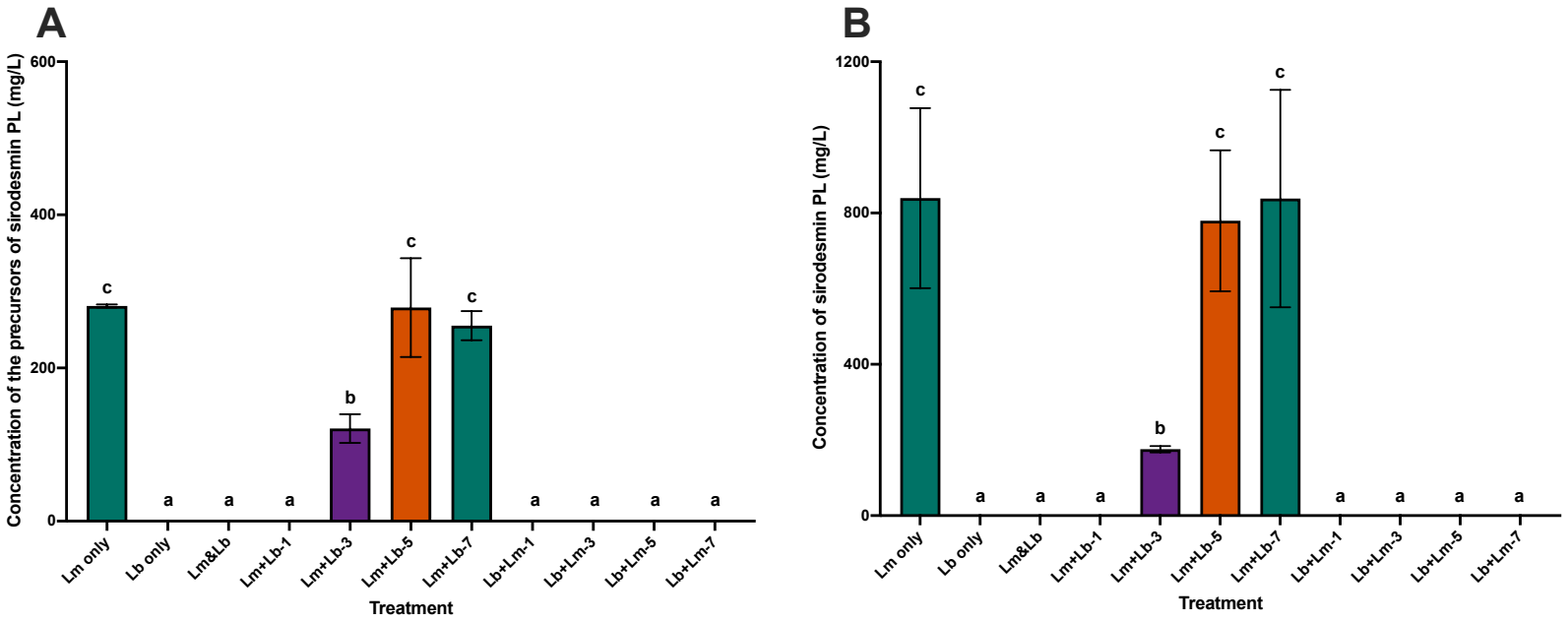

Figure C.7: Concentration of (A) the precursors of sirodesmin PL (mg/L) and (B) sirodesmin PL (mg/L) in secondary metabolite extracts obtained from *in vitro* sequential co-inoculation experiment-1 consisting of liquid cultures inoculated with *Leptosphaeria maculans* only (Lm only), *Leptosphaeria biglobosa* only (Lb only), *L. maculans* & *L. biglobosa* co-inoculated simultaneously (Lm&Lb), initial inoculation with *L. maculans* followed by co-inoculation with *L. biglobosa* sequentially at 1, 3, 5 and 7 days later (Lm+Lb-1, Lm+Lb-3, Lm+Lb-5, Lm+Lb-7), and initial inoculation with *L. biglobosa* followed by co-inoculation with *L. maculans* sequentially at 1, 3, 5 and 7 days later (Lb+Lm-1, Lb+Lm-3, Lb+Lm-5, Lb+Lm-7) at 14 days after the initial inoculation.

Tukey's HSD tests were used to separate the mean concentration of the precursors of sirodesmin PL across different treatments. Columns that do not share a letter are considered significantly different ($P < 0.05$). Error bars show standard error of the mean (SEM) (21 d.f.).

In experiment 1, at 14 dpi, the concentration of sirodesmin PL was significantly different in different treatments ($F_{10,11} = 411.6$, $P < 0.001$). For the treatments 'Lb only', 'Lm&Lb', 'Lm+Lb-1', 'Lb+Lm-1', 'Lb+Lm-3', 'Lb+Lm-5', 'Lb+Lm-7', there were no significant differences between them, since no production of sirodesmin PL was detected in those treatments. For the treatments 'Lm only' (839.2 mg/L), 'Lm+Lb-5' (779.0 mg/L), and 'Lm+Lb-7' (838.2 mg/L), there were no significant differences between them. As with the precursors, 'Lm+Lb-3' (175.6 mg/L) treatment was significantly different from all other treatments (Figure C.7).

Experiment 2

In experiment 2, at 14 dpi, the concentration of the precursors of sirodesmin PL was significantly different in different treatments ($F_{10,22} = 360.6$, $P < 0.001$). For the treatments Lb only', 'Lm&Lb', 'Lm+Lb-1', 'Lb+Lm-1', 'Lb+Lm-3', 'Lb+Lm-5', 'Lb+Lm-7', there were no significant differences between them, since no production of the precursors of sirodesmin PL was detected in those treatments. For the treatments Lm only' (426.5 mg/L), 'Lm+Lb-3' (241.5 mg/L), and 'Lm+Lb-5' (423.93 mg/L), and 'Lm+Lb-7' (491.0 mg/L), there were no significant differences between them. Additionally, Lm+Lb-3' (241.5 mg/L) and 'Lm+Lb-7' (491.0 mg/L) were significantly different (Figure C.8).

In experiment 2, at 14 dpi, the concentration of sirodesmin PL was significantly different in different treatments ($F_{10,22} = 332.6$, $P < 0.001$). For the treatments 'Lb only', 'Lm&Lb', 'Lm+Lb-1', 'Lb+Lm-1', 'Lb+Lm-3', 'Lb+Lm-5', 'Lb+Lm-7', there were no significant differences between them, since no production of sirodesmin PL was detected in those treatments. For the treatments 'Lm only' (889.0 mg/L), 'Lm+Lb-5' (912.5 mg/L) and 'Lm+Lb-7' (958.9 mg/L), there were no significant differences between them. As with the precursors, 'Lm+Lb-3' (416.1 mg/L) treatment was significantly different from all other treatments (Figure C.8).

Experiment 3

In experiment 3, at 14 dpi, the concentration of the precursors of sirodesmin PL was significantly different in different treatments ($F_{10,11} = 995.0$, $P < 0.001$). For the treatments Lb only', 'Lm&Lb', 'Lm+Lb-1', 'Lb+Lm-1', 'Lb+Lm-3', 'Lb+Lm-5', 'Lb+Lm-7', there were no significant differences between them, since no production of the precursors of sirodesmin PL was detected in those treatments.

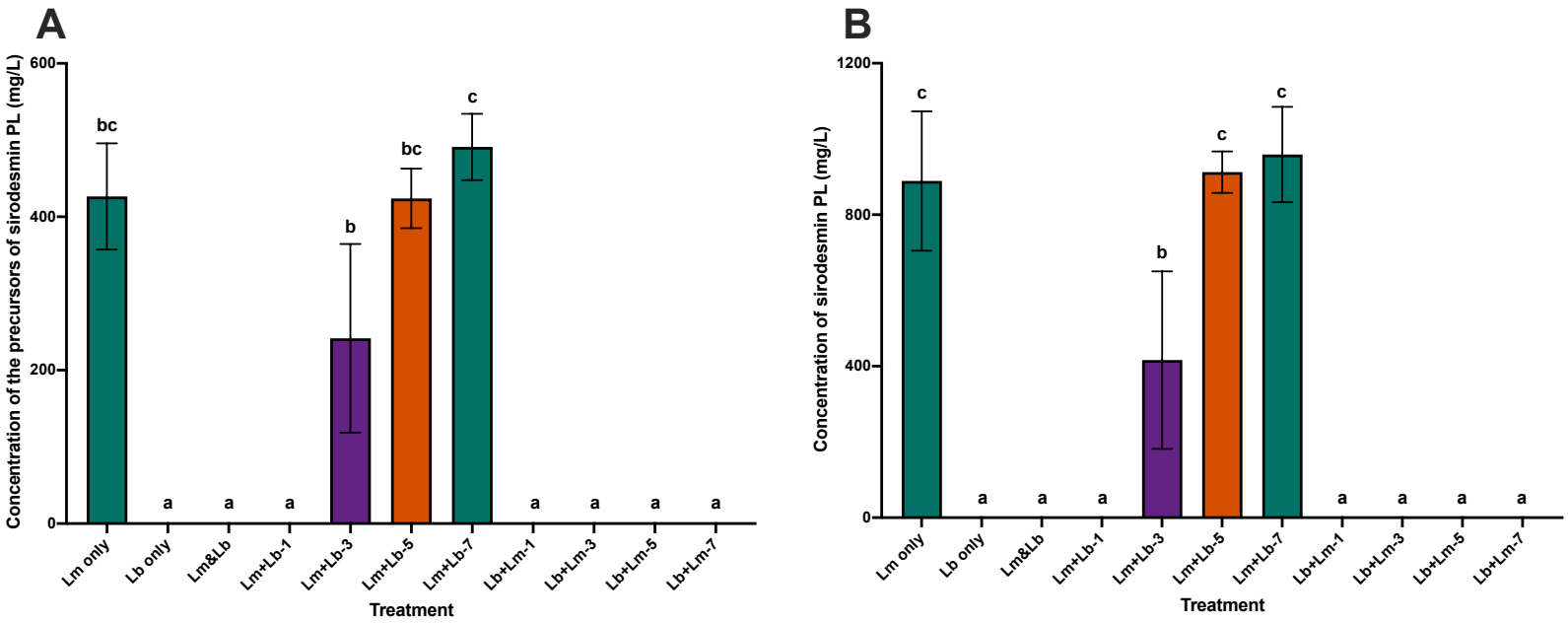

Figure C.8: Concentration of (A) the precursors of sirodesmin PL (mg/L) and (B) sirodesmin PL (mg/L) in secondary metabolite extracts obtained from *in vitro* sequential co-inoculation experiment-2 consisting of liquid cultures inoculated with *Leptosphaeria maculans* only (Lm only), *Leptosphaeria biglobosa* only (Lb only), *L. maculans* & *L. biglobosa* co-inoculated simultaneously (Lm&Lb), initial inoculation with *L. maculans* followed by co-inoculation with *L. biglobosa* sequentially at 1, 3, 5 and 7 days later (Lm+Lb-1, Lm+Lb-3, Lm+Lb-5, Lm+Lb-7), and initial inoculation with *L. biglobosa* followed by co-inoculation with *L. maculans* sequentially at 1, 3, 5 and 7 days later (Lb+Lm-1, Lb+Lm-3, Lb+Lm-5, Lb+Lm-7) at 14 days after the initial inoculation.

Tukey's HSD tests were used to separate the mean concentration of the precursors of sirodesmin PL across different treatments. Columns that do not share a letter are considered significantly different ($P < 0.05$). Error bars show standard error of the mean (SEM) (32 d.f.).

For the treatments Lm only' (414.2 mg/L), 'Lm+Lb-5' (338.9 mg/L), and 'Lm+Lb-7' (361.6 mg/L), there were no significant differences between them. Interestingly, Lm+Lb-3' (165.7 mg/L) treatment was significantly different from all other treatments (Figure C.9).

In experiment 3, at 14 dpi, the concentration of sirodesmin PL was significantly different in different treatments ($F_{10,11}$ = 1148.0, P < 0.001). For the treatments 'Lb only', 'Lm&Lb', 'Lm+Lb-1', 'Lb+Lm-1', 'Lb+Lm-3', 'Lb+Lm-5', 'Lb+Lm-7', there were no significant differences between them, since no production of sirodesmin PL was detected in those treatments. For the treatments 'Lm only' (952.2 mg/L), 'Lm+Lb-5' (765.0 mg/L) and 'Lm+Lb-7' (1031.3 mg/L), there were no significant differences between them. As with the precursors, 'Lm+Lb-3' (371.3 mg/L) treatment was significantly different from all other treatments (Figure C.9).

Effects of sequential co-inoculation on growth of the pathogens

Experiment 1

In experiment 1, at 14 dpi, the percentage of *L. maculans* DNA in total extracted DNA was significantly different in different treatments $F_{10,11}$ = 88.3, P < 0.001. For the treatments 'Lb only' (0.0 %), 'Lm&Lb' (5.0 %), 'Lm+Lb-1' (4.3 %), 'Lb+Lm-1' (0.6 %), 'Lb+Lm-3' (1.4 %), 'Lb+Lm-5' (0.7 %) and 'Lb+Lm-7' (0.4 %), there were no significant differences between them. For the treatments 'Lm only' (100.0 %), 'Lm+Lb-5' (99.3 %), and 'Lm+Lb-7' (97.3 %), there were no significant differences between them. In addition, 'Lm+Lb-3' (60.2 %) treatment was significantly different to all other treatments (Figure C.10).

Experiment 2

In experiment 2, at 14 dpi, the percentage of *L. maculans* DNA in total extracted DNA was significantly different in different treatments $F_{10,22}$ = 223.0, P < 0.001. For the treatments 'Lb only' (0.0 %), 'Lm&Lb' (2.8 %), 'Lm+Lb-1' (9.0 %), 'Lb+Lm-1' (1.7 %), 'Lb+Lm-3' (1.5 %), 'Lb+Lm-5' (1.8 %) and 'Lb+Lm-7' (2.2 %), there were no significant differences between them. For the treatments 'Lm only' (100.0 %), 'Lm+Lb-5' (96.5 %) and 'Lm+Lb-7' (97.4 %), there were no significant differences between them. In addition, 'Lm+Lb-3' (80.9 %) treatment was significantly different to all other treatments (Figure C.10).

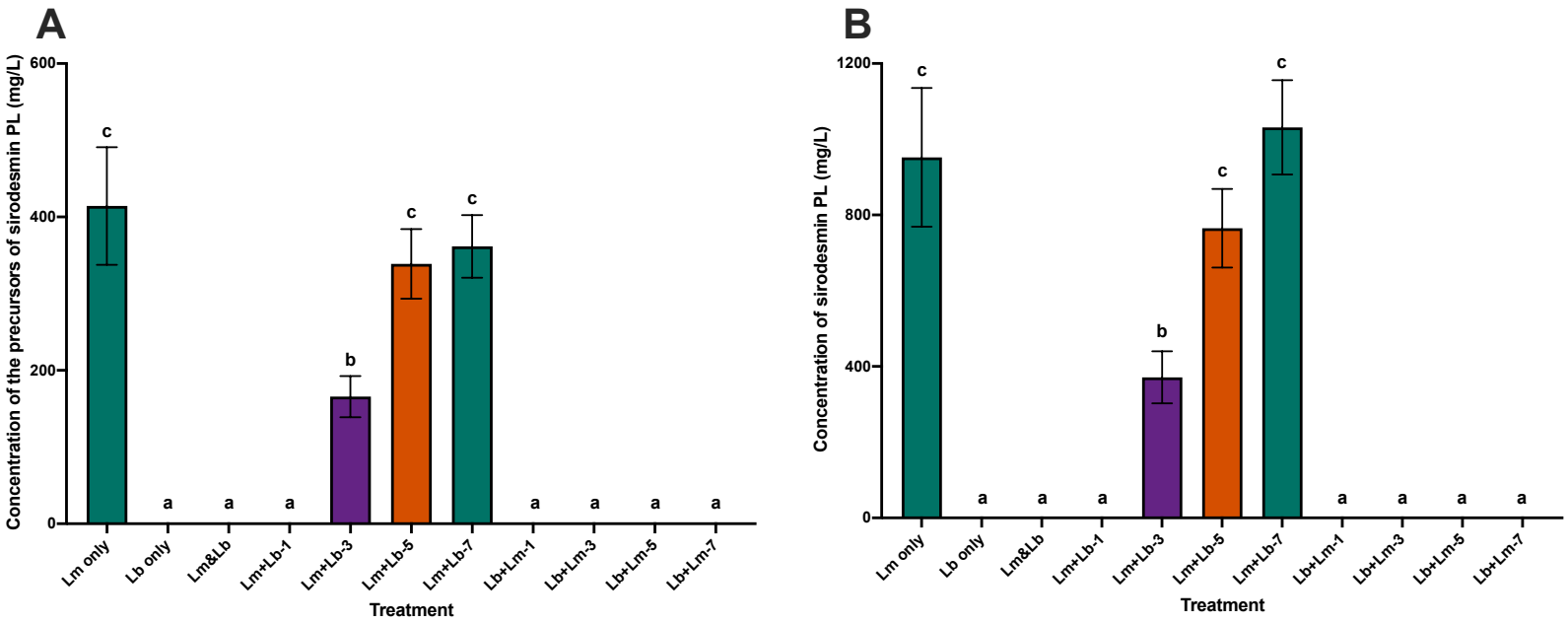

Figure C.9: Concentration of (A) the precursors of sirodesmin PL (mg/L) and (B) sirodesmin PL (mg/L) in secondary metabolite extracts obtained from *in vitro* sequential co-inoculation experiment-3 consisting of liquid cultures inoculated with *Leptosphaeria maculans* only (Lm only), *Leptosphaeria biglobosa* only (Lb only), *L. maculans* & *L. biglobosa* co-inoculated simultaneously (Lm&Lb), initial inoculation with *L. maculans* followed by co-inoculation with *L. biglobosa* sequentially at 1, 3, 5 and 7 days later (Lm+Lb-1, Lm+Lb-3, Lm+Lb-5, Lm+Lb-7), and initial inoculation with *L. biglobosa* followed by co-inoculation with *L. maculans* sequentially at 1, 3, 5 and 7 days later (Lb+Lm-1, Lb+Lm-3, Lb+Lm-5, Lb+Lm-7) at 14 days after the initial inoculation.

Tukey's HSD tests were used to separate the mean concentration of the precursors of sirodesmin PL across different treatments. Columns that do not share a letter are considered significantly different ($P < 0.05$). Error bars show standard error of the mean (SEM) (21 d.f.).

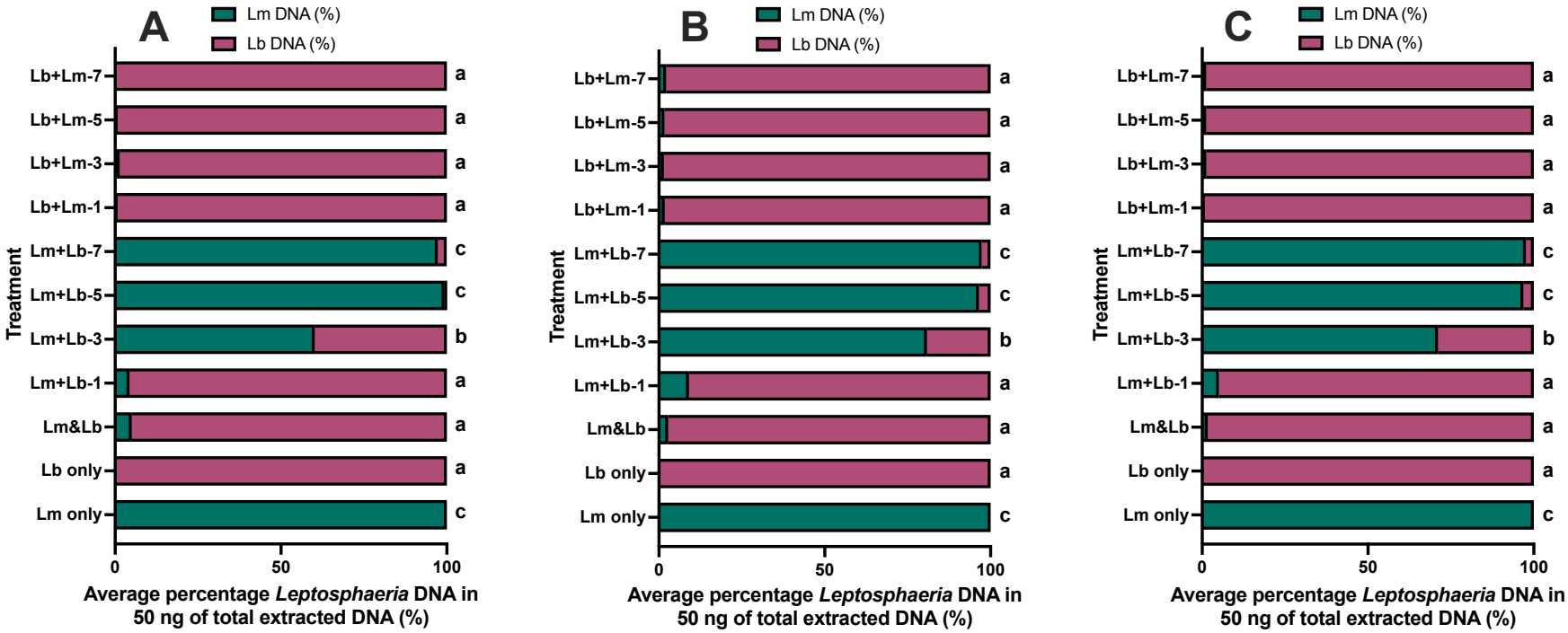

Figure C.10: Percentage of *Leptosphaeria* species DNA (%) in homogenised mycelia obtained from (A) experiment-1, (B) experiment-2, and (C) experiment-3 consisting of liquid cultures inoculated with *Leptosphaeria maculans* only (Lm only), *Leptosphaeria biglobosa* only (Lb only), *L. maculans* & *L. biglobosa* co-inoculated simultaneously (Lm&Lb), initial inoculation with *L. maculans* followed by co-inoculation with *L. biglobosa* sequentially at 1, 3, 5 and 7 days later (Lm+Lb-1, Lm+Lb-3, Lm+Lb-5, Lm+Lb-7), and initial inoculation with *L. biglobosa* followed by co-inoculation with *L. maculans* sequentially at 1, 3, 5 and 7 days later (Lb+Lm-1, Lb+Lm-3, Lb+Lm-5, Lb+Lm-7) at 14 days after the initial inoculation.

Tukey's HSD tests were used to separate the mean percentage of *L. maculans* DNA in total extracted DNA across different treatments. Columns that do not share a letter are considered significantly different ($P < 0.05$) (experiment-1 21 d.f., experiment-2 32 d.f., experiment-3 21 d.f.).

Experiment 3

In experiment 3, at 14 dpi, the percentage of *L. maculans* DNA in total extracted DNA was significantly different in different treatments $F(10,11) = 1173.0$, $P < 0.001$. For the treatments 'Lb only' (0.0 %), 'Lm&Lb' (1.7 %), 'Lm+Lb-1' (5.1 %), 'Lb+Lm-1' (0.7 %), 'Lb+Lm-3' (1.4 %), 'Lb+Lm-5' (1.2 %), and 'Lb+Lm-7' (1.2 %), there were no significant differences between them. For the treatments 'Lm only' (100.0 %), 'Lm+Lb-5' (98.8 %), and 'Lm+Lb-7' (97.7 %), there were no significant differences between them. In addition, 'Lm+Lb-3' (71.1 %) treatment was significantly different to all other treatments (Figure C.10).

8.4 Appendix D – Experimental designs and layouts of experiments in Chapter 4

Layouts of trays for inoculation with different treatments for the *in planta* simultaneous co-inoculation experiment

The experiments were done in a randomised block design, with ten replicates per treatment in each block (Table D.1). The randomisation was done by assigning a number for each treatment group using a random number generator and inoculations were done accordingly. This experiment was done in collaboration with Dr. James Fortune.

Table D.1: Layout of *in planta* simultaneous co-inoculation experiment

Tray 1			
SDW 10 reps	Lm only 10 reps	Lb only 10 reps	Lm&Lb 10 reps
Tray 2			
Lb only 10 reps	Lm&Lb 10 reps	SDW 10 reps	Lm only 10 reps
Tray 3			
Lm&Lb 10 reps	Lb only 10 reps	Lm only 10 reps	SDW 10 reps
Tray 4			
Lm only 10 reps	SDW 10 reps	Lm&Lb 10 reps	Lb only 10 reps

Equipment: Aralab Fitoclima 1200 Growth Cabinet (Aralab, Rio de Mouro, Portugal).

Layouts of trays for inoculation with different treatments for the *in planta* simultaneous and sequential co-inoculation experiments to investigate lesion development and relative growth of the pathogens

The experiments were done in a randomised block design. For the treatments 'Lm only', 'Lb only', 'Lm+Lb-3', 'Lb+Lm-3', 'Lm+Lb-5' and 'Lb+Lm-5', there were five replicates per treatment in three blocks. For the treatments 'Lm+Lb-1' and 'Lb+Lm-1', there were five replicates per treatment in four blocks. For the treatments 'SDW' and 'Lm&Lb', there were fifteen replicates per treatment in one block. The randomisation was done by assigning a number for each treatment group using a random number generator and inoculations were done accordingly (Table D.2).

Table D.2: Layout of *in planta* simultaneous and sequential co-inoculation experiments to investigate lesion development and relative growth of the pathogens

Tray 1							
Lm only 5 reps	Lb only 5 reps	Lm+Lb-1 5 reps	Lb+Lm-1 5 reps	Lm+Lb-3 5 reps	Lb+Lm-3 5 reps	Lm+Lb-5 5 reps	Lb+Lm-5 5 reps
Tray 2							
Lm+Lb-1 5 reps	Lb+Lm-1 5 reps	Lm+Lb-5 5 reps	Lb+Lm-5 5 reps	Lm only 5 reps	Lb only 5 reps	Lm+Lb-3 5 reps	Lb+Lm-3 5 reps
Tray 3							
Lm+Lb-5 5 reps	Lb+Lm-5 5 reps	Lm+Lb-3 5 reps	Lb+Lm-3 5 reps	Lm+Lb-1 5 reps	Lb+Lm-1 5 reps	Lm only 5 reps	Lb only 5 reps
Tray 4							
SDW 15 reps			Lb+Lm-1 5 reps	Lm&Lb 15 reps			Lm+Lb-1 5 reps

Equipment: Conviron Growth Chamber (Conviron, Winnipeg, Manitoba, Canada).

Layouts of trays for inoculation with different treatments for the *in planta* simultaneous and sequential co-inoculation experiments to investigate plant immune responses against co-inoculation by *L. maculans* and *L. biglobosa*

In order to accommodate the sample size required and to avoid mistakes when sampling, the treatments were separated into two groups, and a randomised block design was applied to each group. For the treatments 'SDW', 'Lm only', 'Lb only' and 'Lm&Lb', there were ten replicates per treatment in four blocks. For the treatments 'Lm+Lb-1', 'Lb+Lm-1', 'Lm+Lb-3', 'Lb+Lm-3', 'Lm+Lb-5' and 'Lb+Lm-5', there were ten replicates per treatment in two blocks (Table D.3).

Table D.3: Layout of *in planta* simultaneous and sequential co-inoculation experiments to investigate plant immune responses to against co-inoculation by *L. maculans* and *L. biglobosa*

Tray 1			
SDW 10 reps	Lm only 10 reps	Lb only 10 reps	Lm&Lb 10 reps
Tray 2			
Lm only 10 reps	Lm&Lb 10 reps	SDW 10 reps	Lb only 10 reps
Tray 3			
Lm&Lb 10 reps	Lb only 10 reps	Lm only 10 reps	SDW 10 reps
Tray 4			
Lb only 10 reps	SDW 10 reps	Lm&Lb 10 reps	Lm only 10 reps
Tray 5			
Lm+Lb-1 10 reps	Lb+Lm-1 10 reps	Lm+Lb-5 10 reps	Lb+Lm-5 10 reps
Tray 6			
Lm+Lb-3 10 reps	Lb+Lm-3 10 reps	Lm+Lb-1 10 reps	Lb+Lm-1 10 reps
Tray 7			
Lm+Lb-5 10 reps	Lb+Lm-5 10 reps	Lm+Lb-3 10 reps	Lb+Lm-3 10 reps

Equipment: Aralab Fitoclima 1200 Growth Cabinet (Aralab).

8.5 Appendix E – Recipes of buffers used in DNA extraction protocols

Recipes for spore tape DNA extraction protocol and modified spore tape DNA extraction protocols versions one and two (Huang et al., 2011; Kaczmarek et al., 2009)

Recipe for DNA extraction buffer base (to be activated with 0.1% β-mercaptoethanol before use) – for 500 mL:

- 238 mL of 2X TEN
- 238 mL of Sterilised Distilled Water (SDW)
- 10 g of Polyvinylpyrrolidone (PVP)
- 0.45 g of Phenanthroline
- Allow 30 min – 2 h for solids to dissolve
- Make volume up to 500 mL using SDW if necessary
- Autoclave at 121°C for 15 min

Recipe for 2X TEN – for 500 mL:

- 450 mL of Sterilised Distilled Water (SDW)
- 24.22 g of Tris base
- 9.3 g of $Na_2EDTA2H_2O$
- 14.61 g of NaCl
- Adjust pH to 8.0 using 5 M HCl
- Make volume up to 500 mL using SDW if necessary
- Autoclave at 121°C for 15 min

Recipes for sorbitol pre-wash DNA extraction protocol (Inglis et al., 2018)

Recipe for sorbitol pre-wash buffer base (to be activated with 1% β-mercaptoethanol before use) – for 500 mL:

- 3.03 g of 100 mM Tris-HCl pH 8.0
- 15.9 g of 0.35 M Sorbitol
- 0.47 g of 5 mM EDTA
- 2.5 g of 1% Polyvinylpyrrolidone-40 (PVP-40)
- Make volume up to 500 mL using SDW
- Autoclave at 121°C for 15 min

Recipe for lysis buffer base (to be activated with 1% β-mercaptoethanol before use) – for 500 mL:

- 6.05 g of 0.2 M Tris-HCl pH 8.0
- 4.65 g of 50 mM EDTA
- 29.22 g of 2 M NaCl
- Make volume up to 500 mL using SDW
- Autoclave
- 5 g of 2% Cetyltrimethylammonium bromide (CTAB)
- 2.5 g of 1% Polyvinylpyrrolidone-40 (PVP-40)
- Autoclave at 121°C for 15 min

8.6 Appendix F – Thermocycling profile and standard curves for primer pairs used in gene expression analyses using quantitative polymerase chain reaction (qPCR)

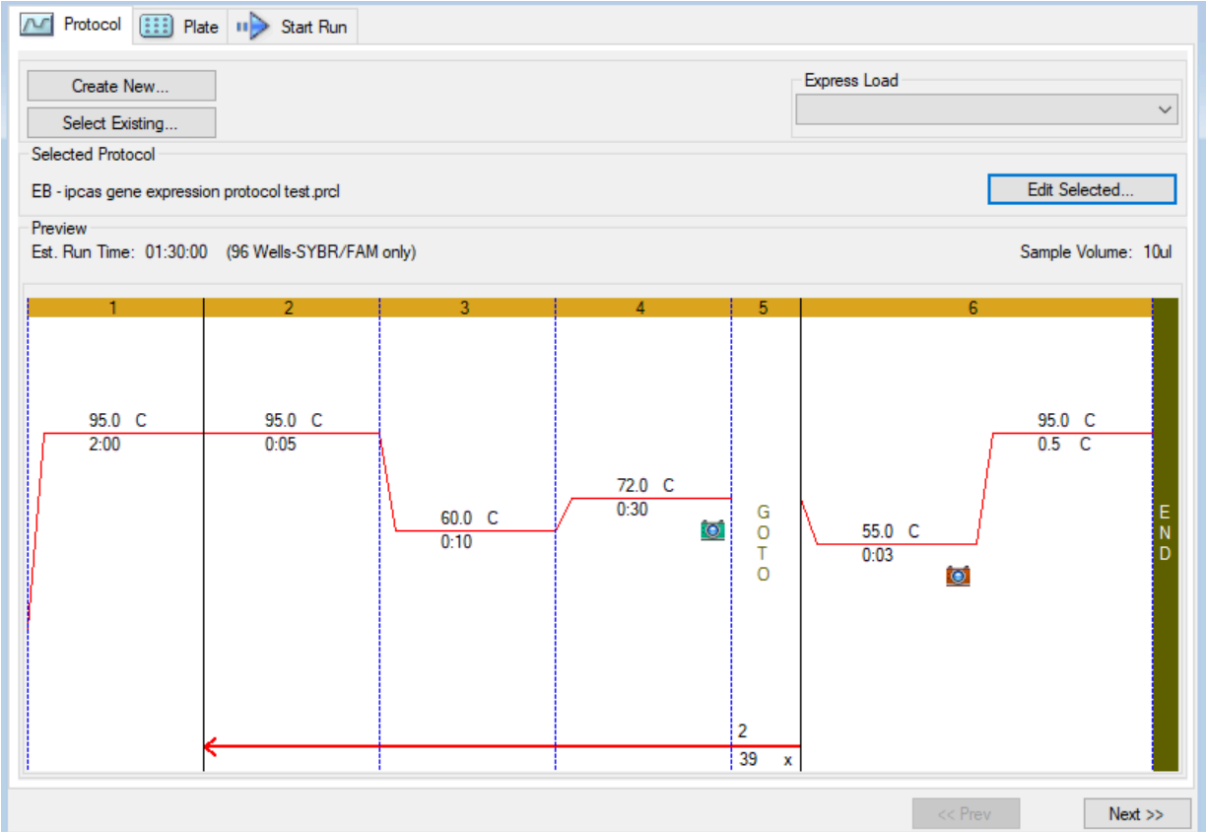

Figure F.1: Thermocycling profile used for all pairs of primers used in gene expression analyses using quantitative polymerase chain reaction (qPCR).

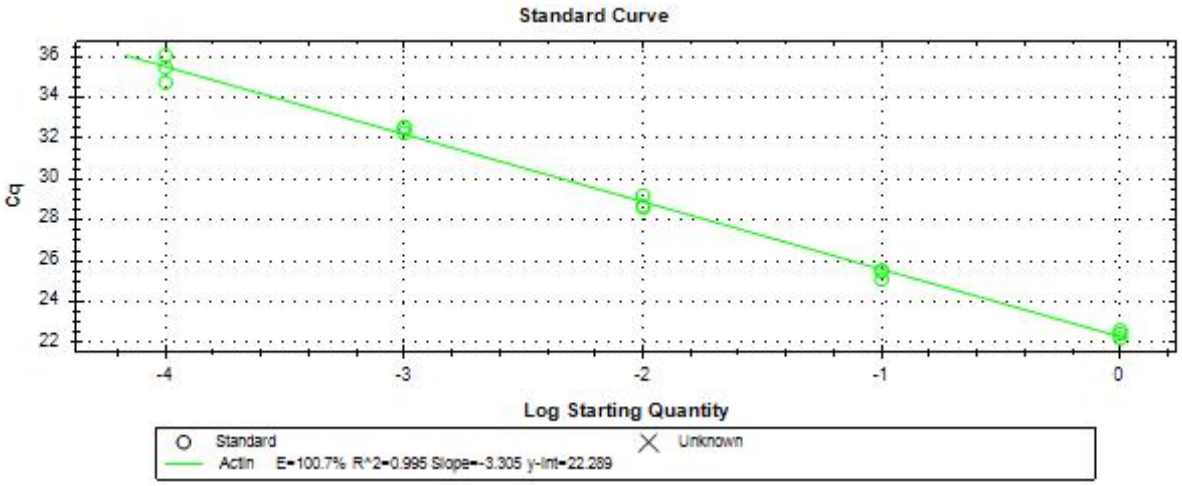

Figure F.2: Standard curve for *Actin* primers used in gene expression analyses.

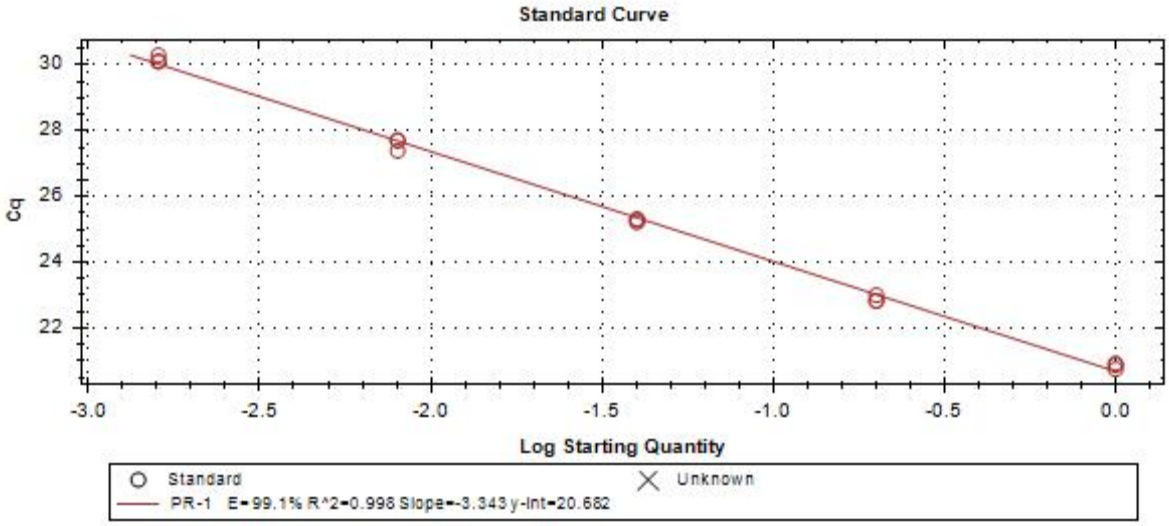

Figure F.3: Standard curve for *PR-1* primers used in gene expression analyses.

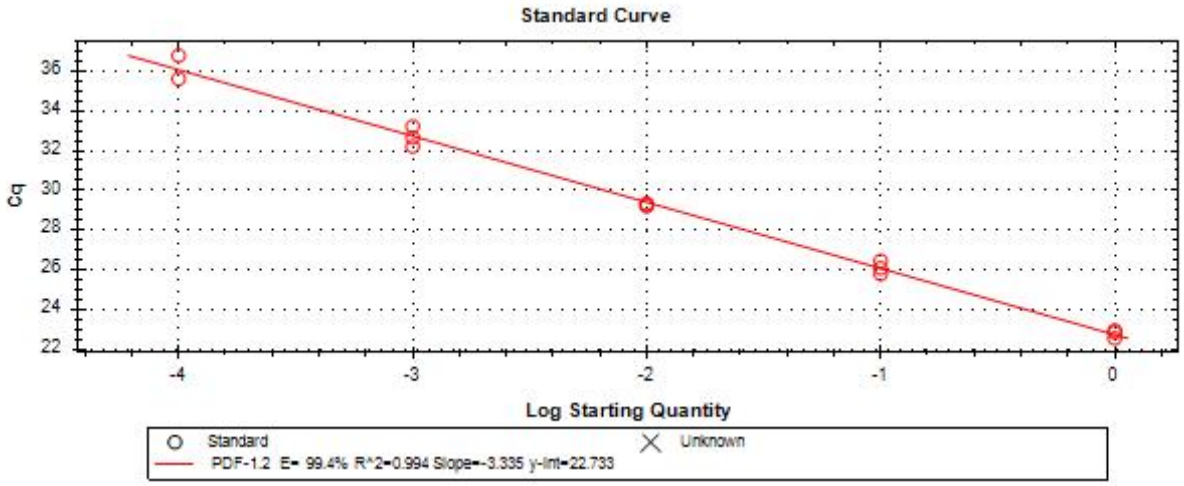

Figure F.4: Standard curve for *PDF-1.2* primers used in gene expression analyses.

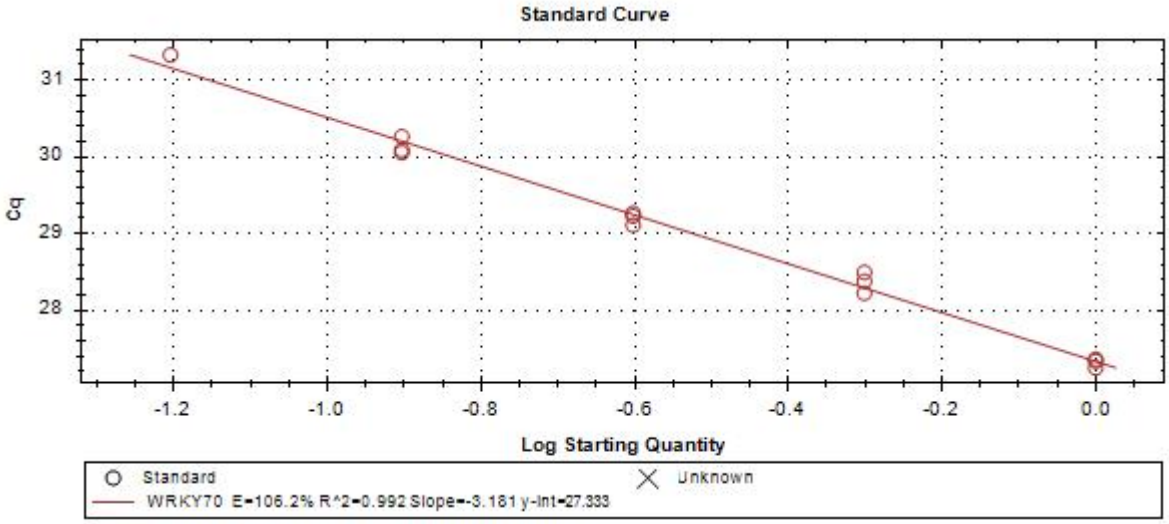

Figure F.5: Standard curve for *WRKY70* primers used in gene expression analyses.

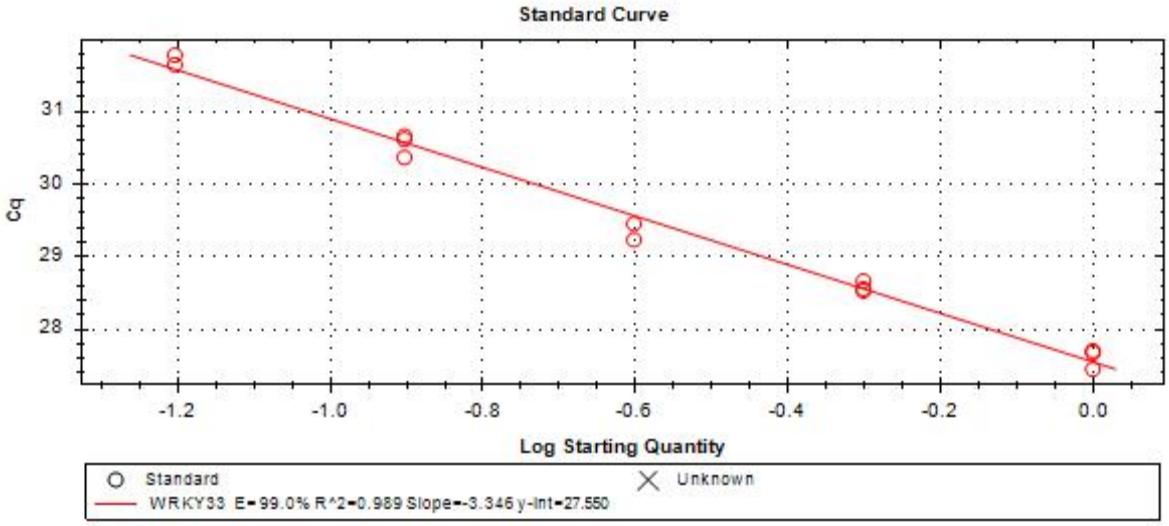

Figure F.6: Standard curve for *WRKY33* primers used in gene expression analyses.

8.7 Appendix G – Individual analyses of experiments in Chapter 4

Effects of simultaneous and sequential co-inoculations on lesion development and phenotype

Experiment 1

In experiment 1, there was no lesion development in 'SDW' control at any time point. For 'Lb only', 'Lm&Lb', 'Lm+Lb-1', 'Lb+Lm-1', 'Lb+Lm-3' and 'Lb+Lm-5', lesion development progressed steadily from 7 dpi to 16 dpi (Figure G.1 B, C, D, G, H, I). Interestingly, despite sharing a similar trend in lesion development with the rest of the treatments in this group, the 'Lm+Lb-1' treatment had smaller lesion areas at all time points. For 'Lm only', 'Lm+Lb-3' and 'Lm+Lb-5', lesion development did not progress significantly between 7 dpi and 10 dpi. However, a rapid increase in lesion area was observed between 10 dpi and 14 dpi for these treatments. The lesions kept expanding rapidly from 14 dpi to 16 dpi (Figure G.1 A, E, F).

Slopes of the fitted simple linear equations were compared to assess the rates of lesion development between the different treatments. There were significant differences in the rates of lesion development between different treatments ($F(9,108) = 22.77$, $P < 0.0001$) (Table G.1). 'SDW' treatment was significantly different from all other treatments, since no lesion development was observed. For the treatments 'Lb only' (0.24), 'Lm&Lb' (0.27), 'Lm+Lb-1' (0.27), 'Lb+Lm-1' (0.27), 'Lb+Lm-3' (0.25) and 'Lb+Lm-5' (0.26), there were no significant differences between them. For the treatments 'Lm only' (0.43), 'Lm+Lb-3' (0.41) and 'Lm+Lb-5' (0.44), there were no significant differences between them (Table G.1).

Experiment 2

In experiment 2, there was no lesion development in the 'SDW' control at any time point. For 'Lb only', 'Lm&Lb', 'Lm+Lb-1', 'Lb+Lm-1', 'Lb+Lm-3' and 'Lb+Lm-5', lesion development progressed steadily from 7 dpi to 16 dpi (Figure G.2 B, C, D, G, H, I). Interestingly, despite sharing a similar trend in lesion development with the rest of the treatments in this group, the 'Lm+Lb-1' treatment had smaller lesion areas at all time points. For 'Lm only', 'Lm+Lb-3' and 'Lm+Lb-5', lesion development did not progress significantly between 7 dpi and 10 dpi. However, a rapid increase in lesion area was observed between 10 dpi and 14 dpi for these treatments. The lesions kept expanding rapidly from 14 dpi to 16 dpi (Figure G.2 A, E, F).

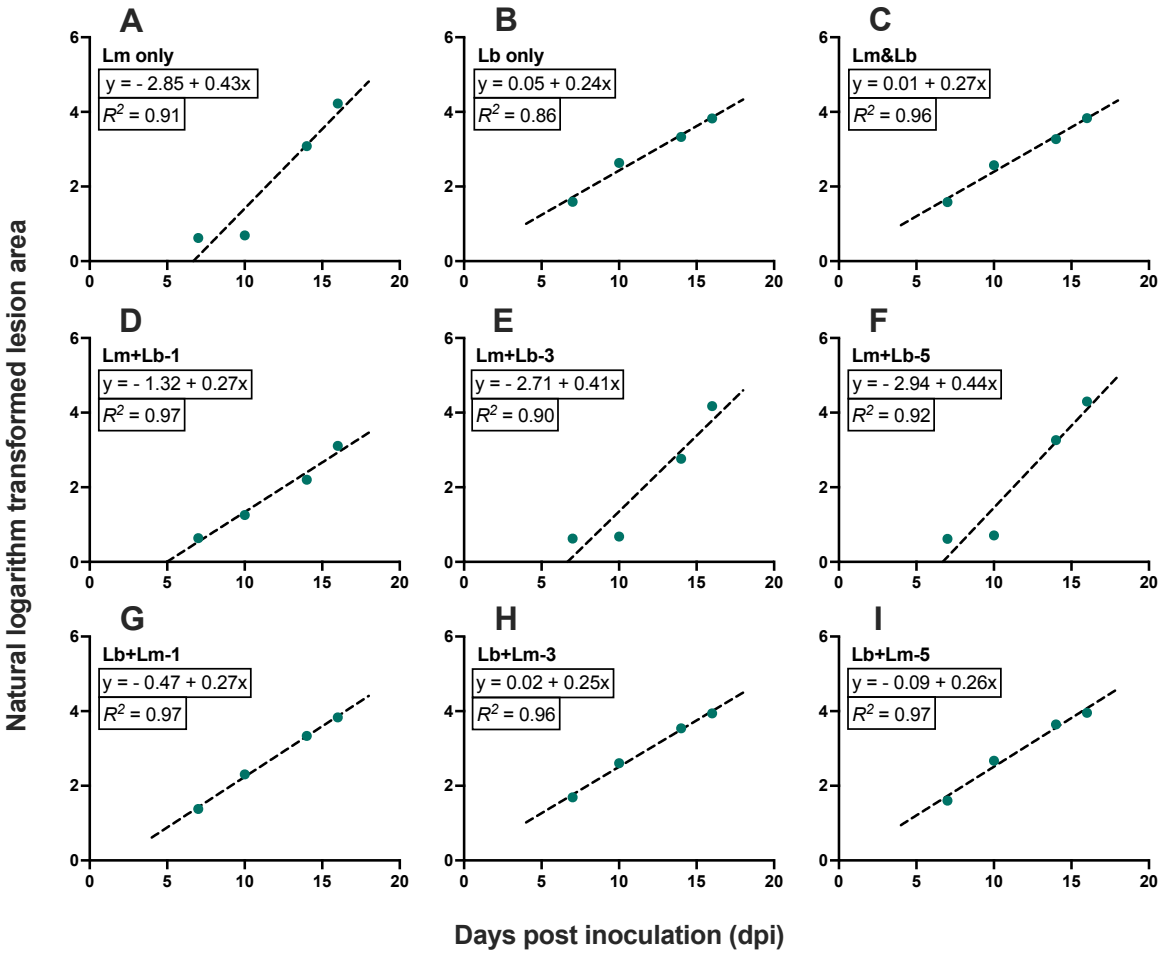

Figure G.1: Simple linear equations (y = a + b*x) showing the relationships between the lesion area (natural logarithm transformed) and days post inoculation (dpi) from experiment-1 for different treatments.

Cotyledons of oilseed rape (*Brassica napus*) cultivar Charger were inoculated with; (A) *Leptosphaeria maculans* only (Lm only), (B) *Leptosphaeria biglobosa* only (Lb only), (C) *L. maculans* & *L. biglobosa* co-inoculated simultaneously (Lm&Lb), (D, E, F) initial inoculation with *L. maculans* followed by co-inoculation with *L. biglobosa* at 1, 3 or 5 days later (Lm+Lb-1, Lm+Lb-3, Lm+Lb-5) and (G, H, I) initial inoculation with *L. biglobosa* followed by co-inoculation with *L. maculans* at 1, 3 or 5 days later (Lb+Lm-1, Lb+Lm-3, Lb+Lm-5). Lesion areas were assessed at 7, 10, 14 and 16 dpi for all treatments (Lm only, Lb only, Lm+Lb-3, Lm+Lb-5, Lb+Lm-3, Lb+Lm-5, n = 12 each) (Lm+Lb-1, Lb+Lm-1, n = 16 each).

Table G.1: The estimated parameter values of intercept (a) and slope (b) in the simple linear equation y = a + b*x fitted to describe the relationship between the natural logarithm transformed lesion area days post inoculation (dpi) from experiment-1 for different treatments.

Cotyledons of oilseed rape (*Brassica napus*) were inoculated with; sterilised distilled water (control), *Leptosphaeria maculans* only (Lm only), *Leptosphaeria biglobosa* only (Lb only), *L. maculans* & *L. biglobosa* co-inoculated simultaneously (Lm&Lb), initial inoculation with *L. maculans* followed by co-inoculation with *L. biglobosa* at 1, 3 or 5 days later (Lm+Lb-1, Lm+Lb-3, Lm+Lb-5) and initial inoculation with *L. biglobosa* followed by co-inoculation with *L. maculans* at 1, 3 or 5 days later (Lb+Lm-1, Lb+Lm-3, Lb+Lm-5). Lesion areas were assessed at 7, 10, 14 and 16 dpi for all treatments. In order to compare the rate of lesion development, line parallel comparisons were done by using Tukey's HSD tests to compare the mean slope values between different treatments. Treatments that do not not share a latter are considered significantly different ($P < 0.05$).

Treatment	Intercept (a)	Slope (b)	Line comparisons
SDW	0.000	0.00	**c**
Lm only	-2.85	0.43	**a**
Lb only	0.05	0.24	**b**
Lm&Lb	0.01	0.27	**b**
Lm+Lb-1	-1.32	0.27	**b**
Lm+Lb-3	-2.71	0.41	**a**
Lm+Lb-5	-2.94	0.44	**a**
Lb+Lm-1	-0.47	0.27	**b**
Lb+Lm-3	0.02	0.25	**b**
Lb+Lm-5	-0.09	0.26	**b**

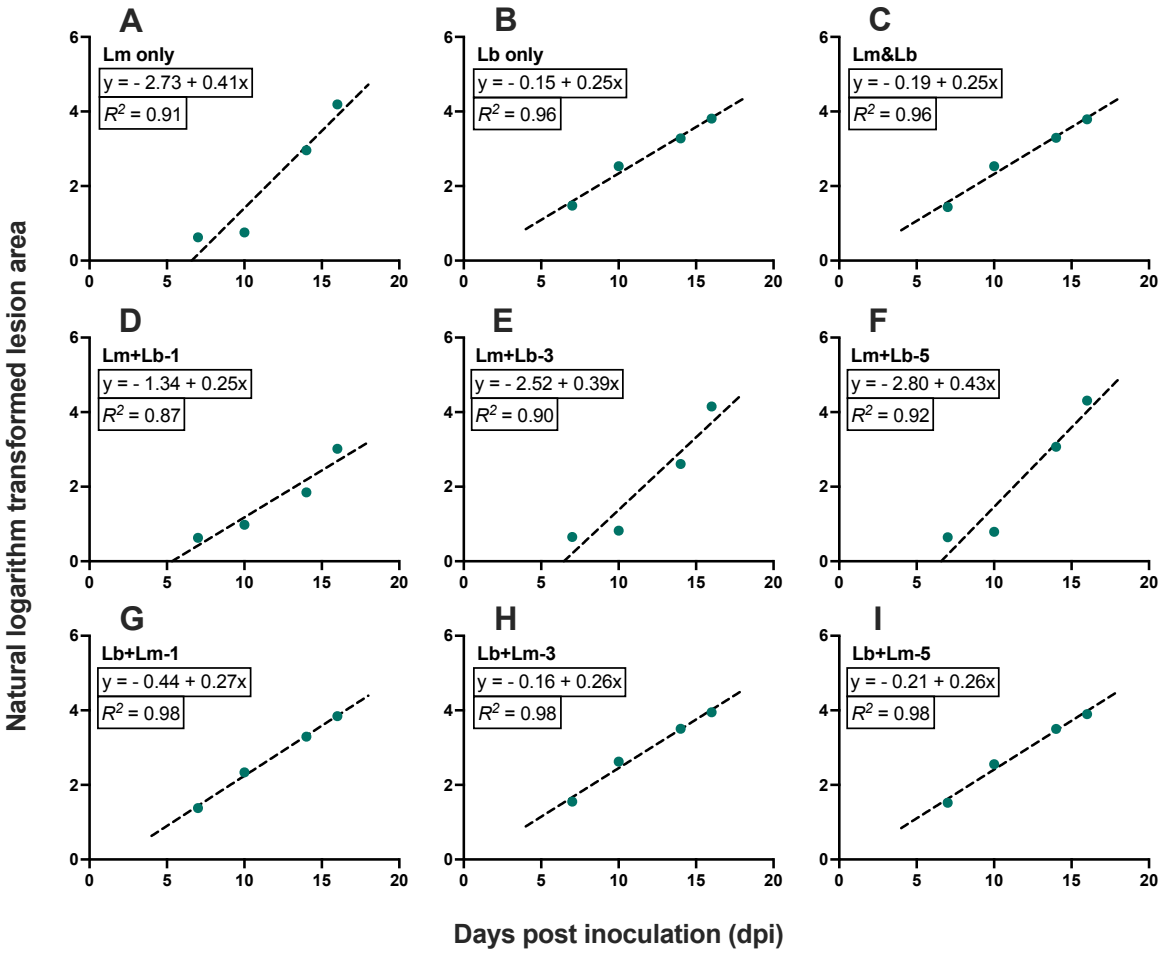

Figure G.2: Simple linear equations (y = a + b*x) showing the relationships between the lesion area (natural logarithm transformed) and days post inoculation (dpi) from experiment-2 for different treatments.

Cotyledons of oilseed rape (*Brassica napus*) cultivar Charger were inoculated with; (A) *Leptosphaeria maculans* only (Lm only), (B) *Leptosphaeria biglobosa* only (Lb only), (C) *L. maculans* & *L. biglobosa* co-inoculated simultaneously (Lm&Lb), (D, E, F) initial inoculation with *L. maculans* followed by co-inoculation with *L. biglobosa* at 1, 3 or 5 days later (Lm+Lb-1, Lm+Lb-3, Lm+Lb-5) and (G, H, I) initial inoculation with *L. biglobosa* followed by co-inoculation with *L. maculans* at 1, 3 or 5 days later (Lb+Lm-1, Lb+Lm-3, Lb+Lm-5). Lesion areas were assessed at 7, 10, 14 and 16 dpi for all treatments (Lm only, Lb only, Lm+Lb-3, Lm+Lb-5, Lb+Lm-3, Lb+Lm-5, n = 12 each) (Lm+Lb-1, Lb+Lm-1, n = 16 each).

Slopes of the fitted simple linear equations were compared to assess the differences in rates of lesion development between the different treatments. There were significant differences in the rates of lesion development between different treatments ($F(9,108) = 21.82$, $P < 0.0001$) (Table G.2). 'SDW' treatment was significantly different to all other treatments, since no lesion development was observed. For the treatments 'Lb only' (0.25), 'Lm&Lb' (0.2515), 'Lm+Lb-1' (0.25), 'Lb+Lm-1' (0.27), 'Lb+Lm-3' (0.26) and 'Lb+Lm-5' (0.2618), there were no significant differences between them. For the treatments 'Lm only' (0.41), 'Lm+Lb-3' (0.39) and 'Lm+Lb-5' (0.43), there were no significant differences between them (Table G.2).

Experiment 1

In experiment 1, at 16 dpi, the average lesion areas were significantly different between different treatments ($F(9,22) = 28.23$ $P < 0.0001$). For the treatments 'Lb only' (45.7 mm^2), 'Lm&Lb' (45.3 mm^2), 'Lb+Lm-1' (45.9 mm^2), 'Lb+Lm-3' (51.0 mm^2) and 'Lb+Lm-5' (51.4 mm^2), there were no significant differences between them. For the treatments 'Lm only' (68.2 mm^2), 'Lm+Lb-3' (64.2 mm^2) and 'Lm+Lb-5' (72.8 mm^2), there were no significant differences between them. Interestingly, 'Lm+Lb-1' (21.6 mm^2) treatment was significantly different to all other treatments (Figure G.3).

Experiment 2

In experiment 2, at 16 dpi, the average lesion areas were significantly different between different treatments ($F(9,22) = 29.21$ $P < 0.0001$). For the treatments 'Lb only' (44.3 mm^2), 'Lm&Lb' (43.6 mm^2), 'Lb+Lm-1' (45.7 mm^2), 'Lb+Lm-3' (51.0 mm^2) and 'Lb+Lm-5' (48.8 mm^2), there were no significant differences between them. For the treatments 'Lm only' (66.1 mm^2), 'Lm+Lb-3' (63.0 mm^2) and 'Lm+Lb-5' (74.1 mm^2), there were no significant differences between them. Interestingly, 'Lm+Lb-1' (19.6 mm^2) treatment was significantly different to all other treatments (Figure G.3).

Table G.2: The estimated parameter values of intercept (a) and slope (b) in the simple linear equation y = a + b*x fitted to describe the relationship between the natural logarithm transformed lesion area days post inoculation (dpi) from experiment-2 for different treatments.

Cotyledons of oilseed rape (*Brassica napus*) were inoculated with; sterilised distilled water (control), *Leptosphaeria maculans* only (Lm only), *Leptosphaeria biglobosa* only (Lb only), *L. maculans* & *L. biglobosa* co-inoculated simultaneously (Lm&Lb), initial inoculation with *L. maculans* followed by co-inoculation with *L. biglobosa* at 1, 3 or 5 days later (Lm+Lb-1, Lm+Lb-3, Lm+Lb-5) and initial inoculation with *L. biglobosa* followed by co-inoculation with *L. maculans* at 1, 3 or 5 days later (Lb+Lm-1, Lb+Lm-3, Lb+Lm-5). Lesion areas were assessed at 7, 10, 14 and 16 dpi for all treatments. In order to compare the rate of lesion development, line parallel comparisons were done by using Tukey's HSD tests to compare the mean slope values between different treatments. Treatments that do not not share a latter are considered significantly different ($P < 0.05$).

Treatment	Intercept (a)	Slope (b)	Line comparisons
SDW	0.00	0.00	**c**
Lm only	-2.73	0.41	**a**
Lb only	-0.15	0.25	**b**
Lm&Lb	-0.19	0.25	**b**
Lm+Lb-1	-1.34	0.25	**b**
Lm+Lb-3	-2.52	0.39	**a**
Lm+Lb-5	-2.81	0.43	**a**
Lb+Lm-1	-0.44	0.27	**b**
Lb+Lm-3	-0.16	0.26	**b**
Lb+Lm-5	-0.21	0.26	**b**

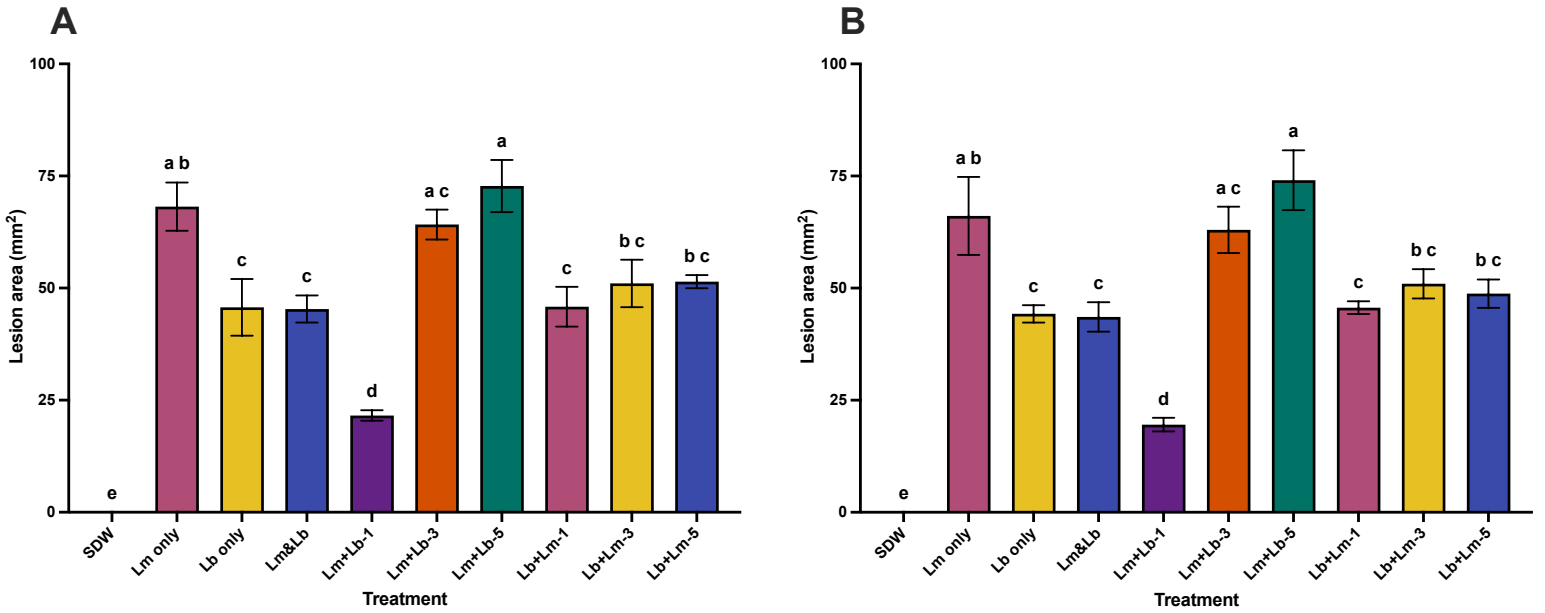

Figure G.3: Average lesion area (mm²) from (A) experiment-1 and (B) experiment-2 for different treatments.

Cotyledons of oilseed rape (*Brassica napus*) were inoculated with; sterilised distilled water (control), *Leptosphaeria maculans* only (Lm only), *Leptosphaeria biglobosa* only (Lb only), *L. maculans* & *L. biglobosa* co-inoculated simultaneously (Lm&Lb), initial inoculation with *L. maculans* followed by co-inoculation with *L. biglobosa* at 1, 3 or 5 days later (Lm+Lb-1, Lm+Lb-3, Lm+Lb-5) and initial inoculation with *L. biglobosa* followed by co-inoculation with *L. maculans* at 1, 3 or 5 days later (Lb+Lm-1, Lb+Lm-3, Lb+Lm-5). Final lesion area was measured at 16 days post inoculation (dpi). Tukey's HSD tests were used to compare the mean lesion area between different treatments. Treatments that do not share a letter are considered significantly different ($P < 0.05$). Error bars show standard error of the mean (SEM) (experiment-1 31 d.f., experiment-2 31 d.f.).

Effects of simultaneous and sequential co-inoculations on pycnidia production on infected cotyledons

Experiment 1

In experiment 1, the average pycnidia density (number of pycnidia/$mm^2 \times 10^{-1}$ area) was significantly different between different treatments ($F(9,20) = 206.8$, $P < 0.0001$). For the treatments 'Lb only', 'Lm&Lb', 'Lm+Lb-1', 'Lb+Lm-1', 'Lb+Lm-3' and 'Lb+Lm-5', there were no significant differences between them. Although there were lesions developed for these treatments, no production of mature pycnidia was observed in microscopic analyses. For the treatments 'Lm only' (37 mature pycnidia/$mm^2 \times 10^{-1}$), 'Lm+Lb-3' (34 mature pycnidia/$mm^2 \times 10^{-1}$) and 'Lm+Lb-5' (35 mature pycnidia/$mm^2 \times 10^{-1}$), there were no significant differences between them (Figure G.4).

Experiment 2

In experiment 2, the average pycnidia density (number of pycnidia/$mm^2 \times 10^{-1}$ area) was significantly different between different treatments. ($F(9,20) = 401.0$, $P < 0.0001$). For the treatments 'Lb only', 'Lm&Lb', 'Lm+Lb-1', 'Lb+Lm-1', 'Lb+Lm-3' and 'Lb+Lm-5', there were no significant differences between them. Although there were lesions developed for these treatments, no production of mature pycnidia was observed in microscopic analyses. For the treatments 'Lm only' (36 mature pycnidia/$mm^2 \times 10^{-1}$), 'Lm+Lb-3' (36 mature pycnidia/$mm^2 \times 10^{-1}$) and 'Lm+Lb-5' (37 mature pycnidia/$mm^2 \times 10^{-1}$), there were no significant differences between them (Figure G.4).

Effects of simultaneous and sequential co-inoculations on relative growth of the pathogens

Experiment 1

In experiment 1, at 19 dpi, the average percentage of *L. maculans* DNA in total DNA of *Leptosphaeria* species extracted from lesions was significantly different between different treatments ($F(8,35) = 8636$, $P < 0.0001$).

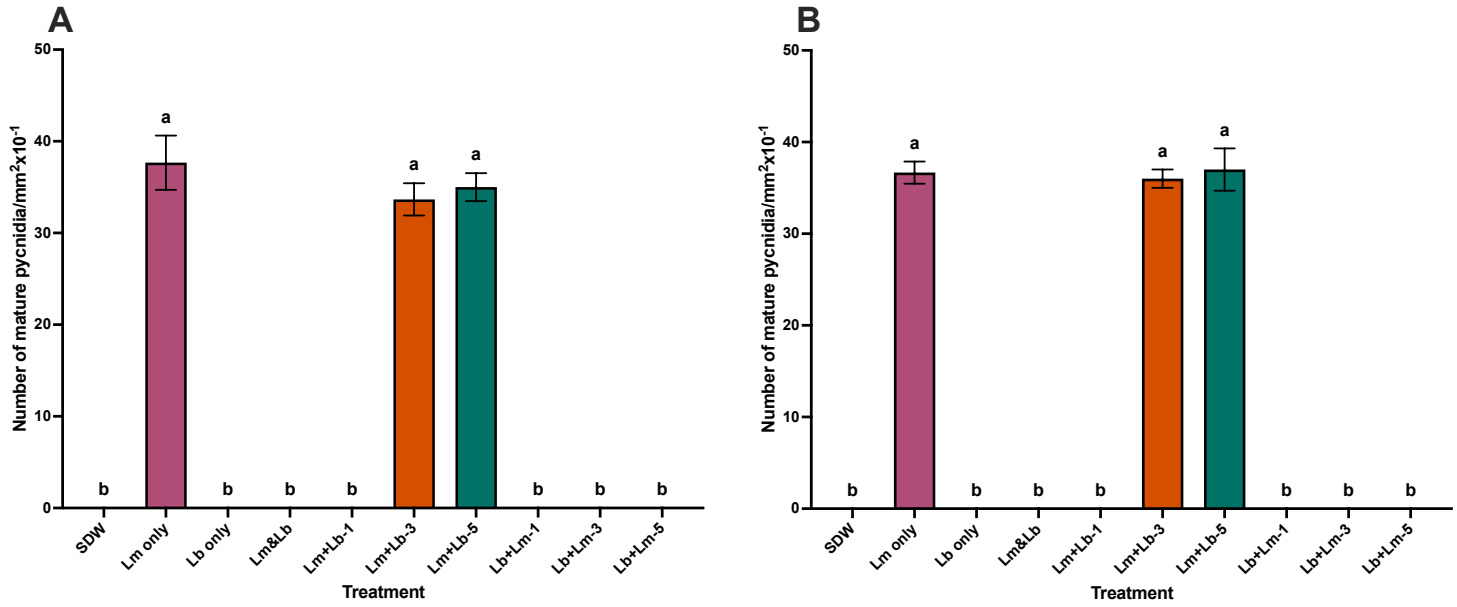

Figure G.4: Average density of pycnidia production (Number of mature pycnidia/mm^2×10^{-1}) from (A) experiment-1 and (B) experiment-2 for different treatments.

Cotyledons of oilseed rape (*Brassica napus*) were inoculated with; sterilised distilled water (control), *Leptosphaeria maculans* only (Lm only), *Leptosphaeria biglobosa* only (Lb only), *L. maculans* & *L. biglobosa* co-inoculated simultaneously (Lm&Lb), initial inoculation with *L. maculans* followed by co-inoculation with *L. biglobosa* at 1, 3 or 5 days later (Lm+Lb-1, Lm+Lb-3, Lm+Lb-5) and initial inoculation with *L. biglobosa* followed by co-inoculation with *L. maculans* at 1, 3 or 5 days later (Lb+Lm-1, Lb+Lm-3, Lb+Lm-5). Cotyledons were removed at 19 days post inoculation (dpi) and incubated at 20°C in darkness for 72 h before microscopic assessment. Tukey's HSD tests were used to compare the mean density of pycnidia production between different treatments. Treatments that do not share a letter are considered significantly different ($P < 0.05$). Error bars show standard error of the mean (SEM)) (experiment-1 29 d.f., experiment-2 29 d.f.).

For the treatments ‘Lb only’ (0.0 %), ‘Lm&Lb’ (1.8 %), ‘Lm+Lb-1’ (1.4 %), ‘Lb+Lm-1’ (1.1 %), ‘Lb+Lm-3’ (1.1 %) and ‘Lb+Lm-5’ (0.6 %), there were no significant differences between them. For the treatments ‘Lm only’ (100.00 %), ‘Lm+Lb-3’ (97.3 %) and ‘Lm+Lb-5’ (98.6 %), there were no significant differences between them (Figure G.5).

Experiment 2

In experiment 2, at 19 dpi, the average percentage of *L. maculans* DNA in total DNA of *Leptosphaeria* species extracted from lesions was significantly different between different treatments ($F(8,35) = 10139$, $P < 0.0001$).

For the treatments ‘Lb only’ (0.0 %), ‘Lm&Lb’ (2.0 %), ‘Lm+Lb-1’ (1.9 %), ‘Lb+Lm-1’ (1.1 %), ‘Lb+Lm-3’ (0.7 %) and ‘Lb+Lm-5’ (0.9 %), there were no significant differences between them. For the treatments ‘Lm only’ (100.00 %), ‘Lm+Lb-3’ (98.3 %) and ‘Lm+Lb-5’ (97.1 %), there were no significant differences between them (Figure G.5).

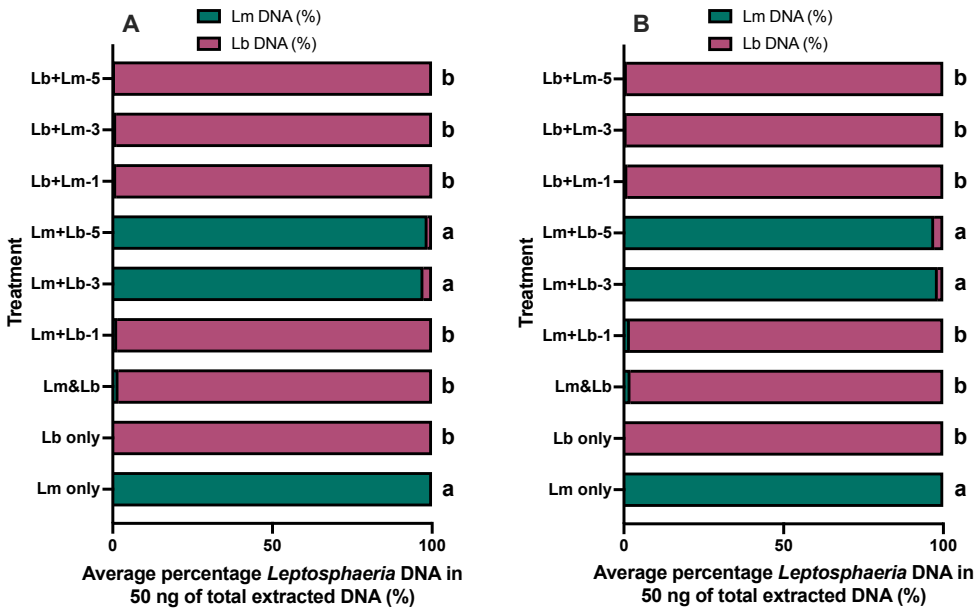

Figure G.5: Average percentage of *Leptosphaeria* species DNA (%) in cotyledons from (A) experiment-1 and (B) experiment-2 for different treatments.

Cotyledons of oilseed rape (*Brassica napus*) were inoculated with; sterilised distilled water (control), *Leptosphaeria maculans* only (Lm only), *Leptosphaeria biglobosa* only (Lb only), *L. maculans* & *L. biglobosa* co-inoculated simultaneously (Lm&Lb), initial inoculation with *L. maculans* followed by co-inoculation with *L. biglobosa* at 1, 3 or 5 days later (Lm+Lb-1, Lm+Lb-3, Lm+Lb-5) and initial inoculation with *L. biglobosa* followed by co-inoculation with *L. maculans* at 1, 3 or 5 days later (Lb+Lm-1, Lb+Lm-3, Lb+Lm-5). Cotyledons were removed at 19 days post inoculation (dpi). Tukey's HSD tests were used to compare the mean percentages of *L. maculans* DNA in total extracted DNA of both *Leptosphaeria* species between different treatments. Treatments that do not share a letter are considered significantly different ($P < 0.05$) (experiment-1 43 d.f., experiment-2 43 d.f.).

Effects of simultaneous and sequential co-inoculations on *Brassica napus* immune responses

Experiment 1 (*PR-1*)

In experiment 1, there were significant differences in relative expression of the *PR-1* gene in different treatments at 2 dpi ($F(3,8) = 247.40$, $P < 0.0001$), 4 dpi ($F(5,12) = 897.50$, $P < 0.0001$) and 6 dpi ($F(5,12) = 249.40$, $P < 0.0001$) (Figure G.6).

All of the remaining treatments were significantly different from each other, with 'Lm&Lb' resulting in the greatest upregulation of this gene, followed by 'Lb only', 'Lm only' and 'SDW', respectively (Figure G.6).

At 4 dpi, for the treatments 'SDW', 'Lm only' and 'Lm+Lb-3', there were no significant differences between them, with all resulting in a very small upregulation. All of the remaining treatments were significantly different from each other, with 'Lb only' resulting in the greatest upregulation of this gene, followed by 'Lm&Lb' and 'Lb+Lm-3', respectively (Figure G.6).

At 6 dpi, for the treatments 'SDW', 'Lm only' and 'Lm+Lb-3', there were no significant differences between them, with all resulting in a very small upregulation. All of the remaining treatments were significantly different from each other, with 'Lm&Lb' resulting in the greatest upregulation of this gene, followed by 'Lb only' and 'Lb+Lm-5', respectively (Figure G.6).

Experiment 2 (*PR-1*)

In experiment 2, there were significant differences in relative expression of the *PR-1* gene in different treatments at 2 dpi ($F(3,8) = 30.19$, $P < 0.0001$), 4 dpi ($F(5,12) = 319.10$, $P < 0.0001$) and 6 dpi ($F(5,12) = 727.50$, $P < 0.0001$) (Figure G.6).

At 2 dpi, 'Lb only' and 'Lm&Lb' resulted in the greatest upregulation of this gene and were not significantly different from each other. 'SDW' and 'Lm only' resulted in a significantly smaller upregulation event and were not significantly different from each other (Figure G.6).

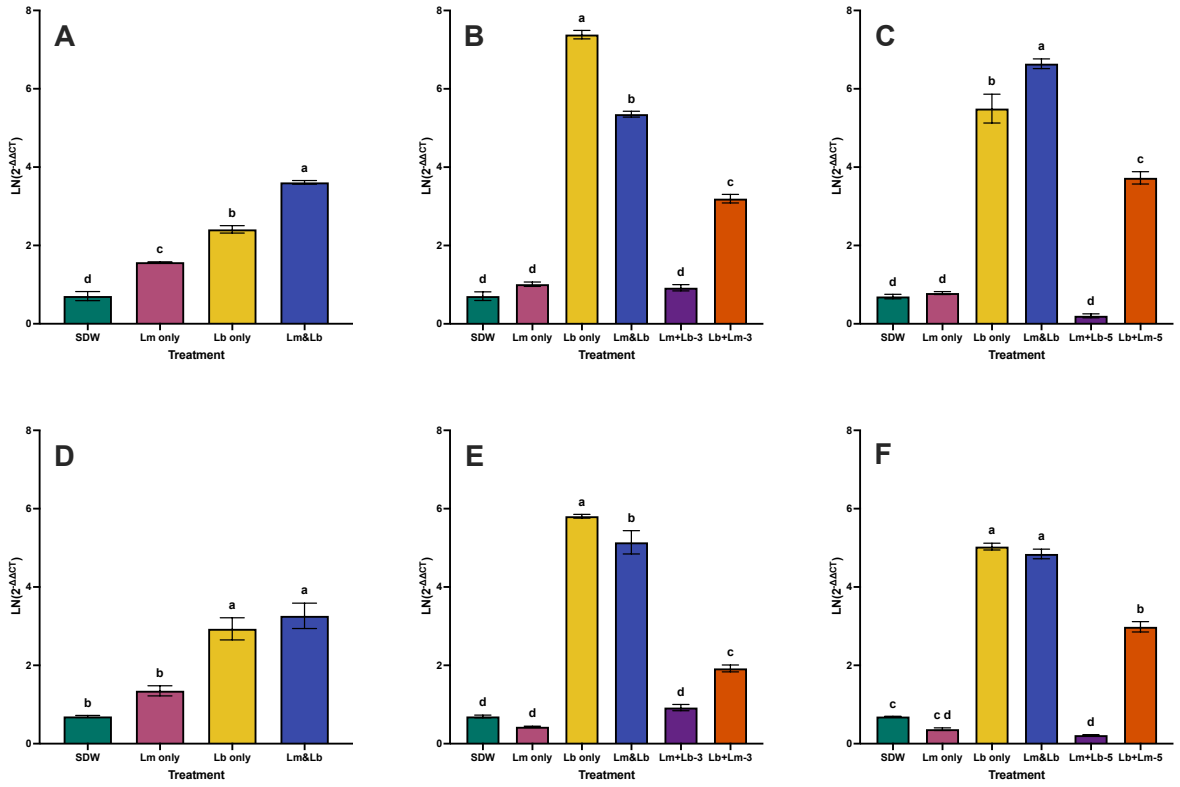

Figure G.6: Relative expression of the *PR-1* gene in cotyledons obtained from experiment-1 (A, B, C) and experiment-2 (D, E, F) consisting of cotyledons of oilseed rape (*Brassica napus*).

Cotyledons were inoculated with Sterilised Distilled Water (SDW) for control, *Leptosphaeria maculans* only (Lm only), *Leptosphaeria biglobosa* only (Lb only), *L. maculans* & *L. biglobosa* co-inoculated simultaneously (Lm&Lb), initial inoculation with *L. maculans* followed by co-inoculation with *L. biglobosa* sequentially at 3 or 5 days later (Lm+Lb-3, Lm+Lb-5) and initial inoculation with *L. biglobosa* followed by sequential co-inoculation with *L. maculans* sequentially at 3 or 5 days later (Lb+Lm-3, Lb+Lm-5) at (A, D) 2 days post inoculation (dpi), (B, E) 4 dpi and (C, F) 6 dpi. Tukey's HSD tests were used to separate the mean relative expression of the *PR-1* gene in across different treatments. Columns that do not share a letter are considered significantly different ($P < 0.05$). Error bars show standard error of the mean (SEM) (experiment-1: 2 dpi 11 d.f., 4 dpi 17 d.f., 6 dpi 17 d.f.) (experiment-2: 2 dpi 11 d.f., 4 dpi 17 d.f., 6 dpi 17 d.f.).

At 4 dpi, for the treatments ‘SDW’, ‘Lm only’ and ‘Lm+Lb-3’, there were no significant differences between them, with all resulting in a very small upregulation. All of the remaining treatments were significantly different from each other, with ‘Lb only’ resulting in the greatest upregulation of this gene, followed by ‘Lm&Lb’ and ‘Lb+Lm-3’, respectively (Figure G.6).

At 6 dpi, ‘Lb only’ and ‘Lm&Lb’ resulted in the greatest upregulation of this gene and were not significantly different from each other. This was followed by ‘Lb+Lm-5’, which was significantly greater than the other treatments except ‘Lb only’ and ‘Lm&Lb’. ‘Lm+Lb-5’ was significantly smaller than ‘SDW’, but not significantly different to ‘Lm only’. ‘SDW’ and ‘Lm only’ were also not significantly different (Figure G.6).

Experiment 1 (*PDF-1.2*)

In experiment 1, there were significant differences in relative expression of the *PDF-1.2* gene in different treatments at 2 dpi ($F(3,8) = 21.55$, $P < 0.001$), 4 dpi ($F(5,12) = 48.00$, $P < 0.0001$) and 6 dpi ($F(5,12) = 27.62$, $P < 0.0001$) (Figure G.7).

At 2 dpi, ‘SDW’ resulted in the greatest upregulation of this gene, followed by ‘Lb only’, which was not significantly different to ‘Lm only’ but was significantly greater than ‘Lm&Lb’ (Figure G.7).

At 4 dpi, ‘Lm+Lb-3’ resulted in the greatest upregulation of this gene and was significantly greater than any other treatment. This was followed by ‘Lb+Lm-3’, which was not significantly different to ‘SDW’. ‘SDW’ was not significantly different to ‘Lm only’, ‘Lb only’ and ‘Lm&Lb’ (Figure G.7).

At 6 dpi, ‘Lb+Lm-5’ resulted in the greatest upregulation of this gene and was significantly greater than any other treatment. This was followed by ‘Lm only’, ‘Lm&Lb’ and ‘Lm+Lb-5’, which were not significantly different from each other. ‘SDW’ and ‘Lb only’ were significantly smaller than the rest of the treatments, but not significantly different to each other (Figure G.7).

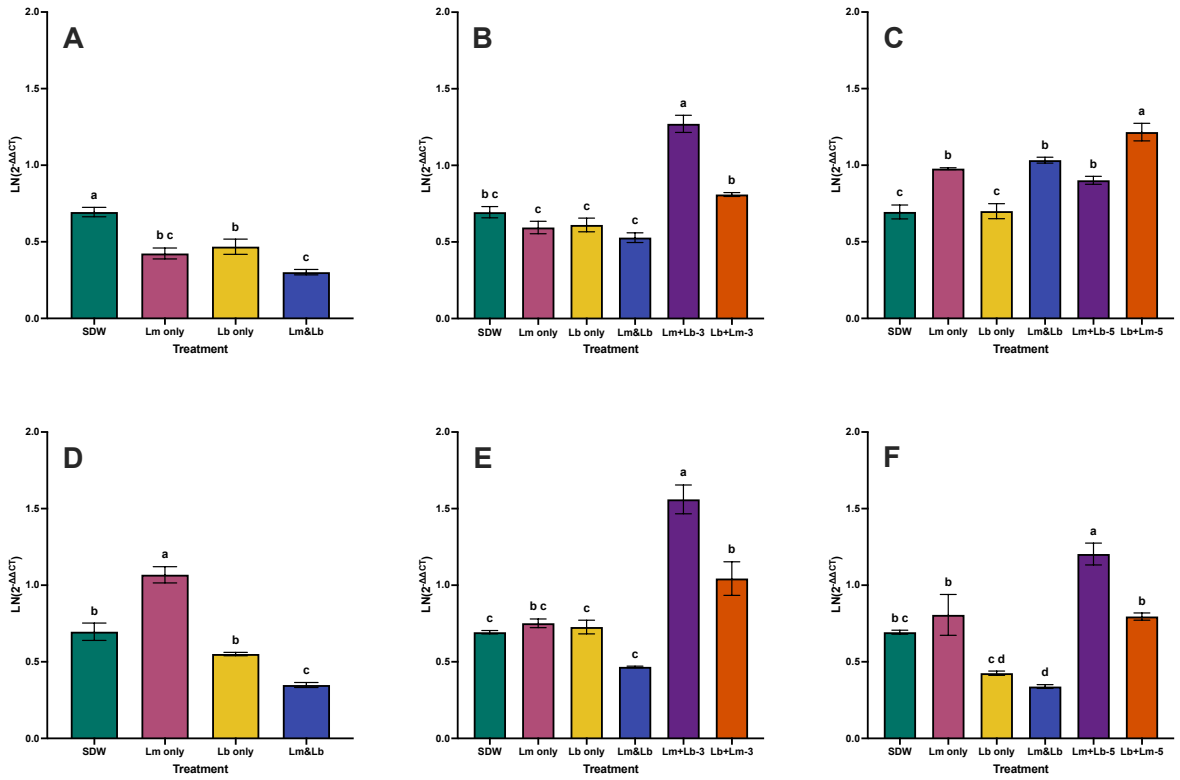

Figure G.7: Relative expression of the *PDF-1.2* gene in cotyledons obtained from experiment-1 (A, B, C) and experiment-2 (D, E, F) consisting of cotyledons of oilseed rape (*Brassica napus*).

Cotyledons were inoculated with Sterilised Distilled Water (SDW) for control, *Leptosphaeria maculans* only (Lm only), *Leptosphaeria biglobosa* only (Lb only), *L. maculans* & *L. biglobosa* co-inoculated simultaneously (Lm&Lb), initial inoculation with *L. maculans* followed by co-inoculation with *L. biglobosa* sequentially at 3 or 5 days later (Lm+Lb-3, Lm+Lb-5) and initial inoculation with *L. biglobosa* followed by sequential co-inoculation with *L. maculans* sequentially at 3 or 5 days later (Lb+Lm-3, Lb+Lm-5) at (A, D) 2 days post inoculation (dpi), (B, E) 4 dpi and (C, F) 6 dpi. Tukey's HSD tests were used to separate the mean relative expression of the *PDF-1.2* gene in across different treatments. Columns that do not share a letter are considered significantly different ($P < 0.05$). Error bars show standard error of the mean (SEM) (experiment-1: 2 dpi 11 d.f., 4 dpi 17 d.f., 6 dpi 17 d.f.) (experiment-2: 2 dpi 11 d.f., 4 dpi 17 d.f., 6 dpi 17 d.f.).

Experiment 2 (*PDF-1.2*)

In experiment 2, there were significant differences in relative expression of the *PDF-1.2* gene in different treatments at 2 dpi ($F(3,8) = 57.89$, $P < 0.0001$), 4 dpi ($F(5,12) = 37.09$, $P < 0.0001$) and 6 dpi ($F(5,12) = 24.08$, $P < 0.0001$) (Figure G.7).

At 2 dpi, 'Lm only' resulted in the greatest upregulation of this gene and was significantly greater than any other treatment. This was followed by 'Lb only' and 'SDW', which were significantly greater than 'Lm&Lb' (Figure G.7).

At 4 dpi, 'Lm+Lb-3' resulted in the greatest upregulation of this gene and was significantly greater than any other treatment. This was followed by 'Lb+Lm-3', which was not significantly different to 'Lm only'. 'Lm only' was not significantly different to 'SDW', 'Lb only' and 'Lm&Lb' (Figure G.7).

At 6 dpi, 'Lm+Lb-5' resulted in the greatest upregulation of this gene and was significantly greater than any other treatment. This was followed by 'Lm only' and 'Lb+Lm-5', which were not significantly different to 'SDW'. 'SDW' was significantly greater than 'Lm&Lb', but not significantly different to 'Lb only'. 'Lb only' was not significantly different to 'Lm&Lb' (Figure G.7).

Experiment 1 (*WRKY70*)

In experiment 1, there were significant differences in relative expression of the *WRKY70* gene in different treatments at 2 dpi ($F(3,8) = 21.03$, $P < 0.001$), 4 dpi ($F(5,12) = 79.01$, $P < 0.0001$) and 6 dpi ($F(5,12) = 231.20$, $P < 0.0001$) (Figure G.8).

At 2 dpi, 'Lb only' resulted in the greatest upregulation of this gene and was greater than any other treatment. 'SDW', 'Lm only' and 'Lm&Lb' were not significantly different from each other (Figure G.8).

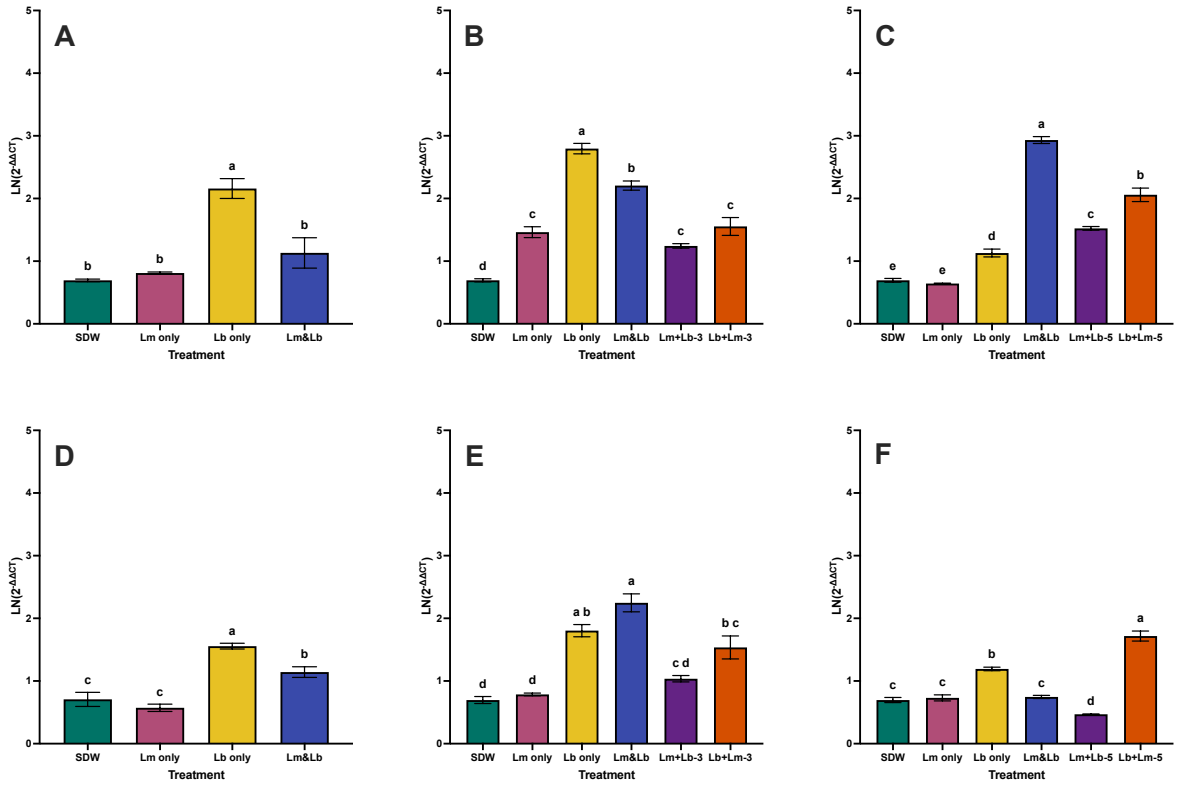

Figure G.8: Relative expression of the *WRKY70* gene in cotyledons obtained from experiment-1 (A, B, C) and experiment-2 (D, E, F) consisting of cotyledons of oilseed rape (*Brassica napus*).

Cotyledons were inoculated with Sterilised Distilled Water (SDW) for control, *Leptosphaeria maculans* only (Lm only), *Leptosphaeria biglobosa* only (Lb only), *L. maculans* & *L. biglobosa* co-inoculated simultaneously (Lm&Lb), initial inoculation with *L. maculans* followed by co-inoculation with *L. biglobosa* sequentially at 3 or 5 days later (Lm+Lb-3, Lm+Lb-5) and initial inoculation with *L. biglobosa* followed by sequential co-inoculation with *L. maculans* sequentially at 3 or 5 days later (Lb+Lm-3, Lb+Lm-5) at (A, D) 2 days post inoculation (dpi), (B, E) 4 dpi and (C, F) 6 dpi. Tukey's HSD tests were used to separate the mean relative expression of the *WRKY70* gene in across different treatments. Columns that do not share a letter are considered significantly different ($P < 0.05$). Error bars show standard error of the mean (SEM) (experiment-1: 2 dpi 11 d.f., 4 dpi 17 d.f., 6 dpi 17 d.f.) (experiment-2: 2 dpi 11 d.f., 4 dpi 17 d.f., 6 dpi 17 d.f.).

At 4 dpi, ‘Lb only’ resulted in the greatest upregulation of this gene and was significantly greater than any other treatment. This was followed by ‘Lm&Lb’, which was significantly greater than the rest of the treatments except ‘Lb only’. ‘Lm only’, ‘Lm+Lb-3’ and ‘Lb+Lm-3’ were not significantly different to each other. ‘SDW’ was significantly smaller than any other treatment (Figure G.8).

At 6 dpi, ‘Lm&Lb’ resulted in the greatest upregulation of this gene and was significantly greater than any other treatment. This was followed by ‘Lb+Lm-5’, ‘Lm+Lb-5’ and ‘Lb only’ respectively, with all being significantly different from each other. ‘SDW’ and ‘Lm only’ were significantly smaller than the rest of the treatments but were not significantly different from each other (Figure G.8).

Experiment 2 (*WRKY70*)

In experiment 2, there were significant differences in relative expression of the *WRKY70* gene in different treatments at 2 dpi ($F(3,8) = 31.10$, $P < 0.0001$), 4 dpi ($F(5,12) = 32.28$, $P < 0.0001$) and 6 dpi ($F(5,12) = 104.40$, $P < 0.0001$) (Figure G.8).

At 2 dpi, ‘Lb only’ resulted in the greatest upregulation of this gene and was significantly greater than any other treatment. This was followed by ‘Lm&Lb’, which was significantly greater than ‘SDW’ and ‘Lm only’, which were not significantly different from each other (Figure G.8).

At 4 dpi, ‘Lm&Lb’ resulted in the greatest upregulation of this gene and was not significantly different to ‘Lb only’. ‘Lb only’ was not significantly different to ‘Lb+Lm-3’, but was significantly greater than the rest of the treatments. ‘Lb+Lm-3’ was not significantly different to ‘Lm+Lb-3’. ‘Lm+Lb-3’’ was not significantly different to ‘SDW’ and ‘Lm only’ (Figure G.8).

At 6 dpi, ‘Lb+Lm-5’ resulted in the greatest upregulation of this gene and was significantly greater than any other treatment. This was followed by ‘Lb only’, which was greater than the other treatments except ‘Lb+Lm-5’. ‘SDW’, ‘Lm only’ and ‘Lm&Lb’ were not significantly different from each other. ‘Lm+Lb-5’ was significantly smaller than any other treatment (Figure G.8).

Experiment 1 (*WRKY33*)

In experiment 1, there were significant differences in relative expression of the *WRKY33* gene in different treatments at 2 dpi ($F(3,8) = 266.90$, $P < 0.0001$), 4 dpi ($F(5,12) = 198.90$, $P < 0.0001$) and 6 dpi ($F(5,12) = 330.20$, $P < 0.0001$) (Figure G.9).

At 2 dpi, 'Lb only' resulted in the greatest upregulation of this gene and was significantly greater than any other treatment. This was followed by 'Lm&Lb', which was significantly greater than 'SDW' and 'Lm only'. 'Lm only' was significantly greater than 'SDW' (Figure G.9).

At 4 dpi, 'Lb+Lm-3' resulted in the greatest upregulation of this gene and was significantly greater than any other treatment. This was followed by 'Lb only' and 'Lm+Lb-3', which were not significantly different from each other. 'Lm+Lb-3' was not significantly different to 'Lm&Lb'. 'SDW' and 'Lm only' were significantly smaller than the rest of the treatments but were not significantly different from each other (Figure G.9).

At 6 dpi, 'Lb+Lm-5' resulted in the greatest upregulation of this gene and was significantly greater than any other treatment. This was followed by 'Lm+Lb-5', which was significantly greater than the rest of the treatments. 'Lm only', 'Lb only' and 'Lm&Lb' were significantly smaller than 'Lm+Lb-5' but were not significantly different from each other. 'SDW' was significantly smaller than any other treatment (Figure G.9).

Experiment 2 (*WRKY33*)

In experiment 2, there were significant differences in relative expression of the *WRKY33* gene in different treatments at 2 dpi ($F(3,8) = 126.40$, $P < 0.0001$), 4 dpi ($F(5,12) = 324.70$, $P < 0.0001$) and 6 dpi ($F(5,12) = 83.51$, $P < 0.0001$) (Figure G.9).

At 2 dpi, 'Lb only' resulted in the greatest upregulation of this gene and was significantly greater than any other treatment. This was followed by 'SDW' and 'Lm only', which were not significantly different from each other but significantly greater than 'Lm&Lb' (Figure G.9).

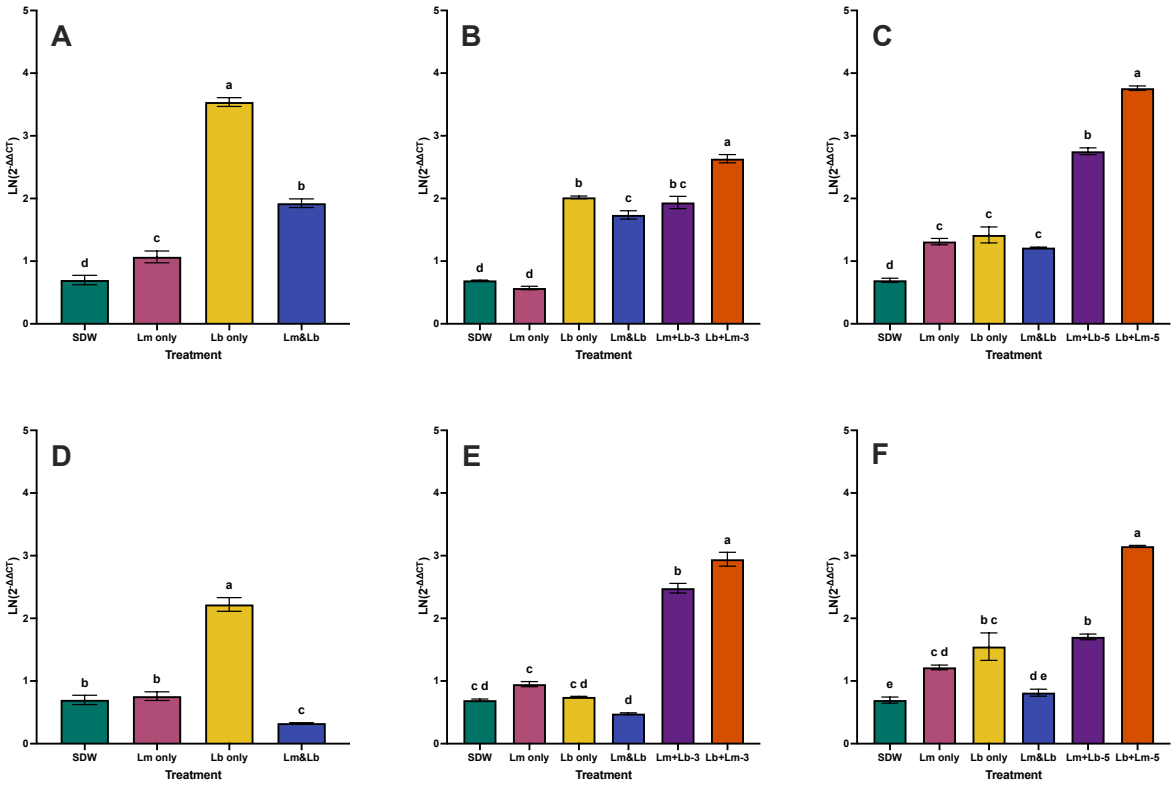

Figure G.9: Relative expression of the *WRKY33* gene in cotyledons obtained from experiment-1 (A, B, C) and experiment-2 (D, E, F) consisting of cotyledons of oilseed rape (*Brassica napus*).

Cotyledons were inoculated with Sterilised Distilled Water (SDW) for control, *Leptosphaeria maculans* only (Lm only), *Leptosphaeria biglobosa* only (Lb only), *L. maculans* & *L. biglobosa* co-inoculated simultaneously (Lm&Lb), initial inoculation with *L. maculans* followed by co-inoculation with *L. biglobosa* sequentially at 3 or 5 days later (Lm+Lb-3, Lm+Lb-5) and initial inoculation with *L. biglobosa* followed by sequential co-inoculation with *L. maculans* sequentially at 3 or 5 days later (Lb+Lm-3, Lb+Lm-5) at (A, D) 2 days post inoculation (dpi), (B, E) 4 dpi and (C, F) 6 dpi. Tukey's HSD tests were used to separate the mean relative expression of the *WRKY33* gene in across different treatments. Columns that do not share a letter are considered significantly different ($P < 0.05$). Error bars show standard error of the mean (SEM) (experiment-1: 2 dpi 11 d.f., 4 dpi 17 d.f., 6 dpi 17 d.f.) (experiment-2: 2 dpi 17 d.f., 4 dpi 17 d.f., 6 dpi 17 d.f.).

At 4 dpi, ‘Lb+Lm-3’ resulted in the greatest upregulation of this gene and was significantly greater than any other treatment. This was followed by ‘Lm+Lb-3’, which was greater than the rest of the treatments. ‘Lm only’ was significantly greater than ‘Lm&Lb’ but not significantly different to ‘SDW’ and ‘Lb only’. ‘SDW’ and ‘Lb only’ were not significantly different to ‘Lm&Lb’ (Figure G.9).

At 6 dpi, ‘Lb+Lm-5’ resulted in the greatest upregulation of this gene and was significantly greater than any other treatment. This was followed by ‘Lm+Lb-5’ and ‘Lb only’, which were not significantly different from each other. ‘Lb only’ was not significantly different to ‘Lm only’. ‘Lm only’ was not significantly different to ‘Lm&Lb’. ‘Lm&Lb’ was not significantly different to ‘SDW’ (Figure G.9).

8.8 Appendix H – Layouts of field experiments in Chapter 5

Layout of field experiment at Rothamsted Research at Harpenden, Hertfordshire in the 2023/2024 growing season

Catana	1	Campus (CMP)	2
Kromerska (KRM)	4	Apex (APX)	3
Acacia	5	Rocket (RKT)	6
Yudal (YDL)	8	POH Bolko (POB)	7
Castille (CST)	9	Kielder (KLD)	10
Rocket (RKT)	12	Kielder (KLD)	11
Yudal (YDL)	13	Acacia	14
Campus (CMP)	16	POH Bolko (POB)	15
Apex (APX)	17	Catana	18
Castille (CST)	20	Kromerska (KRM)	19
Castille (CST)	21	Yudal (YDL)	22
Acacia	24	Catana	23
Campus (CMP)	25	Apex (APX)	26
Kielder (KLD)	28	Rocket (RKT)	27
POH Bolko (POB)	29	Kromerska (KRM)	30
Kromerska (KRM)	32	Campus (CMP)	31
Yudal (YDL)	33	Castille (CST)	34
POH Bolko (POB)	36	Acacia	35
Rocket (RKT)	37	Kielder (KLD)	38
Catana	40	Apex (APX)	39
Rocket (RKT)	41	Kromerska (KRM)	42
Campus (CMP)	44	Kielder (KLD)	43
Apex (APX)	45	POH Bolko (POB)	46
Yudal (YDL)	48	Castille (CST)	47
Acacia	49	Catana	50

Layout of field experiment at Rothamsted Research at Harpenden, Hertfordshire in the 2024/2025 growing season

Rocket (RKT)	1	Acacia	2
Kromerska (KRM)	4	Campus (CMP)	3
Apex (APX)	5	Castille (CST)	6
Catana	8	POH Bolko (POB)	7
Yudal (YDL)	9	Kielder (KLD)	10
Yudal (YDL)	12	Acacia	11
Kielder (KLD)	13	Kromerska (KRM)	14
Apex (APX)	16	Catana	15
Campus (CMP)	17	POH Bolko (POB)	18
Castille (CST)	20	Rocket (RKT)	19
Yudal (YDL)	21	Catana	22
POH Bolko (POB)	24	Acacia	23
Apex (APX)	25	Castille (CST)	26
Rocket (RKT)	28	Campus (CMP)	27
Kromerska (KRM)	29	Kielder (KLD)	30
Yudal (YDL)	32	Kromerska (KRM)	31
Acacia	33	Catana	34
Apex (APX)	36	Castille (CST)	35
Rocket (RKT)	37	Kielder (KLD)	38
Campus (CMP)	40	POH Bolko (POB)	39
POH Bolko (POB)	41	Campus (CMP)	42
Apex (APX)	44	Kielder (KLD)	43
Kromerska (KRM)	45	Castille (CST)	46
Catana	48	Yudal (YDL)	47
Acacia	49	Rocket (RKT)	50

Layout of field experiment at John Innes Centre at Norwich, Norfolk in the 2023/2024 growing season

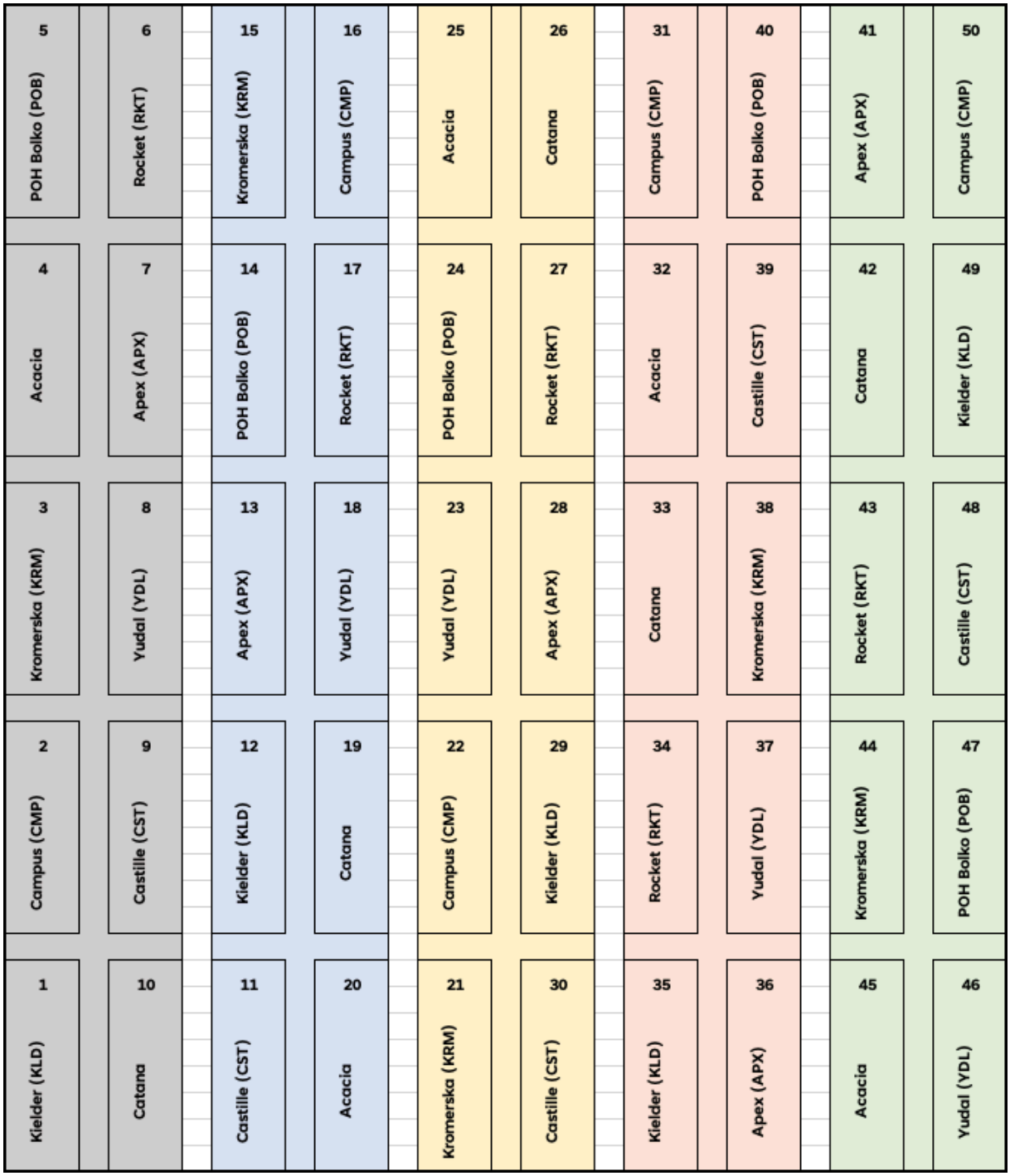

Layout of field experiment at John Innes Centre at Norwich, Norfolk in the 2024/2025 growing season

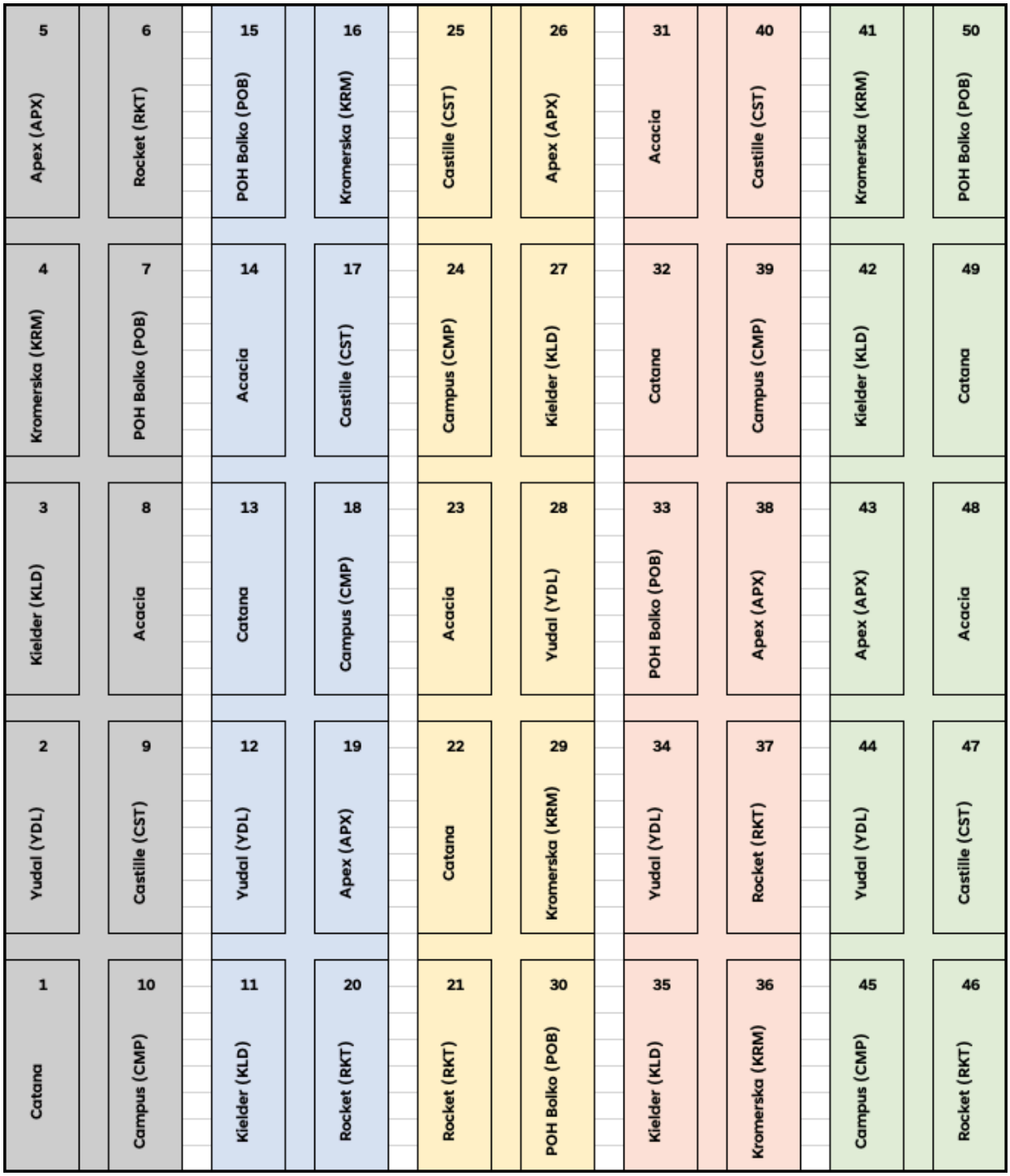

8.9 Appendix I – Comparison of the same cultivars used in field experiments in Huntingdon and Wisbech in the 2021/2022 and 2022/2023 growing seasons presented in Chapter 5

Field experiments at Huntingdon in the 2021/2022 and 2022/2023 growing seasons (cultivar Aquila)

Average phoma stem canker disease score (0-7) and percentage of *Leptosphaeria maculans* DNA (%) in stem basal cankers of cultivar Aquila at Huntingdon in the 2021/2022 and 2022/2023 growing seasons were compared using unpaired t-tests.

Significant differences were found in the average phoma stem canker disease score between the two growing seasons ($t(18) = 10.83$, $P < 0.0001$) (Table I.1) (Figure I.1A). There were no significant differences in the average percentage of *L. maculans* DNA in stem basal cankers between the two growing seasons ($t(12) = 1.16$, $P = 0.268$) (Table I.1) (Figure I.1B).

Field experiments at Wisbech in the 2021/2022 and 2022/2023 growing seasons (cultivars Crocodile, Cromat, Line-A, Murray and Turing)

Average phoma stem canker disease score (0-7) and percentage of *Leptosphaeria maculans* DNA (%) in stem basal cankers of cultivars Crocodile, Cromat, Line-A, Murray and Turing at Wisbech in the 2021/2022 and 2022/2023 growing seasons were compared using unpaired t-tests.

Significant differences were found in the average phoma stem canker disease score between the two growing seasons for cultivars Crocodile ($t(18) = 4.40$, $P < 0.001$), Cromat ($t(18) = 3.97$, $P < 0.001$) and Murray ($t(18) = 4.30$, $P < 0.001$), but not for cultivars Line-A ($t(18) = 1.99$, $P = 0.062$) and Turing ($t(18) = 0.48$, $P = 0.639$) (Table I.2) (Figure I.2A, B, C, D, E). There were no significant differences found in average percentage of *L. maculans* DNA in stem basal cankers between the two growing seasons for cultivars Crocodile ($t(14) = 2.00$, $P = 0.065$), Cromat ($t(14) = 1.44$, $P = 0.172$), Murray ($t(8) = 0.25$, $P = 0.808$) and Turing ($t(13) = 1.70$, $P = 0.113$). Interestingly, average percentage of *L. maculans* DNA in stem basal cankers of cultivar Line-A was significantly different between the two growing seasons ($t(9) = 16.09$, $P < 0.0001$) (Table I.3) (Figure I.3A, B, C, D, E).

Table I.1: Statistical testing output the main effect of growing season on average phoma stem canker disease score (0-7) and percentage of *Leptosphaeria maculans* DNA (%) in stem basal cankers of cultivar Aquila in field experiments at Huntingdon in the 2021/2022 and 2022/2023 growing seasons.

Unpaired t-test was used to test the effect of growing season.

Average phoma stem canker disease score (0-7)			
2021/2022 × 2022/2023 (Aquila)			
Factor	***df***	**t statistic**	**t probability**
Season	18	10.83	< 0.0001
Average percentage of *L. maculans* DNA at stem basal cankers (%)			
2021/2022 × 2022/2023 (Aquila)			
Factor	***df***	**t statistic**	**t probability**
Season	12	1.16	= 0.268

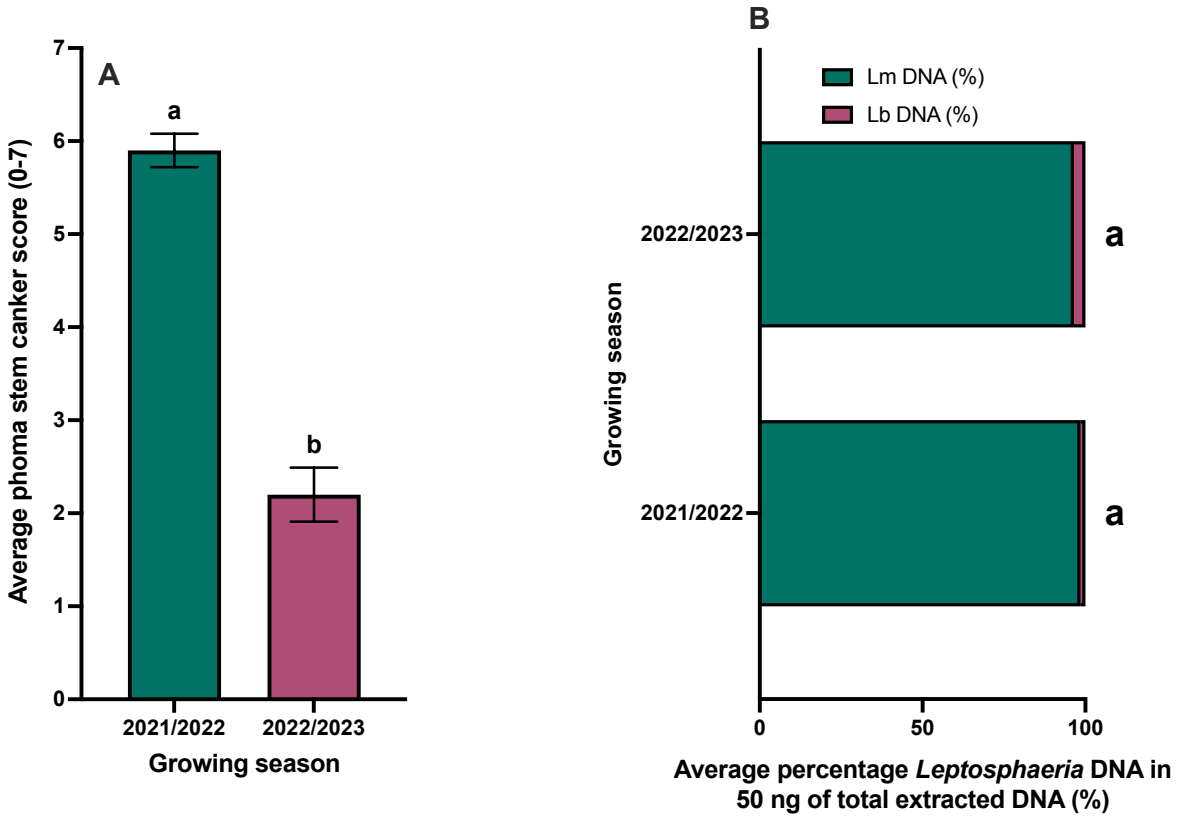

Figure I.1: (A) Average phoma stem canker disease score and (B) percentage of *Leptosphaeria maculans* DNA (%) in stem basal cankers of cultivar Aquila in field experiments at Huntingdon in the 2021/2022 and 2022/2023 growing seasons.

Unpaired t-tests were done to test the effects of growing season. Growing seasons that do not share a letter are considered significantly different ($P < 0.05$). Error bars show standard error of the mean (SEM) (disease score, 18 d.f.; *L. maculans* DNA, 12 d.f.).

Table I.2: Statistical testing outputs for significant probability of the main effects of growing season on average phoma stem canker disease score (0-7) on cultivars Crocodile, Cromat, Line-A, Murray and Turing in field experiments at Wisbech in the 2021/2022 and 2022/2023 growing seasons.

Unpaired t-tests were used for each cultivar to test the effects of growing season.

Average phoma stem canker disease score (0-7)			
2021/2022 × 2022/2023 (Crocodile)			
Factor	***df***	**t statistic**	**t probability**
Season	18	4.30	< 0.001
2021/2022 × 2022/2023 (Cromat)			
Factor	***df***	**t statistic**	**t probability**
Season	18	3.97	< 0.001
2021/2022 × 2022/2023 (Line-A)			
Factor	***df***	**t statistic**	**t probability**
Season	18	1.99	= 0.062
2021/2022 × 2022/2023 (Murray)			
Factor	***df***	**t statistic**	**t probability**
Season	18	4.30	< 0.001
2021/2022 × 2022/2023 (Turing)			
Factor	***df***	**t statistic**	**t probability**
Season	18	0.48	= 0.639

Table I.3: Statistical testing outputs for significant probability of the main effects of growing season on average percentage of *Leptosphaeria maculans* DNA (%) in stem basal cankers of cultivars Crocodile, Cromat, Line-A, Murray and Turing in field experiments at Wisbech in the 2021/2022 and 2022/2023 growing seasons.

Unpaired t-tests were used for each cultivar to test the effects of growing season.

Average percentage of *L. maculans* DNA at stem basal cankers (%)			
2021/2022 × 2022/2023 (Crocodile)			
Factor	***df***	**t statistic**	**t probability**
Season	14	2.00	= 0.065
2021/2022 × 2022/2023 (Cromat)			
Factor	***df***	**t statistic**	**t probability**
Season	14	1.44	= 0.172
2021/2022 × 2022/2023 (Line-A)			
Factor	***df***	**t statistic**	**t probability**
Season	9	16.09	< 0.0001
2021/2022 × 2022/2023 (Murray)			
Factor	***df***	**t statistic**	**t probability**
Season	8	0.25	= 0.808
2021/2022 × 2022/2023 (Turing)			
Factor	***df***	**t statistic**	**t probability**
Season	13	1.70	= 0.113

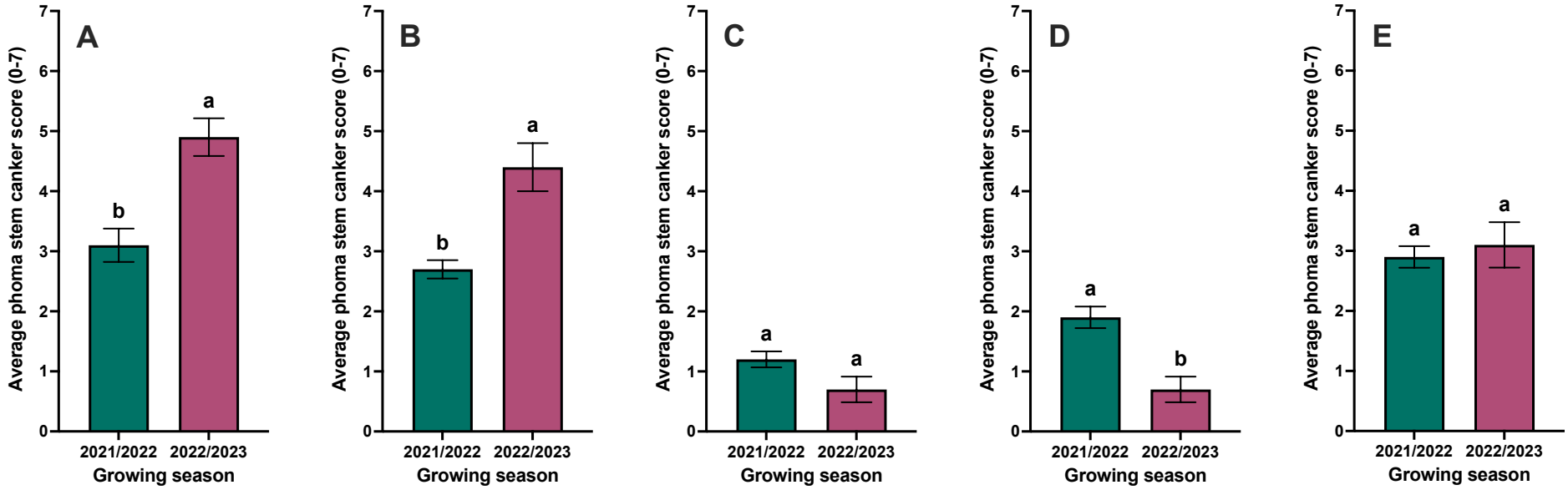

Figure I.2: Average phoma stem canker disease score for cultivar (A) Crocodile, (B) Cromat, (C) Line-A, (D) Murray and (E) Turing in field experiments at Wisbech in the 2021/2022 and 2022/2023 growing seasons.

Unpaired t-tests were used for each cultivar to test the effects of growing season. Growing seasons that do not share a letter are considered significantly different ($P < 0.05$). Error bars show standard error of the mean (SEM) (All cultivars, 18 d.f. each).

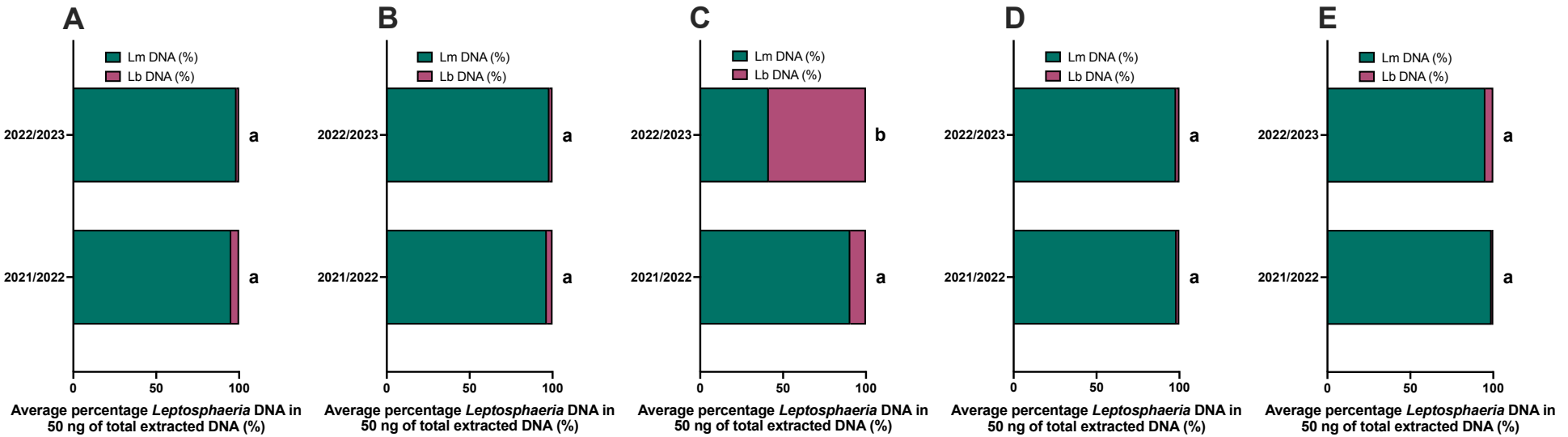

Figure I.3: Average percentage of *Leptosphaeria* species DNA (%) in stem basal cankers of cultivar A) Crocodile, (B) Cromat, (C) Line-A, (D) Murray and (E) Turing in field experiments at Wisbech in the 2021/2022 and 2022/2023 growing seasons.

Unpaired t-tests were used for each cultivar to test the effects of growing season. Growing seasons that do not share a letter are considered significantly different ($P < 0.05$). Error bars show standard error of the mean (SEM) (Crocodile 14 d.f.; Cromat, 14 d.f.; Line-A, 9 d.f.; Murray, 8 d.f.; Turing, 13 d.f.).

8.10 Appendix J – Absolute quantity values of *Leptosphaeria maculans* and *Leptosphaeria biglobosa* DNA in stem basal cankers in field experiments at Hereford, Huntingdon and Wisbech in the 2021/2022 and 2022/2023 growing seasons presented in Chapter 5

Hereford in the 2021/2022 growing season					
Cultivar Aquila					
Stem	**Lm DNA (pg)**	**Lb DNA (pg)**	**Total DNA (pg)**	**Lm DNA (%)**	**Lb DNA (%)**
1	18135.0	0.8	18135.8	100.00%	0.00%
2	12910.0	90.6	13000.6	99.30%	0.70%
3	11115.0	0.2	11115.2	100.00%	0.00%
4	8998.5	8.2	9006.7	99.91%	0.09%
5	13550.0	48.0	13598.0	99.65%	0.35%
6	6262.5	1.9	6264.4	99.97%	0.03%
7	17530.0	0.5	17530.5	100.00%	0.00%
8	9670.0	0.6	9670.6	99.99%	0.01%
9	12565.0	29.8	12594.8	99.76%	0.24%
10	8384.0	1.6	8385.6	99.98%	0.02%
Cultivar Flamingo					
Stem	**Lm DNA (pg)**	**Lb DNA (pg)**	**Total DNA (pg)**	**Lm DNA (%)**	**Lb DNA (%)**
1	12055.0	0.5	12055.5	100.00%	0.00%
2	4724.0	0.3	4724.3	99.99%	0.01%
3	8037.5	0.5	8038.0	99.99%	0.01%
4	0.0	57.9	57.9	0.00%	100.00%
5	18245.0	0.5	18245.5	100.00%	0.00%
6	8910.5	0.9	8911.4	99.99%	0.01%
7	10515.0	0.3	10515.3	100.00%	0.00%
8	9349.0	0.3	9349.3	100.00%	0.00%

Hereford in the 2022/2023 growing season					
Cultivar Aquila					
Stem	**Lm DNA (pg)**	**Lb DNA (pg)**	**Total DNA (pg)**	**Lm DNA (%)**	**Lb DNA (%)**
1	4593.0	95.8	4688.8	97.96%	2.04%
2	3325.0	52.6	3377.6	98.44%	1.56%
3	6152.0	99.1	6251.1	98.41%	1.59%
4	5811.0	120.0	5931.0	97.98%	2.02%
5	76.7	2.7	79.4	96.54%	3.46%
6	4469.0	101.9	4570.9	97.77%	2.23%
7	8266.0	74.3	8340.3	99.11%	0.89%
8	1638.5	65.6	1704.1	96.15%	3.85%
9	3634.0	201.0	3835.0	94.76%	5.24%
Cultivar Flamingo					
Stem	**Lm DNA (pg)**	**Lb DNA (pg)**	**Total DNA (pg)**	**Lm DNA (%)**	**Lb DNA (%)**
1	3202.5	70.9	3273.4	97.83%	2.17%
2	643.9	107.5	751.4	85.69%	14.31%
3	4540.5	338.5	4879.0	93.06%	6.94%
4	4646.0	61.9	4707.9	98.69%	1.31%
5	3145.0	123.5	3268.5	96.22%	3.78%
6	4850.5	103.2	4953.7	97.92%	2.08%
7	398.2	67.2	465.3	85.57%	14.43%
8	2928.5	32.0	2960.5	98.92%	1.08%
9	286.5	13.5	300.0	95.50%	4.50%
10	1450.0	27.9	1477.9	98.12%	1.88%

Huntingdon in the 2021/2022 growing season					
Cultivar Aquila					
Stem	**Lm DNA (pg)**	**Lb DNA (pg)**	**Total DNA (pg)**	**Lm DNA (%)**	**Lb DNA (%)**
1	7847.5	11.2	7858.7	99.86%	0.14%
2	13505.0	1.1	13506.1	99.99%	0.01%
3	14930.0	33.5	14963.5	99.78%	0.22%
4	14640.0	33.5	14673.5	99.77%	0.23%
5	15725.0	38.4	15763.4	99.76%	0.24%
6	10615.0	34.0	10649.0	99.68%	0.32%
7	13525.0	23.2	13548.2	99.83%	0.17%
8	7882.5	638.4	8520.9	92.51%	7.49%
9	3440.5	161.7	3602.2	95.51%	4.49%
Cultivar Flamingo					
Stem	**Lm DNA (pg)**	**Lb DNA (pg)**	**Total DNA (pg)**	**Lm DNA (%)**	**Lb DNA (%)**
1	10422.0	1.7	10423.7	99.98%	0.02%
2	10275.5	5.1	10280.6	99.95%	0.05%
3	23825.0	13.4	23838.4	99.94%	0.06%
4	10800.0	9.0	10809.0	99.92%	0.08%
5	27.8	2140.5	2168.3	1.28%	98.72%
6	21200.0	337.7	21537.7	98.43%	1.57%
7	34180.0	26.2	34206.2	99.92%	0.08%
8	18935.0	15.4	18950.4	99.92%	0.08%

Huntingdon in the 2022/2023 growing season					
Cultivar Aquila					
Stem	**Lm DNA (pg)**	**Lb DNA (pg)**	**Total DNA (pg)**	**Lm DNA (%)**	**Lb DNA (%)**
1	62.4	7.2	69.6	89.61%	10.39%
2	45.9	0.6	46.5	98.72%	1.28%
3	440.0	6.6	446.6	98.51%	1.49%
4	182.8	4.9	187.7	97.39%	2.61%
5	222.9	4.0	226.9	98.24%	1.76%
Cultivar Acacia					
Stem	**Lm DNA (pg)**	**Lb DNA (pg)**	**Total DNA (pg)**	**Lm DNA (%)**	**Lb DNA (%)**
1	3963.5	10.3	3973.8	99.74%	0.26%
2	4471.0	23.5	4494.5	99.48%	0.52%
3	1438.5	4.1	1442.6	99.72%	0.28%
4	2682.0	79.9	2761.9	97.11%	2.89%
5	3406.0	19.2	3425.2	99.44%	0.56%

Wisbech in the 2021/2022 growing season					
Cultivar Adonis					
Stem	**Lm DNA (pg)**	**Lb DNA (pg)**	**Total DNA (pg)**	**Lm DNA (%)**	**Lb DNA (%)**
1	4894.0	121.3	5015.3	97.58%	2.42%
2	3886.0	46.5	3932.5	98.82%	1.18%
3	2892.0	108.1	3000.1	96.40%	3.60%
4	3547.5	32.2	3579.7	99.10%	0.90%
5	6365.0	34.3	6399.3	99.46%	0.54%
6	2167.0	32.7	2199.7	98.51%	1.49%
7	2057.0	99.1	2156.1	95.40%	4.60%
8	2935.5	217.8	3153.3	93.09%	6.91%
Cultivar Crocodile					
Stem	**Lm DNA (pg)**	**Lb DNA (pg)**	**Total DNA (pg)**	**Lm DNA (%)**	**Lb DNA (%)**
1	3251.5	245.4	3496.9	92.98%	7.02%
2	3643.5	155.8	3799.3	95.90%	4.10%
3	35455.0	330.1	35785.1	99.08%	0.92%
4	3441.5	556.1	3997.6	86.09%	13.91%
5	1995.5	39.4	2034.9	98.07%	1.93%
6	5875.0	23.3	5898.3	99.60%	0.40%
Cultivar Cromat					
Stem	**Lm DNA (pg)**	**Lb DNA (pg)**	**Total DNA (pg)**	**Lm DNA (%)**	**Lb DNA (%)**
1	2938.5	54.4	2992.9	98.18%	1.82%
2	3729.0	52.0	3781.0	98.62%	1.38%
3	5735.0	232.7	5967.7	96.10%	3.90%
4	8181.5	110.9	8292.4	98.66%	1.34%
5	5806.0	77.0	5883.0	98.69%	1.31%
6	1288.0	126.1	1414.1	91.09%	8.91%
7	1761.0	115.4	1876.4	93.85%	6.15%
8	1484.5	40.6	1525.1	97.34%	2.66%

Wisbech in the 2021/2022 growing season					
Cultivar Line-A					
Stem	**Lm DNA (pg)**	**Lb DNA (pg)**	**Total DNA (pg)**	**Lm DNA (%)**	**Lb DNA (%)**
1	3550.0	282.5	3832.5	92.63%	7.37%
2	747.5	63.4	810.9	92.18%	7.82%
3	1048.1	55.1	1103.2	95.00%	5.00%
4	529.1	152.3	681.4	77.65%	22.35%
5	1006.8	86.4	1093.2	92.10%	7.90%
6	82.6	5.5	88.1	93.72%	6.28%
Cultivar Murray					
Stem	**Lm DNA (pg)**	**Lb DNA (pg)**	**Total DNA (pg)**	**Lm DNA (%)**	**Lb DNA (%)**
1	6056.5	35.4	6091.9	99.42%	0.58%
2	885.4	60.3	945.6	93.63%	6.37%
3	10753.0	36.1	10789.1	99.67%	0.33%
4	10875.0	36.9	10911.9	99.66%	0.34%
5	7142.5	42.2	7184.7	99.41%	0.59%
Cultivar Turing					
Stem	**Lm DNA (pg)**	**Lb DNA (pg)**	**Total DNA (pg)**	**Lm DNA (%)**	**Lb DNA (%)**
1	948.5	9.5	958.0	99.01%	0.99%
2	8052.5	53.3	8105.8	99.34%	0.66%
3	2593.7	58.3	2652.0	97.80%	2.20%
4	9643.5	139.1	9782.6	98.58%	1.42%
5	6451.5	30.3	6481.8	99.53%	0.47%
6	7427.0	27.3	7454.3	99.63%	0.37%
7	14225.0	46.1	14271.1	99.68%	0.32%
8	8299.0	100.9	8399.9	98.80%	1.20%

Wisbech in the 2022/2023 growing season					
Cultivar Aurelia					
Stem	**Lm DNA (pg)**	**Lb DNA (pg)**	**Total DNA (pg)**	**Lm DNA (%)**	**Lb DNA (%)**
1	6722.5	17.4	6739.9	99.74%	0.26%
2	6883.0	36.0	6919.0	99.48%	0.52%
3	2848.0	10.7	2858.7	99.63%	0.37%
4	121.0	4.2	125.2	96.65%	3.35%
5	713.5	7.9	721.4	98.90%	1.10%
6	772.9	12.8	785.6	98.38%	1.62%
7	4598.0	31.1	4629.1	99.33%	0.67%
Cultivar Crocodile					
Stem	**Lm DNA (pg)**	**Lb DNA (pg)**	**Total DNA (pg)**	**Lm DNA (%)**	**Lb DNA (%)**
1	384.2	2.2	386.4	99.43%	0.57%
2	1845.5	25.0	1870.5	98.66%	1.34%
3	1530.5	50.8	1581.3	96.79%	3.21%
4	2098.0	22.5	2120.5	98.94%	1.06%
5	1279.5	29.2	1308.7	97.77%	2.23%
6	1531.0	18.7	1549.7	98.79%	1.21%
7	3176.5	32.7	3209.2	98.98%	1.02%
8	2260.5	48.8	2309.3	97.89%	2.11%
9	4883.5	20.6	4904.1	99.58%	0.42%
10	1686.5	25.7	1712.2	98.50%	1.50%

Wisbech in the 2022/2023 growing season					
Cultivar Cromat					
Stem	**Lm DNA (pg)**	**Lb DNA (pg)**	**Total DNA (pg)**	**Lm DNA (%)**	**Lb DNA (%)**
1	299.5	15.9	315.4	94.96%	5.04%
2	2664.5	55.0	2719.5	97.98%	2.02%
3	3181.0	23.4	3204.4	99.27%	0.73%
4	4160.5	22.6	4183.1	99.46%	0.54%
5	1812.5	47.6	1860.1	97.44%	2.56%
6	163.7	3.5	167.2	97.89%	2.11%
7	2801.5	24.6	2826.1	99.13%	0.87%
8	2919.5	21.8	2941.3	99.26%	0.74%
Cultivar Line-A					
Stem	**Lm DNA (pg)**	**Lb DNA (pg)**	**Total DNA (pg)**	**Lm DNA (%)**	**Lb DNA (%)**
1	11.5	17.3	28.8	39.98%	60.02%
2	11.4	14.3	25.6	44.32%	55.68%
3	11.5	15.9	27.4	41.82%	58.18%
4	11.3	18.3	29.6	38.18%	61.82%
5	9.9	13.2	23.1	42.82%	57.18%

Wisbech in the 2022/2023 growing season					
Cultivar Murray					
Stem	**Lm DNA (pg)**	**Lb DNA (pg)**	**Total DNA (pg)**	**Lm DNA (%)**	**Lb DNA (%)**
1	1019.2	15.2	1034.4	98.53%	1.47%
2	1291.0	19.1	1310.1	98.54%	1.46%
3	557.1	24.4	581.5	95.80%	4.20%
4	887.0	12.6	899.6	98.60%	1.40%
5	813.3	10.9	824.2	98.68%	1.32%
Cultivar Turing					
Stem	**Lm DNA (pg)**	**Lb DNA (pg)**	**Total DNA (pg)**	**Lm DNA (%)**	**Lb DNA (%)**
1	157.5	11.4	168.8	93.27%	6.73%
2	101.8	22.1	123.9	82.18%	17.82%
3	645.4	27.0	672.4	95.98%	4.02%
4	52.0	0.9	52.9	98.31%	1.69%
5	43.4	0.0	43.4	100.00%	0.00%
6	1118.3	23.0	1141.3	97.99%	2.01%
7	4271.5	24.4	4295.9	99.43%	0.57%

8.11 Appendix K – Poster presentations

BSPP Annual Conference (December 2021 in Birmingham, UK) and Cereals (June 2022 in Herts, UK)

Leptosphaeria biglobosa inhibits production of secondary metabolite sirodesmin PL by *L. maculans in planta*

Fortune, J. A.[1,2] , **Bingol, E.**[1] , Baker, D.[1] , Ritchie, F.[2] , Karandeni Dewage, C. S.[1] , Fitt, B. D. L.[1] and Huang, Y. J.[1]

[1] School of Life and Medical Sciences, University of Hertfordshire, UK, AL10 9AB, [2] ADAS Boxworth, Cambridge, UK, CB23 4NN

Email: e.bingol@herts.ac.uk

Introduction

Phoma stem canker is an economically damaging disease of oilseed rape (*Brassica napus*), caused by two co-existing pathogens *Leptosphaeria maculans* and *L. biglobosa*, with annual yield losses > £80M, despite use of resistant cultivars and fungicides.

L. maculans produces a non-host selective epipolythiodioxopiperazine (ETP) phytotoxin called sirodesmin PL with an *m/z* of 487.2. *L. biglobosa* does not produce sirodesmin PL. *L. maculans* causes more severe cankers (Fig.1), possibly because it produces this phytotoxin.

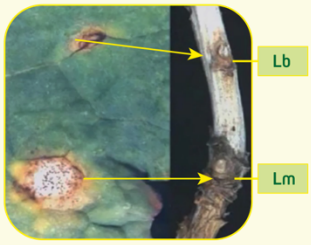

Figure 1: Phoma leaf spots and stem canker caused by *Leptosphaeria maculans* (Lm) and *L. biglobosa* (Lb).

In vitro studies indicated that simultaneous inoculation with *L. biglobosa* inhibits production of sirodesmin PL by *L. maculans*. To investigate novel strategies to improve control of phoma stem canker, this study aimed to determine whether *L. biglobosa* inhibits production of sirodesmin PL by *L. maculans in planta* and reduces severity of disease caused by *L. maculans*.

Materials and Methods

• Oilseed rape cv. Charger plants were grown in a controlled environment. Cotyledons were inoculated with conidial suspensions (10^6 spores/mL) of *L. maculans* only (Lm only), *L. biglobosa* only (Lb only), *L. maculans* and *L. biglobosa* simultaneously (Lm&Lb) or sterilised distilled water (SDW) as a control.

• Severity of lesions was assessed and secondary metabolites were extracted from cotyledons using ethyl acetate at 26 days post inoculation (dpi). Composition of secondary metabolites was assessed using HPLC and LC-MS.

Results

• Plants with 'Lm only' inoculation produced large grey lesions, while plants with 'Lm&Lb' produced small dark, defined lesions, which were similar to lesions with 'Lb only' inoculation (Fig.2).

• The LC-MS chromatograms for *m/z* 487.2 showed unique maxima in the 'Lm only' sample (Fig.3).

• At retention time 5.11 min, the LC-MS positive ion spectrograph indicated presence of ions corresponding to sirodesmin PL and several of its adducts and molecular ions (Fig.4).

• Presence of sirodesmin PL was confirmed only in extracts from cotyledons inoculated with 'Lm only'.

Acknowledgements

University of Hertfordshire UH · ADAS · Perry Foundation · Cobbold Trust

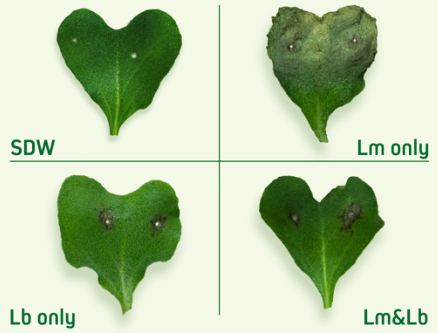

Figure 2: Symptoms on cotyledons of oilseed rape cv. Charger inoculated with sterilised distilled water (SDW), *Leptosphaeria maculans* (Lm only), *L. biglobosa* (Lb only) or *L. maculans* and *L. biglobosa* simultaneously (Lm&Lb) at 26 days post inoculation (dpi).

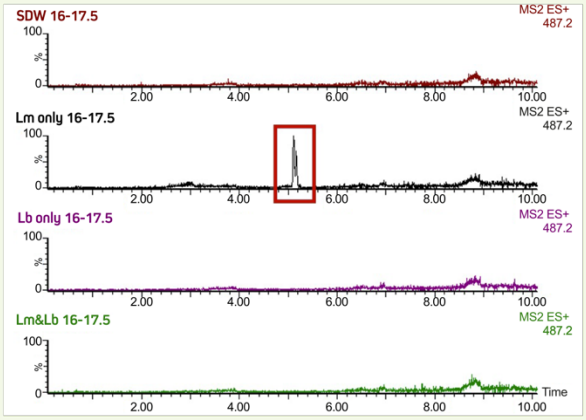

Figure 3: LC-MS chromatograms for *m/z* 487.2 of HPLC fractions at retention time 16-17.5 mins for all treatments. Unique maxima found only in Lm only 16-17.5 sample is highlighted.

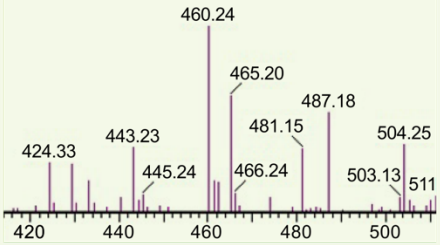

Figure 4: LC-MS positive ion spectrograph of Lm only 16-17.5 sample between *m/z* 420 and 510. Sirodesmin PL (*m/z* 487.18) and several of its adducts and molecular ions (*m/z* 424.33, 445.24, 460.64, 465.20 and 504.25) are identified.

Discussion

• These results indicate that *L. biglobosa* inhibits the production of sirodesmin PL by *L. maculans in planta* when both are inoculated simultaneously. There is a need to further investigate the mechanisms of this inhibition by *L. biglobosa*.

• Understanding the interactions between *L. maculans* and *L. biglobosa* can provide new strategies for effective control of phoma stem canker, alongside resistant cultivars and fungicide applications.

University of Hertfordshire Annual Life and Medical Sciences Conference (June 2022 in Hatfield, UK)

University of Hertfordshire UH

School of Life and Medical Sciences

Leptosphaeria biglobosa inhibits production of secondary metabolite sirodesmin PL by *L. maculans in planta*

Fortune, J. A.[1,2] , **Bingol, E.**[1] , Baker, D.[1] , Ritchie, F.[2] , Karandeni Dewage, C. S.[1] , Fitt, B. D. L.[1] and Huang, Y. J.[1]

[1] School of Life and Medical Sciences, University of Hertfordshire, UK, AL10 9AB, [2] ADAS Boxworth, Cambridge, UK, CB23 4NN

Email: e.bingol@herts.ac.uk

Introduction

Phoma stem canker is an economically damaging disease of oilseed rape *(Brassica napus)*, caused by two co-existing pathogens *Leptosphaeria maculans* and *L. biglobosa*, with annual yield losses > £80M, despite use of resistant cultivars and fungicides.

L. maculans produces a non-host selective epipolythiodioxopiperazine (ETP) phytotoxin called sirodesmin PL with an *m/z* of 487.2 and causes more severe cankers (Fig.1). *L. biglobosa* does not produce sirodesmin PL.

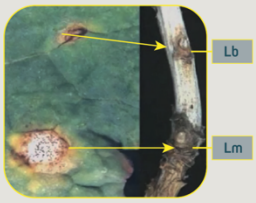

Figure 1: Phoma leaf spots and stem canker caused by *Leptosphaeria maculans* (Lm) and *L. biglobosa* (Lb).

In vitro studies indicated that simultaneous inoculation with *L. biglobosa* inhibits production of sirodesmin PL by *L. maculans*. To investigate novel strategies to improve control of phoma stem canker, this study aimed to determine whether *L. biglobosa* inhibits production of sirodesmin PL by *L. maculans in planta* and reduces severity of disease caused by *L. maculans*.

Materials and Methods

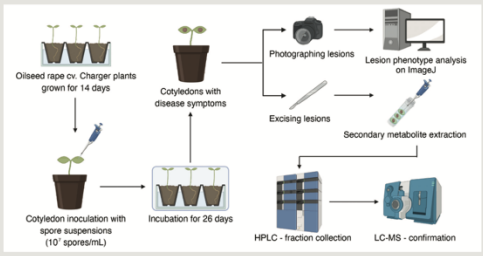

Figure 2: Illustration of method used in this work.

- Treatments were SDW, Lm only, Lb only, and Lm&Lb.

Results

- Plants with 'Lm only' treatment produced large grey lesions, while plants with 'Lm&Lb' produced small, dark lesions, which were similar to 'Lb only' treatment (Fig.3).
- The LC-MS chromatograms for *m/z* 487.2 showed unique maxima in 'Lm only' (Fig.4).
- At retention time 5.11 min, the LC-MS positive ion spectra indicated presence of ions corresponding to sirodesmin PL and several of its adducts and molecular ions (Fig.5).
- Presence of sirodesmin PL was confirmed only in 'Lm only' treatment.

Acknowledgements

University of Hertfordshire UH · ADAS · iPerry Foundation · Cobbold Trust

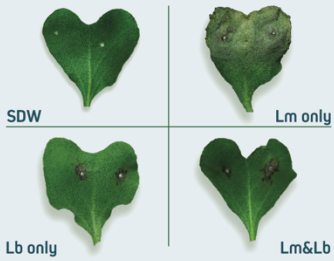

Figure 3: Symptoms on cotyledons of oilseed rape cv. Charger inoculated with sterilised distilled water (SDW), *Leptosphaeria maculans* (Lm only), *L. biglobosa* (Lb only) or *L. maculans* and *L. biglobosa* simultaneously (Lm&Lb) at 26 days post inoculation (dpi).

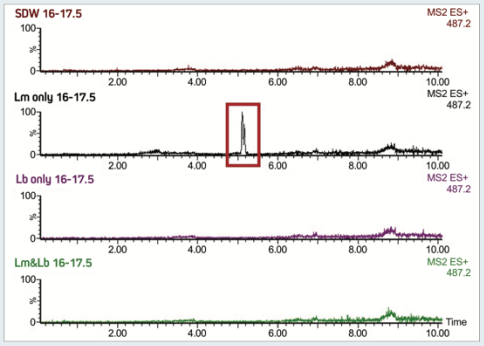

Figure 4: LC-MS chromatograms for *m/z* 487.2 of HPLC fractions at retention time 16-17.5 min for all treatments. Unique maxima found only in Lm only 16-17.5 sample is highlighted.

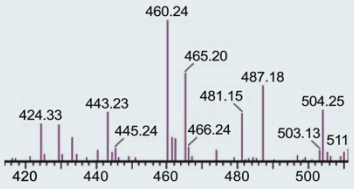

Figure 5: LC-MS positive ion spectra of Lm only 16-17.5 sample between *m/z* 420 and 510. Sirodesmin PL (*m/z* 487.18) and several of its adducts and molecular ions (*m/z* 424.33, 445,24, 460.64, 465.20 and 504.25) are identified.

Discussion

- *L. biglobosa* inhibits the production of sirodesmin PL by *L. maculans in planta* when both are inoculated simultaneously. There is a need to further investigate the mechanisms of this inhibition by *L. biglobosa*.
- Understanding the interactions between *L. maculans* and *L. biglobosa* can provide new strategies for effective control of phoma stem canker, alongside resistant cultivars and fungicide applications.

University of Hertfordshire Annual Life and Medical Sciences Conference (June 2023 in Hatfield, UK)

University of Hertfordshire UH

School of Life and Medical Sciences

Deciphering the influence of co-inoculation timing on antagonistic effects of *Leptosphaeria biglobosa* on *L. maculans*

Evren Bingol[1], Aiming Qi[1], Chinthani Karandeni-Dewage[1], Faye Ritchie[2], Bruce D. L. Fitt[1], Yong-Ju Huang[1]

[1] School of Life and Medical Sciences, University of Hertfordshire, UK, AL10 9AB, [2] ADAS Boxworth, Cambridge, UK, CB23 4NN

Email: e.bingol@herts.ac.uk

Introduction

Phoma stem canker is an economically damaging disease of oilseed rape (*Brassica napus*), caused by two co-existing fungal pathogens *Leptosphaeria maculans* and *L. biglobosa*, with annual yield losses > £80M in the UK, despite the use of fungicides and resistant cultivars.

L. maculans causes severe stem basal cankers, whereas *L. biglobosa* causes less severe upper stem lesions (Fig. 1); *L. maculans* produces a non-host selective phytotoxin called sirodesmin PL while *L. biglobosa* does not.

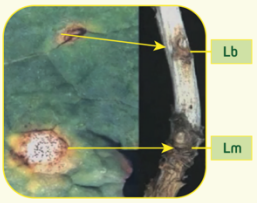

Figure 1: Phoma leaf spots and stem canker caused by *Leptosphaeria maculans* (Lm) and *L. biglobosa* (Lb).

Recent studies showed that *L. biglobosa* can inhibit the production of sirodesmin PL by *L. maculans* if it was simultaneously co-inoculated. In order to further understand the antagonistic effects of *L. biglobosa*, this study investigated the effects of sequential co-inoculation on interspecific interactions between *L. maculans* and *L. biglobosa in vitro*.

Materials and Methods

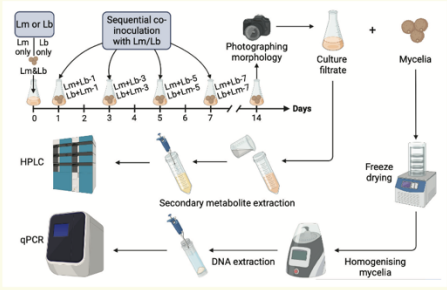

Figure 2: Illustration of method used in this work.

- Data were analysed with Two-Way ANOVA and Tukey's HSD post-hoc tests.

Results

- Morphology of mycelia in cultures initially inoculated with Lb then Lm were similar to 'Lb only', 'Lm&Lb' or 'Lm+Lb-1' (Fig. 3).
- Inhibition of sirodesmin PL and its precursors were congruent with the morphological observations, with 'Lm+Lb-5' and 'Lm+Lb-7' being similar to 'Lm only'. Interestingly, a partial inhibition was found in 'Lm+Lb-3' (Fig. 4).
- *L. biglobosa* has an antagonistic effect on the growth of *L. maculans*, confirmed by species-specific qPCR (Fig. 5).

Acknowledgements

ADAS Chadacre COBBOLD iPerry FOUNDATION University of Hertfordshire UH

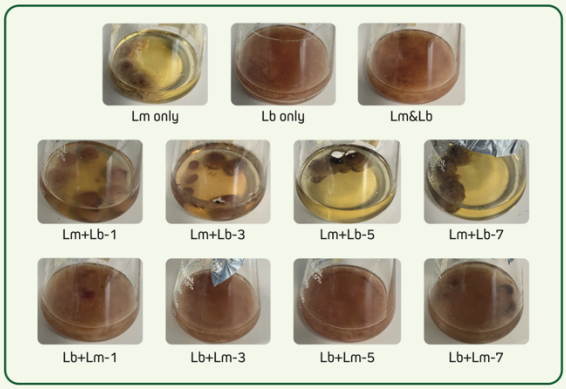

Figure 3: Morphology of mycelia of different treatments in clarified V8 broth at 14 days post inoculation (dpi).

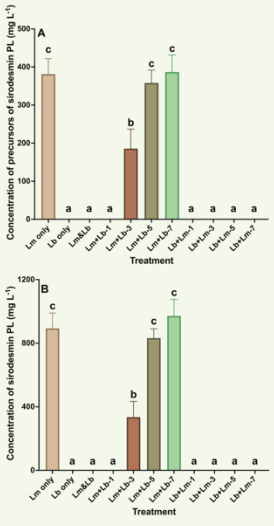

Figure 4: Average concentration of A) The precursors of sirodesmin PL (mg L^{-1}) B) Sirodesmin PL (mg L^{-1}) in secondary metabolite extracts from three independent experiments. Columns that do not share a letter are considered significantly different ($P<0.05$). Error bars show the standard error of the mean (SEM).

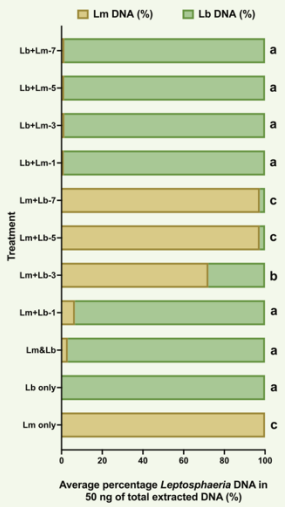

Figure 5: Average percentage of *Leptosphaeria* DNA (%) in homogenised mycelia from three independent experiments. Columns that do not share a letter are considered significantly different ($P<0.05$).

Discussion

- Interspecific interactions between *L. maculans* and *L. biglobosa* are affected by co-inoculation timing, and *L. biglobosa* can exert antagonistic effects on *L. maculans* if it is co-inoculated before or up to 3 days after *L. maculans*.
- There is a need to investigate the mechanism of these antagonistic effects of *L. biglobosa*, for development of novel ideas for sustainable management of phoma stem canker.

Deciphering the influence of co-inoculation timing on antagonistic effects of *Leptosphaeria biglobosa* on *L. maculans*

Evren Bingol[1], Aiming Qi[1], Chinthani Karandeni-Dewage[1], Faye Ritchie[2], Bruce D. L. Fitt[1], Yong-Ju Huang[1]

[1] School of Life and Medical Sciences, University of Hertfordshire, UK, AL10 9AB, [2] ADAS Boxworth, Cambridge, UK, CB23 4NN

Email: e.bingol@herts.ac.uk

Introduction

Phoma stem canker is an economically damaging disease of oilseed rape (*Brassica napus*), caused by two co-existing fungal pathogens *Leptosphaeria maculans* and *L. biglobosa*, with annual yield losses > £80M in the UK, despite the use of fungicides and resistant cultivars.

L. maculans causes severe stem basal cankers, whereas *L. biglobosa* causes less severe upper stem lesions (Fig. 1); *L. maculans* produces a non-host selective phytotoxin called sirodesmin PL while *L. biglobosa* does not.

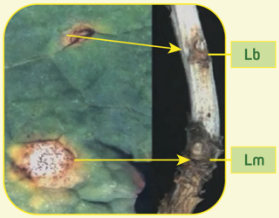

Figure 1: Phoma leaf spots and stem canker caused by *Leptosphaeria maculans* (Lm) and *L. biglobosa* (Lb).

Recent studies showed that *L. biglobosa* can inhibit the production of sirodesmin PL by *L. maculans* if it was simultaneously co-inoculated. In order to further understand the antagonistic effects of *L. biglobosa*, this study investigated the effects of sequential co-inoculation on interspecific interactions between *L. maculans* and *L. biglobosa in vitro*.

Materials and Methods

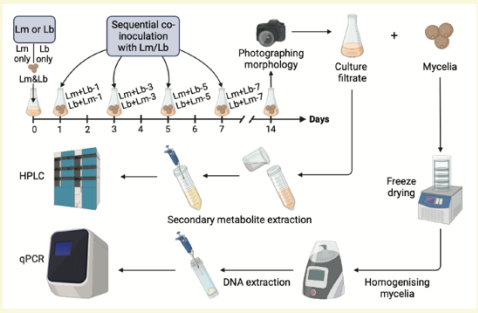

Figure 2: Illustration of method used in this work.

- Data were analysed with Two-Way ANOVA and Tukey's HSD post-hoc tests.

Results

- Morphology of mycelia in cultures initially inoculated with Lb then Lm were similar to 'Lb only', 'Lm&Lb' or 'Lm+Lb-1' (Fig. 3).
- Inhibition of sirodesmin PL and its precursors were congruent with the morphological observations, with 'Lm+Lb-5' and 'Lm+Lb-7' being similar to 'Lm only'. Interestingly, a partial inhibition was found in 'Lm+Lb-3' (Fig. 4).
- *L. biglobosa* has an antagonistic effect on the growth of *L. maculans*, confirmed by species-specific qPCR (Fig. 5).

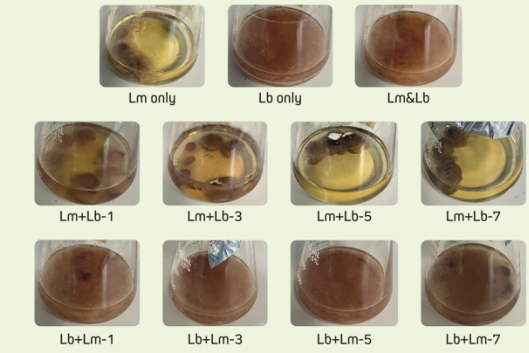

Figure 3: Morphology of mycelia of different treatments in clarified V8 broth at 14 days post inoculation (dpi).

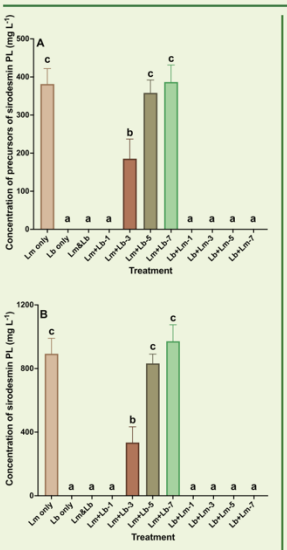

Figure 4: Average concentration of A) The precursors of sirodesmin PL (mg L^{-1}) B) Sirodesmin PL (mg L^{-1}) in secondary metabolite extracts from three independent experiments. Columns that do not share a letter are considered significantly different ($P<0.05$). Error bars show the standard error of the mean (SEM).

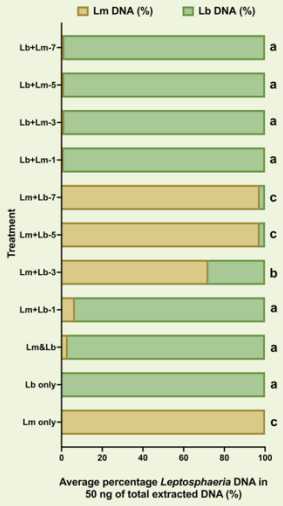

Figure 5: Average percentage of *Leptosphaeria* DNA (%) in homogenised mycelia from three independent experiments. Columns that do not share a letter are considered significantly different ($P<0.05$).

Discussion

- Interspecific interactions between *L. maculans* and *L. biglobosa* are affected by co-inoculation timing, and *L. biglobosa* can exert antagonistic effects on *L. maculans* if it is co-inoculated before or up to 3 days after *L. maculans*.
- There is a need to investigate the mechanism of these antagonistic effects of *L. biglobosa*, for development of novel ideas for sustainable management of phoma stem canker.

Conference Organisers

Acknowledgements

Investigating the effects of co-inoculation timing on interspecific interactions between *Leptosphaeria maculans* and *L. biglobosa*

Evren Bingol[1], Aiming Qi[1], Chinthani Karandeni-Dewage[1], Faye Ritchie[2], Bruce D. L. Fitt[1], Yong-Ju Huang[1]

[1] School of Life and Medical Sciences, University of Hertfordshire, UK, AL10 9AB, [2] ADAS Boxworth, Cambridge, UK, CB23 4NN

Email: e.bingol@herts.ac.uk

Introduction

Phoma stem canker is an economically damaging disease of oilseed rape (*Brassica napus*), caused by two co-existing fungal pathogens *Leptosphaeria maculans* and *L. biglobosa*, with annual yield losses > £80M in the UK, despite the use of fungicides and resistant cultivars.

L. maculans causes severe stem basal cankers, whereas *L. biglobosa* causes less severe upper stem lesions (Fig. 1); *L. maculans* produces a non-host selective phytotoxin called sirodesmin PL while *L. biglobosa* does not.

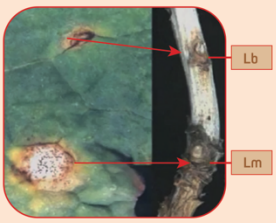

Figure 1: Phoma leaf spots and stem canker caused by *Leptosphaeria maculans* (Lm) and *L. biglobosa* (Lb).

Recent studies showed that *L. biglobosa* can inhibit the production of sirodesmin PL by *L. maculans* if it was simultaneously co-inoculated. In order to further understand the antagonistic effects of *L. biglobosa*, this study investigated the effects of sequential co-inoculation on interspecific interactions between *L. maculans* and *L. biglobosa in vitro*.

Materials and Methods

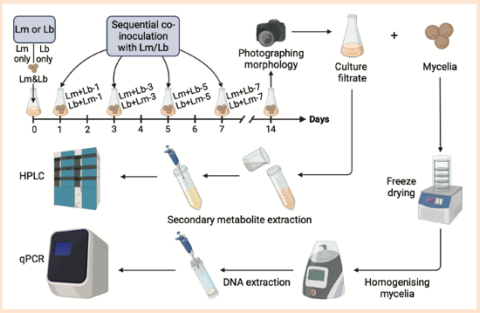

Figure 2: Illustration of method used in this work.

- Data were analysed with Two-Way ANOVA and Tukey's HSD post-hoc tests.

Results

- Morphology of mycelia in cultures initially inoculated with Lb then Lm were similar to 'Lb only', 'Lm&Lb' or 'Lm+Lb-1' (Fig. 3).
- Inhibition of sirodesmin PL and its precursors were congruent with the morphological observations, with 'Lm+Lb-5' and 'Lm+Lb-7' being similar to 'Lm only'. Interestingly, a partial inhibition was found in 'Lm+Lb-3' (Fig. 4).
- *L. biglobosa* has an antagonistic effect on the growth of *L. maculans*, confirmed by species-specific qPCR (Fig. 5).

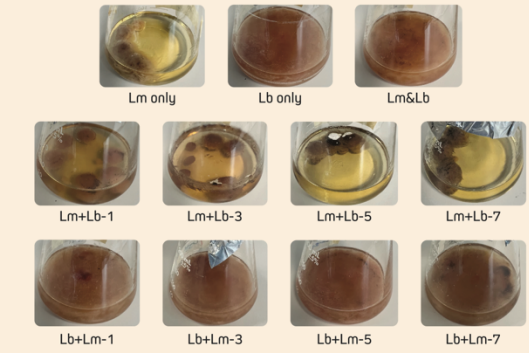

Figure 3: Morphology of mycelia of different treatments in clarified V8 broth at 14 days post inoculation (dpi).

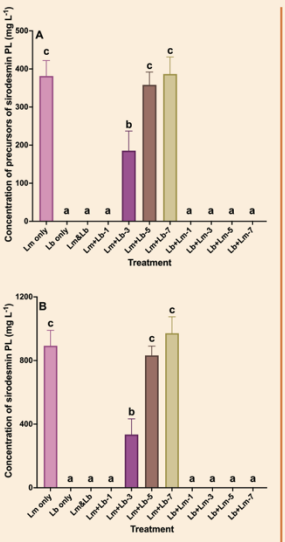

Figure 4: Average concentration of A) The precursors of sirodesmin PL (mg L^{-1}) B) Sirodesmin PL (mg L^{-1}) in secondary metabolite extracts from three independent experiments. Columns that do not share a letter are considered significantly different ($P<0.05$). Error bars show the standard error of the mean (SEM).

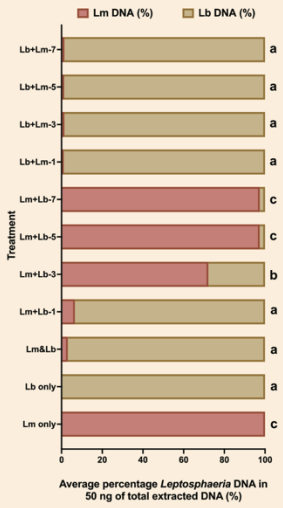

Figure 5: Average percentage of *Leptosphaeria* DNA (%) in homogenised mycelia from three independent experiments. Columns that do not share a letter are considered significantly different ($P<0.05$).

Discussion

- Interspecific interactions between *L. maculans* and *L. biglobosa* are affected by co-inoculation timing, and *L. biglobosa* can exert antagonistic effects on *L. maculans* if it is co-inoculated before or up to 3 days after *L. maculans*.
- There is a need to investigate the mechanism of these antagonistic effects of *L. biglobosa*, for development of novel ideas for sustainable management of phoma stem canker.

Conference Organiser

British Mycological Society promoting fungal science

Acknowledgements

ADAS Chadacre Agricultural Trust COBBOLD TRUST Perry Foundation University of Hertfordshire UH

16th International Rapeseed Congress (IRC2023) (September 2023 in Wagga Wagga, Canberra, Sydney, Australia)

Understanding the effects of co-inoculation timing on interspecific interactions between phoma stem canker pathogens (*Leptosphaeria maculans* and *L. biglobosa*)

Evren Bingol[1], Aiming Qi[1], Chinthani Karandeni-Dewage[1], Faye Ritchie[2], Bruce D. L. Fitt[1], Yong-Ju Huang[1]

[1] School of Life and Medical Sciences, University of Hertfordshire, UK, AL10 9AB, [2] ADAS Boxworth, Cambridge, UK, CB23 4NN

Email: e.bingol@herts.ac.uk

Introduction

Phoma stem canker is an economically damaging disease of oilseed rape (*Brassica napus*), caused by two co-existing fungal pathogens *Leptosphaeria maculans* and *L. biglobosa*, with annual yield losses > £80M in the UK, despite the use of fungicides and resistant cultivars.

L. maculans causes severe stem basal cankers, whereas *L. biglobosa* causes less severe upper stem lesions (Fig. 1); *L. maculans* produces a non-host selective phytotoxin called sirodesmin PL while *L. biglobosa* does not.

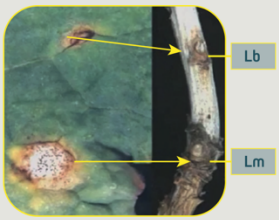

Figure 1: Phoma leaf spots and stem canker caused by *Leptosphaeria maculans* (Lm) and *L. biglobosa* (Lb).

Recent studies showed that *L. biglobosa* can inhibit the production of sirodesmin PL by *L. maculans* if it was simultaneously co-inoculated. In order to further understand the antagonistic effects of *L. biglobosa*, this study investigated the effects of sequential co-inoculation on interspecific interactions between *L. maculans* and *L. biglobosa in vitro*.

Materials and Methods

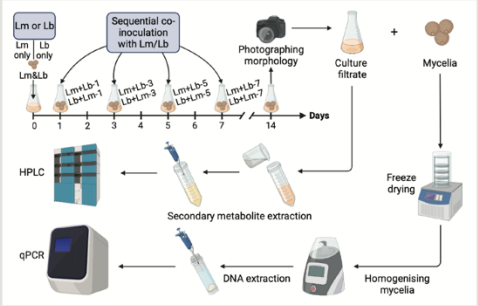

Figure 2: Illustration of method used in this work.

- Data were analysed with Two-Way ANOVA and Tukey's HSD post-hoc tests.

Results

- Morphology of mycelia in cultures initially inoculated with Lb then Lm were similar to 'Lb only', 'Lm&Lb' or 'Lm+Lb-1' (Fig. 3).
- Inhibition of sirodesmin PL and its precursors were congruent with the morphological observations, with 'Lm+Lb-5' and 'Lm+Lb-7' being similar to 'Lm only'. Interestingly, a partial inhibition was found in 'Lm+Lb-3' (Fig. 4).
- *L. biglobosa* has an antagonistic effect on the growth of *L. maculans*, confirmed by species-specific qPCR (Fig. 5).

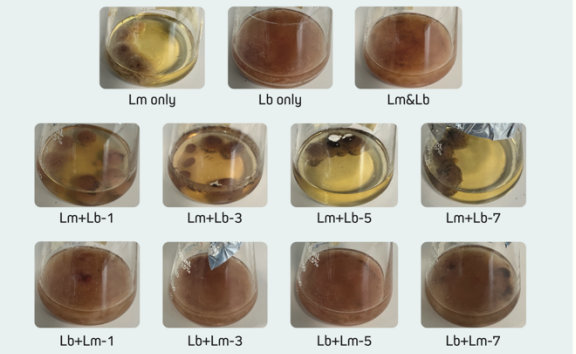

Figure 3: Morphology of mycelia of different treatments in clarified V8 broth at 14 days post inoculation (dpi).

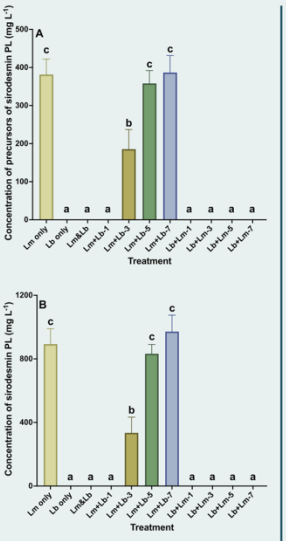

Figure 4: Average concentration of A) The precursors of sirodesmin PL (mg L^{-1}) B) Sirodesmin PL (mg L^{-1}) in secondary metabolite extracts from three independent experiments. Columns that do not share a letter are considered significantly different ($P<0.05$). Error bars show the standard error of the mean (SEM).

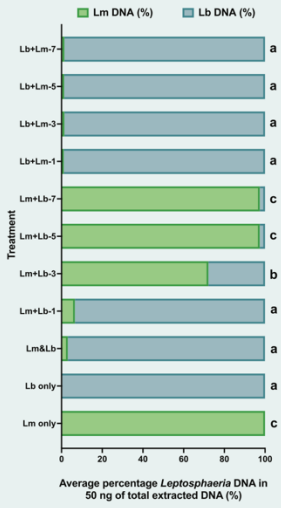

Figure 5: Average percentage of *Leptosphaeria* DNA (%) in homogenised mycelia from three independent experiments. Columns that do not share a letter are considered significantly different ($P<0.05$).

Discussion

- Interspecific interactions between *L. maculans* and *L. biglobosa* are affected by co-inoculation timing, and *L. biglobosa* can exert antagonistic effects on *L. maculans* if it is co-inoculated before or up to 3 days after *L. maculans*.
- There is a need to investigate the mechanism of these antagonistic effects of *L. biglobosa*, for development of novel ideas for sustainable management of phoma stem canker.

Conference Organisers

AOF GCIRC

Acknowledgements

ADAS Chadacre Agricultural Trust COBBOLD TRUST Perry Foundation University of Hertfordshire UH

8.12 Appendix L – Oral presentations

International Organisation for Biological and Integrated Control Meeting on Integrated Control of Oilseed Crops (May 2022 – Remote)

Session 4: OSR diseases and their control

Chair: Birger Koopmann

S4-1: Cultural characteristics and differentiation in virulence pattern of *Sclerotinia sclerotiorum* field isolates

Nazanin ZAMANI NOOR

S4-2: Overview of the joint research project "SkleroPro" - Evaluation of environmental factors affecting *Sclerotinia sclerotiorum*

Sinja BRAND

S4-3: Bacterial volatile mediated dormancy of microsclerotia of *Verticillium longisporum* in soil

Sarenqimuge SARENQIMUGE

S4-4: Azole fungicides sensitivity screening of Irish *Pyrenopeziza brassicae* populations and investigation of molecular mechanisms of insensitivity within *CYP51* gene

Diana BUCUR

S4-5: Systematic map of plant protection management methods in oilseed rape

Anna BERLIN

Session 5: Clubroot and its control

Chair: Ann Charlotte Wallenhammar

S5-1: Disease reaction of different plant species against virulent isolates of *Plasmodiophora brassicae*

Nazanin ZAMANI NOOR

S5-2: Bulk segregant analysis (BSA) for identification of clubroot resistance loci in the rapeseed DH population resynthesis S101 x Raptor

Nazanin ZAMANI NOOR

S5-3: Innovative biocontrol measures against *Plasmodiophora brassicae* Wor.

Pratik DOSHI

POSTERS

Chair: Lenka Burketova

P-1: Leptosphaeria biglobosa inhibits production of secondary metabolite sirodesmin PL by *L. maculans* in planta

Evren BINGOL – FLASH TALK -

P-2: Occurrence of blackleg pathogens in Swedish winter oilseed rape revealed by Loop-mediated Isothermal Amplification

Zahra Saad OMER – FLASH TALK -

P-3: Marker assisted selection in *Brassica napus* breeding for stem canker (*Leptosphaeria* ssp.) resistance

Janetta NIEMANN – FLASH TALK -

P-4: Effects of plant age and inoculum concentration on light leaf spot disease phenotypes on oilseed rape

Laura SAPELLI – FLASH TALK -

P-5: Spectrum of resistance to *Verticillium* wilt in Polish WOSR breeding materials

Joanna KACZMAREK – FLASH TALK -

P-6: Investigating mycovirus-mediated systemic resistance in oilseed rape

Jacob LOCKE-GOTEL – FLASH TALK -

AFCP Student Forum (March 2024 in Cambridge, UK)

University of Hertfordshire Annual Life and Medical Sciences Conference (June 2024 in Hatfield, UK)

BSPP Annual Conference (September 2024 in Oxford, UK)

Understanding interactions between *Leptosphaeria maculans* and *L. biglobosa* for improving control of phoma stem canker on oilseed rape in the UK

Evren Bingol[1], Aiming Qi[1], Chinthani Karandeni-Dewage[1], Faye Ritchie[2], Bruce D. L. Fitt[1] & Yong-Ju Huang[1]

[1] School of Life and Medical Sciences, University of Hertfordshire, Hatfield, AL10 9AB

[2] ADAS Boxworth, Cambridge, CB23 4NN

8.13 Appendix M – Conferences and events

List of conferences and events attended during the course of the PhD

Conference/event	Location	Date
AFCP Forum (OSR Diseases)	Hatfield, UK	June 2021
AFCP Forum (Young Minds and Ideas)	Gloucester, UK	November 2021
BSPP Annual Conference	Birmingham, UK	December 2021
AFCP Student Forum	Cranfield, UK	March 2022
IOBC-ICOC Meeting	Remote	May 2022
UH LMS Conference	Hatfield, UK	June 2022
Cereals	Herts, UK	June 2022
BSPP Annual Conference	Remote	September 2022
AAB Meeting (Climate Mitigation)	Remote	November 2022
AAB Meeting (Biocontrol and IPM)	Remote	November 2022
AFCP/NIAB Meeting	Cambridge, UK	February 2023
UH LMS Conference	Hatfield, UK	June 2023
International Congress of Plant Pathology	Lyon, France	August 2023
BMS Annual Conference	Newcastle, UK	September 2023
International Rapeseed Congress	Sydney, Australia	September 2023
AFCP Student Forum	Cambridge, UK	March 2024
UH LMS Conference	Hatfield, UK	June 2024
Cereals	Herts, UK	June 2024
BSPP Annual Conference	Oxford, UK	September 2024
BCPC Diseases Review Meeting	Cambridge, UK	October 2024

BSPP Annual Conference (December 2021 in Birmingham, UK)

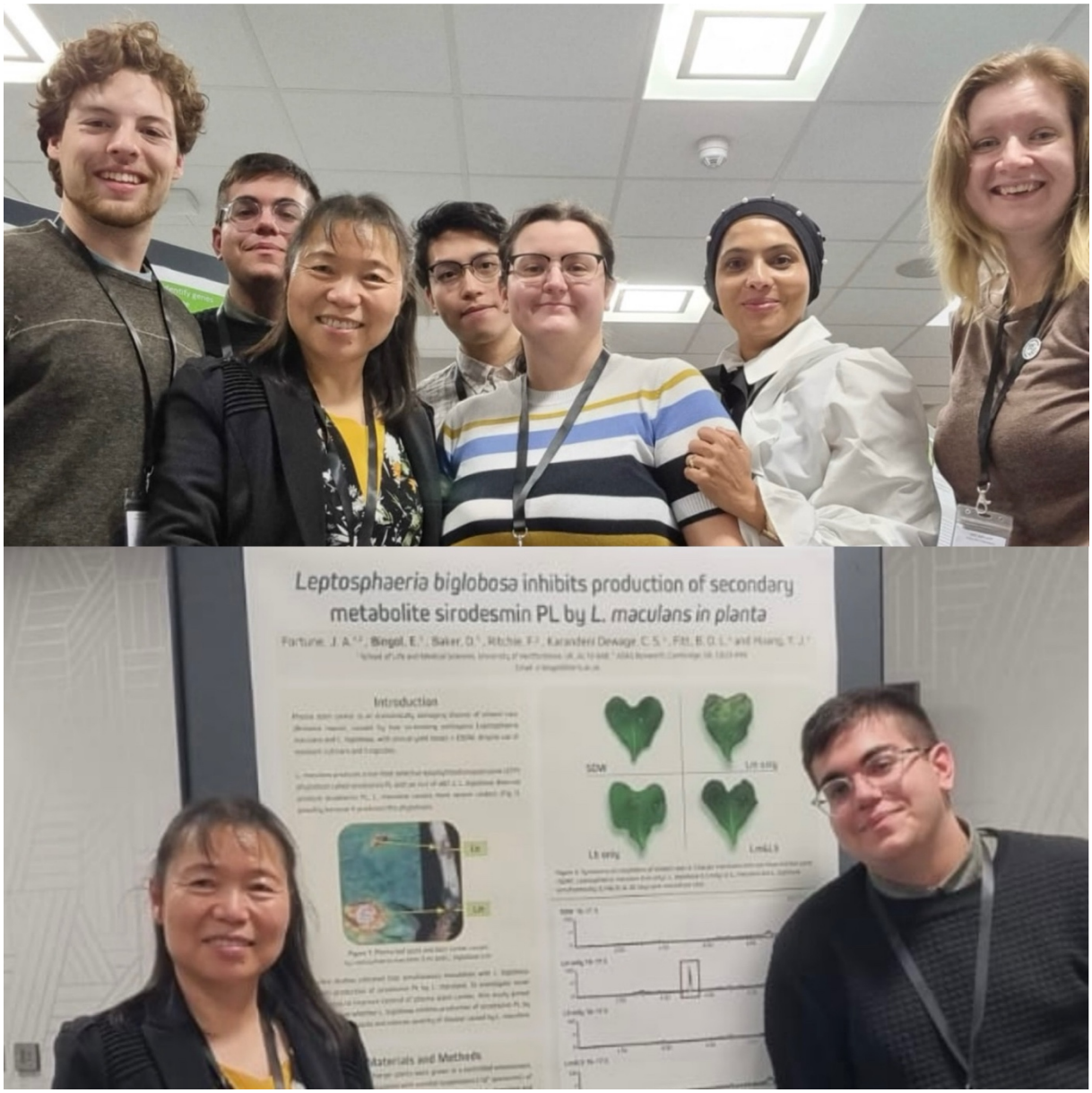

University of Hertfordshire Annual Life and Medical Sciences Conference (June 2022 in Hatfield, UK)

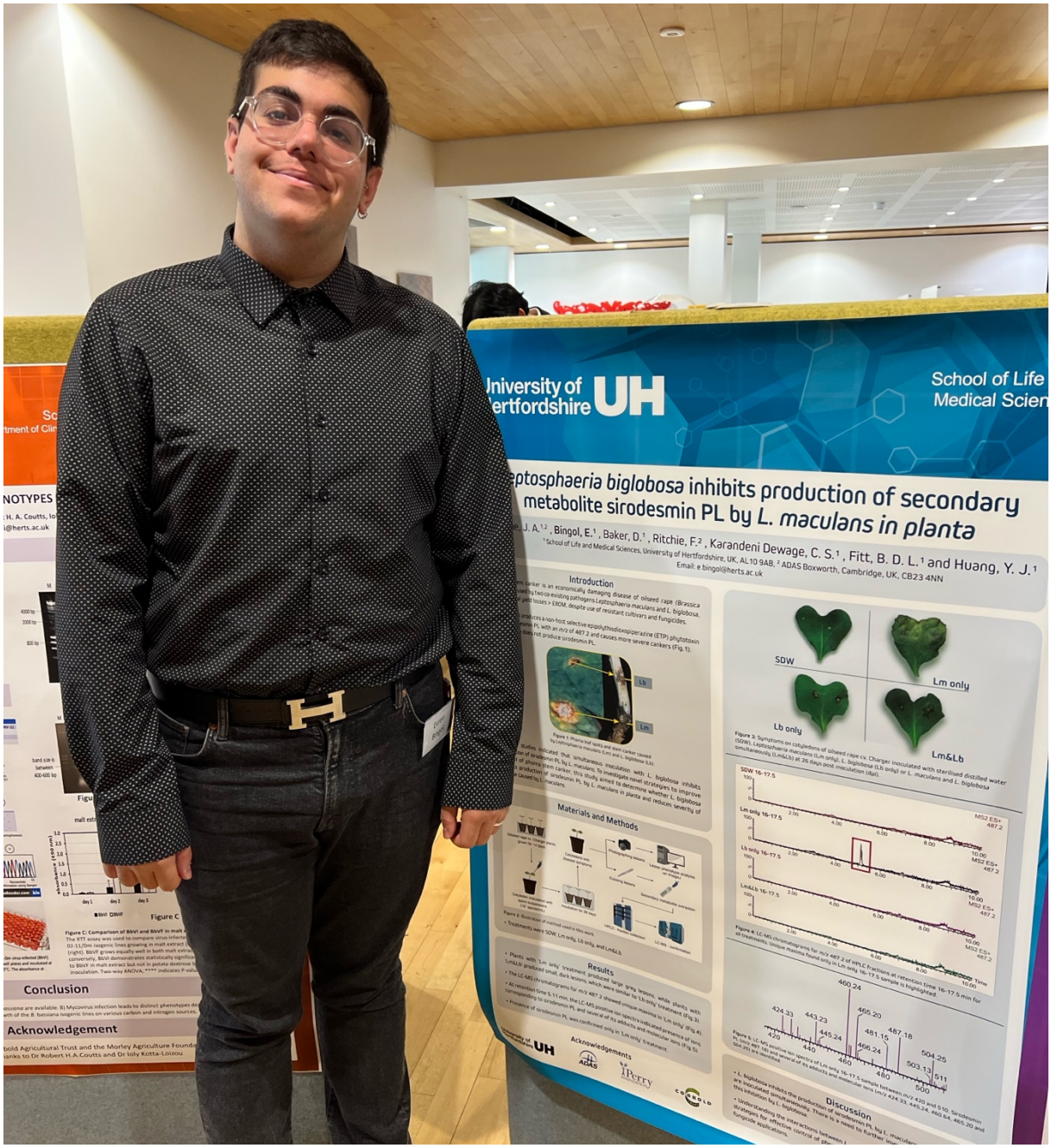

Cereals (June 2022 in Herts, UK)

University of Hertfordshire Annual Life and Medical Sciences Conference (June 2023 in Hatfield, UK)

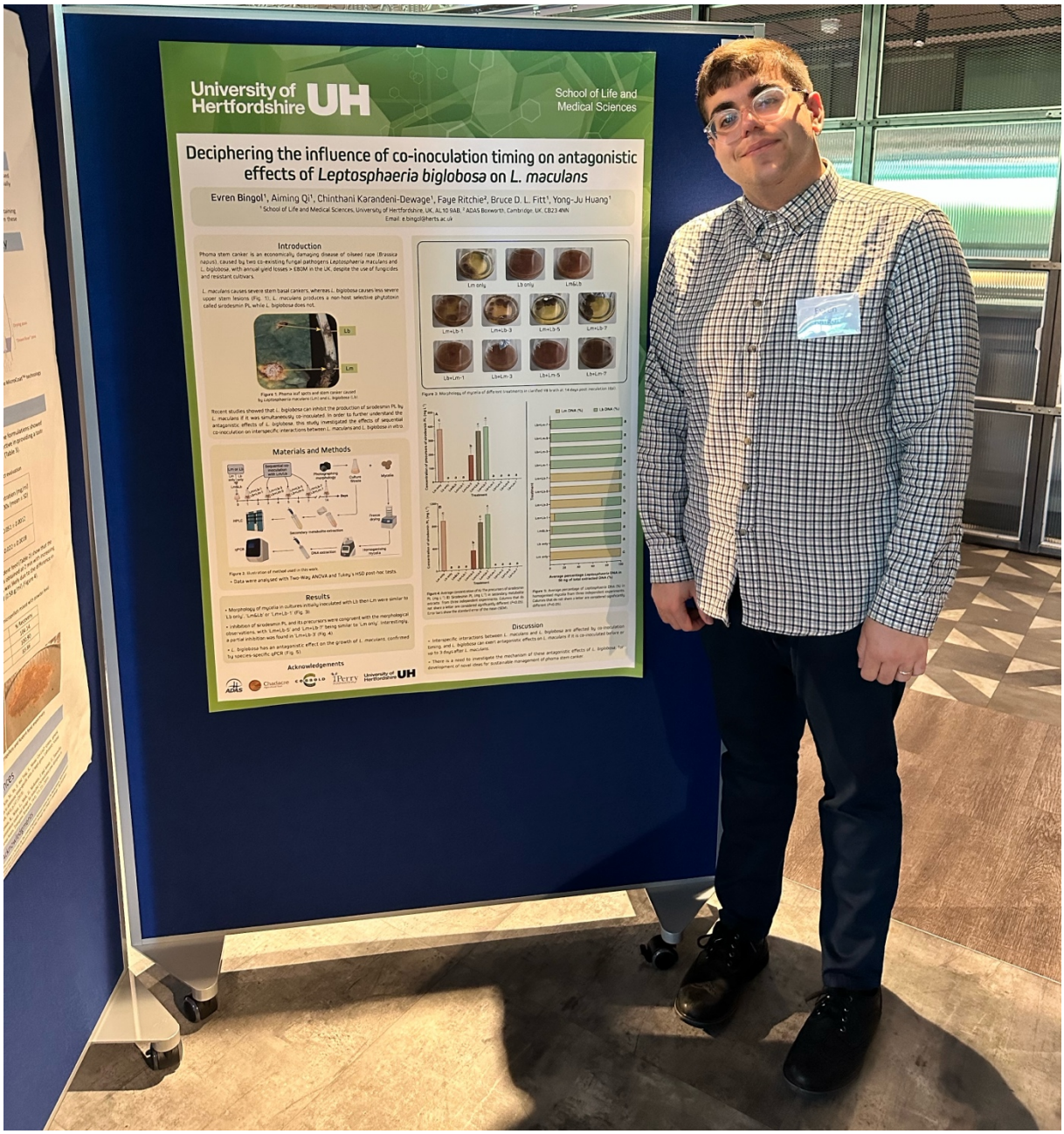

16th International Congress of Plant Pathology (ICPP2023) (August 2023 in Lyon, France)

16th International Rapeseed Congress (IRC2023) (September 2023 in Wagga Wagga, Canberra, Sydney, Australia)

University of Hertfordshire Annual Life and Medical Sciences Conference (June 2024 in Hatfield, UK)

Cereals (June 2024 in Herts, UK)

BSPP Annual Conference (September 2024 in Oxford, UK)

8.14 Appendix N – Awards

Best Poster Presentation (Flash Talk) Award at International Organisation for Biological and Integrated Control Meeting on Integrated Control of Oilseed Crops (May 2022 – Remote)

Evren BINGOL

Leptosphaeria biglobosa inhibits production of secondary metabolite sirodesmin PL by *L. maculans* in planta

Convenor: Małgorzata Jędryczka
SG Entomology Convenor: Sam Cook
SG Pathology Convenor: Małgorzata Jędryczka

Best Poster Presentation Award at University of Hertfordshire Annual Life and Medical Sciences Conference (June 2022 in Hatfield, UK)

Annual School of Life and Medical Sciences

Research Conference

Lindop Building, College Lane Campus, University of Hertfordshire
Tuesday 21st June 2022

Poster Prize Winner

Evren Bingol

Poster title

Leptosphaeria biglobosa inhibits production of secondary metabolite sirodesmin PL by L. maculans in planta

Signature

University of Hertfordshire UH

Health and Wellbeing

Food

Information and Security

Best Oral Presentation Award at University of Hertfordshire Annual Life and Medical Sciences Conference (June 2024 in Hatfield, UK)

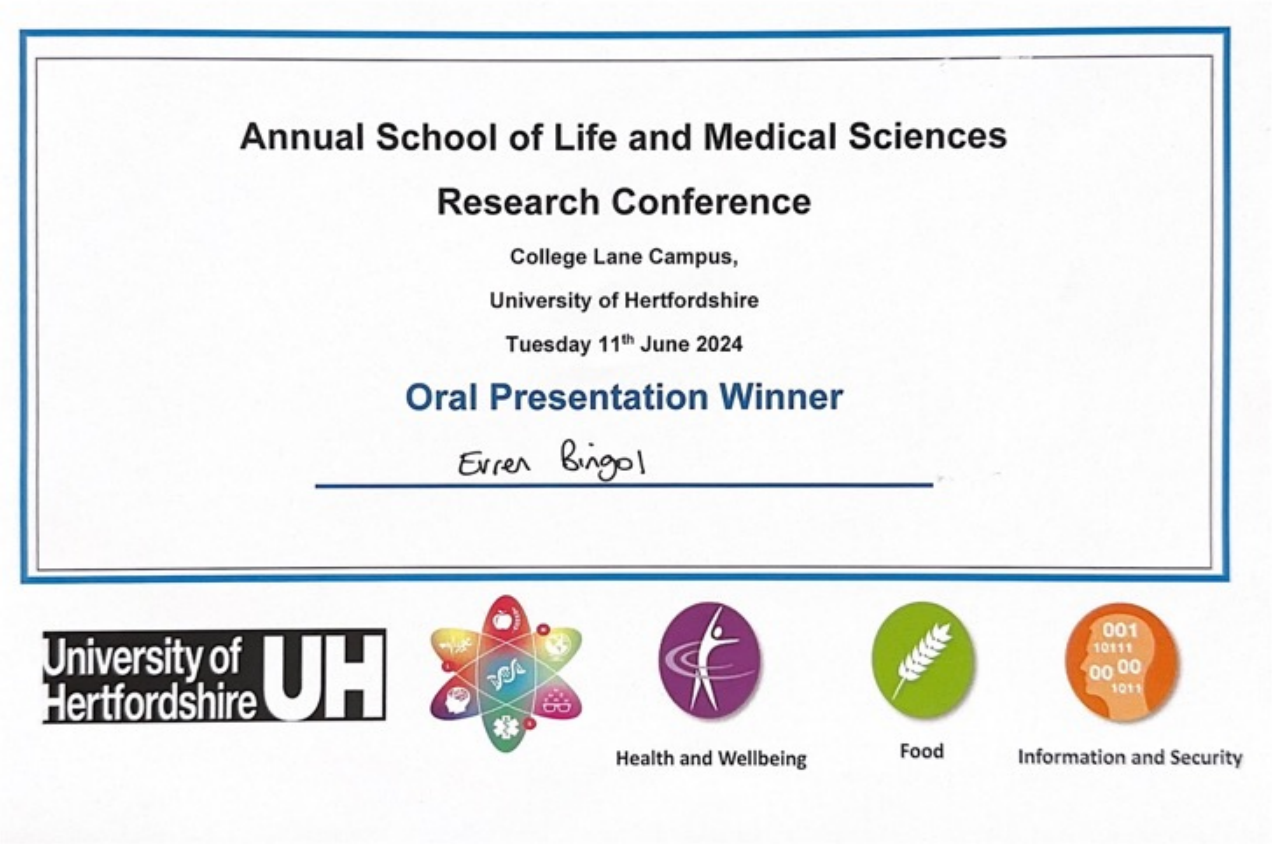

Leptosphaeria biglobosa inhibits the production of sirodesmin PL by *L. maculans* (Pest Management Science, doi: 10.1002/ps.7275)

Research Article

Received: 9 September 2022 Revised: 31 October 2022 Accepted article published: 3 November 2022 Published online in Wiley Online Library:

(wileyonlinelibrary.com) DOI 10.1002/ps.7275

Leptosphaeria biglobosa inhibits the production of sirodesmin PL by *L. maculans*

James A. Fortune,[a,b] Evren Bingol,[a] Aiming Qi,[a] Daniel Baker,[c] Faye Ritchie,[b] Chinthani S. Karandeni Dewage,[a] Bruce D. L. Fitt[a] and Yong-Ju Huang[a*]

Abstract

BACKGROUND: Phoma stem canker is caused by two coexisting pathogens, *Leptosphaeria maculans* and *L. biglobosa*. They coexist because of their temporal and spatial separations, which are associated with the differences in timing of their ascospore release. *L. maculans* produces sirodesmin PL, while *L. biglobosa* does not. However, their interaction/coexistence in terms of secondary metabolite production is not understood.

RESULTS: Secondary metabolites were extracted from liquid cultures, *L. maculans* only (Lm only), *L. biglobosa* only (Lb only), *L. maculans* and *L. biglobosa* simultaneously (Lm&Lb) or sequentially 7 days later (Lm+Lb). Sirodesmin PL or its precursors were identified in extracts from 'Lm only' and 'Lm+Lb', but not from 'Lm&Lb'. Metabolites from 'Lb only', 'Lm&Lb' or 'Lm+Lb' caused significant reductions in *L. maculans* colony area. However, only the metabolites containing sirodesmin PL caused a significant reduction to *L. biglobosa* colony area. When oilseed rape cotyledons were inoculated with conidia of 'Lm only', 'Lb only' or 'Lm&Lb', 'Lm only' produced large gray lesions, while 'Lm&Lb' produced small dark lesions similar to lesions caused by 'Lb only'. Sirodesmin PL was found only in the plant extracts from 'Lm only'. These results suggest that *L. biglobosa* prevents the production of sirodesmin PL and its precursors by *L. maculans* when they grow simultaneously *in vitro* or *in planta*.

CONCLUSION: For the first time, *L. biglobosa* has been shown to inhibit the production of sirodesmin PL by *L. maculans* when interacting simultaneously with *L. maculans* either *in vitro* or *in planta*. This antagonistic effect of interspecific interaction may affect their coexistence and subsequent disease progression and management.

Keywords: interspecific competition; oilseed rape; secondary metabolites; phoma stem canker; *Plenodomus lingam*; *Plenodomus biglobosus*

1 INTRODUCTION

Offspring of most living organisms are provided with enough resources for initial development, but they must obtain resources for the fundamental energy required for further development, growth, survival and reproduction.[1] Resource conservation rules state that resources acquired by one organism are not immediately available to another, so if there is a limited supply of resources, competition will arise – resource competition.[1–3] Interactions between pathogens and host plants do not occur in isolation; a host is likely to interact with many different species.[4] There will be resource competition between different species, called interspecific competition.[3,5] Plant pathogens that share the same host face resource competition for successful infection of the host.

Phoma stem canker is an economically important disease of oilseed rape caused by two closely related hemi-biotrophic ascomycete fungal pathogens: *Leptosphaeria maculans* (*Plenodomus lingam*) and *L. biglobosa* (*P. biglobosus*).[6–8] This disease caused annual yield losses of >£74M in the UK, despite the use of fungicides.[9,10] The distribution of *L. maculans* and *L. biglobosa* varies globally. Whereas in parts of eastern Europe and China only *L. biglobosa* is found, both pathogens can be found to coexist in northern and western Europe, Australia, and Canada.[11] These two pathogens can coexist because they occupy different ecological niches due to slight differences in their biological and epidemiological characteristics.[11] One example is the difference in their temperature optima for pseudothecial (fruiting body) maturation, which causes a temporal separation of ascospore release in Western Europe.[7–12] This enables the resource to be partitioned

* *Correspondence to: Y-J Huang, Centre for Agriculture, Food and Environmental Management Research, School of Life and Medical Sciences, University of Hertfordshire, Hatfield AL10 9AB, UK, E-mail: y.huang8@herts.ac.uk.*

a *Centre for Agriculture, Food and Environmental Management Research, School of Life and Medical Sciences, University of Hertfordshire, Hatfield, UK*

b *Disease and Pest Management, ADAS Boxworth, Cambridge, UK*

c *Centre for Topical Drug Delivery and Toxicology, School of Life and Medical Sciences, University of Hertfordshire, Hatfield, UK*

and the two *Leptosphaeria* spp. to coexist on the same plant because a later *L. biglobosa* ascospore release coincides with the elongation of the stem and emergence of later leaves to infect the upper stems, causing upper lesions. By contrast, while the earlier *L. maculans* ascospore release is associated with stem base cankers due to infection of earlier leaves.[13,14] *L. maculans* is considered economically more important than *L. biglobosa* due to its association with the more damaging stem basal cankers, while *L. biglobosa* is associated with upper stem lesions.[7,13] However, recent reports suggest that *L. biglobosa* can also be detected in stem basal cankers as well as upper stem lesions.[15–18]

There has been limited work investigating the interactions between *L. maculans* and *L. biglobosa*. *In vitro* work has shown that *L. maculans* is able to inhibit the germination of *L. biglobosa* spores due to the presence of a secondary metabolite called sirodesmin PL.[19] *L. maculans* produces sirodesmin PL, a nonhost selective epipolythiodioxopiperazine (ETP) phytotoxin, but *L. biglobosa* does not.[13,20,21] The function of sirodesmin PL is still unknown. Mutant isolates that did not produce sirodesmin PL were still able to cause normal disease symptoms on oilseed rape cotyledons; however, a mild reduction in stem canker severity and 50% reduction in fungal biomass was observed with mutant isolates.[19] This suggests that sirodesmin PL is not required for infection and disease progression. Studies have shown that mutants without sirodesmin PL had less antibacterial and antifungal activity than the wild type but did not have decreased growth or fertility,[22,23] suggesting that it may be used as an interference competition strategy. Interference competition is a strategy of interspecific competition, where a competing pathogen produces a secondary metabolite that is toxic to competing species, limiting access of other pathogens to the resource. For example, early establishment of *F. subglutinans* in maize can reduce the production of the toxic metabolite trichothecene by *F. graminearum* and temporarily protect the plant from colonization by the more toxic and damaging *F. graminearum*.[24] Similarly, previous work has shown that the pre-inoculation of oilseed rape plants with *L. biglobosa* induced resistance to *L. maculans*.[25,26] However, the effectiveness of *L. biglobosa* (weakly virulent type) in inducing resistance to *L. maculans* (highly virulent) infection was compromised if *L. biglobosa* was added at 64 h or later after *L. maculans*.[25] This may be due to the time required for production of sirodesmin PL by *L. maculans* needs up to 3 days,[27] since 64 h is about 2.5 days. This suggests that sirodesmin PL plays an important role in the interactions between *L. maculans* and *L. biglobosa*. There is a need to investigate the interactions between *L. maculans* and *L. biglobosa* in relation to secondary metabolite production, especially sirodesmin PL production by *L. maculans* and its effects on disease development, for improving phoma stem canker control strategies.

2 MATERIALS AND METHODS

2.1 Pathogen and media preparation

2.1.1 Pathogen preparation

L. maculans isolate ME24, obtained from stem canker of oilseed rape cultivar Apex in 2002,[28] and *L. biglobosa* isolate WH17-Why-1, obtained from phoma leaf lesion of oilseed rape cultivar Whisky in 2017, were used in this study. The *L. maculans* and *L. biglobosa* isolates were grown on 20% V8 agar plates for 14 days, and agar plugs were cut at the growth front of the plate for inoculation of liquid culture or agar plates.

2.1.2 Identifying the optimal media for culturing of the pathogens

Agar plugs (10 mm) of *L. maculans* isolate ME24 and *L. biglobosa* isolate WH17-Why-1 were inoculated in the middle of plates (9 cm) containing five different growth media: malt extract agar (MEA), water agar (WA), potato dextrose agar (PDA), 20% V8 juice agar (V8) or 20% clarified V8 agar (V8 Clar). V8 juice was clarified by adding 15 g L^{-1} of calcium carbonate to the V8 juice agitated using a magnetic stirrer for 15 min before being centrifuged at 1400 *g* for 5 min. The pH of the clarified V8 media was 5.86, whereas the pH of the V8 only media was 6.15. The pellet was discarded. The supernatant was stored at −20 °C until required. The supernatant was classed as clarified V8 juice. The inoculated plates were incubated for 7 days at 21 °C in continuous darkness before the colony diameter was measured. Each treatment was replicated three times. The colony diameter was converted to colony area (cm^2).

2.2 Concentration of sirodesmin PL production by *L. maculans*

Three plugs of *L. maculans* (8 mm diameter) were cultured in 250-mL conical flasks containing 75 mL of clarified 20% V8 juice broth in a rotary shaker at 80 rpm and 18 °C for 14 days in continual darkness. Secondary metabolite extractions were taken at six time points. There were three replicates for each time point. The experiment was replicated two times (experiments 1 and 2). The time points for experiment 1 were 1, 3, 7, 8, 10, and 14 days post inoculation (dpi) and for experiment 2 were 1, 3, 6, 8, 10, and 14 dpi. The secondary metabolites were extracted from each sample and analyzed using high-performance liquid chromatography (HPLC).

The secondary metabolites from liquid culture were extracted using ethyl acetate. The culture filtrate from each replicate was split equally into two 50-mL Falcon tubes (~37.5 mL in each). Each Falcon tube was then topped up to 50 mL using ethyl acetate (EtOAc) (~12.5 mL), then gently inverted 30 times to increase secondary metabolite uptake, then left for 1 h so that the phases could settle before being centrifuged at 3200 *g* for 5 min. For each replicate, 20 mL of the organic phase was pipetted into a clean 50-mL Falcon tube and the EtOAc was evaporated under a constant stream of nitrogen using a sample concentrator. The dried metabolites were resuspended in 0.5 mL of EtOAc. Falcon tubes containing the same treatment were combined into sterile plastic sample bottles. Using a syringe, the resuspended metabolites were passed through a 0.45-μm syringe filter into a clean HPLC sample vial. A different HPLC vial was prepared with a glass insert and 200 μL of the resuspended metabolites was pipetted into the insert. The samples were stored at 20 °C until required for HPLC analysis.

To measure the concentration of sirodesmin PL, a gliotoxin standard curve ($R^2 = 0.999$, $y = 2^6x - 56\,900$) was created using maximal areas of gliotoxin samples visualized at 254 nm at concentrations of 0, 10, 50, 100, 250, 500, and 1000 mg L^{-1} using HPLC analysis. This gliotoxin standard curve was used to calculate the concentration of sirodesmin PL at each time point. The level of detection (LOD) and level of quantification (LOQ) were 70 and 200 mg L^{-1}, respectively. The mean concentration at each time point was calculated. Gliotoxin was used for the standard curve because it belongs to the same class of fungal secondary metabolites as sirodesmin PL, ETP, has been used in previous work as a standard curve,[23] and is commercially available.

2.3 Effects of *L. biglobosa* on secondary metabolite production by *L. maculans in vitro*

To investigate the effects of *L. biglobosa* on secondary metabolite production by *L. maculans*, *L. biglobosa* was simultaneously or sequentially inoculated with *L. maculans*. Clarified 20% V8 juice broth was inoculated with four different treatments: *L. maculans* only (Lm only), *L. biglobosa* only (Lb only), *L. maculans* and *L. biglobosa* simultaneously (Lm&Lb), and *L. maculans* and *L. biglobosa* sequentially (Lm+Lb). For the 'Lm+Lb' treatment, the liquid media was inoculated with *L. maculans* followed by *L. biglobosa* inoculation after 7 days. Three plugs of each pathogen were used per corresponding treatment, therefore cultures containing both the pathogens had six fungal plugs. Each inoculation treatment was done in triplicate. The experiment was repeated three times. To identify the secondary metabolite composition of the different treatments, secondary metabolites were extracted from liquid media using ethyl acetate after 14 dpi. The samples were prepared and analyzed using HPLC. To identify the compound responsible for each unique HPLC maximum, individual 1-mL fractions were taken for liquid chromatography–mass spectrometry (LC–MS) analysis.

To identify the secondary metabolite composition, the samples were analyzed using a Shimadzu Prominence HPLC machine (Kyoto, Japan) with a diode array detector (SPD-M20A) using 20-µL injections. Separations were performed on a C_{18} column (Varian pursuit 5, 150 × 4.6 mm). A linear gradient from 85% water and 15% acetonitrile going to 100% acetonitrile in 40 min, then maintaining 100% acetonitrile for 3 min before starting a linear gradient back to 85% water over 5 min was used. It was then held at 85% water before starting the next sample. Each sample had a total run time of 53 min. A flow rate of 1 mL min^{-1} was used. Results were visualized at 254 nm using Lab solution version 5.92 (Shimadzu Corporation) but wavelengths were detected from 190 to 400 nm. The LOD and LOQ were calculated to be 70 and 200 mg L^{-1}, respectively. All samples and chemicals used were passed through a 0.45-µm nylon microfilter before being analyzed, although all chemicals used were of HPLC analytical grade and water was double distilled. The expected pattern of maxima for deacetylsirodesmin PL, phomamide, and sirodesmin PL were identified using information from Pedras *et al.*[27]

2.4 Identification of secondary metabolites using LC–MS

A Waters I-Class UPLC system coupled to a Xevo Micro TQ-S mass spectrometer was used for analysis. Chromatographic separation was performed on a Waters BEH C18 column (2.1 × 50 mm, 1.8 µm) held at 40 °C with mobile phase A = 0.2% formic acid in water, and mobile phase B = acetonitrile. The flow rate was set at 0.4 mL min^{-1} and a gradient separation performed by ramping initial starting conditions of 85% A to 0% A over 9 min, holding 100% B for 1 min, returning to starting conditions of 85% A over 0.1 min, and holding 85% for 4.9 min to re-equilibrate the column. The injection volume was 10 µL. A full mass scan was performed in positive ion mode over the range 50–650 *m/z* using a scan time of 0.2 s. The probe capillary voltage was 3 kV, the cone voltage was fixed at 20 V, and the collision energy was fixed at 3 V. Desolvation gas flow was set at 1000 L h^{-1}, with a temperature of 500 °C, and a cone gas flow of 150 L h^{-1} was used, with source temperature set at 150 °C.

2.5 Effects of secondary metabolite extracts on growth of *L. maculans* and *L. biglobosa* on agar plates

Fungal plugs of *L. maculans* or *L. biglobosa* (8 mm in diameter) were inoculated onto the middle of clarified V8 juice (V8 Clar) agar plates. Each fungal plug was then inoculated with 20 µL of the corresponding secondary metabolite extract from each treatment ('Lm only', 'Lb only', 'Lm&Lb', 'Lm+Lb') or ethyl acetate (control). Each treatment had five replicate plates. Plates were sealed using Parafilm and incubated at 18 °C in continual darkness. Colony diameters for *L. maculans* and *L. biglobosa* were recorded at 7 dpi. The colony diameter was converted to colony area (cm^2). The experiment was repeated three times.

2.6 Effects of *L. biglobosa* on disease development and sirodesmin PL production by *L. maculans in planta*

2.6.1 Preparation of L. maculans *and* L. biglobosa *inoculum and plant material*

L. maculans and *L. biglobosa* conidial inoculum was obtained from 2-week-old cultures grown on 20% V8 juice agar as described by Huang *et al.*[28] The suspensions were measured using a hemocytometer slide under a light microscope and suspensions were adjusted to 1×10^7 conidia mL^{-1}. The 'Lm&Lb' inoculum was prepared by combining a sample of each conidial spore suspension in a 1:1 ratio. Cultivar Charger, which has a moderate disease resistance rating score of 4 according to the AHDB Recommended List resistance ratings (0–9 scale, with 9 being good resistance), was used for this study (https://ahdb.org.uk/knowledge-library/recommended-lists-archive). Cotyledons were prepared by sowing seeds of winter oilseed rape cv. Charger into 40-well plug trays placed in a controlled environment cabinet set at 20/18 °C and 12 h/12 h day/night. Plug trays were filled with John Innes (No. 3) soil and Miracle Grow multipurpose compost mixed in a 1:1 ratio. Plants were regularly watered to ensure soil remained moist. True leaves were removed to prolong the lifespan of cotyledons.

2.6.2 Experimental design and plant inoculation

There were four treatments, 'Lm only', 'Lb only', 'Lm&Lb' and a sterilized distilled water control, 'SDW'. There were 30 plants per treatment. The experiment was designed using a randomized block design with three replicates. Cotyledons of 14-day-old seedlings were inoculated. The inoculation sites were prepared by wounding the cotyledon using a sterilized needle. Each cotyledon was wounded in two locations, therefore there were four inoculation sites per plant. For inoculation, 10 µL of conidial suspension was pipetted onto each inoculation site according to the treatment and experimental design. Inoculated plants were covered with tray covers to maintain high humidity for 48 h. The inoculated plants were kept in a controlled environment cabinet at 18/16 °C and 12 h/12 h day/night.

2.6.3 Assessment of disease development

To measure the size of lesions, cotyledons were excised from each plant at 17 dpi, placed inside a 9 × 9 cm square, and a standardized photograph was taken. The lesion area was calculated by processing the standardized photographs using ImageJ software.[29] The total number of pixels were converted into cm^2. The experiment was repeated three times.

2.6.4 Assessment of sirodesmin PL production in planta

Due to the *in planta* secondary metabolite detection requiring very severely diseased plant tissue, a separate experiment with the same design as those used for disease development experiments was done and the cotyledons were excised from each plant at 26 dpi, rather than at 17 dpi. The standardized photograph was also taken for assessing the lesion area using ImageJ software. After lesion phenotype photographs were taken,

Pest Management Science published by John Wiley & Sons Ltd on behalf of Society of Chemical Industry.

lesions from 30 plants of each treatment were excised. The lesions were excised according to their size. For small (e.g. plants inoculated with Lb only) or no lesions (e.g. control), an 8 mm diameter corer centered over each inoculation site was used. For larger lesions, a scalpel was used to excise the lesion. Lesions from five plants were grouped together and placed into 2-mL screw cap tubes. There was a total of six 2-mL screw cap tubes per treatment. After 48 h of freeze-drying, three small metal balls (3 mm) and 600 µL of ethyl acetate were added to each tube. Each sample was lysed using a FastPrep machine for 40 s at 6.0 m s^{-1}; this step was repeated three times, samples were placed on ice in between runs of the FastPrep. Lysed samples were centrifuged at 15 700 *g* for 5 min and 500 µL of ethyl acetate supernatant was pipetted into a sterile 50 mL Falcon tube. Supernatants for each treatment were combined and evaporated to residue. Each treatment sample was resuspended in 500 µL of ethyl acetate and passed through a 0.45 µm Polytetrafluoroethylene (PTFE) syringe filter into a 2 mL HPLC vial for HPLC analysis. For identification of the compound responsible for each unique HPLC maximum, individual 1.5 mL fractions were taken for between 11–12.5 min and 16–17.5 min for each sample. Fractions were evaporated to residue before being resuspended in 110 µL of ethyl acetate before being analyzed by LC–MS.

2.7 Statistical analysis

The statistical analysis of the data was done using GenStat 22nd edition.[29] To analyse the effects of different media types on colony area of different pathogens, the effect of co-inoculation of *L. maculans* and *L. biglobosa* on the concentration of sirodesmin PL and its precursors, a factorial analysis of variance (ANOVA) was done to determine significant differences between treatments on each pathogen. For the effect of secondary metabolite extracts on colony area, unbalanced ANOVA was used. For data at 17 dpi, a factorial ANOVA was done using 'treatment' and 'experiment number' as factors. For data at 26 dpi, an ANOVA was done using only 'treatment' as the factor. Variance ratio values (i.e., *F*-test) that were significant at $P < 0.05$ were used to provide evidence for significant effects of factors. *Post hoc* Fisher least significant difference tests were applied to separate means between different media and different secondary metabolite extracts for each pathogen.

3 RESULTS

3.1 Optimal media for colony growth

There were significant differences in the colony area on different media for *L. maculans* ($F_{4,13} = 169.37$, $P < 0.001$, LSD = 1.51) and *L. biglobosa* ($F_{4,13} = 21.31$, $P < 0.001$, LSD = 3.55). Both pathogens had significantly larger colony areas when cultured on 20% clarified V8 juice agar than on all other media tested (Fig. 1). For *L. maculans*, the colony area was not significantly different between water agar (5.6 cm^2) and MEA (6.4 cm^2), but was significantly smaller than that on PDA (10.4 cm^2). The largest colony area was on clarified V8 agar, which was significantly larger than that on V8 agar (Fig.1). For *L. biglobosa*, there were no significant differences between MEA (13.6 cm^2), WA (15.4 cm^2) and PDA (15.7 cm^2) or between MEA and V8 (11.6 cm^2). However, the colony area was significantly larger on clarified V8 agar (23.3 cm^2) than those on other media (Fig.1). The clarified V8 was the optimum medium for both *L. maculans* and *L. biglobosa*, therefore clarified V8 was used for liquid culture and agar plates in this study.

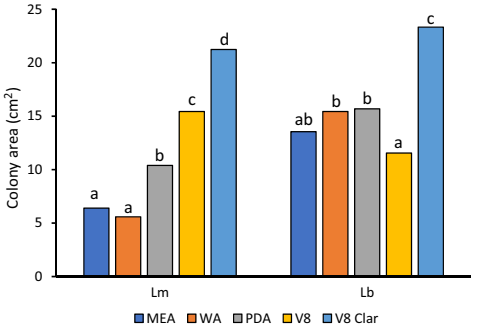

Figure 1. Colony area (cm^2) of *Leptosphaeria maculans* (Lm) or *L. biglobosa* (Lb) when cultured on different media types at 7 days post inoculation. Malt extract agar (MEA), water agar (WA), potato dextrose agar (PDA), 20% V8 juice agar (V8) and 20% clarified V8 agar (V8 Clar) (df = 13, LSD = 1.51 and 3.55 cm^2 for Lm and Lb, respectively). Letters represent Fisher's protected least significant difference test between different media tested on each pathogen. Fisher LSD tests were used to separate the mean values of colony areas for each pathogen. Columns that do not share a letter are significantly different at $P = 0.05$.

3.2 Concentration of sirodesmin PL production by *L. maculans* over 14 days

When the concentration of sirodesmin PL was measured at regular time intervals over 14 days in culture filtrates of *L. maculans*, sirodesmin PL was not detected until 3 dpi. The concentration of sirodesmin PL increased from 3 dpi until 10 dpi and then decreased from 10 dpi (Fig. 2).

3.3 Effects of *L. biglobosa* on sirodesmin PL production by *L. maculans in vitro*

3.3.1 Comparison of secondary metabolite chromatograms

For the secondary metabolites extracted from liquid culture, there were three unique maxima that were present only in the 'Lm only' and 'Lm+Lb' samples (Maximum 1 – Rt 11.2; Maximum 2 – Rt 16.2 and Maximum 3 – Rt 19.25), so these maxima were unique to these samples. When *L. maculans* was cultured simultaneously with *L. biglobosa* ('Lm&Lb') the three maxima unique to 'Lm only' and 'Lm+Lb' were not present and its chromatogram was like that of 'Lb only'.

3.3.2 Identification of maxima found on the chromatograms from extracted secondary metabolites using LC–MS

Maximum 1 contained ions in its LC–MS positive ion spectra (Fig. 3 (a)) at *m/z* 445.20, which corresponds to a monocharged molecule with a molecular weight 444.5 Da; deacetylsirodesmin is a known secondary metabolite produced by *L. maculans* and has a molecular weight of 444.5 Da.[30,31] Additionally, ions were observed at *m/z* 381.24 $[M - S_2 + H]^+$, corresponding to deacetylsirodesmin lacking two sulfur atoms; *m/z* 403.23 $[M - S_2 + Na]^+$, corresponding to the sodium adduct of sirodesmin lacking two sulfur atoms; and *m/z* 467.19 $[M + Na]^+$, corresponding to the sodium adduct of deacetylsirodesmin (Fig. 3(a)). In addition to these, ions were observed at *m/z* 319.26, which corresponds to monocharged molecule with a molecular weight of 318.4 Da. Phomamide is a known secondary metabolite produced by *L. maculans* and has a molecular weight of 318.4 Da.[30,31]

Pest Management Science published by John Wiley & Sons Ltd on behalf of Society of Chemical Industry.

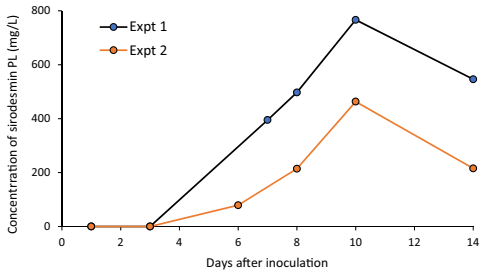

Figure 2. Concentration of sirodesmin PL (mg L^{-1}) produced in clarified V8 liquid media inoculated with *Leptosphaeria maculans* over 14 days post inoculation in experiment 1 (Expt 1) and experiment 2 (Expt 2). Concentrations were calculated using a gliotoxin standard curve ($y = 2^6x - 56900$; $R^2 = 0.999$).

Maximum 2 from the chromatogram contained ions in its LC–MS positive ion spectra (Fig. 3(b)) at *m/z* 487.19 (97%), which corresponds to a monocharged molecule with a molecular weight 486.6 Da. Sirodesmin PL is a known secondary metabolite produced by *L. maculans* with a molecular weight of 486.6 Da.[30,31] Additionally, the following ions were found: *m/z* 423.27 $[M - S_2 + H]^+$, corresponding to sirodesmin PL lacking two sulfur atoms, *m/z* 504.22 $[M + NH_4]^+$, corresponding to the ammonium adduct of sirodesmin PL and *m/z* 509.18 $[M + Na]^+$, corresponding to the sodium adduct of sirodesmin PL.

Maximum 3 from the HPLC chromatogram could not be identified using LC–MS. The fraction was further concentrated by resuspending in only 0.3 mL ethyl acetate, but a unique maximum could not be identified from the LC–MS spectra, therefore the compound responsible for maximum 3 on the HPLC chromatogram remains unknown.

3.3.3 *Secondary metabolite composition and concentration*

There were significant differences between different treatments in concentrations of sirodesmin PL 'precursors' (deacetylsirodesmin and phomamide) ($F_{3,11} = 23.87$, $P < 0.001$, LSD = 125.11) (Fig. 3(c)). The extracts that had concentrations of 'precursors' greater than the level of detection (LOD = 70 mg L^{-1}) and level of quantification (LOQ = 200 mg L^{-1}) were 'Lm only' (283.3 mg L^{-1}) and 'Lm+Lb' (357.5 mg L^{-1}) (Fig. 3(c)), and they were not significantly different from each other. The maxima for precursors were not detected in the 'Lm&Lb' or 'Lb only' treatments.

There were significant differences between treatments in the concentrations of sirodesmin PL ($F_{3,11} = 134.00$, $P < 0.001$, LSD = 128.77) (Fig. 3(c)). The extracts that had concentrations greater than the level of detection (LOD = 70 mg L^{-1}) and level of quantification (LOQ = 200 mg L^{-1}) were 'Lm only' and 'Lm+Lb' (Fig. 3(c)). There was no significant difference in the concentration of sirodesmin PL between 'Lm only' (747.4 mg L^{-1}) and 'Lm+Lb' (831.5 mg L^{-1}). The maxima for sirodesmin PL were not detected in the 'Lm&Lb' or 'Lb only' treatments.

3.3.4 *Effects of secondary metabolite extracts on growth of* L. maculans *and* L. biglobosa *on agar plates*

The secondary metabolites had a significant effect on the colony areas of *L. maculans* ($F_{4,72} = 24.62$, $P < 0.001$, LSD = 2.029) and *L. biglobosa* ($F_{4,73} = 87.10$, $P < 0.001$, LSD = 1.972) (Figs 4 and 5). The secondary metabolite extracts had greater effects on growth of *L. biglobosa* than on growth of *L. maculans* (Fig. 4). For *L. biglobosa*, the extracts that caused significant differences in colony area compared with the 'EtoAc' control (21.3 cm^2) were 'Lm only' (10.1 cm^2) and 'Lm+Lb' (8.7 cm^2) (i.e. 52.7% and 59.3% reduction compared to the EtOAc control in 'Lm only' and 'Lm+Lb', respectively), but they were not significantly different from each other. The Lb only (20.3 cm^2) and Lm&Lb (22.0 cm^2) were not significantly different from each other, nor from the EtOAc control (Fig. 4(b)). For *L. maculans*, the three treatments that differed significantly from the EtOAc control (25.8 cm^2) were 'Lb only' (19.4 cm^2), 'Lm&Lb' (18.2 cm^2) and 'Lm+Lb' (18.2 cm^2) (i.e. 24.8%, 29.5%, and 29.5% reduction, respectively), but they were not significantly different from each other. There was no significant difference between 'Lm only' (24.1 cm^2) and the ethyl acetate control in colony area of *L. maculans* (Fig. 4(a)).

3.4 Effects of *L. biglobosa* on lesion development and sirodesmin PL production by *L. maculans*

3.4.1 *Disease development* in planta

There were differences in lesion phenotypes between the four different treatments (Fig. 6). When cotyledons were inoculated with *L. maculans* conidia only (Lm only), the lesions were large, gray, sunken, and not defined. However, when cotyledons were co-inoculated simultaneously with *L. maculans* and *L. biglobosa* (Lm&Lb), the lesions were small, dark, and well-defined; these were similar to the lesions developed from inoculation with *L. biglobosa* conidia only (Lb only). By 26 dpi, the lesions of 'Lm only' had spread to the whole cotyledons while the lesions of 'Lm&Lb' did not spread and remained similar as lesions of 'Lb only' (Fig. 6). There was a significant difference between treatments in lesion area at 17 dpi ($F_{3.1106} = 181.43$, $P < 0.001$, LSD = 1.603) (Fig. 7(a)). The lesion area was significantly greater for the 'Lm only' (18.1 mm^2) than for 'Lb only' (5.3 mm^2) or 'Lm&Lb' (5.3 mm^2) (Fig. 7(a)). Similarly, at 26 dpi ($F_{3.458} = 690.08$, $P < 0.001$, LSD = 7.35), the lesion area was significantly greater for 'Lm only' (153.3 mm^2) than that for 'Lb only' (24.6 mm^2) or 'Lm&Lb' (27.1 mm^2) (Fig. 7(b)). There was no significant difference between experiments ($F_{2.1106} = 0.81$, $P = 0.444$, LSD = 1.603).

3.4.2 *Production of sirodesmin PL* in planta

There was a difference in the presence or absence of sirodesmin PL and its precursors between treatments *in planta*. Sirodesmin PL and its precursors were present only in the 'Lm only' treatment, and were absent from the 'SDW', 'Lb only' and 'Lm&Lb' treatments (Fig. 8). The LC–MS chromatograms showed that there were three unique maxima at retention times 4.95, 5.03, and 5.11 min in the 'Lm only' sample. At retention time 4.95 min, the positive ion spectra contained ions with *m/z* 242.29 (30%) and 243.35 (5%). These ions remain unidentified.

At retention time 5.03 min (Fig. 8(a)), the positive ion spectra (Fig. 8(b)) contained ions at *m/z* 319.26 (100%) and 320.29 (15%) with a mean *m/z* of 319.4. This corresponds to a monocharged molecule with a molecular weight of 318.4 Da. Phomamide is a known secondary metabolite produced by *L. maculans* and has a molecular weight of 318.4 Da.[30,31]

At retention time 5.11 min (Fig. 8(c)), the positive ion spectra (Fig. 8(d)) contained an ion at *m/z* 487.18, which corresponds to a monocharged molecule with a molecular weight of 486.57 Da. Sirodesmin PL has a molecular weight of 486.6 Da.[30,31] The positive ion spectra (Fig. 8(d)) also contained an ion at *m/z* 445.24, which corresponds to a monocharged molecule with a molecular weight of 444.24 Da. Deacetylsirodesmin PL is a known secondary

Pest Management Science published by John Wiley & Sons Ltd on behalf of Society of Chemical Industry.

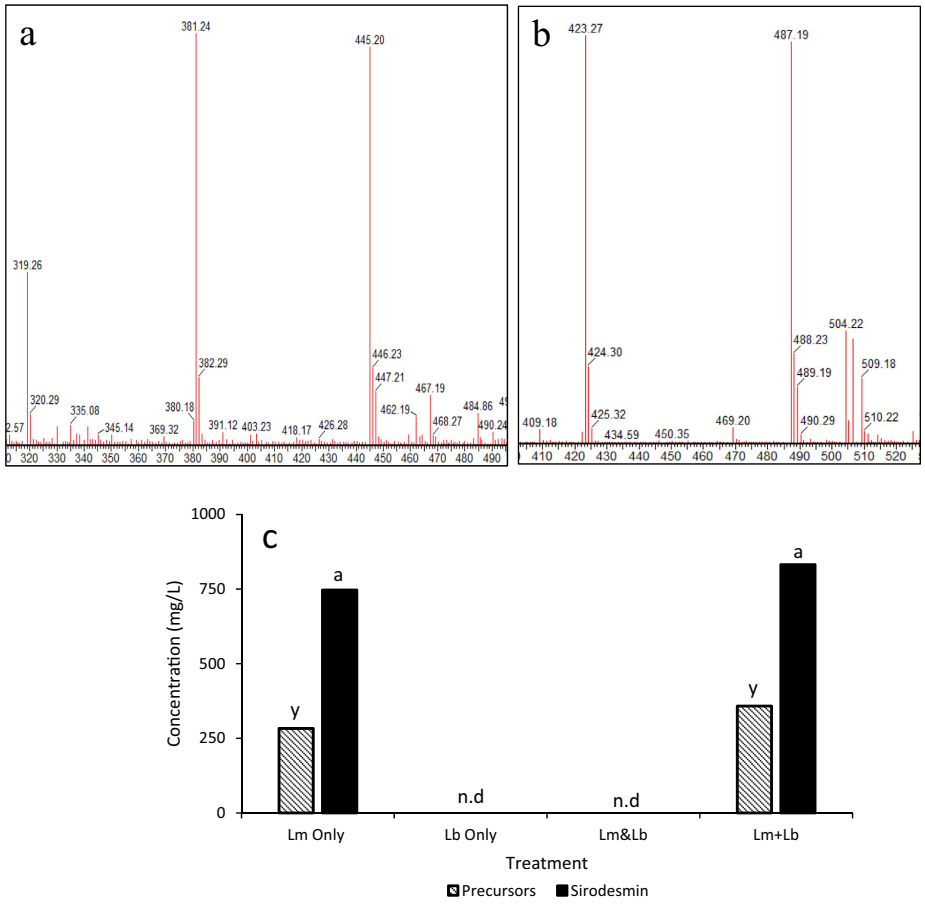

Figure 3. LC–MS positive ion spectra for the 'precursors' HPLC maximum at retention time 11–12 min (a) and 'sirodesmin' HPLC maximum at retention time 16–17 min (b). Concentration of sirodesmin PL and its precursors (mg L^{-1}) (c) extracted from clarified V8 liquid culture inoculated with *Leptosphaeria maculans* only (Lm only), *L. biglobosa* only (Lb only), *L. maculans* and *L. biglobosa* simultaneously (Lm&Lb) or *L. maculans* and *L. biglobosa* sequentially (Lm +Lb). For the Lm+Lb treatment, the liquid media was inoculated with *L. maculans* first then 7 days later with *L. biglobosa*. Fisher LSD tests were used to separate the mean values of concentrations. Columns that do not share a letter are significantly different ($P = 0.05$). Samples where a maxima corresponding to 'precursors' or 'sirodemsin PL' were not detected are indicated (n.d).

metabolite produced by *L. maculans* and has a molecular weight of 444.5 Da.[30,31] The following ions were also found in the positive ion spectra (Fig. 8(d)): *m/z* 424.32 $[M - S_2 + H]^+$, corresponding to sirodesmin PL lacking two sulfur atoms, *m/z* 460.24 $[M - S_2 + K]^+$, corresponding to the potassium adduct of sirodesmin PL lacking two sulfur atoms, 465.20 $[M - S_2 + CH_3CN + H]^+$ corresponding to the acetonitrile adduct of sirodesmin PL lacking two sulfur atoms, and *m/z* 504.25 $[M + NH_4]^+$, corresponding to the ammonium adduct of sirodesmin PL.

4 DISCUSSION

The results of this study for the first time provide evidence that *L. biglobosa* can inhibit *L. maculans* production of sirodesmin PL and its precursors to increase its competitiveness over *L. maculans* both *in vitro* and *in planta*. No sirodesmin PL nor its precursors were produced when *L. maculans* and *L. biglobosa* were grown together simultaneously *in vitro* (liquid culture) or *in planta* (cotyledons of oilseed rape), suggesting that the production of sirodesmin PL and its precursors by *L. maculans* had been inhibited by *L. biglobosa*. The inhibition of sirodesmin PL production has advantages for *L. biglobosa* growth because sirodesmin PL has antibacterial and antifungal properties.[19] There was an inhibition of *L. biglobosa in vitro* growth when secondary metabolite extracts containing sirodesmin PL were applied; this suggests that *L. maculans* uses sirodesmin PL as a form of interference interspecific competition strategy to outcompete *L. biglobosa*. This supports previous findings that *L. maculans*

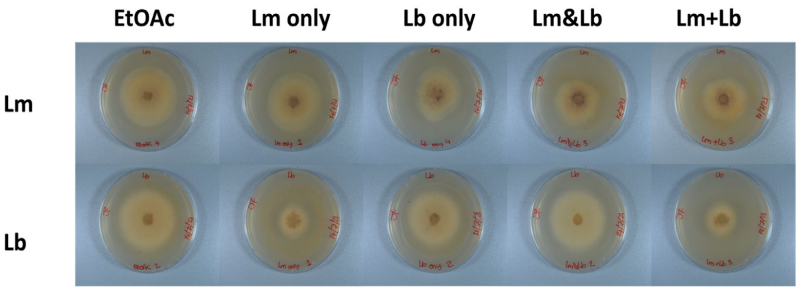

Figure 4. Colony phenotypes of *Leptosphaeria maculans* or *L. biglobosa* on clarified V8 agar plates at 7 days post inoculation (dpi). Fungal plugs of *L. maculans* or *L. biglobosa* were inoculated with different secondary metabolites extracted from liquid cultures inoculated with *L. maculans* only (Lm only), *L. biglobosa* only (Lb only), *L. maculans* and *L. biglobosa* simultaneously (Lm&Lb), *L. maculans* and *L. biglobosa* inoculated sequentially 7 days later (Lm+Lb) or ethyl acetate control (EtOAc).

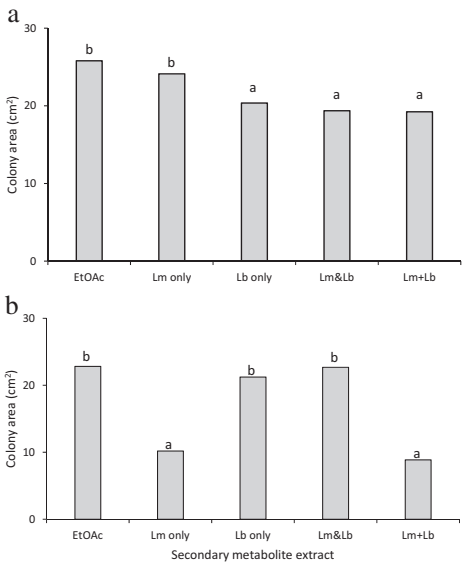

Figure 5. Colony areas (cm^2) of *Leptosphaeria maculans* (a) or *L. biglobosa* (b) on clarified V8 agar plates at 7 days post inoculation. Fungal plugs of *L. maculans* or *L. biglobosa* were inoculated with different secondary metabolites extracted from clarified V8 liquid culture inoculated with *L. maculans* only (Lm only), *L. biglobosa* (Lb only), *L. maculans* and *L. biglobosa* simultaneously (Lm&Lb), *L. maculans* and *L. biglobosa* sequentially (Lm+Lb) or ethyl acetate control (EtOAc). For the 'Lm+Lb' treatment, the liquid media was inoculated with *L. maculans* first then 7 days later with *L. biglobosa*. Data presented are means of three experiments. The *post hoc* Fisher's least significant difference (LSD) tests were done within each pathogen. Columns that share the same letter are not significantly different from each other within each pathogen at $P = 0.05$.

has an inhibitory effect on *L. biglobosa*.[19] Additionally, this study provides evidence that *L. biglobosa* may use an interspecific exploitation competition strategy. *L. biglobosa* had a greater colony area on clarified V8 agar than that of *L. maculans*, suggesting that *L. biglobosa* colonizes the resource more efficiently than

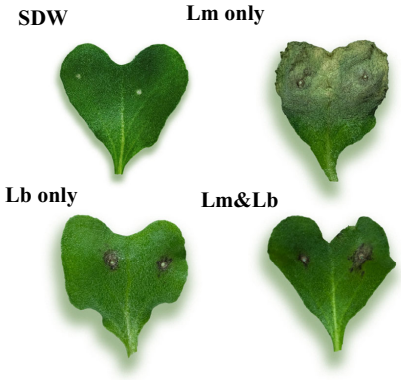

Figure 6. Lesion phenotypes on cotyledons of oilseed rape cultivar Charger at 26 days post inoculation. Cotyledons were inoculated with conidial of *Leptosphaeria maculans* only (Lm only), *L. biglobosa* only (Lb only), *L. maculans* and *L. biglobosa* simultaneously (Lm&Lb) or sterilized distilled water (SDW) as a control.

L. maculans when there is no competition. This is supported by previous studies showing that *L. biglobosa* has a faster colonization rate than *L. maculans*.[7,32,33] The reduced *L. maculans in vitro* growth when secondary metabolite extracts from liquid culture containing *L. biglobosa* were applied suggested that *L. biglobosa* also has antagonistic effects on *L. maculans* growth. Since no specific antibacterial and antifungal compounds were identified from *L. biglobosa* extracts, the effects of *L. biglobosa* on *L. maculans* growth may be due to *L. maculans* detecting *L. biglobosa* pathogen-associated molecular patterns (PAMPS) inducing defense responses, like the mechanism of PAMP-triggered immunity induced in plants,[34] increasing energy use for defense and other strategies, rather than for growth. When *L. maculans* and *L. biglobosa* were inoculated simultaneously (Lm&Lb) onto cotyledons of oilseed rape cv. Charger, the lesion phenotype and lesion size were like lesions of 'Lb only' and not similar to lesions of 'Lm only', suggesting that *L. biglobosa* inhibited the lesion development by *L. maculans*. No sirodesmin PL was detected in plants inoculated with 'Lm&Lb'.

Pest Management Science published by John Wiley & Sons Ltd on behalf of Society of Chemical Industry.

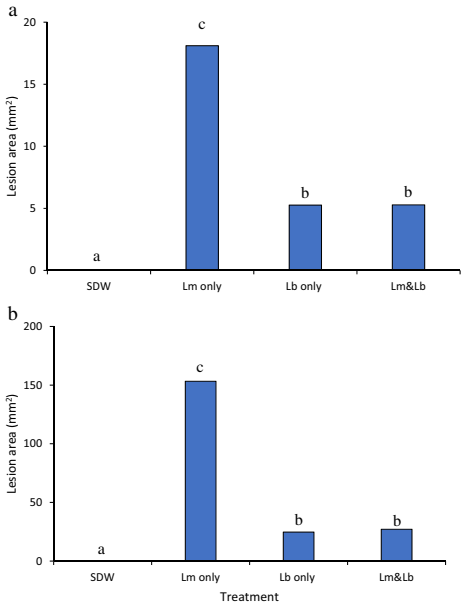

Figure 7. Phoma leaf lesion area (mm^2) on cotyledons of oilseed rape cultivar Charger at 17 (a) or 26 (b) days post inoculation (dpi). Cotyledons were inoculated with conidia suspensions of *Leptosphaeria maculans* only (Lm only), *L. biglobosa* only (Lb only), *L. maculans* and *L. biglobosa* simultaneously (Lm&Lb) or sterilized distilled water (SDW) as a control. Data presented are means of three experiments at 17 dpi (a) or one experiment at 26 dpi (b). The *post hoc* Fisher's least significant difference (LSD) tests were used to separate the mean values of lesion areas. Columns that do not share a letter are significantly different at $P = 0.05$.

The only extracts that contained sirodesmin PL and its precursors were 'Lm only' and 'Lm+Lb' (*L. maculans* followed by *L. biglobosa* inoculation 7 days later), not the 'Lm&Lb' (*L. maculans* and *L. biglobosa* inoculation simultaneously), suggesting that *L. biglobosa* inhibits sirodesmin PL production by *L. maculans* when *L. maculans* and *L. biglobosa* grow together simultaneously. Unique detectable maxima were not identified in the 'Lm&Lb' extracts, suggesting that the production of precursors may have been inhibited. This could be due to inhibition of gene expression of 18 co-regulated genes that have been reported to be involved in the biosynthesis pathway of sirodesmin PL.[23] It has been shown that *O*-prenyl-L-tyrosine is the first committed precursor for sirodesmin PL biosynthesis, a step catalyzed by prenylase (*SirP*).[30] The *sirP* mutants have been shown to inhibit the production of sirodesmin PL[23] so denaturation of *sirP* or another gene involved early in the biosynthesis pathway would probably inhibit the production of the precursors and sirodesmin PL production.[23,30,35] Also, it has been shown that the production of sirodesmin PL is regulated by the cross-pathway control gene cpaA using the transcription factor *sirZ*,[36] therefore if *L. biglobosa* disrupts the expression or products of the genes responsible for the biosynthesis of the sirodesmin PL precursors early in the pathway then downstream products and compounds will not be produced. Once the biosynthesis of sirodesmin PL precursors has started, *L. biglobosa* could not disrupt or inhibit sirodesmin PL production. This hypothesis is supported by the results showing that sirodesmin PL and its precursors were detected in extracts from 'Lm+Lb' but not 'Lm&Lb'. There is a need to investigate the expression of genes related to biosynthesis of sirodesmin PL in the presence of *L. biglobosa* to identify the potential gene inhibitors.

The results of this study suggest that the timing when *L. maculans* and *L. biglobosa* meet and interact is important for the outcome of the interaction between them. In liquid culture, sirodesmin PL and its precursors were identified in the secondary metabolite extracts from 'Lm+Lb' but not from 'Lm&Lb'. This effect of timing is mainly due to the timing of *L. maculans* production of sirodesmin PL since *L. maculans* did not produce sirodesmin PL until 3 dpi, which agrees with the study by Gardiner *et al.*[23] Therefore, if *L. biglobosa* can exploit the resource before *L. maculans* can produce sirodesmin PL, *L. biglobosa* can exploit its exploitation interspecific competitive strategy to use the resource and inhibit the production of sirodesmin PL and its precursors to outcompete *L. maculans*. This is supported by the results from *in planta* experiments. Cotyledons inoculated with 'Lm&Lb' produced lesions like those of *L. biglobosa* but different from those of *L. maculans* and no sirodesmin PL was found. This finding may help to explain why the effectiveness of *L. biglobosa* in inducing resistance to *L. maculans* infection was compromised if *L. biglobosa* was added at 64 h or later after *L. maculans*[24] because 64 h is roughly 2.5 days which is required for sirodesmin PL to be produced (Fig. 2). The production of sirodesmin PL was a maximum at 10 dpi before reducing at day 14; this may be due to conservation of energy because the resource is a relatively nutrient poor by 14 days.[37] Only one cultivar of winter oilseed rape was used in this study. The antagonistic effects of interspecific competition between *L. maculans* and *L. biglobosa* may differ, with cultivars having different resistance ratings or between isolates having different pathogenicity, therefore further investigation is required to fully understand these phenomena.

The results of this study have important practical and agricultural relevance. If the *Leptosphaeria* spp. ascospores are released and infect the host at the same time, then a simultaneous infection will occur that could result in small dark lesions (*L. biglobosa* type of lesions) and affect the timing of fungicide application because the timing of fungicide application is determined based on the *L. maculans* type of lesions (large gray lesions). In the UK, as part of an integrated pest management strategy, growers are advised to accurately apply the first fungicide application when 10–20% of the plants in a crop have *L. maculans* phoma leaf spots in autumn, followed by another application if/when reinfection occurs (https://ahdb.org.uk/knowledge-library/how-to-manage-phoma-in-oilseed-rape). This study showed that when cotyledons were co-infected with *L. maculans* and *L. biglobosa* at the same time, the lesions were small and had an appearance like *L. biglobosa* lesions. Therefore, in seasons where there is simultaneous infection of plants by both *Leptosphaeria* spp., the grower may apply the fungicide later or not at all due to the advised threshold of *L. maculans* lesions not being met. In addition, *L. biglobosa* is less sensitive to azole fungicides than *L. maculans*.[14,38] In the UK, there is substantial reliance on the use of azole fungicides, particularly prothioconazole and tebuconazole.[39] Furthermore, recent studies have shown that *L. biglobosa* can also cause stem basal cankers as well as upper stem lesions[15,18,40,41] and cause yield losses.[16] Therefore, results

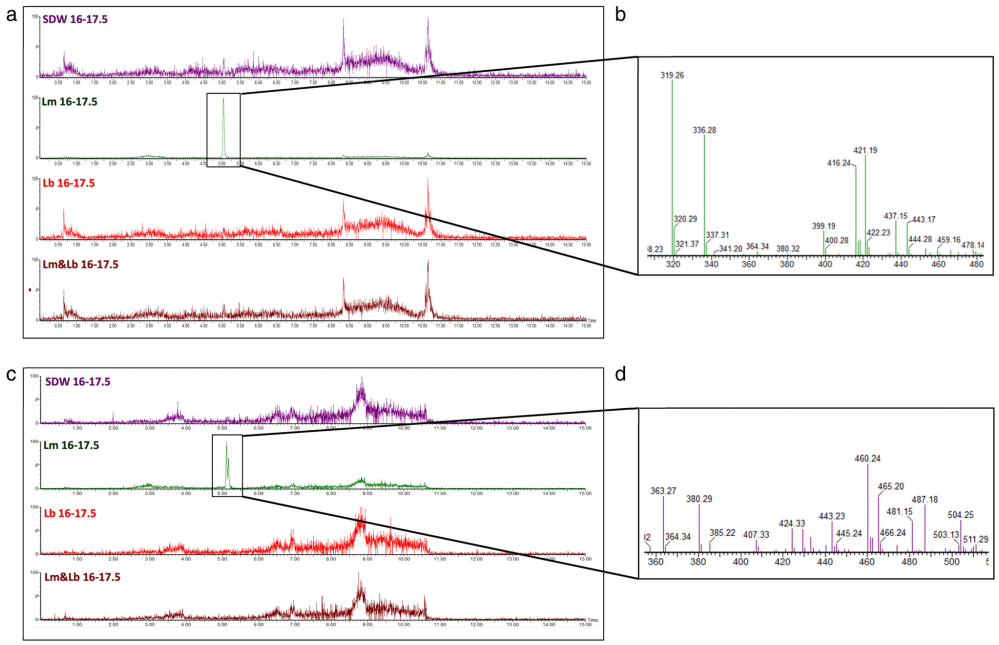

Figure 8. LC-MS chromatograms of HPLC fractions of secondary metabolite extracts from cotyledons of oilseed rape cultivar Charger at 26 days post inoculation. Cotyledons were inoculated with sterilised distilled water (SDW), *Leptosphaeria maculans* only (Lm only), *L. biglobosa* only (Lb only) or *L. maculans* and *L. biglobosa* simultaneously (Lm&Lb). HPLC fractions for 'SDW' (purple), 'Lm only' (green), 'Lb only' (red) or 'Lm&Lb' (brown) were taken from retention time 16.0–17.5 min. Unique maxima were found only in the 'Lm only' sample at retention times 5.03 min (a) and 5.11 min (c) and their ion spectrograms (b and d, respectively).

of this study suggest that the current advice on fungicide application threshold needs to be revised to integrate the appearance of *L. biglobosa* leaf spot lesions to protect the crops from both *Leptosphaeria* spp. because their interspecific interactions and inhibition of sirodesmin PL production may cause unforeseen challenges in the future.

ACKNOWLEDGEMENTS

This research was supported by the Hertfordshire Science Partnership (supported by the Hertfordshire Local Enterprise Partnership), Chadacre Agricultural Trust, Felix Thornley Cobbold Agricultural Trust, the UK Biotechnology and Biological Sciences Research Council (BBSRC, M028348/1 and P00489X/1), Innovate UK (102100 and 102641), AHDB Cereals & Oilseeds (RD-2140021105), and the Department for Environment, Food and Rural Affairs (Defra, CH0110). The authors thank James Stanley and Christine Gigou for technical support and assistance.

CONFLICT OF INTEREST

There is no conflict of interest to report.

DATA AVAILABILITY STATEMENT

The data that support the findings of this study are available from the corresponding author upon reasonable request.

REFERENCES

1 Grover JP, *Resource Competition*. Chapman & Hall, London, UK (1997).
2 Abdullah AS, Moffat CS, Lopez-Ruiz FJ, Gibberd MR, Hamblin J and Zerihun A, Host-multi-pathogen warfare: pathogen interactions in co-infected plants. *Front Plant Sci* **8**:1806 (2017). https://doi.org/10.3389/fpls.2017.01806.
3 Dutt A, Andrivon D and Le May C, Multiple-infections, competitive interactions, and pathogen co-existence. *Plant Pathol* **71**:5–22 (2021). https://doi.org/10.1111/ppa.13469.
4 Kozanitas M, Osmundson TW, Linzer R and Garbelotto M, Interspecific interactions between the sudden oak death pathogen *Phytophthora ramorum* and two sympatric *Phytophthora* species in varying ecological conditions. *Fungal Ecol* **28**:86–96 (2017). https://doi.org/10.1016/j.funeco.2017.04.006.
5 Hortal S, Powell JR, J. Plett M, Simonin A and Anderson IC, Intraspecific competition between ectomycorrhizal *Pisolithus microcarpus* isolates impacts plant and fungal performance under elevated CO_2 and temperature. *FEMS Microbiol Ecol* **92**:fiw113 (2016). https://doi.org/10.1093/femsec/fiw113.
6 Shoemaker RA and Brun H, The teleomorph of the weakly aggressive segregate of *Leptosphaeria maculans*. *Can J Bot* **79**:412–419 (2001). https://doi.org/10.1139/b01-019.
7 Fitt BDL, Huang Y-J, Van Den Bosch F and West JS, Coexistence of related pathogen species on arable crops in space and time. *Ann Rev Phytopathol* **44**:163–182 (2006a). https://doi.org/10.1146/annurev.phyto.44.070505.143417.
8 de Gruyter J, Woudenberg JHC, Aveskamp MM, Verkley GJM, Groenewald JZ and Crous PW, Redisposition of phoma-like anamorphs in Pleosporales. *Stud Mycol* **75**:1–36 (2013). https://doi.org/10.3114/sim0004.
9 Fitt BDL, Evans N, Gladders P, Hughes DJ, Madgwick JW, Jeger MJ *et al.*, Climate change and arable crop disease control: mitigation and

Pest Management Science published by John Wiley & Sons Ltd on behalf of Society of Chemical Industry.

adaptation, in *Paper Presented at 16th International Reinhardsbrunn Symposium*, Freidrichroda, DPG Selbstverlag, pp. 19–26. Germany (2011).
10 CropMonitor. CropMonitor. http://www.cropmonitor.co.uk/?_ga=2.42957989.1876731776.1582020773-1696467554.1575973747 [16 August 2022] (2020).
11 Fitt BDL, Brun H, Barbetti MJ and Rimmer SR, World-wide importance of phoma stem canker (*Leptosphaeria maculans* and *L. biglobosa*) on oilseed rape (*Brassica napus*). *Eur J Plant Pathol* **114**:3–15 (2006b). https://doi.org/10.1007/s10658-005-2233-5.
12 Toscano-Underwood C, Huang YJ, Fitt BDL and Hall AM, Effects of temperature on maturation of pseudothecia of *Leptosphaeria maculans* and *L. biglobosa* on oilseed rape stem debris. *Plant Pathol* **52**:726–736 (2003). https://doi.org/10.1111/j.1365-3059.2003.00930.x.
13 West JS, Fitt BDL, Leech PK, Biddulph JE, Huang YJ and Balesdent MH, Effects of timing of *Leptosphaeria maculans* ascospore release and fungicide regime on phoma leaf spot and phoma stem canker development on winter oilseed rape (*Brassica napus*) in southern England. *Plant Pathol* **51**:454–463 (2002). https://doi.org/10.1046/j.1365-3059.2002.00726.x.
14 Huang YJ, Hood JR, Eckert MR, Stonard JF, Cools HJ, King GJ *et al.*, Effects of fungicide on growth of *Leptosphaeria maculans* and *L. biglobosa* in relation to development of phoma stem canker on oilseed rape (*Brassica napus*). *Plant Pathol* **60**:607–620 (2011). https://doi.org/10.1111/j.1365-3059.2010.02416.x.
15 Liu Z, Latunde-Dada AO, Hall AM and Fitt BDL, Phoma stem canker disease on oilseed rape (*Brassica napus*) in China is caused by *Leptosphaeria biglobosa 'brassicae'*. *Eur J Plant Pathol* **140**:841–857 (2014). https://doi.org/10.1007/s10658-014-0513-7.
16 Cai X, Huang Y, Jiang D, Fitt BDL, Li G and Yang L, Evaluation of oilseed rape seed yield losses caused by *Leptosphaeria biglobosa* in Central China. *Eur J Plant Pathol* **150**:179–190 (2018). https://doi.org/10.1007/s10658-017-1266-x.
17 Kerdraon L, Barret M, Balesdent M-H, Suffert F and Laval V, Impact of a resistance gene against a fungal pathogen on the plant host residue microbiome: the case of the *Leptosphaeria maculans–Brassica napus* pathosystem. *Mol Plant Pathol* **21**:1545–1558 (2020). https://doi.org/10.1111/mpp.12994.
18 Jacques N, Balesdent MH, Rouxel T and Laval V, New specific quantitative real time PCR assays shed light on the epidemiology of two species of the *Leptosphaeria maculans–Leptosphaeria biglobosa* species complex. *Plant Pathol* **70**:643–654 (2021). https://doi.org/10.1111/ppa.13323.
19 Elliott CE, Gardiner DM, Thomas G, Cozijnsen A, Van De Wouw A and Howlett BJ, Production of the toxin sirodesmin PL by *Leptosphaeria maculans* during infection of *Brassica napus*. *Mol Plant Pathol* **8**:791–802 (2007). https://doi.org/10.1111/j.1364-3703.2007.00433.x.
20 Johnson RD and Lewis BG, Variation in host range, systemic infection and epidemiology of *Leptosphaeria maculans*. *Plant Pathol* **43**:269–277 (1994). https://doi.org/10.1111/j.1365-3059.1994.tb02685.x.
21 Williams RH and Fitt BDL, Differentiating a and b groups of *Leptosphaeria maculans*, causal agent of stem canker (blackleg) of oilseed rape. *Plant Pathol* **48**:161–175 (1999). https://doi.org/10.1046/j.1365-3059.1999.00333.x.
22 Rouxel T, Chupeau Y, Fritz R, Kollmann A and Bousquet JF, Biological effects of sirodesmin PL, a phytotoxin produced by *Leptosphaeria maculans*. *Plant Sci* **57**:45–53 (1988). https://doi.org/10.1016/0168-9452(88)90140-9.
23 Gardiner DM, Cozijnsen AJ, Wilson LM, Pedras MSC and Howlett BJ, The sirodesmin biosynthetic gene cluster of the plant pathogenic fungus *Leptosphaeria maculans*. *Mol Microbiol* **53**:1307–1318 (2004). https://doi.org/10.1111/j.1365-2958.2004.04215.x.
24 Cooney JM, Lauren DR and di Menna ME, Impact of competitive fungi on trichothecene production by *Fusarium graminearum*. *J Agric Food Chem* **49**:522–526 (2001). https://doi.org/10.1021/jf0006372.
25 Mahuku GS, Hall R and Goodwin PH, Co-infection and induction of systemic acquired resistance by weakly and highly virulent isolates of *Leptosphaeria maculans* in oilseed rape. *Physiol Mol Plant Pathol* **49**:61–72 (1996). https://doi.org/10.1006/pmpp.1996.0039.
26 Liu SY, Liu Z, Fitt BDL, Evans N, Foster SJ, Huang YJ *et al.*, Resistance to *Leptosphaeria maculans* (phoma stem canker) in *Brassica napus* (oilseed rape) induced by *L. biglobosa* and chemical defence activators in field and controlled environments. *Plant Pathol* **55**:401–412 (2006). https://doi.org/10.1111/j.1365-3059.2006.01354.x.
27 Pedras MSC and Biesenthal CJ, Production of the host-selective phytotoxin phomalide by isolates of *Leptosphaeria maculans* and its correlation with sirodesmin PL production. *Can J Microbiol* **44**:547–553 (1998). https://doi.org/10.1139/w98-034.
28 Huang YJ, Li ZQ, Evans N, Rouxel T, Fitt BDL and Balesdent MH, Fitness cost associated with loss of the *AvrLm4* avirulence function in *Leptosphaeria maculans* (phoma stem canker of oilseed rape). *Eur J Plant Pathol* **114**:77–89 (2006).
29 VSN International, *Genstat for Windows*, 21st edn. VSN International, Hemel Hempstead, UK (2022).
30 Pedras MSC and Yu Y, Mapping the sirodesmin PL biosynthetic pathway – a remarkable intrinsic steric deuterium isotope effect on a ^{1}H NMR chemical shift determines beta-proton exchange in tyrosine. *Can J Chem* **87**:564–570 (2009). https://doi.org/10.1139/V09-019.
31 PubChem. https://pubchem.ncbi.nlm.nih.gov/ [16 August 2022] (2022).
32 Huang YJ, Toscano-Underwood C, Fitt BDL, Todd AD, West JS, Koopmann B *et al.*, Effects of temperature on germination and hyphal growth from ascospores of A-group and B-group *Leptosphaeria maculans* (phoma stem canker of oilseed rape). *Ann Appl Biol* **139**:193–207 (2001). https://doi.org/10.1111/j.1744-7348.2001.tb00396.x.
33 Huang YJ, Toscano-Underwood C, Fitt BDL, Hu XJ and Hall AM, Effects of temperature on ascospore germination and penetration of oilseed rape (*Brassica napus*) leaves by A- or B-group *Leptosphaeria maculans* (phoma stem canker). *Plant Pathol* **52**:245–255 (2003). https://doi.org/10.1046/j.1365-3059.2003.00813.x.
34 Zipfel C and Felix G, Plants and animals: a different taste for microbes? *Curr Opin Plant Biol* **8**:353–360 (2005). https://doi.org/10.1016/j.pbi.2005.05.004.
35 Fox EM and Howlett BJ, Biosynthetic gene clusters for epipolythiodioxopiperazines in filamentous fungi. *Mycol Res* **112**:162–169 (2008). https://doi.org/10.1016/j.mycres.2007.08.017.
36 Elliott CE, Fox EM, Jarvis RS and Howlett BJ, The cross-pathway control system regulates production of the secondary metabolite toxin, sirodesmin PL, in the ascomycete, *Leptosphaeria maculans*. *BMC Microbiol* **11**:169 (2011). https://doi.org/10.1186/1471-2180-11-169.
37 Black WD, A comparison of several media types and basic techniques used to assess outdoor airborne fungi in Melbourne, Australia. *PLOS One* **15**:e0238901 (2020). https://doi.org/10.1371/journal.pone.0238901.
38 Eckert MR, Rossall S, Selley A and Fitt BDL, Effects of fungicides on *in vitro* spore germination and mycelial growth of the phytopathogens *Leptosphaeria maculans* and *L. biglobosa* (phoma stem canker of oilseed rape). *Pest Manag Sci* **66**:396–405 (2010). https://doi.org/10.1002/ps.1890.
39 Fortune JA, Qi A, Ritchie F, Karandeni Dewage CS, Fitt BDL and Huang Y-J, Effects of cultivar resistance and fungicide application on stem canker of oilseed rape (*Brassica napus*) and potential interseasonal transmission of *Leptosphaeria* spp. inoculum. *Plant Pathol* **70**:2115–2124 (2021). https://doi.org/10.1111/ppa.13453.
40 Kerdraon L, Balesdent M-H, Barret M, Laval V and Suffert F, Crop residues in wheat-oilseed rape rotation system: a pivotal, shifting platform for microbial meetings. *Microb Ecol* **77**:931–945 (2019). https://doi.org/10.1007/s00248-019-01340-8.
41 Schneider CA, Rasband WS and Eliceiri KW, NIH image to ImageJ: 25 years of image analysis. *Nat Methods* **9**:671–675 (2012). https://doi.org/10.1038/nmeth.2089.

Research Article

Received: 21 July 2023 Revised: 28 August 2023 Accepted article published: 28 September 2023 Published online in Wiley Online Library:

(wileyonlinelibrary.com) DOI 10.1002/ps.7799

Co-inoculation timing affects the interspecific interactions between phoma stem canker pathogens *Leptosphaeria maculans* and *Leptosphaeria biglobosa*

Evren Bingol,[a] Aiming Qi,[a] Chinthani Karandeni-Dewage,[a] Faye Ritchie,[b] Bruce D. L. Fitt[a] and Yong-Ju Huang[a*]

Abstract

BACKGROUND: Phoma stem canker is an economically important disease of oilseed rape, caused by two co-existing fungal pathogen species, *Leptosphaeria maculans* (*Plenodomus lingam*) and *Leptosphaeria biglobosa* (*Plenodomus biglobosus*). *Leptosphaeria maculans* produces a phytotoxin called sirodesmin PL. Our previous work showed that *L. biglobosa* has an antagonistic effect on the production of sirodesmin PL if it is simultaneously co-inoculated with *L. maculans*. However, the effects of sequential co-inoculation on interspecific interactions between the two pathogens are not understood.

RESULTS: The interactions between *L. maculans* and *L. biglobosa* were investigated in liquid culture by inoculation with *L. maculans* first, followed by *L. biglobosa* sequentially at 1, 3, 5 or 7 days later and vice versa; the controls were inoculated with *L. maculans* only, *L. biglobosa* only, or *L. maculans* and *L. biglobosa* simultaneously. The results showed that *L. biglobosa* inhibited the growth of *L. maculans*, the production of both sirodesmin PL and its precursors if *L. biglobosa* was inoculated before, or simultaneously with, *L. maculans*. However, the antagonistic effects of *L. biglobosa* were lost if it was co-inoculated 5 or 7 days after *L. maculans*.

CONCLUSION: For the first time, the results of this study provided evidence that the timing when *L. maculans* and *L. biglobosa* meet significantly influences the outcome of the interspecific competition between them. *Leptosphaeria biglobosa* can inhibit the production of sirodesmin PL and the growth of *L. maculans* if it is inoculated before *L. maculans* or less than 3 days after *L. maculans* in liquid culture. There is a need to further investigate the timing of co-inoculation on interactions between *L. maculans* and *L. biglobosa* in their host plants for improving the control of phoma stem canker.

Keywords: interspecific interactions; *Leptosphaeria maculans*; *Leptosphaeria biglobosa*; phoma stem canker; secondary metabolites; sirodesmin PL

1 INTRODUCTION

A plant host in nature is subjected to various pest and disease stresses throughout its life cycle, often caused by plant-pathogenic fungi.[1] Oilseed rape, also known as canola (*Brassica napus*) is affected by at least 16 different pathogens worldwide; they infect different parts of the plant in different stages of its life cycle.[2] Phoma stem canker (blackleg) is one of the most economically damaging diseases of oilseed rape globally.[3] In the UK alone, it causes annual yield losses worth > £80M, despite the disease control strategies using fungicides and resistant cultivars.[4] Phoma stem canker is caused by two closely related fungal pathogen species, *Leptosphaeria maculans* (*Plenodomus lingam*) and *Leptosphaeria biglobosa* (*Plenodomus biglobosus*).[5–7] In Europe, phoma stem canker epidemics are initiated by ascospores released from mature pseudothecia developed on previous crop debris in autumn.[8,9] These ascospores get dispersed by wind, land on leaf surfaces and upon successful infection, cause phoma leaf spots.[10,11] Hyphae of *L. maculans* and *L. biglobosa* then grow through the leaf, along the petiole and down to the stem, causing stem cankers at the end of the cropping season.[12,13] Fungicides (most commonly prothioconazole and tebuconazole) are applied at the phoma leaf spotting stage in efforts to stop further pathogen growth into the stem.[14,15] Furthermore, the global distribution of these pathogens varies; only *L. biglobosa* is found in

* *Correspondence to: Y-J Huang, Centre for Agriculture, Food and Environmental Management Research, School of Life and Medical Sciences, University of Hertfordshire, Hatfield, UK. E-mail: y.huang8@herts.ac.uk*

a *Centre for Agriculture, Food and Environmental Management Research, School of Life and Medical Sciences, University of Hertfordshire, Hatfield, UK*

b *Disease and Pest Management, ADAS Boxworth, Cambridge, UK*

China, whereas both of the pathogens are found to co-infect oilseed rape in other parts of the world, such as Europe, Canada and Australia.[16,17]

When co-infection of a single host by multiple pathogens occurs, the interactions between the pathogens can be classified into three groups: competition, co-operation or co-existence.[1,18] Competition can lead to co-existence through niche specialisation, if permitted by the biology of the pathogens. In the case of *L. maculans* and *L. biglobosa*, co-existence in oilseed rape is facilitated by the small differences in the ecological niches they occupy.[6] The optimal temperatures required for pseudothecial maturation of these pathogens are different, with pseudothecia (sexual fruiting bodies) of *L. maculans* maturing faster than those of *L. biglobosa* at low temperatures (e.g., at 5–10 °C), leading to differences in the timing of ascospore release.[19] This produces a temporo-spatial separation in the infection of oilseed rape by these pathogens, and therefore allows their co-existence.[6] Previous studies showed that *L. maculans* has mainly been associated with severe stem basal cankers, whereas *L. biglobosa* has mainly been associated with superficial upper stem lesions; therefore *L. biglobosa* has been considered less damaging than *L. maculans*.[11,16] However, recent studies have found that in the UK, ascospores of *L. maculans* and *L. biglobosa* can be released at similar times, and that *L. biglobosa* can cause stem basal cankers, especially on cultivars with effective resistance genes against *L. maculans*.[20]

When interspecific competition occurs, it can manifest in three different ways.[1] Resource-mediated (exploitation) competition arises when a resource becomes limited, whereby the species that can use the resource most efficiently outcompetes the others and survives, sometimes even leading to competitive exclusion of other species.[21,22] Host-mediated (apparent) competition is when the development of one of the competitors primes the plant immune system against other competing pathogens, reducing their chance of successfully infecting the host.[23] An example of host-mediated competition strategy has been observed between *L. maculans* and *L. biglobosa*. It was reported that pre-inoculation of oilseed rape leaves with *L. biglobosa* primes the plant immune system and induces systemic acquired resistance against *L. maculans*.[24–26] However, if *L. biglobosa* was inoculated 64 h or later after *L. maculans*, the induction of systemic acquired resistance was lost,[26] suggesting that the timing when *L. maculans* and *L. biglobosa* meet and interact affects the outcome of their competition related to disease severity.

The third interspecific competition is interference competition; it occurs when one of the competitors directly interferes with another competitor's access to a limited resource, often by producing toxins.[1] This interference competition strategy has been observed between *L. maculans* and *L. biglobosa*. *Leptosphaeria maculans* produces a non-host selective epipolythiodioxopiperazine (ETP) phytotoxin called sirodesmin PL, while *L. biglobosa* does not.[27–29] Sirodesmin PL has antimicrobial and antifungal properties.[27,28] The sirodesmin PL produced by *L. maculans* was shown to inhibit the growth of *L. biglobosa in vitro*.[29,30] The *in vitro* growth of *L. biglobosa* was inhibited when it was inoculated with liquid culture containing sirodesmin PL.[29] Previous work showed that a mutant isolate of *L. maculans* that did not produce sirodesmin PL was still able to cause disease symptoms on oilseed rape, only with reduced antimicrobial and antifungal activity, suggesting that sirodesmin PL is produced as an interference competition strategy, but not required for disease development.[30] Similar studies were done for another ETP, gliotoxin, which is produced by *Aspergillus fumigatus*, the causative agent of pulmonary aspergillosis.[31] It was shown that mutant isolates of *A. fumigatus* that do not produce gliotoxin were still able to cause invasive aspergillosis, only with reduced cytotoxic effects, suggesting that gliotoxin is not indispensable for disease development.[32]

Recent work showed that *L. biglobosa* can inhibit the production of sirodesmin PL by *L. maculans* both *in vitro* and *in planta*, when it is co-inoculated simultaneously with *L. maculans*.[29] However, when *L. biglobosa* was co-inoculated sequentially 7 days after *L. maculans* in liquid culture, the production of sirodesmin PL by *L. maculans* was not inhibited.[29] Previous work showed that it took approximately 3 days for *L. maculans* to produce sirodesmin PL.[28–30] We hypothesised that the timing when *L. maculans* and *L. biglobosa* meet influences the outcome of the interspecific competition related to sirodesmin PL production and pathogen growth. The aim of this research was therefore to investigate the effects of sequential co-inoculation on interspecific interactions between *L. maculans* and *L. biglobosa* in terms of production of sirodesmin PL and relative growth of the two pathogens *in vitro*, and the impact of the interspecific interactions on phoma stem canker management.

2 MATERIALS AND METHODS

2.1 Pathogen and media preparation

The isolates used in this study were *L. maculans* isolate ME24, which was obtained from phoma stem canker on oilseed rape cultivar Apex in 2002,[12] and *L. biglobosa* isolate WH17-Why-1, obtained from phoma leaf spot of cultivar Whisky in 2017.[29] The *L. maculans* isolate ME24 carries three avirulence (*Avr*) effector genes (*AvrLm1*, *AvrLm6*, *AvrLm7*). These isolates of *L. maculans* and *L. biglobosa* were grown on 20% clarified V8 (CV8) agar plates for 7 days, followed by cutting of agar plugs from growth fronts of the colonies for inoculation of 20% CV8 liquid media.

CV8 media were prepared by the addition of 15 g L^{-1} calcium carbonate ($CaCO_3$) to V8 juice, agitation for 15 min using a magnetic stirrer, then centrifugation at 1400 × *g* for 5 min. The pellet was discarded, and the supernatant was used as the CV8 media. For CV8 agar plates, 12 g L^{-1} agar was added and 15 mL of autoclaved CV8 agar media was poured into each 9 cm diameter Petri dish. For CV8 liquid media, 75 mL of autoclaved CV8 broth was poured into each 250 mL conical flask.

2.2 Inoculation of liquid media

For sequential co-inoculations, the treatments were as follows: *L. maculans* only (Lm only), *L. biglobosa* only (Lb only), *L. maculans* and *L. biglobosa* simultaneous co-inoculation (Lm&Lb), initial inoculation with *L. maculans* followed by sequential co-inoculation with *L. biglobosa* at 1, 3, 5 and 7 days later (Lm + Lb-1, Lm + Lb-3, Lm + Lb-5, Lm + Lb-7), and initial inoculation with *L. biglobosa* followed by sequential co-inoculation with *L. maculans* at 1, 3, 5 and 7 days later (Lb + Lm-1, Lb + Lm-3, Lb + Lm-5, Lb + Lm-7). Three agar plugs (8 mm diameter) of each pathogen were used to inoculate 75 mL of 20% CV8 liquid media in each 250 mL conical flask according to the treatments. Flasks for 'Lm only' and 'Lb only' were inoculated with three agar plugs as sole cultures. Inoculated flasks were placed in a shaking incubator at 80 rpm and 18 °C in continual darkness. Mycelia were harvested and liquid culture filtrates were collected at 14 days from initial inoculation. Three independent experiments were done. There were two replicated flasks for each treatment for two

experiments and three replicated flasks per treatment for one experiment.

To compare the mycelial growth rates of *L. maculans* and *L. biglobosa* in liquid culture, the same inoculation method was used, and the treatments were *L. maculans* only (Lm only), *L. biglobosa* only (Lb only) and *L. maculans* and *L. biglobosa* simultaneous co-inoculation (Lm&Lb). Mycelia were harvested at 1, 3, 5, 7, 10 and 14 days post inoculation (dpi). Two independent experiments were done. There were two replicated flasks for each treatment/time point in each experiment.

2.3 Filtration of mycelia and secondary metabolite extractions from culture filtrates

Mycelia were harvested by filtering the liquid media using a Büchner funnel, pat-dried, placed in a sterile 15 mL Falcon tube and stored at −20 °C overnight before freeze-drying. The necks of the sterile 15 mL Falcon tubes were covered with parafilm and five small holes were pierced before the tubes were placed in a freeze-dryer for 48 h. After freeze-drying, the tubes were weighed using an analytical balance, and the weight of an empty 15 mL Falcon tube was subtracted to obtain the weight of freeze-dried mycelia.

The secondary metabolites were extracted from culture filtrates as previously described.[29] Culture filtrates were aliquoted into sterile tubes in duplicate (35 mL each) and 15 mL of ethyl acetate was added to 35 mL of culture filtrate, inverted 30 times, left in a fume hood for 10 min for the phases to settle, then centrifuged at 1000 × *g* for 5 min. For each replicate, a total of 20 mL of the upper (organic) phase was pipetted into a sterile 50 mL Falcon tube. Ethyl acetate was evaporated under a stream of nitrogen using a sample concentrator. Secondary metabolites were then re-suspended in 500 µL of ethyl acetate.

Using 1 mL syringes, re-suspended secondary metabolites were passed through 0.45 µm syringe filters into high-performance liquid chromatography (HPLC) vials. This was followed by pipetting 150 µL of sample into a new HPLC vial with a 200 µL glass insert and it was stored at 4 °C until required for HPLC analysis.

2.4 Analysis of the composition of secondary metabolites

To identify the composition of secondary metabolites in culture filtrates across different treatments, analysis of samples was done using a Shimadzu Prominence HPLC machine with a diode array detector (SPD-20A; Shimadzu Corporation, Kyoto, Japan). The HPLC column used was a C_{18} column (Varian pursuit 5, 150 mm × 4.6 mm), with 10 µL of sample injection volume and a flow rate of 1 mL min^{-1}.

HPLC-grade water and acetonitrile were used in the HPLC mobile phase. The method started as a linear gradient, going from 85% water and 15% acetonitrile to 100% acetonitrile over 40 min, maintaining there for 3 min, then starting a linear gradient back to 85% water and 15% acetonitrile over 5 min, leading to a total run time of 53 min per sample. The HPLC method was adapted from Pedras and Biesenthal.[33] HPLC analytes were measured by ultraviolet (UV) light absorption in the range of 190–400 nm, and the results were visualised at 254 nm for analysis, using the Lab solution program (version 5.92) by Shimadzu Corporation. The concentrations of sirodesmin PL and its precursors were measured using a gliotoxin standard curve; limit of detection (LOD) was 70 mg L^{-1} and limit of quantification (LOQ) was 200 mg L^{-1}, as described by Fortune *et al.*[29]

2.5 DNA extraction from mycelia

Freeze-dried mycelial samples were ground using a pestle and mortar and approximately 20 mg of each ground sample was transferred into each sterile 2 mL screw-cap tube. DNA extractions from mycelia were done using the DNAmite Plant DNA Extraction Kit (Microzone Ltd, King William St, Amblecote, Stourbridge, UK), according to the manufacturer's guidelines, with minor modifications, described later.

Three sterile metal beads were added to each tube containing a ground mycelial sample and 1 mL of lysis solution was added. The samples were processed using a FastPrep machine at 4.0 m s^{-1} for 40 s. This was followed by the addition of 100 µL of protein precipitant solution into each tube, vortexing for 10 s, and centrifugation at 8000 × *g* for 5 min at 4 °C. Following centrifugation, 500 µL of the supernatant from each tube was transferred into a new sterile 1.5 mL tube containing 500 µL of capture solution. These tubes were inverted ten times and incubated on the bench for 5 min before centrifugation at 11 300 × *g* for 7 min at 4 °C to pellet the DNA. The supernatant was discarded, and any remnants were removed using a pipette. DNA pellets were re-suspended in 60 µL of nuclease-free water after drying in the fume hood for 30 min, then placed at −20°C for 16 h. Extracted DNA samples were then thawed at 20 °C and centrifuged at 7000 × *g* for 10 min at 4 °C, and 50 µL of the supernatants containing the DNA were transferred into a new set of sterile 0.5 mL tubes. DNA concentration of each sample was measured using Qubit DNA Broad Range Assay Kit (Invitrogen, Carlsbad, CA, USA) and diluted to 20 ng μL^{-1} ready for quantitative polymerase chain reaction (qPCR) analyses.

2.6 Relative growth of *L. maculans* and *L. biglobosa* in different treatments

To investigate the relative growth of *L. maculans* and *L. biglobosa* in different treatments, the amounts of *L. maculans* and *L. biglobosa* DNA were quantified using SYBR Green (Agilent, Santa Clara, CA, USA) qPCR, with the primers LmacF (5′- CTTGCCCACCAATTGGATCCCCTA-3′)/LmacR (5′-GCAAAA-TGTGCTGCGCTCCAGG-3′) (for *L. maculans*) and LbigF (5′-CCTTCTAT-CAGAGGATTGGT-3′)/LmacR (5′-CGTTCTTCATCGATGCCAGA-3′) (for *L. biglobosa*).[13] The qPCR reaction mixtures were prepared at a total volume of 20 µL, containing 10 µL of SYBR Green (containing ROX as reference dye), 6.3 µL of nuclease-free water, 0.6 µL of forward primer (10 µM), 0.6 µL of reverse primer (10 µM) and 2.5 µL of DNA sample in duplicate in 96-well plates. To produce standard curves, ten-fold dilutions ranging from 10^4 to 10^{-1} pg of *L. maculans* or *L. biglobosa* DNA obtained from pure cultures were used. The amounts of *L. maculans* or *L. biglobosa* DNA in samples were calculated using the standard curves with the Stratagene MxPro-Mx3000P v3.20 software.

The qPCR reactions were done using a Stratagene 3005P qPCR machine (Agilent). Thermal cycling profiles consisted of one cycle of 95 °C for 2 min, then 40 cycles of 95 °C for 15 s, 60 °C (for *L. maculans*) or 55 °C (for *L. biglobosa*) for 30 s, 72 °C for 45 s, and a reading step of 83 °C for 15 s, then one cycle of 95 °C for 1 min, (60 °C for *L. maculans*/55 °C for *L. biglobosa*) for 1 min, and 95 °C for 15 s to produce a dissociation curve.

2.7 Statistical analysis

To compare the growth rates of *L. maculans* and *L. biglobosa*, a logistic equation was fitted to measurements of mycelial dry weight from each individual replicate against days post inoculation. The data were analysed using the non-linear model directive

Pest Management Science published by John Wiley & Sons Ltd on behalf of Society of Chemical Industry.

in the GenStat program (22nd edition).[34] The fitted logistic equation was:

$$Y = \frac{A}{1 + e^{(-k \times (t - t_0)}}$$

In this logistic equation, Y is the measurement of mycelial dry weight (in grams) at different time points, t is the time in dpi, A is the upper asymptotic mycelial dry weight, k is the slope of the logistic curve at inflection measuring the relative growth rate in mycelial dry weight (i.e., the growth-rate coefficient), and t_0 is the time at which the mycelial dry weight reaches half of the value of A.

To compare the differences between different treatments in mycelial dry weight, production of sirodesmin PL and its precursors, and relative pathogen DNA in homogenised mycelia, analysis of variance was done using the GenStat program (22nd edition).[34] Since three independent experiments were done for the same 11 treatments, experiment was assigned as a factor when analysing the data to assess whether the experiment had a significant effect. For measurements of sirodesmin PL and its precursors, the data were transformed using a common logarithm to homogenise the variance between treatments before they were subjected to analysis of variance. The F-values that were significant at $P < 0.05$ indicated significant effects of the factors. The Tukey *post hoc* test was used to separate the means of the treatments at 5% significant probability.

3 RESULTS

3.1 Morphology of mycelia in liquid cultures and mycelial dry masses of *L. maculans* and *L. biglobosa* in different treatments

The morphology of mycelia in liquid cultures was different between different treatments (Fig. 1). The mycelia of the 'Lm only' treatment were light brown, round and had an intact structure whereas the mycelia of the 'Lb only' treatment were red and spread across the liquid media, without an intact structure. The morphology of mycelia in treatments with initial inoculation of *L. maculans*, followed by sequential co-inoculation by *L. biglobosa* at 1, 3, 5 or 7 days later (Lm + Lb-1, Lm + Lb-3, Lm + Lb-5 and Lm + Lb-7) were more similar to that of the 'Lm only' treatment. The morphology of mycelia in treatments with initial inoculation of *L. biglobosa* followed by sequential co-inoculation by *L. maculans* at 1, 3, 5 or 7 days later (Lb + Lm-1, Lb + Lm-3, Lb + Lm-5 and Lb + Lm-7) and *L. maculans* and *L. biglobosa* simultaneous co-inoculation (Lm&Lb) were similar to that of the 'Lb only' treatment.

At 14 dpi, mycelia were harvested and freeze-dried. There were no significant differences between treatments in mycelial dry weight, except for the treatment 'Lm only' (0.33 g) being significantly greater than all other treatments ($F_{(10,44)} = 4.89$, $P < 0.001$) (Fig. 2). The mycelial dry weights of other treatments ranged from 0.21 to 0.27 g. The interactions between experiments and treatments were not significant ($F_{(20,44)} = 1.60$, $P = 0.095$).

3.2 Effects of sequential co-inoculation of *L. maculans* and *L. biglobosa* on production of secondary metabolites by *L. maculans in vitro*

The colour of culture filtrates from liquid cultures was different between different treatments (Fig. 3). Culture filtrate of the 'Lm only' treatment had a light yellow colour, whereas culture filtrate of the 'Lb only' treatment had a dark yellow/orange colour. This difference was due to production of a pigment by *L. biglobosa*, which was not produced by *L. maculans*.[35] The colours of culture filtrates from liquid cultures where *L. maculans* was inoculated before *L. biglobosa* (Lm + Lb-1, Lm + Lb-3, Lm + Lb-5 and Lm + Lb-7) were similar to that of the 'Lm only' control treatment. However, a slight production of pigment was observed in the Lm + Lb-1 treatment. The colours of culture filtrates from liquid cultures where *L. biglobosa* was inoculated before *L. maculans* (Lb

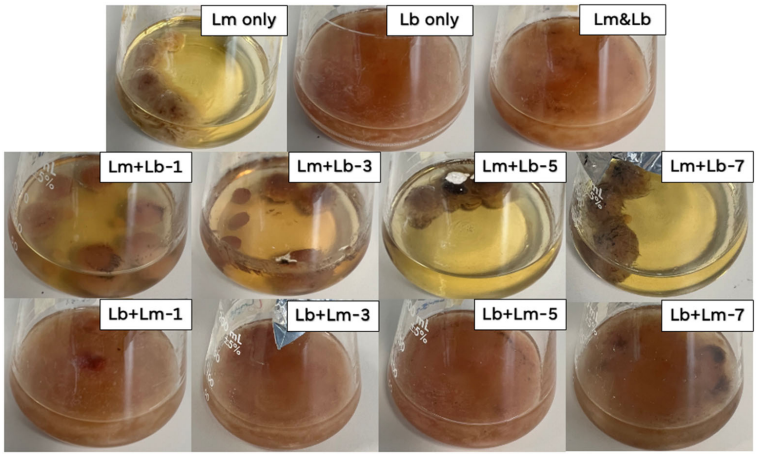

Figure 1. Morphology of mycelia in liquid cultures inoculated with *Leptosphaeria maculans* only (Lm only), *Leptosphaeria biglobosa* only (Lb only), *L. maculans* and *L. biglobosa* co-inoculated simultaneously (Lm&Lb), first inoculation with *L. maculans* followed by co-inoculation with *L. biglobosa* sequentially at 1, 3, 5 or 7 days later (Lm + Lb-1, Lm + Lb-3, Lm + Lb-5, Lm + Lb-7), and first inoculation with *L. biglobosa* followed by co-inoculation with *L. maculans* sequentially at 1, 3, 5 or 7 days later (Lb + Lm-1, Lb + Lm-3, Lb + Lm-5, Lb + Lm-7) at 14 days after the first inoculation.

Pest Management Science published by John Wiley & Sons Ltd on behalf of Society of Chemical Industry.

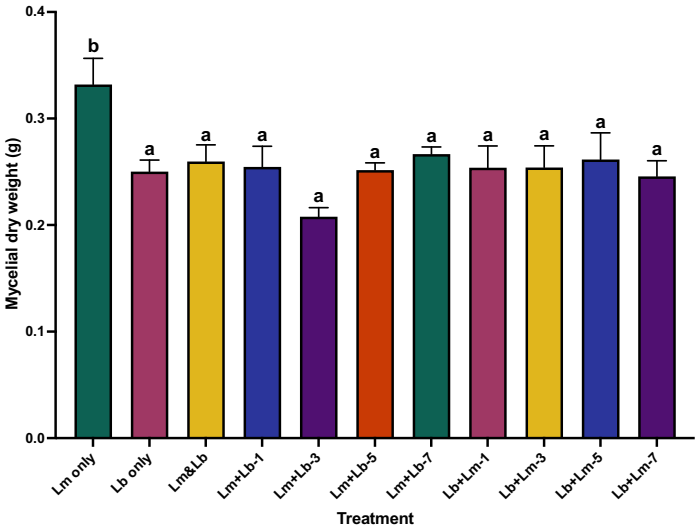

Figure 2. Average dry weight (g) of mycelia obtained from three independent experiments consisting of liquid cultures inoculated with *Leptosphaeria maculans* only (Lm only), *Leptosphaeria biglobosa* only (Lb only), *L. maculans* and *L. biglobosa* co-inoculated simultaneously (Lm&Lb), first inoculation with *L. maculans* followed by co-inoculation with *L. biglobosa* sequentially at 1, 3, 5 or 7 days later (Lm + Lb-1, Lm + Lb-3, Lm + Lb-5, Lm + Lb-7), and first inoculation with *L. biglobosa* followed by co-inoculation with *L. maculans* sequentially at 1, 3, 5 or 7 days later (Lb + Lm-1, Lb + Lm-3, Lb + Lm-5, Lb + Lm-7). Tukey's HSD tests were used to separate the mean dry mycelial weight values across different treatments. Columns that do not share a common letter were considered significantly different ($P < 0.05$). Error bars show standard errors of the mean (SEM).

+ Lm-1, Lb + Lm-3, Lb + Lm-5 and Lb + Lm-7) or simultaneous co-inoculation of both pathogens (Lm&Lb) were similar to that of the 'Lb only' control (Fig. 3).

The composition of secondary metabolites of the culture filtrates was analysed by HPLC. There were significant differences between different treatments in the average concentrations of sirodesmin PL ($F_{(10,44)} = 1129.98$, $P < 0.001$) (Fig. 4(a)) and its precursors ($F_{(10,44)} = 1294.62$, $P < 0.001$) (Fig. 4(b)). For the treatments 'Lb only', 'Lm&Lb', 'Lm + Lb-1', 'Lb + Lm-1', 'Lb + Lm-3', 'Lb + Lm-5' and 'Lb + Lm-7', there were no significant differences between them since no unique maxima corresponding to sirodesmin PL or its precursors were identified in the HPLC chromatograms in those treatments. For all other treatments, unique maxima corresponding to sirodesmin PL were identified at 16.3 min retention time. For the treatments 'Lm only' (892.8 mg L^{-1}), 'Lm + Lb-5' (832.2 mg L^{-1}) and 'Lm + Lb-7' (971.4 mg L^{-1}), there were no significant differences between them in the concentration of sirodesmin PL. However, 'Lm + Lb-3' (334.5 mg L^{-1}) was significantly different from all other treatments (Fig. 4(a)). Although the retention time was similar for the unique maxima corresponding to sirodesmin PL, the 'Lm + Lb-3' treatment had a 62.6% reduction in concentration when compared to the 'Lm only' control treatment. Furthermore, unique maxima corresponding to the precursors of sirodesmin PL were identified at 11.2 min retention time. For the treatments 'Lm only' (381.4 mg L^{-1}), 'Lm + Lb-5' (358.2 mg L^{-1}) and 'Lm + Lb-7' (368.7 mg L^{-1}), there were no significant differences between them in the concentrations of the precursors of sirodesmin PL. Corresponding to the toxin itself, 'Lm + Lb-3' (185.4 mg L^{-1}) was significantly different from all other treatments (Fig. 4(b)). Likewise, even though the retention time was similar for all the unique maxima corresponding to the precursors of sirodesmin PL, the 'Lm + Lb-3' treatment had a 51.4% reduction in concentration when compared to the 'Lm only' control. The interactions between experiments and treatments were not significant, neither for sirodesmin PL ($F_{(20,44)} = 0.46$, $P < 0.969$) nor for its precursors ($F_{(20,44)} = 0.88$, $P = 0.607$).

3.3 Comparison of relative pathogen growth in liquid culture co-inoculated with *L. maculans* and *L. biglobosa*

At 14 days post initial inoculation, mycelia were harvested and freeze dried for DNA extraction and qPCR. The relative growth of *L. maculans* and *L. biglobosa* in liquid cultures with different co-inoculation treatments was assessed by measuring the amounts of *L. maculans* or *L. biglobosa* DNA using qPCR. The amounts of *L. maculans* or *L. biglobosa* DNA in 50 ng DNA extracted from cultures containing both *L. maculans* and *L. biglobosa* were expressed as percentage. There were significant differences between different treatments in percentage of *L. maculans* DNA ($F_{(10,44)} = 545.86$, $P < 0.001$; Fig. 5). For the treatments 'Lb only', 'Lm&Lb', 'Lm + Lb-1', 'Lb + Lm-1', 'Lb + Lm-3', 'Lb + Lm-5' and 'Lb + Lm-7', there were no significant differences between them in percentages of *L. maculans* DNA, with all containing 0 to 7% of *L. maculans* DNA. For the treatments with *L. biglobosa* inoculated first, followed by *L. maculans* at 1, 3, 5 or 7 days later ('Lb + Lm-1', 'Lb + Lm-3', 'Lb + Lm-5' and 'Lb + Lm-7'), the percentage of *L. maculans* DNA was consistently less than that of 'Lm&Lb' (3.10%), with 1.11%, 1.41%, 1.29% and 1.40%, respectively. Moreover, the treatments 'Lm only' (100%), 'Lm + Lb-5' (97.4%) and 'Lm + Lb-7' (97.4%) were not significantly different

Pest Management Science published by John Wiley & Sons Ltd on behalf of Society of Chemical Industry.

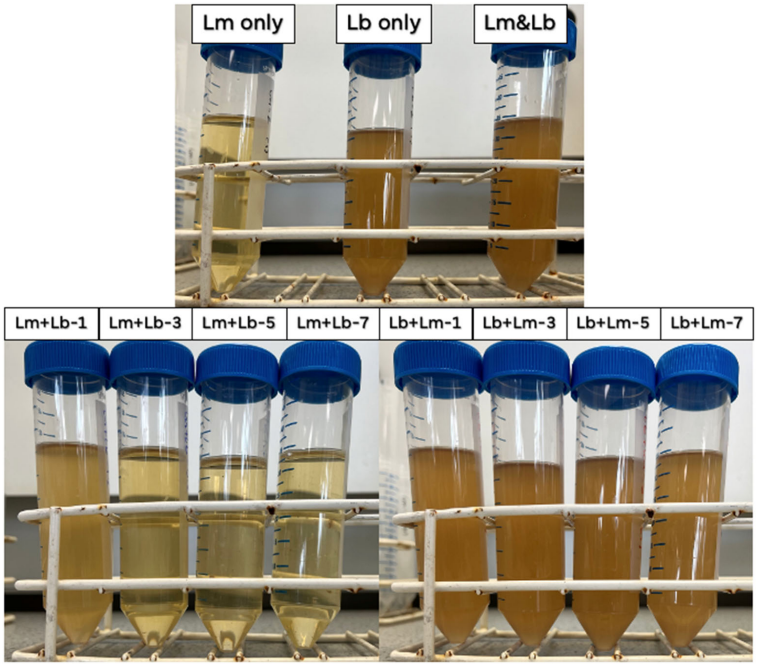

Figure 3. Colour of culture filtrates from liquid cultures inoculated with *Leptosphaeria maculans* only (Lm only), *Leptosphaeria biglobosa* only (Lb only), *L. maculans* and *L. biglobosa* co-inoculated simultaneously (Lm&Lb), first inoculation with *L. maculans* followed by co-inoculation with *L. biglobosa* sequentially at 1, 3, 5 or 7 days later (Lm + Lb-1, Lm + Lb-3, Lm + Lb-5, Lm + Lb-7), and first inoculation with *L. biglobosa* followed by co-inoculation with *L. maculans* sequentially at 1, 3, 5 or 7 days later (Lb + Lm-1, Lb + Lm-3, Lb + Lm-5, Lb + Lm-7), at 14 days after the first inoculation.

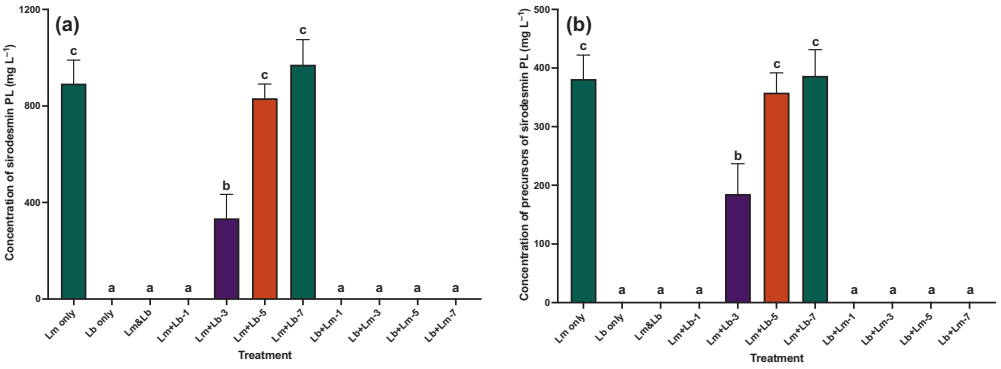

Figure 4. Average concentration of (a) sirodesmin PL (mg L^{-1}) and (b) the precursors of sirodesmin PL (mg L^{-1}) in secondary metabolite extracts obtained from three independent experiments with treatments consisting of liquid cultures inoculated with *Leptosphaeria maculans* only (Lm only), *Leptosphaeria biglobosa* only (Lb only), *L. maculans* and *L. biglobosa* co-inoculated simultaneously (Lm&Lb), first inoculation with *L. maculans* followed by co-inoculation with *L. biglobosa* sequentially at 1, 3, 5 or 7 days later (Lm + Lb-1, Lm + Lb-3, Lm + Lb-5, Lm + Lb-7), and first inoculation with *L. biglobosa* followed by co-inoculation with *L. maculans* sequentially at 1, 3, 5 or 7 days later (Lb + Lm-1, Lb + Lm-3, Lb + Lm-5, Lb + Lm-7). Tukey's HSD tests were used to separate the mean concentration of the precursors of sirodesmin PL across different treatments. Columns that do not share a common letter were considered significantly different ($P < 0.05$). Error bars show standard errors of the mean (SEM).

Pest Management Science published by John Wiley & Sons Ltd on behalf of Society of Chemical Industry.

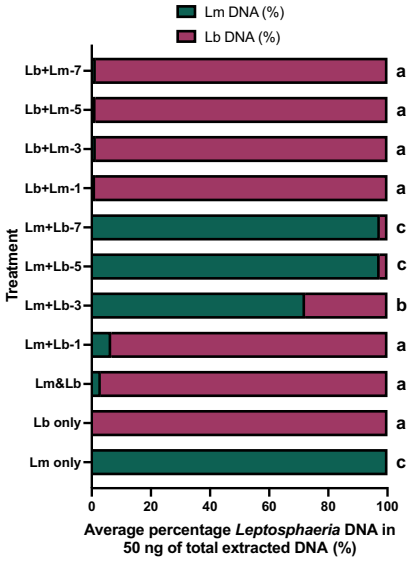

Figure 5. Average percentage of *Leptosphaeria* DNA (%) in homogenised mycelia obtained from three independent experiments with treatments consisting of liquid cultures inoculated with *Leptosphaeria maculans* only (Lm only), *Leptosphaeria biglobosa* only (Lb only), *L. maculans* and *L. biglobosa* co-inoculated simultaneously (Lm&Lb), first inoculation with *L. maculans* followed by co-inoculation with *L. biglobosa* sequentially at 1, 3, 5 or 7 days later (Lm + Lb-1, Lm + Lb-3, Lm + Lb-5, Lm + Lb-7), and first inoculation with *L. biglobosa* followed by co-inoculation with *L. maculans* sequentially at 1, 3, 5 or 7 days later (Lb + Lm-1, Lb + Lm-3, Lb + Lm-5, Lb + Lm-7). Tukey's HSD tests were used to separate the mean percentage of *L. maculans* DNA in total extracted DNA across different treatments. Columns that do not share a common letter were considered significantly different ($P < 0.05$).

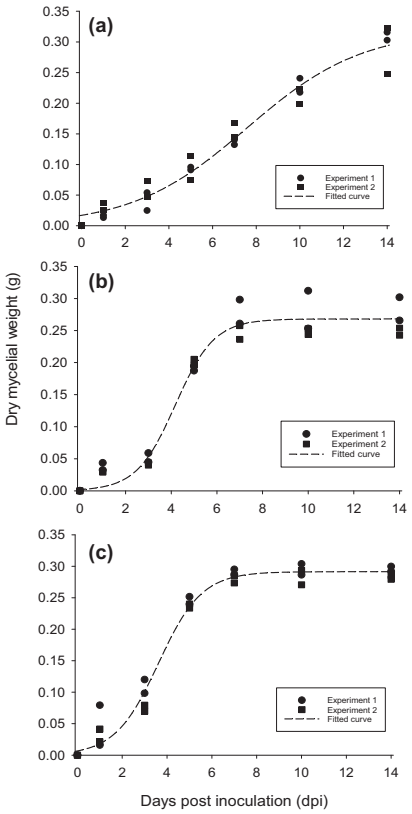

Figure 6. Fitted logistic curves for dry mycelial weight (g) of (a) *Leptosphaeria maculans* only (Lm only), (b) *Leptosphaeria biglobosa* only (Lb only) and C) *L. maculans* and *L. biglobosa* co-inoculated simultaneously (Lm&Lb) treatments from two independent experiments at 1, 3, 5, 7, 10 and 14 days post inoculation (dpi) in liquid culture. Dry mycelial weight in 'Lm only' treatment increased continuously from day 0 to 14 with the growth rate coefficient *k* value of 0.38 and the coefficient of determination (R^2) of 96.6%. Dry mycelial weight in 'Lb only' and 'Lm&Lb' treatments increased from day 0 to 7 to reach an asymptote and maintained the plateau thereafter until the experiment ended in 14 days, with the growth rate coefficient *k* values of 1.18 and 1.03, the coefficients of determination (R^2) of 96.8% and 97.9%, respectively.

from each other. However, 'Lm + Lb-3' (72.2%) was significantly different to all other treatments (Fig. 5). The reduction in *L. maculans* DNA between the 'Lm only' control treatment and 'Lm + Lb-3' was 27.8%; the concentrations of sirodesmin PL and its precursors for 'Lm + Lb-3' were also less than that of the 'Lm only' treatment but the percentage decreases were greater, at 62.6% and 51.4%, respectively. The interactions between experiments and treatments were not significant ($F_{(20,44)} = 0.94$, $P = 0.546$).

3.4 Comparison of mycelial growth rates of *L. maculans* and *L. biglobosa*

Results for the mycelial dry weight showed that there were differences between *L. maculans* and *L. biglobosa* in growth pattern and growth rate (Fig. 6). The mycelial growth of the 'Lm only' treatment increased steadily from day 0 to 14, reaching an average mycelial dry weight of 0.30 g by 14 dpi. The growth rate coefficient '*k*' value, estimated from the fitted logistic equation, was 0.38 (Fig. 6(a)). For the 'Lb only' treatment, mycelial growth rate coefficient was more than three times faster ($k = 1.18$) than for the 'Lm only' treatment. The mycelial growth for the 'Lb only' treatment reached a plateau (i.e., asymptote) at 0.26 g by 7 dpi and did not increase any further from 7 to 14 dpi (Fig. 6(b)). Interestingly, mycelial growth in the 'Lm&Lb' treatment showed a similar growth rate coefficient ($k = 1.03$) to that of the 'Lb only' treatment. Average mycelial dry weight for 'Lm&Lb' reached an asymptote at 0.29 g by 7 dpi and did not increase any further from 7 to 14 dpi (Fig. 6(c)).

4 DISCUSSION

The results of this study provide the first evidence that the timing of co-inoculation (i.e., the timing when *L. maculans* and *L. biglobosa* meet) strongly affects the interspecific interactions between *L. maculans* and *L. biglobosa* in terms of sirodesmin PL production and relative pathogen growth. Under sequential co-inoculation, for treatments where *L. biglobosa* was inoculated first, followed with *L. maculans* at 1, 3, 5 or 7 days later, the production

Pest Management Science published by John Wiley & Sons Ltd on behalf of Society of Chemical Industry.

of sirodesmin PL and its precursors was inhibited in all the treatments (Fig. 4). This research also confirmed previous work that simultaneous co-inoculation of *L. maculans* and *L. biglobosa* (Lm&Lb) inhibited the production of sirodesmin PL and its precursors.[29] However, when *L. maculans* was inoculated first, followed by *L. biglobosa* at 3, 5 or 7 days later, the production of sirodesmin PL and its precursors was not inhibited. These findings indicate that if there was any production of sirodesmin PL, *L. maculans* must be the first pathogen to be inoculated at least 3 days before *L. biglobosa*. This is supported by results from previous studies that it took up to 3 days for *L. maculans* to produce sirodesmin PL.[28,29] This study showed that *L. biglobosa* was still able to inhibit the production of sirodesmin PL and its precursors and retain its competitive advantage even when it was co-inoculated sequentially 1 day after *L. maculans* (Lm + Lb-1). This was because *L. biglobosa* had an antagonistic effect on the growth of *L. maculans*, confirmed by the proportion of the amount of *L. maculans* DNA by species-specific qPCR, with only 6.6% of *L. maculans* DNA detected in 'Lm + Lb-1' (Fig. 5). The antagonistic effect of *L. biglobosa* on the growth of *L. maculans* was also confirmed by both morphology of mycelia and pigment production (Figs 1 and 3). It was previously reported that *L. maculans* mycelia grew more intactly compared to *L. biglobosa* in liquid culture[3] and *L. biglobosa* produced pigmentation whereas *L. maculans* did not.[35] Both morphology of mycelia and pigmentation in culture filtrates suggest that the growth of *L. maculans* was inhibited in liquid cultures where *L. biglobosa* was inoculated before *L. maculans* or the two pathogens were co-inoculated simultaneously (Figs 1 and 3). This is further supported by the results of species-specific qPCR analyses, which showed that those treatments consistently had less than 3.0% *L. maculans* DNA, confirming that the growth of *L. maculans* was inhibited by *L. biglobosa* (Fig. 5). Although the 'Lm + Lb-1' treatment had more *L. maculans* DNA compared to the 'Lm&Lb' treatment, this difference was not significant.

Results showed that *L. biglobosa* started to lose its inhibitory effects when it was co-inoculated sequentially 3 days after *L. maculans*; this was mainly due to some sirodesmin PL and its precursors being produced, even though it was significantly less compared to that of the 'Lm only' control treatment. These results suggest that *L. biglobosa* has a partial antagonistic effect on *L. maculans* at the early stages of sirodesmin PL production since it takes approximately 3 days to produce sirodesmin PL.[28,29] However, *L. biglobosa* completely lost its ability to exert antagonistic effects on *L. maculans* growth and sirodesmin PL production if it was co-inoculated sequentially 5 or 7 days after *L. maculans*. This confirms previous work that *L. biglobosa* could not inhibit sirodesmin PL production by *L. maculans* if it is co-inoculated 7 days after *L. maculans*.[29] This was mainly due to sirodesmin PL already produced by *L. maculans* by 5–7 days, and the competitive advantage 'shifted' in favour of *L. maculans*. Therefore, *L. maculans* produces sirodesmin PL as an interference competition strategy against *L. biglobosa*. In order to out-compete *L. maculans*, *L. biglobosa* needs to act before the production of sirodesmin PL.

Although different hypotheses can be formulated about how these interactions occur, the exact mechanisms of the antagonistic effects of *L. biglobosa* on *L. maculans* remain unknown. Recent investigations have reported differences between *L. maculans* and *L. biglobosa* in terms of metabolic capacities. *Leptosphaeria biglobosa* is more efficient compared to *L. maculans* in terms of nutrient acquisition and utilisation of natural resources,[29,36] which is congruent with past reports indicating tissue colonisation by *L. biglobosa* occurs more rapidly compared to *L. maculans*.[10,37] The findings of this study further support this hypothesis since the mycelial growth rate coefficient of *L. biglobosa* was more than three times greater than that of *L. maculans* (Fig. 6). Furthermore, mycelial weight of the 'Lb only' treatment reached its maximum by 7 dpi and did not increase any further, suggesting that *L. biglobosa* has already utilised all the nutrients in the limited liquid media by 7 dpi. However, the mycelial growth of the 'Lm only' treatment increased steadily and reached its maximum by 14 dpi (Fig. 6). This can explain the reason why the 'Lm only' treatment was significantly greater in mycelial dry weight than all other treatments in the sequential co-inoculation experiments (Fig. 2). Moreover, mycelial growth rate and pattern of 'Lm&Lb' treatment were both similar to those of the 'Lb only' treatment, suggesting that the inhibition of growth of *L. maculans* is because *L. biglobosa* has utilised the nutrients in the condition with limited food source (e.g., limited volume of liquid culture). Previous studies on comparison of *L. maculans* and *L. biglobosa* growth were done by measuring radial growth of mycelia in agar plates.[25,29] However, this work was done in liquid cultures in shaking incubators so that nutrients in the media were equally distributed. Therefore, the differences in metabolic capacity between *L. maculans* and *L. biglobosa* may have been due to differences in their nutritional strategies. Although both *Leptosphaeria* species were characterised to have hemi-biotrophic lifestyles, differences between these two pathogens in terms of nutritional strategies were reported, with some even referring to *L. biglobosa* as a 'necrotroph'.[38,39] Additionally, one of the recent investigations of differences in metabolic capacity between *Leptosphaeria* species reported *L. biglobosa* to be less specialised, with *L. maculans* co-evolving more strictly with the plant host.[36] Therefore, one of the hypotheses to explain the mechanisms of these interactions is that *L. biglobosa* utilised the resources more efficiently and potentially caused competitive exclusion of *L. maculans* by employing a resource-mediated (exploitative) competition strategy.[1] In return, *L. maculans* inhibited the growth of *L. biglobosa* dependent upon successful production of sirodesmin PL by employing an interference competition strategy.[1,27–30] Results of this study supported this hypothesis and highlighted the significant influence of co-inoculation timing on the interspecific interactions between *L. maculans* and *L. biglobosa*.

An additional hypothesis to explain the mechanisms of these interactions between *L. maculans* and *L. biglobosa* is that *L. biglobosa* interferes with the gene expression related to production of sirodesmin PL by *L. maculans*. It was reported that 20 co-regulated genes are involved in the sirodesmin PL biosynthetic gene cluster (BGC) in *L. maculans*.[28,40] Our results showed that *L. biglobosa* inhibits the precursors of sirodesmin PL; this suggests that it would interfere with the expression of genes that are active in early stages of sirodesmin PL biosynthesis. It is known that sirodesmin PL biosynthesis starts with two amino-acids, tyrosine and serine.[28,41] The first step is the O-prenylation of L-tyrosine residue by dimethylallyl pyrophosphate, a reaction catalysed by a 4-*O*-dimethylallyl-L-tyrosine synthase, encoded by *sirD*.[42] The second step is the condensation of dimethylallyl-L-tyrosine and serine, catalysed by a two-module non-ribosomal peptide synthetase known to be indispensable for sirodesmin PL biosynthesis, encoded by *sirP*.[28,30,40] Furthermore, this biosynthetic cluster is regulated by a cross-control pathway gene, encoding for a Zn(II)2Cys6 transcription factor through *sirZ*.[28,30,43,44] There is a need to investigate if expression of one or more of these genes is disrupted, whether sirodesmin PL can be produced or not.

Moreover, competition under limited food source conditions (e.g., liquid culture), the rates of nutrient uptake by *L. maculans* and *L. biglobosa* may also affect the production of sirodesmin PL. Only one isolate of each pathogen was used in this study. There are seven subclades in *L. biglobosa*[17,45]; there is a need to investigate whether other subclades have similar antagonistic effects against *L. maculans*.

The results of this study have potential practical importance for phoma stem canker management. Firstly, this study confirmed the antagonistic effects of *L. biglobosa* on *L. maculans* if it is inoculated before *L. maculans* suggesting that it is possible to identify a weakly pathogenic isolate of *L. biglobosa* and use it as a biocontrol agent against *L. maculans*, which will potentially provide a sustainable and environmentally friendly way to control phoma stem canker by reducing fungicide sprays. Previous work showed that *L. biglobosa* inhibited *L. maculans* growth through inhibiting the production of sirodesmin PL both *in vitro* (liquid culture) and *in planta* (host) when they were co-inoculated simultaneously,[29] which suggests that the antagonistic effects of *L. biglobosa* on *L. maculans* observed in the liquid cultures in sequential co-inoculation, are likely to occur in their host plants. To test this hypothesis, there is a need to do experiments with sequential co-inoculation on host plants. Secondly, results of this study suggest that the difference in timing of *L. maculans* and *L. biglobosa* ascospore release in natural conditions may lead to differences in incidence of simultaneous and/or sequential co-inoculations, which may affect the severity of phoma leaf spotting and subsequently the severity of phoma stem canker. Because phoma stem canker epidemics are initiated by ascospores,[8,19,20,46] if ascospores of *L. biglobosa* are released earlier with a larger amount than ascospores of *L. maculans*, this will be analogous to the sequential co-inoculation with *L. biglobosa* before *L. maculans*, leading to *L. biglobosa* inhibiting the growth of *L. maculans*, subsequently leading to less severe phoma stem canker. This hypothesis is indirectly supported by previous results on timing/abundance of *L. maculans* and *L. biglobosa* ascospore release and the severity of phoma stem canker in field experiments.[20,47] For example, for the field experiments with nine cultivars, the mean severity of stem canker in the summer of 2012 (i.e., 2.28) was less than that in the summer of 2011 (i.e., 4.03). This may have been due to ascospores of *L. biglobosa* being released earlier with a larger amount than ascospores of *L. maculans* in the autumn 2011[20] so that *L. biglobosa* could have inhibited the growth of *L. maculans* leading to less severe canker in the summer of 2012. However, disease severity in field conditions can be affected by many other factors, such as rainfall, temperature, cultivar resistance and composition of pathogen races. Furthermore, the timing of ascospore release is also affected by weather conditions. Although weather-based models have been developed to predict the timing of ascospore release,[8,19,46] those models do not distinguish *L. maculans* from *L. biglobosa* ascospore release. There is a need to develop models specifically for the prediction of *L. maculans* or *L. biglobosa* ascospore release and use data from field experiments with on-site ascospore release monitoring to validate the models for guiding fungicide applications.

ACKNOWLEDGEMENTS

This research work was supported by the University of Hertfordshire, Chadacre Agricultural Trust, Felix Thornley Cobbold Agricultural Trust, the Perry Foundation, the UK Biotechnology and Biological Sciences Research Council (BBSRC, P00489X/1), the Innovate UK (102641), AHDB Cereals & Oilseeds (RD-2140021105), and the Department for Environment, Food and Rural Affairs (Defra, CH0110). The authors thank James Stanley and Christine Gigou for technical support and assistance.

CONFLICT OF INTEREST STATEMENT

There is no conflict of interest to report.

DATA AVAILABILITY STATEMENT

The data that support the findings of this study are available from the corresponding author upon reasonable request.

REFERENCES

1 Dutt A, Andrivon D and Le May C, Multi-infections, competitive interactions, and pathogen coexistence. *Plant Pathol* **71**:5–22 (2021). https://doi.org/10.1111/ppa.13469.
2 Zheng X, Koopmann B, Ulber B and von Tiedemann A, A global survey on diseases and pests in oilseed rape—current challenges and innovative strategies of control. *Front Agron* **2**:1-15 (2020). https://doi.org/10.3389/fagro.2020.590908.
3 Zhang X, White RP, Demir E, Jedryczka M, Lange RM, Islam M *et al.*, *Leptosphaeria* spp., phoma stem canker and potential spread of *L. maculans* on oilseed rape crops in China. *Plant Pathol* **63**:598–612 (2014). https://doi.org/10.1111/ppa.12146.
4 CropMonitor. Secure.fera.defra.gov.uk. (2022). Retrieved 24 February 2022, from https://secure.fera.defra.gov.uk/cropmonitor/.
5 Shoemaker R and Brun H, The teleomorph of the weakly aggressive segregate of *Leptosphaeria maculans*. *Can J Bot* **79**:412–419 (2001). https://doi.org/10.1139/b01-019.
6 Fitt BDL, Huang Y, Bosch F and West J, Coexistence of related pathogen species on arable crops in space and time. *Annu Rev Phytopathol* **44**:163–182 (2006). https://doi.org/10.1146/annurev.phyto.44.070505.143417.
7 de Gruyter J, Woudenberg JHC, Aveskamp MM, Verkley GJM, Groenewald JZ and Crous PW, Redisposition of phoma-like anamorphs in *Pleosporales*. *Stud Mycol* **75**:1–36 (2013). https://doi.org/10.3114/sim0004.
8 Huang Y, Fitt BDL, Jedryczka M, Dakowska S, West J, Gladders P *et al.*, Patterns of ascospore release in relation to phoma stem canker epidemiology in England (*Leptosphaeria maculans*) and Poland (*Leptosphaeria biglobosa*). *Eur J Plant Pathol* **111**:263–277 (2005). https://doi.org/10.1007/s10658-004-4421-0.
9 Bousset L, Jumel S, Garreta V, Picault H and Soubeyrand S, Transmission of *Leptosphaeria maculans* from a cropping season to the following one. *Ann Appl Biol* **166**:530–543 (2015). https://doi.org/10.1111/aab.12205.
10 Huang Y, Toscano-Underwood C, Fitt BDL, Hu X and Hall A, Effects of temperature on ascospore germination and penetration of oilseed rape (*Brassica napus*) leaves by A- or B-group *Leptosphaeria maculans* (phoma stem canker). *Plant Pathol* **52**:245–255 (2003). https://doi.org/10.1046/j.1365-3059.2003.00813.x.
11 West J, Balesdent M, Rouxel T, Narcy J, Huang Y, Roux J *et al.*, Colonization of winter oilseed rape tissues by A/Tox+ and B/Tox0 *Leptosphaeria maculans* (phoma stem canker) in France and England. *Plant Pathol* **51**:311–321 (2002). https://doi.org/10.1046/j.1365-3059.2002.00689.x.
12 Huang Y, Li Z, Evans N, Rouxel T, Fitt BDL and Balesdent M, Fitness cost associated with loss of the AvrLm4 avirulence function in *Leptosphaeria maculans* (phoma stem canker of oilseed rape). *Eur J Plant Pathol* **114**:77–89 (2006). https://doi.org/10.1007/s10658-005-2643-4.
13 Huang YJ, Pirie EJ, Evans N, Delourme R, King GJ and Fitt BDL, Quantitative resistance to symptomless growth of *Leptosphaeria maculans* (phoma stem canker) in *Brassica napus* (oilseed rape). *Plant Pathol* **58**:314–323 (2009).
14 Sewell TR, Hawkins NJ, Stotz HU, Huang YJ, Kelly SL, Kelly DE *et al.*, Azole sensitivity in *Leptosphaeria* pathogens of oilseed rape: the role of lanosterol 14α-demethylase. *Sci Rep* **7**:15849 (2017). https://doi.org/10.1038/s41598-017-15545-9.

Pest Management Science published by John Wiley & Sons Ltd on behalf of Society of Chemical Industry.

15 Fortune JA, Qi A, Ritchie F, Karandeni Dewage CS, Fitt BDL and Huang YJ, Effects of cultivar resistance and fungicide application on stem canker of oilseed rape (*Brassica napus*) and potential interseasonal transmission of *Leptosphaeria* spp. inoculum. *Plant Pathol* **70**:2115–2124 (2021). https://doi.org/10.1111/ppa.13453.
16 Fitt BDL, Brun H, Barbetti M and Rimmer S, World-wide importance of phoma stem canker (*Leptosphaeria maculans* and *L. biglobosa*) on oilseed rape (*Brassica napus*). *Eur J Plant Pathol* **114**:3–15 (2006). https://doi.org/10.1007/s10658-005-2233-5.
17 Dilmaghani A, Balesdent MH, Didier JP, Wu C, Davey J, Barbetti MJ *et al.*, The *Leptosphaeria maculans-Leptosphaeria biglobosa* species complex in the American continent. *Plant Pathol* **58**:1044–1058 (2009). https://doi.org/10.1111/j.1365-3059.2009.02149.x.
18 Abdullah A, Moffat C, Lopez-Ruiz F, Gibberd M, Hamblin J and Zerihun A, Host–multi-pathogen warfare: pathogen interactions in co-infected plants. *Front Plant Sci* **8**:1806 (2017). https://doi.org/10.3389/fpls.2017.01806.
19 Toscano-Underwood C, Huang YJ, Fitt BDL and Hall AM, Effects of temperature on maturation of pseudothecia of *Leptosphaeria maculans* and *L. biglobosa* on oilseed rape stem debris. *Plant Pathol* **52**:727–736 (2003). https://doi.org/10.1111/j.1365-3059.2003.00930.x.
20 Huang YJ, Sidique SN, Karandeni Dewage CS, Gajula LH, Mitrousia GK, Qi A *et al.*, Effective control of *Leptosphaeria maculans* increases importance of L. biglobosa as a cause of phoma stem canker epidemics on oilseed rape. *Pest Manag Sci* (2022). https://doi.org/10.1002/ps.7248.
21 Tan S, Gu Y, Yang C, Dong Y, Mei X, Shen Q *et al.*, *Bacillus amyloliquefaciens* T-5 may prevent *Ralstonia solanacearum* infection through competitive exclusion. *Biol Fertil Soils* **52**:341–351 (2016). https://doi.org/10.1007/s00374-015-1079-z.
22 Dutt A, Anthony R, Andrivon D, Jumel S, Le Roy G, Baranger A *et al.*, Competition and facilitation among fungal plant parasites affect their life-history traits. *Oikos* **130**:652–667 (2021). https://doi.org/10.1111/oik.07747.
23 Aimé S, Alabouvette C, Steinberg C and Olivain C, The endophytic strain *Fusarium oxysporum* Fo47: a good candidate for priming the defense responses in tomato roots. *Mol Plant Microbe Interact* **26**:918–926 (2013). https://doi.org/10.1094/mpmi-12-12-0290-r.
24 Liu S, Liu Z, Fitt B, Evans N, Foster S, Huang Y *et al.*, Resistance to *Leptosphaeria maculans* (phoma stem canker) in *Brassica napus* (oilseed rape) induced by *L. biglobosa* and chemical defence activators in field and controlled environments. *Plant Pathol* **55**:401–412 (2006). https://doi.org/10.1111/j.1365-3059.2006.01354.x.
25 Shah U, Kotta-Loizou I, Fitt BDL and Coutts R, Mycovirus induced hypervirulence of *Leptosphaeria biglobosa* enhances systemic acquired resistance to *Leptosphaeria maculans* in *Brassica napus*. *Mol Plant Microbe Interact* **33**:98–107 (2020). https://doi.org/10.1094/MPMI-09-19-0254-R.
26 Mahuku G, Hall R and Goodwin P, Co-infection and induction of systemic acquired resistance by weakly and highly virulent isolates of *Leptosphaeria maculans* in oilseed rape. *Physiol Mol Plant Pathol* **49**:61–72 (1996). https://doi.org/10.1006/pmpp.1996.0039.
27 Rouxel T, Chupeau Y, Fritz R, Kollmann A and Bousquet JF, Biological effects of sirodesmin PL, a phytotoxin produced by *Leptosphaeria maculans*. *Plant Sci* **57**:45–53 (1988). https://doi.org/10.1016/0168-9452(88)90140-9.
28 Gardiner D, Cozijnsen A, Wilson L, Pedras M and Howlett B, The sirodesmin biosynthetic gene cluster of the plant pathogenic fungus *Leptosphaeria maculans*. *Mol Microbiol* **53**:1307–1318 (2004). https://doi.org/10.1111/j.1365-2958.2004.04215.x.
29 Fortune JA, Bingol E, Qi A, Baker D, Ritchie F, Karandeni Dewage CS *et al.*, *Leptosphaeria biglobosa* inhibits the production of sirodesmin PL by *L. maculans*. *Pest Manag Sci* (2022). https://doi.org/10.1002/ps.7275.
30 Elliott CE, Gardiner DM, Thomas G, Cozijnsen A, van de Wouw A and Howlett BJ, Production of the toxin sirodesmin PL by *Leptosphaeria maculans* during infection of *Brassica napus*. *Mol Plant Pathol* **8**:791–802 (2007). https://doi.org/10.1111/j.1364-3703.2007.00433.x.
31 Gardiner DM and Howlett BJ, Bioinformatic and expression analysis of the putative gliotoxin biosynthetic gene cluster of *Aspergillus fumigatus*. *FEMS Microbiol Lett* **248**:241–248 (2005). https://doi.org/10.1016/j.femsle.2005.05.046.
32 Cramer RA, Gamcsik MP, Brooking RM, Najvar LK, Kirkpatrick WR, Patterson TF *et al.*, Disruption of a nonribosomal peptide synthetase in *Aspergillus fumigatus* eliminates gliotoxin production. *Eukaryot Cell* **5**:972–980 (2006). https://doi.org/10.1128/ec.00049-06.
33 Pedras M and Biesenthal C, Production of the host-selective phytotoxin phomalide by isolates of *Leptosphaeria maculans* and its correlation with sirodesmin PL production. *Can J Microbiol* **44**:547–553 (1998). https://doi.org/10.1139/w98-034.
34 VSN International, *Genstat for Windows*, 22nd edn. VSN International, Hemel Hempstead, UK (2022) Web page: genstat.co.uk.
35 Williams RH and Fitt BDL, Differentiating A and B groups of *Leptosphaeria maculans*, causal agent of stem canker (blackleg) of oilseed rape. *Plant Pathol* **48**:161–175 (1999). https://doi.org/10.1046/j.1365-3059.1999.00333.x.
36 Frąc M, Kaczmarek J and Jędryczka M, Metabolic capacity differentiates *Plenodomus lingam* from *P. biglobosus* subclade 'brassicae', the causal agents of phoma leaf spotting and stem canker of oilseed rape (*Brassica napus*) in agricultural ecosystems. *Pathogens* **11**:50 (2022). https://doi.org/10.3390/pathogens11010050.
37 Eckert M, Maguire K, Urban M, Foster S, Fitt BDL, Lucas J *et al.*, *Agrobacterium tumefaciens*-mediated transformation of *Leptosphaeria* spp. and *Oculimacula* spp. with the reef coral gene dsred and the Jellyfish Gene GFP. *FEMS Microbiol Lett* **253**:67–74 (2005). https://doi.org/10.1016/j.femsle.2005.09.041.
38 Lowe RG, Cassin A, Grandaubert J, Clark BL, Van de Wouw AP, Rouxel T *et al.*, Genomes and transcriptomes of partners in plant-fungal-interactions between canola (*Brassica napus*) and two *Leptosphaeria* species. *PloS One* **9**:e103098 (2014). https://doi.org/10.1371/journal.pone.0103098.
39 Padmathilake K and Fernando W, Less virulent *Leptosphaeria biglobosa* immunizes the canola plant to resist highly virulent *L. maculans*, the blackleg pathogen. *Plan Theory* **11**:996 (2022). https://doi.org/10.3390/plants11070996.
40 Urquhart A, Elliott C, Zeng W and Idnurm A, Constitutive expression of transcription factor SirZ blocks pathogenicity in *Leptosphaeria maculans* independently of sirodesmin production. *PloS One* **16**:e0252333 (2021). https://doi.org/10.1371/journal.pone.0252333.
41 Gardiner DM, Waring P and Howlett BJ, The epipolythiodioxopiperazine (ETP) class of fungal toxins: distribution, mode of action, functions and biosynthesis. *Microbiology* **151**:1021–1032 (2005). https://doi.org/10.1099/mic.0.27847-0.
42 Kremer A and Li S-M, A tyrosine *O*-prenyltransferase catalyses the first pathway-specific step in the biosynthesis of Sirodesmin PL. *Microbiology* **156**:278–286 (2010). https://doi.org/10.1099/mic.0.033886-0.
43 Elliott CE, Fox EM, Jarvis RS and Howlett BJ, The cross-pathway control system regulates production of the secondary metabolite toxin, sirodesmin PL, in the Ascomycete, Leptosphaeria maculans. *BMC Microbiol* **11**:169 (2011). https://doi.org/10.1186/1471-2180-11-169.
44 Fox EM, Gardiner DM, Keller NP and Howlett BJ, A zn(ii)2cys6 DNA binding protein regulates the sirodesmin PL biosynthetic gene cluster in *Leptosphaeria maculans*. *Fungal Genet Biol* **45**:671–682 (2008). https://doi.org/10.1016/j.fgb.2007.10.005.
45 Zou Z, Zhang X, Parks P, du Toit L, Van de Wouw A and Fernando W, A new subclade of *Leptosphaeria biglobosa* identified from *Brassica rapa*. *Int J Mol Sci* **20**:1668 (2019). https://doi.org/10.3390/ijms20071668.
46 Salam MU, Fitt BDL, Aubertot J-N, Diggle AJ, Huang YJ, Barbetti MJ *et al.*, Two weather-based models for predicting the onset of seasonal release of ascospores of *Leptosphaeria maculans* or *L. biglobosa*. *Plant Pathol* **56**:412–423 (2007). https://doi.org/10.1111/j.1365-3059.2006.01551.x.
47 Huang Y, Hood J, Eckert M, Stonard J, Cools H, King G *et al.*, Effects of fungicide on growth of *Leptosphaeria maculans* and *L. biglobosa* in relation to development of phoma stem canker on oilseed rape (*Brassica napus*). *Plant Pathol* **60**:607–620 (2011). https://doi.org/10.1111/j.1365-3059.2010.02416.x.

Pest Management Science published by John Wiley & Sons Ltd on behalf of Society of Chemical Industry.